AES/PE/11-26

Comprehensive reservoir quality assessment of Buntsandstein sandstone reservoirs in the West Netherlands Basin for geothermal applications in Zuid Holland province area

23/08/2011

Peter Stefanov Matev

Department of Geotechnology

Delft University of Technology

Title	:	Comprehensive reservoir assessment of Buntsandstein reservoirs in West Netherlands Basin for geothermal applications in Zuid-Holland province area
Author(s)	:	Peter Stefanov Matev
Date	:	August 2011
Professor(s)	:	Dr. G. J. Weltje
Supervisor(s)	:	Dr. A. Speksnijder
		Dr. G. J. Weltje
		Dr. K.H.A.A. Wolf
TA Report number	:	AES/PE/11-26
Postal Address	:	Section for Applied Geology
		Department of Applied Earth Sciences
		Delft University of Technology
		P.O. Box 5028
		The Netherlands
Telephone	:	(31) 15 2781328 (secretary)
Telefax	:	(31) 15 2781189

Abstract

This report presents the results of a study on the reservoir quality of Main Buntsandstein formations in regard with possible geothermal energy development and exploration in the Zuid Holland area of the West Netherlands Basin. The assessment of the possibility of using the Triassic Buntsandstein sandstone reservoirs for geothermal application is carried out in a similar way of basin exploration for hydrocarbons with major focus on reservoir quality.

Geothermal energy is becoming increasingly important as an alternative source of energy and heat for the Dutch agriculture and urban areas. In order to determine the possibilities for geothermal exploration in the target area the reservoir properties have to carefully studied and assessed. This is done with respect of the original depositional environment of the sediments, the burial history of the basin and the related diagenetic history. The results are summarized in reservoir geologic models and evaluated.

The study on the depositional environment of the Main Buntsandstein formations is the most extensive for the project and covers basin wide well correlations, petrophysical and sedimentological evaluation and interpretation of the encountered facies, and introduction of sequence stratigraphic model for interpretation of the formations. The results of the study include new insights on the formation boundaries and lateral continuity. Each formation member is described separately and examples are provided to support the suggested interpretations.

The burial history study is carried out on three two dimensional seismic surveys in-lines in the offshore and onshore part of the target area. The work is performed using specialized software and the result indicate that specific parts of the basin have experienced significantly stronger effect from the different stages of the tectonic development of the West Netherlands Basin. The major conclusion of the study is that although the Triassic sediments have not been exposed to burial depths of more than 700 meters of their current depth, individual fault blocks have experienced very varied burial histories and have therefore different diagenetic footprint.

The results of the previous studies are used to evaluate and explain the available information for the diagenetic history of the sediments in the target area. The results indicate that significant differences are to be expected between adjacent fault blocks in regard with the late diagenetic processes such as quartz dissolution and precipitation.

The acquired knowledge for the reservoir properties in the target areas in the basin is summarized in extensive reservoir models and grids. The resulting grids represent the observed spatial variations in reservoir quality and also the changes in reservoir thickness across major faults. The resulting grids have also suggested well planning and evaluated for the expected temperatures using available well temperature data.

The time of thermal breakthrough is calculated using a theoretical approach and suggestions are made for further dynamic simulations of the already created reservoir simulation models.

The project is then evaluated in terms of financial planning and expected costs. A suggestion is made and explained for the improved project feasibility and rate of return for co-production of gas and condensates with the hot water.

The report is summarized with an overall evaluation of the project feasibility in terms of reservoir quality and known uncertainties. The final conclusion of the report can be described as conservatively positive as additional studies are required and recommended in order to reduce the still remaining uncertainty.

Acknowledgements

I would like to thank a number of people that contributed positively to this project.

The most important person that made this project possible and contributed greatly to the quality of the results is Dr. Arie Speksnijder. His undisputed expertise in the West Netherlands Basin and Buntsandstein was most valuable guide and help for me. Most of the results and studies that I carried out would have been impossible if it was not for his constructive guidance and shared knowledge.

I would also like to thank all my colleagues in PanTerra Geoconsultants with Dr. Andrew van de Weerd, Wiebe van Driel and Annelies Bender in particular for the professional guidance and helpful suggestions and recommendations for the various parts of the project.

I am very grateful to PanTerra Geoconsultants for providing me with a perfect working environment and professional software tools that helped me carry out the project.

I want to thank all the members of my graduation committee and supervisors in Delft University of Technology for their constructive criticism on the report. I would also want to thank Dr. Andrew van de Weerd and Dr. Arie Speksnijder for their detailed corrections on the report and also for the general guidance while compiling the different parts of the report; Dr. Karl-Heinz Wolf and Dr. Gert Jan Weltje for the final reviewing of the report and constructive and helpful remarks for improving it; and Prof. Dr. Pacelli Zitha for being on the final graduation committee board.

Last but not least I would like to thank my family and close friends for supporting me while I worked on this project.

Table of contents:

List of Abbreviations:

BC	Base Cretaceous
BHM	Base Holland Marl
BFB	Broad Fourteens Basin
BT	Base Tertiary
RD	Rijksdriehoekscoördinaten
RVG	Roer Valley Graben
TNO	Nederlandse Organisatie voor toegepast-natuurwetenschappelijk onderzoek
TTM	Top Texel Marl (Base Chalk)
UMT31	Universal Transverse Mercator, 31
WNB	West Netherlands Basin
SGS	Sequential Gaussian Simulation
SG-CoS	Sequential Gaussian Co-Simulation (concurrent simulation of two parameters)
Geo-grid	Geological grid
Sim-grid	Simulation grid

1. Project introduction and summary of available data

This report presents the results of the regional geologic study including regional well log correlations, burial history restoration, diagenetic history restoration, static geologic modelling of target areas and dynamic reservoir modelling of selected sub-areas. The purpose of the study is to establish a solid framework for planning and development of geothermal resources for very hot water in the south western areas of The Netherlands. The approach is therefore selected such as to include evaluation of the most important factors that influence the geological, engineering and economical conditions related to geothermal applications.

Geothermal energy is a hot topic as it is a sustainable green alternative energy source for the increasing energy demand in the Netherlands. Heat from deep geothermal sources can be used for warming up building, industrial spaces, greenhouses and, given that the produced water temperature is sufficient, also to produce electricity with zero carbon dioxide emissions. Unlike other sources for alternative energy such as photovoltaic panels and wind mills, geothermal energy is available without interruption and most importantly it can benefit from the already existing technological know-how from the oil and gas industry. In comparison other green sources of energy often require large further technological advances in order to achieve sufficient and economically feasible efficiency, making them very expensive alternatives.

The province of Zuid Holland is densely populated and accommodates a significant congestion of greenhouse complexes that require immense amount of energy. From a geological point of view the province lies over the well known hydrocarbon prolific West Netherlands Basin. Exploration and production of hydrocarbons from the basin has been active for more than 50 years already and the geological knowledge of the basin has therefore benefitted well from the large amount of collected data from drilling campaigns and seismic acquisition. The combination of advantageous factor makes the area an important target for development of geothermal energy resources for the benefit of the local agriculture, industry and urban complexes.

The purpose of this study is to evaluate the potential of the reservoirs from Main Buntsandstein subgroup of Lower Triassic age for development of geothermal energy in the area. A successful geothermal project has several important requirements that need to be available in order for the system to operate efficiently. First of all the most important part of a geothermal project is the produced hot water. For a sufficient supply of hot water a reservoir with good petrophysical properties at a sufficient depth is required. In order to be able to use the produced water effectively there should be available onshore location to host the well doublet and heat exchangers. Eventually if all requirements are met the produced energy should exceed the used energy for the production of water and construction of the system in order to make the project efficient and sustainable.

Several factors need to be carefully evaluated in order to give reasonably accurate prediction for the availability and properties of the required reservoirs. This study has its main objective focused towards establishing a steady approach towards achieving this goal. A geological study is required in order to organize the available data into a system with sufficient predictability capabilities for the expected reservoir qualities in areas that have not been penetrated by earlier drilling campaigns. The geological study was designed such as to describe as accurately as possible the depositional environment of the target sediments using well log correlations, well core descriptions and interpretations, evaluation of regional trends, evaluation of petrophysical properties, comparison with analogue systems and comparison with outcrop examples of the same age. The results are also supported by a burial history study which is required given the complex tectonic history of the basin with several stages of extension and basin inversion. The conclusions of both studies are then complemented by a diagenetic history evaluation. As all information is collected and organized the actual geologic modelling is initiated using seismic interpretations from several large 3D seismic surveys. The initial model area is then divided into two smaller study areas which are further modeled using finer geologic grid in order to be able to represent better the spatial variability of reservoir properties. The results from the geologic modelling are then used to create four simulation grids over further limited area. They are the basis for the final dynamic models and simulations that aim to evaluate the actual

potential of the reservoir to provide sufficient flow rates of high temperature water for geothermal applications.

The following overview map gives the contours of the different studies that were carried out as part of this project. The underlay of the map is a map of the south west Netherlands including all the drilled wells. The geographic location of the target areas including the urban areas are shown in Chapter 5 when the actual geologic models are presented.

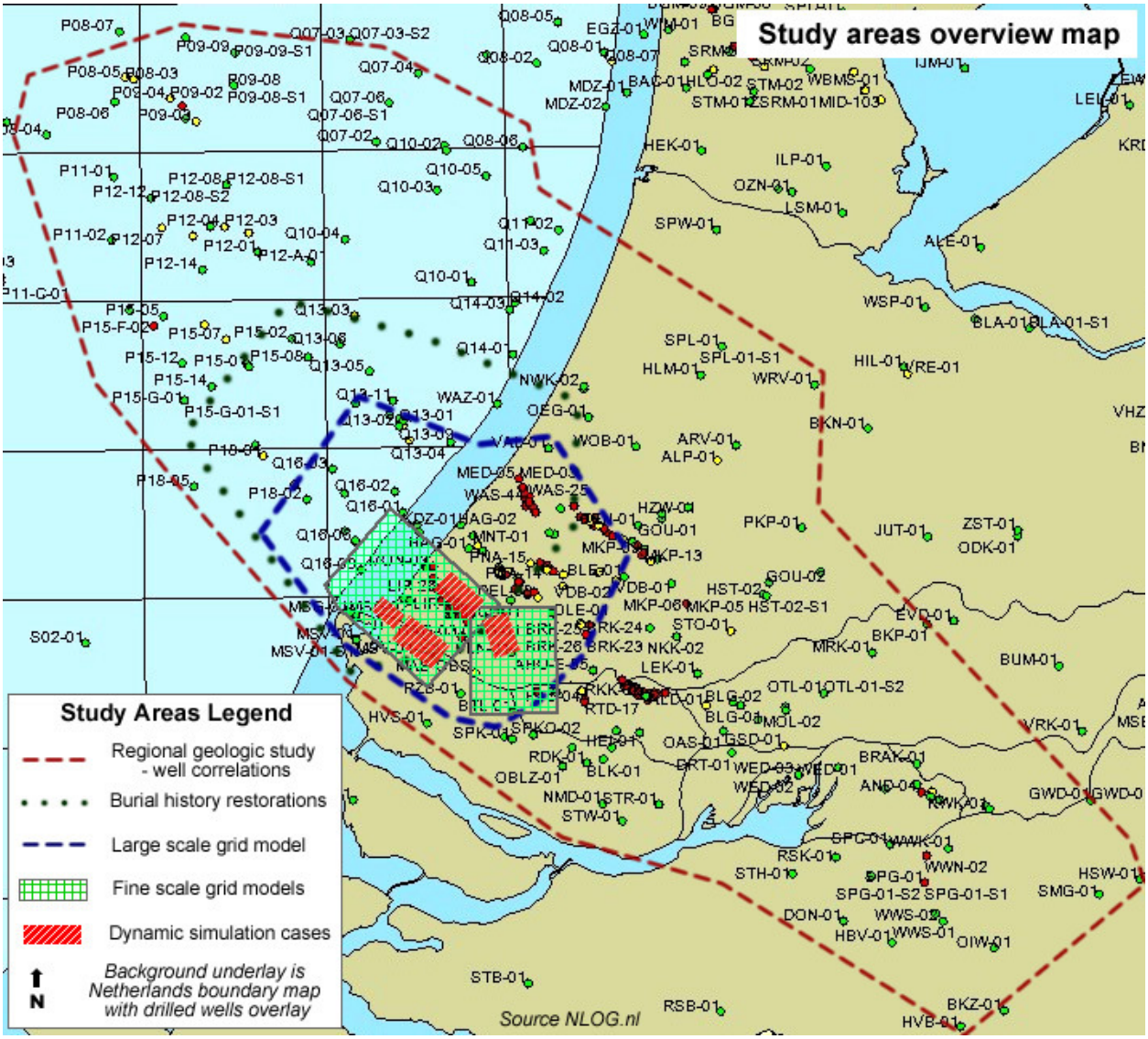

Figure 1: Project areas overview map

The area of the depositional environment geologic study extend towards the Broad Fourteens basin and Roer Valley Graben Basin in order to relate the development of the depositional sedimentary systems in these adjacent to West Netherlands basin areas and thus provide additional controls on the spatial distribution of the different formations. The rest of the studies are concentrated in the south western onshore and offshore areas of the Netherlands where the potential target reservoirs are.

In the following paragraphs an overview of the project approach, used data and used software will be provided in order to outline the project structure and development as well as to be used as reference for further development of the presented concepts.

VISIO

Depositional environment regional study

The regional study is important as the reservoir quality in the project area is directly dependant on the regional basin trends. The only reliable ways to evaluate the regional trends is to starts the study from a broad perspective and gradually direct it towards a more detailed look into the actual target areas.

Available data

The input for this study consists of wireline logs including gamma-ray, bulk density, spontaneous potential, dip-meter surveys and evaluation reports, field petrophysical and sedimentological studies, core analysis data, core photographs and sedimentological descriptions, regional geologic studies for the subsurface of the Netherlands and South North Sea, and for outcrops from Germany and France, and suggested lithostratigraphy from TNO as starting point for interpretations.

The following table gives the list of wells that were used in the project in the regional correlations or in the petrophysical and sedimentological evaluations.

Onshore							
AND-06	ARV-01	BRAK-01	**BRT-02-S1**	**BRTZ-01**	BRTZ-02-S3	BRTZ-03	BSKP-01
BTL-01	**CAP-01**	**GAG-02-S1**	GAG-03	GAG-04	**GAG-05**	HST-02-S1	HSW-01-S1
HVB-01	HVS-01	**IJS-64-S2**	**KDZ-02-S1**	**LIR-45**	**MKP-14**	MOL-02-S2	MON-02
MON-03	MRK-01	**MSG-01**	MSG-02	MSV-01	NWK-02	OAS-01	OBLZ-01
OTL-01	PKP-01	**PRW-01**	PRW-02	PRW-04	PRW-05	RDK-01	**RTD-01**
RZB-01	**SGZ-01-S1**	SPG-01-S2	SPK-01	SPKO-01	**SPKW-01**	STW-01	**VAL-01**
WAA-01	**WAS-23**	WED-02	WED-03	WGD-01	WLK-01	WRV-01	WWK-01
WWN-01-S2	WWN-03	WWS-01-S1	WWS-02				
Offshore							
P08-04	P08-06	P09-07	P11-01	P11-02	P12-01	P12-08-S2	P12-12
P14-A-01	**P15-01**	P15-02	P15-10	P15-F-01	P15-F-02	P15-G-01-S1	P15-12
P15-14	**P18-01**	**P18-02**	Q07-02	Q08-06	Q10-02	Q10-03	Q10-04
Q11-01-S2	Q11-03	Q13-03	**Q13-04**	Q13-06	**Q13-07-S2**	Q14-02	**Q16-02**
Q16-04	**Q16-08**						

Table 1: List of wells used in the project, wells in bold have porosity logs generated for the static geologic modelling. Wells with light grey background are used in the petrophysical evaluation, and wells in darker grey are also used in the sedimentological evaluation for encountered facies.

All of the well wireline logs are taken from the publicly available database from TNO - DINO services website and the actual correlations are carried out in Halliburton Landmark's GeoGraphix Discovery software package.

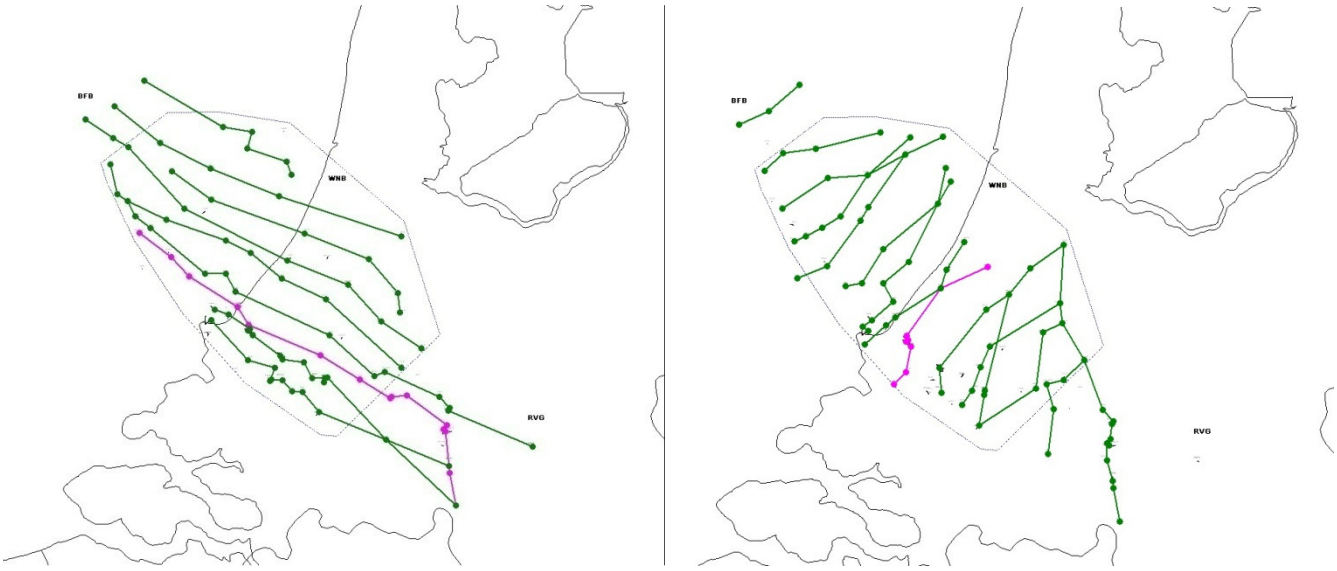

Figure 2: Map of correlation panels in "strike" direction to the left and in "dip" direction to the right.

Approach

The actual approach that was selected for the complete evaluation of the depositional environment of the Main Buntsandstein formations in the West Netherlands Basin is an iterative process between the different components of the study. The workflow includes compilation of available theoretical knowledge about the geologic setting in the basin in regard of the Triassic sediments. In order to provide a consistent and logical interpretation the actual correlation approach was altered from lithostratigraphic to sequence stratigraphic correlations. In order to analyze the individual facies and changes in depositional environment digital core descriptions of the available photographed cores are made and most of the available dip meter and formation micro imager data is collected and analyzed for paleo flow directions.

Results

The outcome of this study includes basin wide correlations for all Triassic formations, thickness maps, detailed Main Buntsandstein formations characterizations with digital core descriptions, combined sequence stratigraphic framework for interpreting the Main Buntsandstein formations, and updated facies probability distribution maps. Results also include a facies petrophysical evaluations that are further discussed in the chapter about porosity-permeability relationships and static geologic modelling.

Burial history restorations and Diagenetic history study

The next part of this study is focussed on second important factor for the current reservoir properties of the target sandstones – the post-depositional diagenetic development of the sediments.

Available data

The input for this part of the reservoir assessment study includes several seismic 2D lines, a number of studies on the structural development of the West Netherlands Basin and other inverted basins, including studies on restoration attempts on such basins, several core analysis reports regarding diagenetic history of Triassic sediments from the West Netherlands Basin (wells SMG-01, WWK-01, NDW-01, P11-02, a number of wells from L, K, P and Q offshore blocks), FMI and AST surveys (wells P18-A-06, VAL-01, Q13-07) and reports including evaluation of fractures availability and descriptions.

Data used in the burial restorations includes:

- In-line 993 from seismic survey Z3AMC1989A
- In-line 1299 from seismic survey L3NAM1991A
- In-line 1778 from seismic survey Z3NAM1990D
- 2D seismic line 142 from seismic survey Z2NAM1983A

The actual restorations are carried out in Midland Valley Exploration's Move (2D) software. Seismic data is taken from the publicly available data from TNO-DINO database. Interpretations are either from PanTerra Geoconsultants database or own work.

Approach and Results

The most important information that this part of the study tries to deliver is the possible mechanisms to improve the predictability of reservoir properties in areas that are not previously reached by drilling campaigns. In order to achieve that, a number of factors are examined and reported including - deepest burial influence from palinspastic restorations; largest combined burial history influence from palinspastic restorations; summarized diagenetic history from several sources; fractures availability, influence and distribution from analysis of AST and FMI studies, and connection to burial history restorations; and evaluation of interaction between burial history and original depositional environment influence for the diagenetic development of different fault blocks in the basin. All of these sub-studies build upon an improved reservoir quality conceptual model that aims to decrease the uncertainty in possible future target areas for geothermal project development. The uncertainty and risk maps are further incorporated in the project evaluation and feasibility chapter.

Building of static geologic models

The construction of the static geologic model presents the combination of all of the previous acquired knowledge about the reservoir properties and qualities. The framework of the reservoirs models is the

seismic interpretation of a number of seismic surveys from the south- south west areas of the West Netherlands Basin but the actual building fabric is based on the results of the previous evaluations from this study. The geologic reservoir models are therefore a manifestation of the combined acquired geologic knowledge and expectations. Although they are based on the available data they are also a product of the authors own perceptions of the basin and geology of the sediments and thus should be considered as only one of the possible realizations of the available data. The risk assessment is further discussed in project feasibility chapter.

Available data

The basis for the project is formed by the seismic interpretation of geologic boundaries reflectors. The seismic surveys that were used in this project can be seen in Figure 2 below. Interpretation of the seismic data, including seismic horizons and faults is owned by PanTerra Geoconsultants. The additional interpretations and adjustments are made by the author of this study. The actual work is carried out in Baker Hughes' software package Jewelsuite Oil & Gas 2011 including seismic horizons construction and interpolation, faults construction and interpolations, additional smoothing, extension, retraction, and connections between horizons and faults, construction of geologic and simulation grids and property modelling of geologic data.

All of the coordinates for the seismic surveys and wells are given in RD New (Rijksdriehoekscoördinaten) coordinate system. Surveys or wells that were available in other coordinate systems such as UMT31 or other have been converted to RD and then imported into the project.

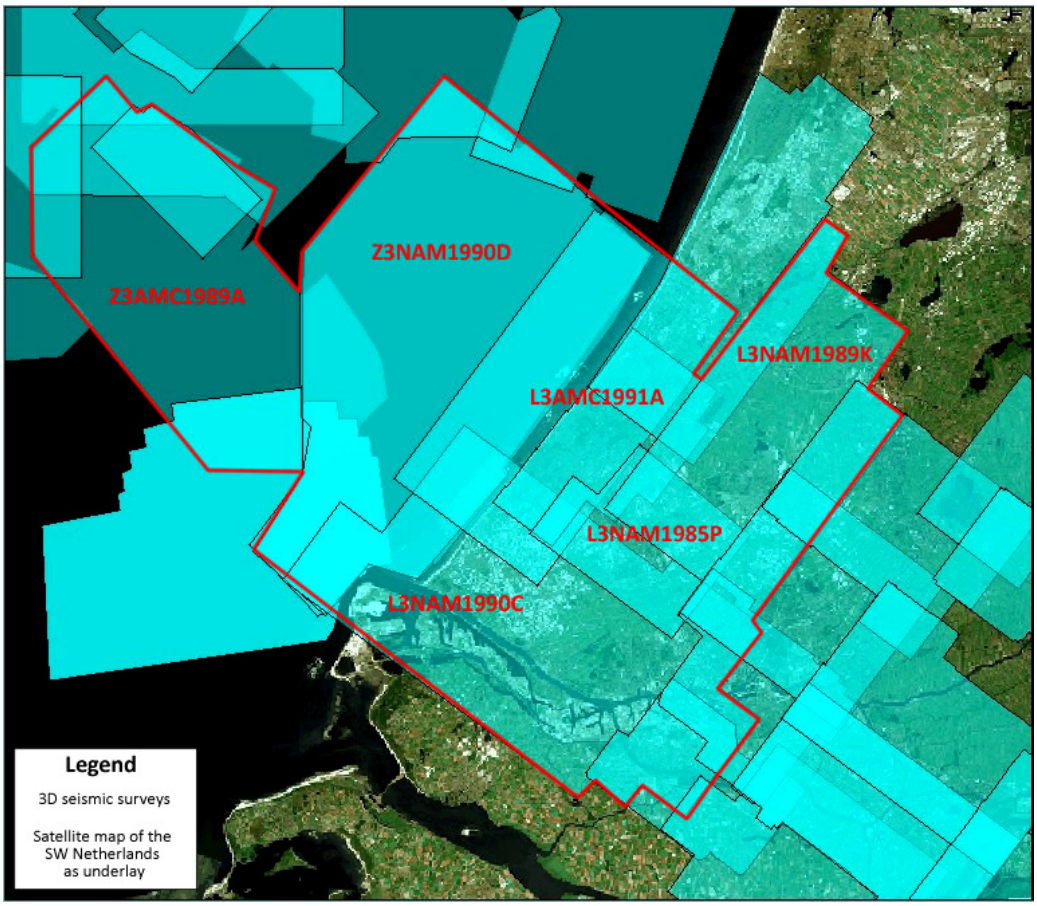

Figure 3: Overview map of the 3D seismic surveys used in the project

Approach

The workflow for the static geologic modelling starts with combining, correcting and merging available seismic interpretations from all of the used seismic surveys. The interpreted surfaces are Base Tertiary, Texel Marl, Posidonia Shale, and Top Triassic. The velocity model that was used in the project is build using interval velocities derived from marker depths and horizon times based on Base Tertiary, Texel Marl and Top Triassic levels. The depth converted Top Triassic horizon is therefore completely accurate at the well locations. The

next steps of the modelling workflow include area definitions, horizon and fault triangulation, structural geologic model building in a number of iterative steps, geologic model definition, and eventually 3D grid modelling in several consecutive steps. The property modelling is also done in several steps starting from the coarse grid cell size regional model and moving towards the fine grid cells size simulation models. The input for the property modelling is prepared using the combined results from the previous parts of the study and is also explained in detail. The detailed workflow steps are further explained in the chapter for reservoir static modelling.

Results

The results of this part of the study include geologic and simulation grids populated with reservoir petrophysical data for the target regions separated into several modelling steps based on the actual amount of detail available in the model. The results of this part of the study also includes evaluation of available bore hole temperature data, evaluation of reservoir petrophysical data and relationships, and evaluation of sources of uncertainty.

Reservoir simulations and evaluation of results

The reservoir simulations and the evaluation of the results is the conclusion of this study as it gives the final touch on the evaluation of the possibility for large scale development of the Main Buntsandstein reservoir for geothermal purposes in the West Netherlands Basin and in Zuid Holland area in particular.

Available data

The input for this part of the study comprises of the results of all of the previous steps in the study – simulation grids, and reservoir properties and temperature models. The simulation model is constructed based on available research studies on geothermal reservoir simulations including the most important considerations that play a role when modelling a geothermal project.

Approach and Results

The first step in preparing the simulations is to plan the possible well locations and optimal trajectories. This is done on basis of the structural geologic model as a combination of depth, porosity and surface location availability. The simulation grids have porosity, horizontal and vertical permeability, and temperature cell properties. Cells in the simulation models are either 25 or 35 meters in lateral and several meters in vertical dimensions based on the structural complexity and the related limitations of the modelling software. The reservoir simulations are designed to evaluate the ability of the targeted reservoir areas to produce fluids at the required production rates and to evaluate the break trough time for the temperature front in the production wells.

The results are presented not only in terms of the calculations but also in respect with the expected economic footprint of the possible project developments and combination of uncertainty evaluations for the risk assessment maps.

2. Depositional environment model of the Main Buntsandstein subgroup in the West Netherlands Basin

The determination of the depositional environment of the Main Buntsandstein subgroup is a very important step towards the thorough understanding of the contemporary reservoir quality of the target reservoirs in the formations. This is achieved by careful analysis of the available information from cores, wireline logs, outcropping analogues from the same formation and inferred information for the paleo-climate and paleo-geography. The regional well correlations are the back bone of the study and are based on 96 gamma ray and density or sonic well logs from the West Netherlands Basin and adjacent regions from Broad Fourteens and Roer Valley Graben Basins. Additionally cores from 31 wells with Main Buntsandstein penetration were analysed and in 17 of them with available core photographs or core description lithofacies were identified and analysed as well. All this data is eventually summarized in a sequence stratigraphic framework for the development of the basin during the studied period based on the classic clastic basin development theories.

2.1. Lithofacies of the Main Buntsandstein subgroup deposited in the Lower Triassic

Interpreted origin of facies	Lithological Composition	Description / Bedding / Divisions
Aeolian Dunes/ Dry sand flats (1)	Well to very well sorted, coarse to fine-grained, subarcosic arenites grading locally to lithic, arcosic arenites – sandstones. Dolomitic and occasionally argillaceous or anhydritic.	Lower portions: Planar cross stratification, with localized slightly wavy bedding and shaly laminations. Bimodal grain size and rounding distributions that can be either segregated or intermixed. Dips to 30°. Upper portions: Decreased bedding, homogeneous grain size distribution and better rounding. Localized diagenetic contacts and generally varied cementation. Top of unit has abundant cement-filled fractures and breccias.
Mixed Aeolian and Fluvial – Unconfined flow (2)	Poorly to well sorted fine-grained sandstones.	Poorly defined horizontal and irregular undulating lamination, interbedded sandstones and siltstones, with thin local clay drapes. Related to sheet flood events such as crevasse splays, fluvial sheet flood or interdune deposits.
Fluvial – Confined flow (3)	Well-sorted, well-stratified fine to medium grained sandstones. Dolomite and anhydrite cement, with localized shows of pyrite cement / inclusions.	Pin-shaped sandstones: Low angle cross-bedding, erosive bases overlain by asymptotic laminations passing up into low angle cross bedding. Related to unconfined sheet sands probably part of fluvial braid bars. Cross-laminated sandstones: Trough cross-laminated with erosive lower contacts containing shale and dolomite rip-clasts and truncation surfaces overlain by horizontally laminated sandstones. Fining-upward sequences with low to medium angle trough cross bedding. Related to confined fluvial flow probably part of fluvial braid bars.
Desert Outwash / Crevasse Splay (4)	Poorly sorted, very fine-to-fine grained sandstone, red-brown siltstones.	Tinily interbedded, with significant accumulations of clays, anhydrite and dolomite, very fine-grained sandstones. Laminated red-brown claystone with minor admixed or interlayered siltstone and fine-grained sandstones. Capped by well-developed palaeosols. Suggested fluvial and lacustrine origin.
Playa / Intermittent Lacustrine / Lacustrine (5)	Dark gray shales, mudstones.	Shales with interbedded very fine-grained sandstones and rippled siltstones. Desert lake.

Table 2: Combined descriptions and interpretations of lithofacies based on data from quadrants F, L, P and Q in the Dutch offshore, based on Spain et al, 1997, Ames et al, 1996, and Purvis et al, 1996

The combined lithofacies associations observed in the Main Buntsandstein subgroup are listed in the following table based on their suggested interpretations from the available literature. A discussion on the similarities and differences in the descriptions from the separate sources follows the table with observations.

As it can be observed from the table above there are a number of variations between the observations and interpretations from different authors. These are as follows:
Purvis et al defines mixed aeolian and fluvial sheet sand deposits, which have horizontal but irregular and undulating lamination. In Spain et al description the facies that come closest to this description are the thinly interbedded and interlaminated shales and very-fine-grained to silty sandstones. In Ames et al article these facies fall in the general group of interdune, floodplain and crevasse splay deposits and are not studied in detail.
Purvis et al makes a distinction between various deposits with fluvial origin related to braided river bars such as pin-shaped sandstones (mid-channel braid bars), cross-laminated sandstones (bank attached bars) and non-stratified sandstones of fluvial origin (undefined). This differentiation is based on whether the flow is presumably confined on not confined. The other authors do not separate the fluvial facies further on, or the information is not published.
Descriptions and differentiations between typical lacustrine deposits and crevasse and outwash deposits vary between the authors and generally create a sense of uncertainty regarding the validity of the interpretations of the more mixed facies.

These differences have at least two origins – the first being the actual horizontal separation between the study areas and the other being the different concepts applied in the facies interpretation process.

The generally accepted concept is that large alluvial fans and braided river systems originating from London-Brabant massive prograded north-northwest-ward into the basin where depending on the availability of accommodation space and climate conditions merged into aeolian sheet sand deposits or lacustrine fine grained deposits (Fisher et al, 1998). Determining the correct actual positions of channel systems and the extent of paleo desert lake requires availability of sufficient subsurface well log and core data in order to build a reasonable model. In the cases where there is not enough relevant correlation data more general assumptions can be applied regarding the interaction between the different lithological units based on the sequence stratigraphical model and analogue data.

2.2. Description of the Main Buntsandstein formations in the West Netherlands Basin based core descriptions, lithofacies descriptions, well correlations, and spatial distribution

In this chapter the complete description of the different formations on the Main Buntsandstein sub-group are presented in a structured framework. The conclusions and suggested concept might deviate in some aspects from what is available in the widely accepted available literature on the subject. These differences will also be addressed and discussed.
Each formation will be evaluated using all of the openly available data in order to make a consistent interpretation over the whole West Netherlands Basin. The eventual goal is to build a detailed sequence stratigraphical framework for the basin during the deposition of the Main Buntsandstein sub-group. The evaluation process starts with the description of available core in terms of sediments and lithofacies. The lithofacies are then related to corresponding log expressions and used to create a consistent basin-wide log correlation using a number of correlation panels. Using the well correlation as a basis facies spatial distribution can be determined and used to establish the depositional environment for the specific formation. When this process is completed for each of the formations the general sequence stratigraphic framework for the whole period and basin can be formulated. Although this is presented in a structured and sequential manner the actual process is flexible and involves constant review of previous results and requires corrections and improvements to the model after new information is accumulated.

The basic steps of the evaluation process will be described below and then the actual evaluation for each formation will follow.

Core descriptions and relation between core lithofacies and log expressions

The fundamental building blocks in sequence stratigraphical framework are the lithofacies and their vertical and lateral stacking. They present a direct reference to the depositional environment and are essential to the proper understanding of important changes in the basin during the deposition of the Main Buntsandstein sub-group.
Images of small outcrops and cores are going to be presented in order to give more detail and visualize the important aspects of the individual formations. The actual cores are only available as photos and are going to be presented as digital interpretations. They are going to be compared with the gamma-ray and sonic and/or density logs so that a relationship can be established between the observed lithologies and corresponding log expressions. This is an important step as the specific log expressions can then be used in the basin well correlations for wells without cores so as to accurately determine the lithology.

Well log correlations – keys to making a consistent basin-wide correlation

In order to determine the spatial distributions of formation in the Main Buntsandstein subgroup, well correlations are made across the West Netherlands Basin in 10 strike and 17 dip directions of major fault pattern. Almost all wells with Triassic penetrations in the West Netherlands Basin were incorporated in the cross-sections. Additionally another 6 strike and 9 dip sections are employed to establish a fine scaled internal correlation for the Hardegsen unconformity in the south west region of the West Netherlands Basin. A total of 96 wells are used for the regional well correlations for all formations. A total of 28 wells were used for the Hardegsen specific correlations and fine scale correlations. All of the data is acquired from the publicly available information from NLOG website. The complete lists of wells and correlation panels are given in the Appendix II.

The available lithostratigraphy of the Main Buntsandstein sub-group was not consistent and varied dramatically between individual well. Therefore each well was separately reviewed and a new basin-wide consistent interpretation is presented. The process of interpreting wireline logs, cores and the general depositional environment is an iterative one. Each interpretation is first checked against adjacent logs and cores. Then it is reconsidered taking into account the sequence stratigraphical framework. If there is an inconsistence the whole process is repeated until a structured and complete interpretation is constructed for the whole basin. This also means that the interpretations for the boundaries of individual formations are a compromise between geologically accurate boundaries and easy to identify log expressions. For example a formation boundary marked by a flooding event is always selected on the highest gamma-gay peak and not at the start of an environmental change.

Initially the major correlation surfaces of the Triassic are pinpointed – Base Lower Buntsandstein, Base Main Buntsandstein (Base Volpriehausen – Volpriehausen unconformity), Base Upper Buntsandstein (Base Solling – Hardegsen unconformity), Base Muschelkalk and Top Sleen. Subsequently the internal sequence boundaries and flooding surfaces are correlated until a consistent model is established for the whole study area. These are Base Rogenstein in Lower Buntsandstein sub-group, Top Volpriehausen sandstone, Top Upper Volpriehausen sandstone/claystone, Top Lower Detfurth sandstone and Top Upper Detfurth claystone in Main Buntsandstein sub-group, and subdivision of Upper, Middle and Lower in Roet and Muschelkalk formations, and Upper and Lower Keuper formation. When these boundaries are determined with sufficient accuracy a more detailed correlation of individual cycles and facies is carried out in order to produce depth and spatial distribution maps of individual facies. These maps together with diagenetic characteristics of different facies are subsequently used to build the porosity and permeability models.

The most important task in this well correlation exercise is to establish a very consistent model for the spatial distribution of the different sub-formations. The way to achieve this is to have a clear idea for the expected

bases and tops for each formation and combine it with general assumptions that formation boundaries are either unconformities or flooding surfaces.

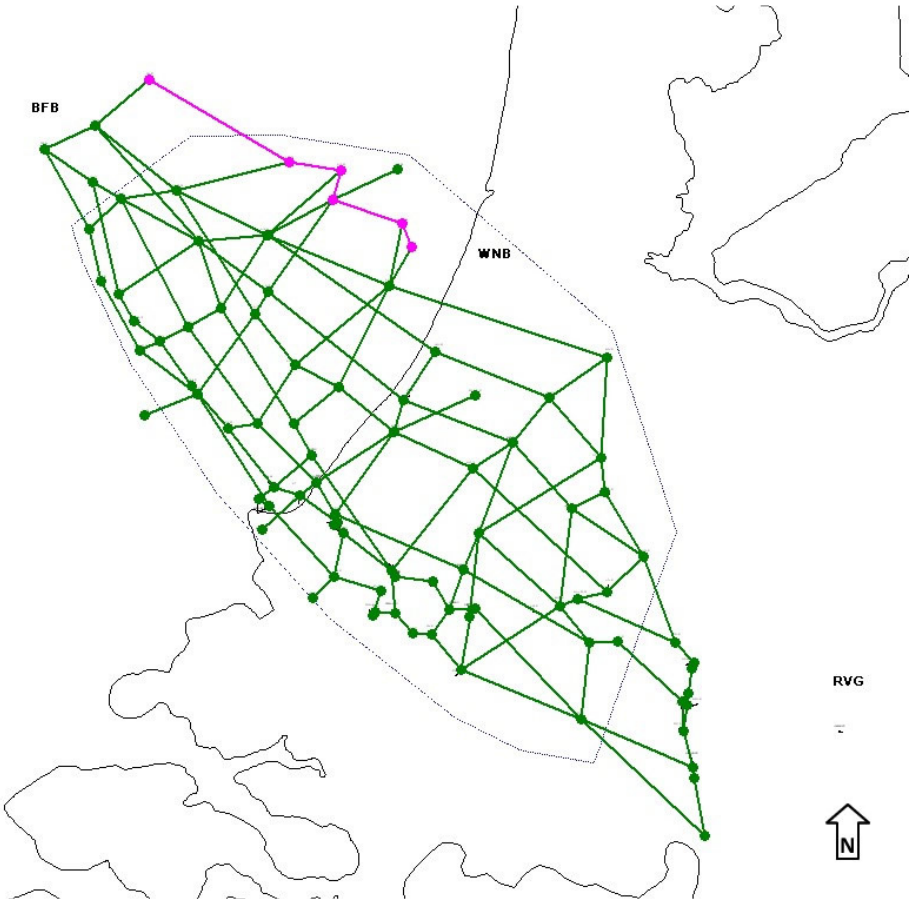

Figure 4: Overview of the strike sections and dip sections used for the well log correlations. The outlines indicate the present Netherlands shore line. Refer to Appendix II.

Formation maps – thickness and possible facies distributions

An important step for determining the depositional environment of a given formation is the construction of maps for the spatial development and preservation of the sediments in it. The well logs and cores provide a good image of the vertical distribution of facies but the more important information that needs to be extracted is the spatial distribution of the formations and lithofacies in them. The workflow involves constructing maps for the top and bottom of the formations and then thickness trend maps. In those maps it is important to identify whether the differences in thickness are caused by tectonic influence or purely by sedimentological processes influence.

It is important to start the description with a basic clarification regarding the naming convention of the different formations from the Main Buntsandstein sub-group. The formations names are given in Table 3 and the names that were encountered in various logs and lithostratigraphic interpretations for the same formations are given in the second column. Even a quick look trough the table can reveal that the amount of confusion regarding the naming of individual formations is tremendous. The reason behind those inconsistencies is the choice of criteria for the naming convention to be based on the observed and interpreted lithologies rather than to be based on time periods or sequence stratigraphic framework. The natural problem that follows this approach is related to the predominantly fluvial and lacustrine environments that deposited these sediments. Often facies in a given formation vary laterally which leads to confusion while interpreting even wells that are adjacent to each other. Moreover the arid climate in the

Lower Triassic has led to very scarce fossil record in the sediments which makes accurate dating of sediment literally impossible.

Sub-formation (member):	Previously referred as:	Formation:
Hardegsen	(Upper cycle) Hardegsen, (Lower cycle) Upper Detfurth Sandstone or Upper Detfurth Claystone	Hardegsen
Upper Detfurth	Lower Detfurth Sandstone, Upper Detfurth Sandstone and Upper Detfurth Claystone	Detfurth
Lower Detfurth	Upper Volpriehausen Sandstone, Lower Detfurth Sandstone and Upper Detfurth Sandstone	
Upper Volpriehausen	Upper Volpriehausen Sandstone, Upper Volpriehausen Claystone, and Lower Detfurth Sandstone	Volpriehausen
Lower Volpriehausen	Lower Volpriehausen Sandstone and Upper Volpriehausen Claystone	

Table 3: Naming convention for formations from Main Buntsandstein as suggested in this report. Previous names are taken from TNO Lithostratigraphy interpretations as seen on NLOG website and interpretation done by company geologists on the original composite logs.

Line name	**Type of boundary**	**Suggested Formation name** *for consistency*	**Sequence Strat Cycle**
Base Solling	Unconformity		
		(Upper) Hardegsen	4
M Buntsandstein C4-2 *Top Upper Detfurth Sandstone or Intra Hardegsen Flooding Surface*	Flooding surface		
		(Lower) Hardegsen	4
M Buntsandstein C4 *Top Upper Detfurth Claystone*	Flooding surface		
		(Upper) Detfurth Claystone	3
M Buntsandstein C3-2 *Top Lower Detfurth Sandstone*	Flooding surface		
		(Lower) Detfurth Sandstone	3
M Buntsandstein C3 *Top Upper Volpriehausen Claystone eq.*	Sequence boundary		
		Upper Volpriehausen Claystone	2
M Buntsandstein C2-2	Flooding surface		
		Upper Volpriehausen Sandstone	2
M Buntsandstein C2	Sequence boundary		
		Lower Volpriehausen Claystone	1
M Buntsandstein C1-2 *Top Lower Volpriehausen Sandstone*	Flooding surface		
		Lower Volpriehausen Sandstone	1
M Buntsandstein Base (C1)	Sequence boundary		

Table 4: Suggested correlation surfaces used in well correlations described in this chapter. Note that the

Volpriehausen claystone members are relatively undeveloped in the West Netherlands Basin in comparison with Roer Valley Graben and Broad Fourteens Basins. The separation of Hardegsen is only for reference regarding the evaluation of possible differential subsidence in the last period of Main Buntsandstein in the West Netherlands Basin. The background colors of the formation names indicate the suggested strength of the tectonic influence in that period with darker green shades for higher influence and lighter for lower.

In the table above (Table 4) the correlation lines used for the basin well correlations and for building the basic formation thickness maps are shown. The naming of the lines is selected so that it does not imply changes in the already accepted naming convention for the formations but rather shows the chosen approach that avoids inconsistent interpretations. The most important difference to the typical approach for correlating formations as suggested by previous works is that the correlated boundaries are either flooding surfaces of sequence boundaries instead of lithology transitions.

Although the number of shown cycles is four, the Lower Volpriehausen Claystone and Upper Volpriehausen Claystone both develop as separate cycles with lower sandstone and upper claystone members in Broad Fourteens and Roer Valley Graben basins. In the West Netherlands Basin those formations are rather limited and are usually observed as a limited shale layer often eroded by the overlying fluvial sequences and intercepted by many small scale shallow channel incisions.

The following diagrams show two examples of the typical West Netherlands Basin Main Buntsandstein formations as seen in well WAS-23-S2 and the so called classical Main Buntsandstein formations differentiation as seen in the well on the border between West Netherlands Basin and Broad Fourteens Basin – P08-04. The interpretations of surfaces are representative for the surfaces used in this work which are described in Table 4.

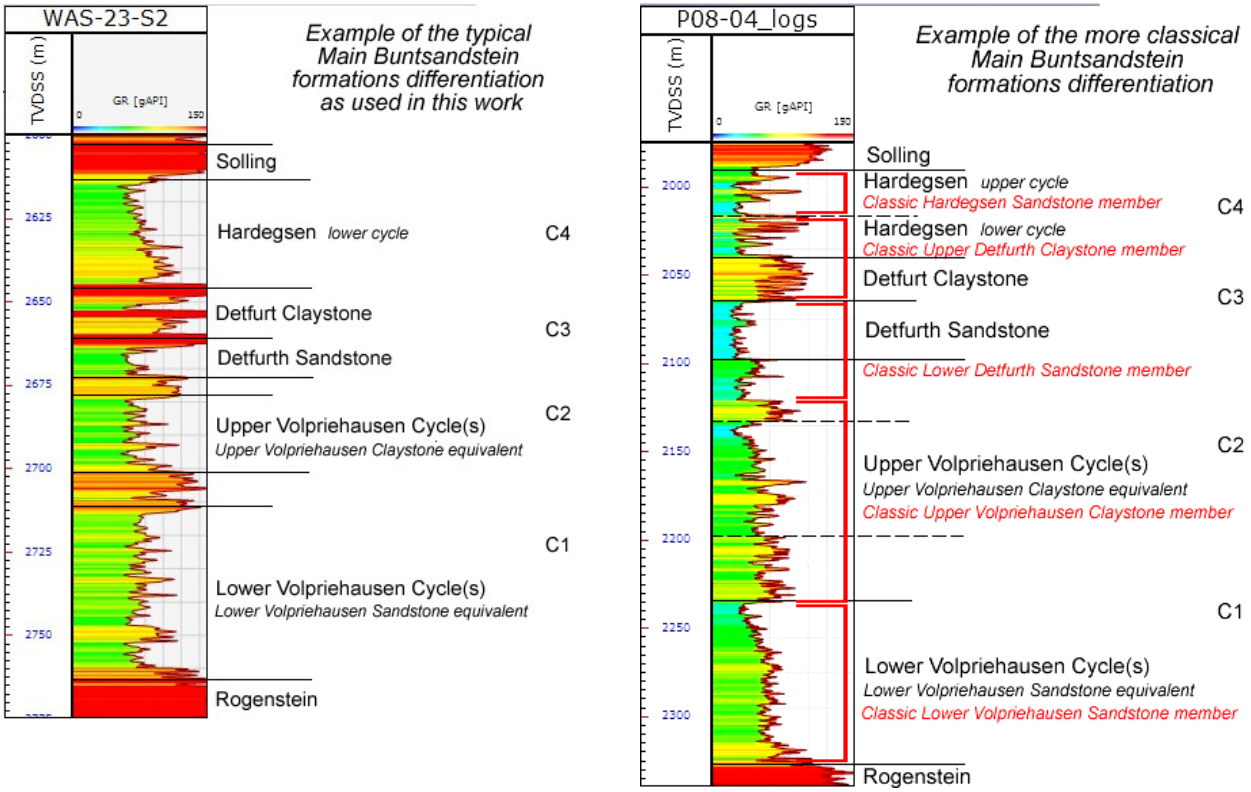

Figure 5a: Comparison of the typical formations interpretations from West Netherlands Basin and Broad Fourteens Basin. Notice that the BFB interpretation fit in a straight forward manner with the so called classical Main Buntsandstein formation interpretation based on lithology and shown in red subdivisions and red text descriptions in this figure.

It is important to note the major differences from the interpretation used in this work to the classical lithological interpretation of the Main Buntsandstein formations. Starting from younger to older formations, the lower cycle of Hardegsen as used in this work is often referred as part of the Upper Detfurth Claystone member. The reasons for this can be related to the slightly higher gamma ray footprint of the lower cycle. However in terms of lithology it is clearly a transition from fluvial to aeolian depositional environment. Based on observed facies, petrophysical properties and wireline log expression this cycle is therefore more appropriate as part of the Hardegsen formation.

In the next diagram the interpretation for a well in the study region is presented – MSG-01 where both Hardegsen cycles are preserved.

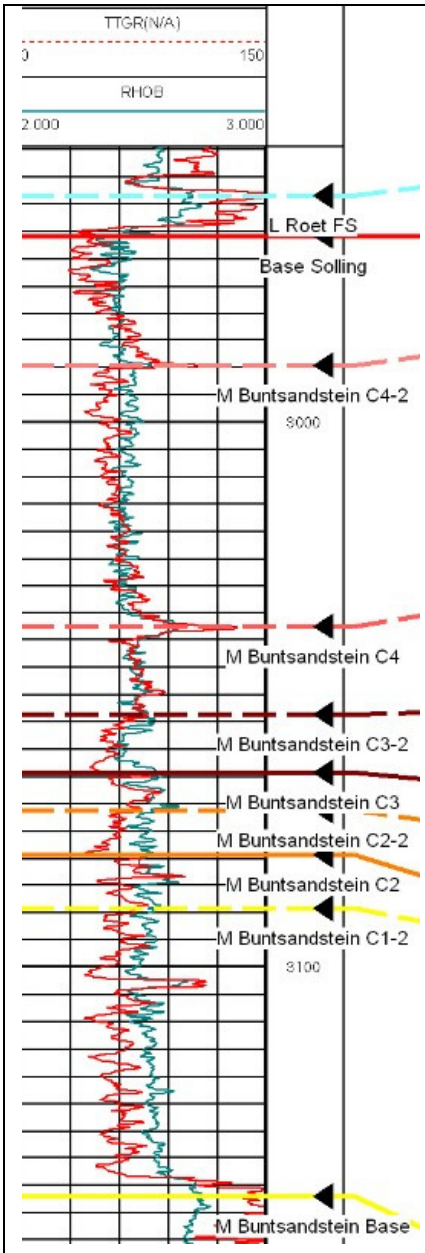

Figure 6b: Screenshot of Main Buntsandstein formations interpretation in well Maasgeul -01

To left is a screenshot from the correlation panel including well MSG-01 where both cycles of Hardegsen are visible. This well is exemplary of the particularly difficult to interpret south-west boundary fault blocks. The reason is that the Main Buntsandstein sequence there is generally referred to as Bunter due to the lack of clay and siltstone intervals typically used to define the claystone members of the Buntsandstein formations. In this study the members and formations are however interpreted not based on the lithological content but rather based on sequence stratigraphical approach.

The interpretation shown to the left is in fact very consistent with the adjacent wells and correlation panels in both directions. It is only possible to interpret the well in a correlation panel as the thick sand rich section offers little options for formation boundaries control based on dominant lithology. This is true for all well proximal to the sediment source towards the south west of the basin.

The upper part of the Main Buntsandstein section consists of two identical intervals with decreasing upwards gamma ray response and very similar overall pattern. It is fairly easy to confuse those intervals given that for example the top one is eroded off or was not deposited at all in the examined well position. Using the basin wide well correlation panels as starting point however the lateral development of the two Hardegsen cycles can be traced and mapped out. They together form a significant reservoir available in the south and south western parts of the West Netherlands Basin. It is therefore of significant importance to be able to accurately determine the upper and lower boundaries of the cycles in order to avoid accidental splitting the relatively homogeneous Hardegsen sands in sections interpreted as with the overlying Solling formation or the underlying Detfurth formation.

Another difference is in regard with the determination of Base Detfurth surface. While in Broad Fourteens Basin it is clearly the transition from floodplain deposits for sandstones, in the West Netherlands Basin it can be easily confused with one of the cycles in the Upper Volpriehausen group. Therefore the Base of the Detfurth Sandstone is considered to the sequence boundary defined as the very distinctive blocky sand on top of the last floodplain deposits of the Upper Volpriehausen Claystone equivalent.
The third and most important difference is related to the Upper Volpriehausen Claystone equivalent in the West Netherlands Basin. Due to the more proximal position of the WNB to the sediment sources this formation develops as a one or more cycles with basal sandstones with erosional bases and overlying claystones with fluvial origin. In the base of the formation is the distinctive claystone sequence which is part of the initial major fluvial cycle. The sandstone part of it is referred also as Lower Volpriehausen Sandstone

member. In order to avoid the obvious possible confusion this work uses a differentiation based of sequence stratigraphy cycles (as suggested in Table 4) instead of direct references to lithology.

2.2.1. Lower Volpriehausen formation

The base of the Lower Volpriehausen formation is considered to be the Volpriehausen unconformity. Although indications for significant erosion are only locally available, the remarkable transition from clay-rich material to coarse grained fluvial sandstones is very easy to identify. The lower boundary can also be referred to as a sequence boundary indicating a substantial change is prevailing climatic and tectonic conditions in the basin and leading to the deposition of blocky sand on top of clay sequence. In other larger basin the base of Volpriehausen is often related to deposition of conglomerates or pebbly sandstones indicating a more proximal position to the major alluvial fans.

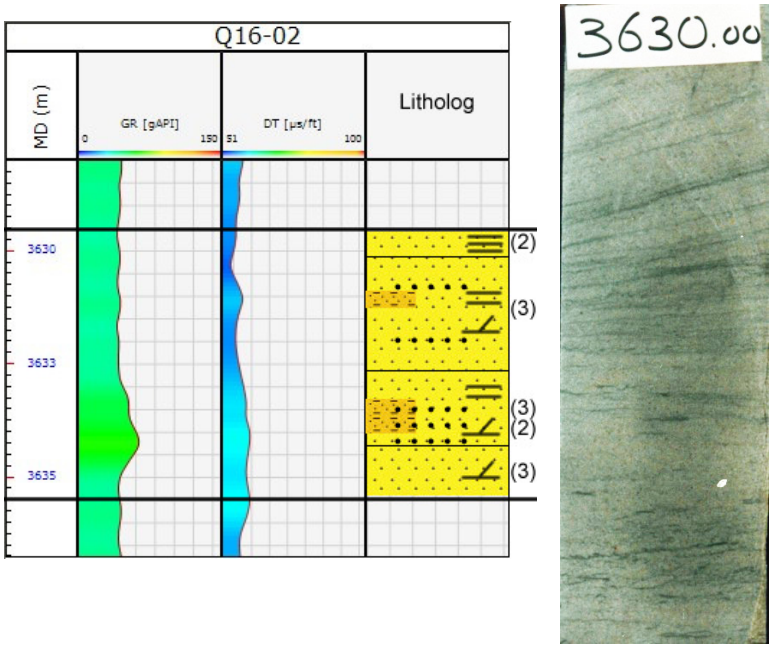

Figure 7: Interpretation of a core taken from well Q16-02 in Lower Volpriehausen formation. On the right there is a photo with indicated depth from the same core. Darker laminations are very fine grained sand to silt.

Core description and lithology

The sandstones of the Lower Volpriehausen formation (Figure 6) are a stacked sequence of trough cross bedded sandstones and parallel cross bedded sandstones. The grain size varies from fine to medium grained with occasional silt laminations. In this particular core it is very clear that there is an abundance of small scale mud clasts in the sandstones. All this indicates a fluvial depositional setting and vertically and laterally stacked fluvial bars and channel bed deposits.

The grain size distribution and rounding of grain is similar for most Volpriehausen sandstone observation due to the fact that the formation is very consistently spread out in the whole West Netherlands basin. Grains in the lower fluvial sandstones are typically medium to fine size in the fluvial bars and channels; fine to very fine size in the parallel laminated sheetflood and crevasse splay sands and range from sub-angular to sub-round. The sorting is also dependent on the facies due to the relation to the continuity and energy of the depositional process. Facies such as braid bars and channel bed deposits deposited by more constant processes have better sorting than facies deposited by flash flooding events.

From dip meter measurements in different wells it can be concluded that the dominant paleo flow direction was towards the north west.

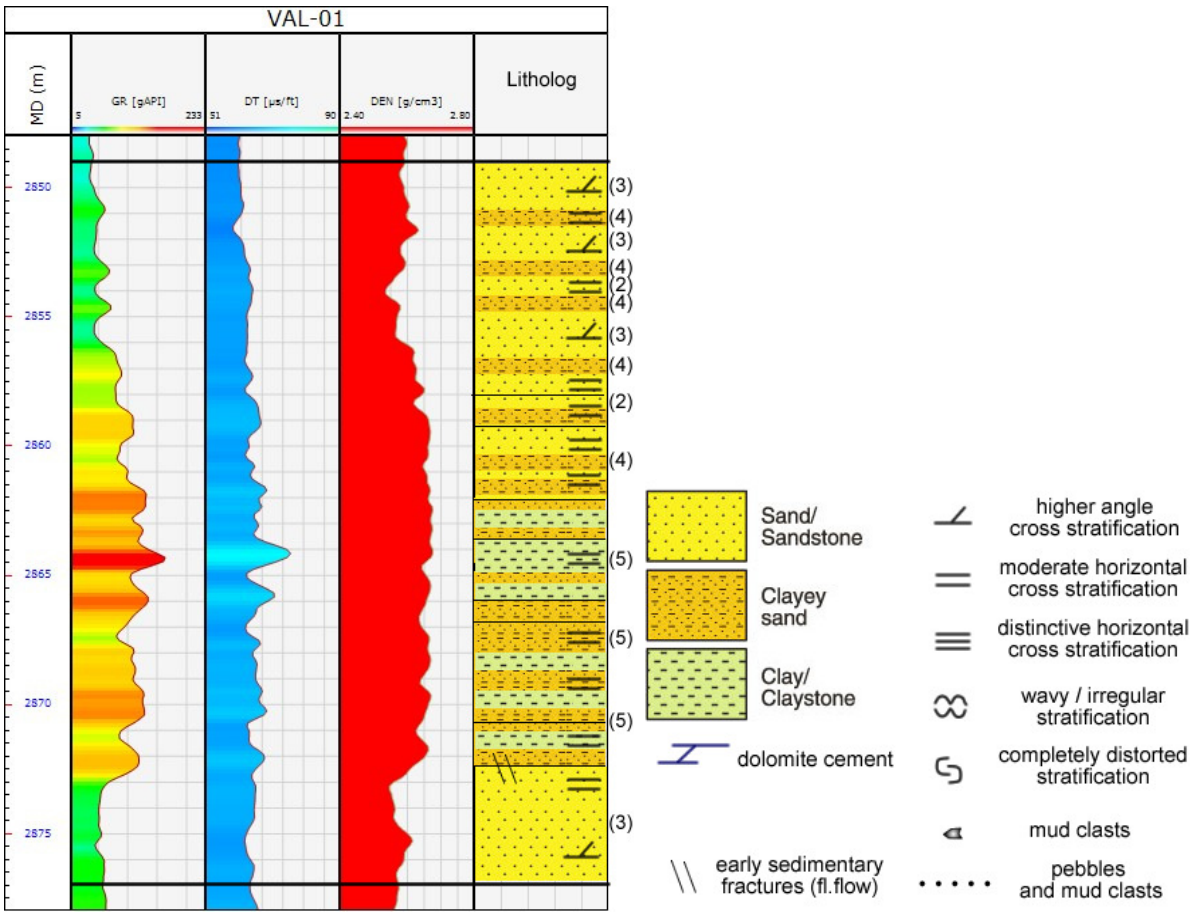

Figure 8: Interpreted core from well VAL-01 compared with Gamma-Ray (GR), Sonic (DT) and Density (DEN) logs. The boundary between Lower and Upper Volpriehausen is the high GR peak at around 2864m MD while the actual sequence boundary is at 2857 m MD. A legend for the symbols used in all subsequent core descriptions is presented underneath. The numbers next to the core description refer to Table 1.

The lower part of core 3 from well VAL-01 contains the upper section of the sandstone sequence of the Lower Volpriehausen formation. The sandstone shows the same properties and stratification as in the previous interpreted well and other wells from the basin. This combined with the very consistent gamma ray profile of the formation over large distances indicates that the sediment supply in the Lower Volpriehausen was sufficient to fill a very large part of the basing with relatively homogeneous lithology deposited in a similar setting.

In well VAL-01 (Figure 7) from depths 2850 m to 2873 m the clay and silt rich upper part of the Lower Volpriehausen formation is visible. The gradual transition towards increasing shale content in the deposited sediments suggests that the formation boundary should be set at the maximum flooding surface as an indication of a turning point in the development of the basin. This shale rich section is also widely spread in the basin and is easily recognizable on gamma ray logs. In Figure 8 a photograph of the core is presented showing that the shales in that sequence have mixed character. The dark brown shales have continental fresh water source while the grey-green-blue shales are related to a salt lake. The close interaction between the two environments is an indication that the deposition of this shale sequence was initiated by an increase of accommodation space in the basin that led to a significant advance of a salt lake boundaries in the basin.

2869.50 (2873) m

Figure 9: Lower section of shale interval in top of Lower Volpriehausen, well VAL-01. Notice the small scale fractures.

2866.29 (2869) m

Figure 10: Shale interval of top Lower Volpriehausen with two shale types, well VAL-01

2854 (2857) m

Figure 11: Lower section of Upper Volpriehausen, well VAL-01. Notice the small scale channel erosion surfaces.

Well correlations

Lower Volpriehausen has a typical log expression that is easy to recognize and trace in the whole West Netherlands Basin. The sand section looks blocky and the individual cycles are easy to correlate over large areas.

The Lower Volpriehausen cycle in the West Netherlands Basin can be divided into lower sandstone unit called for reference Lower Volpriehausen Sandstone member and upper claystone unit called here Lower Volpriehausen Claystone member. The natural continuation of the Lower Volpriehausen Claystone in the

Broad Fourteens Basin is a very thick claystone sequence called there Upper Volpriehausen Claystone. This implies that the Lower Volpriehausen Claystone is what used to be called Upper Volpriehausen Claystone. In the West Netherlands Basin the claystone unit is very poorly developed and followed by a well developed sandstone unit with an overlying claystone unit. This led to the natural conclusion that it is the same unit only with different lithology. It was named Upper Volpriehausen Sandstone member. However the same sandstone unit is also available in BFB and RVG basins and therefore it is not the analogue of Upper Volpriehausen Claystone in the West Netherlands Basin. This is further explained in the next sub-chapters about Upper Volpriehausen and Detfurth.

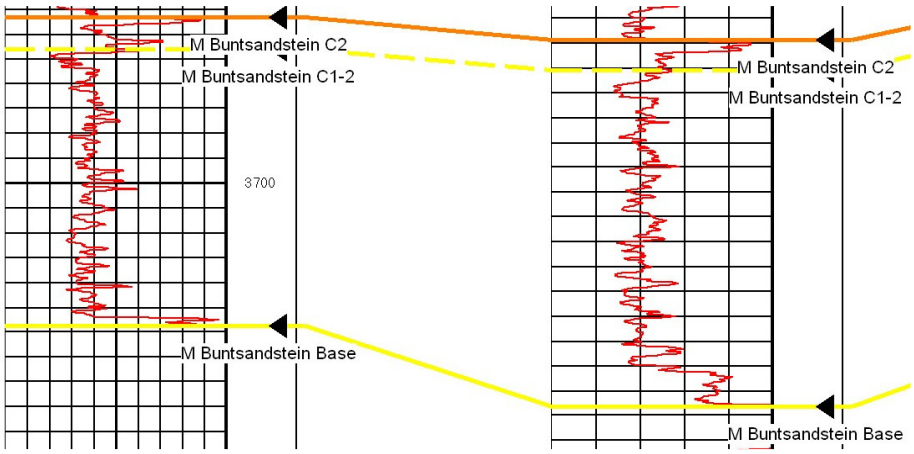

Figure 12: The typical GR pattern of the basal sandstone member of the Main Buntsandstein sequence as seen in the WNB, in this case from wells Q16-08 and SGZ-01-S1. GR scale is from 0(left) to 150(right) API

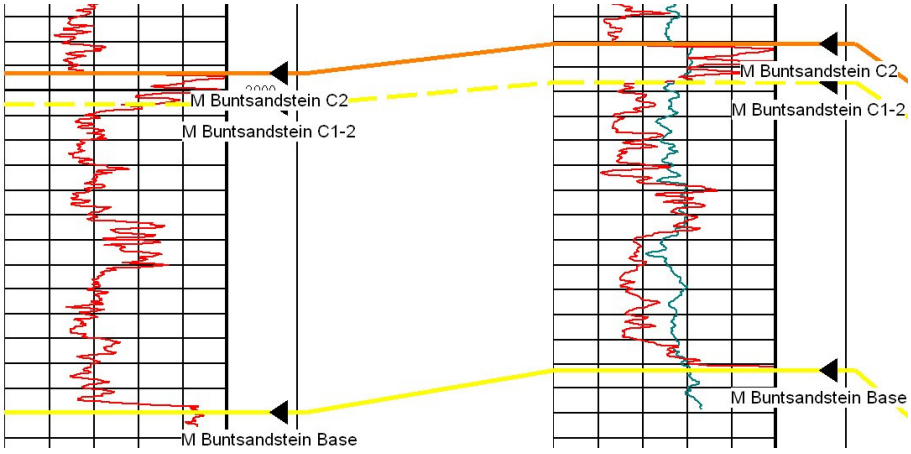

Figure 13: The slightly different GR log pattern of the Lower Volpriehausen Sandstone as seen towards the Roer Valley Graben basin and partially in the northern most areas of the West Netherlands basin.

All of the complete correlation panels can be found in Appendix II.

Thickness maps and Facies distribution

The thickness maps shown below (Figure 13 and 14) represent the extrapolated results of the well correlations. They do not include the major faults and are therefore only considered as intermediate results. The actual thickness models and facies distribution model, including petrophysical properties distribution will be shown and explained further in Chapter 5.

It is interesting to note the more extensive development of the overlying claystone sequence in the Broad Fourteens and Roer Valley Graben basins shown in Figure 14.

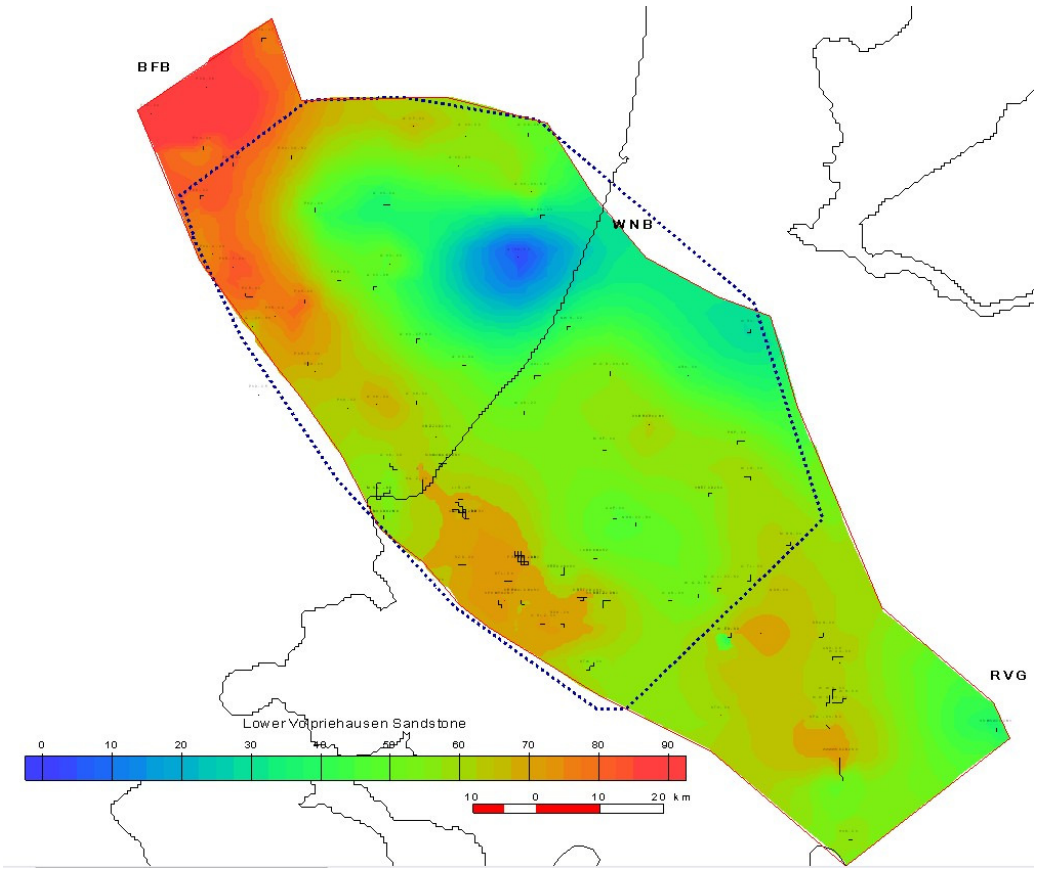

Figure 14: Basic Lower Volpriehausen Sandstone thickness map. North is pointing to the top.

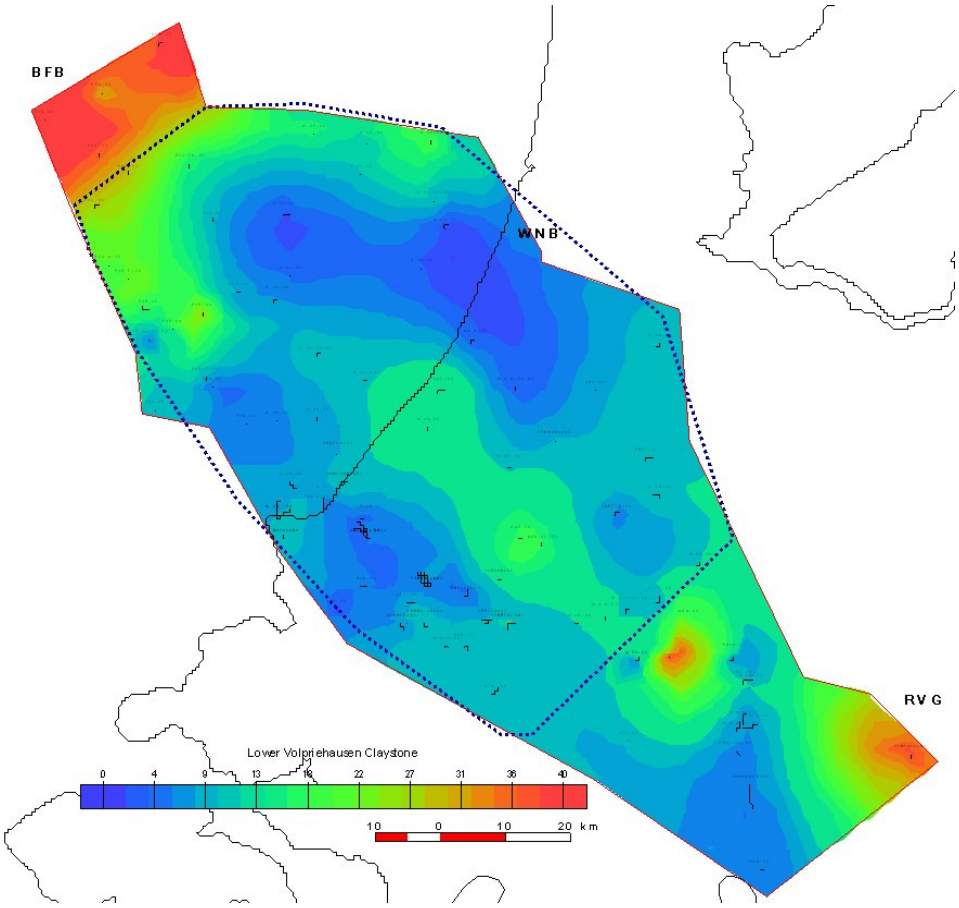

Figure 15: Basic Lower Volpriehausen (Cycle) Claystone thickness map.

2.2.2. Upper Volpriehausen formation

The Upper Volpriehausen is the sequence that follows the Lower Volpriehausen. The base of the formation is generally erosive but it is not an unconformity as the erosional surfaces are more likely to be only local channel incisions. The core section from well VAL-01 (Figure 16) is a good example that in the more distral parts of the basin the incision was limited and was split into several stages.

Core description and lithology

The sediments found in this formation are typically again sandstones with trough and planar crossbedding with several surfaces with abundance of mud clasts. However unlike the Lower Volpriehausen in the formation there are more often clay and silt layers with horizontal stratification that is sometimes undulating. The types of clays are still dependant on the location with salt water clays more abundant in the north and continental floodplain clays in the rest of the basin. Sorting is usually not very good and there is an abundance of anhydrite and dolomite cements.

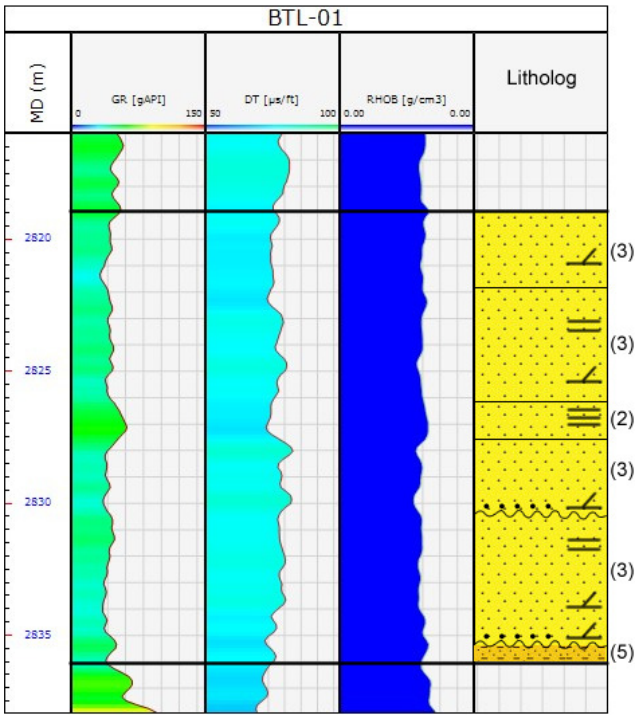

Figure 16: Upper Volpriehausen formation from base upwards as seen in core from well BTL-01. The base of the formation is locally erosive.

In other wells located more towards the south like BTL-01 (Figure 15) the erosional surface are more pronounced and there are better defined stacked massive fluvial bars and channels. The erosional bases observed there also contain significant amount of mud clasts indicating that the fluvial channels were incising into the older flood plains while expanding laterally and reworking previously deposited sediments.

In general the Upper Volpriehausen has a log expression and lithology that is similar to that of the sand rich sequence of the Lower Volpriehausen. The major difference is in the increased lateral variability in the deposits.

The upper boundary of the formation is usually marked by increasing amount of fining upwards silt and shale sequences. They are, however, not as intensive as the shale intervals seen in the upper section of the Lower Volpriehausen.

Furthermore these silt-shale intervals are often interrupted by sand intervals that show no indications of cross stratification and are therefore indicative of sheet flood events rather than channel confined fluvial flow. This is also evidence that accommodation space has increased in the basin while sediment supply did not change drastically. This is one indication that this change was related to a tectonic event and not be shift in climate. In Figure 17 an interval with significant amount of syn-depositional small scale fractures and faults can be seen. A similar interval exists right underneath the shale interval of the Lower Volpriehausen. This is another indication that the changes that marked the shift in lithologies in both formations were triggered by a tectonic event.

The upper section of the Upper Volpriehausen shows significant variability as not only depositional environment was more varied but also the base of the next formation Lower Detfurth is considered to be a local unconformity. The determination of that boundary is very difficult as it is diversified depending on the

location in the basin. While in some areas it has developed as a clear erosional base with blocky sand deposited on top of it, in other locations there are no clear signs of significant erosion and the location of the base can only be inferred by the offset from the overlying easy to recognise triple shale-sand interval of the Upper Detfurth.

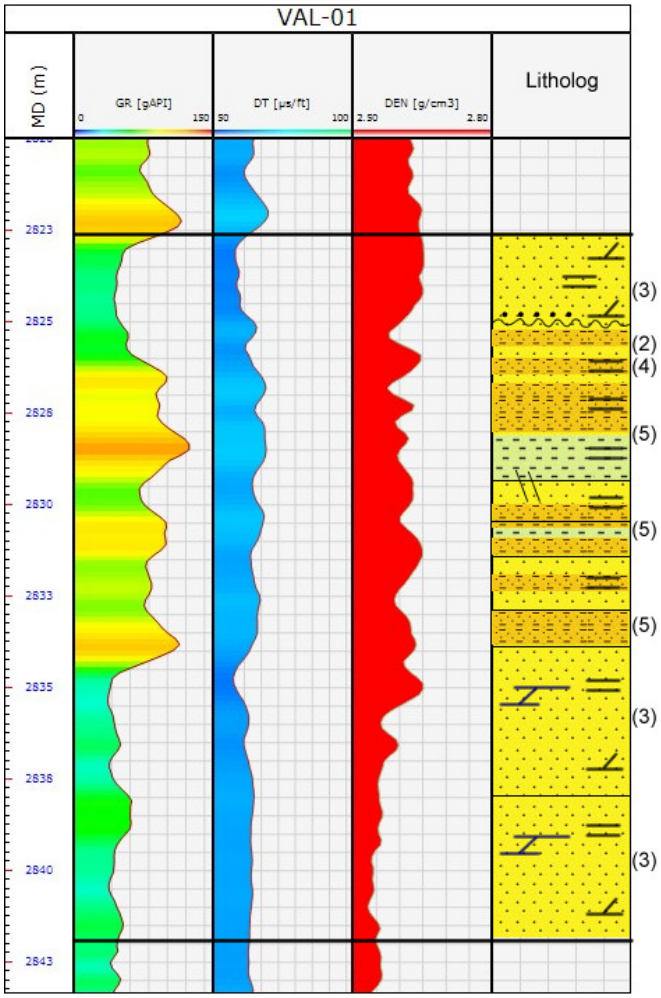

Figure 17: (above) Interpreted core section from well VAL-01 including upper section of Upper Volpriehausen and base of Lower Detfurth. Notice the fractures in the base of shale interval.

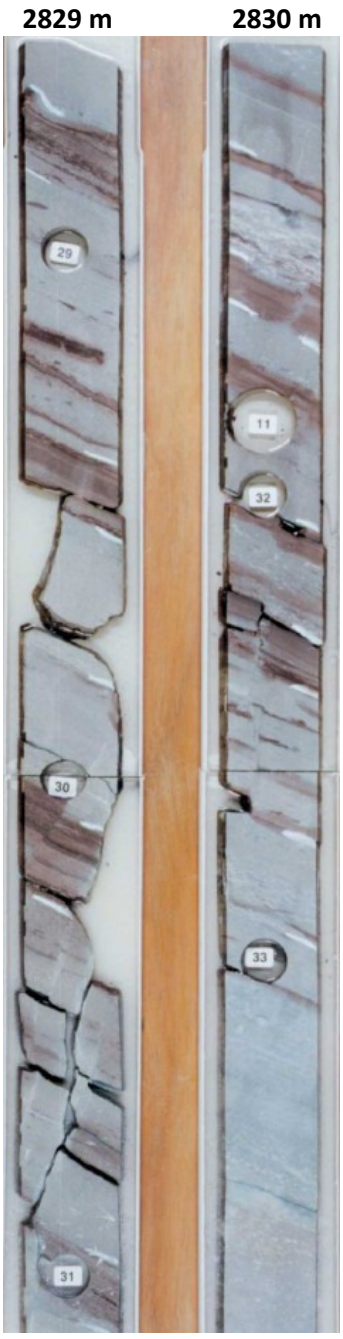

Figure 18: (right) Core photos from fractured interval in well VAL-01. Notice also that the shale rich interval is more sand – shale alternations rather than clear silt-shale layer.

Well correlations

The log expression of the Upper Volpriehausen poses a significant challenge due to the variability depending between the south west, north west and south east regions. The actual correlation of this boundary was made only after attempting it from all possible different directions in order to reach to a consistent and geological sound solution. The biggest problem is the pinpointing of the base of Detfurth or the top of the Upper Volpriehausen in areas where the upper section of the formation has developed as a shale alternating sand interval but rather a sand interval with slightly fining upwards gain size profile.

The most important step in the proper correlation of the Upper and Lower Volpriehausen formations is the recognition of variations in the depositional environment. For example in the south eastern region both

formation have almost completely different profiles than in the south west region. The reason for this that the part of the south west region of the West Netherlands Basin where wells have penetrated the Main Buntsandstein sub-group the Volpriehausen formations are in a more proximal position in regard with the main fluvial channel system. Towards the south east the upper section of the Lower Volpriehausen and the complete Upper Volpriehausen change entirely in terms of dominant lithology and are composed of massive shale intervals. The more confusing problem is that the exact point where the transition occurs is actually different for both formations indicating a lateral shift of the major fluvial system.

The Upper Volpriehausen formation is split into Lower Volpriehausen Sandstone and a limited Upper Volpriehausen Claystone member. The upper member is usually very limited and often eroded by the following formation – Lower Detfurth sandstone. However in the RVG and BFB basins it develops as a separate cycle with lower sandstone and upper claystone member. This difference in the number of distinguishable cycles in the formations is the main source of misinterpretations and confusion regarding the naming of different units in the three basins – RVG, WNB and BFB. The Upper Volpriehausen sandstone is often confused with the Lower Detfurth sandstone leading to tremendous difference in the thicknesses of the two units without any solid geological explanation.

Selecting a representative screenshot for the Upper Volpriehausen cycles is a difficult task due to the many variations that mark this Upper Volpriehausen Claystone equivalent in the West Netherlands Basin. The best way to demonstrate the most important considerations when correlating the different surfaces within the unit is to show the transition from a more homogeneous claystone member with a number of distinguishable individual cycles from Broad Fourteens basin to the limited single or double cycle in the West Netherlands basin.

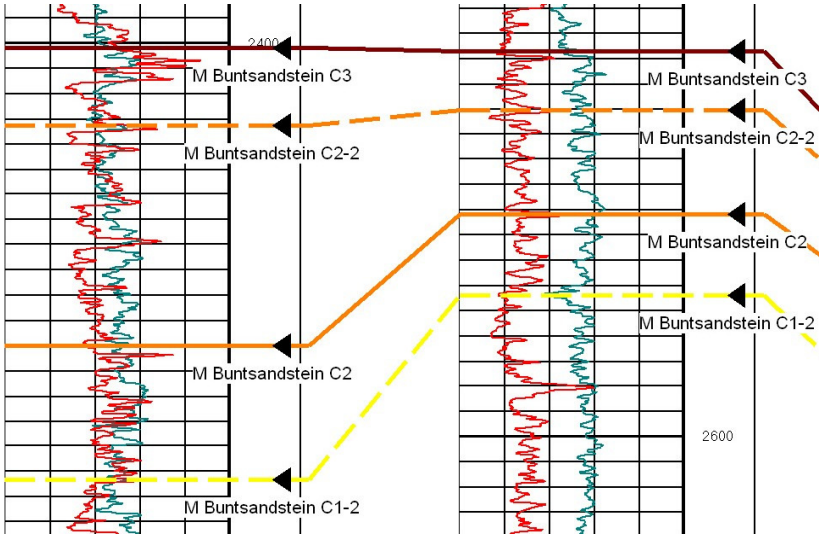

Figure 19: Upper Volpriehausen cycles between surfaces M Buntsandstein C2 and M Buntsandstein C3. Wells P11-02(left) and P14-A-01(right) in the offshore part of WNB. Notice that there is an additional cycle in lower part of Upper Volpriehausen in well P11-02 to the west.

Thickness maps and Facies distribution

The resulting thickness maps is similar to the one created for the first cycle of Volpriehausen and can be seen in the figure below.

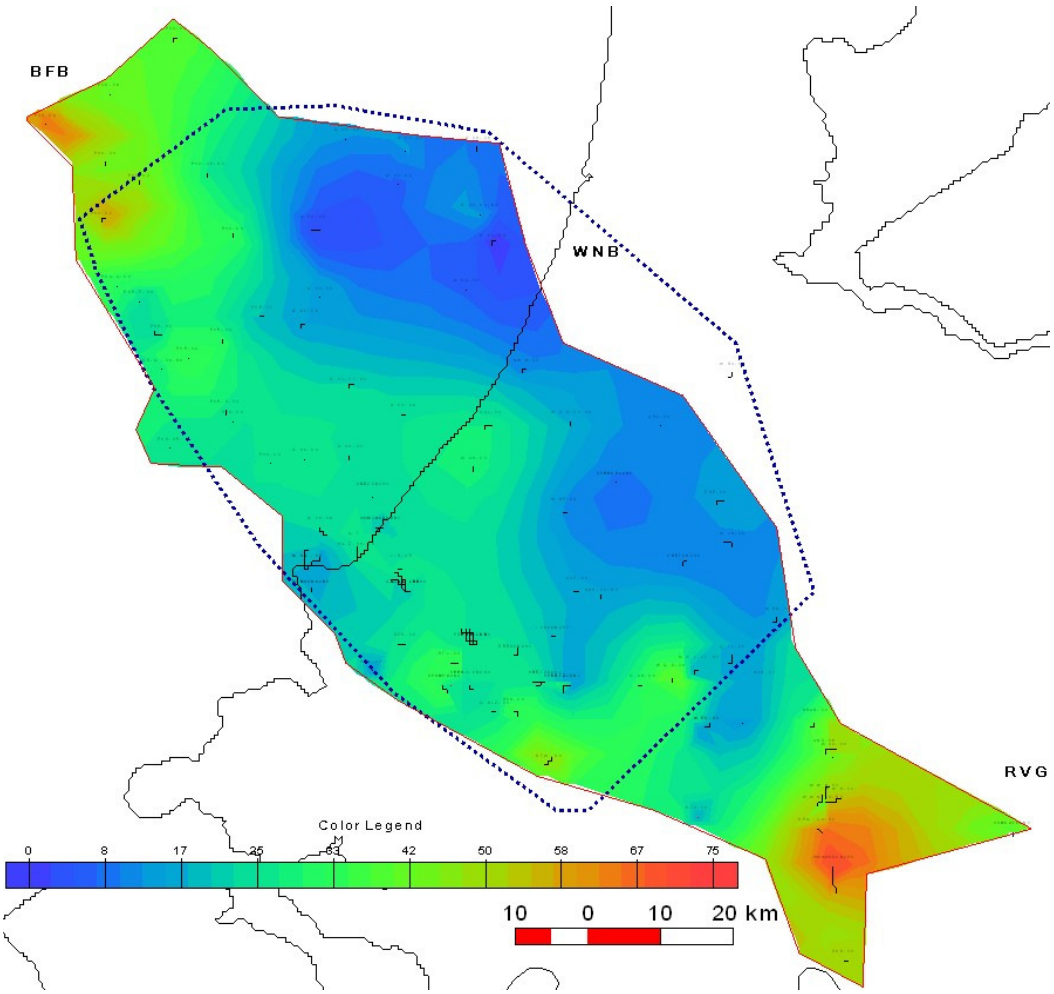

Figure 20: A combined basic thickness map for the Upper Volpriehausen Sandstone and Claystone members in the WNB. The significant increase in thickness towards the adjacent RVG and BFB is related to the expansion of the Upper Volpriehausen Claystone into a complete new cycle. Note that the decrease in thickness around wells MSG-02 and MSV-01 is due to lack of log data and extrapolation effects rather than real decrease of the preserved thickness.

2.2.3. Lower and Upper Detfurth formations

The Lower and Upper Detfurth formations as suggested in this report are significantly different from the previously suggested correlations. The Base of the Lower Detfurth is considered to b a sequence boundary on top of the Upper Volpriehausen claystone sediments. However in several occasions it seems that the Lower Detfurth has either eroded deeper into the Upper Volpriehausen or there have been no shales deposited at the boundary so that the contact below base Detfurth is very difficult to be accurately pinpointed.

Core description and lithology

The full range of lithofacies with all possible variations can be found in the Detfurth formations.

Grain sizes ranging from clay and silt to fine sand and occasional medium sand aeolian layers; usually poor sorting with exception of dune sands; varied quartz content, cements and stratification.

The most important yet also most controversial section to be interpreted is the expected Lower Detfurth – Upper Volpriehausen contact. Several wells have possibly this boundary and the ones that have core photographs have been interpreted and presented below.

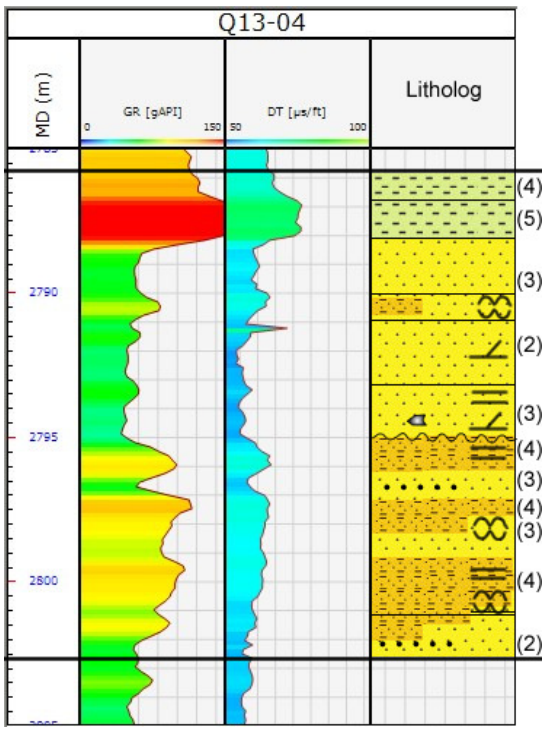

Figure 21: Interpreted log with Lower and Upper Detfurth section from well Q13-04.

The Lower Detfurth is considered to contain one or more sand layers with distinct cross stratification and usually breccias or mud clasts close to the base. This is in accordance with the expectation that base Detfurth is a small scale unconformity with localized erosion of previous sediments. (Figure 20)
Further towards the top of Detfurth the formation becomes highly diversified and harbours almost all of the lithofacies encountered in the Main Buntsandstein sub-group.

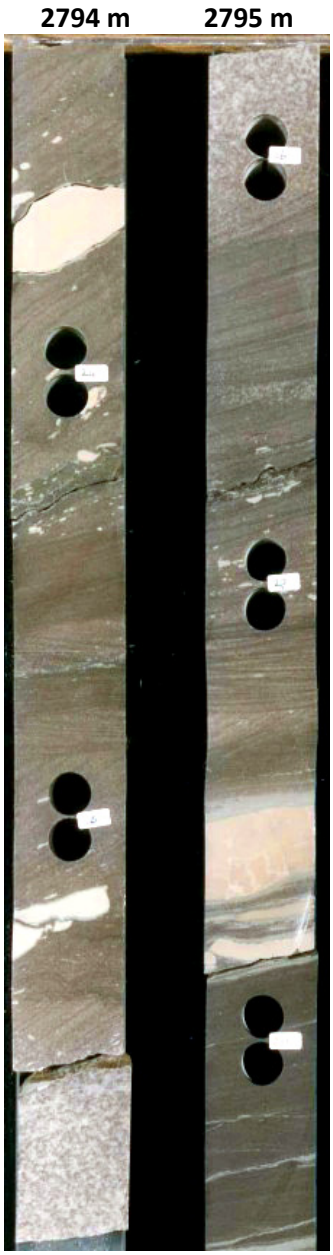

Figure 22: Core photo from well Q13-04 with the expected base of Lower Detfurth. Notice the anhydrite section ~2795m.

Figure 23: Core photo from well Q13-04 with example of the sudden changes of depositional environment.

Although it is true for the complete Main Buntsandstein section the variation in early diagenesis cement composition is best seen in the Detfurth Sandstone. In the more northern areas of the basin closer to the Netherlands swell the Röt formation developed anhydrites unlike the southern areas where it gradually changes from sandy facies to silts and claystones. The result from this is that the meteoric waters penetrating the older Man Buntsandstein formations in the north had abundance of dissolved anhydrite and this led to the development of anhydrite cement is the better reservoir sandstones. An example of that is shown in the lower left corner of photographed cores in Figure 21 where the best original quality fluvial channel sandstones have been completely invaded by so called chicken wire nodular anhydrite.

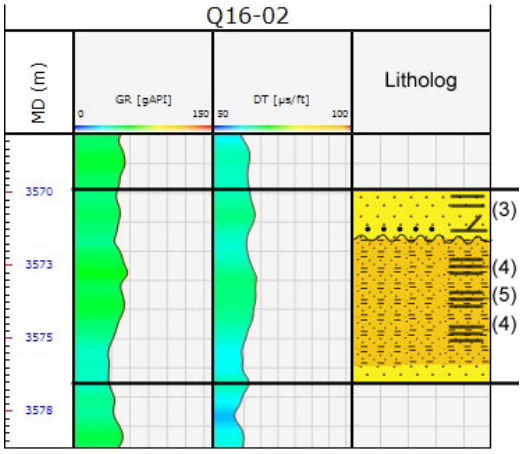

Figure 24: Core with expected base Detfurth from well Q16-02.

This photograph (Figure 24) shows one of the few available core photographs of the expected base of Lower Detfurth marking the onset of mixed fluvial, aeolian and lacustrine deposits rather than the previously dominant fluvial facies in the basin. Although there are no direct indications of large scale tectonic driven erosion like angularly unconformable layers, the concentration of mud clasts and small breccias is indicative of a change in the basin. This boundary is possible to be traced over large distances throughout the basin.

(3572 m)

Figure 25: Small section of first core from well Q16-02 with possible base of Lower Detfurth (the concentration of mud clasts in the very upper part of the image)

Where Lower Detfurth is well developed and easy to recognise it is usually clean sand interval of several meters. However towards the Upper Detfurth both formations become a complete mixture of various depositional environments with gradually increasing amount of aeolian sediments. A good example of this is well Q16-08 where in the range of several meters core length one can observe a sequence of salt lake fluvial fan, fluvial channel, fluvial flooding plain and aeolian dune (Figure 25).

The Detfurth formation can be considered as a transition period with many variations in the depositional environment. It serves as the connection between the fluvial dominated Volpriehausen and more aeolian/desert environment dominated Hardegsen formation. The events that triggered the deposition of such varied formation were probably of varied origin and also very unstable. A combination of climate fluctuations leading to a general shift towards more arid environment without any decrease of accommodation space and increased tectonic activity leading to differential subsidence of the basin but not to an increase in sediment supply could have had the observed influence in terms of deposited sediments. Lower Detfurth sandstone member represents the last significant increase of sediment supply in the West Netherlands Basin before it becomes dominated by a desert environment.

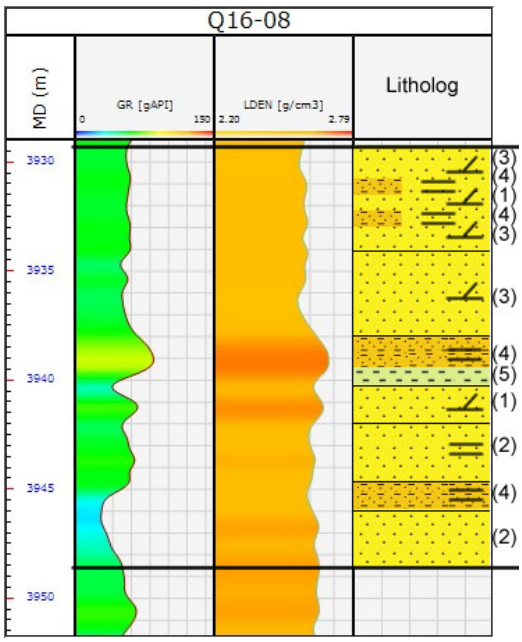

Figure 26: Interpreted core from well Q16-08 with Upper Detfurth section.

Figure 27: Photograph of a section from core from well Q16-08. Notice the extremely varied lithologies over a very short interval.

A good example of the varied facies encountered in the suggested Upper Detfurth formation – starting from bottom to top there is fluvial fan followed by a mixed sand and silt lacustrine deposits until suddenly a clean aeolian sand section follows. It is then flooded again by a fluvial channel or fan that gradually looses any visible stratification and becomes lacustrine deposits. This is interrupted by a sudden influx of fresh water leading to onset of a period when it became fluvial flood plain. The next period is again mixed fluvial channel and fan, and lacustrine deposits.

In the south west region of the basin the last major flooding event is considered as the upper boundary of the Upper Detfurth. Beyond that point aeolian setting dominates the depositional environment and the deposits are referred as Hardegsen formation. In the east and north east however there are very limited amount to preserved aeolian sediments observed in the drilled wells. The deposits continue to show a very varied pattern and the boundary between Detfurth and Hardegsen is very difficult to be determined accurately based on lithologies.

Well correlations

The determination of the Detfurth formation boundaries has been a challenge mainly because of the variability of the contact with the lower Upper Volpriehausen formation. In this correlation exercise the choice is made to interpret Lower Detfurth sandstone as the blocky sandstone unit above the clay rich sequence marking the end of the Upper Volpriehausen Claystone unit. This fits perfectly the approach of selecting sequence boundaries as the bases of new formation and is consistent with the selection of the bases of the previous two Volpriehausen formations/cycles.

The upper boundary of the sandstone unit is easy to find as the first flooding surface above the blocky sandstone. The Upper Detfurth Claystone, or Detfurth Claystone, is very consistently represented by a

sequence of three flooding events that can be found in the whole West Netherlands basin. This approach guarantees a consistent interpretation.
The upper boundary of the formation is fixed at the last flooding surface before onset of the predominantly aeolian sediments with decreasing gamma-ray profile in the south west, or the last of significant flooding surface in the distinctive pattern of three flooding surfaces with high gamma-ray footprint.

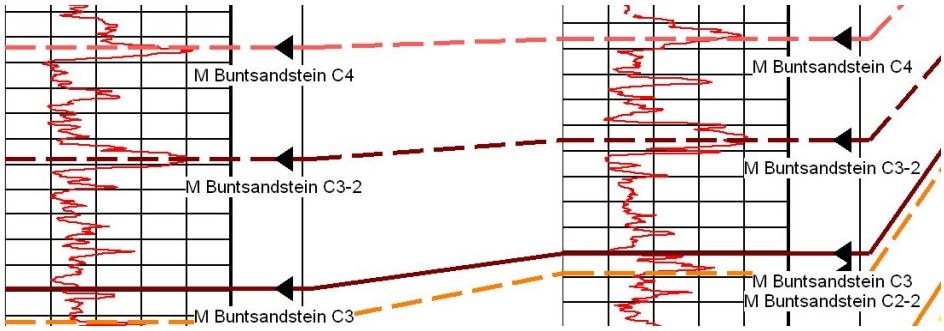

Figure 28: Well correlation screenshot between wells P18-02 and Q16-04 showing Detfurth cycle between lines M Buntsandstein C3 and M Buntsandstein C4. Notice that the base of the Detfurth (Sandstone) is an erosional base and sequence boundary and the very distinctive pattern of the Upper Detfurth (Claystone) with three clear flooding events. The sands in between have often very varied origin ranging from fluvial confined flow, fluvial unconfined flow and even desert dunes or outwash.

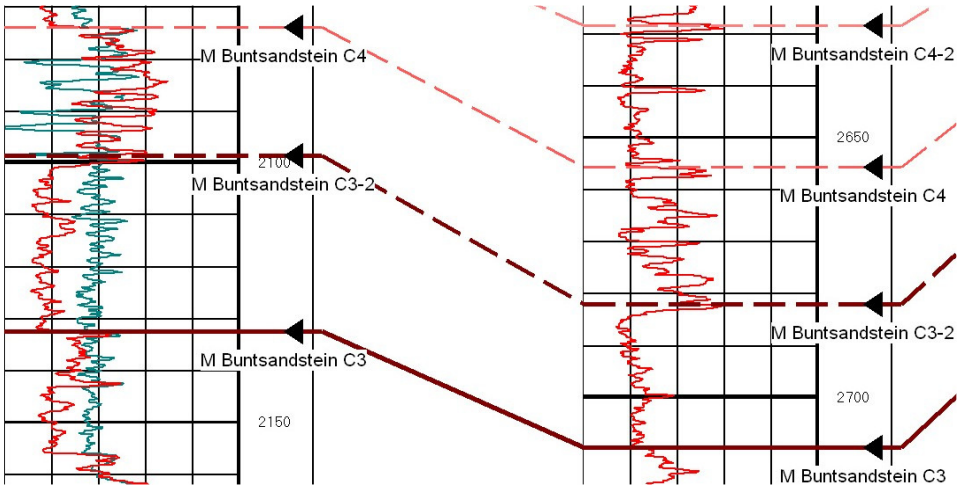

Figure 29: Similar correlation in the more western wells P08-04 (left) and P08-06 (right). Although the base of the Detfurth Sandstone is still relatively easy to be detected, the transition towards aeolian facies which marks the next Hardegsen formation is not so straight forward. Moreover the lithological composition of the Hardegsen is no longer strictly sandstone which already poses a problem for the division of the formation based on lithologies. The key consideration for the further correlation of the Hardegsen is presented in the paragraph devoted to Hardegsen formation.

Thickness maps and Facies distribution

The resulting thickness maps excluding the constraints from the major faults are shown in the figure below. The formation thickness is relatively uniform and changes are gradual which is in accordance with the observations in terms of depositional environments and global changes in the whole basin described further in the final part of this chapter. Another reason for the relatively smooth distribution of the formation is the exclusion of the upper sandstone unit which was generally considered as part of Upper Detfurth Claystone (equivalent) but based on analysis of the rock properties, facies and depositional environment was chosen to be assigned to Hardegsen formation. This is further explained in the next paragraph.

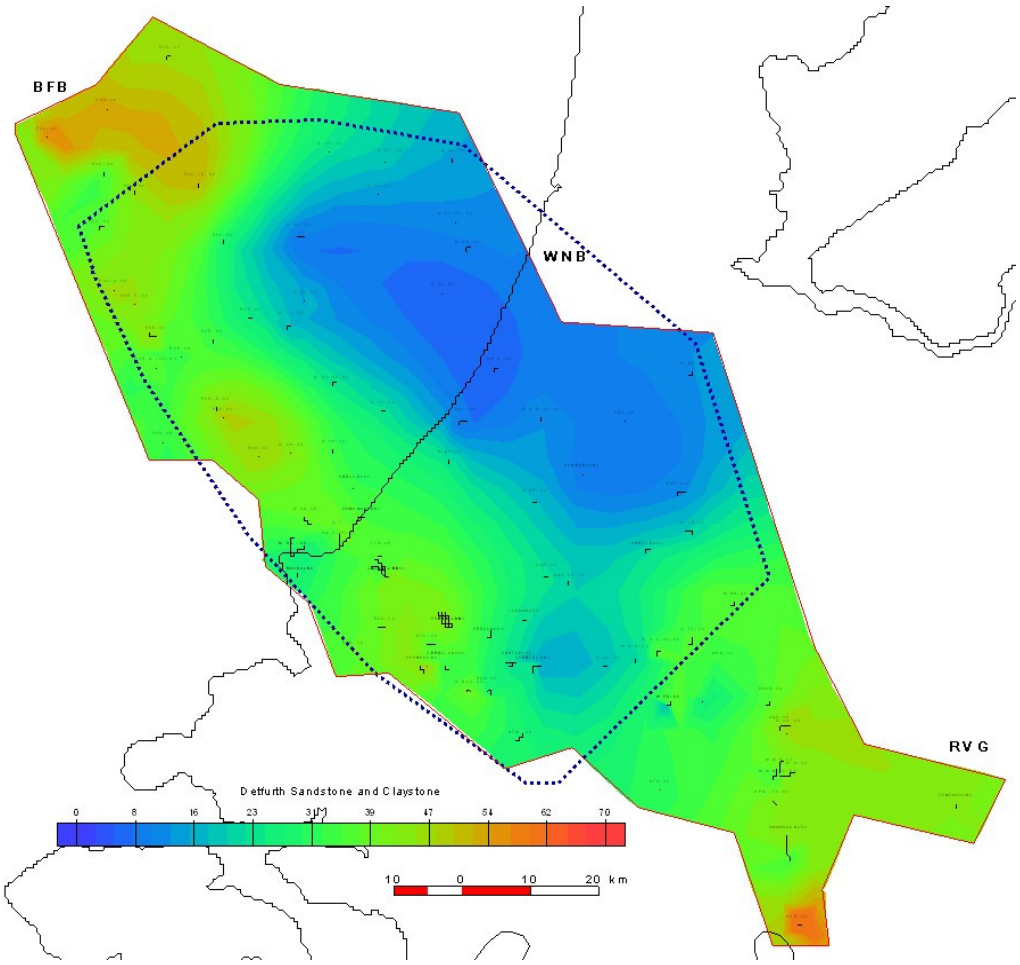

Figure 30: Basin thickness map of both Detfurth sandstone and claystone members. The formation is relatively uniform but again with well distinguishable trend in the WNB and slightly thicker in the RVG and BFB.

2.2.4. Hardegsen formation

Hardegsen formation is considered to be the natural development of Detfurth formation. While the Upper Detfurth represents a very unstable environment with varying conditions allowing a number of different facies to be deposited in very limited time span, the Hardegsen represents a shift towards a clearly defined desert setting with aeolian dunes, damp sand flats and a salt desert lake with unstable boundaries. The shift from Upper Detfurth to Hardegsen is therefore not related to a specific tectonic pulse but rather with the gradual progress of the climatic conditions and their effect on the whole basin.

Core description and lithology

Unlike the previous formation Hardegsen shows a more geographically confined distribution of facies. In the south and west of the basin there are sandstones with high quartz content, fine to coarse gain size, well rounded and with distinct parallel cross stratification. In the north and east of the basin where the dominant lithology is claystones and siltstones, the grain size is clay to very fine sand, horizontal stratification to missing and sorting and rounding of grains is poor.

The typical lithology for the Hardegsen formation in the south and south west of the basin is composed mostly from dry and damp sand flats and sand dunes. Occasional lacustrine sediments interrupt the different cycles. The sandstones are usually with large quartz content, with well sorted and sub-rounded grains. Damp sand flats usually show a distinctive wavy and irregular stratification and they are more compacted and well cemented with dolomite.

Towards the north there are only lacustrine sediments and occasionally fluvial flood plain deposits that start to become more dominant towards the top of the formation.

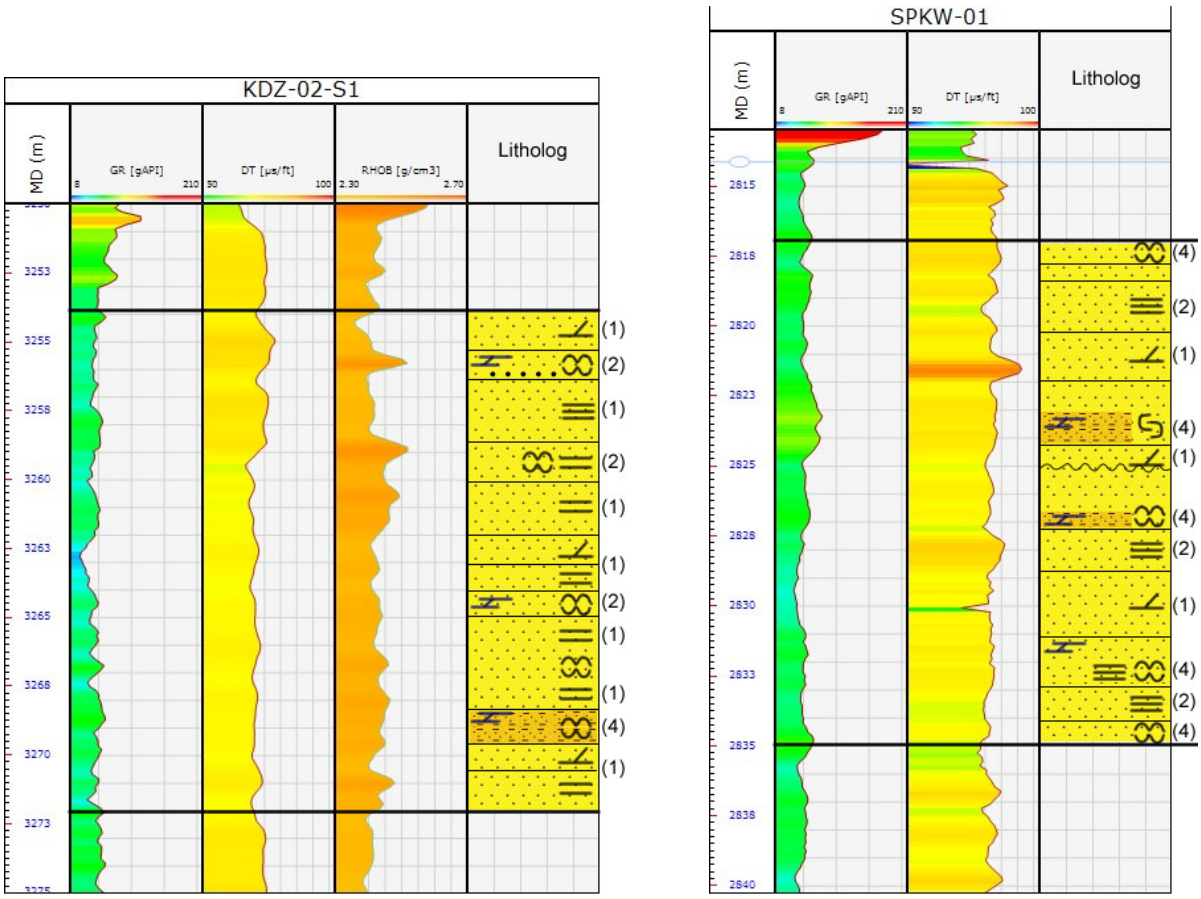

Figure 31: Interpreted cores from top cycle of Hardegsen formation from wells KDZ-02-S1 and SPKW-01

Hardegsen formation contains predominantly sediments deposited in a desert environment. The formation shows a very clear differentiation of facies based on geographical location but also shows signs of notable facies thicknesses and composition differences over adjacent fault block boundaries.
In the south and south west region of the basin where mostly aeolian sediments where deposited, Hardegsen deposits consist usually of alternations of dry and damp sand flats with occasional poorly cemented sand dunes. Dry sand flats are usually cross bedded with either planar or parallel trough stratification while damp sand flats are irregularly stratified and sometimes also with severely distorted stratification. Sand dunes are either trough cross bedded or parallel trough cross bedded with very little binding material between individual strata. (See Figure 29)

In terms of log expression the sand sequences show two major cycles subdivided each into two minor cycles of clear decrease of gamma ray towards the tops coupled with increase of density and sonic travel time. Although the general concept is to associate decreasing gamma ray in a sand sequence of aeolian origin with coarsening upwards of quartz grain sizes, it was found that it can also be related to increased density of occurrence of dolomite cemented zones in damp sand flat layers. (Figure 31)

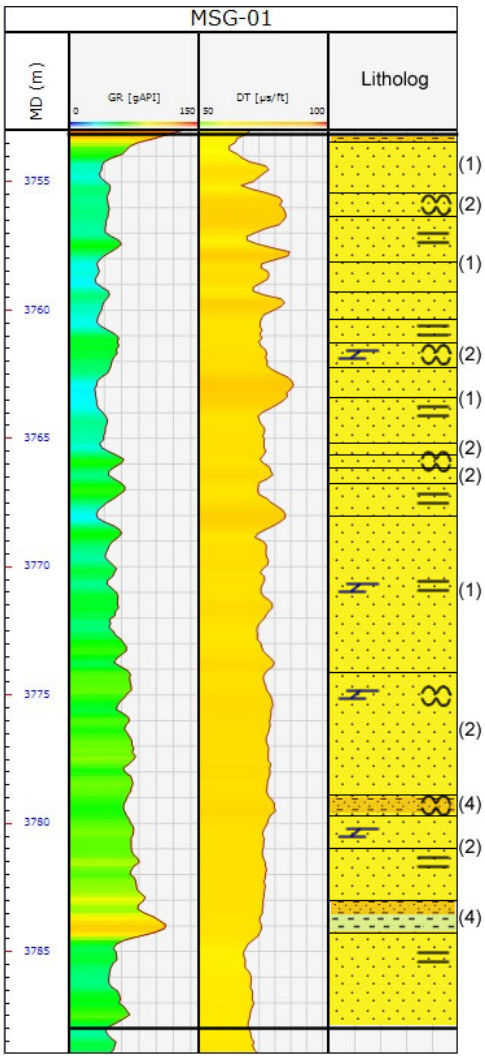

Figure 32: Interpreted core of complete top cycle of Hardegsen formation in well MSG-01. Note that intervals with very low GR profile are coarse grained sands with no visible stratification and slightly darker coloring.

Figure 33: Parts of photograph of core from well MSG-01 showing the sudden transitions from damp sand flats to coarse grained amorphous brown sand intervals.

A complete cycle with decreasing upwards gamma ray expression can be observed in the core from well MSG-01 from 3753 m to 3785 m. (Figure 30) The base of the cycle is marked with a desert lake deposits with distinctive blue-green shales. The rest of the core is sand and resembles other cores from Hardegsen formation with the exception of several intervals towards the top of the core.

These zones are composed of seemingly structure-less, very coarse sands with slightly darker, brownish color. There are occasional horizontal cement laminations with brighter color. (Figure 32) These intervals show very high permeability and porosity values and can be considered as possible enhanced flow highways as the contrast with adjacent sand intervals is significant. These intervals can also be spotted on the sonic log as they have lower transit velocities due to the lack of bonding cement. They seem to interrupt the general pattern of increasing transit velocity towards the top observed in other wells and related to the already mentioned decreasing upwards gamma ray pattern origination from the increased cement content.

The sand rich sections of the Hardegsen found for example in well KDZ-01-S2 (Figure 33) in the south west offshore area of the West Netherlands Basin show a relatively consistent lithological footprint. This combined with the distinctive log expression of these sequence gives sufficient certainty in the correlation attempts in this part of the basin.
The sandstones usually show relatively good reservoir properties with sufficient available porosity and permeability. This makes them primary goals for further evaluation for reservoir targets. The actual porosity and permeability relations including the differences between separate lithofacies and summary per formation and per facies can be found in Chapter 5.

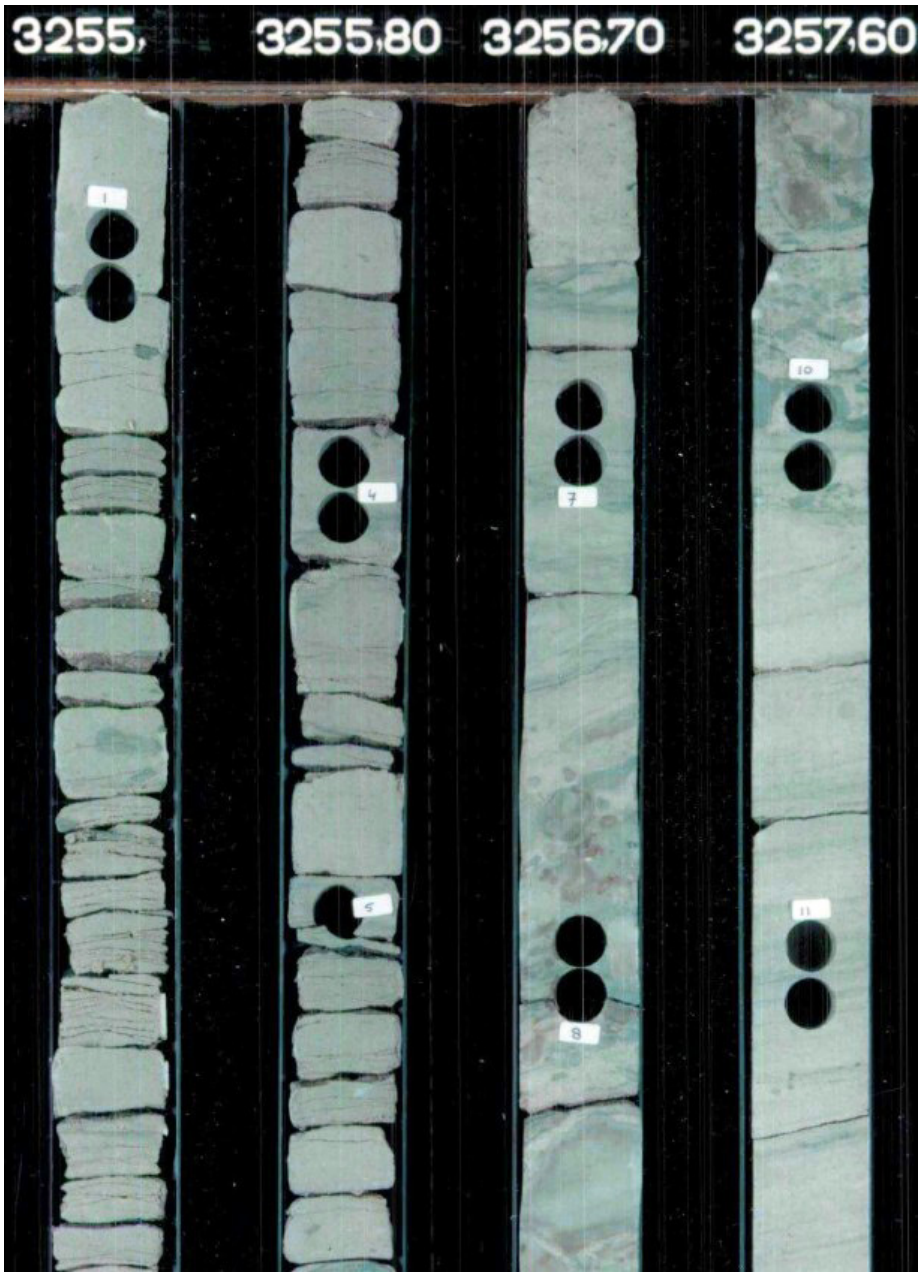

Figure 34: Core photos from well KDZ-01-S1. Notice that the lower sections of the core pieces are cut from the image. From right to left facies include – dry sand flat, damp sand flat with irregular stratification and dolomite cement, and poorly cemented sand dune

In the north and north east of the basin Hardegsen formation contains mostly lacustrine and floodplain deposits with limited thickness. Occasional fine grained sand layers interrupt the clay and siltstones and the general nature of the formation there remains similar to the Detfurth formation. (Figure 33) Although this difference in the preserved lithofacies has previously led to confusion and suggestions for large scale erosion on the Hardegsen unconformity, it is not that odd if considered in terms of typical desert environment depositional models for inland aeolian sediments and large scale facies models for the North Sea are during the Rotliegend. The actual spatial distribution of facies depends on the general shape of the basin and dominant wind direction along with the base level fluctuations. It can be concluded that in fact Hardegsen formation was not predominantly shaped by the erosion on the Hardegsen unconformity but it was rather the result of the accumulation of material released from that erosion.

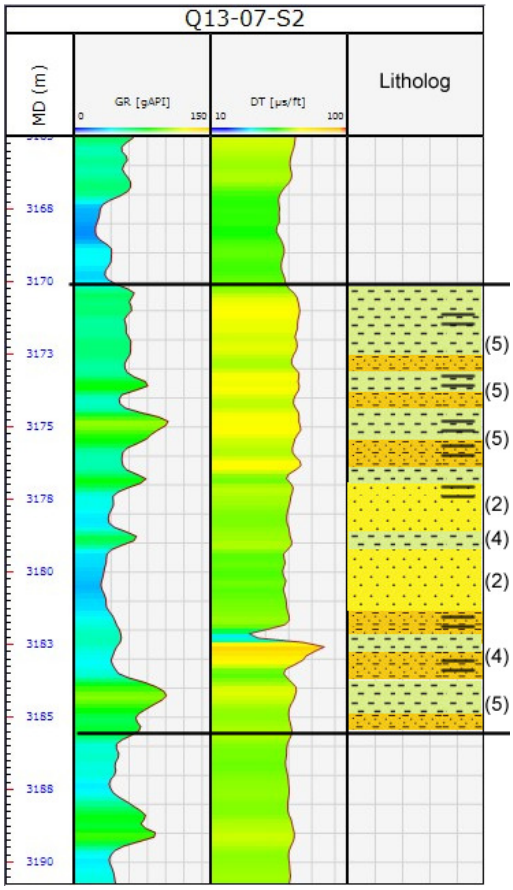

Figure 35: Core from well Q13-07-S2 with lacustrine facies in Hardegsen.

3176,5 m

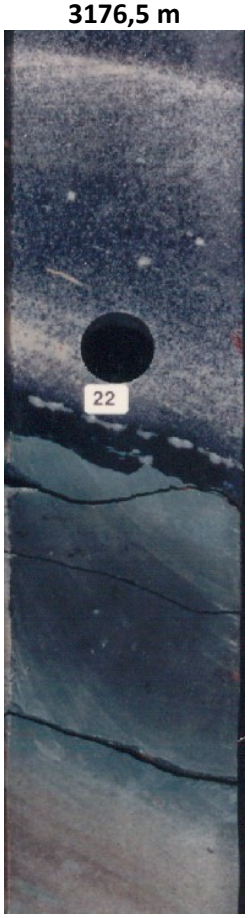

Figure 36: Lacustrine sediments – silts and claystones from core Q13-07-S2. Length is 30cm.

Figure 37: Towards the top of the formation the lake has retreated further to the north and fluvial floodplain facies increase. Wells Q13-07-S2.

Well correlations

Identifying Hardegsen is essentially a relatively easy task using the suggested formation differentiation. The most consistent approach is to recognise the pronounced Hardegsen unconformity or Base Solling for the upper boundary. For the lower boundary of the Hardegsen formation it was already mentioned that is not a sequence boundary but rather a distinctive flooding event. It marks a point beyond which the basin has entered a more stable period in terms of arid climatic conditions and gradual differential subsidence on the major fault blocks. In terms of identifying those events on the wire line logs for the purpose of basin wide correlation, the Hardegsen unconformity occurs as a sharp erosional base overlaid by coarse sediments followed by quick transition towards fine grained sediments. It is relatively easy to spot and follow so that it can be considered as a solid ground for further correlation underneath it.

The lower part of the Hardegsen formation has often been referred as Detfurth Claystone regardless of the fact that in term of lithological characterisation it is typically a very clean desert sheet sands with significant porosity and permeability characteristics. This problem is resolved in this correlation exercise with the proper definition of Detfurth formation. While the desert sands are encountered in the south and south west of the basin in the north of the basin the formation is dominated by lacustrine sediments indicating that the desert lake was still preserved while the fluvial systems have almost disappeared in this final period of the main Buntsandstein sub-group.

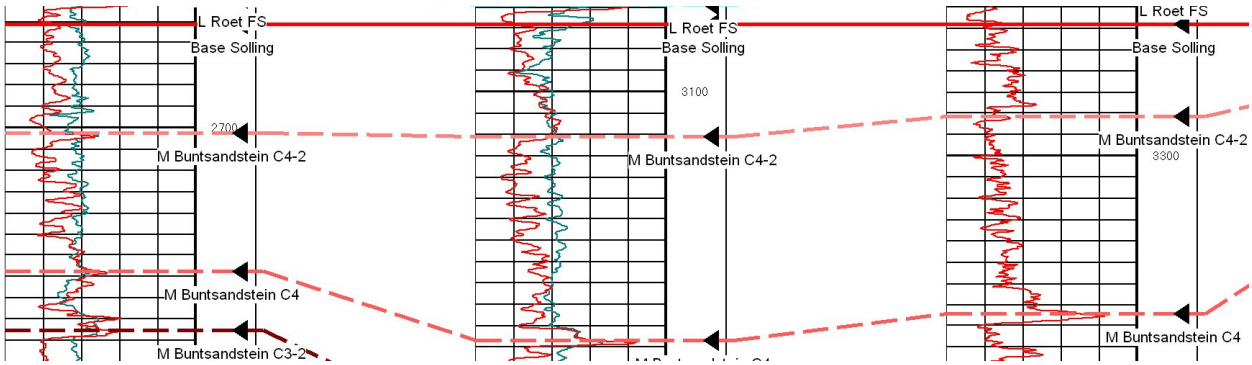

Figure 38: Well correlation for Hardegsen formation between wells P15-G-01-S1, P18-01, P18-02.

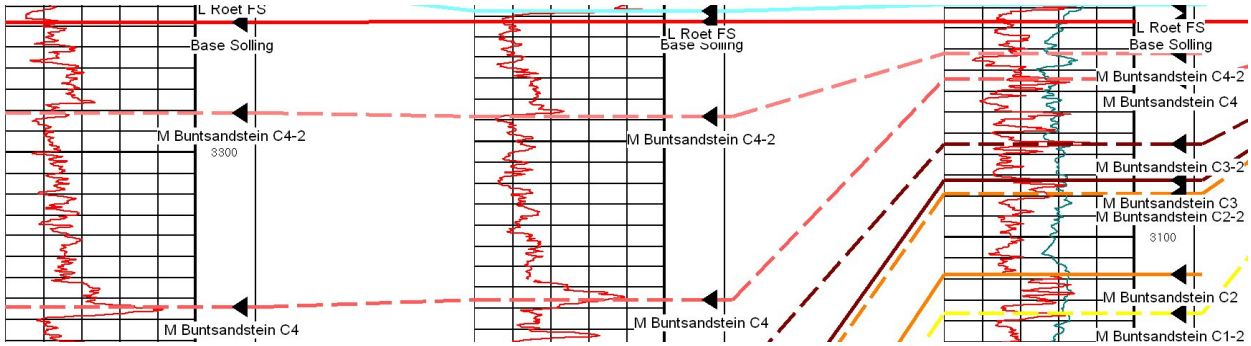

Figure 39: Well correlation along the dip direction of major fault pattern between wells P18-02, Q16-04, Q13-07-S2. Notice the sudden disappearing of large part the formation and change of nature across single fault block between wells Q16-04 and Q13-07-S2 while the pattern of the underlying Upper Detfurth claystone formation remains identical also in terms of formation thickness.

Thickness maps and Facies distribution

The thickness distribution of the preserved Hardegsen formation show great contrasts especially between the southern and northern areas. This is related on one side to the erosion that is expected to have taken place before the deposition of the Base Solling/Hardegsen unconformity transitional lag layer. On the other side it is also related to the significant differences in the depositional environment at the time of deposition with the north parts occupied by an ephemeral desert lake while winds with dominant wind direction towards the west deposited eroded sands in the south and south western regions. The subsidence in those areas was quickly compensated by the accumulation of new sands.

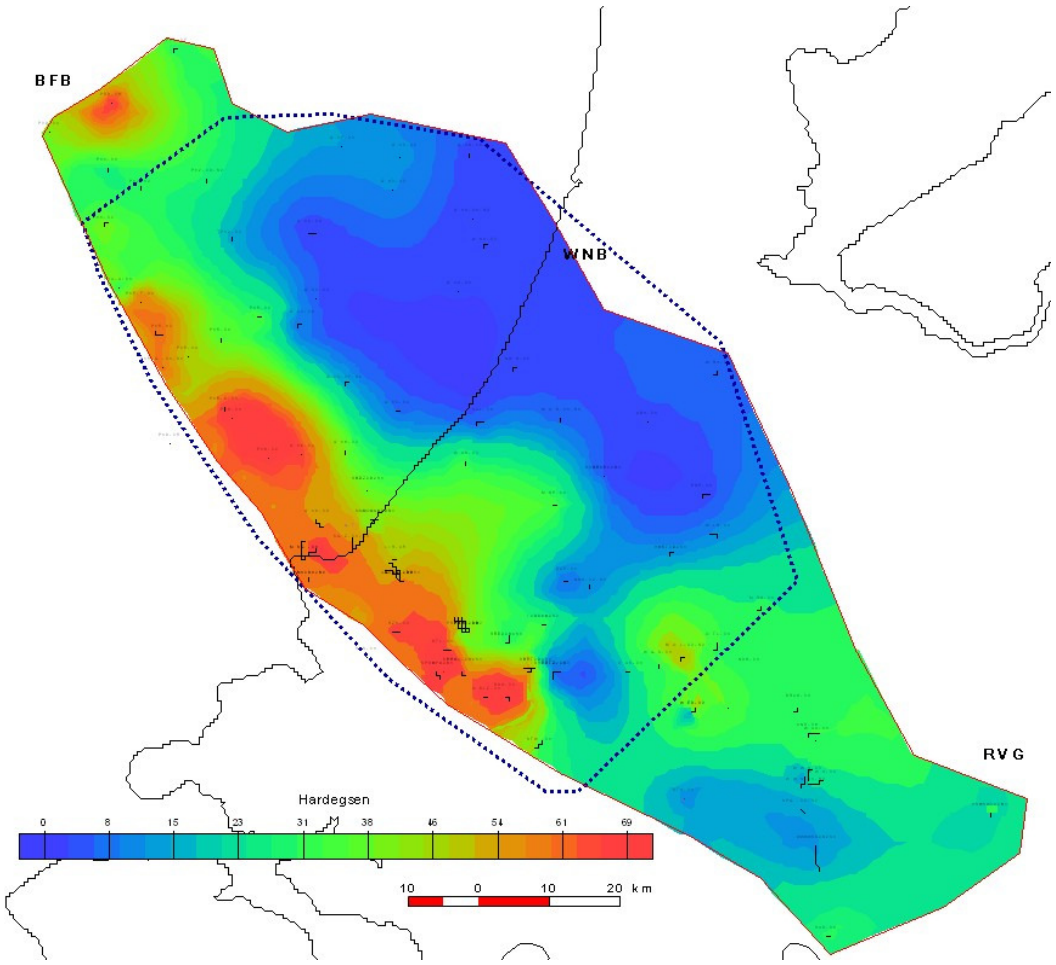

Figure 40: Basic thickness map of Hardegsen formation. It is clear that the formation is only well developed in the south west region of the basin in a much more arid environment than the previous formations of the Main Buntsandstein sub-group.

2.3.5. Middle and Upper Triassic formations

The further subdivision of Röt, Muschelkalk, Keuper and Sleen formations will only be briefly discussed in this chapter, as it is only relevant to this project in regard with the determination of seal capacity of possible reservoirs. The formation boundaries suggested are based on identifying distinctive lithologies changes and sequence boundaries.
The actual correlations can be seen in Appendix II together with the Lower Triassic correlations. It is important to note that the thickness distribution of the Upper Buntsandstein formation differs from those of the Main Buntsandstein with distinctive thickening in the north. This is caused by the specific shape of the basin and adjacent basins together with the different depositional environment of shallow lake/sea. Another important observation is that facies change also from south to north from sandy to evaporate sequences due to the shape of the basin and the difference from proximal to distral position in relevance to the clastic sediment source.

2.3. Conceptual model for the facies distribution and basin development for the West Netherlands Basin during the Lower Triassic

In this sub-chapter the final facies distribution model will be presented based on expected depositional environments in the individual formations of the Main Buntsandstein. There is already an existing model in literature for the spatial probability of encountering a certain facies based on a study of several cored wells in the P and Q offshore quadrants. This study will expand on that model and present a revised model based on the updated well correlations for the whole basin.

2.3.1. Available models for Main Buntsandstein facies distributions per formation

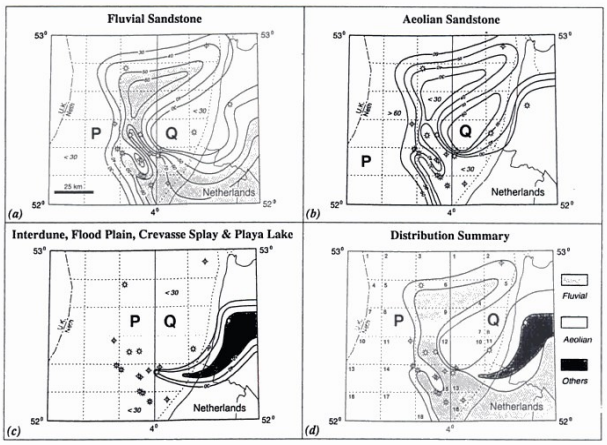

Fig. 11. Distribution of environments of deposition – Volpriehausen Sandstone Member. The distribution map (d) indicates those facies that occupy more than 50% of the rock unit.

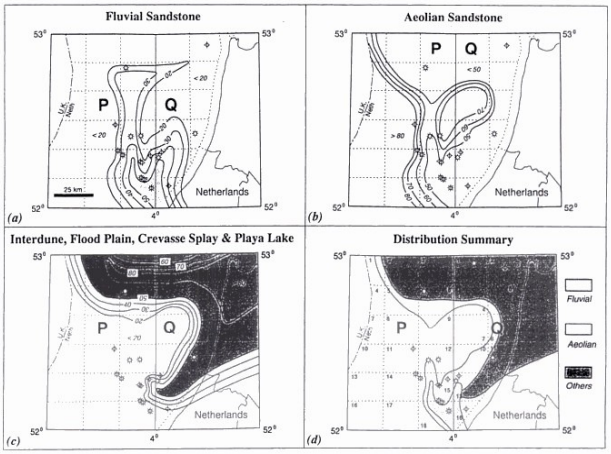

Fig. 12. Distribution of environments of deposition – Volpriehausen Clay-siltstone Member. The distribution map (d) indicates those facies that occupy more than 50% of the rock unit.

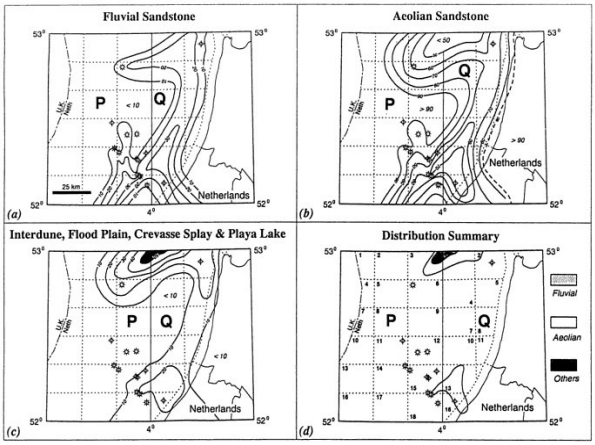

Fig. 13. Distribution of environments of deposition – Detfurth Sandstone Member. The distribution map (d) indicates those facies that occupy more than 50% of the rock unit.

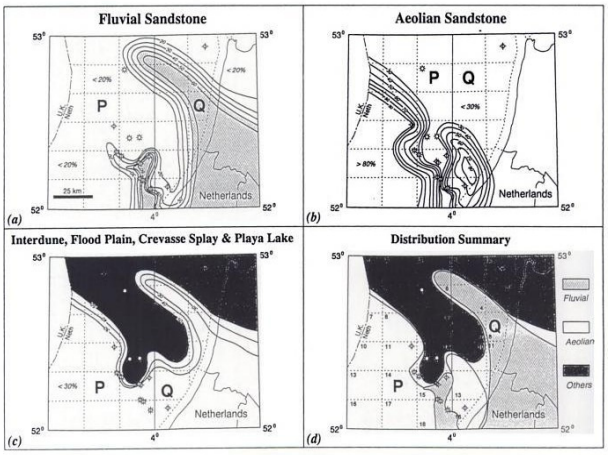

Fig. 14. Distribution of environments of deposition – Detfurth Claystone Member. The distribution map (d) indicates those facies that occupy more than 50% of the rock unit.

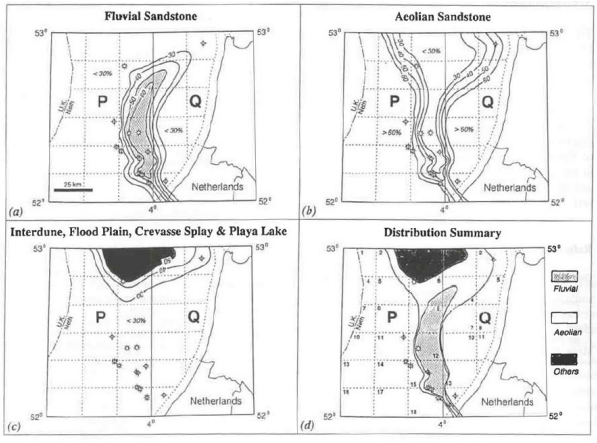

Fig. 15. Distribution of environments of deposition – Hardegsen Sandstone Member. The distribution map (d) indicates those facies that occupy more than 50% of the rock unit.

Figure 41: Suggested facies probability models for all the sandy formations in the Main Buntsandstein after Ames and Farfan, 1996.

These figures (Figure 40) represent suggested probability for encountering a certain lithological facies based on core and log analysis from wells in P and Q quadrants in the Dutch offshore. Although this model is based only on the limited information available to the geologists at that time and is therefore outdated already it is still representative for the Main Buntsandstein facies and formation distributions in terms of the general concept for the basin development.

In order to evaluate the distribution of facies in the study region two factors should be considered. The first and most important is the one taken into account in the distribution chance diagrams presented above is the frequency of occurrence of individual facies in cores. The quality of the interpretation is directly related to the quality of the interpretation of the original cores and might differ between different authors. In order to avoid over-complication of the model, facies should be grouped into combinations based on similarities of the depositional environment.

The second factor to be considered in the evaluation is the dip and orientation measurements from all wells that can give clues about the paleo channel flow directions and wind directions. In the figure below (Figure 41) a summarized collection of all orientation measurements separated by the different formations are

presented. There are two distinctive regions analyzed – south west region and the rest of the study area in the basin. This is done in order to evaluate the most considerable difference in the depositional environment namely the difference between the south west region bounded by the major boundary normal fault and the other parts of the basin.

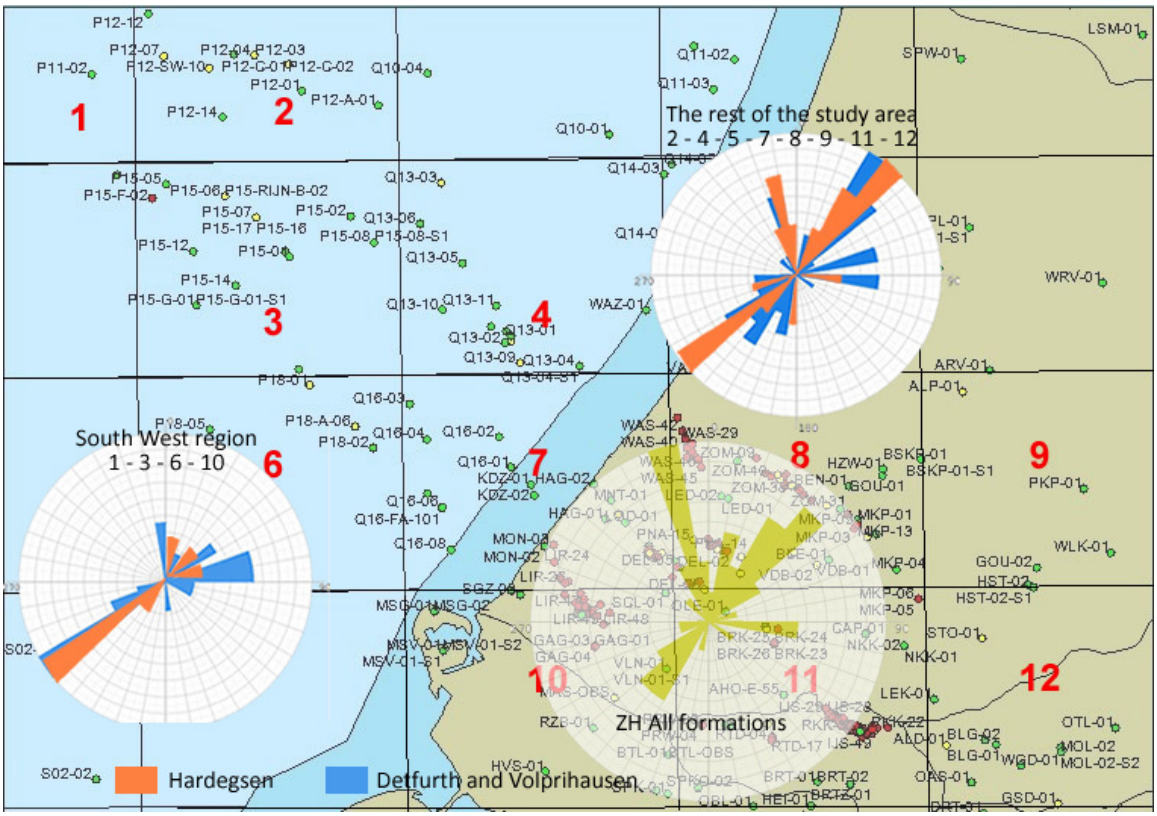

Figure 42: List of rose diagrams of azimuths separated by location and formation.

When all data is collected and analyzed it can be summarized into a conceptual model that depicts the generalized knowledge for the whole basin. In order to honor the difference between the first fluvial systems in arid environment dominated part of the main Buntsandstein and the second aeolian system arid desert environment dominated part two separate models are developed. The basic concepts are taken from the depositional environment and the morphological outlook is guided by present day analogues of similar environments.

Conceptual models (Figures 42 and 43) are based on a supposed environment resembling the current conditions around lake Chad in Africa or lake Eyre in Australia. Although there is sufficient rainfall in the mountain hinterland to supply sufficient amount of sediment to the basin, the climate is relatively arid. The reason for this is probably similar to nowadays similar cases where large mountain chains serve as barriers to more humid masses coming from the oceans and therefore desert or semi desert environment are created behind them. Braid channel systems existed in the Volpriehausen and Detfurth times with fluctuating lateral positions and two major flow directions. One was coming from the Roer valley Graben basin and the other was of smaller significance but still constantly active coming directly from the London-Brabant mountain range. The is little evidence of significant aeolian desert conditions on the areas between the channel but it is also not excluded as possibility. The arid climate prevented the development of significant vegetation and animal life so such areas were subjected to constant dry wind.
In Hardegsen times the sediment supply decrease caused the channel systems to become completely dormant and probably seasonal turning the areas not covered by the fluctuating desert lake in the center of the basin into desert sand flat with relatively limited dune development. Most probably sandy sediment deposited on seasonal basis were often eroded by the desert winds and deposited against the foot wall of the south boundary fault. It is very probable that the activity along that fault was increasing towards the end of the Main Buntsandstein deposition period.

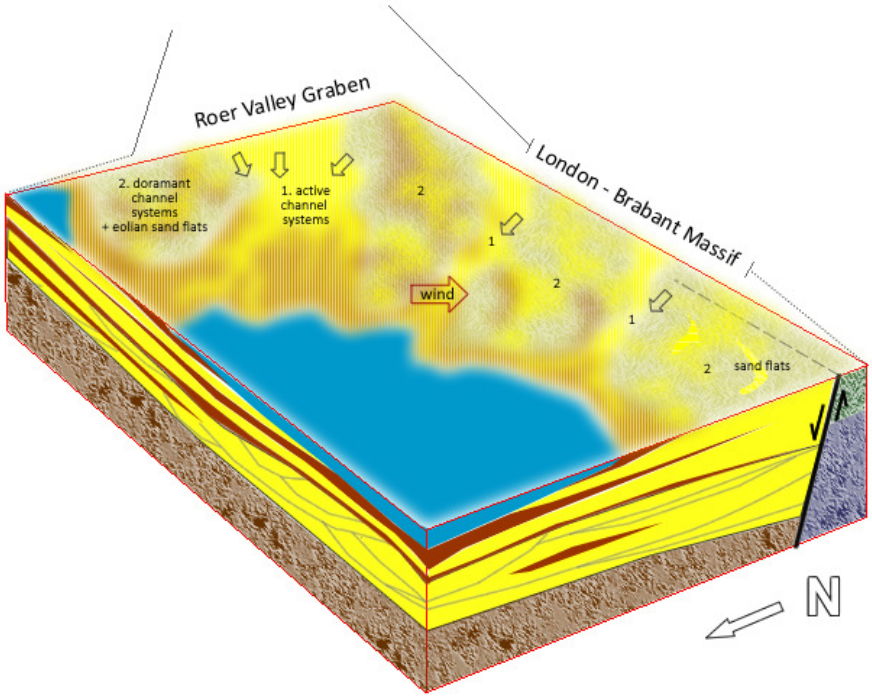

Figure 43: Conceptual geologic model for the period when Volpriehausen and Detfurth formation were deposited in the West Netherlands Basin.

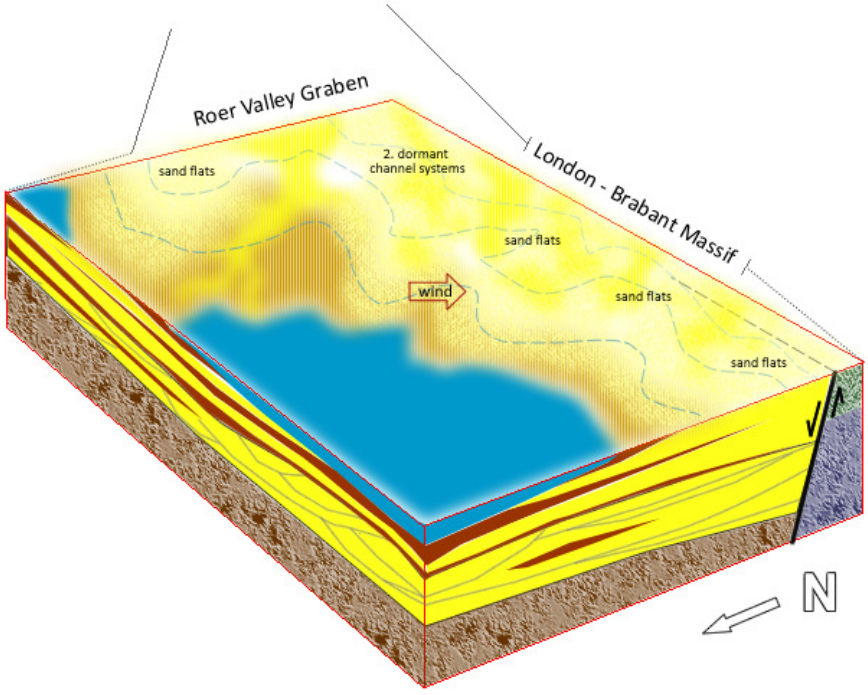

Figure 44: Conceptual model for the period when Hardegsen formation was deposited in the West Netherlands Basin. Dashed blue lines indicate fluctuating ground water table.

2.3.2. Revised model for spatial distribution of lithofacies

Due time limitations, lack of automated software workflow and insufficient core sedimentological interpretations density in the study area no updated facies probability and spatial distribution model is presented. The ideas and expectations for the facies distributions are however applied to the static geologic modelling as described in chapter 5.

2.4. Revised sequence stratigraphical framework model for Main Buntsandstein in the West Netherlands Basin

The building elements in a sequence stratigraphical framework are the sediment supply and availability of accommodation space. They control the way sedimentological processes occur and type and intensity of deposition of different facies. The factors that control them can be summarized based on their origin – it can be tectonic, climatic or geomorphologic. A basic schematic representation of the complex interactions that exists between the factors can be seen in the figure below. (Figure 44)

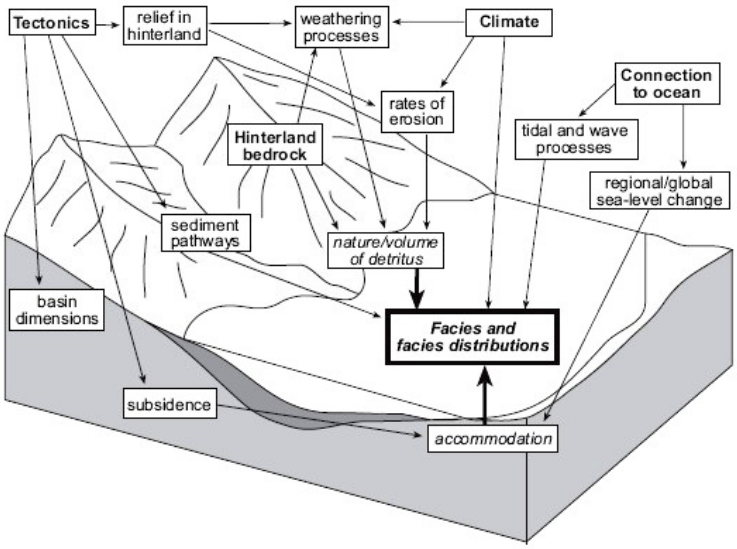

Figure 45: Schematic model of factors influencing the depositional environment in a basin leading to the facies variations and distribution. (Nichols, 2009)

Geomorphologic profile of the basin determines the general shape thus it controls the initial amount of accommodation space available and the way it would change in reactions on influence from other factors. This also includes the connections to the regional or global sea and oceans. It also determines the possible travel paths for sediment to be transported to and in the basin with water, wind or gravity.

The impact of tectonic activity on a sedimentary basin is very strong. It controls the rate of subsidence or uplift of the basin and the sediment source bedrock.

This way it shapes the basin and the sediment transport pathways while also triggering more erosion or on the contrary – reducing the amount of erosion in the hinterland.

The last major control is given by the climate. Rate of weathering and erosion, energy and capacity of sediment transport systems, changes in accommodation space, sedimentary processes that shape the eventual lithofacies are the factors that are directly influenced by the climatic conditions in a sedimentary basin.

In the next paragraphs the way these factors interact in the West Netherlands Basin during the deposition of the Main Buntsandstein subgroup will be evaluated and presented as sequence stratigraphical framework for regional understanding of the subdivisions in the basin and the probabilities of encountering certain facies at locations without already drilled exploration wells. As it was mentioned earlier although this summary is presented as a final conclusion the actual process of gathering and incorporating all the information is an iterative one involving constant review of previous work.

2.4.1. Analysis of factors that have influence on the depositional environment

Sediment supply

Sediment supply is generally a function of the tectonic influence in regard with erosion in the hinterland and of the paleo climatic conditions also in regard with rate of erosion in the hinterland and sediment transport capacity to the basin. The sediment supply in the West Netherlands Basin during the deposition of the Main Buntsandstein sub-group was controlled by the conditions in the major sediment source – the London Brabant Massif. Direct control over such factors as the sediment composition and rate of sediment supply is controlled by the rate of erosion is the hinterland. Indirect influence on the depositional environment in the basin include the effect that paleo high had on the local climatic conditions. It served as a natural barrier for the flow of the damp atmospheric currents coming from the south, while on the other hand it confined the already dry atmospheric current coming from the east. As a result of this the climate was becoming steadily more arid throughout the deposition of the Main Buntsandstein. The major alluvial fans developed in south

and east directions leaving out the West Netherlands basin with more monsoonal sediment supply rather than persistent all year round sediment influx.

Accommodation space

The accommodation space is a function mostly of the tectonic influence in regard with the rate of subsidence or uplift in the basin and of the paleo climate in regard with the local base level changes. As the West Netherlands Basin did not have a direct connection to the global ocean during the deposition of the Main Buntsandstein sub-group, the global eustatic fluctuations did not play a direct role in the changes in the accommodation space. The basin was part of the Southern North Sea basin which in turn was a part of the general North Sea Basin. A number of ephemeral salt lakes existed in the big basin and the fluctuations of their boundaries controlled the variations in accommodation space in the local smaller basins. As there was no connection to the global ocean the changes in the basin climate had direct consequences on fluctuations of the boundaries.

The tectonic development of the basin during the Lower Triassic is related to the onset of the Pangaea break up marked by the Hardegsen unconformity.

2.4.2. Sequence stratigraphical model combining tectonic and sedimentological influences

This sub-chapter will present a suggested model for the complex interaction of the different factors mentioned previously. Graphs for the suggested development of the sediment supply, accommodation space and corresponding graphs for tectonic development and climate changes will be presented as a summary of the evaluation of individual factors.

The starting point for this evaluation is the base of the Main Buntsandstein sub-group. It is a distinctive change in lithology indicating a drastic change in conditions in the basin. The shales of the Rogenstein formation are cut by the fluvial sandstones of the Lower Volpriehausen which indicates that the sediment supply has increased significantly along with the general energy in the sediment transport systems. In this case those are alluvial fans and braided rivers which originate from the northern slopes of the London-Brabant Massif. This is in accordance with the development of the base of the Middle Buntsandstein equivalent in other adjacent regions where the increase of the energy in the system is even more emphasized by the deposition of conglomerates and pebbly sandstones.

The accommodation space in the basin should also have decreased prior to the onset of the deposition in order to trigger the changes. The reason for this decrease is most probably due to tectonic subsidence. Indications for this conclusion are the later significant subsidence of the basin and also the fact that the basin did not have a direct connection to the global ocean. It is thus not influenced by eustatic fluctuations but rather by climate induced changes of local lake water level and groundwater water table. On the other hand the increase in sediment supply is directly related to increase in humidity in the hinterland and therefore a general drying out of the basin cannot be expected as a source for the decrease in accommodation space at that time.

During the lower period of the Volpriehausen the sediment supply was sufficient for the deposition of sand rich sediments in very broad scale. Towards the next period the accommodation space gradually increased until the more distral areas became completely submerged underneath the lake or system of lakes. Indication for this is the preserved thicknesses and lithologies in the areas adjacent to Broad Fourteens Basin and Rour Valley Graben Basin in West Netherlands Basin. While there the upper parts of the formations have developed as distinctive claystone members, towards the West Netherlands basin the same time period those members are in fact complete individual cycles with erosive base followed by a sandstone rich lower section and clay rich upper section terminating in small scale flooding surfaces.

Upper Volpriehausen sandstone and Detfurth sandstone members are all indications of new periods with decrease in accommodation space with overall gradually decreasing strength of the sediment supply. The triggering event for the onset of these periods and can be of tectonic or combined tectonic and climatic origin.

West Netherlands Basin unlike the adjacent basins experience much greater variation of the deposited sediments and corresponding depositional environments as it has more proximal position to the major

sediment source. The unstable response of the basin to the changes in conditions also contributes to the abundance of sheetflood deposits in the different formations instead of development of distinctive channel belts of braid bars and channels.
This overall greater sensitivity to the slight changes in the conditions makes the correct interpretation of the different formations a challenge. However the overall trends in the Early Triassic remain similar. The climate towards the final stage of the deposition of the Main Buntsandstein sub-group becomes drier. This led to reduction of sediment supply and decrease in accommodation space. The combination of these two conditions has triggered wide scale erosion in areas that were not covered by the few remaining river systems or the lake. This effect was also enhanced by a more significant subsidence of the south western parts of the basin. The result was a significant accumulation of redeposited sand in the south western margin of the basin in a typical desert depositional environment.
Due to the relatively close position of the lake and expected high levels of the groundwater level most of the sand was deposited in sheet-like sand flats and relatively few small scale dunes could develop. While the river systems were flowing from south / south east towards the north / north west, results from dip measurements in the desert sand deposits indicate a dominant wind direction towards the west / south west. The London Brabant Massif served as a natural barrier for the damp atmospheric currents coming from the south west, but also as a confining boundary for the dry currents coming from the north east.

Figure 45 below shows a suggested schematic graphical representation of the already presented development of the West Netherlands Basin in terms of the major considered factors.

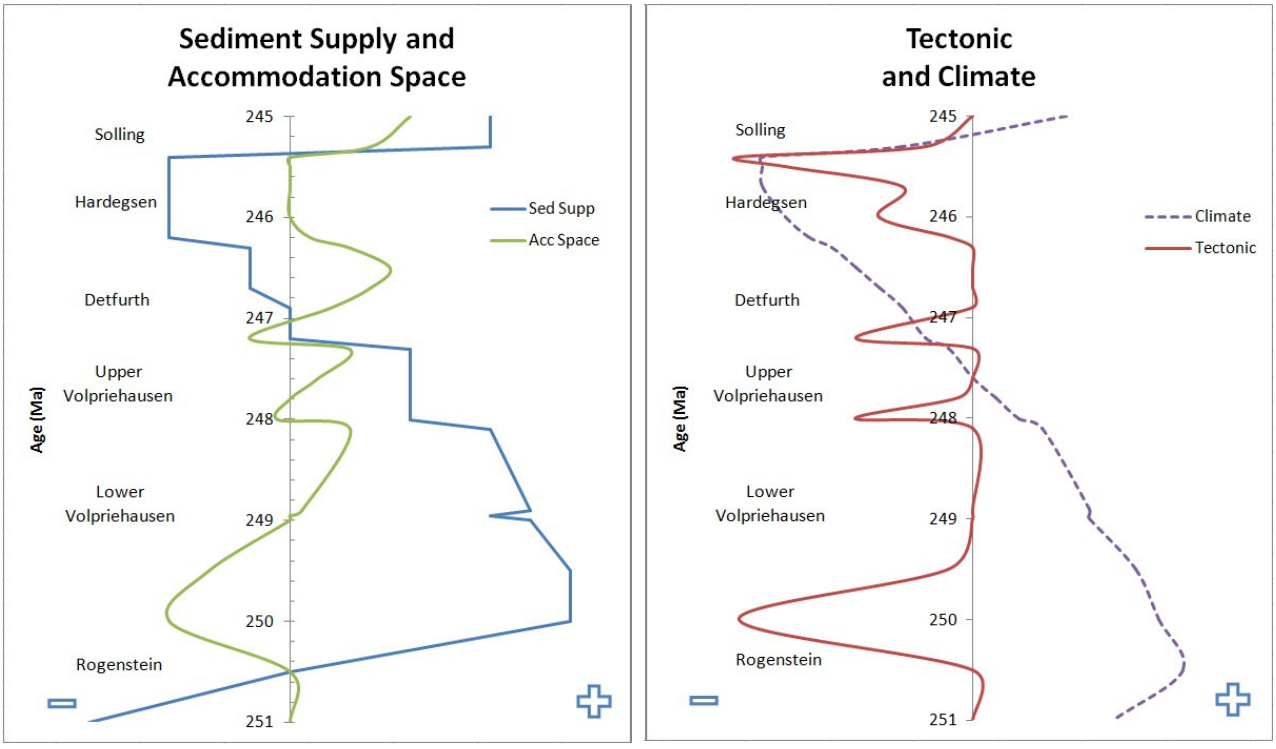

Figure 46: On the left side: Schematic graphs with suggested relation between sediment supply and accommodation space changes during the deposition of the Main Buntsandstein subgroup formations. A negative position of sediment supply curve means reduction or no supply at all. Negative position of the accommodation space curve indicates decease of accommodation space and positive position of the curve indicates increase in accommodation space. On the right side: The controlling elements that influence most the sediment supply and accommodation space – tectonic influence and climate conditions. A negative influence for the tectonic curve indicates subsidence. A negative influence of the climate curve indicates dry climate, positive influence indicate humid climate including climate in the hinterland.

2.5. Conclusions and recommendations

In this chapter it is shown that the proper evaluation of the Main Buntsandstein formations requires an integrated approach where a number of different aspects are simultaneously taken into account. The already available lithostratigraphy of the sub-group showed a wide variety of inconsistencies and inaccuracies. In order to be able to interpret the formation boundaries a different approach is suggested and applied. The Main Buntsandstein sub-group is evaluated using system sequence stratigraphic approach and individual formations are identified according to their corresponding upper and lower boundaries. Those boundaries are selected so that they represent sequence stratigraphic surfaces such as flooding surfaces or sequence boundaries. As the basin was not in direct contact with the world ocean during the deposition of the Main Buntsandstein the major controlling mechanisms are sediment supply from the sediment source and variations in the accommodation space availability triggered by tectonic subsidence or fluctuations of the ground water level related to the ephemeral desert lake towards the north.

This report suggests not only a revised and consistent interpretation of the formation boundaries but also presents solutions to several problems related to the vertical extent of Hardegsen and Detfurth formations in the basin. The major differences that are proposed to the already existing models are related to the identification and mapping of the two cycles in the Hardegsen formation and determination of a consistent base Detfurth boundary. Hardegsen formation is proposed as the major exploration target for geothermal energy and is therefore a major topic of interest of this report. The formation of predominantly desert environment origin is only fully developed in the south and south west parts of the basin and is unique in its features to the West Netherlands Basin. Base of Detfurth formation is considered to be a sequence boundary most distinctly recognizable in more proximal to the sediment source parts of the basin towards the south. It is typically a distinctive coarse sand incision into the underlying shales or silts to silty sands of the upper Volpriehausen formations. While Volpriehausen formations have clear indications for fluvial depositional environment dominated by braided rivers, Detfurth formations are more related to a period when the basin experienced gradual reduction of humidity leading to the deposition of the Hardegsen formation in the south parts of the basin in already complete desert climate.

It is important to note that although Hardegsen is associated with desert environment and aeolian sandstones there are no distinctive dune deposition but desert sand flats with limited relief variations in relatively very flat setting. Early stages of basin extension have influenced the basin during the deposition of the Hardegsen formation and are most probably related to activation of the major base faults including significant activity along the south boundary faults. These conclusions are based on the analysis of the thickness maps of the formations and also include the observation that erosion has taken place on some of the fault blocks on the Hardegsen unconformity leading to complete erosion of the upper cycle of Hardegsen. The actual separation of Hardegsen in two cycles is also related to major shift in tectonic activity rather than drastic change in climate conditions.

Individual formations with their revised vertical boundaries are then described in terms of sedimentological features and dominant facies. The detailed descriptions are intended to give a more clear idea of the exact depositional environment and dominant facies deposited in the basin at the given geological time. These descriptions serve as the basis for further evaluations of the reservoir potential of the Main Buntsandstein formations in terms of diagenetic development related to depositional environment or burial history.

From the evaluation of the depositional environment it becomes evident that the basin has been influenced by the individual development of fault bocks. This is indicated by the notable changes in formation thicknesses and dominant facies across major faults. It becomes reasonable to consider fault blocks as natural limits for possible reservoir division based on facies distribution, burial development, and eventually resulting reservoir properties characterization.
In the next chapter the individual development of fault blocks is taken one step further with the complete evaluation of the burial history of Triassic sediments trough the most significant stages in the tectonic development of the West Netherlands Basin including the basin inversion.

Further improvements on the sequence stratigraphic model are recommended before it can be tested used as prediction tool for future drilling and exploration campaigns. Several suggestions for additional work that can be carried out in order to achieve the desired advancement in the understanding of the depositional environment include – better understanding of the connection between tectonic influence and the shift in lithofacies and formations, better controls on the sediment supply sources and more profound analysis on the spatial facies distribution as combination of conceptual geological model and log sedimentological observations as suggested in this work.

References:

Ames, R., Farfan, P.F., 1996, The environment of deposition of the Triassic Main Buntsandstein formation in P and Q quadrants, offshore Netherlands, in Rondeel, H.E., Batjes, D.A.J. et al, Geology of oil and gas under the Netherlands, Kluwer, p167-178, Dordrecht.

Bourquin, S., Peron, S., Durand, M., 2006, Lower Triassic sequence stratigraphy of the western part of the Germanic Basin: Fluvial system evolution trough time and space, Sedimentary Geology 186, p187-211, Elsevier

Einsele, G., 2000, Sedimentary basins – Evolution, facies, and sediment Budget, 2nd edition, Springer, Germany

Fisher, M.J., Mudge, D.C., 1998, Triassic, Petroleum geology of the North Sea, 4th edition, K.W. Glennie, JAPEC, UK

Geluk, M.C., 2005, Stratigraphy and tectonics of Permo-Triassic basins in the Netherlands and surrounding areas, University of Utrecht, PhD Thesis.

Geluk, M.C., Röhling, H-.G., 1997, High-resolution sequence stratigraphy of the Lower Triassic Buntsandstein in the Netherlands and North West Germany, Geologie en Mijnbouw 76

Mader, D., 1983, Evolution of fluvial sedimentation in the Buntsandstein (Lower Triassic) of the Eifel (Germany), Sedimentary Geology 37, Elsevier

Nichols, G., 2009, Sedimentology and Stratigraphy (second edition), Wiley-Blackwell, p.324-381

Purvis, K., Okkerman, J.A., Inversion of reservoir quality by early diagenesis: an example from the Triassic Buntsandstein, offshore the Netherlands, in Rondeel, H.E., Batjes, D.A.J. et al, Geology of oil and gas under the Netherlands, Kluwer, p179-191

Spain, D. Conrad, C., 1997, Quantitative analysis of top seal capacity, offshore Netherlands, Southern North Sea, Geologie en Mijnbouw 76

Szulies, M., 2004, Magnetostratigraphy: the key to a global correlation of the classic Germanic Trias – case study Volpriehausen formation, Middle Buntsandstein, Central Germany, EPSL, Elsevier

Williams, B., McKie, T., 2009, Triassic palaeogeography and fluvial dispersal across the North-West European Basins, in Triassic basins of the Central and North Atlantic borderlands - models for exploration, Geology Journal 44, Issue 6.

Williams, B., 2009, Large scale alluvial architecture and correlation in a Triassic pebbly braided river (Lower Wolfville formation, Fundy Basin), Journal of Sedimentary Research, SEPM

www.nlog.nl – Netherlands Oil and Gas Portal, source for all wireline logs and core photos.

3. Determination of maximum burial depth and influence from differential subsidence of the Lower Triassic Bunter sandstone deposits using 2D palinspastic reconstructions

An important step in the correct determination of the reservoir qualities for the sandstones of the Main Buntsandstein formation of the Lower Germanic Trias subgroup is the estimation of the maximum burial depth to which they were exposed in the course of geological history. West Netherlands Basin is an inverted basin. As such it has experienced reactivation of already available normal fault structures from the rifting phase into reverse faults. The correct amount of uplift can be accurately determined only if the geological development of the basin is closely examined in regard with the reconstruction of the different rifting and compaction stages.

3.1. Geological development of West Netherlands Basin during the Mesozoic and Cenozoic, and effects on Triassic deposits

West Netherlands Basin has been an active depositional basin during the most of the rifting phase in the Triassic, Jurassic and Lower Cretaceous. The basin is superimposed on an ancient tectonic lineament formed due to the wrench movement after the Variscan orogeny (Ziegler at al, 1990). The shallower subsurface manifestation of this weakness zone is the Mid Netherlands fault zone that plays an important part of the structural forming of the West Netherlands Basin (Worum et al, 2005). The extensional movement along the fault zone has continuously influenced the basin and with its full effect started by middle Triassic when the Atlantic crust extension prograded into the southern North Sea area.

The possible target reservoirs in the Main Buntsandstein formation were deposited in the Early Triassic. They are overlying conformably the Lower Buntsandstein succession consisting mainly of small scale fining upwards succession ranging from fine to very fine-grained sandstones to siltstones and claystones (Geluk, 2005). The Main Buntsandstein sub-group, also known as Main Bunter in the southern parts of the basin, consists of coarser clastic sediments. The source of the sediments was the London Brabant Massif. Sediments were transported into the basin by low sinuosity braided river systems and mixed with aeolian and lacustrine deposits. The exact depositional patterns will be discussed in the chapter dedicated to depositional and diagenetic history of the lower Triassic sediments in the West Netherlands Basin.

A very important part of the development of the basin is the sequence of tectonic events in the area during the time of deposition of the Lower Triassic sediments and after they were already deposited and buried. As it was already mentioned the basin has experienced several stages of tectonic subsidence and uplift. During the time of deposition of the Main Buntsandstein sub-group the already existing structural features in earlier formations reaching down to the basement were reactivated (Jager, 2005*; Geluk, 2005*; Worum, 2005). A clear proof for this is the observed syn-depositional features in individual formations in the Main Buntsandstein sub-group. The differential subsidence continued further with increased intensity in the Middle Jurassic and Early Cretaceous, until Late Cretaceous when the stress field in the basin was gradually changed to compressional because of the Alpine inversion. The cause for that was the collision between Africa and Europe continents. This inversion makes the West Netherlands Basin a transtensional basin (Van Balen, 1999). The inversion of major stress directions led to reactivation of the already existing structural features with reversed direction. This can be observed best at major faults in the basin reaching deep towards the basement that show normal offsets at greater depths and reversed offsets at younger layers. As a result of the different influences the basin has developed a specific structural pattern. The basement oblique and predominantly dextral strike slip faults have caused and echelon pattern faults at shallower depths with pronounced popup and NW-SE trending flower structures. The resulting major fault pattern is anastomosing with dominant WNW-ESE to NNW-SSE direction in the southern part and predominantly NW-SE direction on the northern part of the basin (Worum, 2005). It appears that both trends have been simultaneously reactivated as none of them was perfectly aligned with the changing major stress directions and it is believed that only a few new faults were formed at Permian level in favour of reactivation of already existing faults. It is important to mention also that it is believed that the Pyrenean inversion did not result in reactivation of faults but rather took place as uniform uplift of the whole basin (Jager, 2005*). This assumption is based on the lack of evidence that the major basin faults continue into Early Tertiary deposits (Worum, 2005; De Jager, 2005*). All this resulted in the creation of elongated fault blocks with trends in NW-SE direction on Lower Triassic level and often tilted and juxtaposed with younger deposits (Van Balen, 1999).

The finer scale tectonic events are related to the regional unconformities separating the individual formations that constitute the Main Buntsandstein formation and will be discussed in the chapter about depositional environment.

These structural elements are important in order to understand the factors that influenced the diagenetic footprint of the targeted formations. Faults blocks with deposits from the Lower Triassic are believed to have been uplifted more than 1 kilometre up to 1.5 kilometres thus they have been buried to greater depth than

the ones we find them today at (Jager, 2005*). The exact amount of uplift in the West Netherlands Basin is required to determine the temperatures, pressures and fluids to which the targeted reservoirs have been in contact with. The greater temperatures they have been exposed to have led to facilitated precipitation of inter-granular cement in the available pore space. The pressures at greater depths are also higher leading to increased compaction and grain rearrangement that reduces the available pore space and fluid flow pathways affecting the permeability of the formations. The availability of overpressures and expected contact with different older or younger formations can give an insight into the nature of the formation fluids and that have passed through the reservoirs. The relatively easy passage of fluids can lead to dissolution of some cements and grains but also to the precipitation of new cements and grain overgrowths.

There are several methods known to be used to determine the burial history of given sediments. Some of them are vitrinite-reflectance (temperature history analysis based on organic matter maturity), fission-track (radiometric dating and provenance determination based on damage trails from fission fragments in uranium bearing minerals) and fluid-inclusion analysis (analysis of trapped liquids within crystals). Although they are accurate their validity is limited to the vicinity of the well whose core data was examined. In order to get a more basin wide idea of the burial history balanced reconstructions of basin cross-sections are required either in 2D or 3D. In this report the results of the palinspastic reconstructions of several 2D seismic lines across the West Netherlands Basin are presented and the results are discussed.

3.2. Palinspastic reconstructions of 2D seismic lines across the West Netherlands Basin on several studied time levels – problems & approach

The initial analysis is carried out on ordinary paper sections with the main purpose to test the already known information from the geological development of the basin and to get a better idea of the structural features such as faults that can be observed on the available seismic with sufficient confidence. After the completion of this stage the basic expectations for this restoration exercise are established and the approach is set for the following detailed digital reconstruction. It is chosen to restore of the basin on four time steps during the inversion period in Cretaceous and Tertiary epochs. The three 2D seismic in-lines to be used in the restorations are selected to be perpendicular to the major structural trend of the basin and to cover the centre of the basin as well as the sides with sufficient lateral coverage.

3.2.1. Purpose of study and objectives

The ultimate purpose of this restoration exercise is to establish a database of the variations in burial depth of the Triassic Bunter sandstones in geologic time and recover the maximum achieved depth for the deeper fault blocks. Additional objectives include creating contour maps of the depths of the fault blocks in different geologic times, calculating the amount inverted extension and subsequently calculating the β-factor. This information can be used after that for tracing the complete development of the Triassic Bunter sandstones and correlate this information to the diagenetic processes and available trends for permeability and porosity from petrophysical data.

3.2.2. Proposed process and workflow for restorations

The proposed restoration attempt was proposed to be carried out using the software package 2DMove, part of the Move 2010.1 program issued by Midland Valley Exploration Ltd on reinterpreted seismic in-lines 993 from survey Z3AMC1989A (referred as inline993), in-line 1778 from survey Z3NAM1990D (referred as inline1778), and in-line 1299 from survey L3NAM1991A (referred as inline1229). The initial reconstruction on paper was performed on a 2D seismic line 142 from survey Z2NAM1983A. The coordinates of the sections were translated to RD coordinate system so that each point on the sections can be traced with x and y coordinates and used later in other geologic software (Figure 46).

Figure 47: Geographic position of restored digital seismic sections with Google Earth map as underlay. Coordinates are given in RD coordinate system.

The workflow was designed as follows:

- The paper seismic line was interpreted and inspected for geologic time lines where it would be best to proceed with restoration. The logic behind the choices was agreed to be that the restoration should recover the eroded missing material and it should restore the uplift caused by the inversion. The experiments with the paper sections lead to the following decisions for the restoration workflow.
- It was chosen to carry out the reconstruction on five different steps – four major unconformities that have eroded significant amounts of sediments and that are easily distinguishable on seismic – end of Tertiary, end of Chalk group, end of Holland Marl group, end of Lower Cretaceous. The last one was designed to include erosion at the end of the previous period – end Upper Jurassic. The final paper reconstruction was carried out on Posidonia shale level and was used only to confirm the concepts applied to the other reconstructions.
- The restoration process focuses on reconstructing the original dimensions of the target group using the assumption that the top unconformity has been relatively flat at the start of deposition of the new period, and the base has been deformed to reflect for the tectonic changes that occurred in the recovered period. This implies that each formation or group of formations is defined by its top and its base. The four groups are as follows: Tertiary with Tertiary/Quaternary unconformity as top and with Base Tertiary as reconstruction base, Chalk group with Base Tertiary as top and with Top Texel Marl as base, Holland Marl group with flattened Top Texel Marl as top and with Base Holland Marl as base, Lower Cretaceous with flattened Base Holland Marl as top and with Base Rijswijk unconformity as base. The last period also includes recovery of eroded material from Delft unconformity, Pijnacker unconformity and Schieland unconformity.
- The processes that are going to be used for the restorations are Unfold with Simple Shear and Flextural Slip algorithms.
- It will be attempted to decompact the formation groups using estimated initial porosity and expected reduction. The available decompaction algorithm in the software did not deliver satisfactory results in the initial attempts.

An important observation regarding the chosen workflow is that each formation is defined best by a flat top, usually an unconformity, and deformed base, also usually an unconformity. Initially it was assumed that the restored base of the younger formation or group can be used directly as a top to the older formation or group. However this implies that the tectonic influence accountable for the eroded material on the top of the younger formation and reflected by the shape of the younger formation target base is included twice. The second time is the influence it has on the predicted depth of the restored older formation. Therefore each formation or group is defined by individually defined top and base only related but not completely equal to the boundaries of the overlying and underlying formations.

3.2.3 Assumptions and limitations of processes and software

A number of assumptions are made in order to achieve acceptable results from the restorations. First of all the initial attempt to restore the basin was carried out on the section while the faults and horizons were interpreted as closely as possible to their real seismic reflection. This realistic model combined with the fact that most of the movement along the faults in the basin has been oblique turned out to be a big challenge for the restoration software and the result were not satisfactory. It was decided to simplify the model with the main focus on straightening and preserving only the faults with significant offset to define the major fault blocks. The following graph (Figure 47) show how the original complete and the updated simplified section compare for the case of section Z3NAM1990D in-line1778.

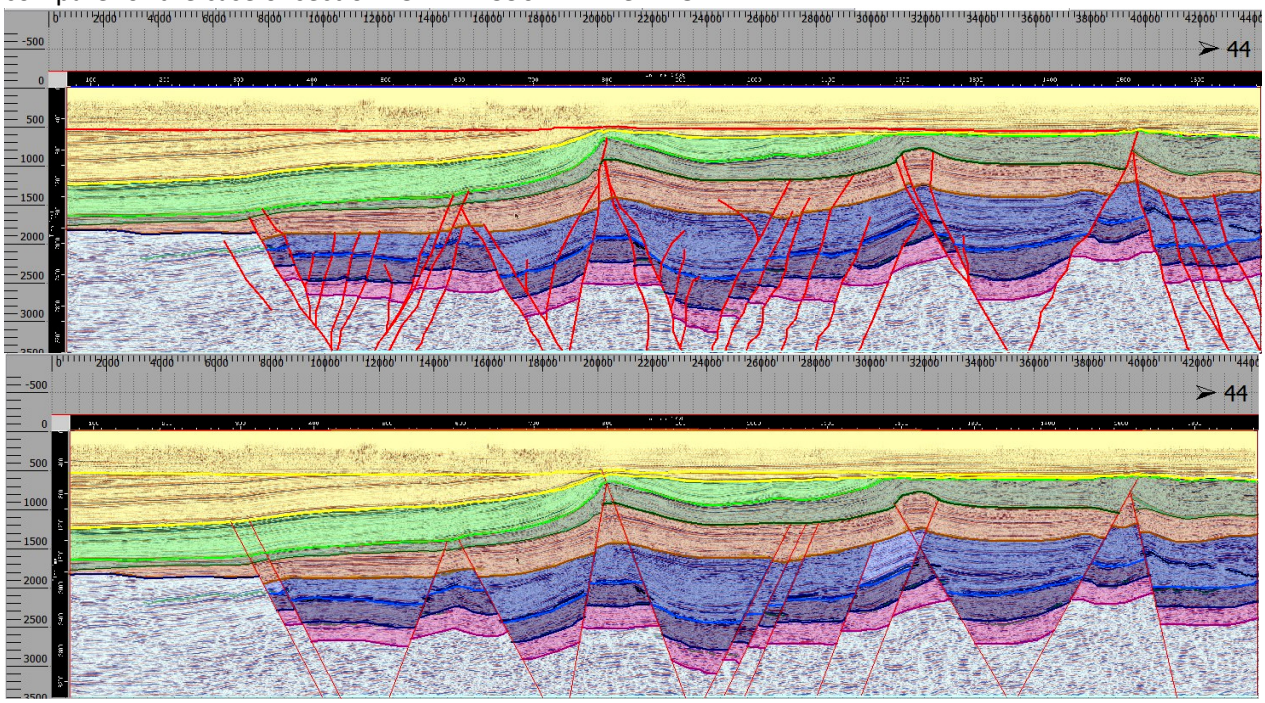

Figure 48: Comparison between complete and simplified interpretation of inline 1778 in time.

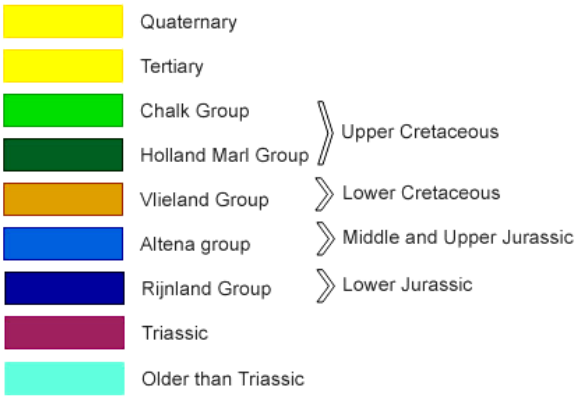

Figure 49: Color codes used in all graphics

This is the colour code for all the polygons as used in the graphics shown in this document.
In general the horizons show slightly darker shade of the colour assigned to the formation or group. Also target horizons for top and bottom of a given formation are a shade darker than the colours used for the horizon interpretations.
Horizons that represent the expected continuation of missing layers under the unconformities at the tops of given formation are given is darker shade of the same colour.

An additional requirement to the simplified model is that the restoration process can only be executed in small step taking a single fault block at a time. This is the only

way that can preserve the realistic position of the faults not artificially influenced by the restoration movements of the fault blocks. On several occasions it is also possible to apply a single operation to a couple of fault blocks at the same time but this is only limited to restorations of formations or groups where the amount of erosion on the base is very limited, for instance Base Holland Marl. This approach was chosen after the restoration was attempted initially taking multiple fault blocks at the same time. In that case the faults were not correctly honoured by the software and their position was not correct.

Another important assumption is related to the recovery of eroded missing sediments is that layers that are cut off by an unconformity can be used as a guide to the original shape of the sediment package. Several of those imaginary continuations of missing tops have been made in each section and used to construct the target tops ad bases (Figure 50). In Table 2 in Appendix I all the measurements of minimal visible, reconstructed maximal using visual lines and averaged optimal value for the layer thickness for each inline can be found. The shape of these imaginary horizons is completely based on the visible trends in the seismic with the maximum one actually equal to the minimum visible trend. In this manner the maximum line is actually a conservative choice that is not exceeding the data that can be derived directly from the available seismic. It is possible that there is more missing material but as there are not reliable indications for that it is not taken into account.

As a result of this assumption the restoration is carried out as two separate scenarios. The first is called "Minimal" and represents the case of the maximal preserved vertical thickness, usually in the left stable side of the sections that was not affected by the rifting or inversion stages. The second is called "Optimal" and uses the already explained concept that visible layer trends and shapes can be continued over the eroded parts as imaginary tops.

Horizon	Colour	Velocity	k Value
SeaBed		0	0
MidCenozoic		1821	0.5
BaseTertiary		1821	0.5
TopTexelMarl		2349	0.5
BaseHollandMarl		2082	0.5
BaseCretaceous-Rijswijk		3100	0.5
PosidoniaShale		3556	0.5
TopTriassic		3490	0.5
BaseTriassic		4826	0.5
Older		4781	0.5

Figure 50: Velocity model used, velocity given in m/s.

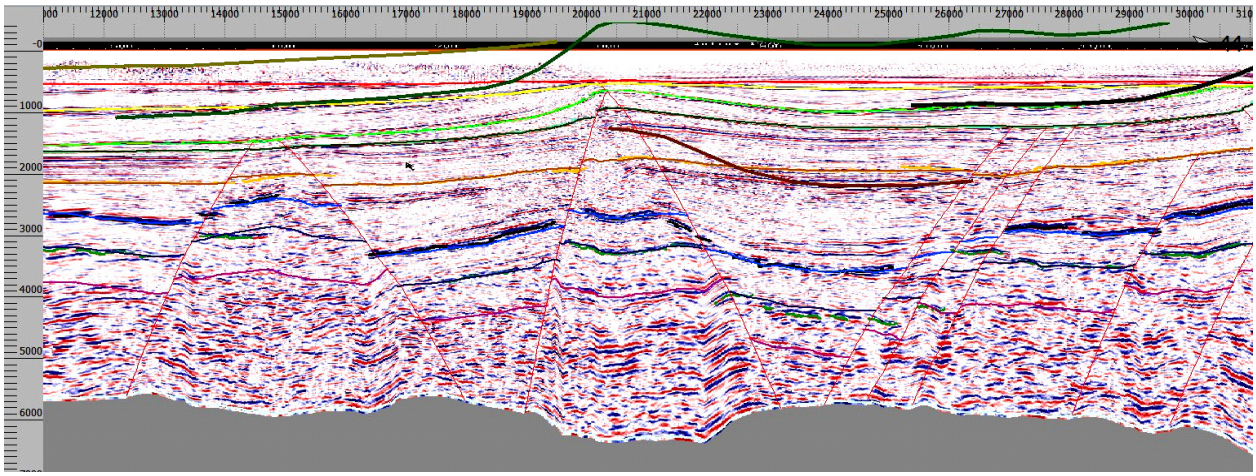

Figure 51: Imaginary missing tops in section inline1299. Note dark grass green above red horizon for base North Sea super-group, the dark green horizon rising above the yellow Base Tertiary, and the dark red horizon representing an unconformity below Base Rijswijk.

The seismic sections are interpreted in time. In order to determine the variations in burial depth the reconstructions have to be carried out in the depth domain. Therefore, after the completion of the interpretation and after the model is populated with the corresponding polygons representing the formation fault blocks it is converted to depth using the velocity model available (Figure 49). This should also be considered as possible source for very large inaccuracies as the restoration software is not full featured seismic interpretation software. (Figure 51)

The processes used in the restorations are chosen and adjusted to fit each separate fault block. This is a source of significant slowdown regarding the restoration workflow. Unfortunately it is inevitable to be avoided due to the oblique movements of the fault blocks making it not only difficult to interpret the correct movement but also requiring individual approach to each fault block in each separate time period. Other indications for the importance of this assumption are the differences between the tectonic processes that were active. The result that proves that this assumption works well is the beta- stretching factor graphs for both scenarios indicating back the nature of the reconstructed tectonic events.

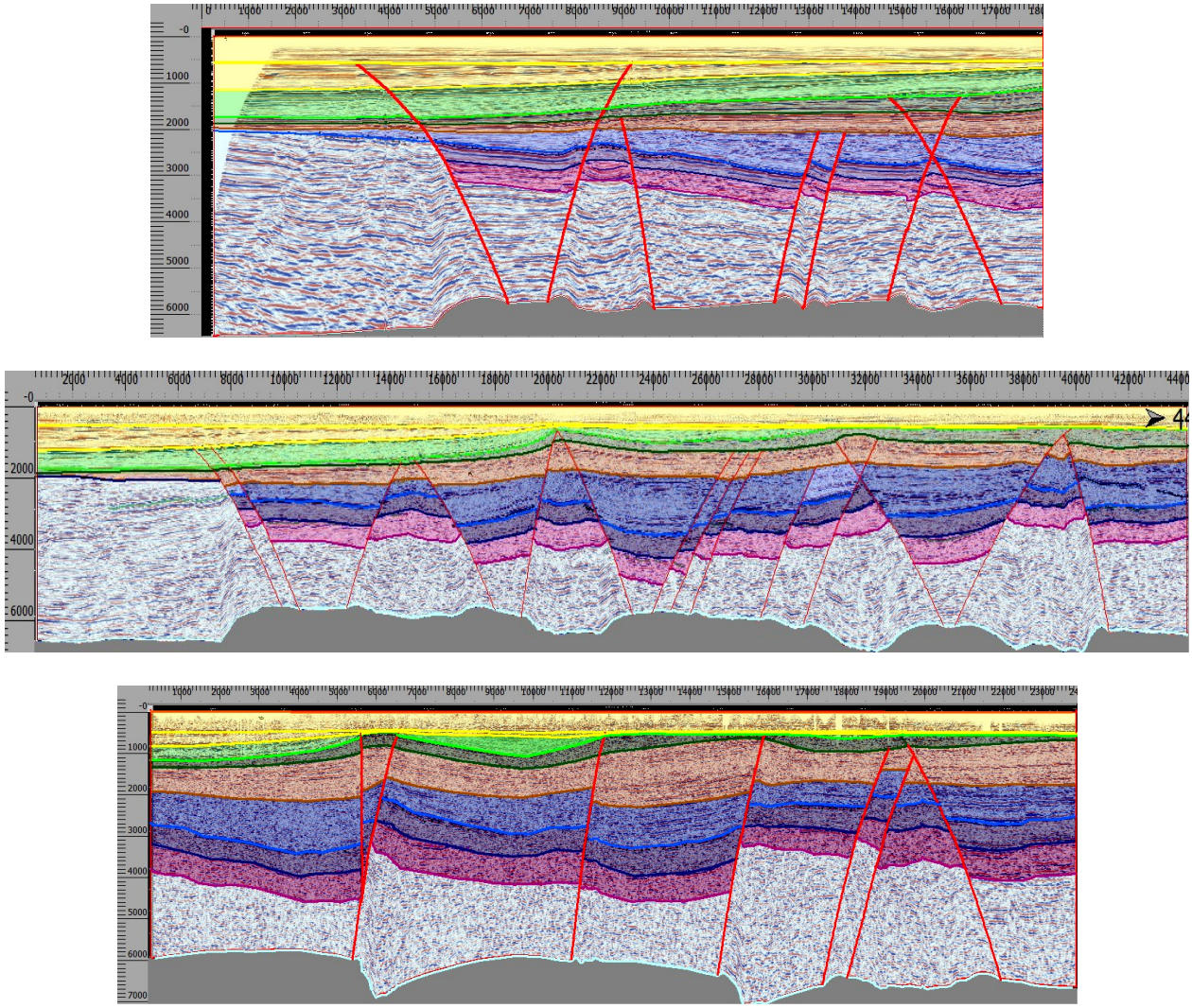

Figure 52: Final depth models for Inline 993 (above) – total length 23.6 km, Inline 1778 (middle) – total length 43.6 km, Inline 1299 (below) – total length 23.6 km

3.3. Results

This chapter will present the results from the restoration first as the direct graphic products of the restoration procedure, and then as the exact measured depths of Top Bunter including graphic analysis of the collected data and differences between scenarios.

3.3.1. Used processes in 2DMove

The process used for the restoration is Unfold with Simple Shear and Flextural Slip algorithms. The dip angles used in the Simple shear and pins for Flextural slip are chosen for each individual restored fault block. During the restoration several general trends emerged regarding where is certain algorithm more successful including trends also in the dominant shear angle directions applied. The table with the entire restoration track can be found in Appendix I, Table 1.

- Simple Shear was the dominant algorithm for the Base Tertiary, Top Texel Marl and Base Holland Marl as base targets.
- Flextural Slip was applied only close to blocks that have still preserved the normal offset.
- Flextural Slip was the algorithm of choice in the restoration on Base Cretaceous target. This is probably related to the fact that during that period there was still active rifting thus the normal movement on the faults was dominant.
- Shear angles often showed shift across large offset faults.
- Relatively quiet tectonic periods such as the deposition of the Holland Marl group tend to be restored with shear angles close to 90 degrees, while periods of more active tectonic events such as the Subhercynian, Laramide and Pyrenean inversion phases require angles between 45 and 70 degrees with either positive or negative offset from the vertical.

3.3.2. Restorations – results from both scenarios

Below are the final results of the restoration for each Time level and each seismic section. The restoration procedure starts with designing the target base horizon for the specific inline and scenario. After the shape of the base, as it was at the end of the restored time period, is constructed and backed up by the available regional geologic data the top target is designed as well. In some cases the top horizon is directly the previous base target. This is acceptable, however, only in the first two target base horizons. The reason for this is that the basin underwent a uniform uplift during the final compressional phases. As a result the fault offsets are not dramatically influenced until the restoration above Base Cretaceous target.

The next step in the process, after the individual fault blocks have been properly reconstructed at their expected original positions for that time period, is to determine the relative amount of compaction to be recovered. Zero sea level is then set at the top of the already decompacted layer, while the above lying layers are removed. The final step is to measure and record the depth of the horizon of interest.

It is important to note that reflections of Top Triassic are relatively poor and places where reflections were missing has been interpreted using relatively constant thickness of the Lower Jurassic group. Base Triassic is interpreted only for representational purposes.

Minimal cases – Base Tertiary base: (the same for Optimal cases – Base Tertiary base)

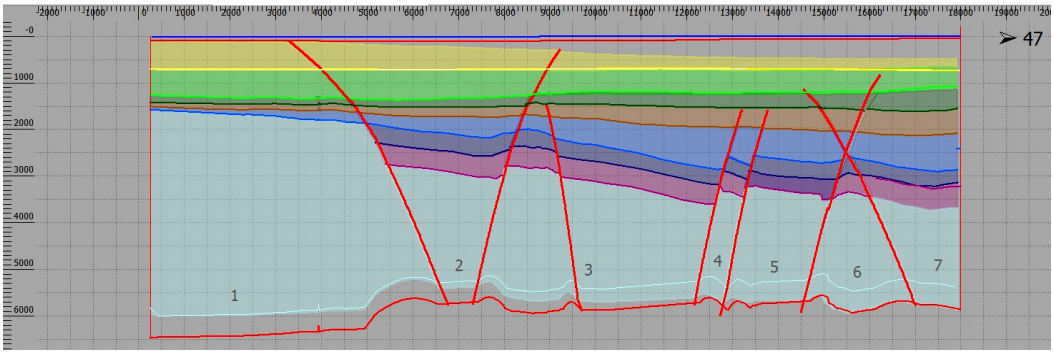

Figure 53: Inline 993, restoration on Base Tertiary level. Restored eroded and decompacted material is the transparent separation between Sea Bottom and the yellow horizon Base Tertiary. Note that the grid size is the same for all graphics ad is 500x500 meters

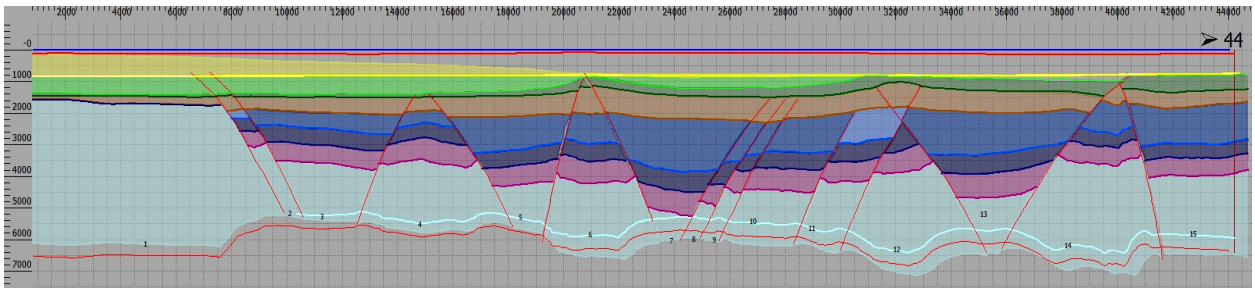

Figure 54: Inline 1778, restoration on Base Tertiary level. Restored eroded and decompacted material is the transparent separation between Sea Bottom and the yellow horizon Base Tertiary

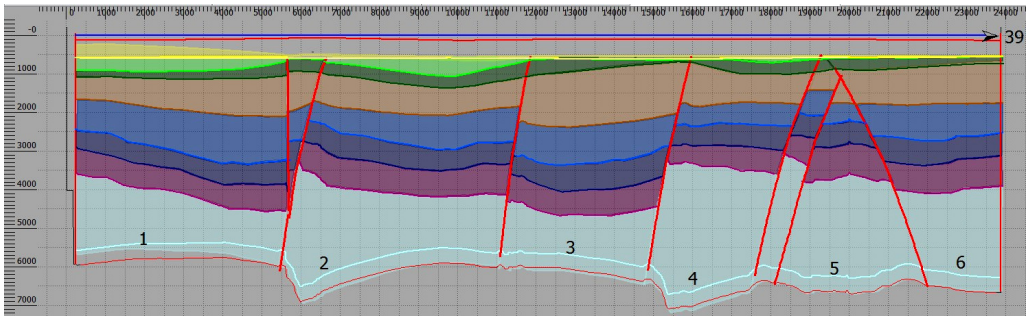

Figure 55: Inline 1299, restoration on Base Tertiary level. Restored eroded and decompacted material is the transparent separation between Sea Bottom and the yellow horizon Base Tertiary

The first restoration with Base Tertiary as target base (Figures 52, 53 and 54) is common for Minimal and Optimal scenarios. The reason for this is that there is no visual indication that the layers thicken towards the eroded central parts. Even though the layers have uniform thickness the amount of eroded material still exceeds the amount of removed material above. As a result the central parts of the section are pushed deeper beyond the current depth. This conclusion is only applicable in the centre of the basin presented in Inline1778.

The amount of added eroded material is visible in the transparent separation between the Sea Bottom horizon (usually blue or orange colour) and the top of the layer polygon representing the preserved sediments. This eroded material is also visible in some of the sections as the separation between the light blue base line and the bases of the light blue polygons. The separation between the bases of the light blue polygons and the red base line, which always represents the original current position of the bases of the light blue polygons and is kept constant, is the amount of gained or lost burial depth at that time period compared to now.

Minimal cases – Top Texel Marl base:

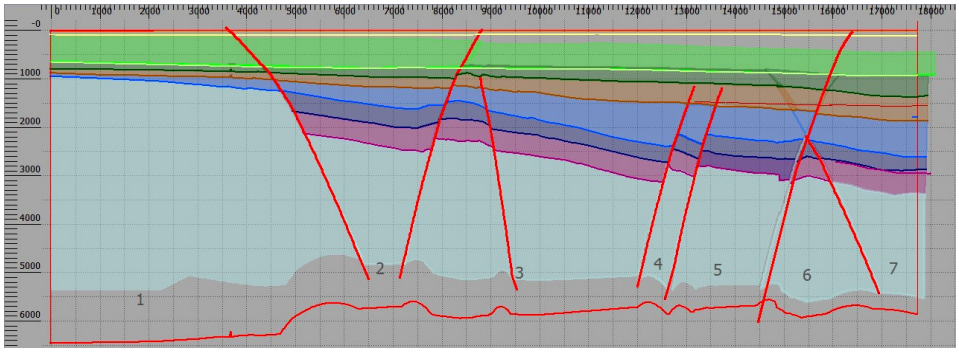

Figure 56: Inline 993, restoration on Top Texel Marl level

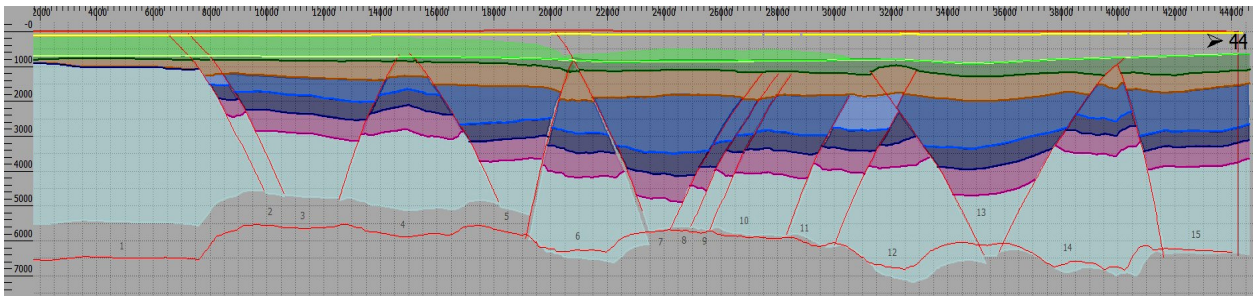

Figure 57: Inline 1788, restoration on Top Texel Marl level

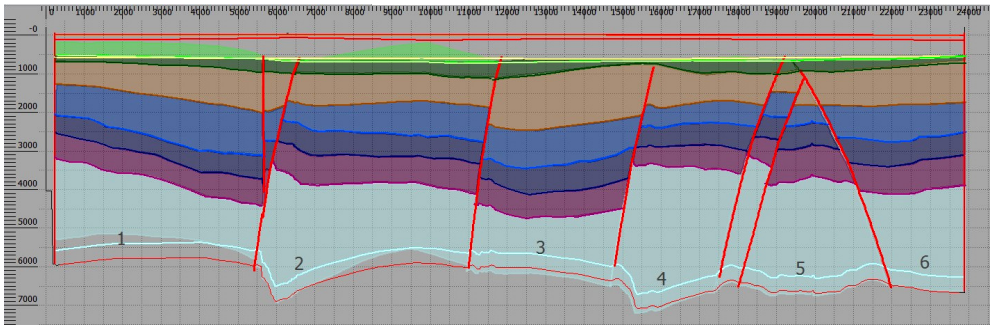

Figure 58: Inline 1299, restoration on Top Texel Marl level

In the restoration of the Top Texel Marl base (Figures 55, 56 and 57) target (Base Chalk) the first significant differences between minimal and optimal cases occur. The shape of the target horizon has only a gentle lens form, slightly thickening towards the centre of the basin. Although this approach can be described as the most conservative regarding the estimation of missing material, the sediments in the centre of the basin are still at deeper positions that the current ones.

Minimal cases – Base Holland Marl base:

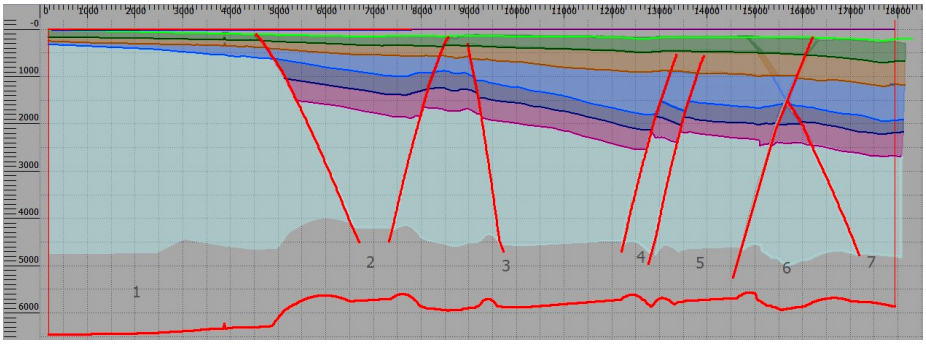

Figure 59: Inline 993, restoration on Base Holland Marl level

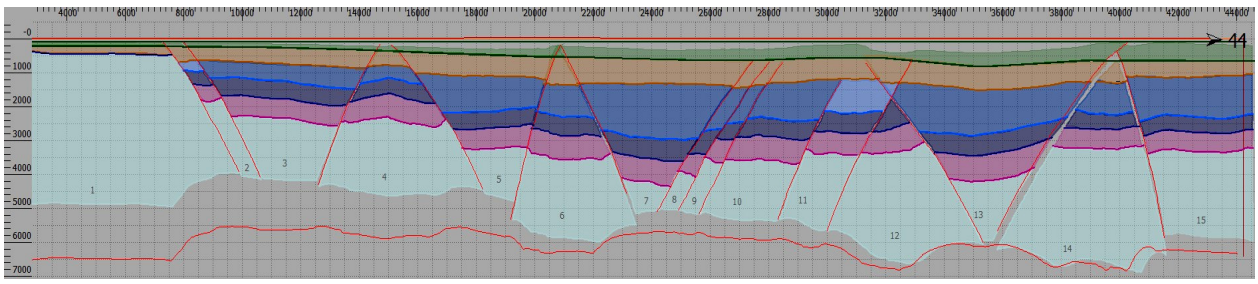

Figure 60: Inline 1788, restoration on Base Holland Marl level

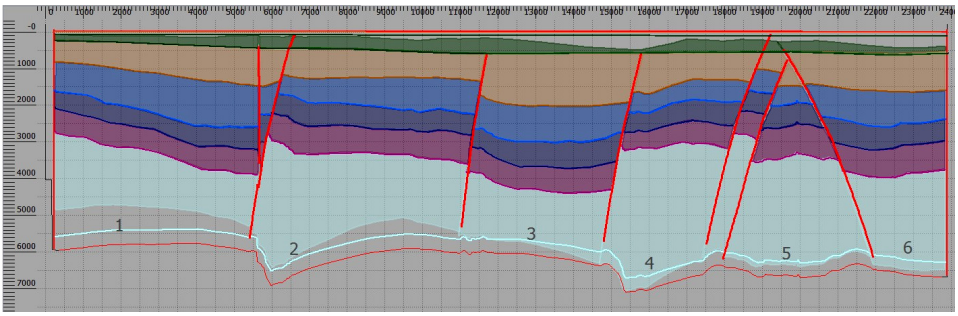

Figure 61: Inline 1299, restoration on Base Holland Marl level

The target for the Base Holland Marl restoration (Figure 58, 59 and 60) is also common for both scenario but the reconstruction was done separately as there were inherited differences from the previous step. In general this period is relatively tectonically quiet and there is not much erosion or subsidence.

Minimal cases – Base Cretaceous - Rijswijk base:

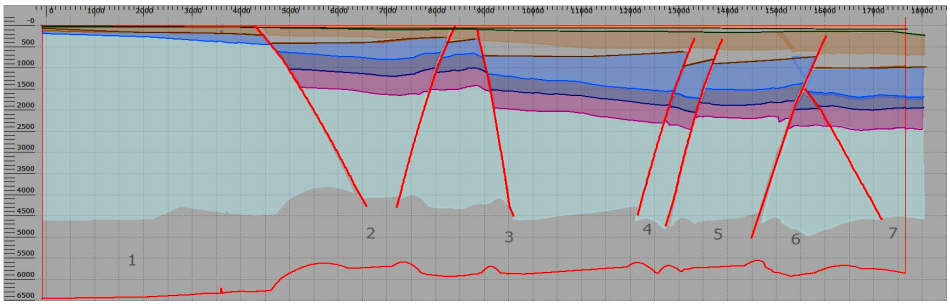

Figure 62: Inline 993, restoration on Base Cretaceous-Rijswijk level

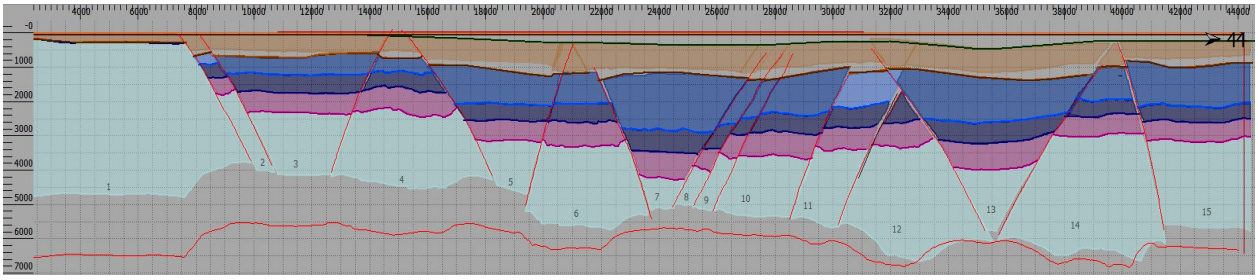
Figure 63: Inline 1778, restoration on Base Cretaceous-Rijswijk level

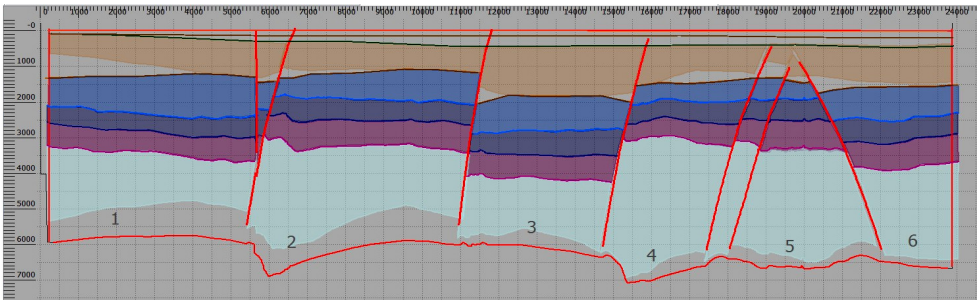

Figure 64: Inline 1299, restoration on Base Cretaceous-Rijswijk level

Base Cretaceous-Rijswijk restoration (Figures 61, 62 and 63) is an important step as it includes erosion in the Lower Cretaceous as well as in Upper Jurassic. Moreover during that period there had been still active differential subsidence in the basin. This effect is more actively applied to the optimal scenario.

In this final restoration step the fault blocks are eventually moved and rotated towards more horizontal positions reflecting the assumption that most of the fault blocks have endured differential subsidence at a certain angle and therefore they have also been differentially reactivated. This had led to the creation of the series of the angular unconformities around Base Cretaceous and Upper Jurassic. The restoration process brings the fault blocks closer to their pre-deformation state as normal fault blocks in an extensional setting.

Some minor space and material problems occur close to areas where major faults cross each other. Those can be recognised on restoration figures are places where restored blocks are detached from the local bounding faults or where edges of adjacent blocks are overlapping. These occurrences are probably result of the fact that the actual movement along the fault has been oblique and the true movement restoration can be only made in three dimensions.

Optimal cases – Base Tertiary base – see Minimal Case
Optimal cases – Top Texel Marl base:

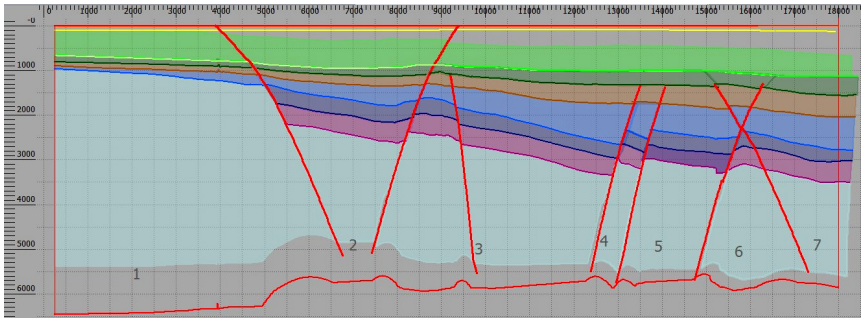

Figure 65: Inline 993, optimal restoration on Top Texel Marl level

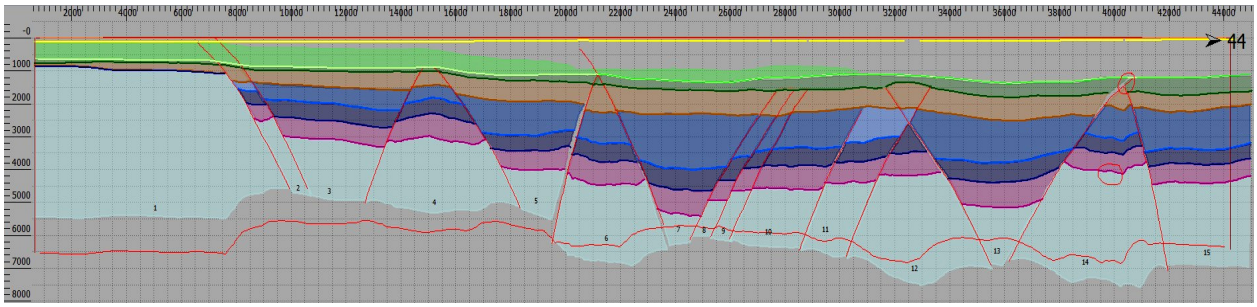

Figure 66: Inline 1788, optimal restoration on Top Texel Marl level

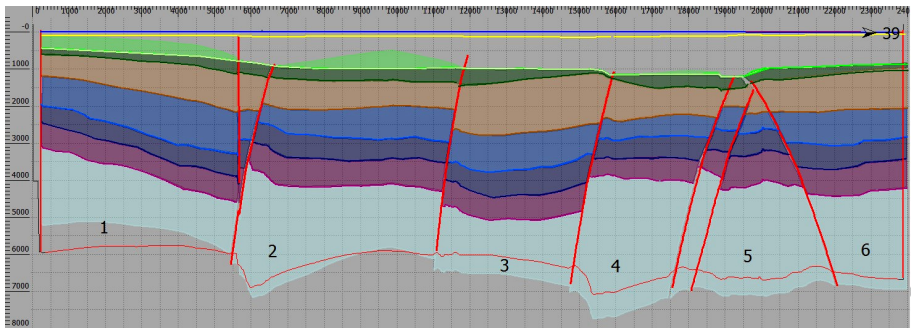

Figure 67: Inline 1299, optimal restoration on Top Texel Marl level

The restoration of Top Texel Marl as target base for the optimal restored thickness scenarios (Figures 64, 65 and 66) is the first step where the effect from the expected general thickening towards the centre of the basin shows its strong influence to the possible maximal burial depth of Bunter sandstones. Clearly the major part of the Triassic sediments in the basin has been buried deeper than the current level. This is represented by the overlap of the light blue polygons and the current level red base line.

The target itself has been design so that the basin is deepening towards the centre but the gain in depth is strongly related to the major faults in the area. The amount of extension is increased but is still limited due to the assumption that the basin is uniformly uplifted in the central parts with strong reactivation of faults.

Optimal cases – Base Holland Marl base:

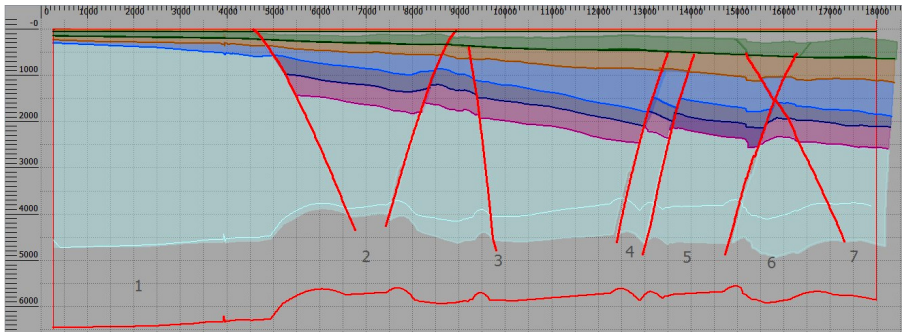

Figure 68: Inline 993, optimal restoration on Base Holland Marl level

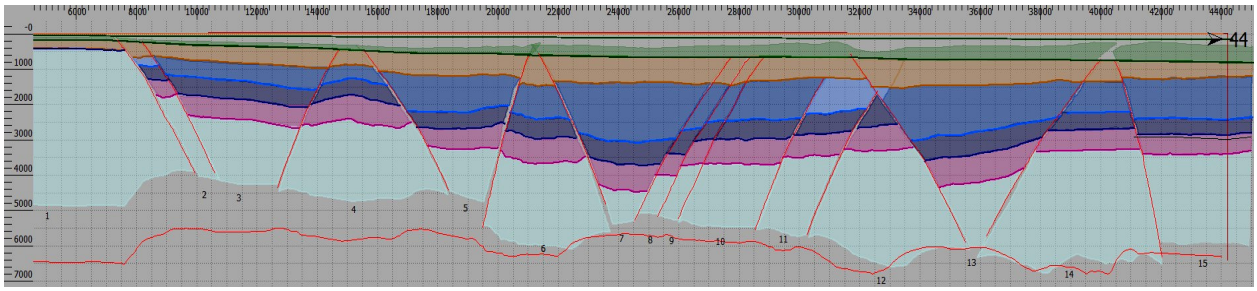

Figure 69: Inline 1788, optimal restoration on Base Holland Marl level

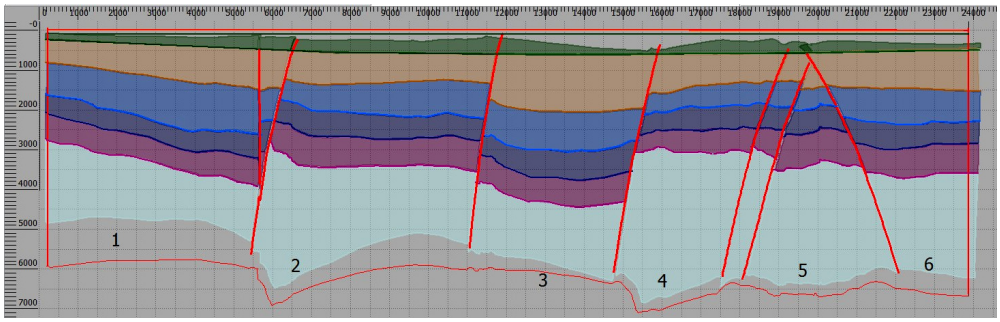

Figure 70: Inline 1299, optimal restoration on Base Holland Marl level

The restoration on Base Holland Marl base (Figures 67, 68 and 69) is similar to the minimal case with the exception that the effect from the added extension in the previous optimal restoration step is preserved.

Optimal cases – Base Cretaceous - Rijswijk base:

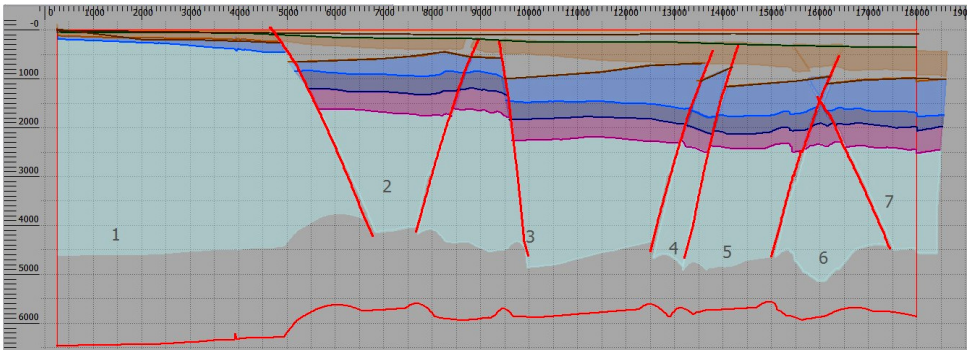

Figure 71: Inline 993, optimal restoration on Base Cretaceous-Rijswijk level

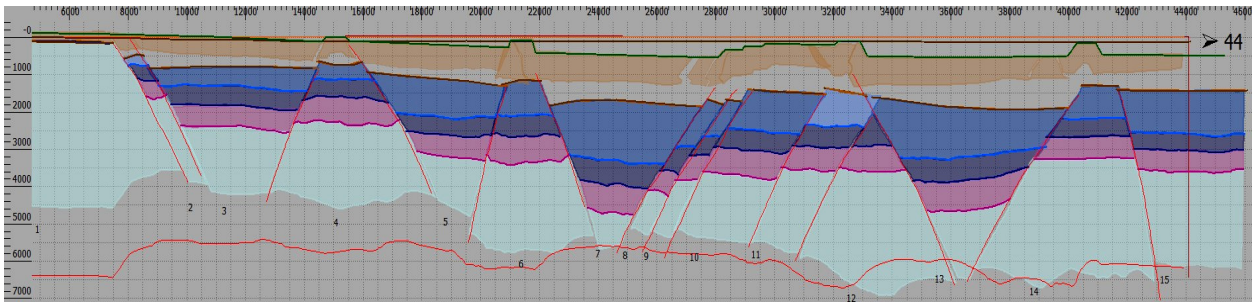

Figure 72: Inline 1778, optimal restoration on Base Cretaceous-Rijswijk level

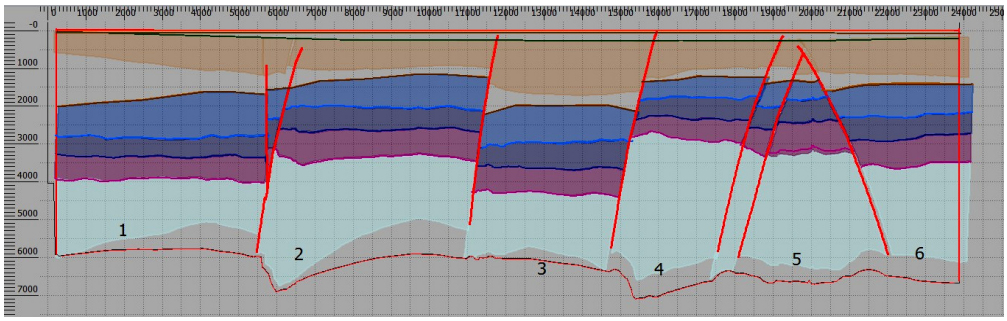

Figure 73: Inline 1299, optimal restoration on Base Cretaceous-Rijswijk level

The final restoration on Base Cretaceous-Rijswijk level (Figures 70, 71 and 72) again includes effects of erosion in both Lower Cretaceous and Upper Jurassic level, and takes into account that there was active subsidence during that period. The effect from the still ongoing rifting and differential subsidence in the initial stages of the period is best visible in the varying separation in individual fault blocks and the large amount of lateral extension gain.

Fault blocks are restored closer to their original shapes and dips as normal fault blocks from the previous rifting periods. Horizons and polygon boundaries have been gradually restored in each restoration step to their original non-deformed flat shapes which is the source for large parts of the additional extension gain.

3.3.3. Measured depths of Top Bunter at different restored ages

The depths of Top Triassic are measured and then a uniform depth of 242m is added to calculate the depth of Top Bunter subgroup. The measurements are made every 500m. The complete data for each scenario,

section and time period is presented in Appendix I, Table 3. Please refer also to the graphical visualization of the depth data that can be found under the tables – Figures 1 to 6, Appendix I.

The following graphs represent the summary of the depth measurement and serve as a guide to understanding the development of the burial depth of Bunter sandstones. The measurements are averaged depth over three fault blocks in Inline1778 that were originally subsided and then uplifted. Please bear in mind while reviewing these graphs that the actual depth can vary up to -200 meters due to differences in the complexity of the velocity model used for the Time to Depth conversion. This effect is increasing towards NE thus only Blocks 7 and 13 are affected.

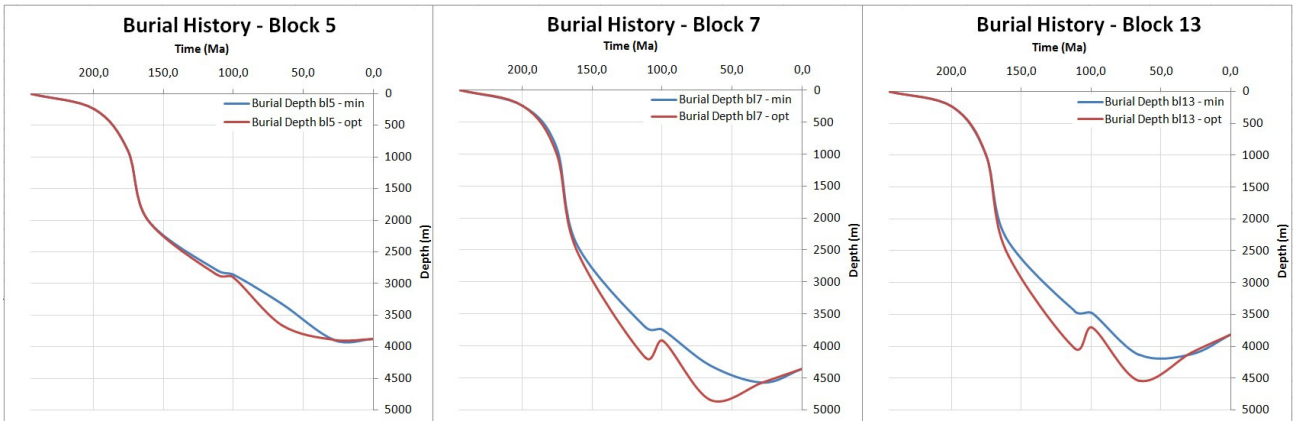

Figure 74: Burial depth history of three fault blocks (5, 7 and 13) at three different positions in section Inline1778.

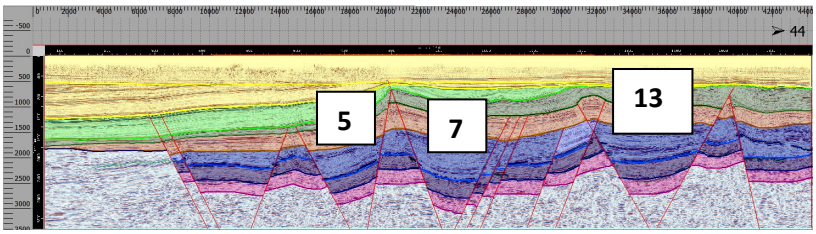

Block 5 is close to the SW more stable part of the basin, while Block 7 is in the centre of the basin, and Block 13 is slightly to the NE from the centre.

The maximum depth that was reached by Block 7 is close to 4880 m and is the largest depth that Bunter sandstones have been according to this restoration. Bunter sandstones have not been to depth exceeding the current burial depth by more than 700 m. However the sandstones have been buried to a depth of 4000 m and more 120 million years ago and have not been uplifted above this depth regardless of the inversion of the basin.

3.3.4. Contour maps of depths of Top Bunter

The following maps are based on the restoration results and should not be considered as representative for the current depth of Top Bunter Horizon. The most important aspect of the restoration is that it gives a basic idea for the development of the basin and the results are well representative for the dominating processes. This is further discussed and explained in Chapter 3.4.2.

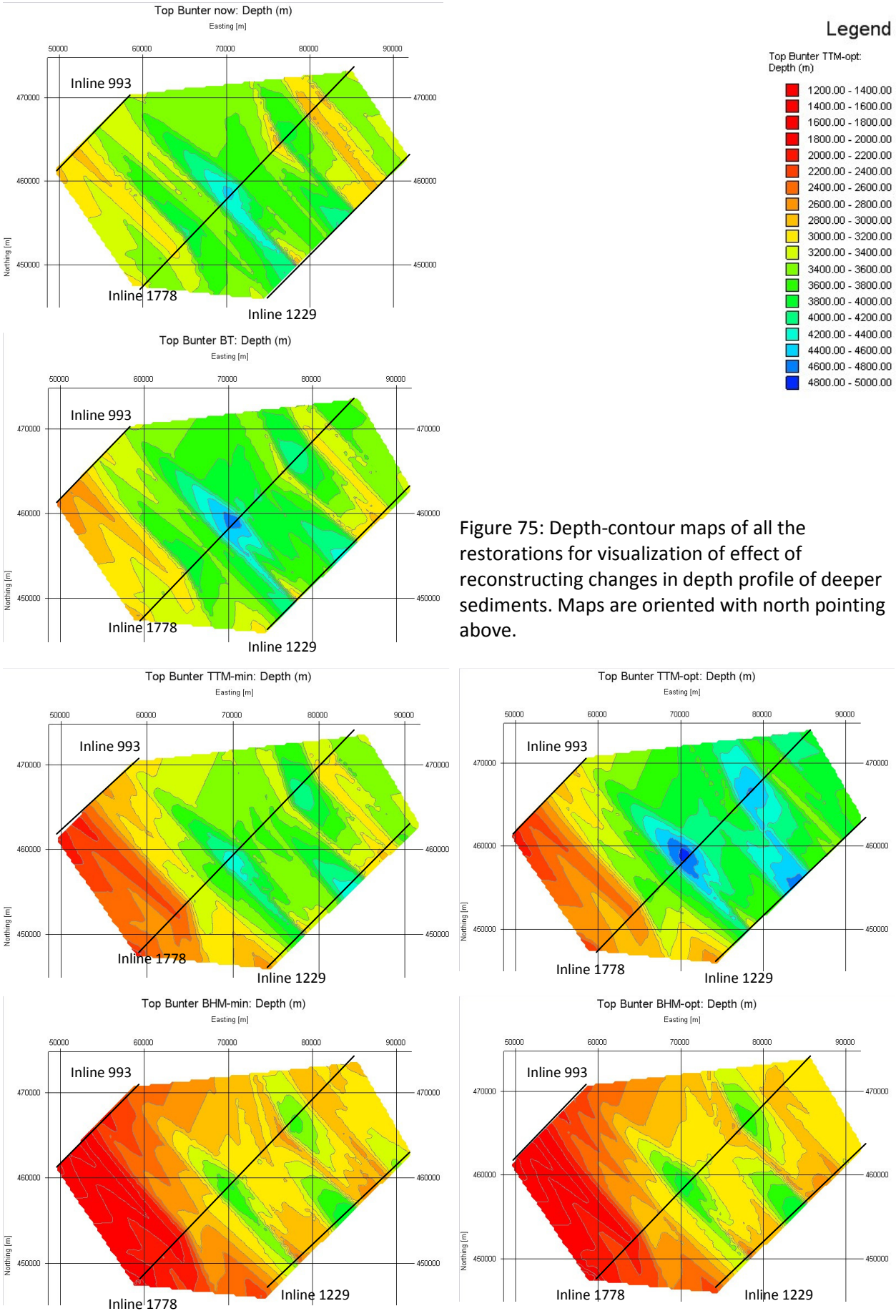

Figure 75: Depth-contour maps of all the restorations for visualization of effect of reconstructing changes in depth profile of deeper sediments. Maps are oriented with north pointing above.

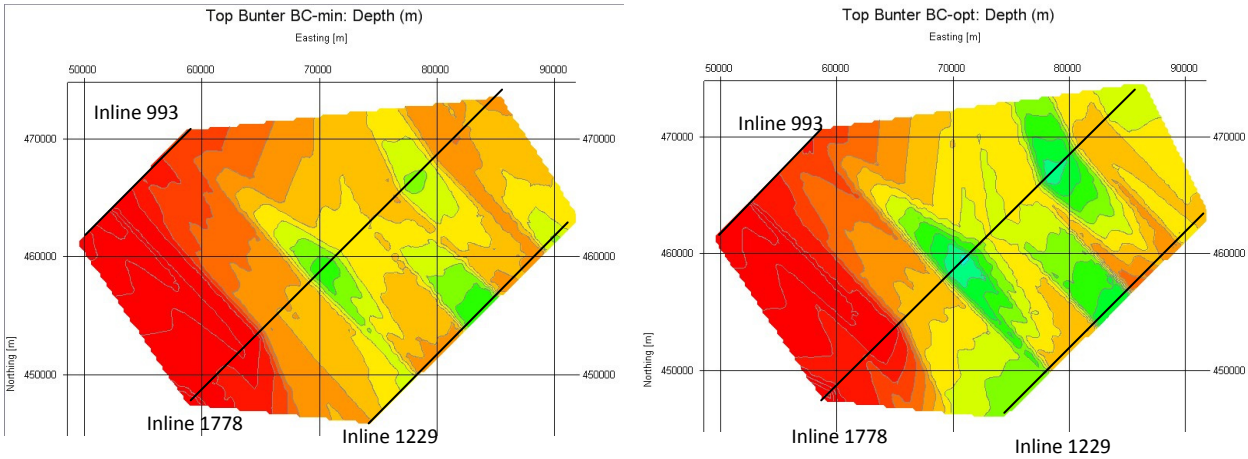

3.3.5. Recovered compaction, recovered extension and β-factor

The percentage assumed and recovered compaction is given in the list below. The complete table with applied compaction data can be found in Appendix I, Table 6.

- Tertiary – 13%
- Chalk – 20%
- Holland Marl – 25%
- Lower Cretaceous – 25%

The complete record for the reconstructed extension and calculated volume of restored eroded material can be found in Appendix I, Table 4. Figure 75 is an example with indications what is considered restored eroded material - given as red area polygon, and extension - given as a red arrow on the graphic.

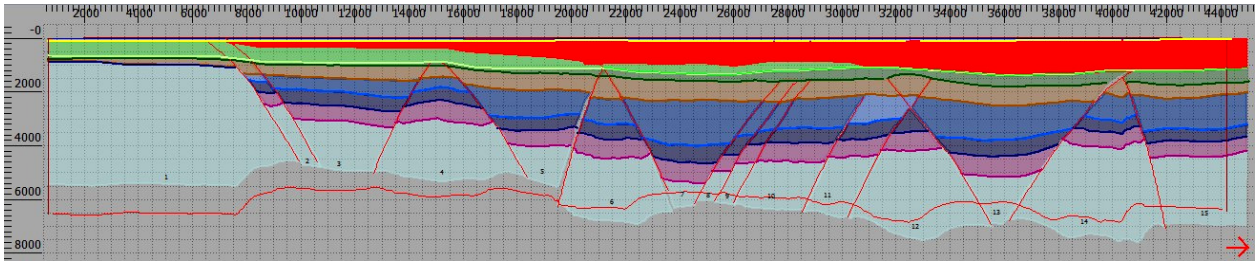

Figure 76: Example of eroded material (red area) and lateral extension (red arrow)

A commonly accepted tool for evaluating the severity of the influence of a tectonic process is the stretching beta factor. The following graphs (Figure 76) show the beta factors for the optimal and minimal cases for all three in-lines. The most important one to be considered is Inline1778 – given as slightly thicker and darker line. The reason is that it includes the stable south west side of the basin as well as the tectonically active centre of the basin.

The boundary values of 1.03 – minimal and 1.05 – optimal cases are representative for the slight extension during the Quaternary. The lower boundary values of 1.08 – minimal and 1.10 –optimal cases are representative for the rifting phase active in the most part of Early Mesozoic. The values are derived from a measurement of the additional extension gain from further restoring the seismic sections on Posidonia shale level beta factor 1.086 and other available regional data dependant on the position and ranging from 1.40 in the triple junction in the North Sea to 1.10 in more distral basins (Hendrie et al.) These graphs can be used to compare with the already existing geological history of the basin and also analyse the differences between different parts of the basin.

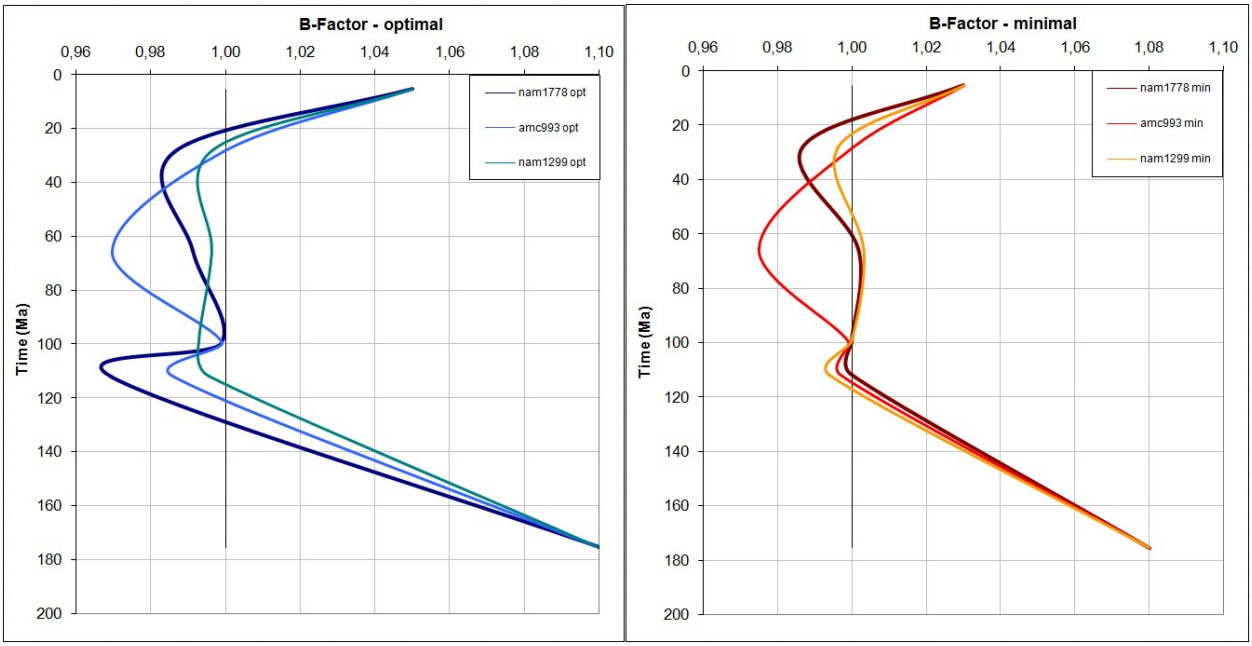

Figure 77: β-factor for Optimal case (left) and Minimal case (right)

3.4. Explanation of results and discussion

From the results of the restorations several conclusions can be drawn.

- Inline 993 from survey Z3AMC1898A covers the southern edge of the basin where it is clear that the effect of the rifting and subsequently the inversion becomes stronger towards the north.
- Similar pattern emerges from the analysis of Inline 1778 from survey Z3NAM1990D. This restored inline contains the centre of the basin as well and it is visible that it has been subject to most of the tectonic influences. Some of the blocks in the centre of the basin (Block 13) have been exposed to 960 m greater paleo burial depth than the current one.
- Inline 1299 from survey L3NAM1991A covers the region further from the northern part of the basin centre. The amount of compensated uplift there becomes less accurate due to increased uncertainty regarding the amount of eroded material. The maximum difference between the paleo burial depth and current depth of blocks corresponding to Block 13 from inline 1778 is 700 m.
- The best way to relate the influence of the greater burial depth to current rock properties of the target formations is to compare trend map.

3.4.1. Tracing the development of Bunter sandstones and possible diagenetic effects from middle Jurassic to end of Tertiary

This topic is further discussed in Chapter 4 – Diagenetic history of Main Buntsandstein formations of this work.

3.4.2. Effects of maximal burial depths of Bunter sandstones at given ages

The maximal burial depth achieved by Top Bunter is at 4880 (4680) m (- 200 m from Time-to-Depth conversion inaccuracies) in Block 7 of Inline1778. However that block is relatively at great depth from End of Lower Jurassic and thus it is better to compare the blocks for the largest difference between the maximum achieved burial depth and current depth. The following graph (Figure 77) gives the largest depth difference between a restored time and current depth.

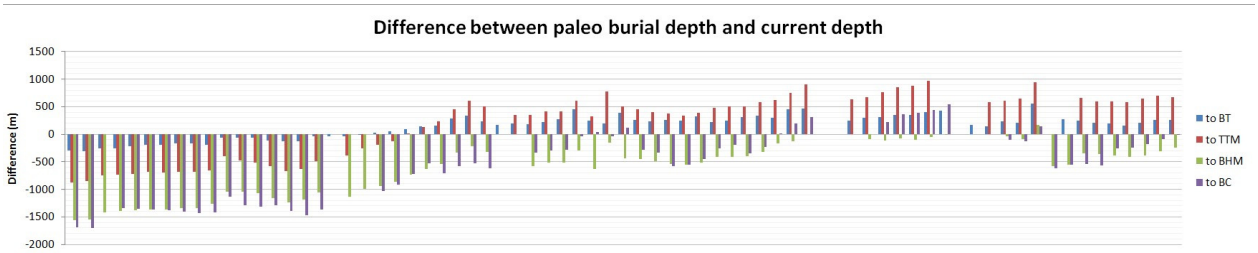

Figure 78: Differences between paleo burial depth and current depth along Inline1778. Left side is SW.

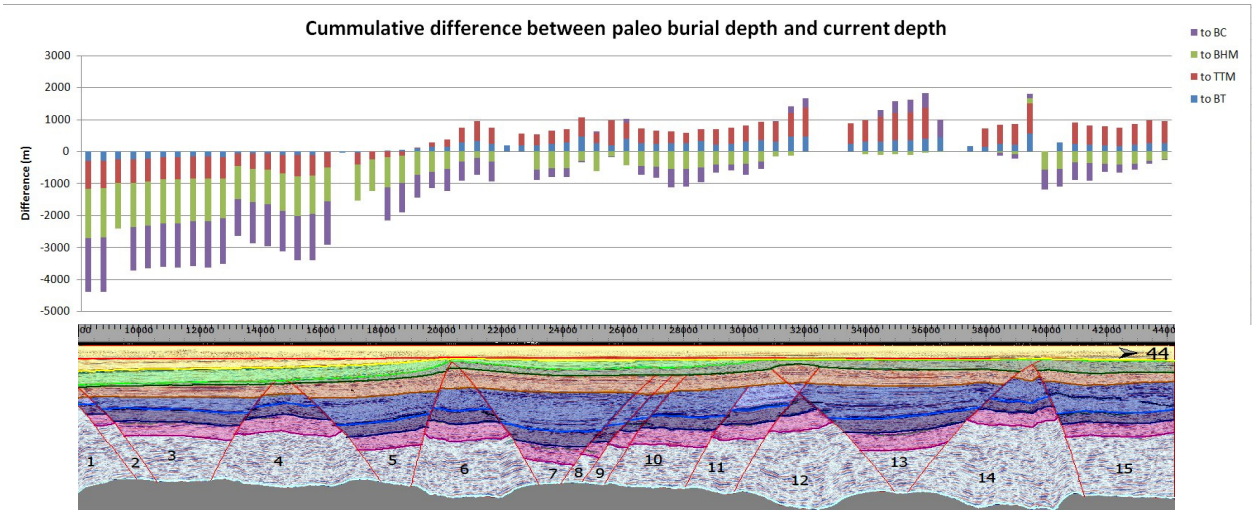

Figure 79: Combined effect of differences between paleo burial depth and current depth along Inline 1778.

From the graphs (Figure 77 and 78) it becomes visible which parts of the inline have been continuously at greater depth. This data can be used to evaluate which blocks are expected to show more influence of the deeper burial such as increased exposure to higher temperatures and subsequent amplified dissolution of minerals and re-precipitations in available pore spaces.
Using this way of representing the differences the cumulative effect of the deeper burial can be evaluated in more general terms. Deviations in the burial of different faults blocks can be summed up and represented as a fraction of the highest number. The resulting fraction varying from 0 to 1 can represent the different burial influence.

3.4.3. Trends based on burial depths maps and comparison with permeability and porosity trends maps

It was shown that there is a clear difference between different fault blocks and different positions in the study area regarding the amount of change in burial depth in geological time. The next step in utilizing this data is by creating a cumulative trend map of the amount of change and compares it with other available trend data. The graph below (Figure 79) shows an example of cumulative evaluation of the effect seen in the palinspastic restorations. Several different trends can be observed – general trend with increased influence in the centre of the basin, and finer scaled trend within every individual fault block due to the tilting.

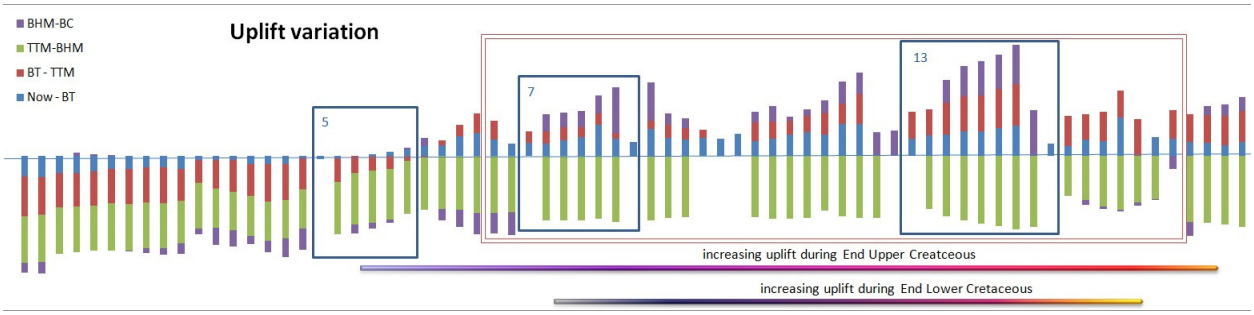

Figure 80: Qualitative evaluation of cumulative effect of variations between the different restoration steps along Inline 1778 – Optimal scenario. Left side is SW. Area of largest influence is enclosed in double red line. Position of analyzed blocks is given enclosed in blue line.

The resulting trend map is shown below (Figure 80).

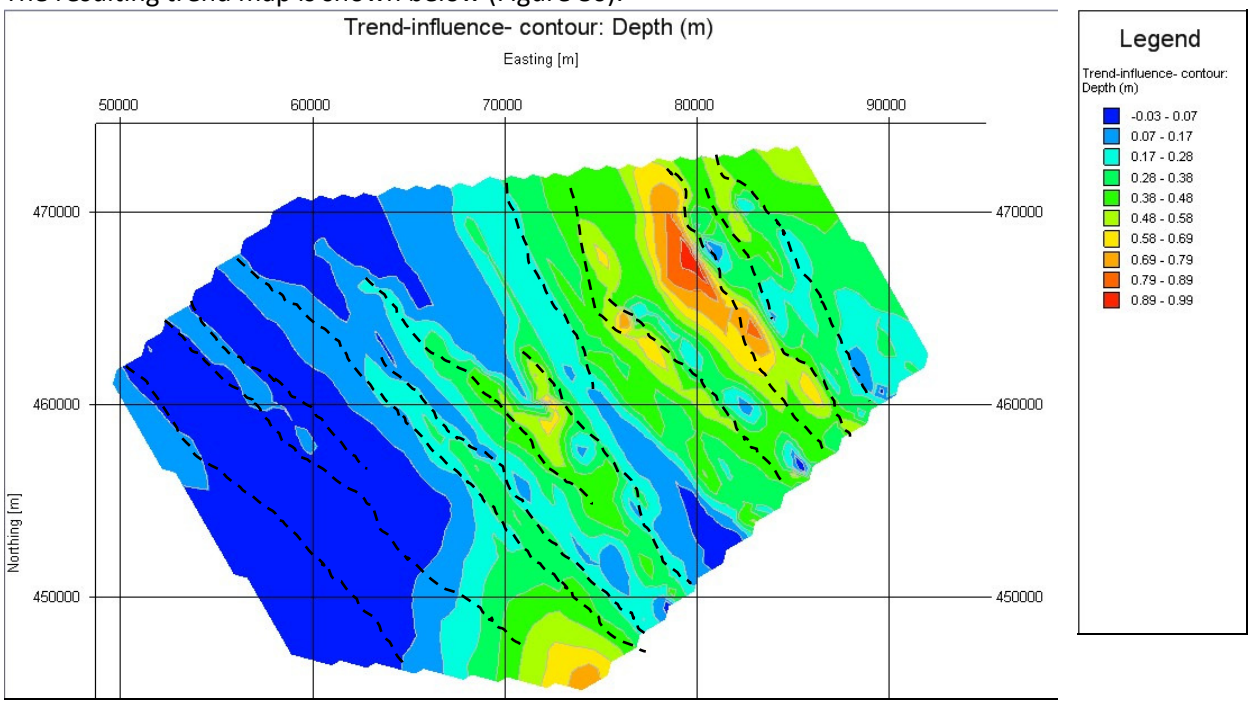

Figure 81: Trend map of area between studied sections - Optimal. Red represents most strong expected effect from greater burial depth, whereas blue represents the weakest. Interpolation between data points done with Distance Weighting with power 0.30 and 5000 points trend analysis using Jewell suite software 2D Gridding algorithm. Major faults are given schematically. 1 indicates maximum expected effect and 0 no influence.

This contour map also clearly depicts the general conclusion that influence from greater burial depth is guided by the fault blocks and it follows the general NW trend of the field as well as that there is also trends within major fault blocks.

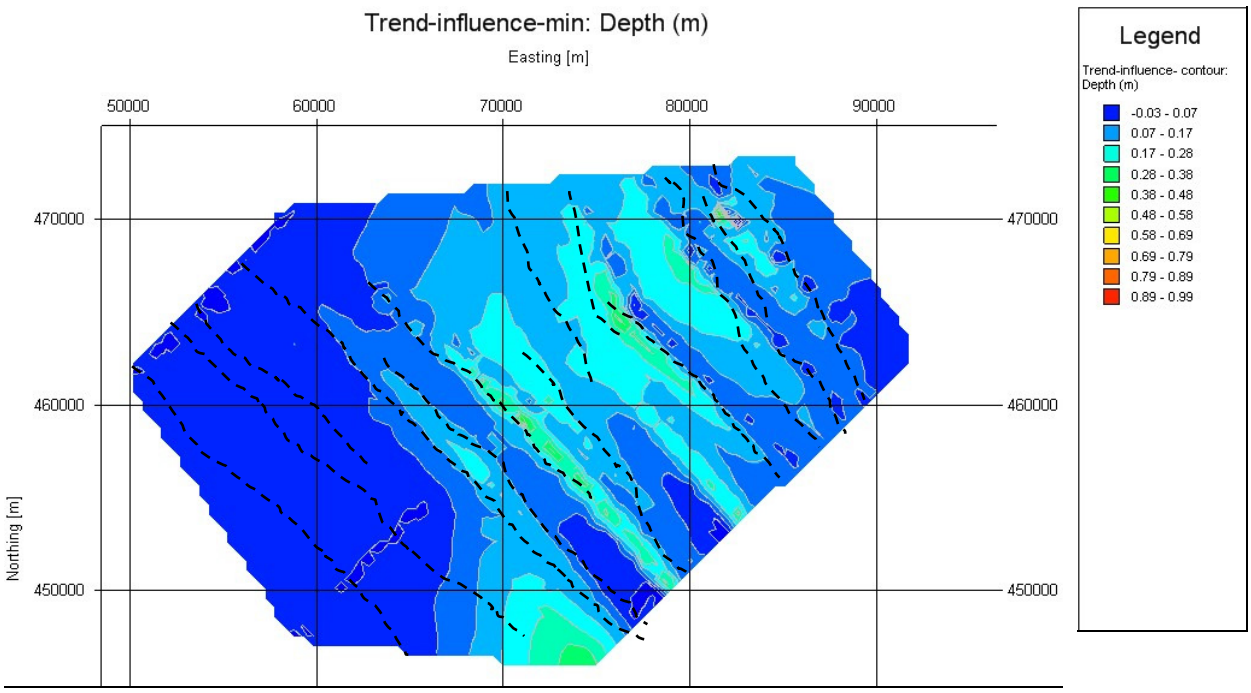

Figure 82: Trend map of area between studied sections - Minimal. Red represents most strong expected effect from greater burial depth, whereas blue represents the weakest. Interpolation between data points done with Distance Weighting with power 0.30 and 5000 points trend analysis using Jewell suite software 2D Gridding algorithm. Major faults are given schematically.

From the two trend maps (Figure 80 and 81) it can be observed that the fault blocks that were most greatly affected by the tectonic processes are the same but the extent of the effect is different. In the optimal case where the effect is stronger we can also easily observe that the most prominent influence is focused in the centre of the elongated fault blocks.

3.5. Conclusions and recommendations

Palinspastic restorations along 3 seismic in-lines showed that the basin is strongly influenced by the different stages of inversion and most importantly that individual fault blocks have been influenced differently. This provides a basis for further evaluation of the reservoir quality of sandstones in the Main Buntsandstein sub-group with strong constrained based on major faults. The amount of expected influence can be qualitatively inferred by the results of the restorations presented in this chapter.

Further recommendations for additional work for the burial history understanding include complete studies on individual fault blocks and considering them as individual units in term of reservoirs, seals, migration path and possibilities, and stress regime development.

References:

Barr, D., 1985, 3-D palinspastic restoration of normal faults in the Inner Moray Firth; implication for extensional basin development, EPSL, Elsevier

Bulnes, M., McClay, K., 1999, Benefits and limitations of different 2D algorithms used in cross-secton restoration of inverted extensional faults; application to physical experiments, Tectonophysics 312, Elsevier

De Jager, J., 2007, Geological Development, in Geology of the Netherlands, KNAW
* Based on earlier publication of the author

Geluk, M.C., 2005, Stratigraphy and tectonics of Permo-Triassic basins in the Netherlands and surrounding areas, University of Utrecht, PhD Thesis.

Van Balen, R.T., et al, 1999, Modelling the hydrocarbon generation and migration in the West Netherlands Basin, the Netherlands, Geologie en Mijnbouw/ Netherlands journal of Geosciences 79 (1) p29-44, 2000

Van Wijhe, D.H., 1987, Structural evolution of inverted basins in Dutch offshore, Tectonophysics 137, Elsevier

Worum, G. et al, 2005, Pre-Neogene controls on present-day fault activity in the West Netherlands Basin and Roer Valley Graben System (southern Netherlands): role of variations in fault orientation in a uniform low-stress regime, Quaternary Science Reviews 24, Elsevier

Hendrie, D.B., Kusznir, N.J., Hunter, R.H., 1993, Jurassic rifting extension in the North Sea triple junction from flextural backstripping: implications for decompression melting models, EPSL, Elsevier

Turner, J.P., Williams, G.A., 2004, Sedimentary basin inversion and intra-plate shortening, Earth Science Reviews, Elsevier

2DMove 2010.1, Manual and Tutorials, Midland Valley Exploration Ltd., Glasgow

4. Diagenetic history and tectonic events influence on the sandstones of the Main Buntsandstein subgroup in the West Netherlands Basin

The evaluation of the diagenetic development of the rocks from the formation of the Main Buntsandstein sub-group is closely related to the depositional environment, burial history and composition of older formations. Part of the information presented in this chapter has actually been already used in the analysis of the depositional environments in the basin. However the complete diagenetic development description serves as a summary of the previous chapters and is therefore presented as an individual topic.

This chapter will present the results of several published studies as well as conclusions that can be drawn from the combination those studies and the acquired knowledge from previous chapters about burial and depositional history.

4.1. Diagenetic history model

There are several studies available for the diagenetic history of the Man Buntsandstein from both onshore and offshore areas. The most extensive studies in selected wells from the offshore blocks L, K, P and Q are presented by the articles from Spain et al., 1997 and Purvis et al., 1996. Also individual well core report from well P11-02 is considered. It presents an important view over the reservoir diagenetic development of the sandstones in the most southern deep fault block. The onshore studies are based on the diagenetic studies on wells SMG-01, WWK-01 and NDW-01 presented by Emery, 1987.

4.1.1. Summary of diagenetic history for the Main Buntsandstein formations

Time of occurrence of diagenetic process	Early	Middle	Late
Compaction			
Illite			
Feldspar overgrowths			
Feldspar dissolution			
Nodular anhydrite			
Pyrite			
Anhydrite dissolution			
Anhydrite			
Dolomite – non ferroan			
Dolomite – ferroan			
Quartz dissolution			
Quartz overgrowths			
Siderite			
Hydrocarbon migration		* * *	

Table 5: Summary of diagenetic processes and their relevant time of occurrence for Main Buntsandstein / Middle Bunter core from West Netherlands Basin

These are the summarized results of the different studies done on Middle Bunter core. Although the list of different cements and processes is significant individual wells differ from each other regarding the sequence of diagenetic events and also in the severity of the individual processes.

Different minerals that were encountered have different effect on the resulting reservoir properties. Although most cements have generally detrimental influence on the available pore space and thus on the porosity and permeability, the dissolution process often create secondary porosity and improve the permeability along established flow paths.

Early diagenesis processes are related to the effects of meteoric water invasion. The expected climate conditions during the Early Triassic are such of arid desert environment. Initially the diagenesis is dominated by precipitation of illite grain coating and dissolution of feldspar grains. This has led to replacement of

feldspars by illite and subsequent precipitation of feldspar overgrowths. Typical early cement for the Main Buntsandstein sandstones is also dolomite. It has developed as both aggregations and zoned crystals in open pore spaces. Dolomite crystals often exhibit hematite rims and that indicates that they were formed under oxidizing conditions with contact to meteoric water. Dolomite is generally more abundant in the fluvial sandstone facies. Anhydrite is common in Buntsandstein sediments in different forms. It is believed that it has served as early framework-stabilizing cement to counteract the effects of compaction in the sandstones.

After the inversion of the basin, Buntsandstein sediments were exposed again to meteoric waters. This has led to dissolution of grains and cements, and subsequently to new precipitation of cements dependant on the area. The more northern regions have experienced stronger influence of precipitation and replacement of evaporate cements due to the availability of evaporates in the overlying sediments. This has led to significant reduction of reservoir quality in those areas in comparison to the south west.
Hydrocarbon migration is believed to have taken place in the middle range period but it is highly dependent on the individual structural characteristics.

At later stages, under higher temperatures different cements such as quartz cements and platy illite have formed. Further leaching of formation fluids has led to dissolution of more feldspar, quartz and anhydrite grains and cements and has formed secondary porosity in some of the sandstones.

4.1.2. Influence of diagenetic and burial history on reservoir properties and implications for their predictability

The diagenetic history is directly related to the depositional environment of the studied sediments but also with that of the overlying deposits. The proper understanding of the depositional facies and processes has a key role in the successful determination which processes have the strongest influence on the diagenetic development of the reservoir sandstones. When the later stages of the diagenesis are considered the burial history of the basin starts to play a more important role as significantly inverted fault blocks tend to be more exposed to a variety of geomechanic and chemical processes.

Differences in reservoir quality for identical formation intervals across major faults are best observed in cored wells on the SW-NE dip sections. There are strong indications that the depositional environments encountered for the Main Buntsandstein changed over the large faults. This leads to the conclusion that the faults were syndepositional – sufficiently active also during deposition so that they can influence the development of sedimentary systems.

Example of such effect can be any pair of wells across one of the many large offset faults in the basin. For the purpose of being relevant to the target area wells SGZ-01-S1 and KDZ-02-S1 are selected. The cored interval in the Main Buntsandstein in those wells includes sandstones from the lower cycle of Hardegsen formation (referred also as the upper section of the Upper Detfurth Claystone equivalent or also Upper Detfurth Sandstone). The thickness of the formation to the southern well SGZ-01 is 45 meters and in the northern well KDZ-02 is 35 meters. The GR log profile has identical shape and individual peaks can easily be correlated between the two wells although the interval seen in the northern well KDZ-02 seems to be less developed in terms of thickness of individual layers. The resulting plot of the petrophysical properties is shown below.

It is very clear that there is a remarkable separation of the measurements from both wells in respect to porosity and, to a smaller extent, permeability values. The difference is so significant that it can lead to exclusion of the section seen in well KDZ-02 as net reservoir in the case for oil or water reservoir evaluation.
Such a clear separation based on porosity can originate from the abundant availability of pore-filling cement in well KDZ-02 in contrast to well SGZ-01.

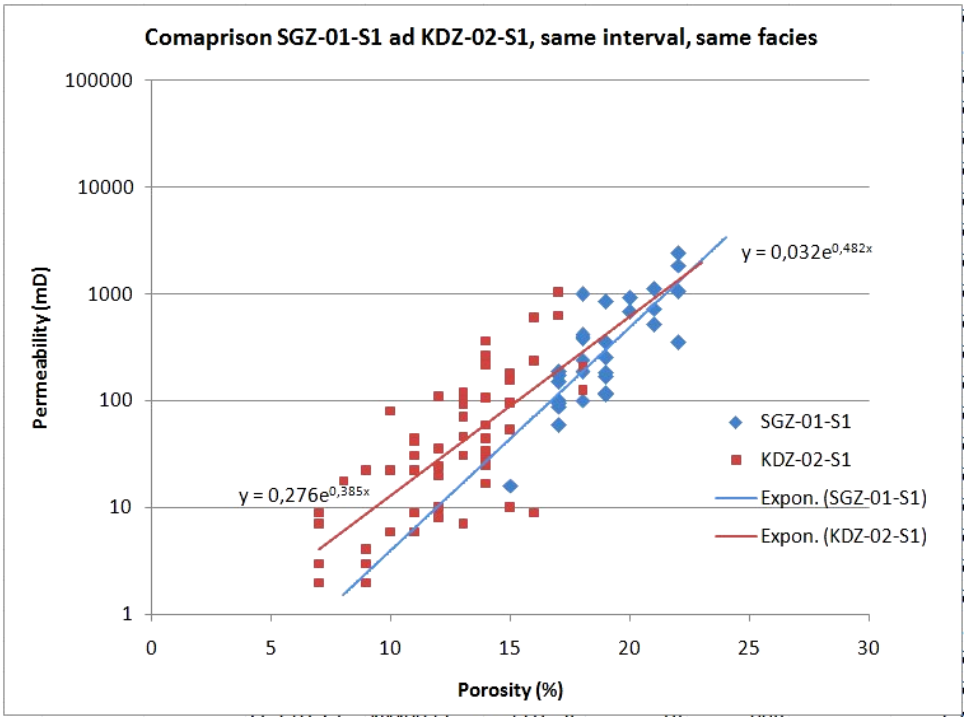

Figure 83: Comparison of core petrophysical data from wells SGZ-01-S1 and KDZ-02-S1 with clear separation of measurements while the cored interval is identical and also encountered facies are similar. Cores contain only sand facies and overall GR for the interval of well KDZ-02-S1 is actually lower that in SGZ-01-S1. Permeability axis is logarithmic scale.

Comparing the grain density and porosity from those two wells shows that there is a possible separation on grounds of grain density as well but it is more subtle. That leads to the conclusion that the source for the difference cannot be carbonate cement as it will give more striking grain density separation but rather another type of pore filling cement. Although it is also possible to explain the difference with extensive leaching and precipitation from meteoric waters it is more likely the source for the pore-filling cement to already available at the time of deposition. The proximity of the desert lake and more importantly the possible restriction of the fluctuations of the desert lake boundaries due to the paleo geomorphology of the basin are more likely to be the reasons for this remarkable difference is reservoir quality between these otherwise comparable sections of aeolian sandstones.

Not only deposits differ across major faults but also there seems to be significant differences in adjacent fault blocks in direction parallel to the fault strike. The only difference in such situations is related to the different amount of uplift and subsequent subsidence that one part of a given fault block has experienced in comparison with other part of the same fault block or adjacent fault block.

An example for remarkable difference in reservoir quality of similar in terms of sand composition, net thickness and lithological facies sediments deposited in similar depositional setting are core from wells MSG-01 to the west and RZB-01 to the east situated on a strike section. These wells are relatively close to each other but show significant deviations in terms of reservoir permeability in the very high permeability range. In well MSG-01 there are zones with very high permeability in the range of 2 to 18 Darcy while core analysis of well RZB-01 has not shown any exceptionally permeable zones. From the results of the study on the burial history of the Triassic sediments it is clear that well RZB-01 is situated in the upper end of a deeper fault block and is of significantly higher expected impact from the basin inversion. This could lead to the precipitation of additional cements in the RZB-01 area in comparison to the area of MSG-01. Other than that both wells are dry with traces of hydrocarbon migration.

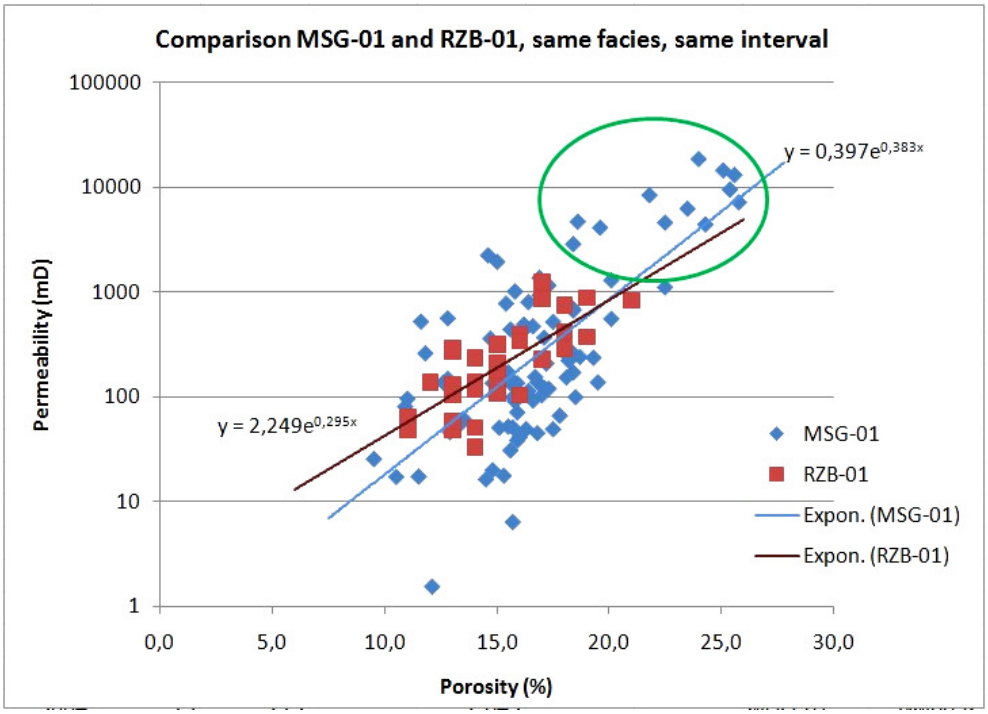

Figure 84: Comparison of core petrophysical data from wells RZB-01 and MSG-01 with indication of sand intervals with exceptionally better porosities and permeabilities in well MSG-01. Note that these measurements fall relatively good inside the trend of the rest of the measurements in well MSG-01. Only sand facies are encountered in the both cored intervals. Permeability axis is logarithmic scale.

The figure above shows the comparison of the basic petrophysical properties of both wells with the exceptionally permeable intervals circled in green. It is clear that that they are unique to well MSG -01 while the rest of the measurements from both wells are relatively well grouped, with a lightly larger spread in well MSG-01 due to the larger number of measurements.
These examples give another reason to consider the study area to be separated by the major basin faults not only in structural sense but also in terms of depositional environment, diagenetic history and reservoir properties.

Another consideration that needs to be taken into account when considering the diagenetic history in a basin with complex burial history such as the West Netherlands Basin is that diagenetic processes of different time periods can interact with each other provided with the proper conditions. A typical late diagenetic process that leads to considerable reduction of reservoir quality such as quartz dissolution at greater depth can for example be counteracted by early diagenetic clay mineral grain occlusion. This creates controversy as clay minerals are usually considered detrimental to the reservoir properties for their tendency to clog pore spaces and throats. It is therefore important to consider each reservoir target individually and carry out comprehensive evaluations of individual fault blocks.

4.2. Fractures – possibility for occurrence and distribution model

Fractures are typically created as a result of the effect of local stress condition. In a broader sense fractures are zones of critical instability in the rock matrix and their orientation and shapes are strongly related to the stress conditions that have been active during the time of creation. Most of the sands of the Main Buntsandstein formations are very heavily cemented and their porosities and especially permeabilities are rather low. The existence of a fracture network in those otherwise tight sandstones is probably the only way to make them suitable for a geothermal project. There are a number of indications of fractures that are going to be discussed and evaluated in this chapter. There are also different considerations to be taken into account regarding fractured reservoirs that are going to be mentioned as well.

As the West Netherlands basin has experienced a significant period of inversion leading to alternating stages of subsidence and uplift it is expected that this could have led to the creation of a possible fracture network. The reactivation of faults is can also lead to local creation of fractures or fracture zones.

4.2.1. Indications of fractures or small scale faults in Bunter sandstones

Common indications for existence of open fractures are the sudden and unexpected mud losses during drilling. Not all cases of recorded mud losses are related to fractures but it is always a good practice to investigate such occurrences for further clarification. In the scope of this study a large number of mud, composite, lithological and drilling logs have been reviewed in order to record any mud losses in the Main Buntsandstein interval and their exact locations. Due to lack of complete data only a limited amount of recorded mud losses was collected. The results are presented in the following table.

Well	MD	Loss rate (m3/hr)	Total (m3)	Formation and Notes
Q13-07-S1	3216	18	246	Upper Volpriehausen
Q13-07-S1	3256	? - unknown	? - substantial	Lower Volpriehausen
P18-A-05	4843	23.85	100%	Hardegsen
P18-02	3270	?	?	Hardegsen
P15-16	2964	?	4.13	Hardegsen
P15-16	2978	3.66	?	Upper Detfurth (?)
MON-02	2990	?	100	Lower Volpriehausen

Table 6: List of recorded mud losses in Buntsandstein formations in areas proximal to Zuid-Holland region in West Netherlands Basin

While the mud losses observed in Hardegsen seem to be related to layers of poorly consolidated coarse sand with very high permeability, the ones in Volpriehausen formation are situated right underneath the claystone intervals overlying the fluvial sandstones. Further inspection of those locations in adjacent wells that have cores including those intervals has revealed that those zones often contain a number of small scale syndepositional faults. However it was also found that those faults are usually completely cemented. Similar syndepositional faults in the claystone intervals have been observed also in outcrops in Germany.
Such features occur when the sediments are exposed to structural stress shortly after the early diagenesis has taken place. Their positions can be indicative for influences from the tectonic regime at given periods but the accuracy of the conclusions is limited to the good understanding of the diagenetic history of the sediments. More importantly due to the early development of these fractures and micro faults they become cemented with pore filling cements during later diagenetic events.
As almost all of the observed examples are normal faults, or fractures with extensional offsets it is likely that they are related to the early stages of the basin subsidence.
A number of figures of those observations are selected and displayed below (Figure 84).

Figure 85: Examples of syndepositional micro faults from well VAL-01 (left side) and syndepositional cemented fractures from well PKP-01 (right side)

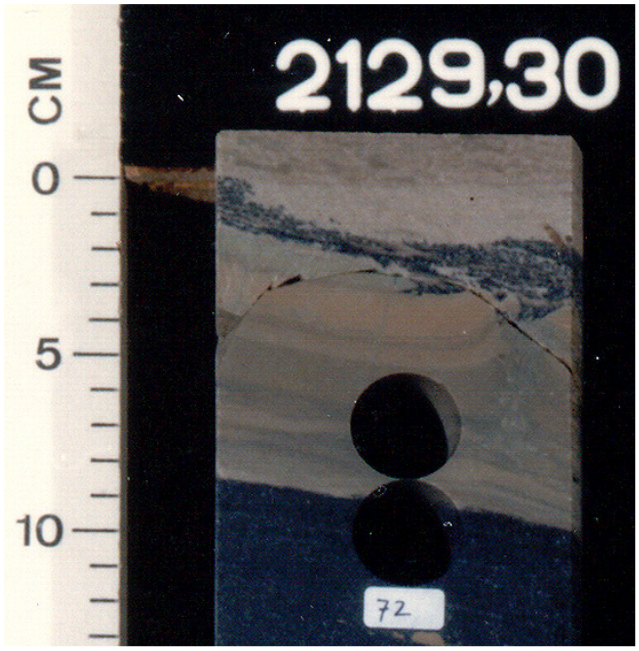

Figure 86: An example for a real open fracture observed in well PKP-01. The change in lithology is clear across the sinusoidal curve that represents the fault/fracture plane cut obliquely in the core slab.

There are rarely such clear examples of open fractures in core as the one that can be seen in core from Upper Volpriehausen interval in well Papekop-01 (PKP-01) shown in Figure 85. The usual reason that such open fractures are not preserved lies in the fact that cores typically break at loosely cemented or completely detached surfaces. It becomes impossible to determine whether there is broken material missing in the core, or if the break was induced by the coring process and is not natural.
The observed fracture image – a part of a sinusoid, resembles the typical image of fractures observed in borehole imaging surveys. There are different types of such tools – borehole images, formation micro images, acoustic images and other tools. They are a more common source for information over formation dips and fracture availability and orientations.

Wells from the list above have also been logged with borehole image analyser and with borehole image analyser and equivalents in order to confirm the expectations for fractures and to evaluate their orientation and frequency of occurrence.

The images of the intervals with mud losses from the first well in the list Q13-07 are displayed below.

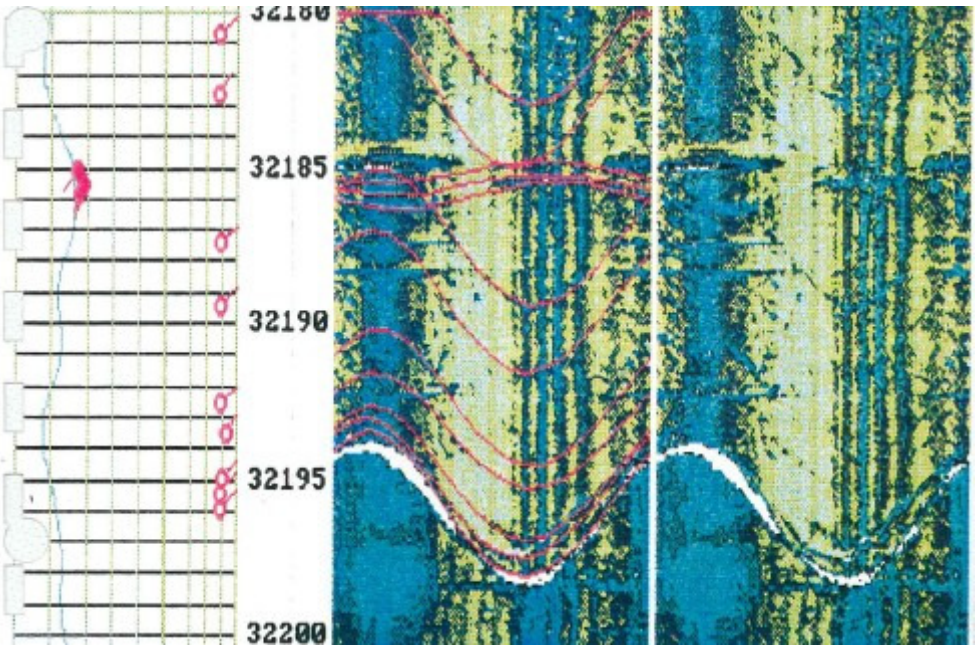

Figure 87: Example of fracture as seen on a FMI/Borehole Image Analyzer log. Notice that apart from the large fracture/fault at 3219m there are also smaller ones in the whole interval above.

Borehole image instruments are powerful tools for detection of fractures and they can also be used to summarize fracture orientation data for complete intervals.

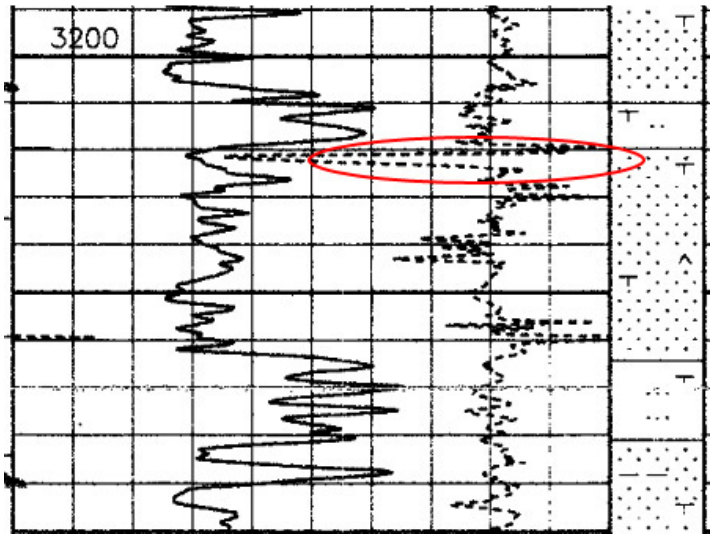

Figure 88: The same interval with the observed large fracture with GR log (scale 0-150 API) on the left side and sonic log (scale 140-40 mics/f) on the right side. Positive peak is circled with red.

Open fractures with sufficient offset just as faults can also be detected by the sonic logging tools and represent a distinctive positive peak in the sonic log as the empty space in the fracture significantly slows down the signal.
An example of such effect can be seen in Figure 87. The image shown is a screen shot of the composite log of well Q13-07 presenting the same interval as depicted from the borehole image analyzer in Figure 86. It is important to note that the area of well Q13-07 is expected to be relatively affected by the inversion of the basin based on the results of the burial history restoration.
The findings of fractures in well Q13-07 and the significant recorded mud losses in the interval are good indications that the expected effect of the strong inversion influence in the fault blocks in the center of the basin is realistic and the result can be used in areas not yet penetrated by exploration or production wells.
The images of the intervals with mud losses from an adjacent to the second well in the list (P18-A-05), well P18-A-06 are shown below.

Fractures in well P18-A-06 are located on the expected places as observed in other wells – fractures in base of Lower Volpriehausen Claystone and increased dips although not interpreted as fractures at the almost missing claystone part right below the Detfurth base (base of Upper Volpriehausen Claystone). What is unique in this survey is that there is record of fractures in the two flooding surfaces signifying the two flooding events at the onset of Hardegsen and at the base of the second cycle of Hardegsen. It is possible

that the reason for the existence of these fractures is similar to the other ones – early cementation and brittle deformation due to a tectonic event that led to limited partial subsidence of the basin.

Although positions where fractures can be expected are already becoming evident it is still unclear what factors determine whether the fractures will be open or closed. In general fractures and micro faults that were created at an early stage tend to be completely cemented whereas fractures that were created at later stages have better chance to be still open. There is also a possibility that older fractures have better chances to serve as instability zones where younger fractures have formed.

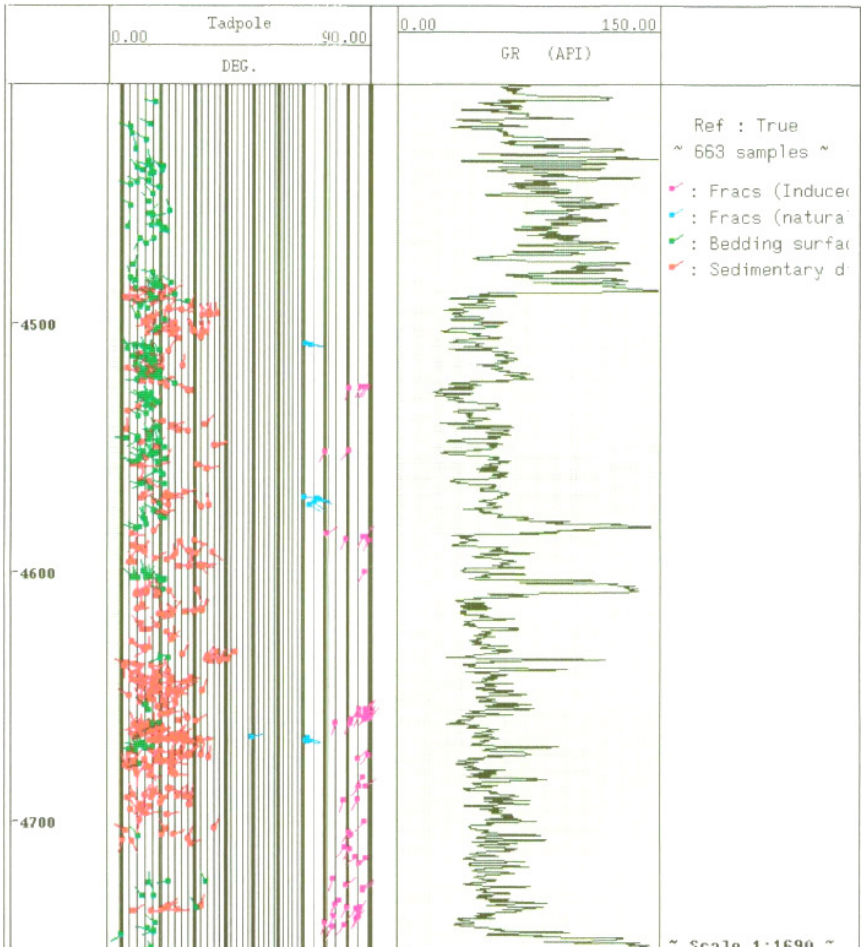

Figure 89: Summary of recorded dips and fractures from the whole Main Buntsandstein interval from well P18-A-06. Notice the positions of the observed fractures are in accordance with previous observations – close to the bases of flooding periods.

In the other wells mentioned in the table with observed mud losses there is also record of unusual dips recorded with continuous dip-meter surveys indicating possible fractures. A summary of the formation and fracture dips from well VAL-01 is shown below.

In well VAL-01 the observed fractures from the borehole imaging survey are again distributed mostly in the already know zones prone to development of fractures. Most of the fractures are cemented; however there are indications of open fractures in the Upper Detfurth Sandstone – or lower cycle of Hardegsen as used in this work. This is in accordance with the observations from well P18-A-06 and further proves that reservoir quality in zones with typical low porosity and permeability due to abundant cementation can be partially improved by the availability of fracture network. A possible effect from this conclusion can be that such zones can also be perforated although from petrophysical point of view they might fall outside of the interest zones.

In the next paragraph a short summary of the fractures observations is offered along with concluding suggestions over the spatial distribution and factors influencing spread of fractured zones.

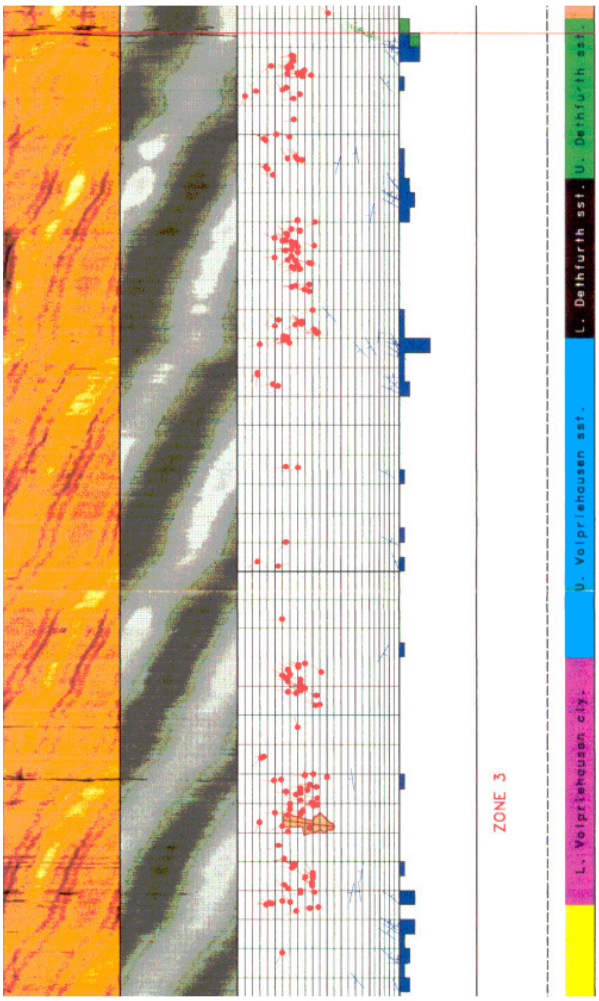

Figure 90: Summary of stratigraphic dips and fractures in the Buntsandstein interval from well VAL-01. Notice that the positions of the fractures are again where expected.

4.2.2. Suggested model for spread of fractures

In the previous paragraph it became evident which zones tend to be more prone to contain closed or open fractures. It is clear that these are typically the bases of the more claystone or siltstone rich layers or the upper parts of the underlying sandstone layers. Although the usual formations that show fractures on borehole images and dip-meter surveys are Volpriehausen and less frequently Detfurth, it is also possible to observe recorded fractures in the more shale rich layer separating the two sandstone layers in Hardegsen.

Factors that influence the spread of fracture and micro fault zones can be considered in several groups based on the type of rock and formation, the amount of cement related to early diagenesis, individual fault block, and actual position in the fault block in regard with the local stress field development.

The following figure (Figure 90) show a basic diagram for the expectation for encountering fractures based on the different mentioned factors. The suggested model is based on the observations described in all of the previous chapters. Note that most zones with expected fractures are situated close to the center of the inversion axis in the basin and on uplifted fault blocks. Such fractures are more likely to be of younger origin, namely the last inversion stage. In comparison there also widespread cemented fractures related to early diagenesis of the sediments and minor tectonic influences during deposition. However those fractures do not pose interest for the further exploration of the basin as they do not improve reservoir performance in any

way. Open fractures on the other hand can possible be associated to significant improvements of production rates from otherwise tight sand reservoirs in Detfurth and Volpriehausen formations.

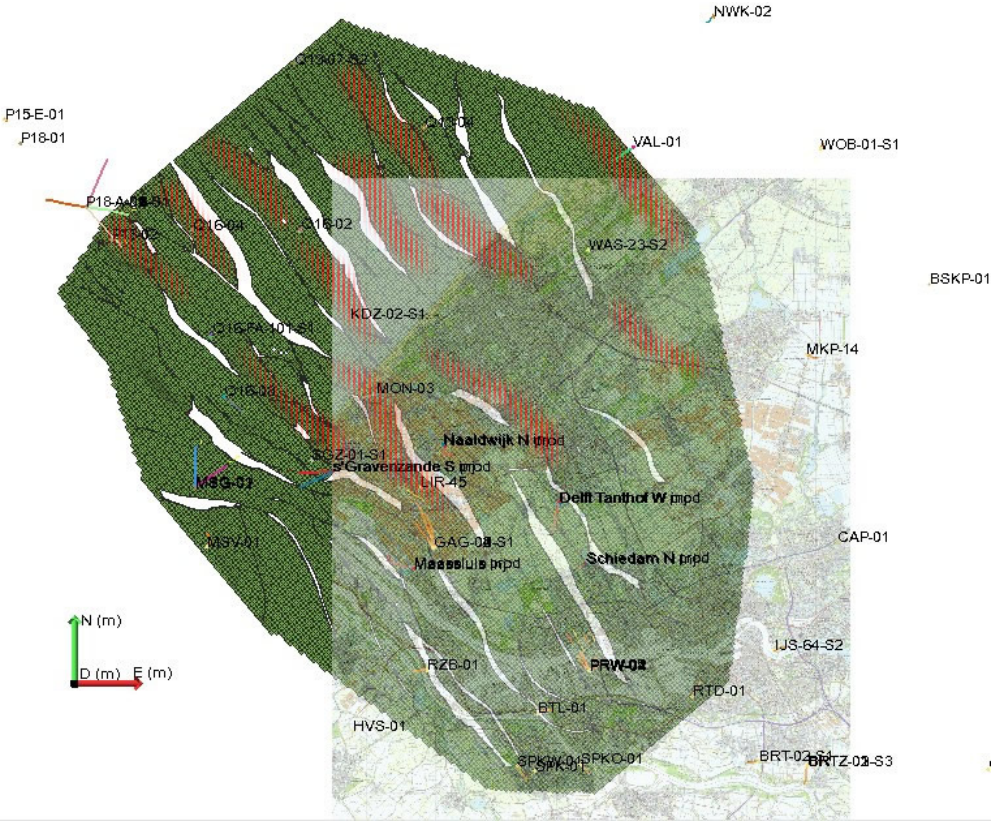

Figure 91: Suggested areas of high fracture probabilities based on conclusions in this and previous chapters.

4.3. Conclusions and recommendations

The diagenetic history of the targeted reservoir is a very important factor in the evaluation of the current reservoir properties. A whole range of different possibilities of different developments exist and each of them might lead to considerable differences in the final result. For example it was already shown that the Main Buntsandstein sediments have been buried to a significant depth for a long period of time and although they have not been buried to much greater depth than the current one the conditions for late diagenetic processes have been available for a considerable time. However it was also shown that the original depositional environment of the sediments plays a very important role for the early diagenetic processes but also for the late ones as it can introduce different scenarios for the late diagenetic effect influences.

Several of the observations include that nodular anhydrite is more probable towards the north while late diagenetic quartz dissolution is possible in the deep faults blocks in the south west in sandstones with low clay content during deposition. In general each individual reservoir target requires an evaluation of the diagenetic history in combination with the knowledge for the depositional environment and burial history in order to be able to accurately predict reservoir quality and spatial variations.

Additional work on the individual diagenetic development of target fault blocks and areas is essential in order to improve the predictability of reservoir qualities in not explored regions. A very important consideration in regard with this is the possibly very varied development between higher and lower faults blocks triggered by both burial history differences and middle and later diagenetic processes differences due to the unrelated contacts with adjacent formations.

References:

Emery, D., 1987, The Sedimentology and reservoir characteristics of the middle and upper Bunter formations, Waalwijk-1, onshore Netherlands, BP

Faulkner, D., Jackson, C., Lunn, R., Schlische, R., Shipton , Z., Wibberley, C., Withjack, M., 2010, A review of recent developments concerning the structure, mechanics and fluid flow properties of fault zones, Journal of Structural Geology 32, Elsevier

Henk, A., Nemcok, M., 2008, Stress ad fracture prediction in inverted half-graben structures, Journal of Structural Geology 30, Elsevier

Purvis, K., Okkerman, J.A., 1996, Inversion of reservoir quality by early diagenesis: an example from the Triassic Buntsandstein, offshore the Netherlands, in Rondeel, H.E., Batjes, D.A.J. et al, Geology of oil and gas under the Netherlands, Kluwer, p179-191.

Reuver, F. de, 1996, Sedimentology, petrography and reservoir properties of cores 1 to 4 from well P11-02 – Final Report, GAPS/Amoco

Spain, D. Conrad, C., 1997, Quantitative analysis of top seal capacity, offshore Netherlands, Southern North Sea, Geologie en Mijnbouw 76

Sullivan, M., Haszeldinet, S., Boyce, A., Rogers G., Fallick A., 1994, Late anhydrite cements mark basin inversion: isotopic and formation water evidence, Rotliegend Sandstone, North Sea, Marine and Petroleum Geology 11

5. Porosity and Permeability relationships and static models for the Main Buntsandstein subgroup in the West Netherlands Basin with reservoir data

After the completion of the geological research on the depositional environment, burial and diagenetic history of the Main Buntsandstein formations the next step is the incorporation of the collected information into a static reservoir model or models. It should contain the most important petrophysical properties and be separated for different areas of interest.

The petrophysical data is a very important component in the static model and therefore it is very important to successfully combine the geological information with the laboratory petrophysical data. In this chapter the analysis of the data is presented and a way is suggested for the combination of the geological ideas with actually collected petrophysical data. The resulting model is designed to be as accurate as possible by including all the accumulated and analyzed data into a single entity.

5.1. Analysis of petrophysical data and references to depositional facies

After interpreting the basin in terms of depositional environment and diagenetic development it is important to incorporate this information in the eventual reservoir model. In order to achieve this all of the available cores with photographs and sedimentological descriptions are included in a database with the corresponding porosity and permeability measurements. This way it is possible to determine the porosity and permeability relationships for individual facies and formations. Such a relation is a stable basis for the creation of an accurate reservoir model using all of the available data.

5.1.1. Combining petrophysical measurements with sedimentological cores

Almost all collected core have available petrophysical analysis carried out on them. These include porosity, horizontal and also in some cases vertical permeability, and grain density measurements. These measurements are made on core plug taken roughly every 30 to 50 cm in a given core. When a core sedimentological description and/or core photograph is available the petrophysical data can be coupled to the sedimentological description. The result is that porosity – permeability relationships can be calculated for individual facies in the same or in different formations and also regions in the basin. Seventeen wells have been used for the interpretation of petrophysical properties of facies.

List of facies	
A	**desert sand dune**
B	**dry desert sand flat**
C	**fluvial braid bar**
D	**damp desert sand flat**
E	**fluvial fan/sand flat**
F	**floodplain/overbank**
G	**lacustrine clay/silt**

A complete list of used wells and corresponding formations encountered in the cores is available in Appendix III. The following table gives a rough idea how the results look like including the used differentiation of facies. The complete table is listed in Appendix III. Dry sand flat refers to desert sand flat no affected by ground water fluctuations whereas damp sand flat is similar desert sand flat that is affected by those fluctuations.

Well	Plug Num	Depth m MD	Porosity %	Kh mD	Kv mD	RHOB g/cm3	GR API	Formation	Facies
...	...	...	...	...	...	...	...	...	...
GAG-05	NM0047	4101.15	6.6	0.26		2.67	70	Hardegsen	D
GAG-05	NM0048	4101.45	5.5	0.66		2.66	75	Hardegsen	E
GAG-05	NM0049	4101.80	3.2	0.39		2.69	75	Hardegsen	E
GAG-05	NM0050	4102.10	6.9	1.00		2.67	90	Hardegsen	F
GAG-05	NM0051	4102.57	5.0	0.42		2.70	90	Hardegsen	F
GAG-05	NM0052	4102.92	2.6	0.32		2.70	90	Hardegsen	F
GAG-05	NM0053	4103.32	11.6	15.96		2.67	90	Hardegsen	F
GAG-05	NM0054	4103.50	11.1	2.52		2.66	85	Hardegsen	E
GAG-05	NM0055	4103.80	9.1	32.34		2.67	80	Hardegsen	D
GAG-05	NM0056	4104.13	11.1	38.32		2.66	75	Hardegsen	D
KDZ-02-S1	NM0001	3255.10	13.8	28.10		2.65	45	Hardegsen	A
KDZ-02-S1	NM0004	3256.00	13.5	25.40		2.66	45	Hardegsen	A
KDZ-02-S1	NM0005	3256.30	12.0	25.00		2.67	40	Hardegsen	A

KDZ-02-S1	NM0007	3256.90	17.5	210.50		2.65	45	Hardegsen	B
KDZ-02-S1	NM0008	3257.20	7.3	7.50		2.75	45	Hardegsen	D
KDZ-02-S1	NM0009	3257.50	6.5	6.50		2.74	50	Hardegsen	D
KDZ-02-S1	NM0010	3257.80	14.0	43.60		2.66	45	Hardegsen	D
KDZ-02-S1	NM0011	3258.10	12.8	31.10		2.65	40	Hardegsen	B
...	...	...	...	...	...	...	...	...	...

Table 7: Example of facies interpretation in two wells core sections, full list is in Appendix III

After all the available cores are interpreted and data is collected and analyzed it can be sorted per formation and facies. The results are separated in individual graphs and then the entire data is presented in order to show the clear separation based on the different depositional environment lithologies.

5.1.2. Sorting of results and comparison with complete data

The following graphs represent the summarized results of the petrophysical and sedimentological evaluation of the different formations. The most important separation is between good quality sands and lower quality sands – for Hardegsen formation the separation is mostly between sands deposited in a dry desert environment or with low groundwater level (referred to as dry sands), and sands deposited in more humid desert environment or high groundwater level.

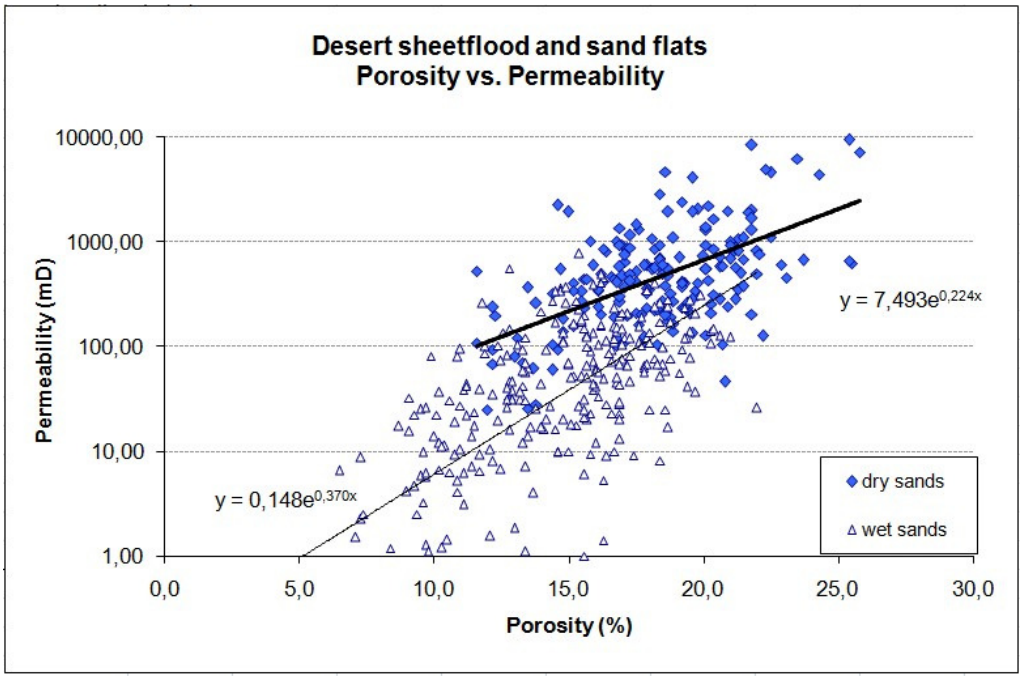

Figure 92: Porosity – permeability relations from cores in Hardegsen formation

The separation of the two different facies types is very clear in core photograph as well as on the reservoir properties plots with a clear advantage of the aeolian dry sand flat sandstones over the aeolian damp sand flat sandstones. The explanation for this separation can easily be related to the amount of available cement in the sediments and that is visible on the cross plot between porosity and grain density (Figure 92). It is assumed that this effect is triggered predominantly from the abundant calcite cement and that s directly related to the depositional environments. Areas with high groundwater level in contact with the open environment were more predisposed to facilitated precipitation of minerals.

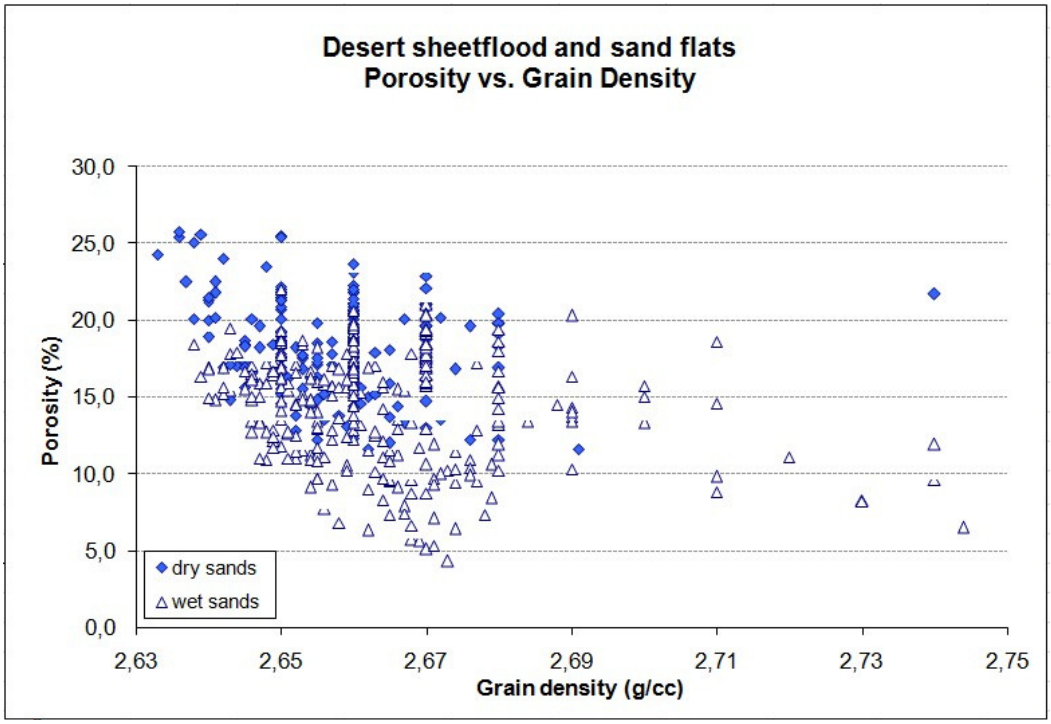

Figure 93: Porosity – bulk density relations from cores in Hardegsen formation

Although sediments from the Hardegsen formation are considered in this work as predominantly of aeolian origin there are no indications for the development of large scale desert dunes. Most of the sands were deposited in sand flats or sheets sands with minor small scale dunes and lamination. The explanation for this phenomenon can be found in the strength of the dominant winds as well as in the general availability of sand in the region.
In general the porosity in the Hardegsen formation is favorable for fluid flow. It is therefore the target formation for the development of geothermal reservoirs.

The next formation is the Detfurth and the same procedure was also applied to the available cores and core analysis data. The following graph (Figure 93) presents the porosity permeability relations for the two major united groups of facies observed in Detfurth formation – braided river sand bars and fluvial sheet flood sands.
It is clearly visible that unlike in the previous formation the major separation between facies here is not based on their depositional origin but rather on their current geographic position. This effect is more likely to be a result of the different diagenetic development rather than on any more significant difference in the facies composition of the original sediments. In general the depositional environment of this formation can be summarized as fluvial or fluvial/transitional environment. This implies that minerals that could have been later dissolved and precipitated as cements were readily available in all of the deposited sedimentological facies. If the effect of the deep burial and several stages of subsidence and inversion are also considered, it can be concluded that the reservoir quality of the sandstones is controlled by the amount of diagenetic steps experienced by the individual fault block or compartment.

From the cross plot it is also visible that wells situated in the south west of the basin have consequently better porosities and permeabilities leading to a completely different poro-perm relationships. This effect is also taken into account in the later stages of the reservoir modelling as the reservoir models in the south-south west parts of the basin have different relationship applied in comparison with the reservoir model in the rest of the basin.

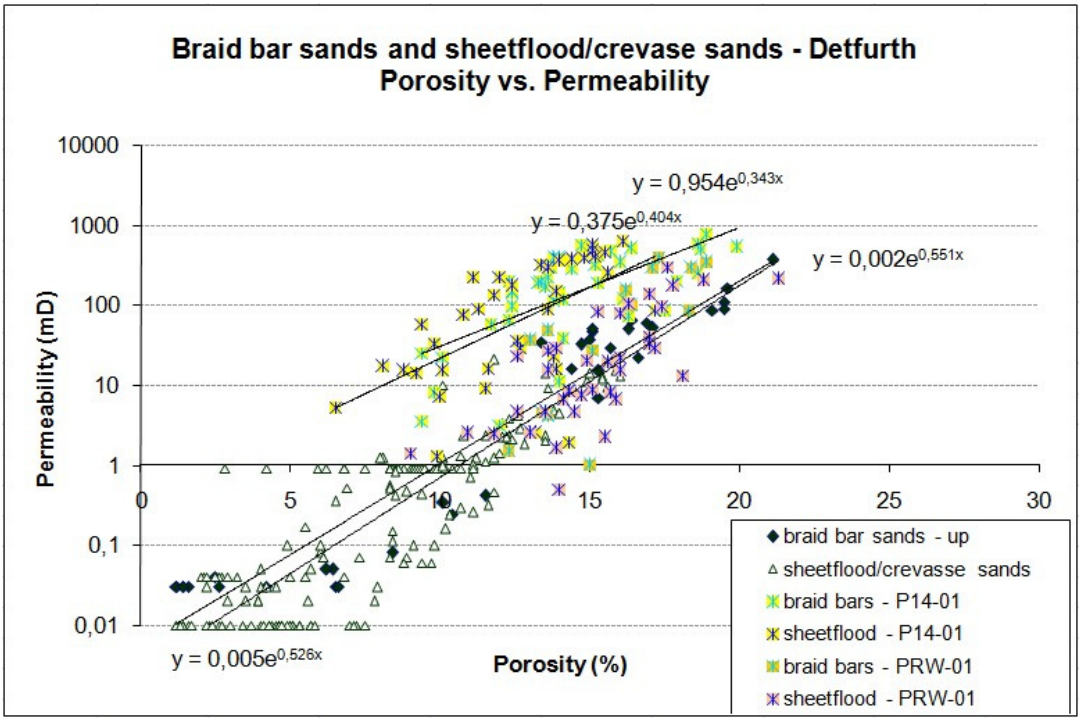

Figure 94: Porosity-permeability relations from cores in Detfurth (sandstone) formation

The next graph (Figure 94) shows the results of the summary of the core interpretation from Volpriehausen formations where the same effect as observed in Detfurth sandstones is visible.

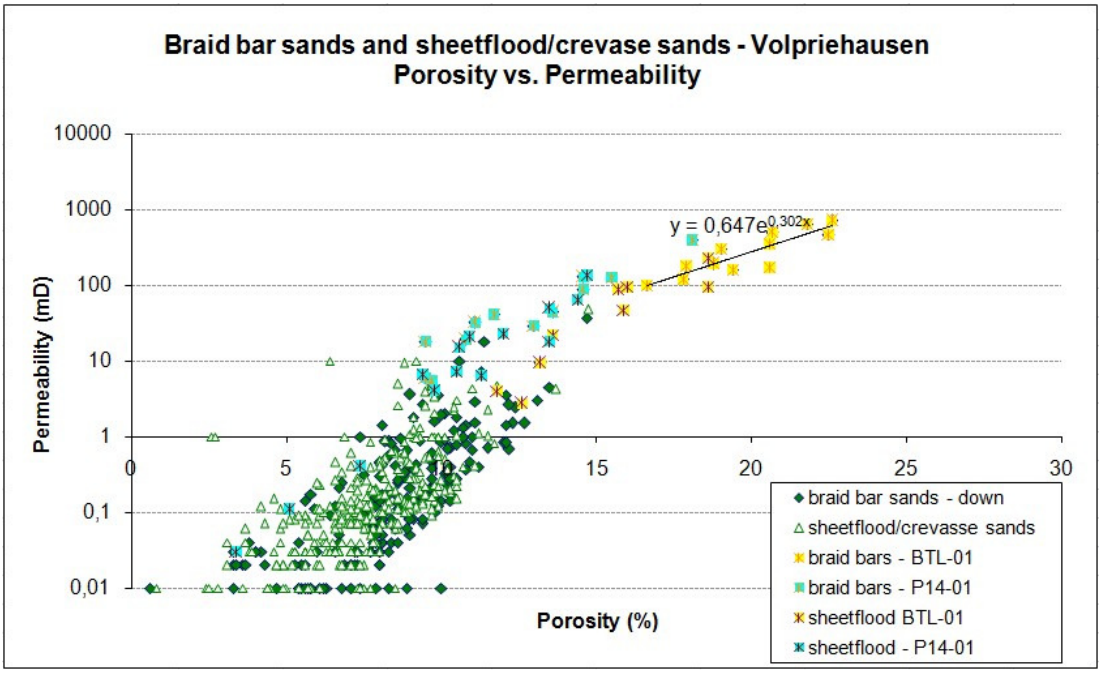

Figure 95: Porosity – permeability relations from cores in Volpriehausen (sandstones) formation

The presented relations give a detailed summary of the quality of the sandstones in relation to the observed sedimentological facies. In order to get a more complete idea for the whole range of sediments in the target area all of the available petrophysical data has to analyzed and evaluated. The following graphs (Figure 95) show a summary of all of the analyzed facies data from the geologic study region. The clear separation between the different facies encountered in the sandstones is already quite remarkable which gives additional reassurance that the depositional environment spatial variations and development in times plays an important role in the current reservoir qualities of Main Buntsandstein sandstone reservoirs in the West Netherlands Basin.

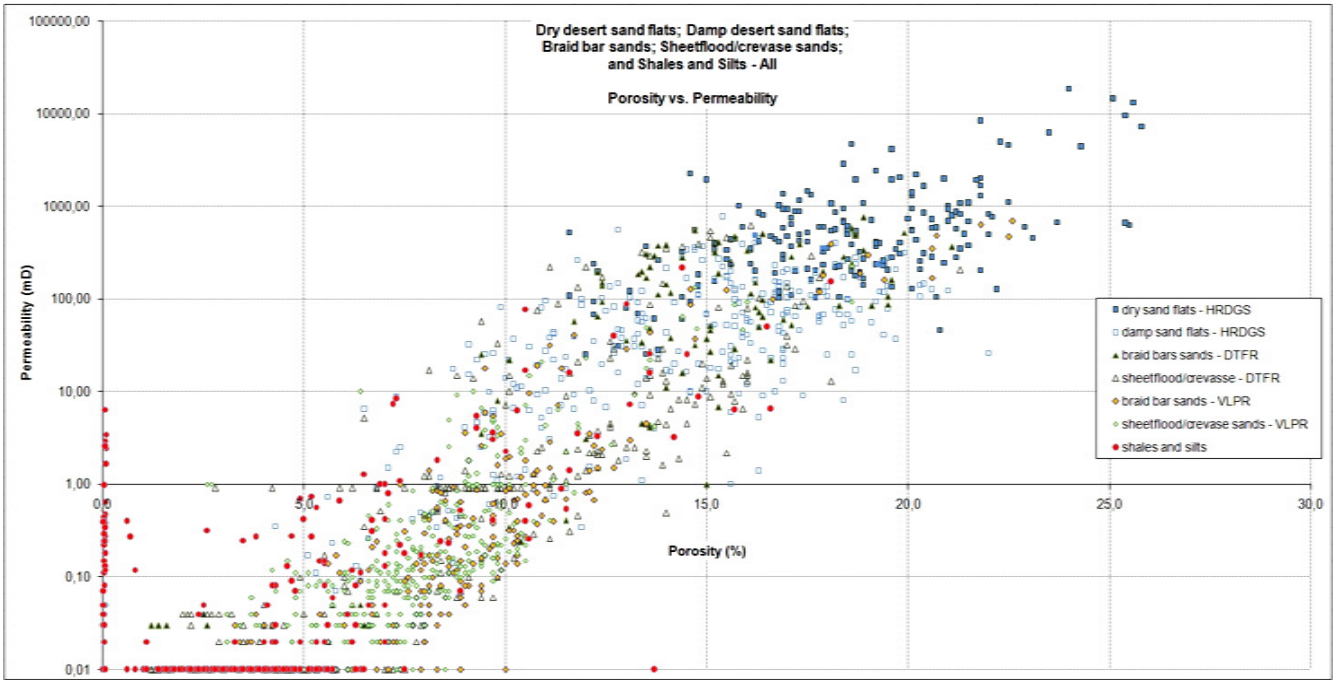

Figure 96: Summary of porosity-permeability relations for all of the observed facies in different formations in the study area. Data is representative for cores from 17 wells with available core photographs.

As expected aeolian sands show the best reservoir qualities while the fluvial sands have moderate quality and are more homogeneous in terms of differences between different facies. If the data is evaluated only in terms of sediments from different formations the already extracted relationships from the facies models can be tested against the combined data so that more general relations are derived for the complete reservoir intervals. Note that the formations division is according to the formation separation suggested in the chapter about the depositional environment of the Man Buntsandstein subgroup in the West Netherlands Basin.

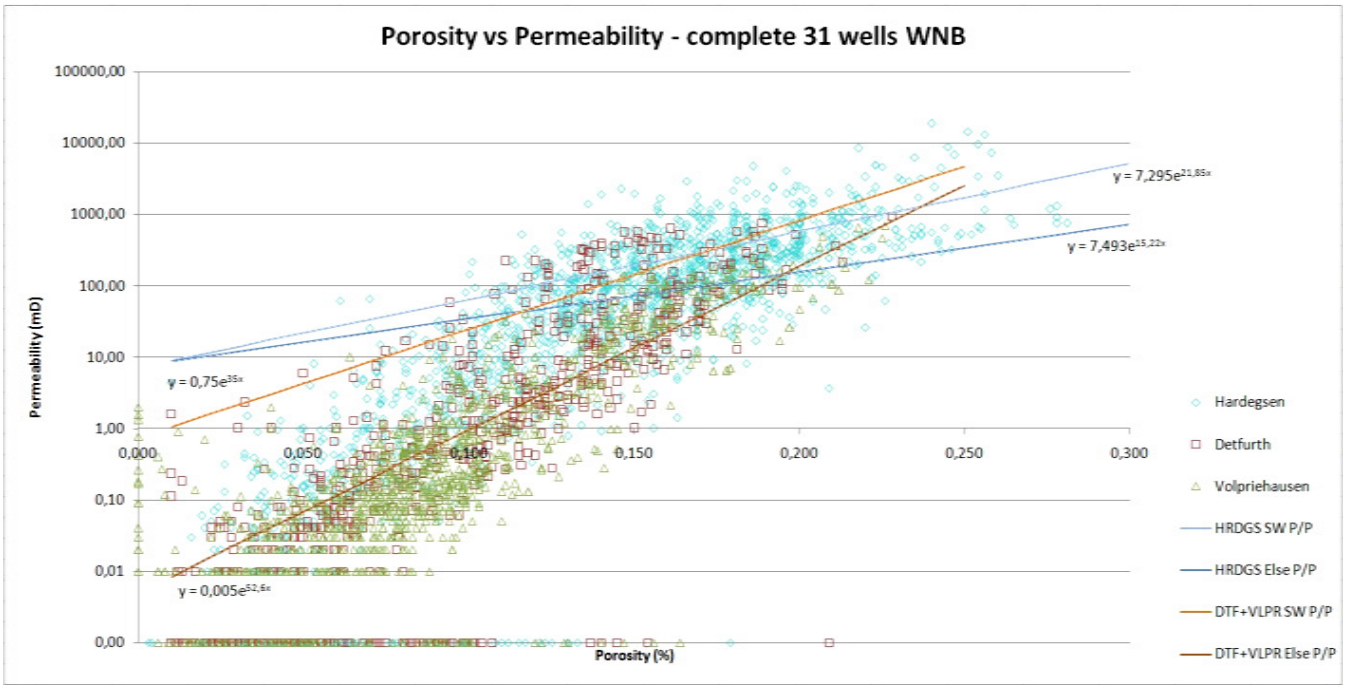

Figure 97: Summary of porosity-permeability relations for all available core analysis data separated on basis of formations from the study area. Data is representative for 31 wells with available core analysis data.

The complete combined porosity-permeability relationships graph (Figure 96) for all of the available core analysis data from the study area gives the more general relations for the different formations. For practical purposes Detfurth and Volpriehausen sediments are combined. However there are different relationships proposed based on spatial position in the basin, namely focusing on the differences between the south western fault blocks and the rest of the basin. This separation is also applied for the Hardegsen sediments although the differences are more limited. A further explanation for the relations and the resulting porosity and permeability models are presented in Chapter 5.2.6.

5.1.3. Collection and evaluation of available bottom hole temperature data

A good grip on the temperature distribution in the subsurface is very important for geothermal projects. In order to provide a sufficient database of observed bottom hole temperature data for Buntsandstein sandstones from 27 wells from the study area is collected and analyzed. This database includes BHTs from wireline logging tools, RFT and DST tests and production tests. Although the general geothermal gradient for the Netherlands is relatively accurate, areas that were subjected to periods of basin extension show slightly higher geothermal gradient. The evaluation of the results from the south west of the basin shows that this is also true for the West Netherlands Basin. The complete list of all analyzed data with depth references can be found in Appendix III.

The results of the evaluation are separated into three different sections – all of the temperature data without correction for hour from circulation for measurements from wireline logging tools, all of the temperature data with correction applied and only RFT/DST/Production tests data.

BRT-02-S1	BRTZ-01	BTL-01	GAG-02-S1	GAG-03	GAG-04	GAG-05
IJS-64-S2	KDZ-02-S1	MKP-14	MON-02	MON-03	MSG-01	MSG-02
OBLZ-01	P15-01	P18-01	P18-02	PRW-01	PRW-02	PRW-03
Q13-04	Q13-07-S2	Q16-08	RZB-01	SGZ-01-S1	SPKW-01	

Table 8: List of wells where BHT data is extracted for Upper and Main Buntsandstein depth

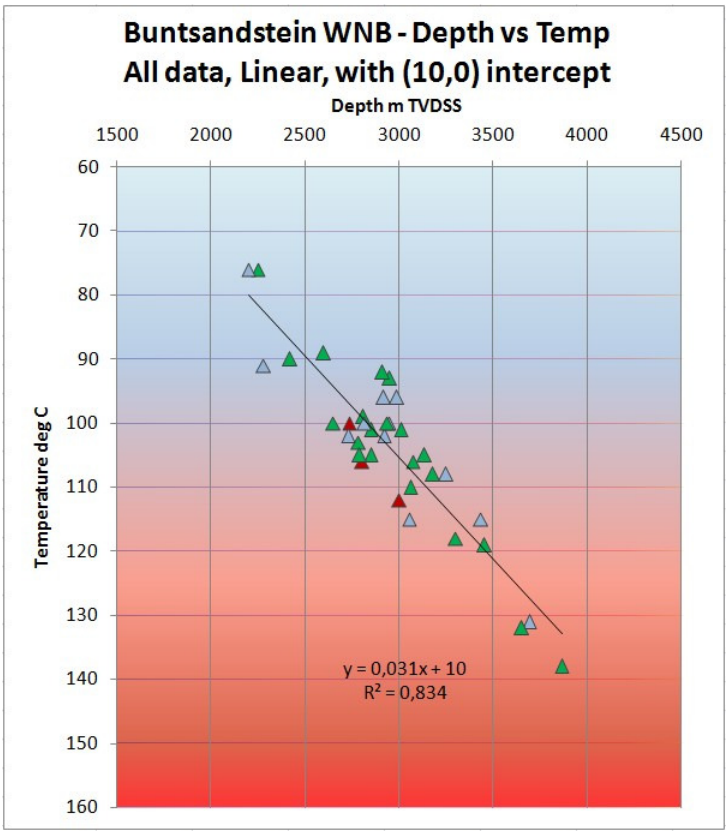

Figure 98: Cross plot graph for the relationship between depth and bottom hole temperature for all BSMB measurements, no correction applied, with 10 degrees surface temperature.

From the first graph (Figure 97) evaluation the resulting geothermal gradient comes in accordance with the widely accepted gradient for the Netherlands up to 2000 meter depth. However the measurements derived from wireline logging tools cannot be considered accurate as they measure the temperature of the drilling mud in the borehole. The actual temperature of the drilling mud in the borehole is actually slightly lower that the surrounding formation temperature unless it has been given sufficient time to come to equilibrium. Therefore it is important to also take into account the time from last circulation before the wireline tool was submerged to the position where the temperature was taken.

There are two possible approaches to avoid this problem. The first is to apply a correction for the wireline logging tool measurements and the second is to use only formation test or production test temperature data

which should be much more accurate. Both possibilities were evaluated and the results are presented in the graphs below.

There several published approaches for introducing a correction factor based on the time since last circulation and true vertical depth of the measurement. The one that was used in this study is proposed by Douglas W. Waples in 2004 and is calibrated for deep temperature measurements in the Gulf of Mexico.

$$T_{true} = T_{surf} + f \cdot (T_{meas} - T_{surf}) - 0.001391(Z - 4498) \text{ with } f = 1.32866^{\,-0.005289 * TSC}$$

Where T_{true} is the actual temperature in degrees C, T_{surf} is the surface temperature in degrees C, T_{meas} is the bottom hole temperature measured by the wireline logging tool in degrees C, Z is the true vertical depth of the measurement in meters, and TSC is the Time since last circulation measured in hours. (Waples et al.)

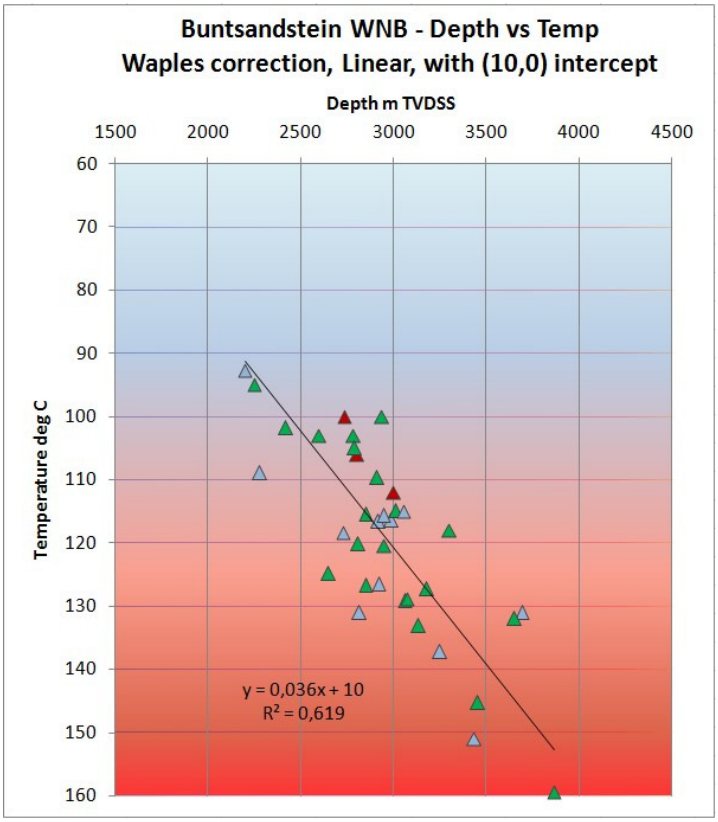

Figure 99: Cross plot graph for the relationship between depth and bottom hole temperature for all BSMB measurements, wireline logging tool measurements corrected using Waples correction and 10 degrees surface temperature.

In this graph (Figure 98) the results from the improved measurements with Waples correction for the temperatures applied are shown. The geothermal gradient is higher but the coefficient of determination R^2 has decreased. That is an indication that the variability in the data has increased and the correlation is worse. A possible reason for this is probably the amount of correction that is calculated by the Waples correction algorithm is in the range of 15 and 25 degrees C. This is possible an overestimation of the temperatures and the resulting linear trend relationship should be considered with caution.

In order to avoid introducing error in the temperature model due to the applied correction the input data can be filtered so that only temperature measurements from RFT\DST and production test are used. Such data is usually much more reliable and no correction is required. The final evaluation of the bottom hole temperature measurements data is therefore based solely on formation evaluation tests and complete production tests from Main Buntsandstein reservoirs that are taken after a sufficiently long time after last drilling mud circulation of at least 18 hours.

The resulting graph is show in the figure below (Figure 99) is the calculated linear relationship with 10 degrees Celsius surface temperature is selected as the relationship to be used in further calculation including temperature estimation in this project. It is also clearly visible that the coefficient R^2 for the relationship is also the highest from all of the previously determined relationships which gives even further confidence in the accuracy of the estimation.

$$\text{Temperature (C)} = 0.0326 * \text{Depth (m)} + 10$$

The actual input data for the calculations can be found in Appendix III.

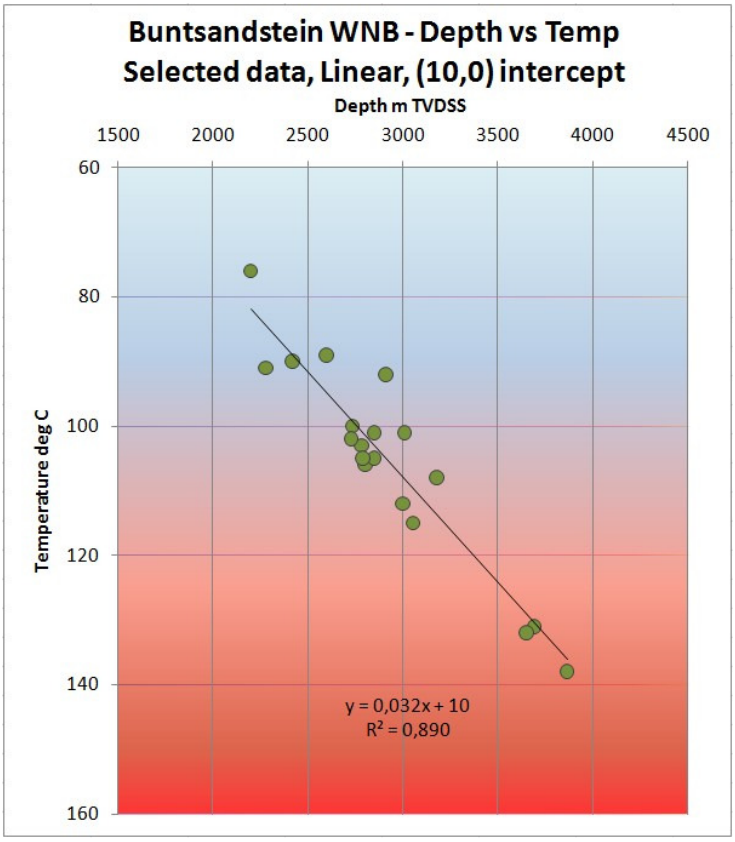

Figure 100: Cross plot graph of the relationship between depth and bottom hole temperature for Main Buntsandstein reservoirs measurement only from formation evaluation tests and production flow tests. The relationship is calculated with 10 degrees Celsius surface temperature.

5.2. Building the static models

This part of the report will follow the actual steps for the complete construction of the structural geologic model and the geologic property grids used in this project. The resulting models are representative for the results from previous chapters that are part of this study and serve as a combined summary of previous conclusion. The accuracy of the results presented is limited to the accuracy of the input data, limits of the modelling software and authors personal interpretation choices.

5.2.1. Seismic interpretation and horizons and fault models

The first step in the modelling process is the seismic interpretation of geologic horizons and faults. The interpretations from 3D seismic surveys L3NAM1985P, Z3AMC1989A, L3NAM1989K, L3NAM1990C, Z3NAM1990D and L3NAM1991A of Base Tertiary, Top Texel Marl, Posidonia Shale and Top Triassic horizons and 170 faults were available from PanTerra Geoconsultants. They served as the basis for the further work that included merging of horizons and faults from adjacent surveys and correcting the resulting model for inaccuracies. In most cases the faults required also extension in upward or downward direction.

The initial input for the surface interpolations consists of poly line seismic interpretation. In order to use then in the model as surfaces they are turned into triangulated meshes. The amount of details or the size of the building triangles is corresponding to the structural complexity of the individual area. The triangles boundary sizes vary therefore from parts of a meter close to fault junctions to several hundreds of meters in large flat areas in the horizons.

The following figure presents some of the poly line sets used as input for the modelling workflow.

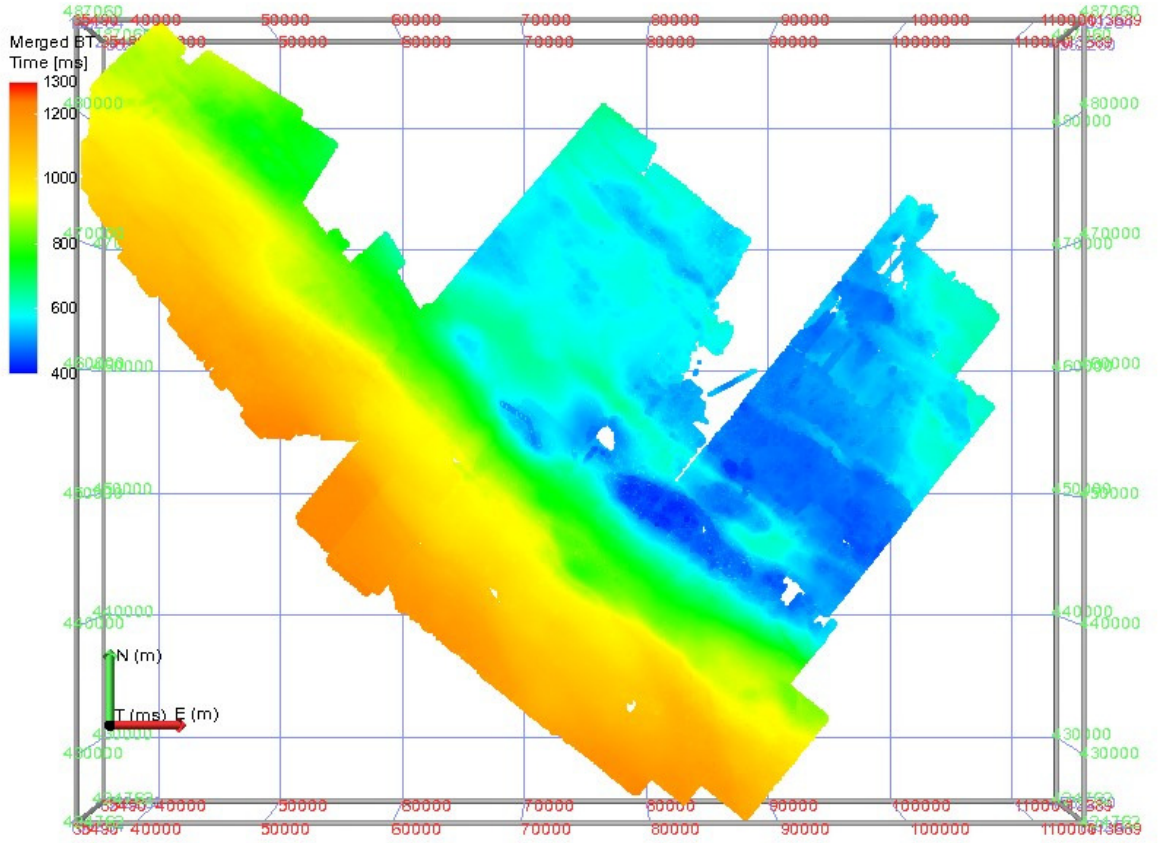

Figure 101: Base Tertiary poly line set interpretation used as input for the horizon construction

5.2.2. Velocity model

There are several options for the actual structural modelling workflow. The general difference between them is in the selection between working in time and working in depth. It is essentially recommended to work in time until the definite structural model is completed and approved. The reason for this is to be able to go back to the seismic interpretation and if required to make changes on the original input data for the model. In the case of this project it was chosen to work in depth for a number of practical considerations. First of all the input data has already been reviewed for quality approval in earlier projects and therefore no significant changes were expected to be required. Secondly the size of the model required some compromises with the amount of data left available in the working project due to limitations of the workstation available and software productivity consideration as suggested from the software developer.

The eventual workflow for the structural modelling starts with construction of triangulated surfaces in time for the horizons and faults. The next step was to constrain the data within the suggested project area and calculate the velocity model. After the surfaces were converted in the depth domain the further modelling was carried out only in depth.

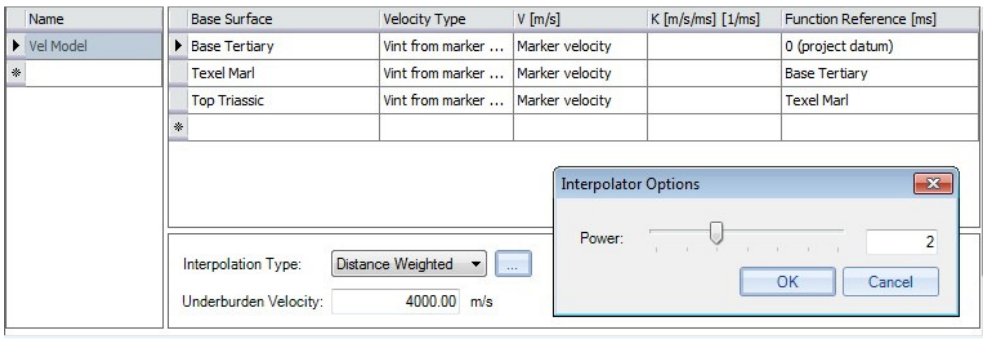

Figure 102: Screenshot for the velocity model calculation input screen

The resulting model from the input data (Figure 101) has the following statistics – Layer above Base Tertiary has a mean velocity of 1606.22 m/s, mean time of 0.820045 s with standard deviation of 0.17011. Layer above Texel Marl has a mean velocity of 2795.55 m/s, mean time 1.04455 s with standard deviation of 0.250215. Layer above Top Triassic has a mean velocity of 3099.71 m/s, mean time of 2.36648 s with standard deviation of 0.144011.

The resulting marker velocity model is presented below (Figure 102).

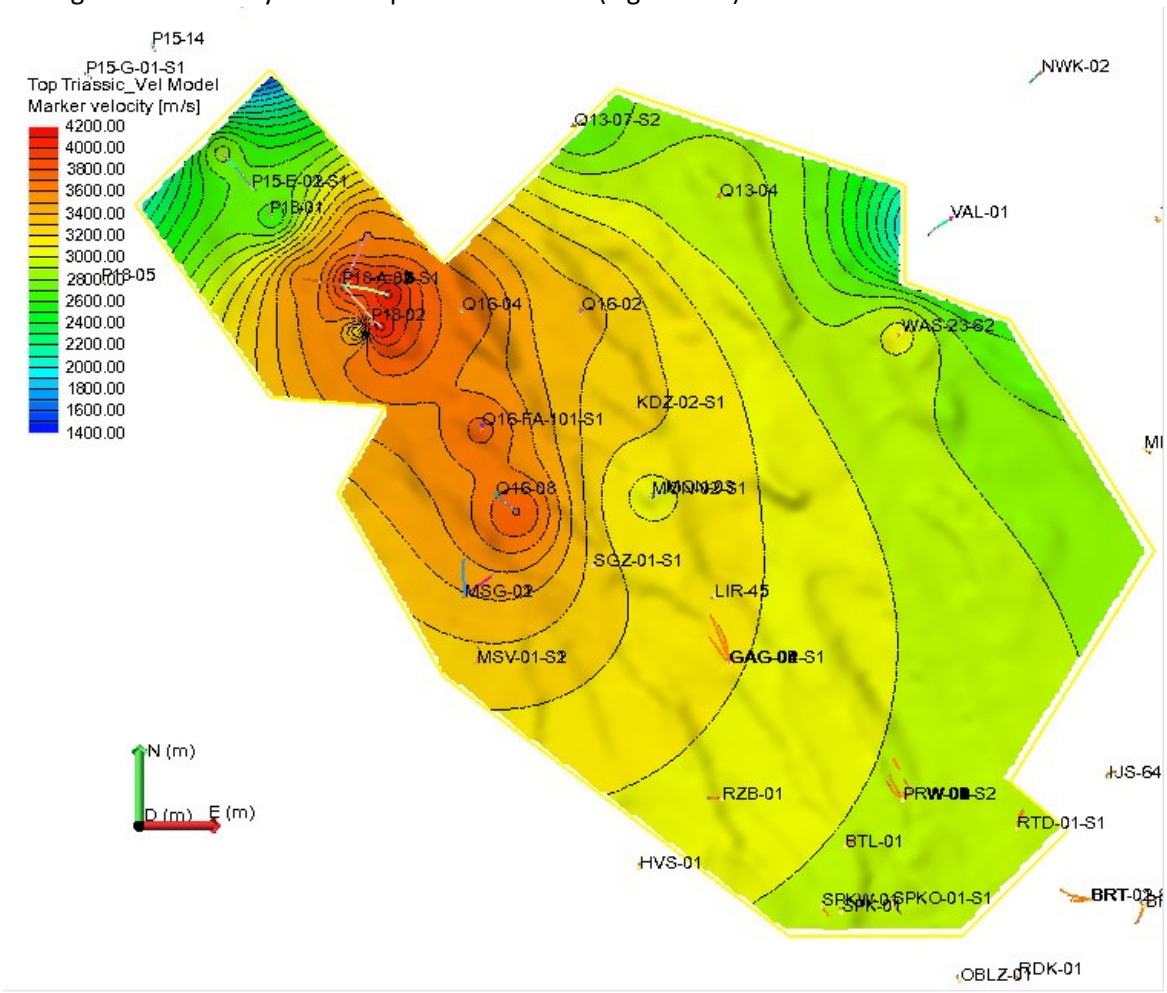

Figure 103: Marker velocity map for Top Triassic resulting from selected velocity model.

5.2.3. Constructing the structural geologic model and geological grids

After the velocity model is completed and tested the seismic interpretation of the important recognizable surfaces and faults are converted in the depth domain. The structural geologic model is constructed in a stepwise manner using the Top Triassic depth converted surface as a basis and guide for the underlying surfaces. The process requires that each level of the reservoir model is completed in hierarchical consequential order so that there is always a triangulated surface to guide the well picks interpolation that are used as basis for the construction of the new surfaces. The initial model that is used to the construction of the main surfaces is shown in Figure 103 with Top Triassic as the first step. The next surface that is included in the model is Base Solling followed by Base Main Buntsandstein (M Buntsandstein Base). Together they give the upper and lower boundaries of the reservoir section and are further used to guide the rest of the surface in the Main Buntsandstein section.

The original surface for Top Triassic does not contain discontinuities for the fault offsets and separations. It is very important to correct the initial guide surface so that it connects properly to the faults in order to be able to guide the following steps in the grid model workflow. The sequence for the correction of the surface starts

with creating cuts in the vicinity of the faults in the horizon. It is important to remove the parts of the horizon that are non-geological and show very steep dip angles in relative close distance from a fault. If required additional processes can be used to remove parts of the triangulated surface that are not affected by the fault distance tri-mesh removal process such as removal based on dip angle.

In order for this part of the procedure to be completed successfully, the fault model should be completed in such a way so that all of the faults connect to each other in a geologically reasonable way. It is important that they do not extend trough each other creating additional fault compartments as this would mislead the gridding and interpolation modules to create additional reservoir section at nonexistent locations. The faults are therefore merged, smoothed, extended or retracted until the fault model is complete and geologically correct. Also several additional faults have been added to the model as they were missing in the original seismic interpretation. The finalized model is shown in the figure below (Figure 99)

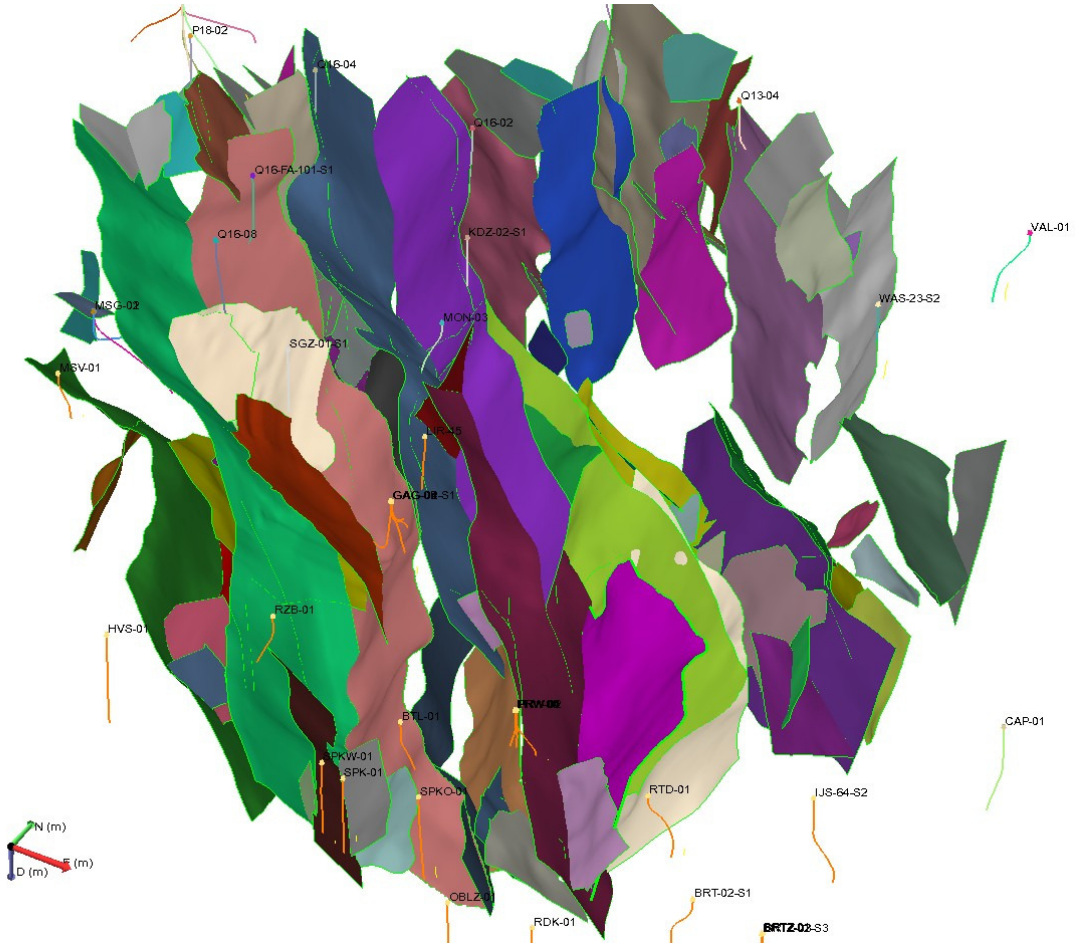

Figure 104: Fault model with already merged large faults. Faults area also soothed and edited for non-geological artifacts of the time to depth conversion and triangulation procedures.

The next step in the surface preparation for the structural geologic model is extending the horizons towards the faults or retracting the parts which are extending on the opposite side of a fault. The procedure is relatively straight forward but the actual work required may vary depending on the amount of detail and the amount of required corrections as almost each connection has to be reviewed in order to avoid introduction of leaking horizon to fault connection or non-geological extrapolations of horizons. A crucial role in the successful completion of this part of the workflow plays the resolution of the triangulated surfaces at the more difficult areas, or in other words the boundary triangle size or node frequency.

The most important consideration in this modelling exercise is to keep the model as close as possible to the realistic geological situation. The workflow is repeated until all of the interpreted surfaces from the well correlation study have their corresponding tridimensional triangulated surfaces in the structural and grid

models. The reservoir definition models for the whole study region (Figure 104) and for the more detailed target development regions (Figure 105) are shown below.

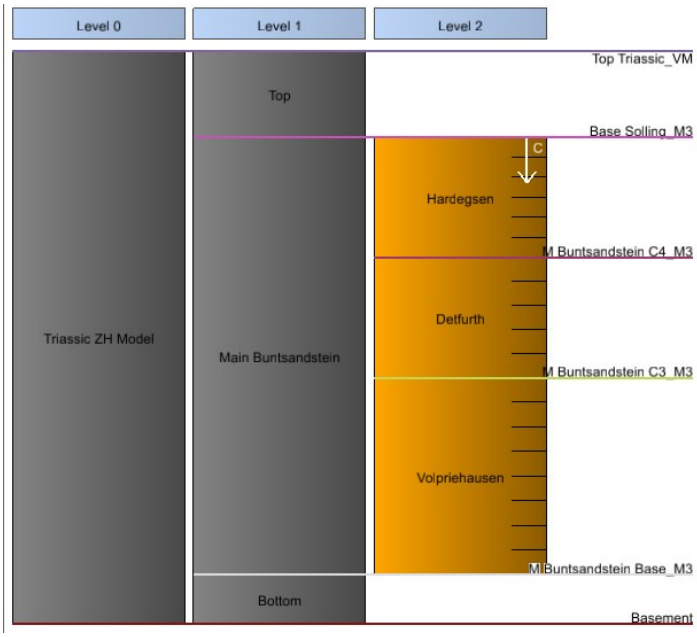

Figure 105: Reservoir layer definition model for coarse grid cell size model over the whole modeled area.

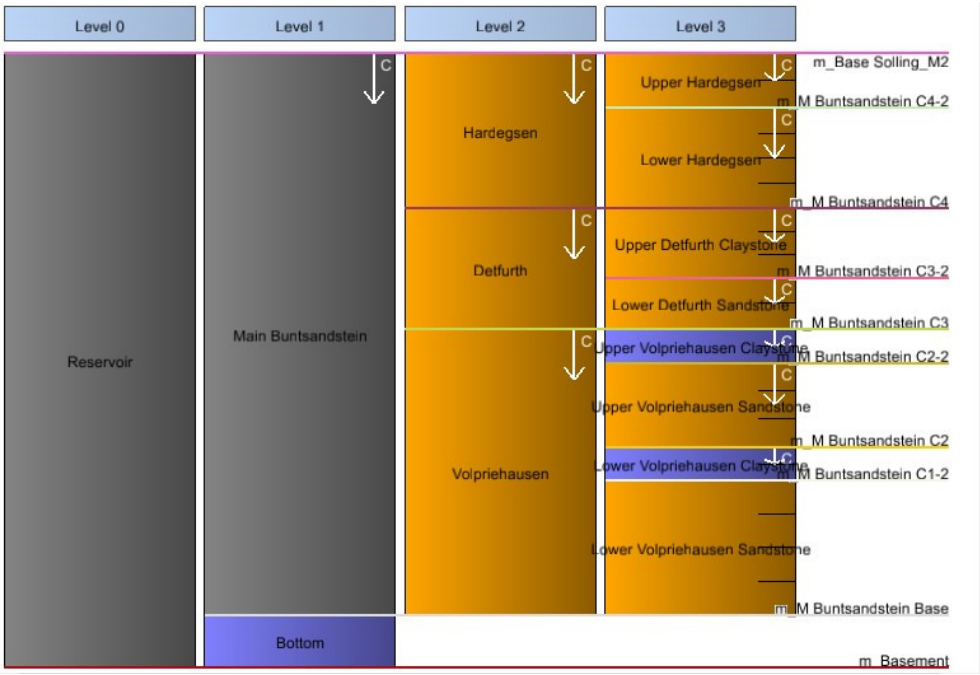

Figure 106: Reservoir layer definition model for all of the fine scale grid cell size geological and simulation grids. Note that name of the used surfaces varies according to the particular model.

An overview of the resulting structural geologic model can be seen in Figure 106. The final structural model is used as input for the final gridding processes for the different target areas. A complete list of all of the created grids including grid cell dimensions, grid area and basic list of reservoir properties modeled for that grid can the found in Table 9 below. The first grid that was created is called WNB Coarse which is short for West Netherlands Basin south west study region Coarse grid cell size grid. This grid is used to interpolate the porosity property using the largest amount of available wells in the area. The next two geological grids are called Maasland - Den Haag and Delfland respectively in order to refer to the major administrative areas that are found in their boundaries. With each level the amount of detail increases with the decreasing grid cell size dimensions. The final four grids are created as simulation grids and also include permeability property

models. They are more focused on the target fault blocks and therefore they contain little detail from the structural model.

	Grid type	Grid cell dimensions	Grid area	Porosity prop.	Perm. Prop.
WNB Coarse	Geological – master	200 x 200 m	1518.468 km^2	Yes	No
Maasland – Den Haag	Geological	75 x 75 m	281.291 km^2	Yes	No
Delfland	Geological	50 x 50 m	151.395 km^2	Yes	No
Delfland - SimGrid	Simulation	30 x 30 m	21.083 km^2	Yes	Yes
Maasland - SimGrid	Simulation	35 x 35 m	25.206 km^2	Yes	Yes
Haagland - SimGrid	Simulation	35 x 35 m	29.487 km^2	Yes	Yes
H v/n Holland SimGrid	Simulation	30 x 30 m	8.035 km^2	Yes	Yes

Table 9: List of created grids for the different project areas with basic dimensions and modeled properties.

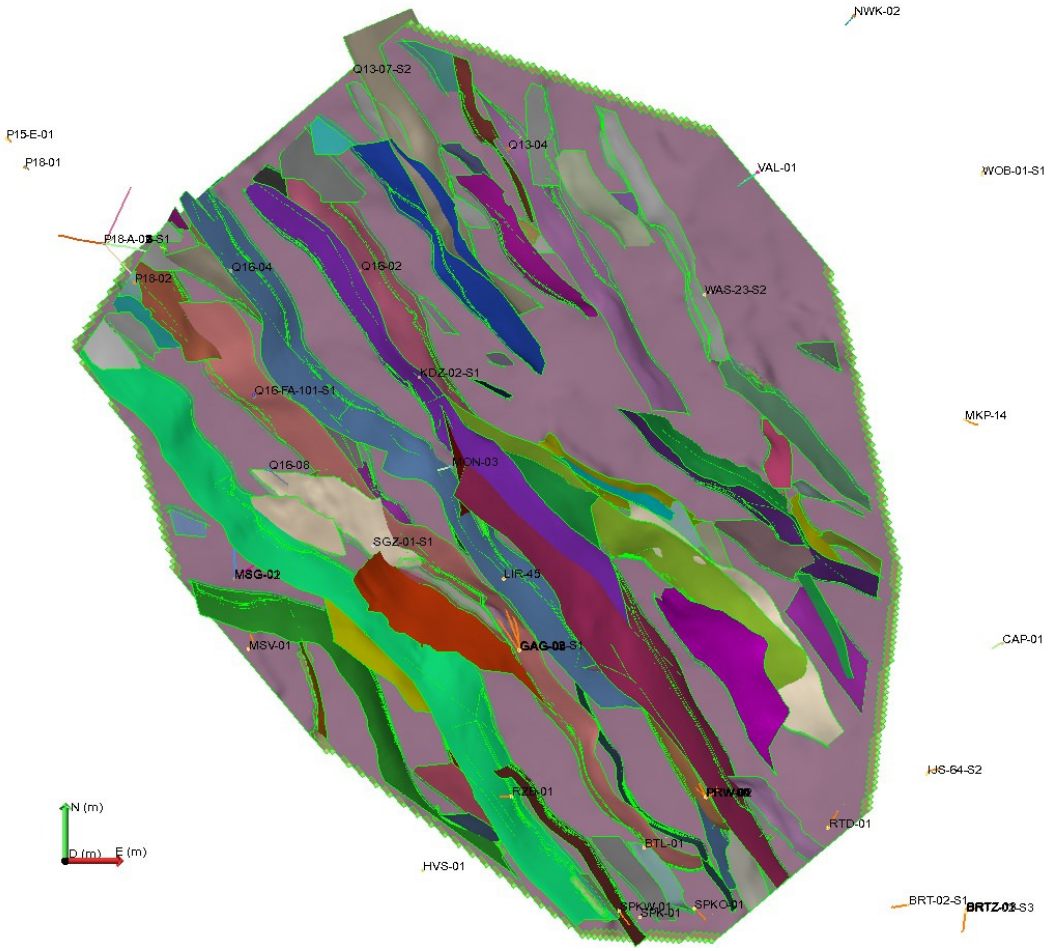

Figure 107: Faults and horizons model in depth in top view. Notice the area in the center of the model with only a few faults and relatively smoother horizon. This is area directly underneath Den Haag urban area and the quality of the seismic does not allow proper interpretation of faults and horizons.

The resulting surfaces for Base Solling or top of the reservoir section for the WNB Coarse (Figure 107) including the position of the target areas for the two detailed geological grids, and also the Base Solling surfaces for the Maasland – Den Haag and Delfland grids (Figure 108 and Figure 109) are shown below. Four additional fake wells called Interpolation wells D/M are used in the modelling process in order to help guide the software create correct reservoir thickness in fault blocks without available wells. Unfortunately the resulting models still show considerable amount of thickness discrepancies in such unexplored fault blocks and thus introduce additional uncertainty in those areas. This will be further reflected in the convoluted risk maps in the project feasibility evaluation chapter.

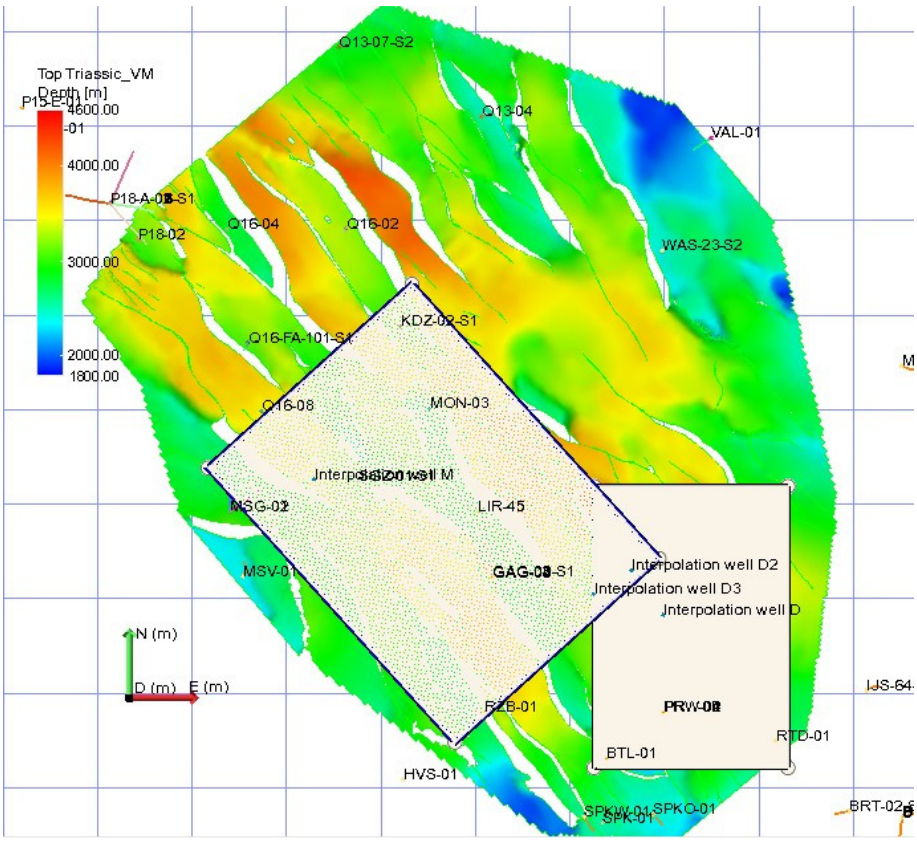

Figure 108: Horizon Top Triassic from general coarse grid cell size grid with target project areas Maasland-Den Haag on the left and Delfland on the right (in white). Additional fake wells called Interpolation well in both areas are also visible in this graphic.

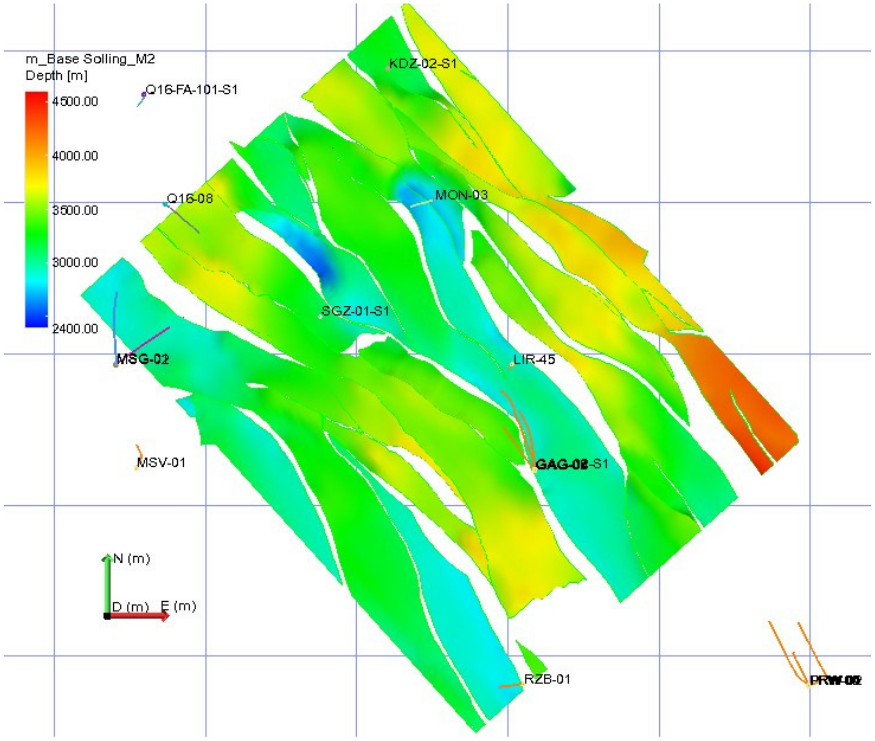

Figure 109: Base Solling horizon with depth property map for Maasland-Den Haag project area

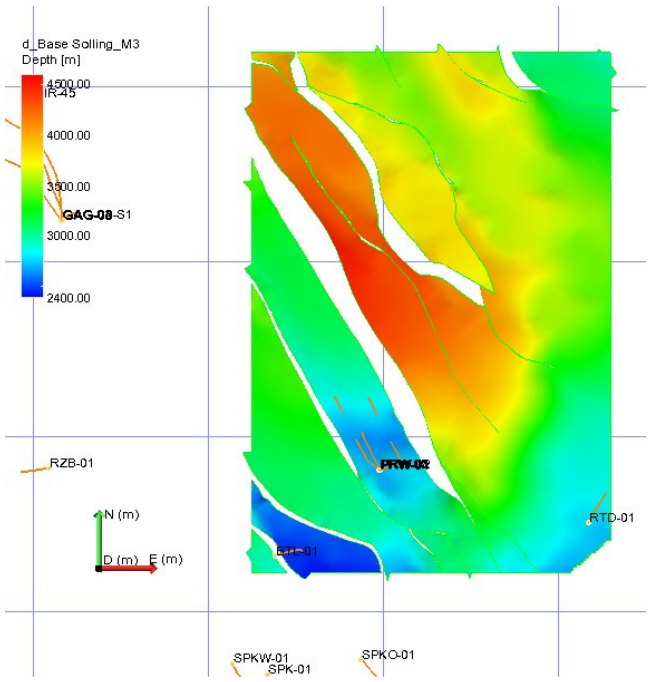

Figure 110: Base Solling horizon with depth property map for Delfland project area

The resulting detailed geological grids will be presented in detail in chapter 5.2.5 and 5.2.6 and the resulting simulation grid in chapter 5.2.4. In the figure below (Figure 110) the calculated from the already described relationship temperature is shown in top layer of Hardegsen in WNB Coarse grid.

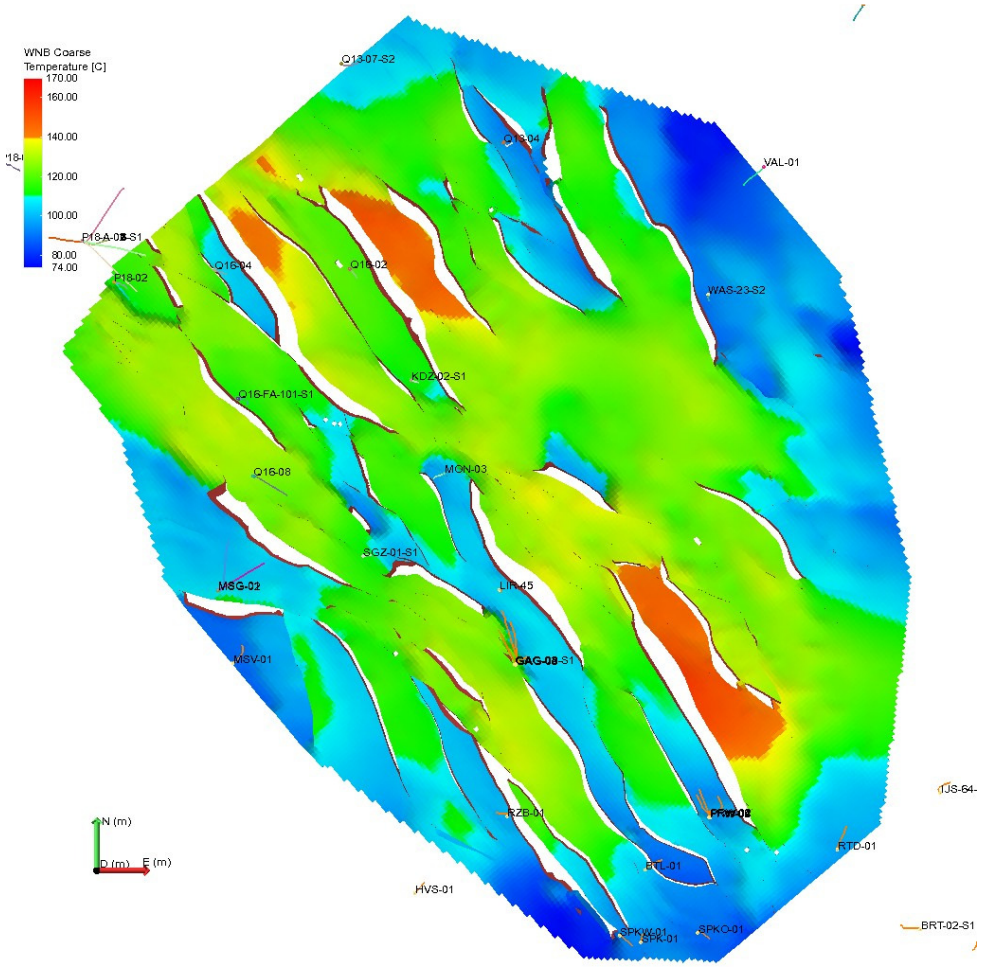

Figure 111: Temperature map for Top grid layer in Hardegsen. Red means suitable for heat and electricity production and yellow to green means suitable only for heat production.

5.2.4. Reservoir locations and considerations

The reservoir locations are selected using a number of criteria. The leading one is logically the temperature map which is used as starting basis for all evaluation maps as it provides the initial constraining requirement for this project. The second overlay is the expected reservoir quality guided by the available porosity data and the final consideration is given by the possibility for construction of surface facility and the proximity to possible users for the produced heat.

The following figures represent the results for the evaluation of the different factors and also show the suggested well trajectories and surface locations for the drilling operations.

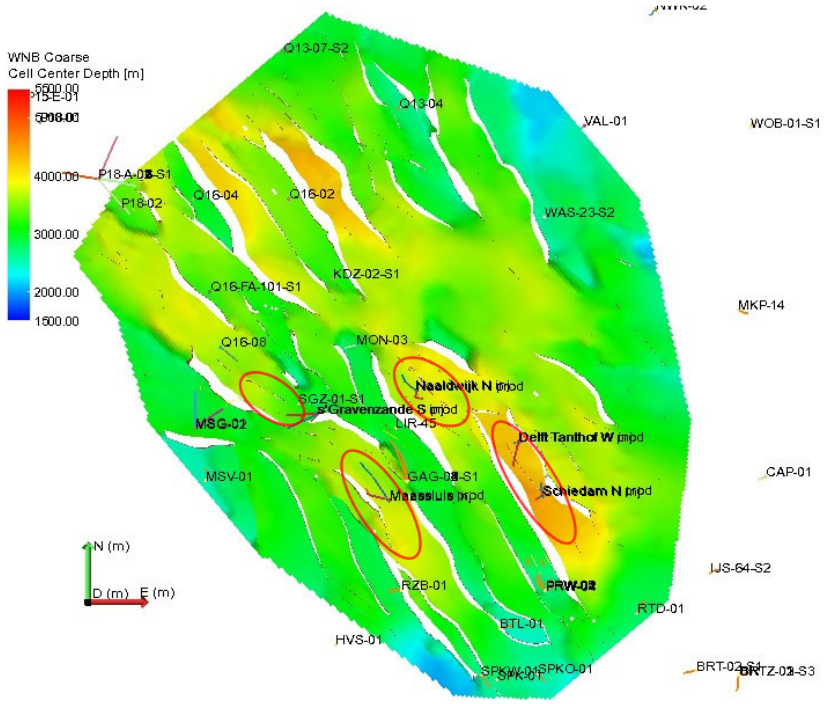

Figure 112: Suitable location for production of hot water from Triassic reservoir including suggested well locations in each target area.

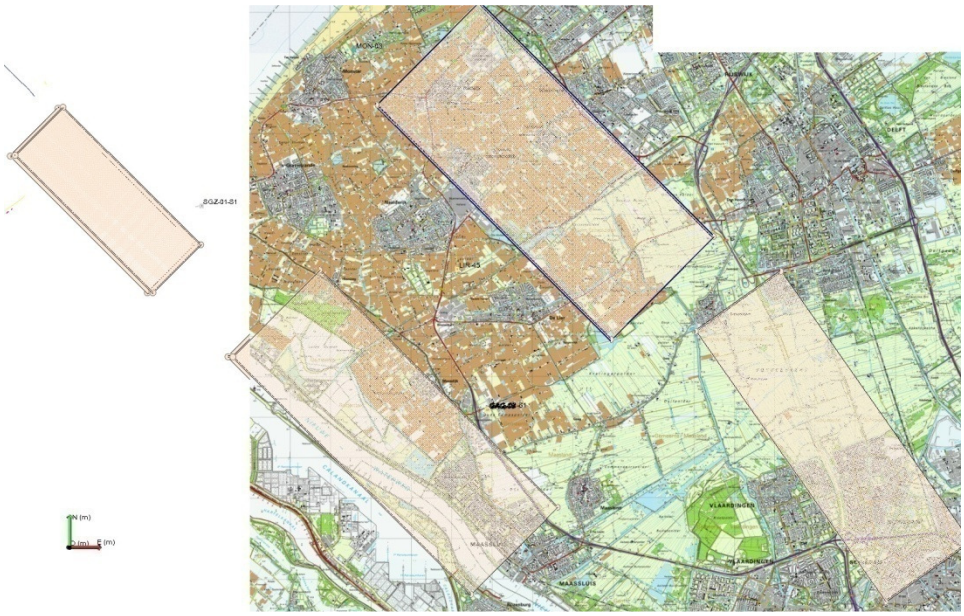

Figure 113: Surface administrative map with greenhouse clusters and target simulation areas. Note that the red ellipses from Figure 107 fall within the limits of the white rectangular meshes.

Figures 111 and 112 show a selection of four areas that qualify as possible target location for the development of geothermal facilities for hot water above 120 degrees C. The areas are also presented in terms of the surface location of the subsurface targets. It is important to plan ahead the project geographical locations as the lack of availability construction and drilling sites can lead the whole project to a halt. In the next figure (Figure 113) the selected surface locations are presented together with suggested well trajectories and the target reservoir layers with porosity property.

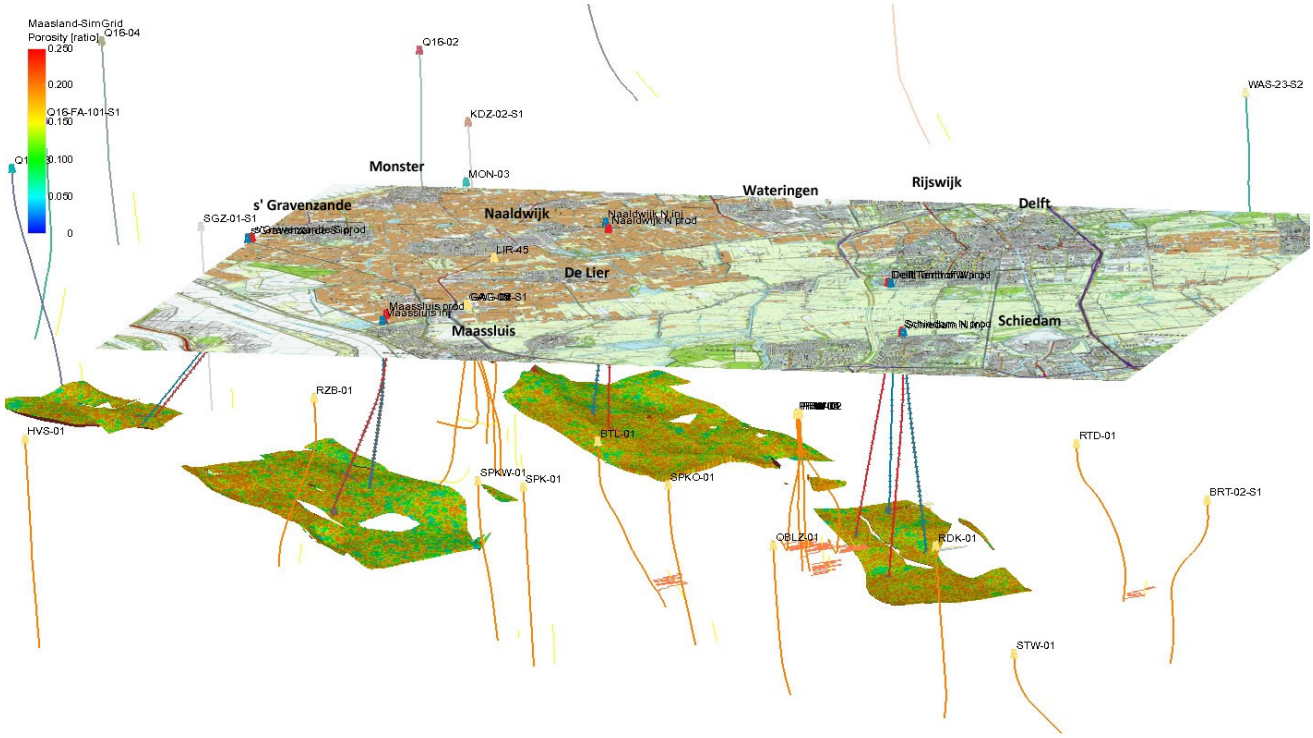

Figure 114: Target well locations and well trajectories with Hardegsen grid layers with porosity realization.

The suggested locations are focused on being only suggestive for the best possible zones for geothermal developments. There are other locations that can be developed especially in the south western region of the study area but they require special attention in order to avoid drilling into existing structural traps with gas accumulations as the area is known to be prolific in Carboniferous gas resources. This topic is further discussed in the chapter about risks and uncertainties.

5.2.5. Geostatistical considerations for the porosity property modelling

This sub-chapter describes the approach for the porosity property interpolation from the existing well locations into the whole study area. The model is build using the porosity logs calculated from combination of wireline logs and core analysis results. The porosity logs themselves are created in petrophysical software using a number of different methods depending on which method works best for the particular well data. The full list with the wells with logs and used methods can be seen below (Table 10)

Well ID	Core?	Cored Formation	Porosity method
BRT-02-S1	X		Shaly sand
BRTZ-01	yes	Hardegsen	Shaly sand
BTL-01	yes	Volpriehausen	Shaly sand
CAP-01	yes	multiple	o Sonic
GAG-02-S1	yes	Hardegsen	Sonic-Neutron
GAG-05	yes	Hardegsen	o Neutron
IJS-64-S2	yes	Hardegsen	Shaly sand (ed)

The porosity logs are calculated for wells in the study region. Most of them have also cored sections where the calculated logs can be calibrated towards the core analysis data. This calibration is however only accurate for the formations with cored intervals. Some discrepancy is observed for the other not cored formation leading to

KDZ-02-S1	yes	Hardegsen	o	Neutron
LIR-45	X			Shaly sand (ed)
MKP-14	X			Density-Neutron (ed)
MON-03	X			Shaly sand (ed)
MSG-01	yes	Hardegsen	o	Shaly sand (ed)
OBLZ-01	yes	Hardegsen		Sonic-Neutron
P15-01	X			Neutron (ed)
P18-01	yes	Hardegsen	o	Sonic
P18-02	yes	multiple		Sonic (ed)
PRW-01	yes	multiple	o	Shaly sand (ed)
Q13-04	yes	Detfurth	o	Neutron
Q13-07-S2	yes	Hardegsen +	o	Shaly sand (ed)
Q16-02	yes	Detfurth	o	Sonic
Q16-04	X			Sonic
Q16-08	yes	Detfurth		Density-Neutron (ed)
RTD-01	yes	Hardegsen	o	Shaly sand (ed)
RZB-01	yes	Hardegsen		Sonic
SGZ-01-S1	yes	Hardegsen		Density
SPKO-01-S1	yes	Hardegsen		Shaly sand (ed)
SPKW-01	yes	Hardegsen	o	Density
VAL-01	yes	Volpriehausen		Sonic
WAS-23-S2	X			Density

Table 10: List of wells for which PHI logs are created and list of methods used for porosity calculation. Wells with cores have the PHI logs calibrated to the core analysis data.

local over- or underestimation of the porosity property in the model. This is further taken into consideration in the uncertainty evaluation in later chapters.

In the table to the left wells with cores and core photographs are shown with a sign next to them (o). Such wells can be used in a more detailed modelling attempt where individual facies can be digitized in the well logs and then simulated in the target formation in order to get even more accurate model for the property distributions in the study area.

Short explanations for the used methods for the porosity calculation as used in the petrophysical software (Tigress) are presented below. Note that these explanations are only very basic view on the procedures in order to clarify the approach for calculations.

The general workflow for the petrophysical evaluation starts with the calculation of the clay volume. In this study the V clay is derived using gamma-ray method with individual minimum GR (clean sand) and maximum GR (shale) lines for each separate formation.

$$V_{clay} = (GR_{value} - GR_{min\text{-}formation}) / (GR_{max\text{-}formation} - GR_{min\text{-}formation})$$

This approach was selected in order to reduce the possibility of cross-influences between porosity calculations in different formations. After the V clay curve is derived for the whole studied interval it is used as a basis for the further calculations.

It is generally preferred to use a cross plot or density corrected method for the calculation. Only in the cases where there is only single wireline log available for the targeted interval a single log method is used. Such are Sonic, Density and Neutron. For example Sonic Wyllie method uses the sonic (slowness) log to calculate porosity log and then it is corrected for the calculated V clay. An example workflow is presented below:

$$PHI_{eff}\ (\text{Sonic Wyllie}) = PHI_{sonic} - V_{clay} * PHI_{sonic\ shale}, \text{ where:}$$

- DTC is the sonic reading from the sonic tool
- KCP is the sonic compaction factor = max(1, DTC_{shale}/(328 – metric, 100 – English))
- $PHI_{sonic} = (DTC - DTC_{matrix}) * KCP / (DTC_{water\ sat} - DTC_{matrix})$
- $PHI_{sonic\ shale} = (DTC_{shale} - DTC_{matrix}) * KCP / (DTC_{water\ sat} - DTC_{matrix})$

The method that was used most often was open hole porosity calculation using shaly sand method. This method calculates porosity from V clay curve as derived from Density Neutron cross plot analysis. The following workflow is representative for Shaly Sand but also for Density, Neutron and different cross plot methods so the references for the reading are shown in a more generalized way below:

$$PHI_{eff}\ (\text{Shaly Sand/Density Neutron/Other}) =$$
$$PHI_{effective} * S_{xo} * PHI_{water\ saturated} + V_{clay} * PHI_{shale} + (1 - V_{clay} - PHI_{effective}) * SUM\ (V_{matrix} * PHI_{matrix})$$

In the case where Density-Neutron combination is used if $PHI_{neutron} > PHI_{density}$ then:

$PHI_{cross\ plot} = (PHI_{density} * PHI_{neutron\ shale} - PHI_{neutron} * PHI_{density\ shale}) / (PHI_{neutron\ shale} - PHI_{density\ shale})$, where:

- $PHI_{(log)\ shale} = (Reading_{shale} - Reading_{matrix})$ [* *Compaction f.*] / $(Reading_{water\ sat} - Reading_{matrix})$
- $PHI_{(log)} = (Reading_{(log)} - Reading_{matrix})$ [* *Compaction f.*] / $(Reading_{water\ sat} - Reading_{matrix})$
- $PHI_{(log)\ corrected} = PHI_{(log)} - V_{clay} * PHI_{(log)\ shale}$
- Compaction factor is applied for calculations involving sonic log methods.

In the cases where other logs are cross plotted the corresponding reading are used in the formulas.
Correction for total porosity: $V_{clay} * (RHO_{matrix} - RHO_{clay}) / (RHO_{matrix} - RHO_{fluid})$ where RHO is bulk density has not been applied due to time limitations and only effective porosity logs were used in the modelling.
The choice of the method used for each well is based on the actual match between the depth corrected core analysis data and calculated PHI log with all available porosity calculation methods for the well.

After the PHI logs are prepared and edited for unnatural peaks and other oddities they are imported into the static geologic modelling software. The porosity property is used as the main modelling parameter and guide for the rest of the modelled reservoir parameters. The next step of the modelling process has the purpose to analyse the input porosity log data and to prepare the geostatistical modelling parameters. Two different processes are used in the modelling approach – Distance weighted interpolation and Sequential Gaussian Co-Simulation using ordinary kriging interpolation algorithm. They are further explained in the modelling flowchart (Figure 118).

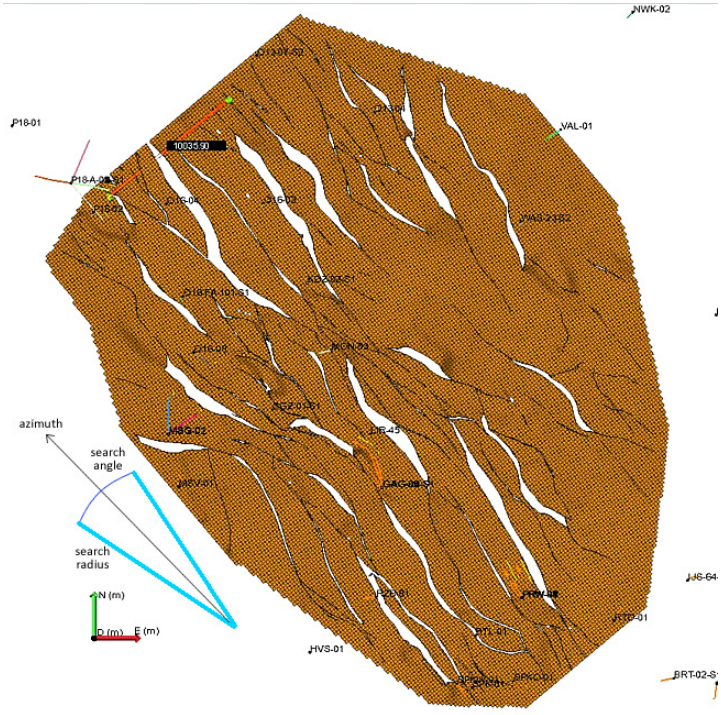

Figure 115: Schematic presentation of the geostatistical parameters for the SGS simulation

List of parameters that were modified for the SGS co-simulations for porosity measurements.

Covariance kriging statistical parameters:

Sill is the value for the squared variance (γ) of the examined variable at maximum correlation range. Nugget is the initial value for the variance. Nugget was selected to be 0 while the sill varies between different grids and formations and is typically in the range of 0.0025 and 0.0035 ratio^2.

$$\gamma(x,y) = E[(Z(x) - Z(y))^2]$$

Search radius for correlation statistics is defined in lateral and vertical direction with maximum and minimal values. In the case of this modelling study larger models have radii of 12500 to 15000 meters, while smaller model only of 5000 meters.

Azimuth for the correlations is used to give the orientation for the statistical evaluation search algorithm. In the case the usual value for the azimuth has been chosen to be 315 degrees following the fault trend in the basin.
Search ellipsoid neighbourhood parameters are also defined with corresponding to the current model values. These include maximum, mean and minimum radii and around X Y and Z angles.
The kriging process calculates the estimator based on the assigned variance from the derived variogram and interpolates property values guided from the available data and limiting factors.

$\hat{Z}(x^*) = [\lambda_{1...n}]' * [Z(x_1) ... Z(x_n)]$ where λ are the weights calculated from the variogram.

The workflow for the property modelling starts with analysis of the log input data statistics. This includes analyzing the porosity property distribution histogram (Figure 116) and correlation variogram (Figure 115). The results from the analysis are used as input for the geostatistical interpolation modelling methods such as Kriging, Co-Kriging, Sequential Gaussian Simulation and Sequential Gaussian Co-Simulation.
It was already mentioned that in order to meet the requirements for geothermal applications in terms of hourly flow rate only reservoirs of relatively good quality are considered. In the case of Main Buntsandstein subgroup this implies that the main target is Hardegsen formation. It is therefore logical to put the largest amount of effort to create a consistent and effective model for the porosity distribution. The depositional environment as discussed in chapter 2 of this work is considered to be of an arid desert environment with ephemeral lake in the basin center causing regular fluctuations in the ground water level and abruptly terminating seasonal channel systems. The resulting relief is expected to be slightly undulating with no distinctive large scale desert dune systems. If the effect of the early diagenesis is considered as the cause of variations in cementation and compaction it can be assumed that the resulting pattern of better reservoir quality zones will be relatively patchy. This means that zones of better porosities and permeabilities will be spread out in the formation in relatively random manner. It is therefore safe to assume that a Sequential Gaussian simulation and co-simulation can deliver a reasonably accurate model for the Hardegsen formation porosity model.

The connectivity of zones with high permeability is not completely clear and requires further work. It is not considered as constraining factor for the modelling study. In other words the amount of connected zones is controlled by the random Gaussian field simulation and is a direct derivative of the log input statistics.

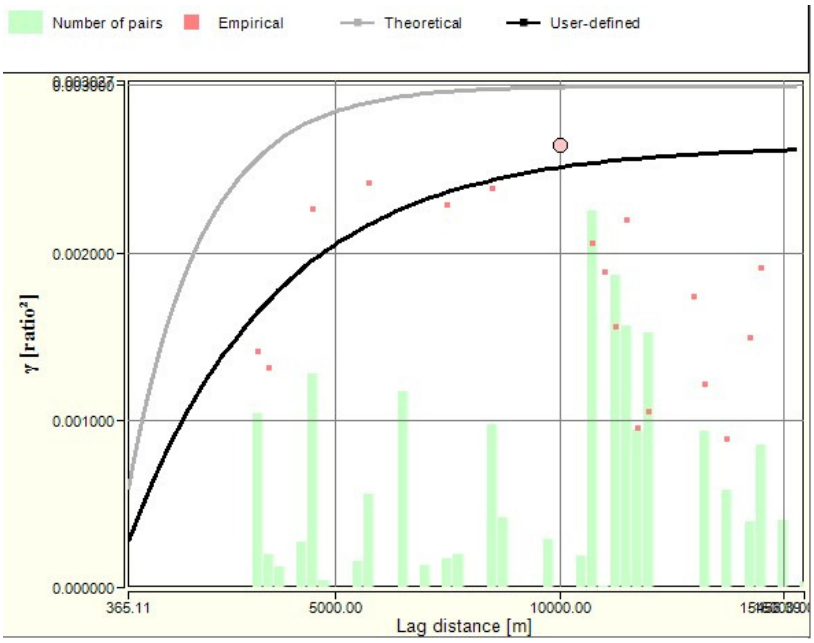

Figure 116: Variogram calculated from the original log PHI data.

The histogram for the original data (Figure 116) shows that it is relatively normally distributed. The large amount of values between 0.000 and 0.026 is attributed to the fact that some wells don't penetrate the whole Main Buntsandstein section while the statistical evaluation includes the complete interval. As a result parts of the studied interval have values automatically set to zero for the statistical analysis while in reality there is no data to be used in the modelling algorithm there.
On the second histogram (Figure 116) the porosity from the interpolated model is shown. The mean value is the same but now the whole model is populated and the histogram is closer to the normal distribution.

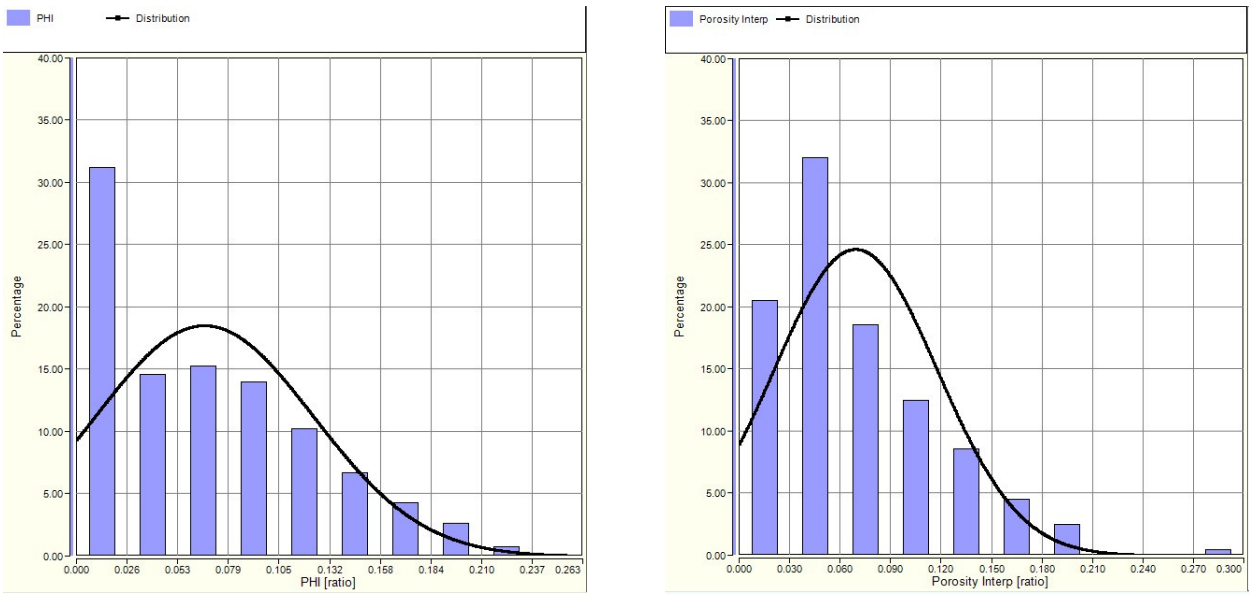

Figure 117: Histograms for PHI (porosity) from logs and Porosity interpreted in the WNB Coarse geological grid using Distance weighted interpolation with power 2. Note the shift towards the average value.

5.2.6. Porosity and permeability models

In this sub-chapter the modelling approach for the porosity and permeability models will be presented and explained. There are several important considerations that need to be taken into account for the models. The first and most important one is focused on the general decision to model only porosity in the models while other properties are only linked to the porosity model with relationships that are location and formation dependant. Although this approach saves time and gives very good control over the amount of detail and random factor influence on the resulting models, it can also introduce additional problems such as over-parameterization of the models. This means that there is very high direct correlation between different parameters in the model. As a result of that the risk of error propagation in the model is significantly increased and might lead to inaccurate results. This issue is taken into consideration in the modelling process and has been solved by implementing several different modelling steps at different detail levels. Each steps incorporates introduction of small random seed in the geostatistical interpolation and therefore helps avoid

The actual modelling approach for the porosity property is given in the following two flowcharts. The second one is a continuation of the first as it covers level two and three grid models. Each following level has finer grid cell size.

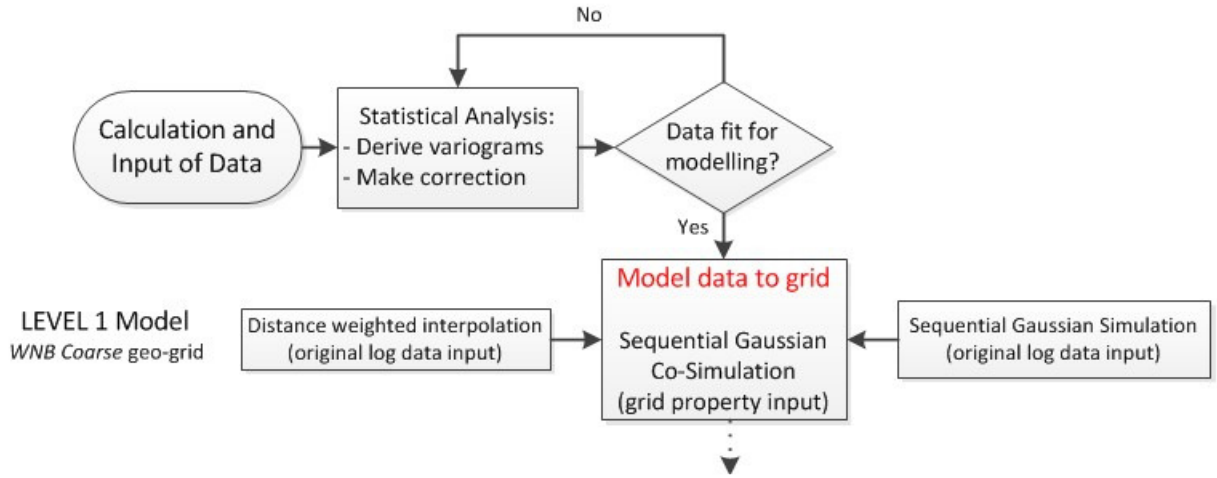

Figure 118: Workflow for the first level grid that covers the whole study region (WNB Coarse)

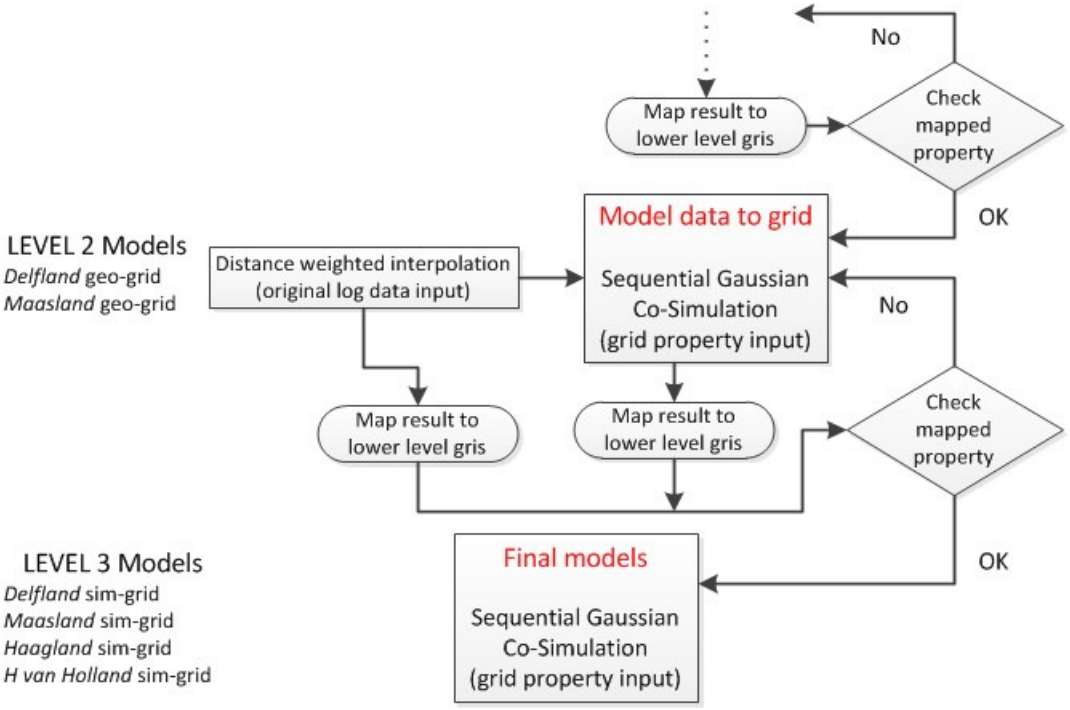

Figure 119: Workflow for the next two level of the modelling approach for the finer grid models

From the presented flow charts it can be observed that each modelling level incorporates a Sequential Gaussian Co-Simulation of the distance weighted interpolated log data and Gaussian field simulation with the derived statistical parameters of the original log data. In principle this constrains the eventual outcome of the modelling to the PHI log data, however the introduction of four subsequent steps of random seed multiplication and two of grid refinement keeps the bias of the modelling results at sufficiently low level.

The results of the first level modelling are shown in the figures below (Figure 119 and Figure 120)

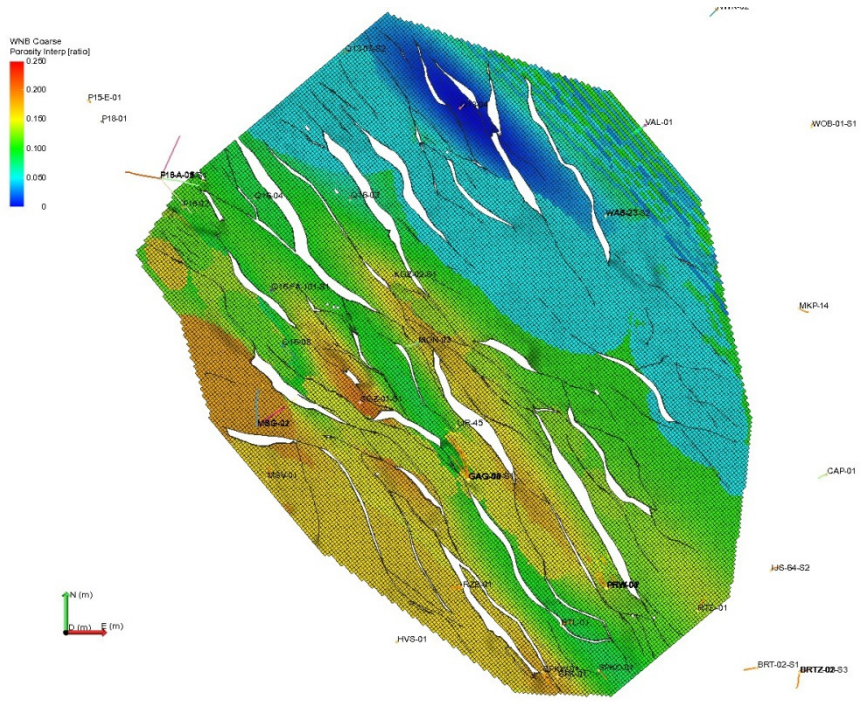

Figure 120: Porosity property as modeled by Distance weighted interpolation with power 2 using all of the available wells in the study region. Layer is top layer of Hardegsen.

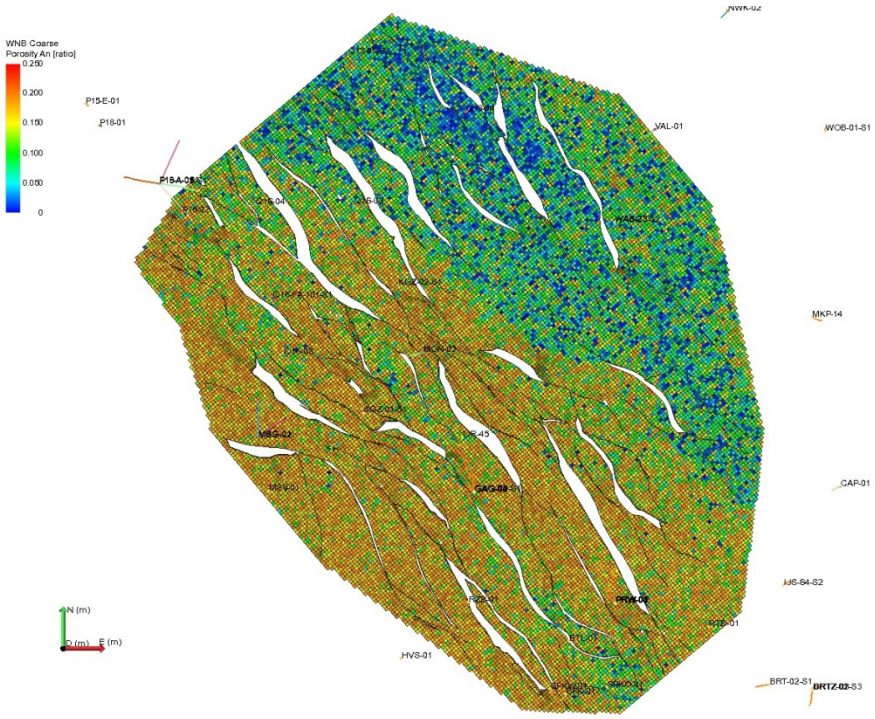

Figure 121: A co-simulation of the result from the interpolated porosity results and Sequential Gaussian simulation outcome using the interpolated results. Layer is top layer of Hardegsen

After each Sequential Gaussian Co-Simulation the results are mapped to the finer lower level grids and reviewed from two points of view. The first criterion for the evaluation of the modelling result is oriented towards determining of the model fits the original geological expectations for the porosity distribution based on the depositional environment and diagenetic history. The second criterion is to evaluate the mapping algorithm as the next level finer grid cell size grid requires introduction of more detail in the property distribution. As these new details are inferred from the previous level model some error can be introduced. If any discrepancies are found the modelling is repeated and remapped so that the eventual result satisfies the requirements for the next step of the modelling process. In general this iterative approach is applied to most of the modelling and interpretation studies part of this work as it is considered very robust way to avoid introduction of unexpected errors in the results.

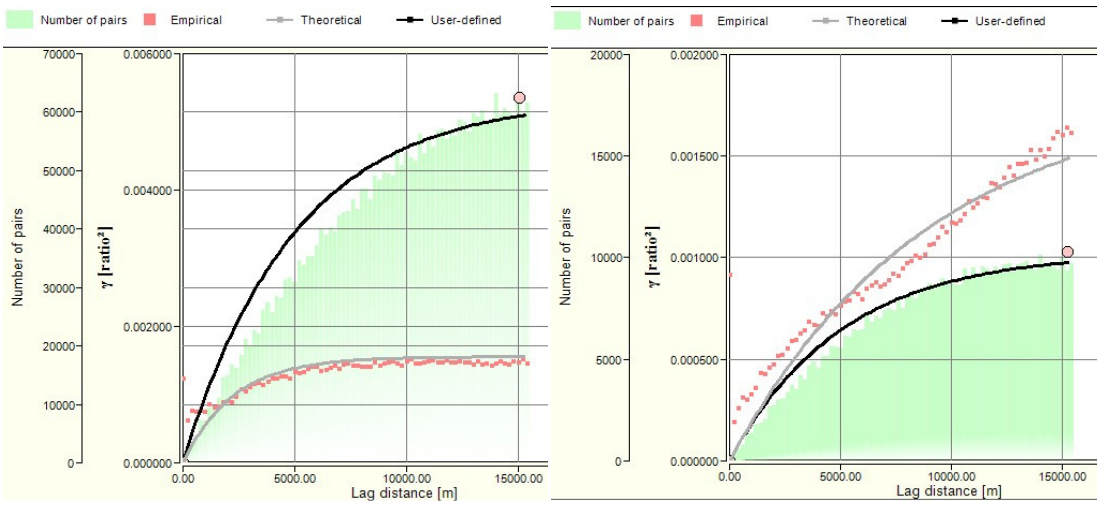

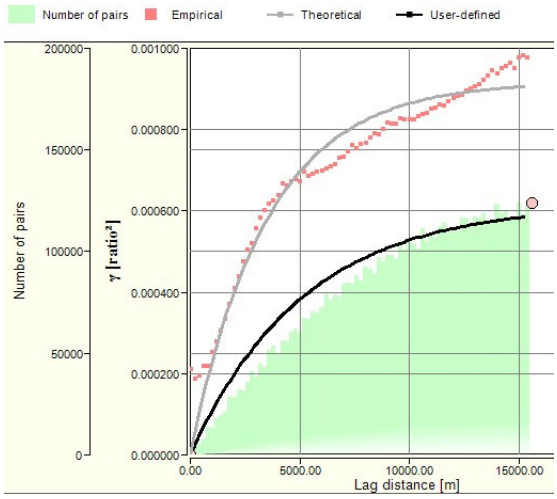

Figure 122: Variograms for the porosity models in (left to right) Hardegsen, Detfurth and Volpriehausen (on the second row) formations in the WNB Coarse grid combined Distance weighted interpolation with Sequential Gaussian field co-simulation.

After the creation of the models for each level the statistics for the resulting property distributions are examined in order to determine if the models fit the expectations. The variograms of the modeled porosity for the first level models per formation are shown below. The reason to show the variograms divided per formation is because porosity is modeled separately for each formation in order to incorporate the presented ideas for the different depositional nature of the sediments of the different formations of the Main Buntsandstein sub-group.

The porosity models for the level 2 grids are presented below. Figure 122 shows the porosity property result in Hardegsen formation. This is the model before mapping it to the next level grids.

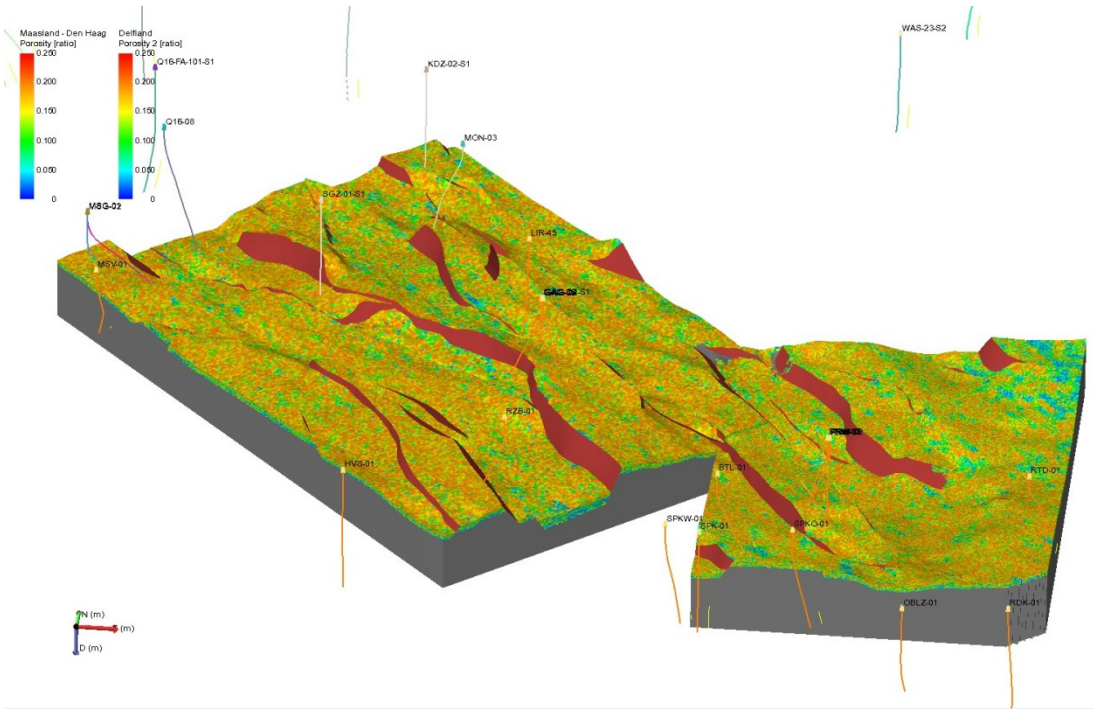

Figure 123: Porosity models for Hardegsen formation in both fine grid cell geological target area grids.

Below (Figure 123) a comparison for the original PHI log data and the modeled grid porosity property for the WNB Coarse and for Delfland geological fine grid is presented. It is clearly visible that the fine grid cells size grid offers a better upscaled representation of the original PHI logs.

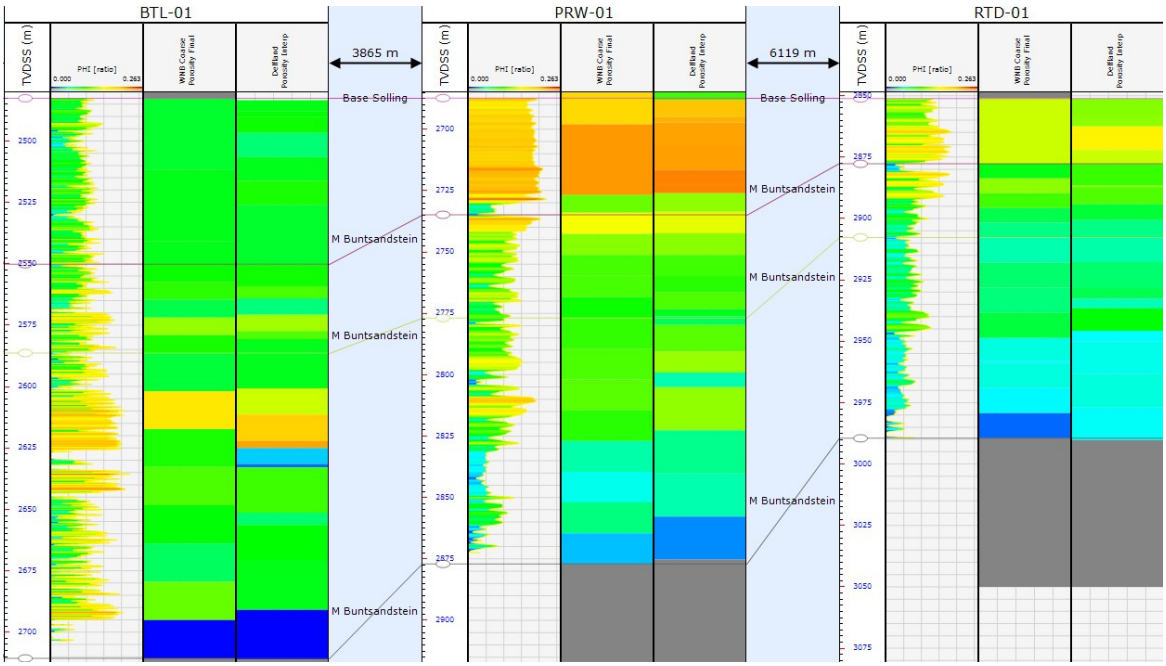

Figure 124: Comparison for the amount of detail in the coarse grid cell size grid (second column) and finer grid cell size grid from Delfland (third column) upscaled interpolations and the original PHI log (left)

After the final porosity models are prepared and evaluated for the quality of the result other properties can be modeled to the simulation grid. The porosity is used as the guiding property for all of the other properties which include horizontal permeability ($k_x = k_y$), vertical permeability (k_z) and net over gross (ntg). For the horizontal permeability the already described relationships derived from the petrophysical evaluations are used. They are shown in the table below (Table 11), and for graphical representation of the relationships refer to Figure 96 in sub-chapter 5.1.2.

	Hardegsen	Detfurth & Volpriehausen	
South West region	$\mathbf{k} = 7.295 * e^{(21.85 * \mathbf{PHI})}$	$\mathbf{k} = 0.75 * e^{(35 * \mathbf{PHI})}$	• Maasland SimGrid • Hoek van Holland SimGrid
Anywhere else	$\mathbf{k} = 7.493 * e^{(15.224 * \mathbf{PHI})}$	$\mathbf{k} = 0.005 * e^{(52.6 * \mathbf{PHI})}$	• Haagland SimGrid • Delfland SimGrid

Table 11: Porosity – permeability relationships used in this study per formation and region (grid)

Vertical permeability is considered as derivative of the horizontal according to the relation $k_z = 0.1*k_y$. The choice is made after analyzing the limited available data for k_v / k_h measurements from core analysis. Values for the ratio recorded are highly dependent on the type of lithofacies and range from 0.001 to 0.3. Therefore an average value of 0.1 is selected for the purposes of this study. Net over gross is based on the porosity model and is calculated with 9% porosity as cut-off value.

The resulting models for the porosity and permeability are presented in the figures below (Figure 124 and Figure 125). The whole workflow for the modelling is designed so that the general basin trends can be applied to the target interest areas although they contain no wells or other directly collected data. It is important to keep this remark in mind as different target areas are also subjects to different amount of accumulated uncertainty and therefore the amount of total risk related to them is also different. This topic is further explained in the next sub-chapter.

Underneath the porosity and permeability models, the net over gross model is also shown (Figure 126). White represents net reservoir and black non-reservoir. This is not directly correlatable to net sand model as some of the tightly compacted and cemented sands are excluded from the net reservoir calculation.

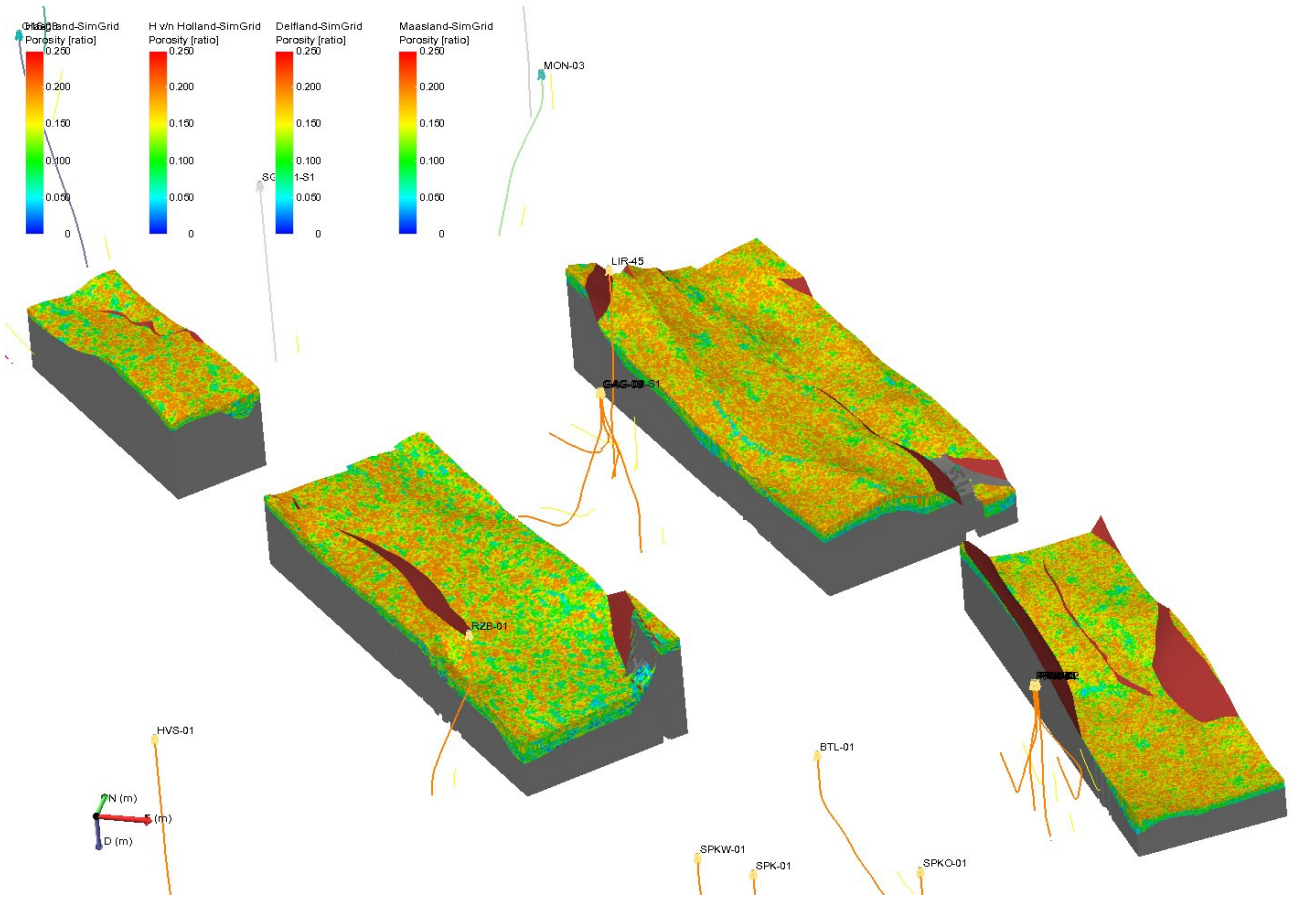

Figure 125: Target simulation grids final porosity models after the last SGCoS modelling step.

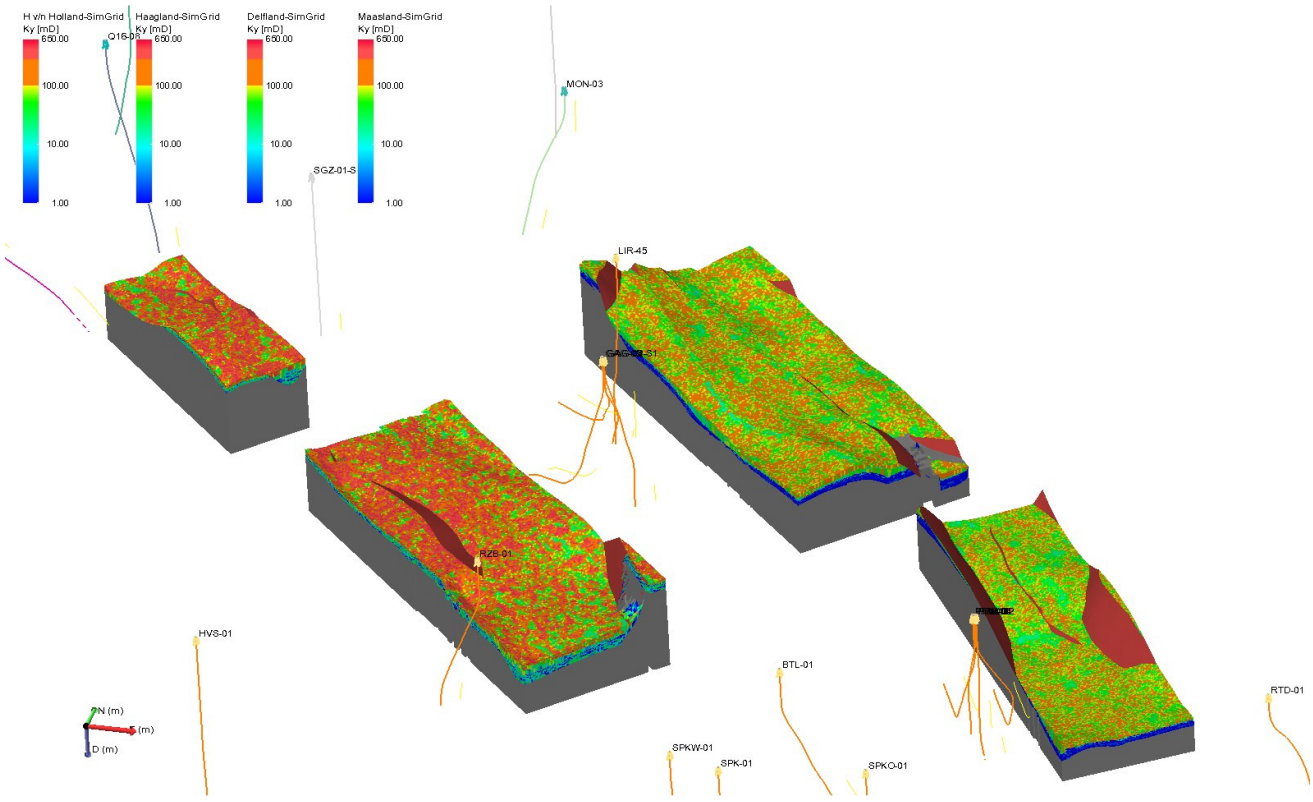

Figure 126: Target simulation grids permeability models created from the described relationships per region.

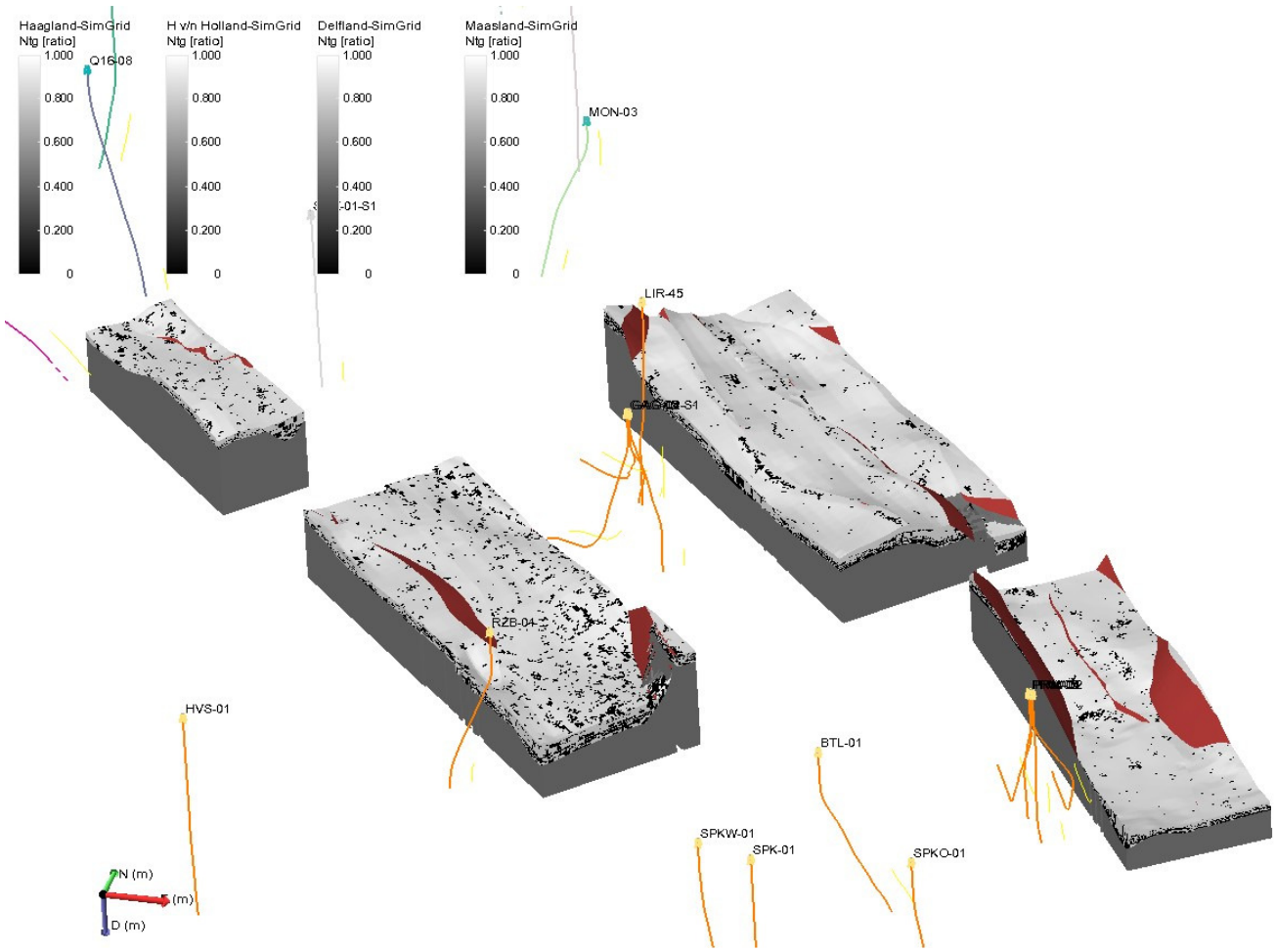

Figure 127: Net over gross models based on porosity cut off value of 9%

5.2.7. Evaluation of uncertainty in models

There are several major sources of uncertainty for the models in this study. They all relate to the fact that deeper fault blocks have almost never been penetrated by exploration wells. On the other hand they are the targets for future exploration related to geothermal energy exploitation and thus require careful analysis of all of the factors that influence the risks associated to reservoir quality and structure.
The main uncertainties that are going to be evaluated in this section are therefore

- The depth of the target reservoir
- The reliability of the modeled reservoir properties
- The lateral continuation of the target formation
- The quality of the input seismic data

The way the suggested uncertainties maps are going to be presented is as convoluted risk map. The basal fundament for the map is the calculated temperature map while the rest of the factors are given as areas of strong risk and areas of less risk. The final figure that combines the result of the convoluted map assessment is a map of total evaluated risk over the study region.

The underlay basal map also contains uncertainties related to the quality of the time to depth conversion velocity model that was used to convert Top Triassic seismic interpretation. The major problem with the velocity model is related to the difficulties in determining which actual formation pick corresponds to the seismic reflector that was interpreted. Although it is assumed that Top Triassic reflector corresponds to the Dolomitic Keuper formation, the lateral discontinuities of the formation might lead to some misinterpretations. Another source of uncertainty is related to the actual interpolation techniques used by the modelling software to calculate the velocity model. The same type of error is also expected to have influence on the actual horizon interpolation from the gridding algorithm. It is observed that the modelling software has considerable difficulties with interpolation of horizons in fault blocks that are completely

disconnected by surrounding fault blocks and have no existing wells drilled in them. The amount of error can range between 200 and 400 meters. This issue has been addressed in the modelling process by inclusion of fake interpolation wells in those fault blocks in order to guide the algorithm to better results.

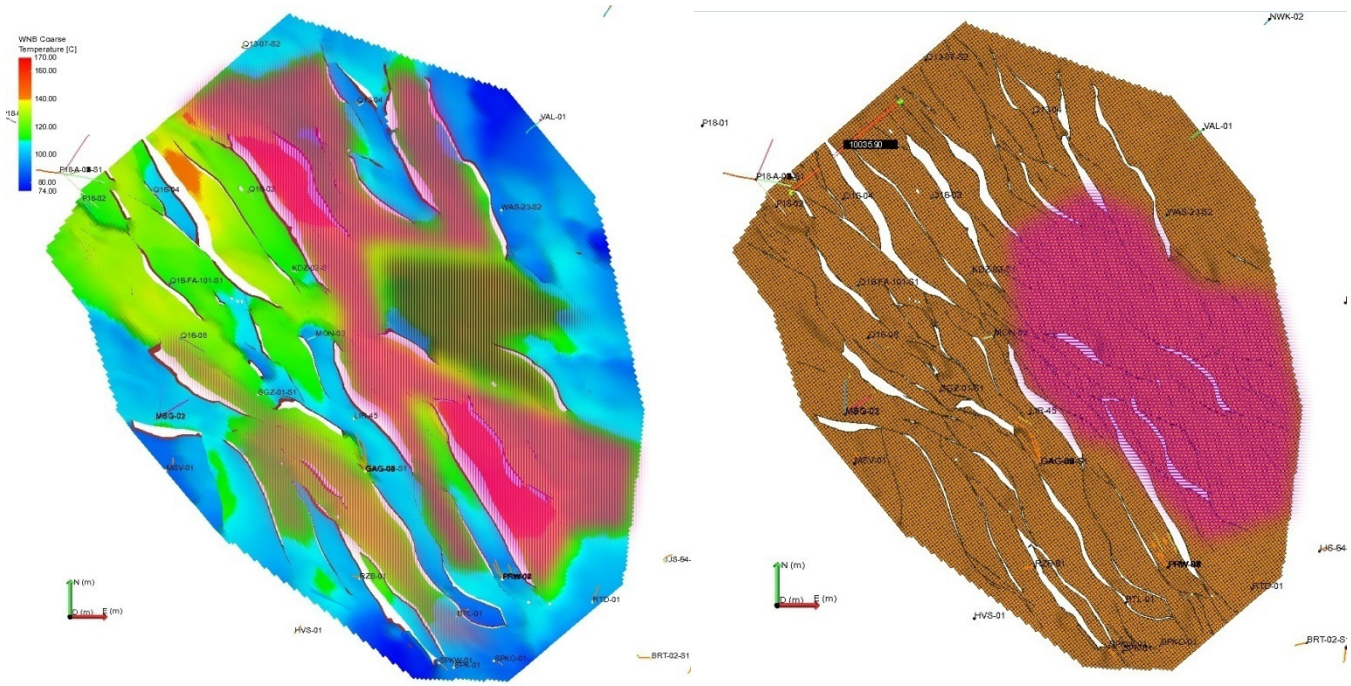

Figure 128: (to the left) Uncertainty map for the structural and depth uncertainty based on the velocity model interpolations and software horizons interpolation errors both influenced by the lack of well data. (to the right) Area of uncertainty related to property spatial distribution uncertainty due to severe lack of well data given as a purple stripped area. In the rest of the modeled are a sufficiently good prediction can be made based on the depositional environment analysis and expectations.

In the figure above (Figure 127) three different degrees of uncertainty are visible. In the south corner the uncertainty for the structural model is least, whereas the next deep fault block without well penetration to the north has larger uncertainty due to the decreased density of drilled wells and thus has a darker shade of purple. There is a region in the centre of the northern region of uncertainty where the available seismic data quality is significantly affected by the densely urbanized area. This introduces even more uncertainty on all levels and therefore this region has yet darker shade of purple. The northern target areas are also affected in terms of model uncertainty by the unknown spatial distribution of the reservoir qualities and formation thicknesses due to the complete lack of data over a very large region.

All this information combined can be used to evaluate the risk in individual simulation grids. In order to give a quick and easy to understand estimation of the convoluted risk a system involving a grading scale of 1 to 4 is used to describe the results in each simulation-target grid. The scale is such that 1 means “There are risks involved but the predictability of the model is good”, 2 means “There are risks but the predictability of the model is sufficient”, 3 means “There are risks and the predictability of the model is questionable. The target area is still a good prospect”, and 4 means “There are risks and serious question for the predictability of the model. Additional analysis is required in order to render the model a prospect”.
Risk level 1 and 2 are generally related to areas that have sufficient density of available well data in the vicinity. The spatial separation from the drilled exploration wells is the factor controlling the choice of risk level. Levels 3 and 4 are related to areas of limited amount of exploration wells. Level 4 in particular is also related to significant questionability of the input data.

The result of the evaluation is shown in the next figure (Figure 128). Recommendations for decreasing the amount of risk in the high risk models are given in the last sub-chapter of this modelling chapter.

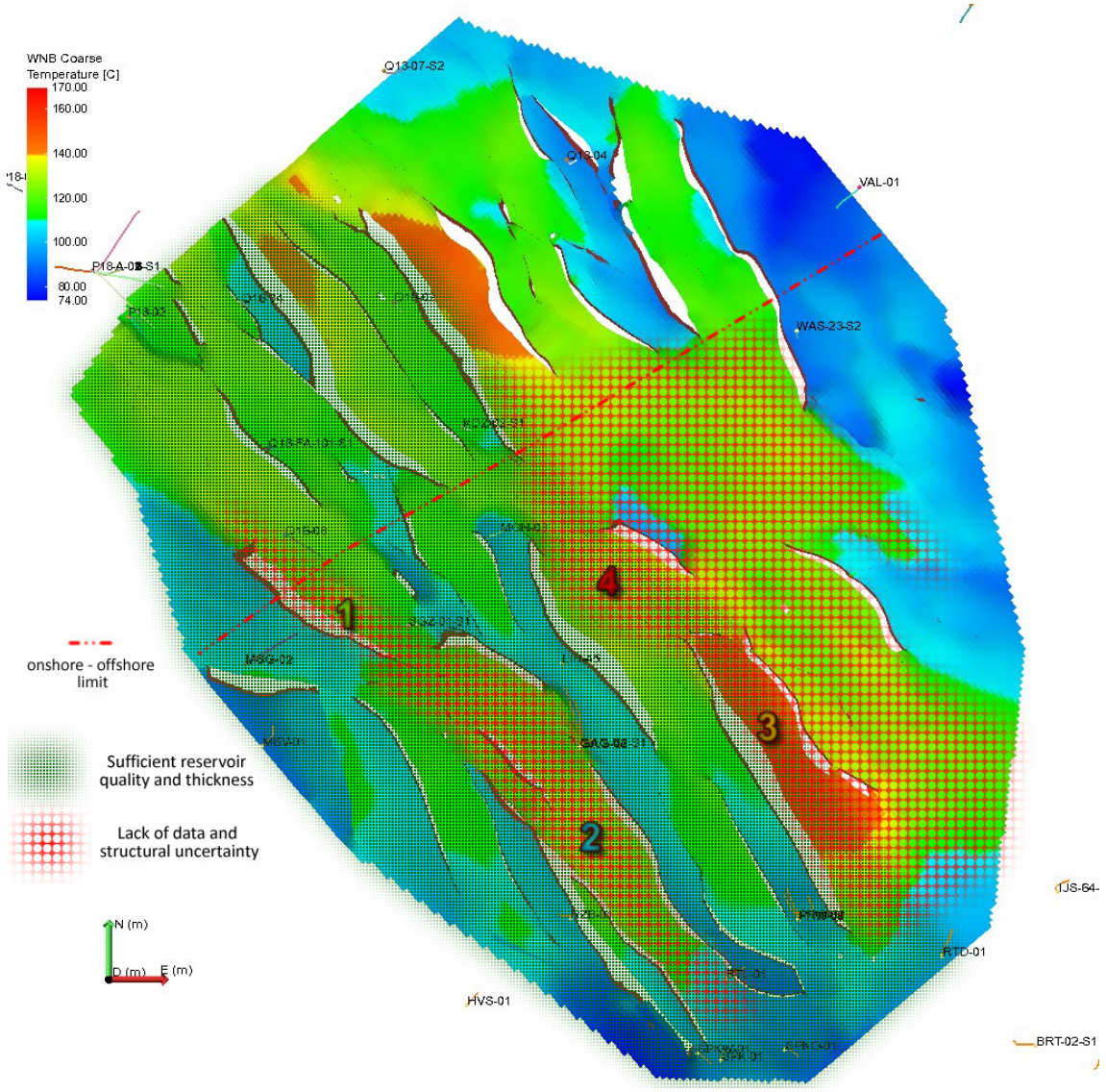

Figure 129: Convoluted map for the potential and uncertainty. Base map is temperature map at top Hardegsen formation where red (140 deg C +) means that both electricity and hot production is possible and green-yellow (120-140 deg C) means that only hot water production is possible. The green mesh overlay gives the relative expectation for good reservoir quality and sufficient reservoir thickness. The red circle hatch indicates areas of structural uncertainty and lack of exploration well data.

5.3. Conclusions and recommendations

The geologic static reservoir modelling is a very important part of total evaluation of the region potential for development of geothermal resources as is combines and summarizes all of the conclusions from previous chapters in the study. In it of vital importance to incorporate all of the available data and assumptions in the models in order to assure that no information is ignored and can lead to increase in the eventual total model uncertainty.

The modelling workflow presented is an iterative process that includes frequent revision of already completed steps in order to quality monitor the process at each step. Using this approach the possibility of introducing unexpected errors that are left unnoticed in the model is limited. In general this is a prerequisite for the final risk evaluation. When all of the uncertainty and possible error are well known and easy to predict the total risk and uncertainty is only a direct function of them.

There are several recommendations for the further development of the models and for the reduction of the evaluated uncertainty in the models. As it is clear from the last sub-chapter the risk in different models is also different due to the local data density and structural certainty. In order to bring each model to the same level

of low uncertainty a few additional improvements can be introduced. For example in order to bring the risk level for the southern models to both level 1 additional study is required on wells Q16-08 and GAG-05 as they are the only well that really also penetrate a deep fault block. Well GAG-05 also penetrates a higher fault block and a deeper fault block with Main Buntsandstein section and is therefore very important for the comparison or reservoir qualities such as porosity depth trend. This can improve the knowledge over reservoir quality distribution in simulation target grid Maasland.

In order to reduce the amount of uncertainty in the northern simulation target grids to similar to the ones in the south additional information should be assessed and included in the study. This includes evaluation and interpretation of 2D seismic lines in the areas where the 3D seismic is of very poor quality. It is almost impossible to get additional information over the reservoir quality and availability in those areas without the drilling of new exploration wells. Thus the risk in the northern simulation target grids will always remain higher, also given the fact that the general trend in the basin is of rapid reservoir quality deterioration towards the north.

References:

Crain, E.R., 1986, The Log Analysis Handbook, Pennwell Books, Tulsa

Davis, J.C., 2002, Statistics and Data Analysis in Geology, Third Edition, Kansas Geological Survey, John Wiley and Sons, New York

Waples, D., Pacheco, J., Vera, A., 2004, A method for correcting log-derived temperatures in deep wells, calibrated in the Gulf of Mexico, Petroleum Geoscience v 10, 2004.

Anonymous, 2009, User manual, Tigress v.5.1.1

Anonymous, 2011, User manual, JOA Oil and Gas, JewelSuite 2011

www.nlog.nl – Netherlands Oil and Gas Portal, source for all composite logs, core photos and core analyses

6. Building the dynamic models and consideration for geothermal energy, reservoir simulations and evaluations of results

After the simulation models are created they need to be evaluated using appropriate fluid models for the reservoir fluids. The most important parameters to be determined are production flow rate and temperature front propagation. However in a complicated situation with varying and uncertain reservoir parameters and availability of hydrocarbons in the system there are more implications to the regular approach. Each aspect of the reservoir production profile needs to be analyzed independently and all of the input parameters have to be reconsidered so that they match the geothermal specific requirements.
In this chapter some ideas for geothermal reservoir simulations are presented and summarized as well as a basic approach is suggested for simulating the reservoir models created in previous chapter.

Table of used symbols in this chapter:

A	Cross sectional area	$[m^2]$
Cp	Material specific heat at constant pressure	$[J.\ Kg^{-1}.\ K^{-1}]$
g	Gravitational acceleration	$[m.\ s^{-2}]$
e_x	Direction vector	-
h	Height/Well open section length	[m]
k	Permeability	[Darcy]
m	Mass	[kg]
P	Pressure	[Pa]
q_x	Heat flux	$[W.m^{-2}]$
Q	Flow rate	[m/s]
U	Local Darcy velocity	$[m.\ s^{-1}]$
T	Temperature	[K]
v	Velocity	$[m.\ s^{-1}]$
Z	Height of perforated section	[m]
α	Heat transfer coefficient	$[W.\ m^{-2}.\ K^{-1}]$
Δ	Difference/Step	
λ (k_T)	Conductivity	$[W.m^{-1}.K^{-1}]$
φ	Porosity	-
μ	Viscosity	[Pa.s]
ϕ	Massa flux	$[kg.m^{-2}]$
ρ	Material density	$[kg.\ m^{-3}]$

6.1. Considerations for geothermal reservoir simulations

From theoretical point of view reservoir simulations of geothermal reservoirs is very similar to a conventional reservoir simulation. In practice the major focus of geothermal reservoir simulations is directed to propagation of the thermal front in the reservoir. The applications of the laws for mass and energy conservation are still the same, however geothermal numerical simulations are intended to evaluate the heat conduction and convection taking place between the fluids in the reservoir and the grains of the reservoir rock and fluids in the pore space. The actual displacement of fluids in the pores has less importance than the development of the thermal balance and therefore numerical geothermal simulations are quite often limited to one or two dimensional problems. Such approach reduces the amount of calculations while it put more attention to the heat equilibrium in the system that is generally of secondary importance in more common multiphase fluids displacement simulators.

An example of widely accepted geothermal specific simulator is iTOUGH2 – Inverse modeling of transport of unsaturated groundwater and heat, which can handle irregular unstructured meshes. This simulator can use various types of input grids and can be adjusted to simulate a wide variety of test parameters. (Ketilsson et al.) On the other hand more common simulators using rectangular input reservoir meshes that are used in geothermal research and simulations are STARS (Salimi et al.) and TETRAD. Although the limit on the input grid either simulator can handle multiphase and multi component reservoir simulations and output detailed data on the compositional and heat balance in the system.
More general simulator that is often used in geothermal reservoir simulations is Eclipse. It is a full featured reservoir simulation package that can also handle thermal modeling and can be used to directly simulate on geologic reservoir grids thus taking into account the expected geological variations in the target reservoir (Brouwler et al.)

Different reservoir studies require individual approaches in terms of choice of simulators and balances to be evaluated. Each study requires an initial analysis of the set targets and the requirements from the expected results.
The results from the studies part of this project so far can therefore be used to select the most important aspects to be evaluated in the reservoir simulations. The major considerations can be grouped in three important topics:

- Thermal front breakthrough given the specific expected reservoir properties
- Simultaneous gas and hot water production
- Influence of the formation heterogeneities on thermal from propagation

These three aspects will be the focus of this chapter. The general thermal front propagation will be evaluated using analytical approach and several basic reservoir simulations. The possibility of simultaneous gas and hot water production will be discussed using a literature study and theoretical approximations. The influence of the heterogeneities typical for the Triassic formations will also be evaluated with theoretical approach.

6.2. Geothermal specific requirements of the project

In order to accomplish the goals set for this project several approaches can be taken. Due to the limited amount of available time only one reservoir scale simulation is carried out for two different well separation distances. The choice of reservoir simulator is given to Eclipse due to the possibility to model and simulate
This approach will be used to solve target number one. The reservoir simulator essentially calculates the mass influx into the reservoir and determines the cooling down of the porous media due to the temperature difference from the injected fluid.

The theoretical background for this simulation will be explained in this subchapter and in the workflow also problems number two and three will be addressed. As it was already mentioned geothermal simulations for hot water production are rather similar in the basics to ordinary reservoir simulations employed in

hydrocarbon reservoir evaluations. The starting point is the basic laws for the flow in porous media and well injectivity and productivity.
The following derivations are entirely based on the approach chosen by H. Salimi in his work.

Darcy Law: $u_x = (Q/A) = -\frac{k}{\mu}(\frac{dP}{dx} + \rho g e_x)$

Injection and production wells influx and injection is derived from the local velocity calculated for radial flow with given uniform height and identical volumetric rates. Other assumptions that are required in order to simplify the problem include the thickness of the injection area and the injection are uniform. The medium is considered infinite in radial extent so that no additional boundary conditions are required.

Flow rate production well: $$Q = \frac{k.2\pi.r_{well}.H.(\Delta P)}{\mu.\ln(\frac{r_\infty}{r_{well}})}$$

The estimation for the flow rate and front propagation from the injection well requires introducing first the laws for heat conduction and energy balance.

Fourier heat conduction: $$q_x = -k_T.\frac{dT}{dx}$$

Energy balance: $$\frac{\partial}{\partial t}(\rho C_p T) + \nabla.(\rho \bar{u} C_p T) - \nabla.(k_T \nabla T) = 0$$

If only a single phase flow is considered with homogeneous reservoir properties and a number of additional simplifications such as properties independent of temperature, horizontal medium, no influence at the boundaries and only heat transfer by convection, an expression for the velocity of the thermal front can be calculated as a function of the water front. Therefore the expression can also be called retardation coefficient for the thermal front as opposed to the actual compositional front of the injected water.

Velocity of thermal front: $$v_T = \left(\frac{1}{1 + \left(\frac{1-\varphi}{\varphi}\right)\left(\frac{\rho_s C_{ps}}{\rho_l C_{pl}}\right)} \right) v_W$$

The expression in the brackets is called the retardation factor, K.

The next step is to derive the expression for the arrival time of the Thermal front in a situation with a doublet including the overall drift flux from the aquifer. The drift flux can be estimated from the expression for injection well in infinite medium. The total velocity is equal to the interstitial injection velocity (v_x) originating from the injection well and the ambient aquifer velocity (v_∞) called drift flux. This can be substituted in the expression for the position of the thermal or compositional front from the injection well. The expression for the position where the injection velocity is then equal to the drift flux is:

$$v_x = \frac{-Q.\cos\theta}{2.\pi.h.\varphi.r} \text{ then } r = \frac{Q}{2.\pi.h.\varphi.v_\infty}$$

The position of the thermal front is given by the following expression derived from well index:

$$r_T = \sqrt{\frac{Q.t}{h.\pi.\varphi}.K_{retardation}}$$

Therefore the arrival time at the production well in the case of a doublet can be derived and is equal to:

$$t_T = \frac{\pi.h.\varphi.L^2}{3.Q}\left[1+\left(\frac{1-\varphi}{\varphi}\right)\left(\frac{\rho_s C_{ps}}{\rho_l C_{pl}}\right)\right]$$

There are a number of additional factors that need to be taken into account. As the target Hardegsen formation show significant permeability variation in vertical direction observed in exploration wells but also permeability variations in horizontal direction seen in horizontal gas production wells, additional estimation have to be made for the influence of conduction between layers with different permeability. Also the effect of thermal front dispersion needs to be estimated as it is going to play a role in setting with many small layers with significant permeability contrast.
The radial inflow in the production well have to be calculated for two phase flow in order to estimate the minimum required perforated or open hole section in the well. The experience from the gas production wells in s'Gravenzande and Pernis gas fields has shown that horizontal or highly deviated wells in Hardegsen formation might be required to achieve the required flow rates.

A rough estimation of the time for thermal front breakthrough based on average porosity and permeability in the southwest deep fault block of 13% and 125 mD indicates that a production period of 42 years is possible given a 1 kilometer well separation. This is calculated for flow rate of 150 m^3/h, 100 meters well open section, rock density of 2650 kg/m^3, heat capacity 1000 J/(kg.K), density of the water 1000 kg/m^3, and heat capacity of water 4180 J/(kg.K). It is important to note that density of water could increase with increased mineral content; also the heat capacity of the sandstone is strongly influenced by the quartz content. Geothermal surface facilities usually have planned life span of 15 years, subsurface installations of 30 years.

Flow between two horizontal wells might have additional implications and should be considered along with two phase flow of water and gas in the further reservoir modelling and simulations estimations.

6.3. Reservoir simulations

Due to lack of available software licenses and conflict of interest regarding the use of certain software licenses, actual reservoir simulations are not presented in this report. The reservoir models generated can still be used in further projects focused in specific areas of interest.

6.4. Conclusions and recommendations

Evaluation of the sandstone reservoir in the Triassic Buntsandstein formations in terms of thermal front propagation and possible flow rates needs to be taken up as a separate study. A number of additional factors should be taken out of the assumptions and evaluated in order to have a reliable estimation of the project time span. These additional factors include use of horizontal wells, two phase inflow into production wells, well performance with two phase mixture, and influence of permeability variations on thermal front dispersion.

References:

Brouwer, G., Lokhorst, A. Orlic, B., 2005, Geothermal Heat and Abandoned Gas Reservoirs in the Netherlands, TNO Netherlands, Proceedings World Geothermal Congress 2005, Antalya, Turkey

Chun, N., 2009, Petrofysische sediment- en chemische wateranalyse van de Berkel zandsteen, Onder Krijt, Zuid Holland, BSc Thesis, TU Delft / DAP.

Den Boer, C., 2010, Doublet spacing in the Delft Aardwarmte Project, BSc Thesis, TU Delft / DAP

Garcia-Valladares, O., Sanchez-Upton, P., Santoyo, E., 2005, Numerical modeling of flow processes inside geothermal wells: An approach for predicting production characteristics with uncertainties, Morella, Mexico, Energy Conservation and Managment v 47, 2006, Elsevier

Ketilsson, J., Axelsson, G., Palsson, H., Jonsson, M., 2008, Production Capacity Assessment: Numerical modelling of geothermal resources, Orkustofnun, Iceland, Proceedings of 33rd Worksop on Geothermal Reservoir engineering 2008, Stanford, California

Leeuwen, W. A. Van., Buik, N., Gutierrez-Neri, M., Lokhorst, A., Willemsen, G., 2010, Subsurface Spatial Planning for Geothermal Heat Production in Greenport Westland-Oostland, the Netherlands, IF Technology, Arnhem, Netherlands, Proceedings World Geothermal Congress 2010, Bali, Indonesia

O'Sullivan, M., Pruess, K., Lippmann, M., 2001, State of the art of geothermal reservoir simulation, Geothermics v 30, Pergamon/ Elsevier

Ryley, D. J., 1982, Geothermal energy problems in heat and fluid flow, University of Liverpool, England

Salimi, H., Groenenberg, R., Wolf, K.H., 2011, Compositional flow simulations of mixed CO2 – water injection into geothermal reservoirs: Geothermal energy combined with CO2 storage, TU Delft, Netherlands, Proceedings of 36th Workshop on Geothermal Reservoir Engineering 2011, Stanford, California

Uzun, I., Akin, S., 2005, Pore Network Modelling of Adsorption Effect in Geothermal Reservoirs, METU Ankara, Proceedings of 13th Workshop on Geothermal Reservoir Engineering 2005, Stanford, California

Vogt, C., Mottaghy, D., V., Rath, Wolf, A., Pechnig, R., Clauser, C., 2010, Quantifying Uncertainty in Geothermal Reservoir Modeling, RWTH Aachen and EON Energy Germany, Proceedings World Geothermal Congress 2010, Bali, Indonesia

7. Economic evaluation and risk assessment of the different possible project scenarios and developments

One of the most important limiting factors for geothermal projects is the financial expression of the required investment and operation costs. Unlike hydrocarbon exploration project a geothermal project has more limited capabilities to return the initial investment and is more vulnerable to unexpected complications that can affect the production of hot water or the effectiveness of the surface facilities. In this chapter a basic estimation of the costs associated with geothermal project in the Triassic reservoirs in the West Netherlands basin will be presented.
This chapter will also present a summary of the risk assessment from previous chapters and how it could affect the investment decision making process in terms of uncertainties and their influences.

In addition to that a comparison will be made between a possible geothermal project cash flow case and the development of a small gas field as well as the idea of simultaneous development will be covered and explained. The stress will be put on the benefits that such a project can have in terms of reduction of uncertainty and improvement of the rate of return of the initial investments.

7.1. Summary of expected project costs

The cost related to the execution of a geothermal project can be split into several major groups. The first step is the planning and exploration stage of the project when the major focus is on feasibility in terms of geological setting, reservoir properties and surface location availability. It is a very important stage as it determines not only if the project is actually possible to carry out but also sets the major targets for the production rates and life span of the endeavor.
After the expected production rates in terms of hot water flow rates and produced heat flux are determined the next step is to actually drill and complete the production and injection wells. It is considered a separate step from the construction of surface facilities which comes next as it is an expensive operation. This is especially true for deep drilling target such as in the Triassic in the West Netherlands Basin. The final step in the evaluation and construction process respectively is the connection between the production site and the final users for the generated heat.
This chapter will give a short and basic estimation of the associated cost with each step as well as a short introduction to each step and some recommendations or suggestions related to being more cost effective or to possible cost savings.
The following cost citations are taken from the feasibility study done by Marco van de Weerdhof (Van de Weerdhof et al.) and are current for the end of 2010.

7.1.1. Cost of geological evaluation, model setup and engineering consulting

This project on its own is essentially a predecessor for eventual geological studies and planning projects related to geothermal hot water exploitation in the Zuid-Holland province. The actual geological surveys are more focused on the target area and describe in detail the expected reservoir characteristics and properties. The reservoir size and preferred perforation sites are carefully determined so that the final report of the study can be directly used to guide the drilling process and the surface facility planning. Projects in the West Netherlands Basin can benefit greatly from the fact that most seismic data and geological knowledge is publicly available which is a major reduction in the actual cost of the study.
A typical value that is often cited as charge for the set up of geological models is 100.000 euro. However when the costs for engineering of most of the systems are also taken into account the cost can easily exceed 700.000 euro or more in total. This includes the design of wells, production facilities and heat exchanger and electricity production system.

7.1.2. Cost of drilling and geothermal specific requirements

Drilling cost make the largest fraction of the required investment costs. The total cost for the drilling of the required doublet can be rounded up to close to 10.000.000 euro and this includes steel casing completion and basic well heads for the wells. It is clear that the drilling of the doublet accounts for more than 80% of the required minimum CAPEX (Capital expenditures) costs and is thus the best candidate for any cost reduction attempts. A number of options exist such as drilling with casing for reduced rig time and using composite casing instead of steel one to reduce cost and possible corrosion during exploitation (Leijnse et al.).

There are a number of factors that can make the drilling and completion campaign more expensive. For example the final section of the wells in the Triassic reservoir might be completed horizontally or with high deviation angle in order to keep the production interval in the Hardegsen and Detfurth formations. Other options that might require significant additional investments are related to stimulation of the tighter Detfurth and Volpriehausen formations using hydraulic fracturing techniques. This possibility will also be discussed in this chapter in terms of the additional risks it is associated with and also the possible decrease in public acceptance of geothermal projects that it might lead to. A well simulation procedure might make the wells more expensive with up to 5.000.000 euro. Completing the wells with gas production well standards can also increase the required initial investment.
The electric submersible pumps are also included in the costs related to drilling and completion of the wells and sum up to another 250.000 euro.

7.1.3. Cost of surface facilities and heat exchangers

The surface facilities as used in this subchapter include the production installations for separation of different produced fluids from each other and transferring the heat from the produced water to a binary system for electricity production and hot water network for greenhouses or living premises. The heat exchangers and the Organic Rankine Cycle installation for electricity production including turbines cost approximately 1.500.000 euro in total. The complete installation including buildings and other infrastructure can cost additional 1.000.000 euro.

In addition to these costs a project in the Triassic reservoirs in the West Netherlands Basin that incorporates simultaneous hot water and natural gas (methane) production will require at least one two phase (water-gas) separator installed before the heat exchangers. In is highly recommended to have such separator installed even if the project is not intended to utilize the produced natural gas as it is readily available also in the deeper fault blocks and is going to be produced as by-product. This can be concluded from the two available exploration wells in the southern deep fault block where the bounding faults have sufficient offsets to be sealing and thus gas is trapped in stratigraphic traps towards the faults or gentle anticlinal structures against the overlying Röt formation. Separation of gas and liquid phase is further very important in order to increase the efficiency of the heat exchangers and to prevent difficulties related to the injection well performance. Injection of two phase mixture requires higher injection pressures and thus additional compressors or pumps in order to achieve the designed flow rates. The costs for separators can vary between 50.000 and 300.000 euro depending on the requirements of the installation design and the availability of CO_2 or H_2S in the produced gas phase.

If gas is produced it can be used directly on site to produce electricity, heat or both. Although the required adjustments and additions to the installations will cost extra capital investment the added heat production will also generate more electricity and hot water and thus add to the profit cash flow of the project.

The cost for the construction of hot water supply systems or updates to the already available heating systems in greenhouses and in living quarters will not be added to the calculations at the moment as it can be managed and organized by another party such as an utility company.

7.1.5. Cash flow estimation for geothermal project in the Triassic

In the calculation for total expenses and revenues from a possible geothermal project targeting Triassic Buntsandstein sandstones in the West Netherlands Basin also cost of insurance and license acquisition expenses are taken into account. The calculation of the expected revenues from eventual electricity generation and hot water production combined with a basic estimate of the OPEX (operational expenditures) for the project is included in the following table. Also the already discussed CAPEX expenses are included. The data is then summarized in a bar chart.

	CAPEX First Year	OPEX per Year	Electricity production	Heat production
Expenditures	-15000	-500	0	0
Revenue	0	0	500	2000
Total	-15000	-500	500	2000

Table 12: Summary of cash flow for geothermal project in thousands Euro

The calculations for the expected revenues are made on basis of 150 m3/h flow rate of 120 degrees C hot water. The power of the electric plant is generating 0,5 MW energy and the hot water installation produces 9 MW energy. Gas price is used as a conversion factor for the heat generation calculations in terms of investment return.
Additional costs for reservoir stimulation or additional benefits for sustainable energy development are not included in the calculations.

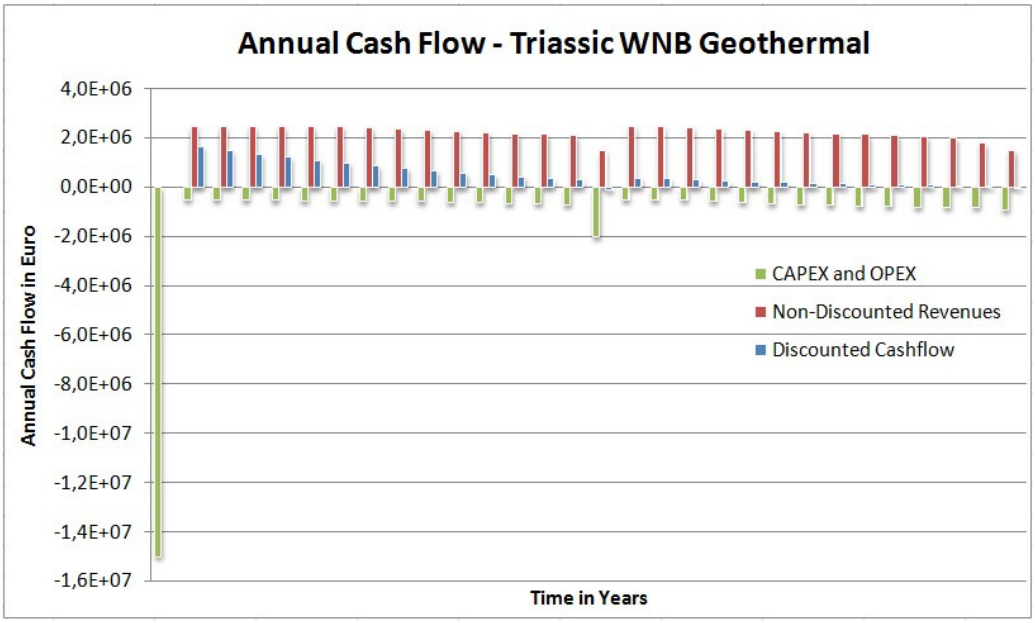

Figure 130: Annual cash flow for Triassic project in WNB

In the figure above (Figure 129) the annual cash flow is given using discount rate of 15%. A number of additional factors are not taken into account such as rent on outside financing and additional taxes on the profits. It can be observed that the revenues per year are gradually decreasing in order to account for reduction in well performance and heat exchangers performance. In year 15 there is a planned maintenance activity in the surface facilities to improve performance and efficiency of the equipment.

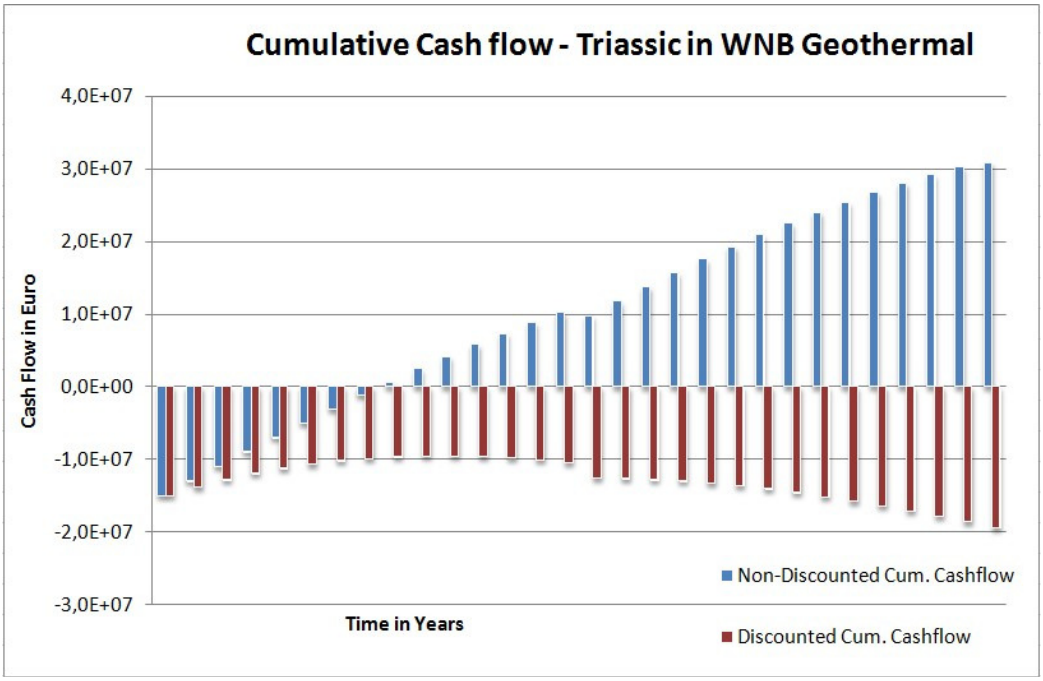

Figure 131: Cumulative cash flow, with and without discount, for geothermal project in Triassic in WNB

As it can be seen on the cumulative cash flow graph (Figure 130) the breakeven point for the project is around the eighth year of the project. This calculation excludes additional financial burden from dept accumulated by the rent on the external financing which should also be taken into account.

It is clear that the breakeven point comes at a later point compared to a typical hydrocarbon project. The reason for this is in the specifics of the revenue cash flow. The generation of revenues is relatively slow but steady and continuous. The peak production is achieved right away and the decline in production is only a minor factor. However the capital expenditures are still very high and cannot be spread out in a longer

period as all of the installations are required prior to commencing of the production. As a result of this discounting the profits leads to considerable reduction of the profit. In fact as it can be seen on the discounted cumulative cash flow diagram the overall cash flow of the project remains negative. This however is deceiving presentation of the information as the actual calculation should involve a different approach and set of financial market tools in order to correctly evaluate the feasibility of the project. The main reason for this is the fact that the heat generation is not a investment targeting pure profit but rather an investment into cost reduction and greenhouse gas emission reduction. The heat is required and it will be generated with other sources at higher cost if geothermal is not available. Therefore it is not accurate to apply simple discount algorithm to the economic evaluation of the project but rather compare the costs of a geothermal project to costs of using natural gas for the generation of heat for greenhouses and domestic homes.

7.2. Comparison between geothermal and small gas filed development cash flow

Another way to deal with the negative economic profile of geothermal projects is to try to combine hot water production with gas production. The Buntsandstein reservoirs are known to contain gas deposits and Carboniferous gas is still being generated in the south-west areas of the West Netherlands Basin. The two wells drilled in the deeper south western fault block indicate that there are gas accumulations in the deeper fault blocks as well as the faults with large offsets tend to be sealing.

If a geothermal project is modified to produce and use natural gas that is being co-produced this will require some adjustments in the installations design. First of all the wells should be drilled up to standard oil industry requirements for gas wells and the power plant area will have to conform to certain requirements. On the other hand the additional work required is not very much compared to the already constructed facilities for geothermal power plant. The produced gas can either sold or used directly on site for co-generation of electricity and heat.
The following graph shows an example of cash flow diagram for geothermal project including production of gas and utilization in the heat generation facilities.

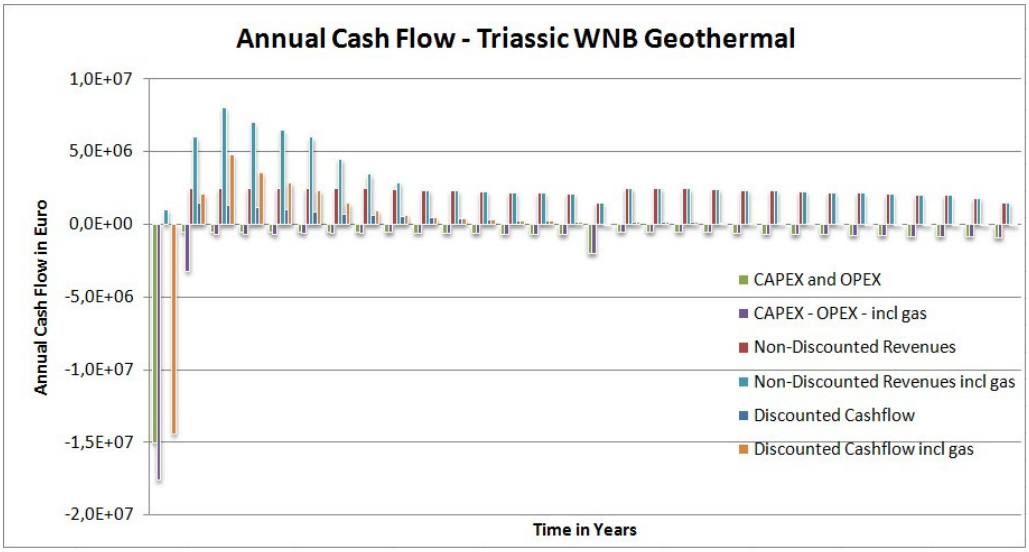

Figure 132: Example of possible Annual cash flow including gas production

The suggested model is representative for a field containing 0.5 billion Sm^3 assuming the gas is sold to the market and taxes are paid. Developing a gas field also requires obtaining the required licenses or operating is shared contract with the license holder. Targeting areas expected to have gas accumulations and producing the gas along with the formation water will lead to reduction of water flow rate in the first years but the gas is expected to have significant influence only in the first six to eight years of the project. Nevertheless the benefit from properly including the gas production in the calculations is visible on the next graph (Figure 132) for the cumulative cash flow of the project including gas production. The breakeven point is achieved in the fifth year making the project more financially attractive.

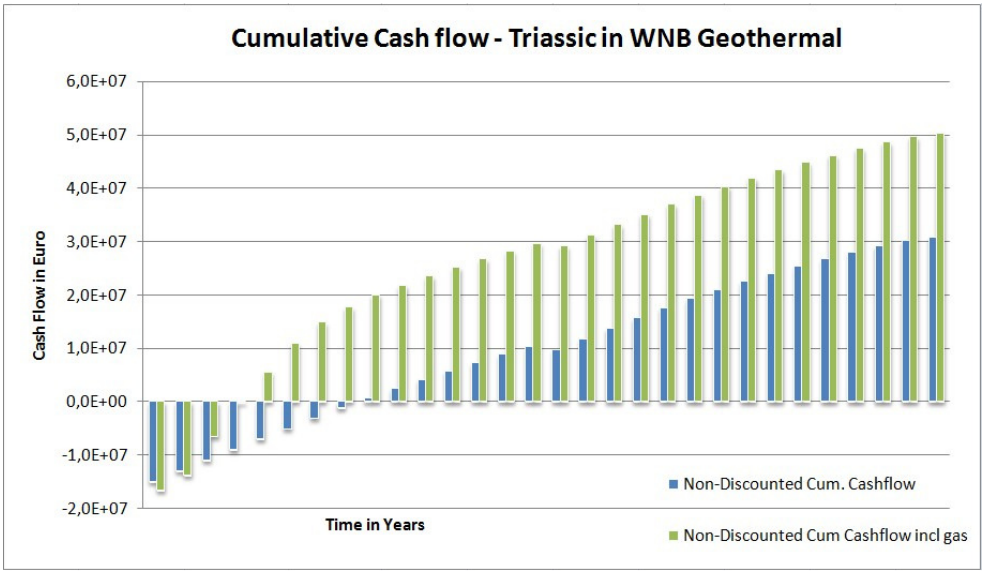

Figure 133: Example of possible cumulative cash flow including production of gas

The calculations presented in this report regarding possible gas production are however only suggestive of the opportunities. An actual development study must be carried out in order to determine the available amounts of gas and the possibility to combine the production. If sufficient amounts of gas are available the CAPEX expenditures can be spread out in a larger period of time as the electric submersible pumps might not be required in the first years of production as the wells can be designed to use natural or artificial gas lift.

7.3. Evaluations of the reliability of results and risk assessment

A geothermal project in the Zuid-Holland province area of the West Netherlands Basin would require careful planning and good public presentation. As geothermal projects are not able to generate quick revenues but rather have steady income cash flow for a longer period the financial planning for them should be guided by different principles in comparison with standard hydrocarbon exploitation project. Although both type of project share many similarities and even surface and subsurface equipment, the incentive to venture into such a geothermal project is fueled by different goals. Geothermal energy exploitation requires long term commitment to the community and long term financial planning capability.

This report provides only preliminary conclusions regarding the potential of the area for deep geothermal exploitation. Most of the sources of uncertainty were explained in the previous chapter. In many regards they are related to the subsurface part of the project. The correct long term financial planning for a geothermal project should therefore account for the sensitivity of the project success with regard to subsurface limits and specifics.

7.4. Conclusions and recommendations

The economic evaluation of a future geothermal project in the Triassic Buntsandstein sandstone reservoirs shows that a project is feasible under the current economic condition provided that the wells can produce and inject at the required rates. Furthermore it is possible to combine the project with development of small gas resources in the area. The co-production of hot water and gas can make the overall project more beneficial and financially attractive. Most importantly possible gas production will decrease the time before the initial investment is returned and thus make such a project more attractive to a larger variety of investors.

Additional work is required in exploring the possibilities of joint licences and financing project aimed at combining geothermal with small gas field development in the area.

Additional work is required on the risk evaluation and feasibility sensitivity to reservoir performance rather than coupling project success with gas price fluctuations. A geothermal project will become more attractive for investors given that the gas price is rising however this will not actually affect the project success.

References:

Leijnse, S., 2008, Drilling hazards for the DAP geothermal wells, BSc Thesis, TU Delft / DAP

Van de Weerdhof, M., 2011, Haalbaarheidsonderzoek elektriciteitsproductie Oostland, Grontmij, Waddinxveen, www.energiek2020.nu

8. Evaluation of project feasibility – conclusions and recommendations

The final chapter of this report is a summary of the conclusions from previous chapters as well as a general evaluation of the potential of the area for further geothermal development.

As a result of the different studies carried out in this project a number of ideas were generated. They will be presented again in the final part of this chapter as recommendations for further studies and developments in the area.

8.1. Geothermal potential in Zuid Holland area for very hot water production

The final recommendation for the further development of the basin for geothermal exploration in the deeper fault blocks is based on the combined conclusions from the evaluation of the depositional environment, burial history, diagenetic history and observed petrophysical properties of the reservoir sandstones of the Main Buntsandstein formations. It was shown that consistent basin wide interpretation of the formation boundaries is essential for the determination of the target reservoirs. The most prospective formation to form the major reservoir rock was determined to be Hardegsen formation. It is mostly deposited and preserved in the south western parts of the basin which is convenient for the project target areas underneath the southern parts of Zuid-Holland province area. Based on the depositional environment of the formation it is expected to show very good reservoir quality also at significant depths. As the targets for the geothermal exploration are in the deeper fault blocks the expected reservoir properties are going to be affected by the more complicated burial history there and thus the additional diagenetic processes that have taken place. The expected reduction of reservoir quality can push the reservoir properties very close to the threshold minimum for the achieving the desired production and injection flow rates. It is essential that every target reservoir is individually assessed before drilling is started.

The thickness of the target formation can vary between 40 and 80 meters in the target area and compared to the total Main Buntsandstein interval thickness of close to 200 meters is only a small fraction. Drilling trough the deeper formations in the sequence is recommended only in the very south west margin of the basin. In all other locations additional reservoir rock stimulation is required in order to achieve the required flow rates. In order to make maximum use of the target Hardegsen formation horizontal or highly deviated drilling is recommended similar to the development of s'Gravenzande and Pernis-West gas fields.

The few available wells in the deeper fault blocks show that hydrocarbons are readily available in the Hardegsen formation. The situation is similar to the higher fault blocks and therefore gas accumulations are possible in structural and stratigraphical traps as the faults with large offsets are likely to be sealing. In the marginal southwest regions seal is not available for the Main Buntsandstein sub-group due to the high sand and silt content of the overlying formations caused by the proximity to the basin sediment source London-Brabant massif. It is recommended to develop geothermal project in combination of small gas field development. Specialized reservoir simulations have to evaluate the additional requirements for such development and determine the possible producible quantities. Such development is likely to bring significant financial benefits for the geothermal project due to earlier return of investment with only very minor additional capital expenditures.

8.2. Recommendations for further studies and project development planning

This chapter presents a summary of all the different recommendation suggested for additional work in the previous chapters. The order of the suggestions is the same as the order of the chapters in the report starting with Depositional environment. Next paragraph covers palinspastic reconstruction, then diagenetic history study. The next paragraph continues with the suggestions from the chapter on static geologic modelling. The final paragraphs cover dynamic modelling and overall project economic and technical feasibility evaluation recommendations.

Further improvements on the sequence stratigraphic model are recommended before it can be tested used as prediction tool for future drilling and exploration campaigns. Several suggestions for additional work that can be carried out in order to achieve the desired advancement in the understanding of the depositional environment include – better understanding of the connection between tectonic influence and the shift in lithofacies and formations, better controls on the sediment supply sources and more profound analysis on the spatial facies distribution as combination of conceptual geological model and log sedimentological observations as suggested in this work.

Further recommendations for additional work for the burial history understanding include complete studies on individual fault blocks and considering them as individual units in term of reservoirs, seals, migration path and possibilities, and stress regime development.

Additional work on the individual diagenetic development of target fault blocks and areas is essential in order to improve the predictability of reservoir qualities in not explored regions. A very important consideration in regard with this is the possibly very varied development between higher and lower faults blocks triggered by both burial history differences and middle and later diagenetic processes differences due to the unrelated contacts with adjacent formations.

There are several recommendations for the further development of the models and for the reduction of the evaluated uncertainty in the models. As it is clear from the last sub-chapter the risk in different models is also different due to the local data density and structural certainty. In order to bring each model to the same level of low uncertainty a few additional improvements can be introduced. For example in order to bring the risk level for the southern models to both level 1 additional study is required on wells Q16-08 and GAG-05 as they are the only well that really also penetrate a deep fault block. Well GAG-05 also penetrates a higher fault block and a deeper fault block with Main Buntsandstein section and is therefore very important for the comparison or reservoir qualities such as porosity depth trend. This can improve the knowledge over reservoir quality distribution in simulation target grid Maasland.

In order to reduce the amount of uncertainty in the northern simulation target grids to similar to the ones in the south additional information should be assessed and included in the study. This includes evaluation and interpretation of 2D seismic lines in the areas where the 3D seismic is of very poor quality. It is almost impossible to get additional information over the reservoir quality and availability in those areas without the drilling of new exploration wells. Thus the risk in the northern simulation target grids will always remain higher, also given the fact that the general trend in the basin is of rapid reservoir quality deterioration towards the north.

Evaluation of the sandstone reservoir in the Triassic Buntsandstein formations in terms of thermal front propagation and possible flow rates needs to be taken up as a separate study. A number of additional factors should be taken out of the assumptions and evaluated in order to have a reliable estimation of the project time span. These additional factors include use of horizontal wells, two phase inflow into production wells, well performance with two phase mixture, and influence of permeability variations on thermal front dispersion.

Additional work is required in exploring the possibilities of joint licences and financing project aimed at combining geothermal with small gas field development in the area.

Additional work is required on the risk evaluation and feasibility sensitivity to reservoir performance rather than coupling project success with gas price fluctuations. A geothermal project will become more attractive for investors given that the gas price is rising however this will not actually affect the project success.

List of Figures:

List of Tables:

Complete References list:

2DMove 2010.1, Manual and Tutorials, Midland Valley Exploration Ltd., Glasgow

Ames, R., Farfan, P.F., 1996, The environment of deposition of the Triassic Main Buntsandstein formation in P and Q quadrants, offshore Netherlands, in Rondeel, H.E., Batjes, D.A.J. et al, Geology of oil and gas under the Netherlands, Kluwer, p167-178, Dordrecht.

Anonymous, 2009, User manual, Tigress v.5.1.1

Anonymous, 2011, User manual, JOA Oil and Gas, JewelSuite 2011

Barr, D., 1985, 3-D palinspastic restoration of normal faults in the Inner Moray Firth; implication for extensional basin development, EPSL, Elsevier

Bourquin, S., Peron, S., Durand, M., 2006, Lower Triassic sequence stratigraphy of the western part of the Germanic Basin: Fluvial system evolution trough time and space, Sedimentary Geology 186, p187-211, Elsevier

Brouwer, G., Lokhorst, A. Orlic, B., 2005, Geothermal Heat and Abandoned Gas Reservoirs in the Netherlands, TNO Netherlands, Proceedings World Geothermal Congress 2005, Antalya, Turkey

Bulnes, M., McClay, K., 1999, Benefits and limitations of different 2D algorithms used in cross-secton restoration of inverted extensional faults; application to physical experiments, Tectonophysics 312, Elsevier

Chun, N., 2009, Petrofysische sediment- en chemische wateranalyse van de Berkel zandsteen, Onder Krijt, Zuid Holland, BSc Thesis, TU Delft / DAP.

Crain, E.R., 1986, The Log Analysis Handbook, Pennwell Books, Tulsa

Davis, J.C., 2002, Statistics and Data Analysis in Geology, Third Edition, Kansas Geological Survey, John Wiley and Sons, New York

De Jager, J., 2007, Geological Development, in Geology of the Netherlands, KNAW

Den Boer, C., 2010, Doublet spacing in the Delft Aardwarmte Project, BSc Thesis, TU Delft / DAP

Einsele, G., 2000, Sedimentary basins – Evolution, facies, and sediment, Budget, 2nd edition, Springer, Germany

Emery, D., 1987, The Sedimentology and reservoir characteristics of the middle and upper Bunter formations, Waalwijk-1, onshore Netherlands, BP

Faulkner, D., Jackson, C., Lunn, R., Schlische, R., Shipton , Z., Wibberley, C., Withjack, M., 2010, A review of recent developments concerning the structure, mechanics and fluid flow properties of fault zones, Journal of Structural Geology 32, Elsevier

Fisher, M.J., Mudge, D.C., 1998, Triassic, Petroleum geology of the North Sea, 4th edition, K.W. Glennie, JAPEC, UK

Garcia-Valladares, O., Sanchez-Upton, P., Santoyo, E., 2005, Numerical modeling of flow processes inside geothermal wells: An approach for predicting production characteristics with uncertainties, Morella, Mexico, Energy Conservation and Managment v 47, 2006, Elsevier

Geluk, M.C., 2005, Stratigraphy and tectonics of Permo-Triassic basins in the Netherlands and surrounding areas, University of Utrecht, PhD Thesis.

Geluk, M.C., Röhling, H-.G., 1997, High-resolution sequence stratigraphy of the Lower Triassic Buntsandstein in the Netherlands and North West Germany, Geologie en Mijnbouw 76

Hendrie, D.B., Kusznir, N.J., Hunter, R.H., 1993, Jurassic rifting extension in the North Sea triple junction from flextural backstripping: implications for decompression melting models, EPSL, Elsevier

Henk, A., Nemcok, M., 2008, Stress ad fracture prediction in inverted half-graben structures, Journal of Structural Geology 30, Elsevier

Ketilsson, J., Axelsson, G., Palsson, H., Jonsson, M., 2008, Production Capacity Assessment: Numerical modelling of geothermal resources, Orkustofnun, Iceland, Proceedings of 33rd Worksop on Geothermal Reservoir engineering 2008, Stanford, California

Leeuwen, W. A. Van., Buik, N., Gutierrez-Neri, M., Lokhorst, A., Willemsen, G., 2010, Subsurface Spatial Planning for Geothermal Heat Production in Greenport Westland-Oostland, the Netherlands, IF Technology, Arnhem, Netherlands, Proceedings World Geothermal Congress 2010, Bali, Indonesia

Leijnse, S., 2008, Drilling hazards for the DAP geothermal wells, BSc Thesis, TU Delft / DAP

Mader, D., 1983, Evolution of fluvial sedimentation in the Buntsandstein (Lower Triassic) of the Eifel (Germany), Sedimentary Geology 37, Elsevier

Nichols, G., 2009, Sedimentology and Stratigraphy (second edition), Wiley-Blackwell, p.324-381
O'Sullivan, M., Pruess, K., Lippmann, M., 2001, State of the art of geothermal reservoir simulation, Geothermics v 30, Pergamon/ Elsevier

Purvis, K., Okkerman, J.A., 1996, Inversion of reservoir quality by early diagenesis: an example from the Triassic Buntsandstein, offshore the Netherlands, in Rondeel, H.E., Batjes, D.A.J. et al, Geology of oil and gas under the Netherlands, Kluwer, p179-191.

Purvis, K., Okkerman, J.A., Inversion of reservoir quality by early diagenesis: an example from the Triassic Buntsandstein, offshore the Netherlands, in Rondeel, H.E., Batjes, D.A.J. et al, Geology of oil and gas under the Netherlands, Kluwer, p179-191

Reuver, F. de, 1996, Sedimentology, petrography and reservoir properties of cores 1 to 4 from well P11-02 – Final Report, GAPS/Amoco

Ryley, D. J., 1982, Geothermal energy problems in heat and fluid flow, University of Liverpool, England

Salimi, H., Groenenberg, R., Wolf, K.H., 2011, Compositional flow simulations of mixed CO2 – water injection into geothermal reservoirs: Geothermal energy combined with CO2 storage, TU Delft, Netherlands, Proceedings of 36th Workshop on Geothermal Reservoir Engineering 2011, Stanford, California

Spain, D. Conrad, C., 1997, Quantitative analysis of top seal capacity, offshore Netherlands, Southern North Sea, Geologie en Mijnbouw 76

Spain, D. Conrad, C., 1997, Quantitative analysis of top seal capacity, offshore Netherlands, Southern North Sea, Geologie en Mijnbouw 76

Sullivan, M., Haszeldinet, S., Boyce, A., Rogers G., Fallick A., 1994, Late anhydrite cements mark basin inversion: isotopic and formation water evidence, Rotliegend Sandstone, North Sea, Marine and Petroleum Geology 11

Szulies, M., 2004, Magnetostratigraphy: the key to a global correlation of the classic Germanic Trias – case study Volpriehausen formation, Middle Buntsandstein, Central Germany, EPSL, Elsevier

Turner, J.P., Williams, G.A., 2004, Sedimentary basin inversion and intra-plate shortening, Earth Science Reviews, Elsevier

Uzun, I., Akin, S., 2005, Pore Network Modelling of Adsorption Effect in Geothermal Reservoirs, METU Ankara, Proceedings of 13th Workshop on Geothermal Reservoir Engineering 2005, Stanford, California

Van Balen, R.T., et al, 1999, Modelling the hydrocarbon generation and migration in the West Netherlands Basin, the Netherlands, Geologie en Mijnbouw/ Netherlands journal of Geosciences 79 (1) p29-44, 2000

Van de Weerdhof, M., 2011, Haalbaarheidsonderzoek elektriciteitsproductie Oostland, Grontmij, Waddinxveen, www.energiek2020.nu

Van Wijhe, D.H., 1987, Structural evolution of inverted basins in Dutch offshore, Tectonophysics 137, Elsevier

Vogt, C., Mottaghy, D., V., Rath, Wolf, A., Pechnig, R., Clauser, C., 2010, Quantifying Uncertainty in Geothermal Reservoir Modeling, RWTH Aachen and EON Energy Germany, Proceedings World Geothermal Congress 2010, Bali, Indonesia

Waples, D., Pacheco, J., Vera, A., 2004, A method for correcting log-derived temperatures in deep wells, calibrated in the Gulf of Mexico, Petroleum Geoscience v 10, 2004.

Williams, B., 2009, Large scale alluvial architecture and correlation in a Triassic pebbly braided river (Lower Wolfville formation, Fundy Basin), Journal of Sedimentary Research, SEPM

Williams, B., McKie, T., 2009, Triassic palaeogeography and fluvial dispersal across the North-West European Basins, in Triassic basins of the Central and North Atlantic borderlands - models for exploration, Geology Journal 44, Issue 6.

Worum, G. et al, 2005, Pre-Neogene controls on present-day fault activity in the West Netherlands Basin and Roer Valley Graben System (southern Netherlands): role of variations in fault orientation in a uniform low-stress regime, Quaternary Science Reviews 24, Elsevier

www.nlog.nl – Netherlands Oil and Gas Portal, source for all composite logs, core photos and core analyses
www.nlog.nl – Netherlands Oil and Gas Portal, source for all wireline logs and core photos.

Appendix I – Palinspastic restorations and Burial history data

1.1. Restoration process overview

Software 2Dmove 2010.1 (64bit)

Inline 993 - AMC1989A

Base Tertiray base			Top Texel Marl base -min			Top Texel Marl base - opt			Base Holland Marl base -min		
Block	Process	Shear dip Corrections	Block	Process	Shear dip Corrections	Block	Process	Shear dip Corrections	Block	Process	Shear dip Corrections
1	Flextural Slip		1	Flextural Slip		1	Flextural Slip		1		
2	Simple Shear	-77	2	Flextural Slip		2	Simple Shear	-50	2		
3	Simple Shear	75	3	Simple Shear	-42	3	Simple Shear	-50	3	Simple Shear (single)	90
4	Simple Shear	-72	4	Simple Shear +rotate 1.5	-48	4	Simple Shear	-55	4	Simple Shear (single)	90
5	Simple Shear	-72	5	Simple Shear	-45	5	Simple Shear + rotate 1	-55	5	Simple Shear (single)	90
6	Simple Shear	81	6	Simple Shear	-55	6	Simple Shear + rotate 1	-60	6	Simple Shear (single)	90
7	Simple Shear	81	7	Simple Shear	-55	7	Simple Shear	-60	7	Simple Shear (single)	90

Inline 1778 - NAM1990D

Base Tertiray base			Top Texel Marl base -min			Top Texel Marl base - opt			Base Holland Marl base -min		
Block	Process	Shear dip Corrections	Block	Process	Shear dip Corrections	Block	Process	Shear dip Corrections	Block	Process	Shear dip Corrections
1	Flextural Slip		1	Flextural Slip		1	Simple Shear	90	1	Simple Shear	90
2	Simple Shear	-58	2	Simple Shear	-85	2	Simple Shear	-63	2	Simple Shear	90
3	Simple Shear	-69	3	Simple Shear	-80	3	Simple Shear	-56	3	Simple Shear	90
4	Simple Shear	-85	4	Simple Shear	-80	4	Simple Shear	-56	4	Simple Shear	90
5	Simple Shear	-60	5	Simple Shear	-70	5	Simple Shear	-56	5	Simple Shear	90
6	Flextural Slip + rotate 1.5		6	Flextural Slip + rotate 1		6	Simple Shear +rotate 2.5	-70	6	Simple Shear	90
7	Simple Shear +rotate 1.5	-63	7	Flextural Slip (single loop)		7	Simple Shear +rotate 1	-75	7	Simple Shear	90
8	Simple Shear +rotate 2.0	-50	8	Flextural Slip (single loop)		8	Simple Shear	-72	8	Simple Shear	90
9	Simple Shear +rotate 1.5	-70	9	Flextural Slip (single loop)		9	Simple Shear	-72	9	Simple Shear	90
10	Flextural Slip		10	Flextural Slip (single loop)		10	Simple Shear	-72	10	Simple Shear	90
11	Simple Shear +rotate 1.5	-70	11	Flextural Slip (single loop)		11	Simple Shear	-70	11	Simple Shear	90
12	Simple Shear +rotate 1.5	-70	12	Flextural Slip (single loop)		12	Simple Shear	-70	12	Flextural Slip	
13	Flextural Slip		13	Simple Shear	90	13	Simple Shear	-70	13	Flextural Slip + rotate 1	
14	Simple Shear +rotate 1.5	-80	14	Simple Shear +rotate 1	85	14	Simple Shear	-75	14	Simple Shear	90
15	Simple Shear +rotate 1.5	-72	15	Simple Shear +rotate 1	85	15	Simple Shear	-77	15	Simple Shear	90

Inline 12993 – NAM1991A

Base Tertiray base			Top Texel Marl base - min			Top Texel Marl base - opt			Base Holland Marl base -min		
Block	Process	Shear dip Corrections	Block	Process	Shear dip Corrections	Block	Process	Shear dip Corrections	Block	Process	Shear dip Corrections
1	Flextural Slip		1	Flextural Slip		1	Flextural Slip		1	Simple Shear	90
2	Simple Shear	-82	2	Simple Shear	90	2	Simple Shear	90	2	Simple Shear	90
3	Simple Shear	-85	3	Simple Shear	80	3	Simple Shear	85	3	Simple Shear	90
4	Simple Shear	-82	4	Simple Shear	80	4	Simple Shear	88	4	Simple Shear	90
5	Simple Shear	-80	5	Simple Shear	82	5	Simple Shear	88	5	Simple Shear	90
6	Simple Shear	-80	6	Simple Shear	82	6	Simple Shear	90	6	Simple Shear	90

Inline 993 - AMC1989A

Base Holland Marl base -opt			Base Cretaceous base - min			Base Cretaceous base -opt		
Block	Process	Shear dip Corrections	Block	Process	Shear dip Corrections	Block	Process	Shear dip Corrections
1	Simple Shear (single)	90	1	Flextural Slip (varying pins)		1	Flextural Slip (varying pins)	
2	Simple Shear (single)	90	2	Flextural Slip		2	Flextural Slip	
3	Simple Shear (single)	90	3	Flextural Slip		3	Flextural Slip	
4	Simple Shear (single)	90	4	Flextural Slip		4	Flextural Slip	
5	Simple Shear (single)	90	5	Flextural Slip		5	Flextural Slip	
6	Simple Shear (single)	90	6	Flextural Slip		6	Flextural Slip	
7	Simple Shear (single)	90	7	Flextural Slip		7	Flextural Slip	

Inline 1778 – NAM1990D

Base Holland Marl base -opt			Base Cretaceous base -min			Base Cretaceous base -opt		
Block	Process	Shear dip Corrections	Block	Process	Shear dip Corrections	Block	Process	Shear dip Corrections
1	Simple Shear	90	1	Flextural Slip (varying pins)		1	Flextural Slip (varying pins)	
2	Simple Shear	90	2	Flextural Slip		2	Flextural Slip	
3	Simple Shear	90	3	Flextural Slip		3	Flextural Slip	
4	Simple Shear	80	4	Flextural Slip		4	Flextural Slip	
5	Flextural Slip		5	Flextural Slip		5	Flextural Slip	
6			6	Flextural Slip		6	Flextural Slip	
7	Simple Shear	90	7	Flextural Slip		7	Flextural Slip	
8	Simple Shear	90	8	Flextural Slip		8	Flextural Slip	
9	Simple Shear	90	9	Flextural Slip		9	Flextural Slip	
10	Simple Shear	83	10	Flextural Slip		10	Flextural Slip	
11	Simple Shear	-83	11	Flextural Slip		11	Flextural Slip	
12	Simple Shear	-83	12	Flextural Slip		12	Flextural Slip	
13	Simple Shear	-83	13	Flextural Slip		13	Flextural Slip	
14	Simple Shear	-69	14	Flextural Slip		14	Flextural Slip	
15	Simple Shear	-80	15	Flextural Slip		15	Flextural Slip	

Inline 1299 - NAM1991A

Base Holland Marl base -opt			Base Cretaceous base -min			Base Cretaceous base -opt		
Block	Process	Shear dip Corrections	Block	Process	Shear dip Corrections	Block	Process	Shear dip Corrections
1	Simple Shear	72	1	Flextural Slip (varying pins)		1	Flextural Slip (varying pins)	
2	Simple Shear	90	2	Flextural Slip		2	Flextural Slip	
3	Simple Shear	70	3	Flextural Slip		3	Flextural Slip	
4	Simple Shear	80	4	Flextural Slip		4	Flextural Slip	
5			5	Flextural Slip		5	Flextural Slip	
6	Simple Shear	-57	6	Flextural Slip		6	Flextural Slip	

Table 13: Processes used in the restoration procedure

1.2. Restoration data

Table 14: Recorded minimal visible vertical, and expected realistic vertical thicknesses of layers used to determine the amount of eroded material

Z3AMC1989A Inline 1299:

Target Horizon (depths) (interpretation)	**at 1/3 of section**			**at 2/3 of section**		
	min (m)	***opt (m)***	***max (m)***	***min (m)***	***opt (m)***	***max (m)***
Base Tertiary Target	1161	1268	1278	1281	1391	1450
Top Texel Marl Target	1668	1948	2068	1788	2071	2240
Base Holland Marl Target	2064	2348	2478	2184	2471	2650
Base Cretaceous Target	2566	3075	3430	2686	3198	3602
Posidonia Shale (including eroded)						
Top Triassic (Rifting stages)						

** Missing thicknesses add up downwards*

** Pattern for relation between 1/3 and 2/3 based on remarks*

** Excluding compaction infuence*

**** These are only guiding points, actual targets show less separation except at paleo depo centers - actively subsiding fault blocks, later uplifted and heavily eroded***

Observed data

Horizons (thickness)	***min (m)***	***opt (m)***	***max (m)***		
Lower Tertiary	583	690	700	uniform	<- already missing section in the left side
Upper Cretaceous	507	680	790	mostly left side	
Middle Cretaceous	396	400	410	mostly left side	
Lower Cretaceous including effect from Upper Jurassic	502	727	952	mostly left side	
	observed	estimated	visualized		
		averaged	copied		

Z3NAM1990D Inline 1778:

Target Horizon (depths) (interpretation)	at 1/3 of section			at 2/3 of section		
	min (m)	***opt (m)***	***max (m)***	***min (m)***	***opt (m)***	***max (m)***
Base Tertiary Target	1197	1210	1220	1197	1260	1320
TopTexelMarl Target (Base Chalk)	1679	2010	2402	1729	2110	2552
BaseHollandMarl Target	2035	2480	2991	2185	2680	3241
Base Cretaceous Target	2785	3430	4241	2935	3630	4491
Posidonia Shale (including eroded)						
Top Triassic (Rifting stages)						

** Missing thicknesses add up downwards*

** Pattern for relation between 1/3 and 2/3 based on remarks*

** Excluding compaction infuence*

**** These are only guiding points, actual targets show less separation except at paleo depo centers - actively subsiding fault blocks, later uplifted and heavily eroded***

Observed data

Horizons (thickness)	***min (m)***	***opt (m)***	***max (m)***	***remarks****
Lower Tertiary	677	690	700	uniform
Upper Cretaceous (Chalk)	482	800	1182	mostly at center
Middle Cretaceous (Holland Marl) - Rijnland	356	470	589	mostly at left side
Lower Cretaceous	750	950	1250	only at center and left, includes erosion on Altena Group
(including Upper Jurassic contribution)				see p.114 Geology of Netherlands

observed	estimated	visualized
	averaged	

plus 500 m

A3NAM1991A Inline 1299:

Target Horizon (depths) (interpretation)	at 1/3 of section			at 2/3 of section		
	min (m)	***opt (m)***	***max (m)***	***min (m)***	***opt (m)***	***max (m)***
Base Tertiary Target	801	1059	1089	851	1109	1139
Top Texel Marl Target	1267	1574	1687	1317	1624	1737
Base Holland Marl Target	1689	2030	2165	1739	2080	2215
Base Cretaceous Target	2429	3030	3570	2479	3080	3620
Posidonia Shale (including eroded)						
Top Triassic (Rifting stages)						

** Missing thicknesses add up downwards*

** Pattern for relation between 1/3 and 2/3 based on remarks*

** Excluding compaction infuence*

**** These are only guiding points, actual targets show less separation except at paleo depo centers - actively subsiding fault blocks, later uplifted and heavily eroded***

Observed data

Horizons (thickness)	***min (m)***	***opt (m)***	***max (m)***		
Lower Tertiary	332	590	620	not clear*	
Upper Cretaceous (Chalk)	466	515	598	mostly at center	
Middle Cretaceous (Holland Marl) - Rijnland	422	456	478	mostly right side	
Lower Cretaceous - Schieland	740	1000	1405	unreliable*	<- highly dependant on fault blocks
Upper Jurassic					

Copied from another section - 100m

* low quality seismic, missing picks

1.3. Depth table

MINIMAL CASE

Top Middle Bunter depths at end of given reconstructed periods

1	NOW - For comparison to avoid influence from time-depth conversion and interpretation
2	Mid Tertiary - Oligocene - end Rupelian/Chattian - 28.4 Ma ago
3	Upper Creataceous - end Cenomanian - 65.5 Ma ago
4	Lower Creatacoues - end Albian - 99.6 Ma ago
5	Lower Creataceous - end Barriasian - 112.0 Ma ago (including erosion on Upper jurassic (Altena) from 145.5 Ma to 161.2 Ma ago)

Inline993

SW — Section direction = **46**

			1		2		3		4		5	
Distance from right post	x (RD)	y (RD)	Depth of Top Triassic (m)	Depth of Top Middle Bunter (m)	Depth of Top Triassic (m)	Depth of Top Middle Bunter (m)	Depth of Top Triassic (m)	Depth of Top Middle Bunter (m)	Depth of Top Triassic (m)	Depth of Top Middle Bunter (m)	Depth of Top Triassic (m)	Depth of Top Middle Bunter (m)
0.00												
0.50												
1.00												
1.50												
2.00												
2.50												
3.00												
3.50												
4.00												
4.50												
5.00												
5.50	49775	461072	2685	2927	2329	2571	1752	1994	1089	1331	1050	1292
6.00	50126	461428	2753	2995	2390	2632	1862	2104	1177	1419	1094	1336

6.50	50476	461785	2791	3033	2442	2684	1899	2141	1241	1483	1138	1380
7.00	50827	462141	2844	3086	2503	2745	1994	2236	1322	1564	1201	1443
7.50	51177	462498	2887	3129	2555	2797	2008	2250	1370	1612	1156	1398
8.00	51528	462855	2774	3016	2459	2701	1906	2148	1314	1556	1041	1283
8.50	51878	463211	2662	2904	2364	2606	1847	2089	1241	1483	1067	1309
9.00	52229	463568	2683	2925	2425	2667	1913	2155	1281	1523	1094	1336
9.50	52579	463925	2839	3081	2633	2875	2103	2345	1491	1733	1565	1807
10.00	52929	464281	2877	3119	2685	2927	2169	2411	1555	1797	1591	1833
10.50	53280	464638	2941	3183	2763	3005	2279	2521	1635	1877	1627	1869
11.00	53630	464994	3006	3248	2849	3091	2374	2616	1732	1974	1662	1904
11.50	53981	465351	3086	3328	2962	3204	2498	2740	1852	2094	1742	1984
12.00	54331	465708	3183	3425	3075	3317	2615	2857	1973	2215	1795	2037
12.50	54682	466064	3274	3516	3161	3403	2710	2952	2102	2344	1875	2117
13.00	55032	466421	3016	3258	2953	3195	2542	2784	1868	2110	1955	2197
13.50	55383	466778	2990	3232	2901	3143	2505	2747	1860	2102	1849	2091
14.00	55733	467134	3065	3307	2997	3239	2593	2835	1925	2167	1875	2117
14.50	56084	467491	3081	3323	3031	3273	2622	2864	1965	2207	1875	2117
15.00	56434	467847	3097	3339	3066	3308	2637	2879	1997	2239	1822	2064
15.50	56784	468204	3011	3253	2953	3195	2608	2850	2021	2263	1982	2224
16.00	57135	468561	3033	3275	2987	3229	2666	2908	2005	2247	1973	2215
16.50	57485	468917	3097	3339	3076	3318	2768	3010	2029	2271	1964	2206
17.00	57836	469274	3194	3436	3194	3436	2878	3120	2134	2376	2000	2242

17.50	58186	469631	3221	3463	3206	3448	2885	3127	2198	2440	1964	2206
18.00	58537	469987	3129	3371	3117	3359	2856	3098	2190	2432	1964	2206
18.50	58887	470344							2166	2408	1965	2207

NE

inline 1778

SW Section direction = **44**

			1		2		3		4		5	
Distance from right post	x (RD)	y (RD)	Depth of Top Triassic (m)	Depth of Top Middle Bunter (m)	Depth of Top Triassic (m)	Depth of Top Middle Bunter (m)	Depth of Top Triassic (m)	Depth of Top Middle Bunter (m)	Depth of Top Triassic (m)	Depth of Top Middle Bunter (m)	Depth of Top Triassic (m)	Depth of Top Middle Bunter (m)
0.00												
0.50												
1.00												
1.50												
2.00												
2.50												
3.00												
3.50												
4.00												
4.50												
5.00												
5.50												
6.00												

6.50												
7.00												
7.50												
8.00												
8.50	63520	450165	2855	3097	2561	2803	1926	2168	1347	1589	1260	1502
9.00	63877	450515	2855	3097	2551	2793	1935	2177	1337	1579	1275	1517
9.50	64234	450866	3143	3385	2892	3134	2241	2483	1680	1922	1693	1935
10.00	64590	451216	3153	3395	2902	3144	2241	2483	1671	1913	1683	1925
10.50	64947	451566	3183	3425	2963	3205	2299	2541	1726	1968	1723	1965
11.00	65304	451916	3193	3435	3003	3245	2341	2583	1745	1987	1754	1996
11.50	65661	452266	3203	3445	3013	3255	2366	2608	1772	2014	1754	1996
12.00	66018	452616	3250	3492	3083	3325	2424	2666	1837	2079	1764	2006
12.50	66375	452966	3312	3554	3143	3385	2482	2724	1902	2144	1765	2007
13.00	66732	453317	3352	3594	3164	3406	2540	2782	1958	2200	1755	1997
13.50	67089	453667	3104	3346	3043	3285	2399	2641	1865	2107	1713	1955
14.00	67446	454017	2985	3227	2922	3164	2258	2500	1810	2052	1621	1863
14.50	67803	454367	2895	3137	2832	3074	2175	2417	1698	1940	1520	1762
15.00	68160	454717	2885	3127	2772	3014	2109	2351	1615	1857	1571	1813
15.50	68517	455067	3004	3246	2882	3124	2250	2492	1717	1959	1632	1874
16.00	68874	455417	3084	3326	2963	3205	2341	2583	1828	2070	1672	1914
16.50	69231	455768	3044	3286	3013	3255	2399	2641	1921	2163	1723	1965

17.00	69588	456118	3799	4041	3756	3998						
17.50	69944	456468	3769	4011	3736	3978	3145	3387	2652	2894	2528	2770
18.00	70301	456818	3690	3932	3686	3928	3104	3346	2661	2903	2548	2790
18.50	70658	457168	3620	3862	3646	3888	3071	3313	2615	2857	2507	2749
19.00	71015	457518	3541	3783	3596	3838	3054	3296	2605	2847	2558	2800
19.50	71372	457868	3390	3632	3485	3727	3004	3246	2578	2820	2589	2831
20.00	71729	458219	3163	3405	3310	3552	3278	3520	2652	2894	2517	2759
20.50	72086	458569	3292	3534	3443	3685	3369	3611	2744	2986	2579	2821
21.00	72443	458919	3252	3494	3534	3776	3485	3727	2865	3107	2619	2861
21.50	72800	459269	3173	3415	3509	3751	3468	3710	2846	3088	2609	2851
22.00	73157	459619	3233	3475	3468	3710	3460	3702	2828	3070	2579	2821
22.50	73514	459969	3948	4190	4124	4366	3435	3677	2855	3097	2599	2841
23.00	73871	460319	4057	4299	4249	4491	3983	4225	3411	3653		
23.50	74228	460670	4167	4409	4348	4590	4057	4299	3485	3727	3424	3666
24.00	74585	461020	4206	4448	4431	4673	4074	4316	3522	3764	3464	3706
24.50	74941	461370	4216	4458	4489	4731	4132	4374	3587	3829	3475	3717
25.00	75298	461720	4028	4270	4481	4723	3875	4117	3346	3588	3495	3737
25.50	75655	462070	4008	4250	4257	4499	3858	4100	3392	3634	3383	3625
26.00	76012	462420	3561	3803	3759	4001	3361	3603	2902	3144		
26.50	76369	462770	3441	3683	3833	4075	3460	3702	2966	3208	2955	3197

27.00	76726	463121	3451	3693	3717	3959	3370	3612	2892	3134	2935	3177
27.50	77083	463471	3481	3723	3717	3959	3344	3586	2846	3088	2894	3136
28.00	77440	463821	3501	3743	3759	4001	3410	3652	2883	3125	2874	3116
28.50	77797	464171	3521	3763	3767	4009	3452	3694	2929	3171	2894	3136
29.00	78154	464521	3481	3723	3800	4042	3510	3752	2976	3218	2935	3177
29.50	78511	464871	3292	3534	3509	3751	3261	3503	2698	2940	2762	3004
30.00	78868	465221	3283	3525	3526	3768	3319	3561	2726	2968	2762	3004
30.50	79225	465572	3233	3475	3543	3785	3402	3644	2772	3014	2772	3014
31.00	79582	465922	3143	3385	3485	3727	3419	3661	2791	3033	2752	2994
31.50	79939	466272	2925	3167	3227	3469	3245	3487	2744	2986	2650	2892
32.00	80295	466622	2776	3018	3235	3477	3245	3487	2698	2940	2640	2882
32.50	80652	466972	2607	2849	3069	3311	3095	3337	2559	2801	2619	2861
33.00	81009	467322			2920	3162	2979	3221	2411	2653	2507	2749
33.50	81366	467672	3620	3862								
34.00	81723	468023	3640	3882	3883	4125	3891	4133	3355	3597	3149	3391
34.50	82080	468373	3630	3872	3925	4167	3941	4183	3411	3653	3210	3452
35.00	82437	468723	3600	3842	3908	4150	3941	4183	3457	3699	3220	3462
35.50	82794	469073	3532	3774	3883	4125	3883	4125	3411	3653	3200	3442
36.00	83151	469423	3481	3723	3833	4075	3808	4050	3327	3569	3179	3421
36.50	83508	469773	3372	3614	3775	4017	3717	3959	3253	3495	3149	3391

37.00	83865	470123	3233	3475	3667	3909	3568	3810	3124	3366	3027	3269
37.50	84222	470474	2518	2760								
38.00	84579	470824	2648	2890	2820	3062	2772	3014	2615	2857	2405	2647
38.50	84936	471174	2736	2978	2878	3120	2822	3064	2605	2847	2446	2688
39.00	85292	471524	2776	3018	3011	3253	2905	3147	2652	2894	2456	2698
39.50	85649	471874	2816	3058	3028	3270	2921	3163	2670	2912	2365	2607
40.00	86006	472224	2547	2789	3103	3345	2913	3155	2661	2903	2343	2585
40.50	86363	472574	3283	3525	2845	3087	2706	2948	2587	2829	2365	2607
41.00	86720	472925	3213	3455	3485	3727	3402	3644	2828	3070	2548	2790
41.50	87077	473275	3183	3425	3426	3668	3311	3553	2698	2940	2538	2780
42.00	87434	473625	3203	3445	3410	3652	3328	3570	2747	2989	2599	2841
42.50	87791	473975	3223	3465	3418	3660	3294	3536	2744	2986	2599	2841
43.00	88148	474325	3253	3495	3410	3652	3294	3536	2772	3014	2619	2861
43.50	88505	474675	3213	3455	3418	3660	3294	3536	2791	3033	2619	2861
44.00	88862	475025	3124	3366	3385	3627	3236	3478	2754	2996	2497	2739
44.50	89219	475376	3054	3296	3320	3562	3129	3371	2661	2903	2497	2739
45.00	89576	475726			3227	3469	3054	3296	2633	2875	2497	2739
45.50	89933	476076										
46.00	90290	476426										
46.50	90646	476776										
47.00												
47.50												

NE

inline 1299

SW Section direction = **44**

1					2		3		4		5	
Distance from right post	x (RD)	y (RD)	Depth of Top Triassic (m)	Depth of Top Middle Bunter (m)	Depth of Top Triassic (m)	Depth of Top Middle Bunter (m)	Depth of Top Triassic (m)	Depth of Top Middle Bunter (m)	Depth of Top Triassic (m)	Depth of Top Middle Bunter (m)	Depth of Top Triassic (m)	Depth of Top Middle Bunter (m)
0.00	73961	446075	3062	3304	2818	3060	2416	2658	1978	2220	2512	2754
0.50	74321	446423	3248	3490	2970	3212	2595	2837	2140	2382	2626	2868
1.00	74680	446770	3349	3591	3094	3336	2710	2952	2264	2506	2684	2926
1.50	75040	447117	3484	3726	3227	3469	2831	3073	2406	2648	2751	2993
2.00	75400	447465	3585	3827	3342	3584	2946	3188	2502	2744	2780	3022
2.50	75759	447812	3619	3861	3427	3669	3046	3288	2597	2839	2808	3050
3.00	76119	448159	3686	3928	3704	3946	3146	3388	2701	2943	2818	3060
3.50	76479	448507	3855	4097	3856	4098	3346	3588	2920	3162	2914	3156
4.00	76838	448854	3956	4198	3847	4089	3539	3781	3101	3343	2990	3232
4.50	77198	449201	3905	4147	3866	4108	3568	3810	3092	3334	3000	3242
5.00	77558	449549	3888	4130	3847	4089	3647	3889	3149	3391	2981	3223
5.50	77917	449896	3821	4063	2694	2936	3704	3946	3177	3419	2990	3232
6.00	78277	450243	2642	2884	2875	3117	2702	2944	2216	2458	2387	2629

6.50	78637	450591	2844	3086	3170	3412	2903	3145	2378	2620	2445	2687
7.00	78996	450938	3080	3322	3227	3469	3117	3359	2559	2801	2540	2782
7.50	79356	451285	3164	3406	3303	3545	3103	3345	2559	2801	2473	2715
8.00	79716	451633	3248	3490	3427	3669	3110	3352	2568	2810	2483	2725
8.50	80075	451980	3400	3642	3485	3727	3132	3374	2625	2867	2540	2782
9.00	80435	452327	3450	3692	3513	3755	3132	3374	2644	2886	2530	2772
9.50	80795	452675	3467	3709	3475	3717	3153	3395	2673	2915	2530	2772
10.00	81154	453022	3450	3692	3351	3593	3189	3431	2721	2963	2559	2801
10.50	81514	453369	3332	3574	3342	3584	3189	3431	2692	2934	2521	2763
11.00	81874	453717	3366	3608	3637	3879	3282	3524	2778	3020	2607	2849
11.50	82233	454064	3585	3827	3837	4079	3733	3975	3168	3410	3383	3625
12.00	82593	454411	3787	4029	4018	4260	3961	4203	3463	3705	3469	3711
12.50	82953	454759	3956	4198	4009	4251	4112	4354	3653	3895	3469	3711
13.00	83312	455106	3939	4181	4028	4270	4069	4311	3663	3905	3478	3720
13.50	83672	455453	3905	4147	3980	4222	4033	4275	3691	3933	3517	3759
14.00	84032	455801	3855	4097	3951	4193	3997	4239	3710	3952	3517	3759
14.50	84391	456148	3753	3995	3875	4117	3911	4153	3672	3914	3478	3720
15.00	84751	456495	3602	3844	3723	3965	3740	3982	3549	3791	3517	3759
15.50	85111	456843	2759	3001	2846	3088	2903	3145	2730	2972	2607	2849
16.00	85470	457190	2776	3018	2865	3107	28	3138	2701	2943	2502	2744

16.50	85830	457537	2759	3001	2856	3098	2896028	3102	2530	2772	2435	2677
17.00	86190	457885	2810	3052	2865	3107	2846	3088	2445	2687	2512	2754
17.50	86549	458232	2827	3069	2894	3136	2853	3095	2454	2696	2579	2821
18.00	86909	458579	2894	3136	2941	3183	2946	3188	2549	2791	2626	2868
18.50	87269	458927	2574	2816	2598	2840	2624	2866	2368	2610	2473	2715
19.00	87628	459274	2625	2867	2646	2888	2702	2944	2663	2905	2550	2792
19.50	87988	459621	2861	3103	2903	3145	2960	3202	2606	2848	2531	2773
20.00	88348	459969	2759	3001	2808	3050	2846	3088	2511	2753	2531	2773
20.50	88707	460316	2864	3106	2875	3117	2946	3188	2597	2839	2512	2754
21.00	89067	460663	3256	3498	3284	3526	3325	3567	3035	3277	3095	3337
21.50	89427	461011	3325	3567	3332	3574	3375	3617	3149	3391	3124	3366
22.00	89786	461358	3336	3578	3351	3593	3389	3631	3225	3467	3201	3443
22.50	90146	461705	3302	3544	3294	3536	3332	3574	3158	3400	3134	3376
23.00	90506	462053	3175	3417	3199	3441	3210	3452	3073	3315	3009	3251
23.50	90865	462400	3152	3394	3151	3393	3160	3402	3025	3267	2917	3159
24.00	91225	462747	3071	3313	3094	3336	3074	3316	2958	3200	2885	3127
24.50	91585	463095									2818	3060

OPTIMAL CASES

inline 993

SW Section direction =

1	46				2		3		4		5	
Distance from right post	x (RD)	y (RD)	Depth of Top Triassic (m)	Depth of Top Middle Bunter (m)	Depth of Top Triassic (m)	Depth of Top Middle Bunter (m)	Depth of Top Triassic (m)	Depth of Top Middle Bunter (m)	Depth of Top Triassic (m)	Depth of Top Middle Bunter (m)	Depth of Top Triassic (m)	Depth of Top Middle Bunter (m)
0.00												
0.50												
1.00												
1.50												
2.00												
2.50												
3.00												
3.50												
4.00												
4.50												
5.00												
5.50	49775	461072	2685	2927	2329	2571	1765	2007	1001	1243	1198	1440
6.00	50126	461428	2753	2995	2390	2632	1875	2117	1095	1337	1218	1460
6.50	50476	461785	2791	3033	2442	2684	1965	2207	1161	1403	1258	1500
7.00	50827	46214	2844	308	2503	2745	2014	22	1204	1446	1267	1509

		1		6				56				
7.50	51177	462498	2887	3129	2555	2797	2125	2367	1355	1597	1307	1549
8.00	51528	462855	2774	3016	2459	2701	2125	2367	1195	1437	1317	1559
8.50	51878	463211	2662	2904	2364	2606	1978	2220	1197	1439	1238	1480
9.00	52229	463568	2683	2925	2425	2667	2007	2249	1329	1571	1228	1470
9.50	52579	463925	2839	3081	2633	2875	2220	2462	1490	1732	1336	1578
10.00	52929	464281	2877	3119	2685	2927	2315	2557	1563	1805	1830	2072
10.50	53280	464638	2941	3183	2763	3005	2389	2631	1630	1872	1810	2052
11.00	53630	464994	3006	3248	2849	3091	2484	2726	1681	1923	1790	2032
11.50	53981	465351	3086	3328	2962	3204	2609	2851	1784	2026	1790	2032
12.00	54331	465708	3183	3425	3075	3317	2748	2990	1901	2143	1810	2052
12.50	54682	466064	3274	3516	3161	3403	2881	3123	1989	2231	1820	2062
13.00	55032	466421	3016	3258	2953	3195	2624	2866	2102	2344	1919	2161
13.50	55383	466778	2990	3232	2901	3143	2646	2888	1895	2137	2047	2289
14.00	55733	467134	3065	3307	2997	3239	2726	2968	1916	2158	2086	2328
14.50	56084	467491	3081	3323	3031	3273	2785	3027	1982	2224	2136	2378
15.00	56434	467847	3097	3339	3066	3308	2829	3071	2026	2268	2077	2319
15.50	56784	468204	3011	3253	2953	3195	2866	3108	2136	2378	2057	2299
16.00	57135	468561	3033	3275	2987	3229	2690	2932	1938	2180	1919	2161
16.50	57485	468917	3097	3339	3076	3318	2778	3020	1982	2224	1938	2180

17.00	57836	469274	3194	3436	3194	3436	2895	3137	2033	2275	1938	2180
17.50	58186	469631	3221	3463	3206	3448	3020	3262	2092	2334	1998	2240
18.00	58537	469987	3129	3371	3117	3359	3027	3269	2114	2356	2037	2279
18.50	58887	470344					2998	3240	2136	2378	1988	2230
19.00												
19.50												
20.00												

NE

Inline1778

1	Section angle: **44**				**3**		**4**		**5**	
Distance from right post	x (RD)	y (RD)	Depth of Top Triassic (m)	Depth of Top Middle Bunter (m)	Depth of Top Triassic (m)	Depth of Top Middle Bunter (m)	Depth of Top Triassic (m)	Depth of Top Middle Bunter (m)	Depth of Top Triassic (m)	Depth of Top Middle Bunter (m)	Depth of Top Triassic (m)	Depth of Top Middle Bunter (m)
0.00												
0.50												
1.00												
1.50												
2.00												
2.50												
3.00												
3.50												
4.00												
4.50												
5.00												
5.50												
6.00												

6.50														
7.00														
7.50														
8.00														
8.50	63520	450165	2855	3097	2561	2803	1983	2225	1300	1542	1167	1409		
9.00	63877	450515	2855	3097	2551	2793	2003	2245	1313	1555	1155	1397		
9.50	64234	450866	3143	3385	2892	3134	2398	2640	1721	1963				
10.00	64590	451216	3153	3395	2902	3144	2418	2660	1758	2000	1806	2048		
10.50	64947	451566	3183	3425	2963	3205	2458	2700	1808	2050	1829	2071		
11.00	65304	451916	3193	3435	3003	3245	2509	2751	1820	2062	1829	2071		
11.50	65661	452266	3203	3445	3013	3255	2509	2751	1833	2075	1818	2060		
12.00	66018	452616	3250	3492	3083	3325	2570	2812	1907	2149	1841	2083		
12.50	66375	452966	3312	3554	3143	3385	2630	2872	1969	2211	1875	2117		
13.00	66732	453317	3352	3594	3164	3406	2701	2943	2089	2331	1932	2174		
13.50	67089	453667	3104	3346	3043	3285	2711	2953	2055	2297	1969	2211		
14.00	67446	454017	2985	3227	2922	3164	2509	2751	1944	2186	1692	1934		
14.50	67803	454367	2895	3137	2832	3074	2378	2620	1820	2062	1578	1820		
15.00	68160	454717	2885	3127	2772	3014	2307	2549	1721	1963	1601	1843		
15.50	68517	455067	3004	3246	2882	3124	2337	2579	1771	2013	1612	1854		
16.00	68874	455417	3084	3326	2963	3205	2448	2690	1894	2136	1612	1854		
16.50	69231	455768	3044	3286	3013	3255	2560	2802	1993	2235	1681	1923		

17.00	69588	456118	3799	4041	3756	3998					1703	1945
17.50	69944	456468	3769	4011	3736	3978	3389	3631	2637	2879		
18.00	70301	456818	3690	3932	3686	3928	3439	3681	2699	2941	2560	2802
18.50	70658	457168	3620	3862	3646	3888	3429	3671	2674	2916	2594	2836
19.00	71015	457518	3541	3783	3596	3838	3409	3651	2674	2916	2628	2870
19.50	71372	457868	3390	3632	3485	3727	3409	3651	2650	2892	2674	2916
20.00	71729	458219	3163	3405	3310	3552	3288	3530	2526	2768	2640	2882
20.50	72086	458569	3292	3534	3443	3685	3520	3762	2749	2991	2583	2825
21.00	72443	458919	3252	3494	3534	3776	3702	3944	2922	3164	2674	2916
21.50	72800	459269	3173	3415	3509	3751	3783	4025	2959	3201	2651	2893
22.00	73157	459619	3233	3475	3468	3710	3743	3985	2910	3152	2617	2859
22.50	73514	459969	3948	4190	4124	4366	3763	4005	2947	3189	2617	2859
23.00	73871	460319	4057	4299	4249	4491	4410	4652				
23.50	74228	460670	4167	4409	4348	4590	4520	4762	3591	3833	3839	4081
24.00	74585	461020	4206	4448	4431	4673	4622	4864	3690	3932	3907	4149
24.50	74941	461370	4216	4458	4489	4731	4633	4875	3700	3942	3930	4172
25.00	75298	461720	4028	4270	4481	4723	4643	4885	3727	3969	3987	4229
25.50	75655	462070	4008	4250	4257	4499	4339	4581	3380	3622	4044	4286
26.00	76012	462420	3561	3803	3759	4001	4339	4581	3405	3647	3530	3772
26.50	7636	462770	3441	368	3833	4075	3945	4187	3009	3251	3565	380

	9			3								7
27.00	76726	463121	3451	3693	3717	3959	3904	4146	3000	3242	3165	3407
27.50	77083	463471	3481	3723	3717	3959	3884	4126	2996	3238	3142	3384
28.00	77440	463821	3501	3743	3759	4001	3874	4116	2959	3201	2925	3167
28.50	77797	464171	3521	3763	3767	4009	3864	4106	2972	3214	2971	3213
29.00	78154	464521	3481	3723	3800	4042	3864	4106	2972	3214	3028	3270
29.50	78511	464871	3292	3534	3509	3751	3773	4015	2885	3127	3039	3281
30.00	78868	465221	3283	3525	3526	3768	3783	4025	2872	3114	3097	3339
30.50	79225	465572	3233	3475	3543	3785	3743	3985	2835	3077	2891	3133
31.00	79582	465922	3143	3385	3485	3727	3722	3964	2823	3065	2914	3156
31.50	79939	466272	2925	3167	3227	3469	3551	3793	2761	3003	2937	3179
32.00	80295	466622	2776	3018	3235	3477	3530	3772	2650	2892	2971	3213
32.50	80652	466972	2607	2849	3069	3311	3510	3752	2612	2854	2914	3156
33.00	81009	467322			2920	3162	3470	3712	2575	2817	2914	3156
33.50	81366	467672	3620	3862					2538	2780	2902	3144
34.00	81723	468023	3640	3882	3883	4125	4279	4521			2902	3144
34.50	82080	468373	3630	3872	3925	4167	4309	4551	3541	3783		
35.00	82437	468723	3600	3842	3908	4150	4370	4612	3492	3734	3827	4069
35.50	82794	469073	3532	3774	3883	4125	4390	4632	3454	3696	3896	4138
36.00	83151	469423	3481	3723	3833	4075	4360	4602	3380	3622	3873	4115

36.50	83508	469773	3372	3614	3775	4017	4339	4581	3318	3560	3816	4058
37.00	83865	470123	3233	3475	3667	3909	4279	4521	3219	3461	3782	4024
37.50	84222	470474	2588	2830			4097	4339	3071	3313	3736	3978
38.00	84579	470824	2648	2890	2820	3062					3610	3852
38.50	84936	471174	2736	2978	2878	3120	3318	3560	2736	2978		
39.00	85292	471524	2776	3018	3011	3253	3379	3621	2736	2978	2674	2916
39.50	85649	471874	2816	3058	3028	3270	3460	3702	2724	2966	2686	2928
40.00	86006	472224	2547	2789	3103	3345	3490	3732	2712	2954	2686	2928
40.50	86363	472574	3283	3525	2845	3087	3379	3621	2702	2944	2663	2905
41.00	86720	472925	3213	3455	3485	3727	3288	3530	2665	2907	2663	2905
41.50	87077	473275	3183	3425	3426	3668	3844	4086	2832	3074	2640	2882
42.00	87434	473625	3203	3445	3410	3652	3803	4045	2842	3084	2640	2882
42.50	87791	473975	3223	3465	3418	3660	3813	4055	2842	3084	2971	3213
43.00	88148	474325	3253	3495	3410	3652	3834	4076	2840	3082	3005	3247
43.50	88505	474675	3213	3455	3418	3660	3864	4106	2830	3072	3028	3270
44.00	88862	475025	3124	3366	3385	3627	3824	4066	2820	3062	3039	3281
44.50	89219	475376	3054	3296	3320	3562	3733	3975	2810	3052	3039	3281
45.00	89576	475726			3227	3469	3631	3873	2800	3042	3085	3327
45.50	89933	476076					3600	3842	2790	3032	3039	3281
46.00	90290	476426									3005	3240

46.50	0 90646	476776								2994	7 3236	
47.00												
47.50												

NE

inline 1299

SW Section direction =

1	44				2		3		4		5	
Distance from right post	x (RD)	y (RD)	Depth of Top Triassic (m)	Depth of Top Middle Bunter (m)	Depth of Top Triassic (m)	Depth of Top Middle Bunter (m)	Depth of Top Triassic (m)	Depth of Top Middle Bunter (m)	Depth of Top Triassic (m)	Depth of Top Middle Bunter (m)	Depth of Top Triassic (m)	Depth of Top Middle Bunter (m)
0.00	73961	446075	3062	3304	2818	3060	2371	2613	2017	2259	3227	3469
0.50	74321	446423	3248	3490	2970	3212	2524	2766	2171	2413	3309	3551
1.00	74680	446770	3349	3591	3094	3336	2642	2884	2307	2549	3344	3586
1.50	75040	447117	3484	3726	3227	3469	2795	3037	2426	2668	3344	3586
2.00	75400	447465	3585	3827	3342	3584	2896	3138	2512	2754	3332	3574
2.50	75759	447812	3619	3861	3427	3669	3015	3257	2614	2856	3321	3563
3.00	76119	448159	3686	3928	3704	3946	3150	3392	2734	2976	3309	3551
3.50	76479	448507	3855	4097	3856	4098	3380	3622	2921	3163	3356	3598

4.00	76838	448854	3956	4198	3847	4089	3556	3798	3058	3300	3344	3586
4.50	77198	449201	3905	4147	3866	4108	3624	3866	3006	3248	3309	3551
5.00	77558	449549	3888	4130	3847	4089	3759	4001	3075	3317	3321	3563
5.50	77917	449896	3821	4063	2694	2936	3878	4120	3177	3419	3344	3586
6.00	78277	450243	2642	2884	2875	3117	2965	3207	2239	2481	2620	2862
6.50	78637	450591	2844	3086	3170	3412	3085	3327	2426	2668	2620	2862
7.00	78996	450938	3080	3322	3227	3469	3370	3612	2665	2907	2690	2932
7.50	79356	451285	3164	3406	3303	3545	3421	3663	2682	2924	2620	2862
8.00	79716	451633	3248	3490	3427	3669	3421	3663	2648	2890	2620	2862
8.50	80075	451980	3400	3642	3485	3727	3472	3714	2734	2976	2667	2909
9.00	80435	452327	3450	3692	3513	3755	3472	3714	2734	2976	2632	2874
9.50	80795	452675	3467	3709	3475	3717	3455	3697	2716	2958	2620	2862
10.00	81154	453022	3450	3692	3351	3593	3387	3629	2699	2941	2609	2851
10.50	81514	453369	3332	3574	3342	3584	3370	3612	2631	2873	2550	2792
11.00	81874	453717	3366	3608	3637	3879	3506	3748	2734	2976	2655	2897
11.50	82233	454064	3585	3827	3837	4079	4013	4255	3160	3402	3566	3808
12.00	82593	454411	3787	4029	4018	4260	4267	4509	3450	3692	3589	3831
12.50	82953	454759	3956	4198	4009	4251	4284	4526	3655	3897	3636	3878
13.00	83312	455106	3939	4181	4028	4270	4470	4712	3689	3931	3659	3901
13.50	83672	455453	3905	4147	3980	4222	4444	4662	3723	3965	3671	3913

		53		7			20					13
14.00	84032	45801	3855	4097	3951	4193	4403	4645	3757	3999	3671	3913
14.50	84391	45648	3753	3995	3875	4117	4386	4628	3706	3948	3624	3866
15.00	84751	45695	3602	3844	3723	3965	4301	4543	3569	3811	3671	3913
15.50	85111	45643	2759	3001	2846	3088	4115	4357	2614	2856	2317	2559
16.00	85470	45790	2776	3018	2865	3107	3448	3690	2512	2754	2270	2512
16.50	85830	45737	2759	3001	2856	3098	3438	3680	2512	2754	2305	2547
17.00	86190	45785	2810	3052	2865	3107	3421	3663	2545	2787	2363	2605
17.50	86549	45832	2827	3069	2894	3136	3387	3629	2450	2692	2328	2570
18.00	86909	45879	2894	3136	2941	3183	3387	3629	2450	2692	2363	2605
18.50	87269	45927	2574	2816	2598	2840	3421	3663	2450	2692	2574	2816
19.00	87628	45974	2625	2867	2646	2888	3201	3443	2497	2739	2632	2874
19.50	87988	45921	2861	3103	2903	3145	3218	3460	2640	2882	2422	2664
20.00	88348	45969	2759	3001	2808	3050	3389	3631	2509	2751	2398	2640
20.50	88707	46016	2864	3106	2875	3117	3252	3494	2509	2751	2363	2605
21.00	89067	46063	3256	3498	3284	3526	3289	3531	2616	2858	2375	2617
21.50	89427	46111	3325	3567	3332	3574	3641	3883	2925	3167	2900	3142
22.00	89786	46158	3336	3578	3351	3593	3692	3934	2985	3227	2947	3189
22.50	90146	46205	3302	3544	3294	3536	3709	3951	2925	3167	2877	3119
23.00	90506	46253	3175	3417	3199	3441	3641	3883	2842	3084	2772	3014

23.50	90865	462400	3152	3394	3151	3393	3489	3731	2842	3084	2749	2991
24.00	91225	462747	3071	3313	3094	3336	3472	3714	2842	3084	2737	2979
24.50	91585	463095					3404	3646	2830	3072	2702	2944
25.00												

NE

Figure 134: Depth profile for minimal scenario on Inline 993

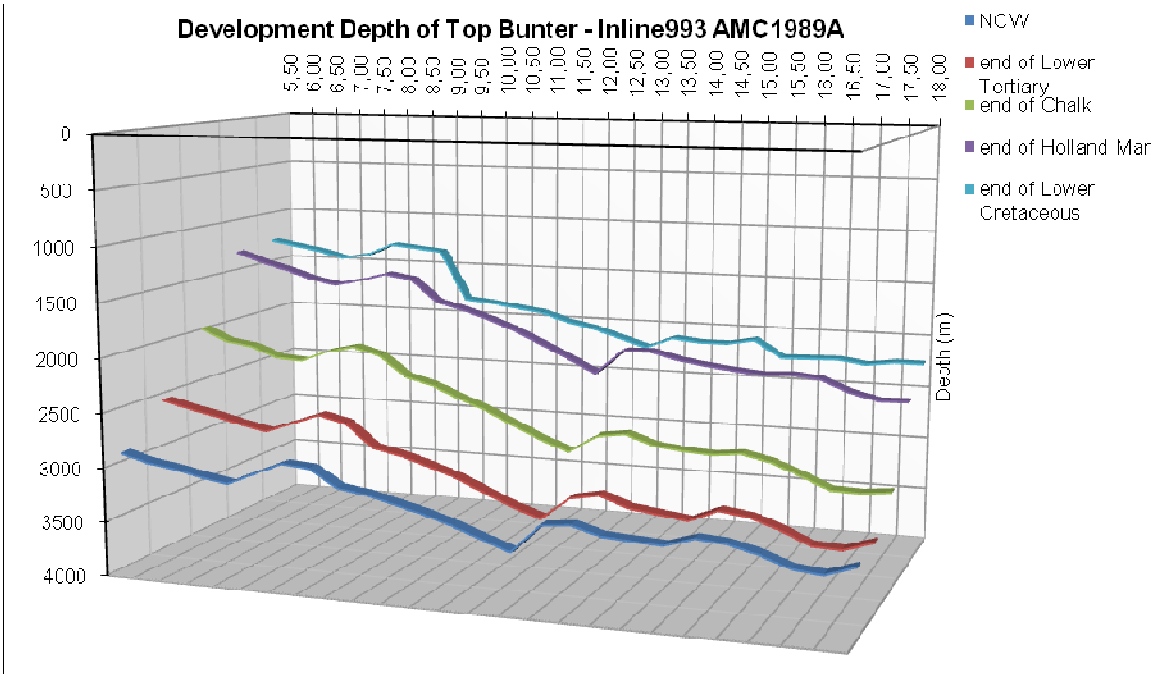

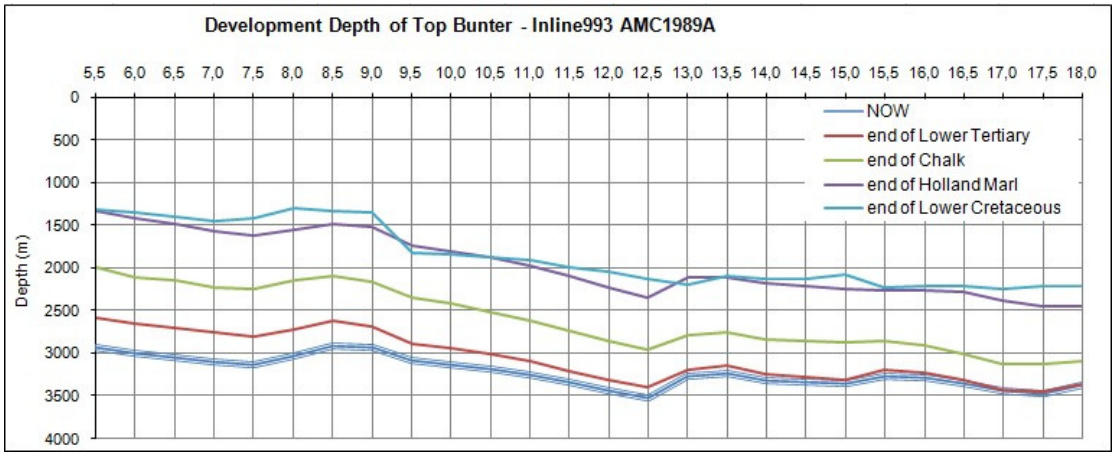

Figure 135: Depth profile for minimal scenario on Inline 1778

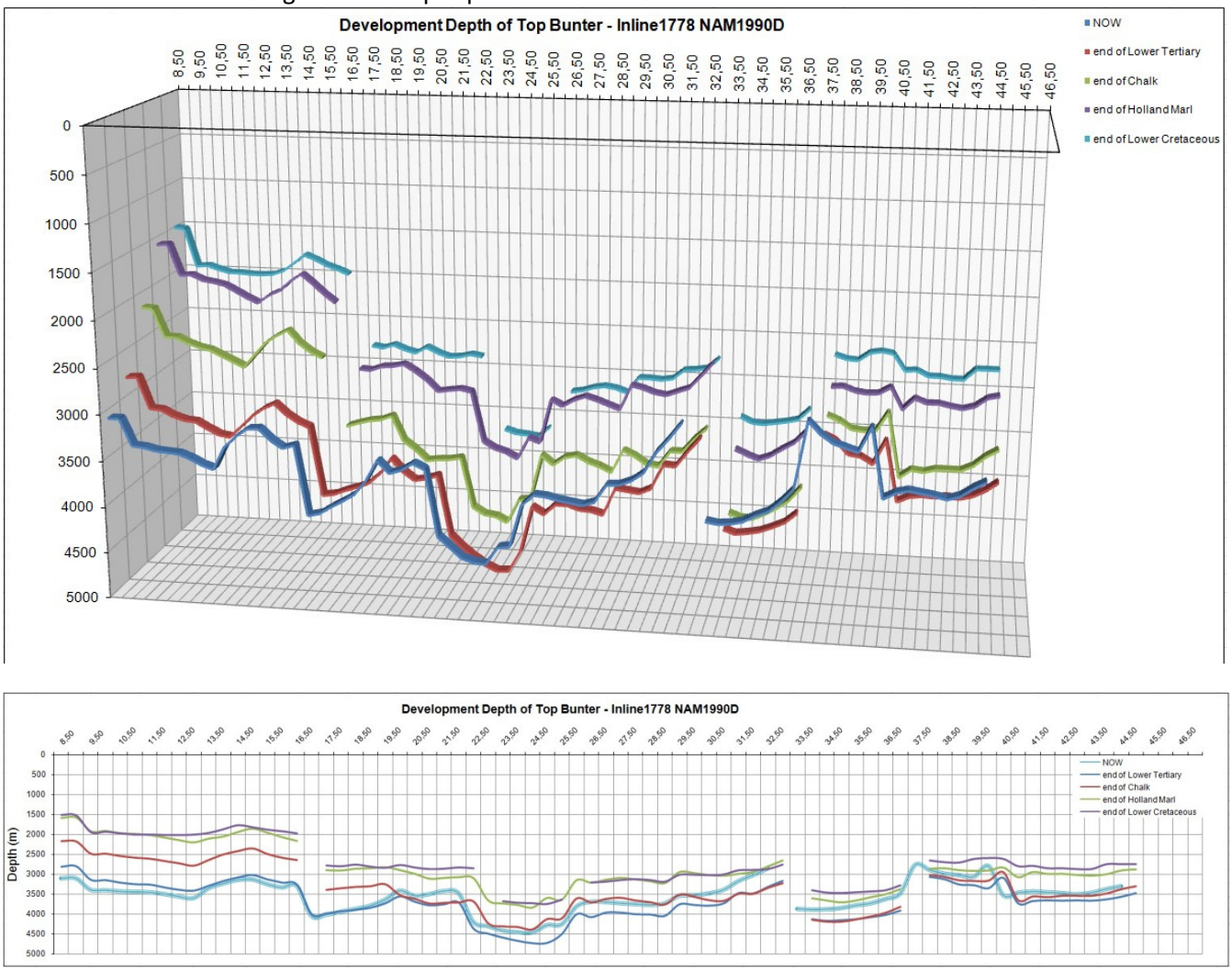

Figure 136: Depth profile for minimal scenario on Inline 1299

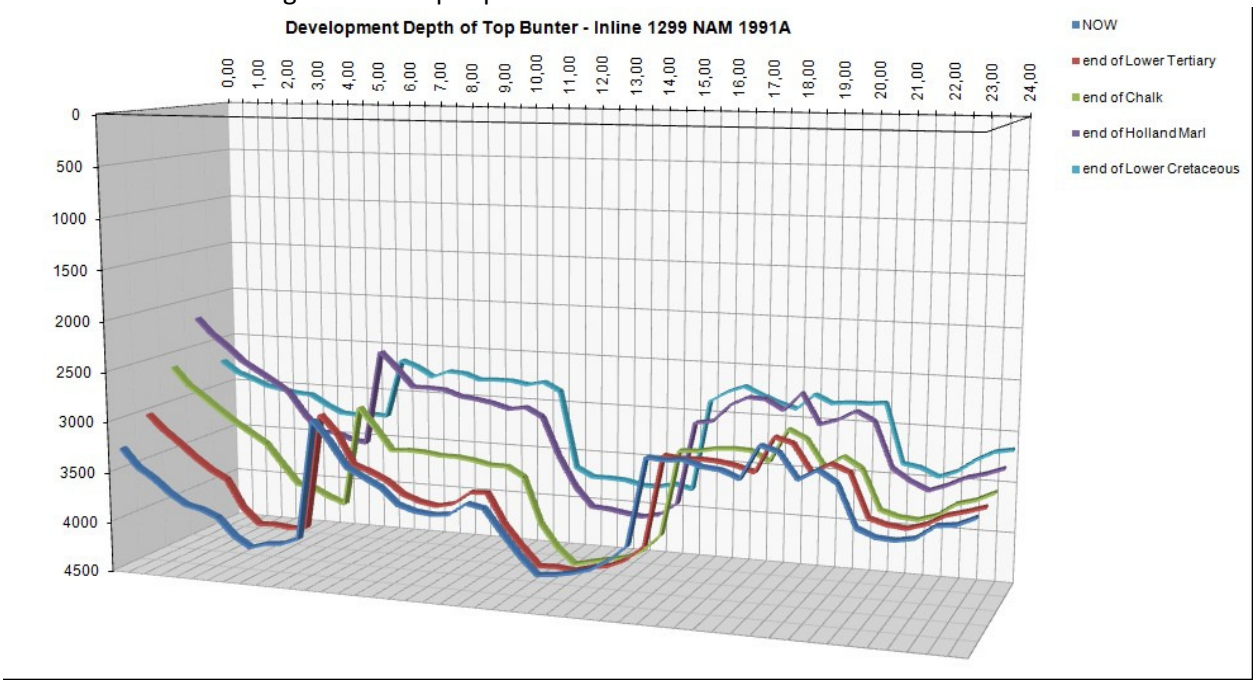

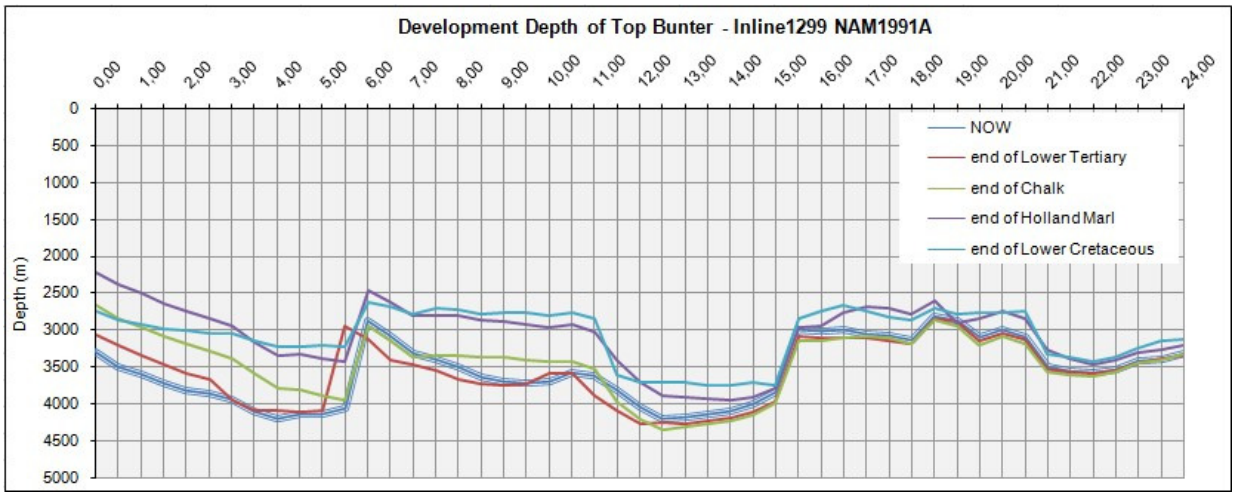

Figure 137: Depth profile for optimal scenario on Inline 993

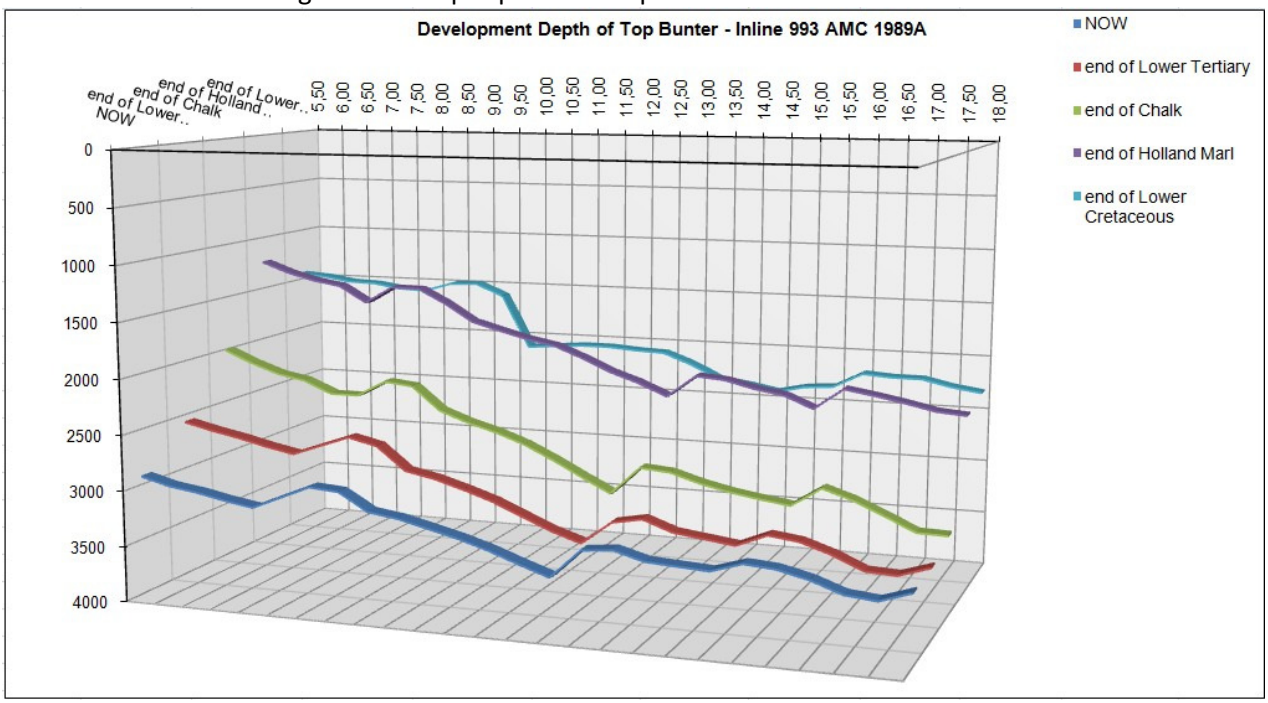

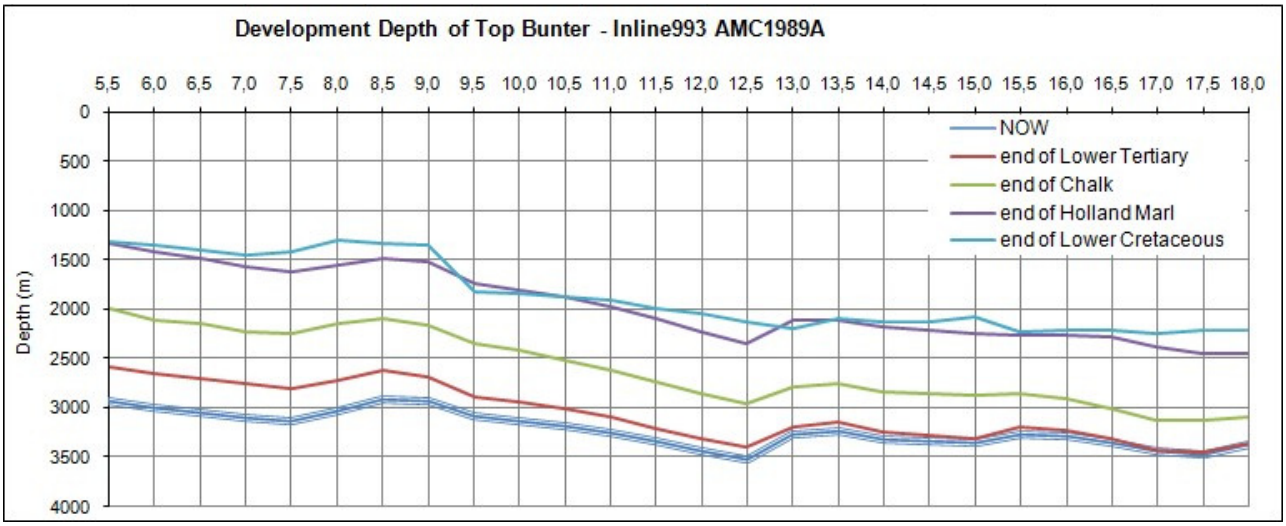

Figure 138: Depth profile for optimal scenario on Inline 1778

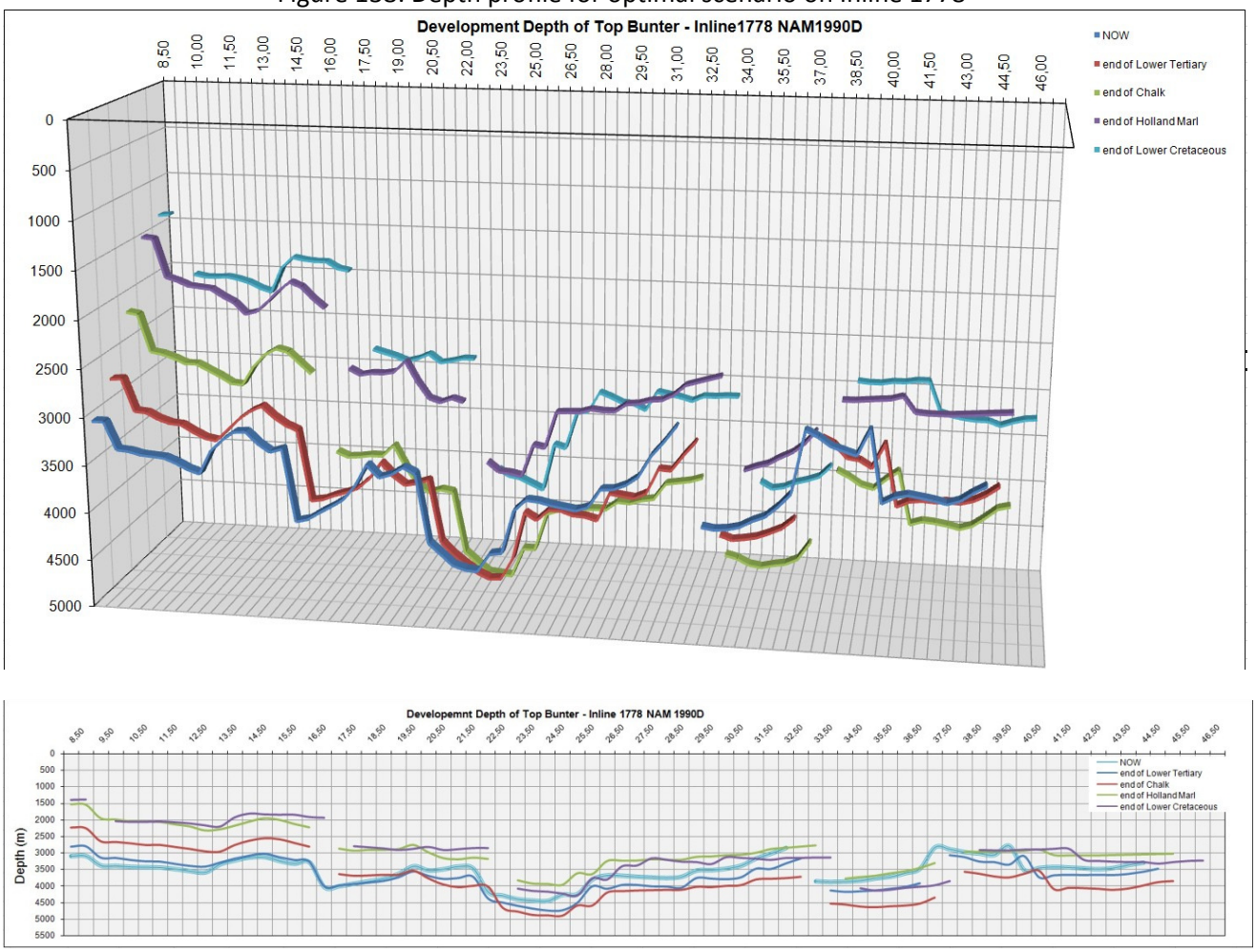

Figure 139: Depth profile for optimal scenario on Inline 1299

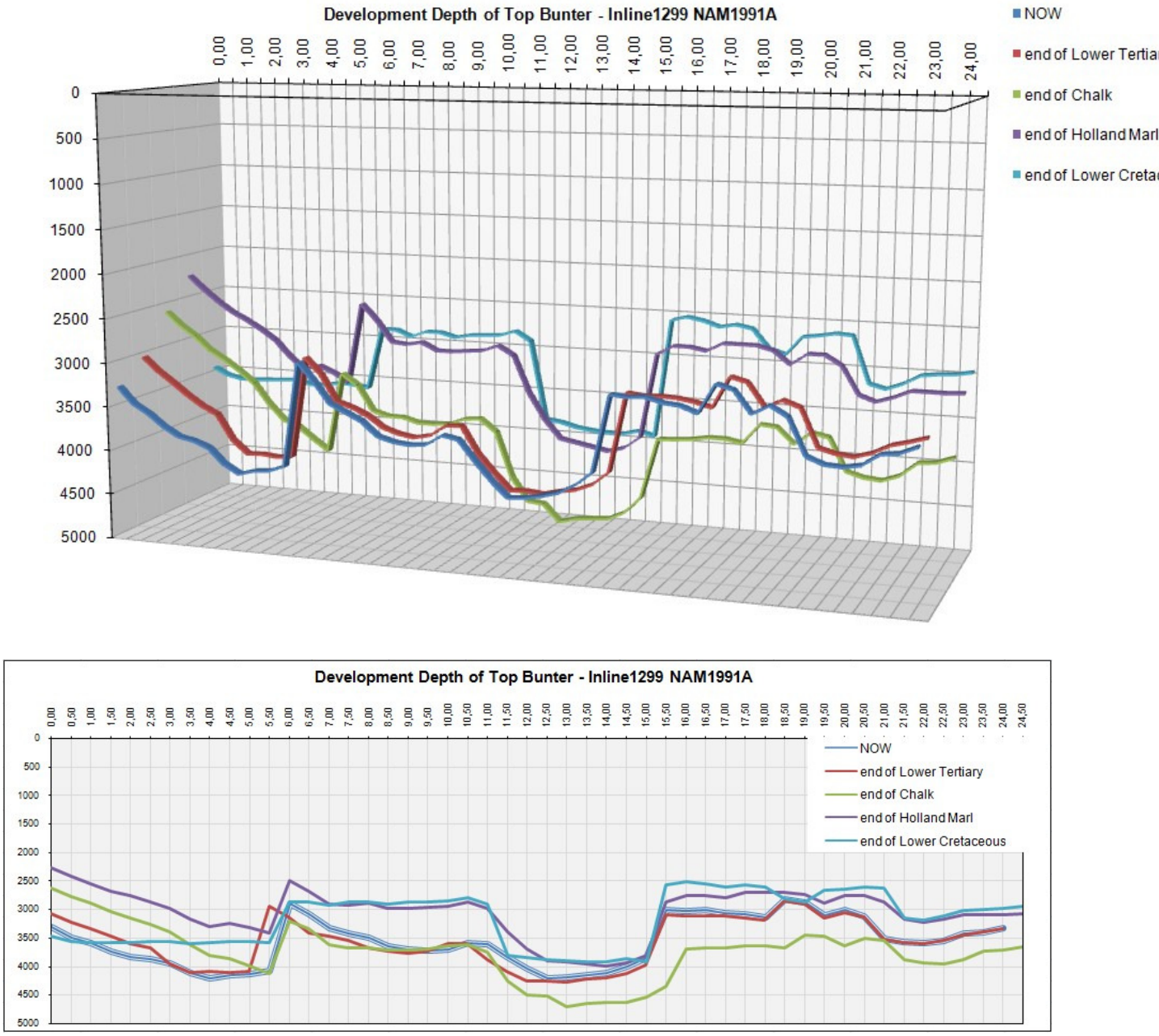

Table 15: Differences between burial depth throughout geologic time and qualitative analysis of the effect – OPTIMAL

Inlin
e993

Now
all

max 267

fraction

to BT	to TTM	to BHM	to BC	now - BT	BT - TTM	TTM - BHM	BHM - BC						
-356	-920	-1684	-1487	-356	-564	-764	197	0	0	0	197	197	0.122
-363	-878	-1658	-1535	-363	-515	-780	123	0	0	0	123	123	0.076
-349	-826	-1630	-1533	-349	-477	-804	97	0	0	0	97	97	0.060
-341	-830	-1640	-1577	-341	-489	-810	63	0	0	0	63	63	0.039
-332	-762	-1532	-1580	-332	-430	-770	-48	0	0	0	0	0	0.000
-315	-649	-1579	-1457	-315	-334	-930	122	0	0	0	122	122	0.076
-298	-684	-1465	-1424	-298	-386	-781	41	0	0	0	41	41	0.025
-258	-676	-1354	-1455	-258	-418	-678	-101	0	0	0	0	0	0.000
-206	-619	-1349	-1503	-206	-413	-730	-154	0	0	0	0	0	0.000
-192	-562	-1314	-1047	-192	-370	-752	267	0	0	0	267	267	0.166
-178	-552	-131	-113	-178	-374	-759	180	0	0	0	180	180	0.112

		1	1										
		-	-										
		132	121										
-157	-522	5	6	-157	-365	-803	109	0	0	0	109	109	0.068
		-	-										
		130	129										
-124	-477	2	6	-124	-353	-825	6	0	0	0	6	6	0.004
		-	-										
		128	137										
-108	-435	2	3	-108	-327	-847	-91	0	0	0	0	0	0.000
		-	-										
		128	145										
-113	-393	5	4	-113	-280	-892	-169	0	0	0	0	0	0.000
			-										
			109										
-63	-392	-914	7	-63	-329	-522	-183	0	0	0	0	0	0.000
		-											
		109											
-89	-344	5	-943	-89	-255	-751	152	0	0	0	152	152	0.094
		-											
		114											
-68	-339	9	-979	-68	-271	-810	170	0	0	0	170	170	0.106
		-											
		109											
-50	-296	9	-945	-50	-246	-803	154	0	0	0	154	154	0.096
		-	-										
		107	102										
-31	-268	1	0	-31	-237	-803	51	0	0	0	51	51	0.032
-58	-145	-875	-954	-58	-87	-730	-79	0	0	0	0	0	0.000
		-	-										
		109	111										
-46	-343	5	4	-46	-297	-752	-19	0	0	0	0	0	0.000
		-	-										
		111	115										
-21	-319	5	9	-21	-298	-796	-44	0	0	0	0	0	0.000
		-	-										
		116	125										
0	-299	1	6	0	-299	-862	-95	0	0	0	0	0	0.000
		-	-										
		112	122										
-15	-201	9	3	-15	-186	-928	-94	0	0	0	0	0	0.000
-12	-102	-	-	-12	-90	-913	-77	0	0	0	0	0	0.000
		101	109										

			5	2											

Inline 1778

Now - all				Largest variation - all times								max	160 9	
												min	21	influence fraction
to BT	to TTM	to BHM	to BC	Now - BT	BT - TTM	TTM-BHM	BHM-BC							
-294	-872	-1555	-1688	-294	-578	-683	-133	0	0	0	0	0	0.000	
-304	-852	-1542	-1700	-304	-548	-690	-158	0	0	0	0	0	0.000	
-251	-745	-1422		-251	-494	-677		0	0	0	0	0	0.000	
-251	-735	-1395	-1347	-251	-484	-660	48	0	0	0	48	48	0.030	
-220	-725	-1375	-1354	-220	-505	-650	21	0	0	0	21	21	0.013	
-190	-684	-1373	-1364	-190	-494	-689	9	0	0	0	9	9	0.006	
-190	-694	-1370	-1385	-190	-504	-676	-15	0	0	0	0	0	0.000	
-167	-680	-1343	-1409	-167	-513	-663	-66	0	0	0	0	0	0.000	
-169	-682	-1343	-1437	-169	-513	-661	-94	0	0	0	0	0	0.000	
-188	-651	-1263	-1420	-188	-463	-612	-157	0	0	0	0	0	0.000	

-61	-393	-1049	-1135	-61	-332	-656	-86	0	0	0	0	0	0.000
-63	-476	-1041	-1293	-63	-413	-565	-252	0	0	0	0	0	0.000
-63	-517	-1075	-1317	-63	-454	-558	-242	0	0	0	0	0	0.000
-113	-578	-1164	-1284	-113	-465	-586	-120	0	0	0	0	0	0.000
-122	-667	-1233	-1392	-122	-545	-566	-159	0	0	0	0	0	0.000
-121	-636	-1190	-1472	-121	-515	-554	-282	0	0	0	0	0	0.000
-31	-484	-1051	-1363	-31	-453	-567	-312	0	0	0	0	0	0.000
-43				-43				0	0	0	0	0	0.000
-33	-380	-1132		-33	-347	-752		0	0	0	0	0	0.000
-4	-251	-991		-4	-247	-740	-139	0	0	0	0	0	0.000
26	-191	-946	-1026	26	-217	-755	-80	26	0	0	0	26	0.016
55	-132	-867	-913	55	-187	-735	-46	55	0	0	0	55	0.034
95	19	-740	-716	95	-76	-759	24	95	0	0	24	119	0.074
147	125	-637	-523	147	-22	-762	114	147	0	0	114	261	0.162
151	228	-543	-709	151	77	-771	-166	151	77	0	0	228	0.142
282	450	-330	-578	282	168	-780	-248	282	168	0	0	450	0.280
336	610	-214	-522	336	274	-824	-308	336	274	0	0	610	0.379
235	510	-323	-616	235	275	-833	-293	235	275	0	0	510	0.317
176				176		-816	-330	176	0	0	0	176	0.109
192	353			192	161			192	161	0	0	353	0.219

181	353	-576	-328	181	172	-929	248	181	172	0	248	601	0.374		
225	416	-516	-299	225	191	-932	217	225	191	0	217	633	0.393		
273	417	-516	-286	273	144	-933	230	273	144	0	230	647	0.402		
453	615	-301	-41	453	162	-916	260	453	162	0	260	875	0.544		
249	331	-628	36	249	82	-959	664	249	82	0	664	995	0.618		
198	778	-156	-31	198				198	0	0	0	198	0.123		
392	504	-432	124	392	112	-936	556	392	112	0	556	1060	0.659		
266	453	-451	-286	266	187	-904	165	266	187	0	165	618	0.384		
236	403	-485	-339	236	167	-888	146	236	167	0	146	549	0.341		
258	373	-542	-576	258	115			258	115	0	0	373	0.232		
246	343	-549	-550	246				246	0	0	0	246	0.153		
319	383	-509	-453	319				319	0	0	0	319	0.198		
217	481	-407	-253	217	264	-888	154	217	264	0	154	635	0.395		
243	500	-411	-186	243	257	-911	225	243	257	0	225	725	0.451		
310	510	-398	-342	310	200	-908	56	310	200	0	56	566	0.352		
342	579	-320	-229	342	237	-899	91	342	237	0	91	670	0.416		
302	626	-164	12	302	324	-790	176	302	324	0	176	802	0.498		
459	754	-126	195	459	295	-880	321	459	295	0	321	1075	0.668		
462	903		307	462	441	-898	302	462	441	0	302	1205	0.749		
						-895	339	0	0	0	339	339	0.211		
							364	0	0	0	364	364	0.226		
243	639			243	396			243	396	0	0	639	0.397		
295	679	-89		295	384	-768		295	384	0	0	679	0.422		
308	770	-108	227	308	462	-878	335	308	462	0	335	1105	0.687		
351	858	-78	364	351	507	-936	442	351	507	0	442	1300	0.808		
352	879	-101	392	352	527	-980	493	352	527	0	493	1372	0.853		

403	967	-54	444	403	564	-1021	498	403	564	0	498	1465	0.911
434		-14	549	434	612	-1060	563	434	612	0	563	1609	1.000
						-1026	665	0	0	0	665	665	0.413
172				172				172	0	0	0	172	0.107
142	582			142	440	-582		142	440	0	0	582	0.362
235	603	-40	-102	235	368	-643	-62	235	368	0	0	603	0.375
212	644	-92	-130	212	432	-736	-38	212	432	0	0	644	0.400
556	943	165	139	556	387	-778	-26	556	387	0	0	943	0.586
		-581	-620		534	-677	-39	0	534	0	0	534	0.332
272		-548	-550	272		-623	-2	272	0	0	0	272	0.169
243	661	-351	-543	243	418		-192	243	418	0	0	661	0.411
207	600	-361	-563	207	393	-961	-202	207	393	0	0	600	0.373
195	590	-381	-252	195	395	-971	129	195	395	0	129	719	0.447
157	581	-413	-248	157	424	-994	165	157	424	0	165	746	0.464
205	651	-383	-185	205	446	-1034	198	205	446	0	198	849	0.528
261	700	-304	-85	261	439	-1004	219	261	439	0	219	919	0.571
266	679	-244	-15	266	413	-923	229	266	413	0	229	908	0.564

Inline 1229

Now to all

to BT	to TTM	to BHM	to BC	now - BT	BT - TTM	TTM - BHM	BHM - BC					fraction
-244	-691	-1045	165	-244	-447	-354	1210	0	0	0	1210	1210	0.752
-278	-724	-1077	61	-278	-446	-353	1138	0	0	0	1138	1138	0.707

-255	-707	-1042	-5	-255	-452	-335	1037	0	0	0	1037	1037	0.644
-257	-689	-1058	-140	-257	-432	-369	918	0	0	0	918	918	0.571
-243	-689	-1073	-253	-243	-446	-384	820	0	0	0	820	820	0.510
-192	-604	-1005	-298	-192	-412	-401	707	0	0	0	707	707	0.439
18	-536	-952	-377	18	-554	-416	575	18	0	0	575	593	0.369
1	-475	-934	-499	1	-476	-459	435	1	0	0	435	436	0.271
-109	-400	-898	-612	-109	-291	-498	286	0	0	0	286	286	0.178
-39	-281	-899	-596	-39	-242	-618	303	0	0	0	303	303	0.188
-41	-129	-813	-567	-41	-88	-684	246	0	0	0	246	246	0.153
-1127	57	-644	-477					0	0	0	0	0	0.000
233	323	-403	-22	233	90	-726	381	233	90	0	381	704	0.438
326	241	-418	-224	326	-85	-659	194	326	0	0	194	520	0.323
147	290	-415	-390	147	143	-705	25	147	143	0	25	315	0.196
139	257	-482	-544	139	118	-739	-62	139	118	0	0	257	0.160
179	173	-600	-628	179	-6	-773	-28	179	0	0	0	179	0.111
85	72	-666	-733	85	-13	-738	-67	85	0	0	0	85	0.053
63	22	-716	-818	63	-41	-738	-102	63	0	0	0	63	0.039
8	-12	-751	-847	8	-20	-739	-96	8	0	0	0	8	0.005
-99	-63	-751	-841	-99	36	-688	-90	0	36	0	0	36	0.022
10	38	-701	-782	10	28	-739	-81	10	28	0	0	38	0.024
271	140	-632	-711	271	-131	-772	-79	271	0	0	0	271	0.168
252	428	-425	-19	252	176	-853	406	252	176	0	406	834	0.518
231	480	-337	-198	231	249	-817	139	231	249	0	139	619	0.385
53	328	-301	-320	53	275	-629	-19	53	275	0	0	328	0.204

89	531	-250	-280	89	442	-781	-30	89	442	0	0	531	0.330
75	515	-182	-234	75	440	-697	-52	75	440	0	0	515	0.320
96	548	-98	-184	96	452	-646	-86	96	452	0	0	548	0.341
122	633	-47	-129	122	511	-680	-82	122	511	0	0	633	0.393
121	699	-33	69	121	578	-732	102	121	578	0	102	801	0.498
87		-145	-442					0	0	0	0	0	0.000
89	672	-264	-506	89	583	-936	-242	89	583	0	0	672	0.418
97	679	-247	-454	97	582	-926	-207	97	582	0	0	679	0.422
55	611	-265	-447	55	556	-876	-182	55	556	0	0	611	0.380
67	560	-377	-499	67	493	-937	-122	67	493	0	0	560	0.348
47	493	-444	-531	47	446	-937	-87	47	446	0	0	493	0.306
24	847	-124	0	24	823	-971	124	24	823	0	124	971	0.603
21	576	-128	7	21	555	-704	135	21	555	0	135	711	0.442
42	357	-221	-439	42	315	-578	-218	42	315	0	0	357	0.222
49	630	-250	-361	49	581	-880	-111	49	581	0	0	630	0.392
11	388	-355	-501	11	377	-743	-146	11	377	0	0	388	0.241
28	33	-640	-881	28	5	-673	-241	28	5	0	0	33	0.021
7	316	-400	-425	7	309	-716	-25	7	309	0	0	316	0.196
15	356	-351	-389	15	341	-707	-38	15	341	0	0	356	0.221
-8	407	-377	-425	-8	415	-784	-48	0	415	0	0	415	0.258
24	466	-333	-403	24	442	-799	-70	24	442	0	0	466	0.290
-1	337	-310	-403	-1	338	-647	-93	0	338	0	0	338	0.210
23	401	-229	-334	23	378	-630	-105	23	378	0	0	401	0.249

Normal Depth - Porosity Trend

Depth – Porosity Trend influenced by eroded material

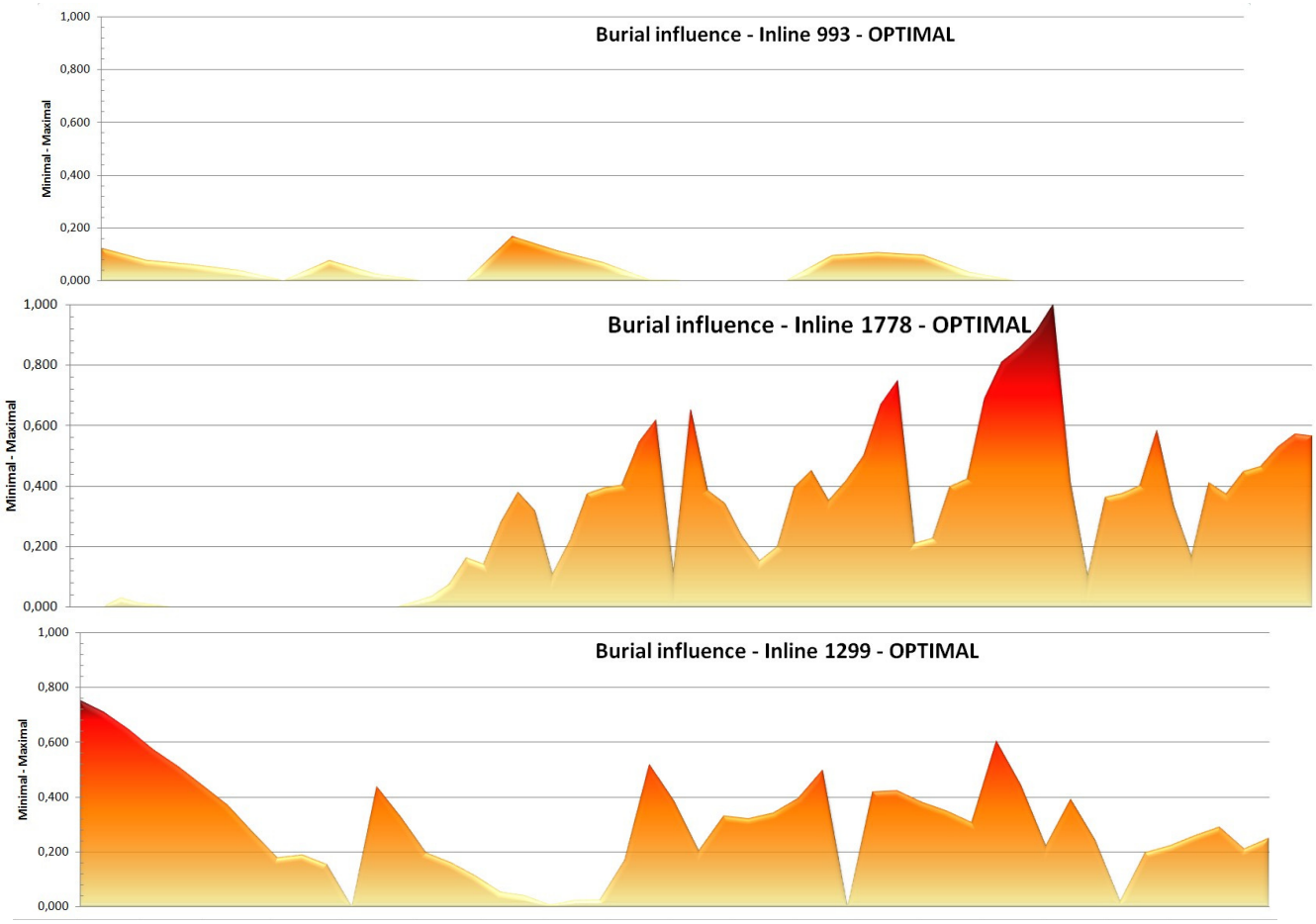

Inline993

Now all max 87

fraction

to BT	to TTM	to BHM	to BC	now - BT	BT - TTM	TTM - BHM	BHM - BC						
-356	-933	-1596	-1635	-356	-577	-663	-39	0	0	0	0	0	0.000
-363	-891	-1576	-1659	-363	-528	-685	-83	0	0	0	0	0	0.000
-349	-892	-1550	-1653	-349	-543	-658	-103	0	0	0	0	0	0.000
-341	-850	-1522	-1643	-341	-509	-672	-121	0	0	0	0	0	0.000
-332	-879	-1517	-1731	-332	-547	-638	-214	0	0	0	0	0	0.000
-315	-868	-1460	-1733	-315	-553	-592	-273	0	0	0	0	0	0.000
-298	-815	-1421	-1595	-298	-517	-606	-174	0	0	0	0	0	0.000
-258	-770	-1402	-1589	-258	-512	-632	-187	0	0	0	0	0	0.000
-206	-736	-1348	-1274	-206	-530	-612	74	0	0	0	74	74	0.046

-192	-708	-1322	-1286	-192	-516	-614	36	0	0	0	36	36	0.022
-178	-662	-1306	-1314	-178	-484	-644	-8	0	0	0	0	0	0.000
-157	-632	-1274	-1344	-157	-475	-642	-70	0	0	0	0	0	0.000
-124	-588	-1234	-1344	-124	-464	-646	-110	0	0	0	0	0	0.000
-108	-568	-1210	-1388	-108	-460	-642	-178	0	0	0	0	0	0.000
-113	-564	-1172	-1399	-113	-451	-608	-227	0	0	0	0	0	0.000
-63	-474	-1148	-1061	-63	-411	-674	87	0	0	0	87	87	0.054
-89	-485	-1130	-1141	-89	-396	-645	-11	0	0	0	0	0	0.000
-68	-472	-1140	-1190	-68	-404	-668	-50	0	0	0	0	0	0.000
-50	-459	-1116	-1206	-50	-409	-657	-90	0	0	0	0	0	0.000
-31	-460	-1100	-1275	-31	-429	-640	-175	0	0	0	0	0	0.000
-58	-403	-990	-1029	-58	-345	-587	-39	0	0	0	0	0	0.000
-46	-367	-1028	-1060	-46	-321	-661	-32	0	0	0	0	0	0.000
-21	-329	-1068	-1133	-21	-308	-739	-65	0	0	0	0	0	0.000
0	-316	-1060	-1194	0	-316	-744	-134	0	0	0	0	0	0.000
-15	-336	-1023	-1257	-15	-321	-687	-234	0	0	0	0	0	0.000
-12	-273	-939	-1165	-12	-261	-666	-226	0	0	0	0	0	0.000

Inline 1778

Now - all

Largest variation - all times

ma x 160 9

min 21

influence fraction

to BT	to TTM	to BHM	to BC	Now - BT	BT - TTM	TTM- BHM	BHM- BC						
-294	-929	-1508	-1595	-294	-635	-579	-87	0	0	0	0	0	0.000
-304	-920	-1518	-1580	-304	-616	-598	-62	0	0	0	0	0	0.000
-251	-902	-1463	-1450	-251	-651	-561	13	0	0	0	13	13	0.008
-251	-912	-1482	-	-251	-661	-570	12	0	0	0	12	12	0.007

			1470										
-220	-884	-1457	-1460	-220	-664	-573	-3	0	0	0	0	0	0.000
-190	-852	-1448	-1439	-190	-662	-596	9	0	0	0	9	9	0.006
-190	-837	-1431	-1449	-190	-647	-594	-18	0	0	0	0	0	0.000
-167	-826	-1413	-1486	-167	-659	-587	-73	0	0	0	0	0	0.000
-169	-830	-1410	-1547	-169	-661	-580	-137	0	0	0	0	0	0.000
-188	-812	-1394	-1597	-188	-624	-582	-203	0	0	0	0	0	0.000
-61	-705	-1239	-1391	-61	-644	-534	-152	0	0	0	0	0	0.000
-63	-727	-1175	-1364	-63	-664	-448	-189	0	0	0	0	0	0.000
-63	-720	-1197	-1375	-63	-657	-477	-178	0	0	0	0	0	0.000
-113	-776	-1270	-1314	-113	-663	-494	-44	0	0	0	0	0	0.000
-122	-754	-1287	-1372	-122	-632	-533	-85	0	0	0	0	0	0.000
-121	-743	-1256	-1412	-121	-622	-513	-156	0	0	0	0	0	0.000
-31	-645	-1123	-1321	-31	-614	-478	-198	0	0	0	0	0	0.000
-43				-43				0	0	0	0	0	0.000
-33	-624	-1117	-1241	-33	-591	-493	-124	0	0	0	0	0	0.000
-4	-586	-1029	-1142	-4	-582	-443	-113	0	0	0	0	0	0.000
26	-549	-1005	-1113	26	-575	-456	-108	26	0	0	0	26	0.016
55	-487	-936	-983	55	-542	-449	-47	55	0	0	0	55	0.034
95	-386	-812	-801	95	-481	-426	11	95	0	0	11	106	0.066
147	115	-511	-646	147	-32	-626	-135	147	0	0	0	147	0.091

151	77	-548	-713	151	-74	-625	-165	151	0	0	0	151	0.094
282	233	-387	-633	282	-49	-620	-246	282	0	0	0	282	0.175
336	295	-327	-564	336	-41	-622	-237	336	0	0	0	336	0.209
235	227	-405	-654	235	-8	-632	-249	235	0	0	0	235	0.146
176				176			-256	176	0	0	0	176	0.109
192	-74	-646		192	-266	-572		192	0	0	0	192	0.119
181	-110	-682	-743	181	-291	-572	-61	181	0	0	0	181	0.112
225	-132	-684	-742	225	-357	-552	-58	225	0	0	0	225	0.140
273	-84	-629	-741	273	-357	-545	-112	273	0	0	0	273	0.170
453	-153	-682	-533	453	-606	-529	149	602	0	0	149	602	0.374
249	-150	-616	-625	249	-399	-466	-9	249	0	0	0	249	0.155
198	-200	-659		198	-398	-459		198	0	0	0	198	0.123
392	19	-475	-486	392	-373	-494	-11	392	0	0	0	392	0.244
266	-81	-559	-516	266	-347	-478	43	309	0	0	43	309	0.192
236	-137	-635	-587	236	-373	-498	48	284	0	0	48	284	0.177
258	-91	-618	-627	258	-349	-527	-9	258	0	0	0	258	0.160
246	-69	-592	-627	246	-315	-523	-35	246	0	0	0	246	0.153
319	29	-505	-546	319	-290	-534	-41	319	0	0	0	319	0.198

								9						
217	-31	-594	-530	217	-248	-563	64	217	0	0	64	281	0.175	
243	36	-557	-521	243	-207	-593	36	243	0	0	36	279	0.173	
310	169	-461	-461	310	-141	-630		310	0	0	0	310	0.193	
342	276	-352	-391	342	-66	-628	-39	342	0	0	0	342	0.213	
302	320	-181	-275	302	18	-501	-94	302	18	0	0	320	0.199	
459	469	-78	-136	459	10	-547	-58	459	10	0	0	469	0.291	
462	488	-48	12	462	26	-536	60	462	26	0	60	548	0.341	
					59	-568	96	0	59	0	96	155	0.096	
								0	0	0	0	0	0.000	
243	251	-285	-491	243	8			243	8	0	0	251	0.156	
295	311	-219	-420	295	16	-530	-201	295	16	0	0	311	0.193	
308	341	-143	-380	308	33	-484	-237	308	33	0	0	341	0.212	
351	351	-121	-332	351	0	-472	-211	351	0	0	0	351	0.218	
352	327	-154	-302	352	-25	-481	-148	352	0	0	0	352	0.219	
403	345	-119	-223	403	-58	-464	-104	403	0	0	0	403	0.250	
434	335	-109	-206	434	-99	-444	-97	434	0	0	0	434	0.270	
				0				0	0	0	0	0	0.000	
172	124	-33	-243	172	-48	-157	-210	17	0	0	0	172	0.107	

								2							
142	86	-131	-290	142	-56	-217	-159	142	0	0	0	142		0.088	
235	129	-124	-320	235	-106	-253	-196	235	0	0	0	235		0.146	
212	105	-146	-451	212	-107	-251	-305	212	0	0	0	212		0.132	
556	366	114	-204	556	-190	-252	-318	556	0	0	0	556		0.346	
								0	0	0	0	0		0.000	
272	189	-385	-665	272	-83	-574	-280	272	0	0	0	272		0.169	
243	128	-485	-645	243	-115	-613	-160	243	0	0	0	243		0.151	
207	125	-456	-604	207	-82	-581	-148	207	0	0	0	207		0.129	
195	71	-479	-624	195	-124	-550	-145	195	0	0	0	195		0.121	
157	41	-481	-634	157	-116	-522	-153	157	0	0	0	157		0.098	
205	81	-422	-594	205	-124	-503	-172	205	0	0	0	205		0.127	
261	112	-370	-627	261	-149	-482	-257	261	0	0	0	261		0.162	
266	75	-393	-557	266	-191	-468	-164	266	0	0	0	266		0.165	

Inline 1229

Now to all

to BT	to TTM	to BHM	to BC	now - BT	BT - TTM	TTM - BHM	BHM - BC						fraction
-244	-646	-1084	-550	-244	-402	-438	534	0	0	0	534	534	0.332

-278	-653	-1108	-622	-278	-375	-455	486	0	0	0	486	486	0.302
-255	-639	-1085	-665	-255	-384	-446	420	0	0	0	420	420	0.261
-257	-653	-1078	-733	-257	-396	-425	345	0	0	0	345	345	0.214
-243	-639	-1083	-805	-243	-396	-444	278	0	0	0	278	278	0.173
-192	-573	-1022	-811	-192	-381	-449	211	0	0	0	211	211	0.131
18	-540	-985	-868	18	-558	-445	117	18	0	0	117	135	0.084
1	-509	-935	-941	1	-510	-426	-6	1	0	0	0	1	0.001
-109	-417	-855	-966	-109	-308	-438	-111	0	0	0	0	0	0.000
-39	-337	-813	-905	-39	-298	-476	-92	0	0	0	0	0	0.000
-41	-241	-739	-907	-41	-200	-498	-168	0	0	0	0	0	0.000
-1127	-117	-644	-831			-527	-187	0	0	0	0	0	0.000
233	60	-426	-255	233	-173	-486	171	233	0	0	171	404	0.251
326	59	-466	-399	326	-267	-525	67	326	0	0	67	393	0.244
147	37	-521	-540	147	-110	-558	-19	147	0	0	0	147	0.091
139	-61	-605	-691	139	-200	-544	-86	139	0	0	0	139	0.086
179	-138	-680	-765	179	-317	-542	-85	179	0	0	0	179	0.111
85	-268	-775	-860	85	-353	-507	-85	85	0	0	0	85	0.053
63	-318	-806	-920	63	-381	-488	-114	63	0	0	0	63	0.039
8	-314	-794	-937	8	-322	-480	-143	8	0	0	0	8	0.005
-99	-261	-729	-891	-99	-162	-468	-162	0	0	0	0	0	0.000
10	-143	-640	-811	10	-153	-497	-171	10	0	0	0	10	0.006

271	-84	-588	-759	271	-355	-504	-171	271	0	0	0	271	0.168
252	148	-417	-202	252	-104	-565	215	252	0	0	215	467	0.290
231	174	-324	-318	231	-57	-498	6	231	0	0	6	237	0.147
53	156	-303	-487	53	103	-459	-184	53	103	0	0	156	0.097
89	130	-276	-461	89	41	-406	-185	89	41	0	0	130	0.081
75	128	-214	-388	75	53	-342	-174	75	53	0	0	128	0.080
96	142	-145	-338	96	46	-287	-193	96	46	0	0	142	0.088
122	158	-81	-275	122	36	-239	-194	122	36	0	0	158	0.098
121	138	-53	-85	121	17	-191	-32	121	17	0	0	138	0.086
87	144	-29	-152		57	-173	-123	0	57	0	0	57	0.035
89	120	-75	-274	89	31	-195	-199	89	31	0	0	120	0.075
97	101	-229	-324	97	4	-330	-95	97	4	0	0	101	0.063
55	36	-365	-298	55	-19	-401	67	55	0	0	67	122	0.076
67	26	-373	-248	67	-41	-399	125	67	0	0	125	192	0.119
47	52	-345	-268	47	5	-397	77	47	5	0	77	129	0.080
24	50	-206	-101	24	26	-256	105	24	26	0	105	155	0.096
21	77	38	-75	21	56	-39	-113	21	56	0	0	77	0.048
42	99	-255	-330	42	57	-354	-75	42	57	0	0	99	0.062
49	87	-248	-228	49	38	-335	20	49	38	0	20	107	0.067
11	82	-267	-352	11	71	-349	-85	11	71	0	0	82	0.051

28	69	-221	-161	28	41	-290	60	28	41	0	60	129	0.080
7	50	-176	-201	7	43	-226	-25	7	43	0	0	50	0.031
15	53	-111	-135	15	38	-164	-24	15	38	0	0	53	0.033
-8	30	-144	-168	-8	38	-174	-24	0	38	0	0	38	0.024
24	35	-102	-166	24	11	-137	-64	24	11	0	0	35	0.022
-1	8	-127	-235	-1	9	-135	-108	0	9	0	0	9	0.006
23	3	-113	-186	23	-20	-116	-73	23	0	0	0	23	0.014

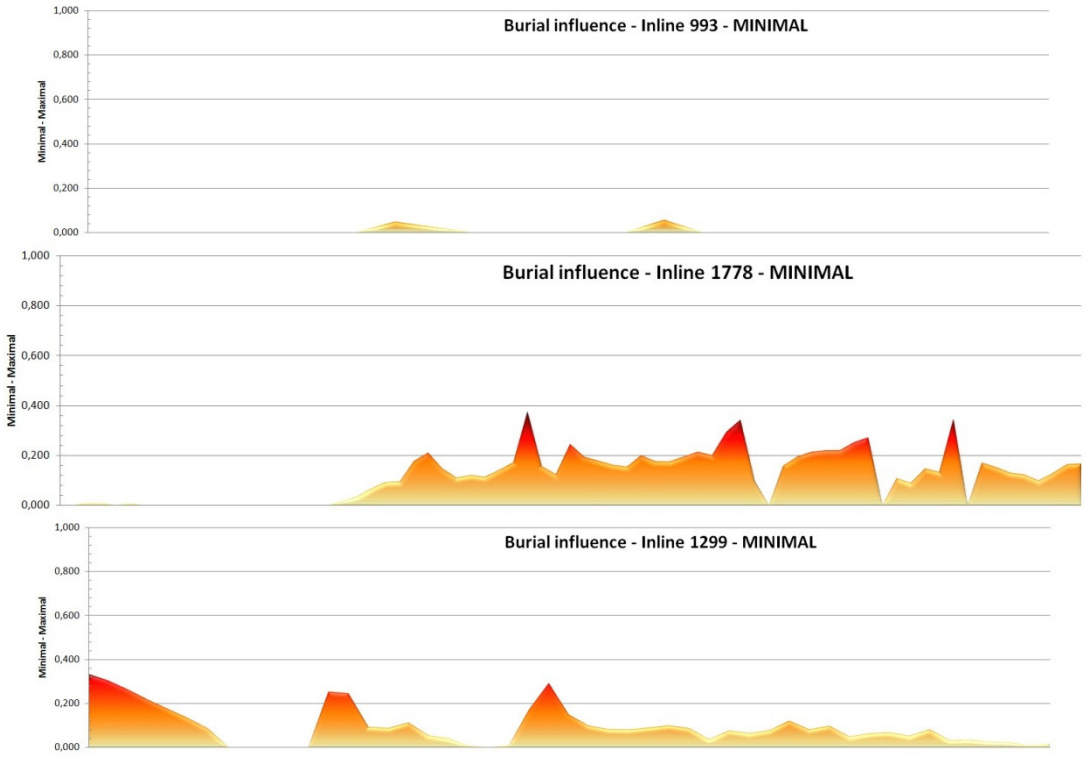
Burial influence - Inline 993 - MINIMAL
Minimal - Maximal
1,000
0,800
0,600
0,400
0,200
0,000
Burial influence - Inline 1778 - MINIMAL
Minimal - Maximal
1,000
0,800
0,600
0,400
0,200
0,000
Burial influence - Inline 1299 - MINIMAL
Minimal - Maximal
1,000
0,800
0,600
0,400
0,200
0,000

1.4. Tables

Table 16: Extension and amount of restored eroded sediments per 1 m thick volume

Restored extension after given time:

Base restoration	**AMC1989A Inline 993**				**NAM1990D Inline 1778**				**NAM1991A inline 1299**			
	Extension on right side (m)		**Volume erosion per 1m thickness (10^6 m^3)**		**Extension on right side (m)**		**Volume erosion per 1m thickness (10^6 m^3)**		**Extension on right side (m)**		**Volume erosion per 1m thickness (10^6 m^3)**	
(in meters)	**Minimal**	**Optimal**	**Minimal**	**Optimal**	**Minimal**	**Optimal**	**Minimal**	**Optimal**	**Minimal**	**Optimal**	**Minimal**	**Optimal**
Base Tertiary	1	1	3.982482	3.982482	501	501	20.788236	20.788236	88	88	9.647794	9.647794
Top Texel Marl	362	442	2.768815	4.397874	441	825	15.958961	29.361793	20	172	8.315288	15.402884
Base Holland Marl	375	455	2.154389	1.620001	445	867	5.229343	7.018411	25	324	3.509.917	4.240107
Base Cretaceous	415	643	2.690529	2.811637	450	2019	5.720537	16.811436	169	428	3.696423	9.487114

** Note that the amount of restored inverted extension is adding up with increasing time for the period of active compression. However in the last period the basin was still in the end of the rifting stage so there was also non-inverted extension.*

** Note that the increase in extension of the restored basin the last period is most prominent. This effect is also to be partially considered related to the restoration process itself, namely in Inline 1778 that is the longest and with best quality so it contains the most indications for eroded material and additional subsidence of blocks. The major reason for this difference is however the fact that it is the only section that includes the center of the basin which the part that has experienced the largest amount of extension and subsequently reduction of extension.*

Table 17: B-Factor data

B-Factor	**original** = restored (flat line)	**deformed** = as seen on seismic (flat line)	excludes extension not accompanied by rift fault activity

AMC1989A Inline 993	**Minimal**			**Optimal**				
	deformed (m)	**original (m)**	**B-factor**	**deformed (m)**	**original (m)**	**B-factor**	**Age (Ma)**	
Quaternary			1.030			1.050	**5.33**	
Base Tertiary	14088	14089	1.000	14088	14089	1.000	**28.4**	
Top Texel Marl	14001	14362	0.975	14088	14529	0.970	**65.5**	**Estimated**
Base Holland Marl	14088	14101	0.999	14151	14164	0.999	**99.6**	Quaternary
Base Cretaceous	13390	13430	0.997	13243	13431	0.986	**112.0**	Upper Jurassic
Upper Jurassic			1.080			1.100	**175.6**	

NAM1990D Inline 1778	**Minimal**			**Optimal**				
	deformed (m)	**original (m)**	**B-factor**	**deformed (m)**	**original (m)**	**B-factor**	**Age (Ma)**	
Quaternary			1.030			1.050	**5.33**	1
Base Tertiary	36652	37153	0.987	36652	37153	0.987	**28.4**	1
Top Texel Marl	36240	36180	1.002	36652	36976	0.991	**65.5**	1
Base Holland Marl	36920	36924	1.000	36931	36973	0.999	**99.6**	1
Base Cretaceous	36458	36463	1.000	36585	37737	0.969	**112.0**	1
Upper Jurassic			1.080			1.100	**175.6**	1

NAM1991A inline 1299	**Minimal**	**Optimal**

	deformed (m)	original (m)	B-factor	deformed (m)	original (m)	B-factor	Age (Ma)
Quaternary			1.030			1.050	**5.33**
Base Tertiary	22579	22667	0.996	23578	23666	0.996	**28.4**
Top Texel Marl	22218	22150	1.003	22377	22461	0.996	**65.5**
Base Holland Marl	21058	21063	1.000	21072	21224	0.993	**99.6**
Base Cretaceous	23550	23694	0.994	23649	23753	0.996	**112.0**
Upper Jurassic			1.080			1.100	**175.6**

Table 18: Applied decompaction thicknesses

	Z3AMC1989A inline 993			Z3NAM1990D inline 1778			L3NAM1991A inline 1299		
	Visible thickness	**Uplifted thickness**	**Decomp %**	**Visible thickness**	**Uplifted thickness**	**Decomp %**	**Visible thickness**	**Uplifted thickness**	**Decomp %**
Base Tertiary	583	670	**13.0**	677	777	**12.9**	332	385	**13.8**
Top Texel Marl	586	725	**19.2**	544	676	**19.5**	348	456	**23.7**
Base Holland Marl (left)	155	207	**25.1**	155	209	**25.8**	201	266	**24.4**
Base Cretaceous (left)	142	194	**26.8**	275	375	**26.7**	639	783	**18.4**

Appendix II – Depositional environment and Diagenetic history data

1. Depositional environment summary from other sources

Description of formations of Main Buntsandstein according to available literature

Main Buntsandstein formation is divided into three distinct periods – Volpriehausen further split in the Northern part of the basin into Volpriehausen Upper and Lower Sandstone and Volpriehausen Claystone members, Detfurth formation also split into Detfurth Sandstone and Detfurth Claystone members and finally Hardegsen formation. The group is cut by the Hardegsen unconformity and overlying Solling formation.

The Volpriehausen sandstone is the first formation in the sequence that cuts unconformable the underlying Lower Buntsandstein subgroup. The thickness in the West Netherlands basin varies from 60 meters in the southern parts to less than 20 meters in the north. The formation consists of arcosic sandstones with quartz content less than 50%. The sandstones are usually cemented with high percentages of calcite and dolomite cement. A trend in distribution of dominant facies is also present with more fluvial sandstones in the southern part and more aeolian sandstones in the north (Geluk, 2005).
Volpriehausen claystone represents the more fine-grained lacustrine siltstone and marl facies deposited on the coarser sandstones. The Claystone member is more prominent in the north while in the southern offshore areas on the Netherlands in the West Netherlands Basin it is referred to as Volpriehausen Upper Sandstone because it consists mostly of silt and clay rich sandstones and claystones. Sandstones are usually abundantly cemented with calcite and dolomite cement.

The next formation is Detfurth also divided into Lower Sandstone member and Upper Sandstone member or Claystone member. The division between different formations is driven by tectonic events leading to occurrence of erosion and unconformities that mark the transition from one formation to the other. Within the formation there is a clear pattern of cyclisity governed by climate cycles, which can be used for fine scale correlation between wells.

The base of Detfurth Lower Sandstone formation is marked by an unconformity best visible in the southern offshore areas of the West Netherlands Basin. The thickness of the formation varies between 20 and 30 meters also thickening towards the south. Sandstones have higher quartz content and are more loosely quartz cemented.
The formation that follows is Detfurth Claystone or Detfurth Lower Sandstone in the southern margins in West Netherlands Basin.

The last formation in the Main Buntsandstein subgroup is Hardegsen formation. In this formation the lateral variations are very clear. The more abundant sandstones occur only close to active basin margins and turn into alternations of siltstones and sandstones towards the centre. In the West Netherlands Basin Hardegsen formation reaches thicknesses of around 70 meters in the south west offshore areas. The thickening towards the south might indicate that the south major boundary fault was an active growth fault in the Lower Triassic. (Geluk et al, 2005)
The distinctive variations in thickness of Hardegsen formation can be appointed to a number of different factors. The most important one turns out to be misinterpretation of the Hardegsen – Upper Detfurth boundary. It was reviewed and reinterpreted in order to represent better the distinctive lithologies of the two formations. This is further explained in the next paragraph offering a complete sequence stratigraphy framework for the Main Buntsandstein sub-group.
Other factors include differential subsidence of the major fault blocks in the basin and erosion on Hardegsen unconformity.

In total there are three tectonically driven erosional unconformities – Base Volpriehausen unconformity marking the lower boundary of the group, Base Detfurth is the internal boundary separating Detfurth and Volpriehausen formations, and finally Hardegsen unconformity marking the onset of the next Upper Buntsandstein sub-group. Within the formations there are a number of flooding surfaces marking a number

of climate-driven cycles in each of the formations. In the paleo depositional centres where the formations are best developed the full range of cycles is visible while closer towards the paleo highs several of the cycles can be missing.

This is the most current summary of the sequence stratigraphical framework accepted for the West Netherlands Basin. Although formations deposited during the Lower Triassic in adjacent basins show similar features, the fine scale cyclisity model cannot be directly applied to basins other than the studied one without taking considerable precautions.

Dating the sediments using fossils is not possible due to the relatively arid desert depositional setting during the Early and Lower Triassic. However if the major unconformities and distinctive characteristics of the individual formations are properly recognised this can serve as a basis for more broad scale correlations and better naming convention. This can prove useful as outcrops of Triassic rocks are found only from relatively very distant basins where the developments of the individual formations were largely controlled by the local conditions.

When a division based on the tectonic driven unconformities is used to subdivide the Main Buntsandstein sub-group (or Middle Bunter) two distinctive formations are formed.
The first is Volpriehausen formation that is confined between the Base Volpriehausen unconformity and Detfurth unconformity. It has predominantly fluvial influence and the paleo relief governs the deposition of the individual cycles within the formation. Correlation between different regions is sometimes hindered by the more extensive development of the formation in one of the regions. This usually leads to the deposition of an additional cycle that can be confused as part of another formation. The uncertainties regarding the sediment source and possible transport directions are the major source of error while correlating the formation close to the boundary between two major depositional centres such as West Netherlands Basin and Roer Valley Graben. Another typical difference in Volpriehausen formation in other larger than West Netherlands Basin other larger basins is that the basal section of the sequence is usually marked by the deposition of a pronounced conglomerate layer related to alluvial fans.

The second formation is Detfurth and Hardegsen formations combined and confined by the corresponding unconformities. While Detfurth formation is mostly defined by stronger fluvial influence with several upward increasing gamma-ray sandstone cycles in the south and grading into claystones towards the north, Hardegsen is usually seen as two major upward decreasing gamma-ray cycles of possible aeolian origin. It can be further subdivided into more cycles that gradually disappear towards the northeast and southeast. In general formation thicknesses increase significantly with increased availability of accommodation space. The internal boundaries within the formations and between Detfurth and Hardegsen are typically maximum flooding surfaces.
This part of the Main Buntsandstein is considered a transitional phase where the depositional setting has changed by the advance of an arid aeolian setting over the previous fluvial dominated setting.

In either situation a saline lake controlled the boundaries of fluvial and aeolian sediment deposition zones. The constant fluctuations of the lake served as limiting factor for the availability of accommodation space, erosional and transport energy of the systems.

In general typical depositional system of the lower Triassic can be described, proximal to distral – very coarse grained alluvial fan grading into sandy braided river system diminishing in power until it disappears in a dessert setting with aeolian dunes and evaporate desert lakes. The major difference between the north and south North Sea regions is in the amount of precipitation in the areas that served as sediment source. In the north there was excess of precipitation securing a constant influx of sediment in the basin while in the south conditions were much warmer and arid, making the fluvial discharge monsoonal. (Szulies et al, 2004, Bourquin et al, 2006, McKie et al, 2009, Williams et al, 2009)

2. Correlation panels:

Correlation panels are listed in the following manner:

- First sections along the basin strike called Strike sections, ordered North to South.
- Second sections on the basin dip direction called Dip Sections, ordered West to East

Bellow there is a map of all sections with reference for the naming/section numbers:

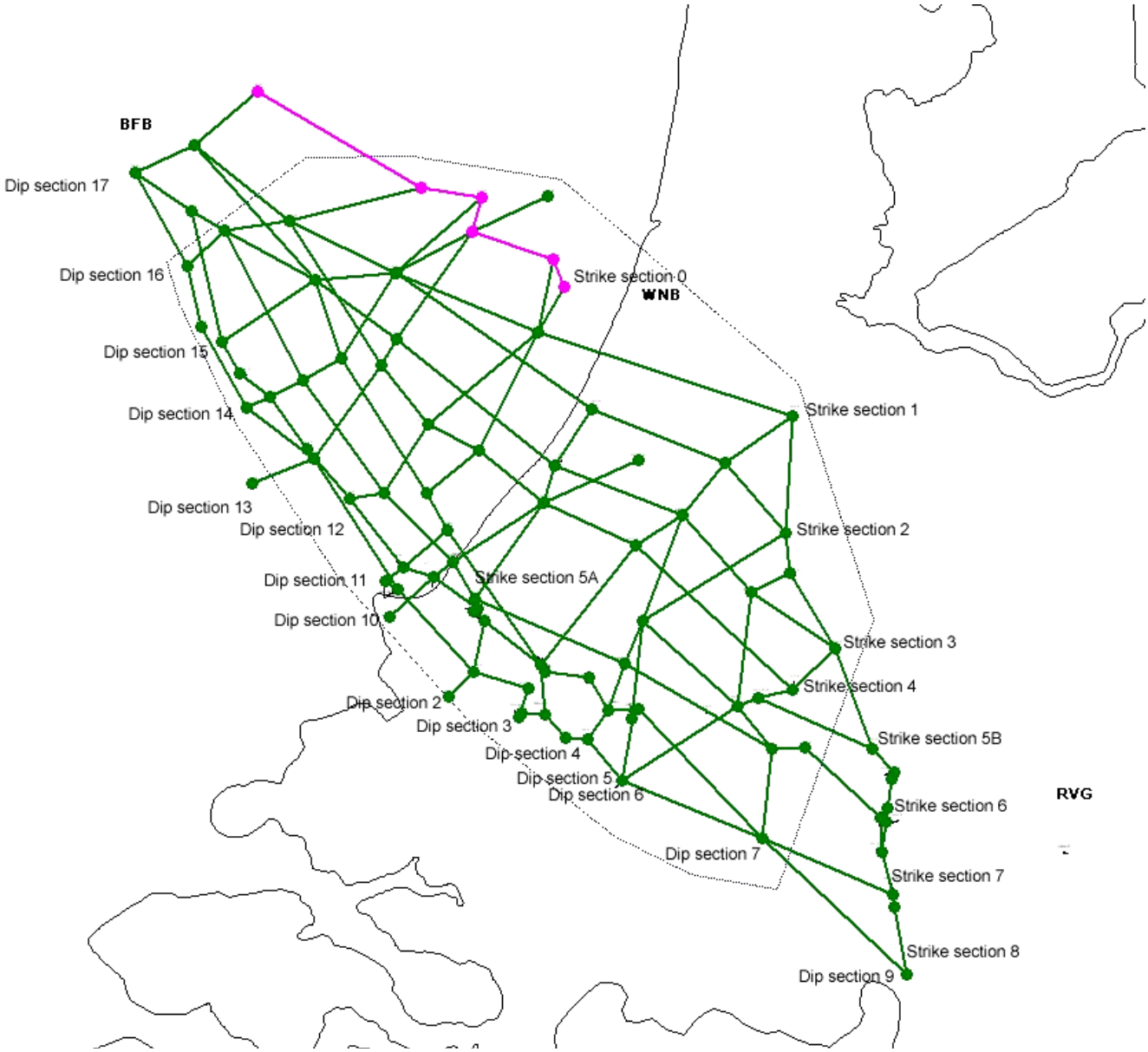

Figure 140: Legend for correlation section locations – see explanation above. North points upwards.

Figure 141: Strike section 0

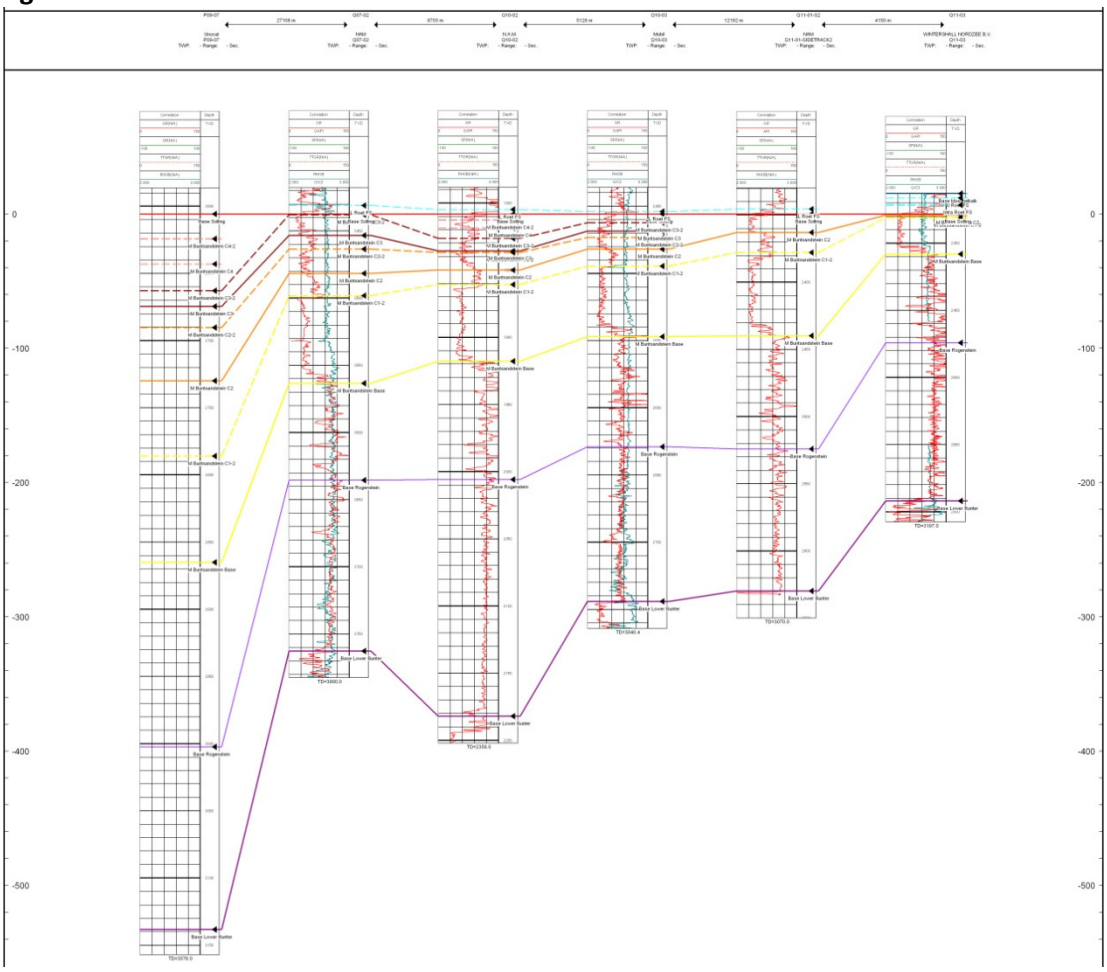

Figure 142: Strike section 1

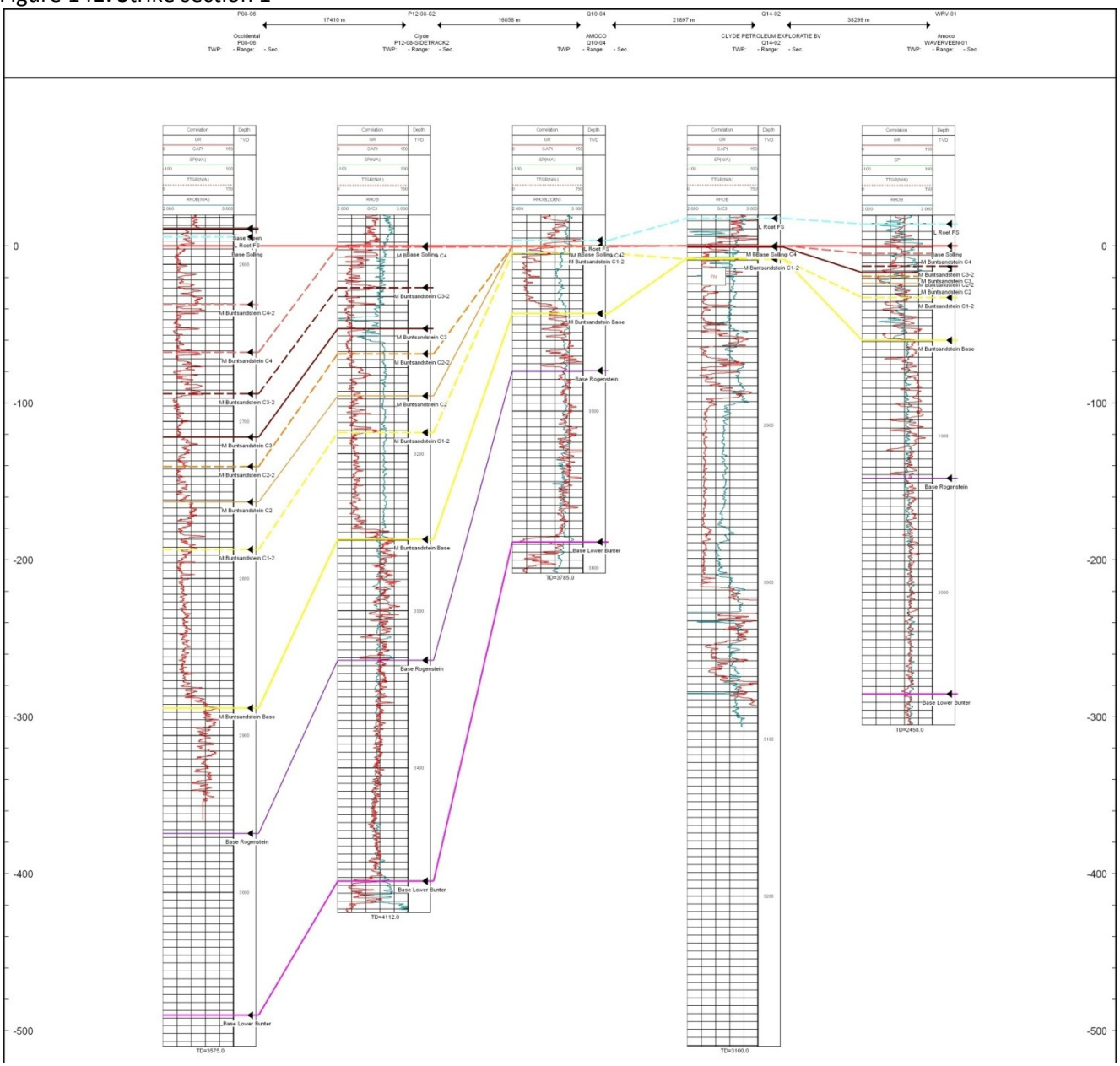

Figure 143: Strike section 3

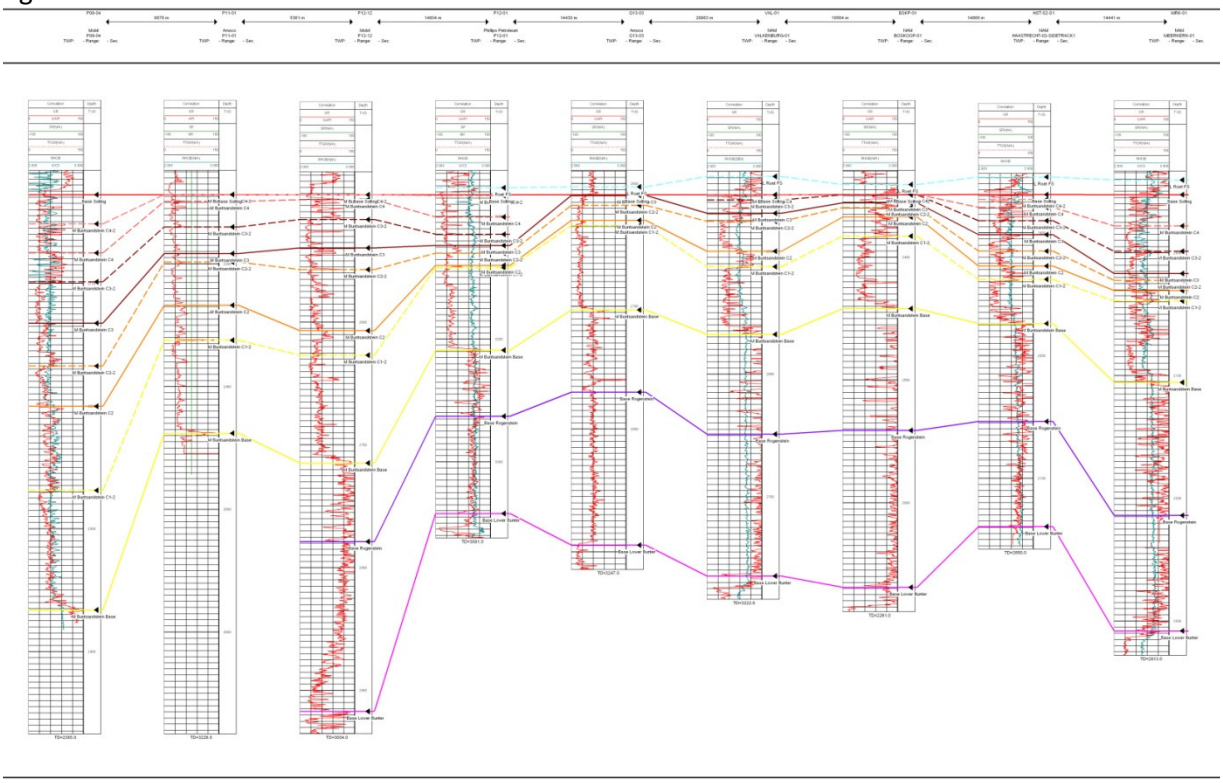

Figure 144: Strike section 4

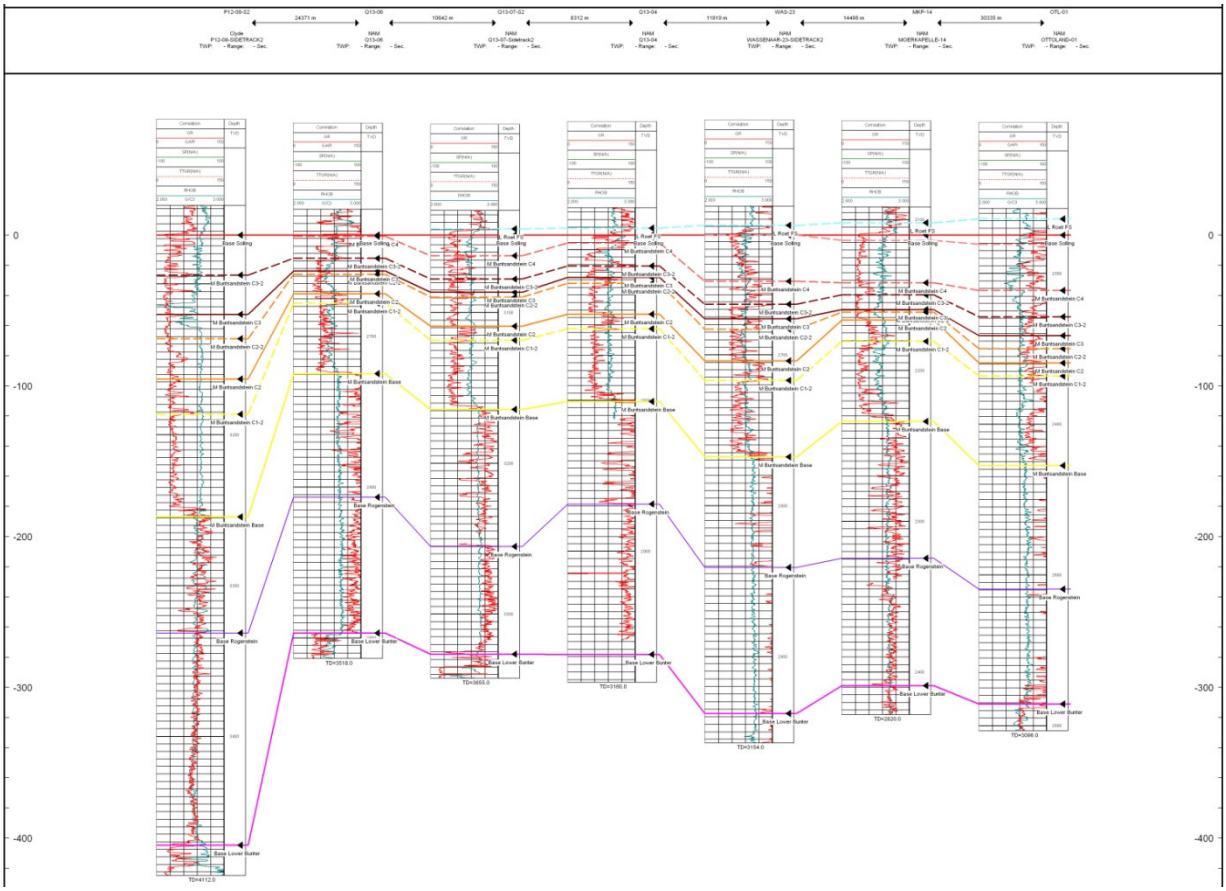

Figure 145: Strike section 5A

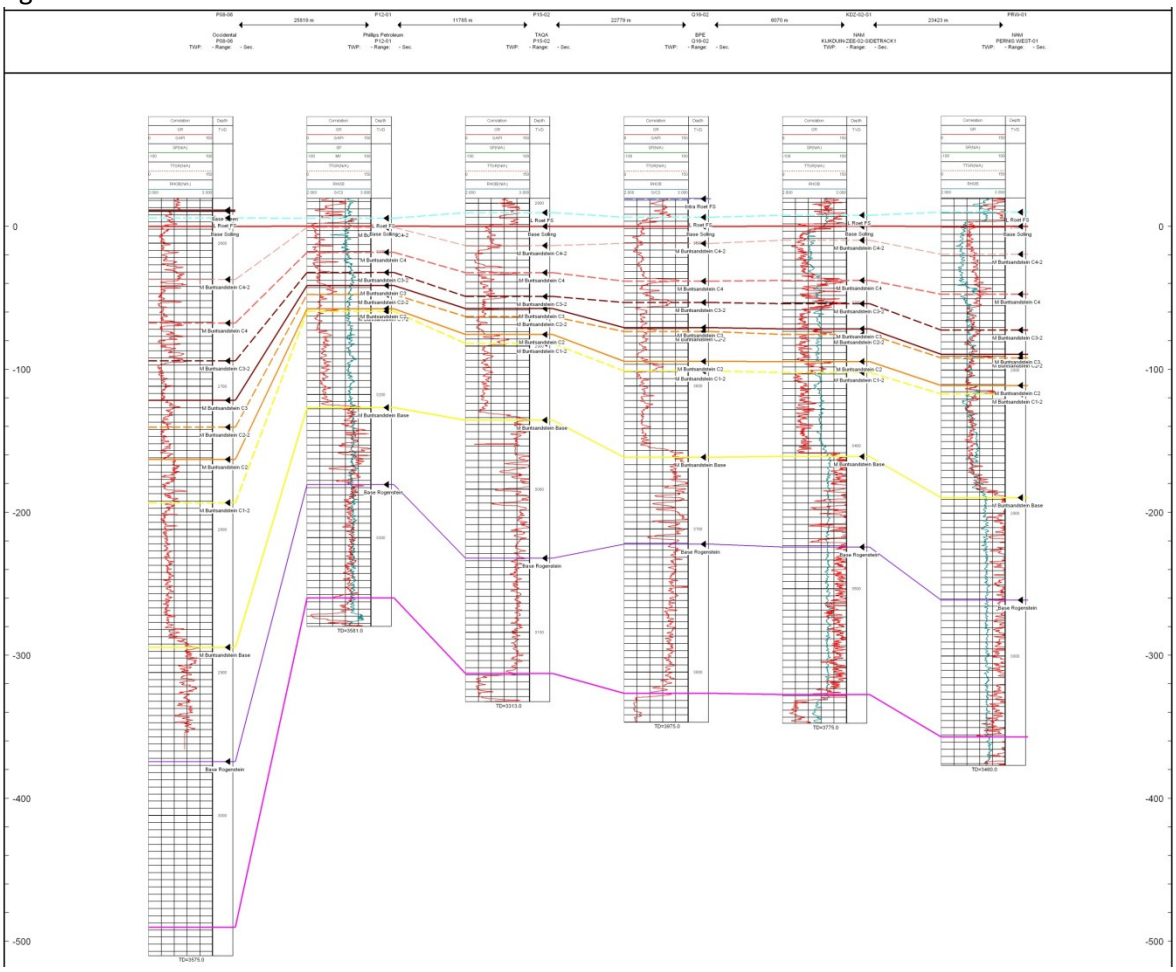

Figure 146: Strike section 5B

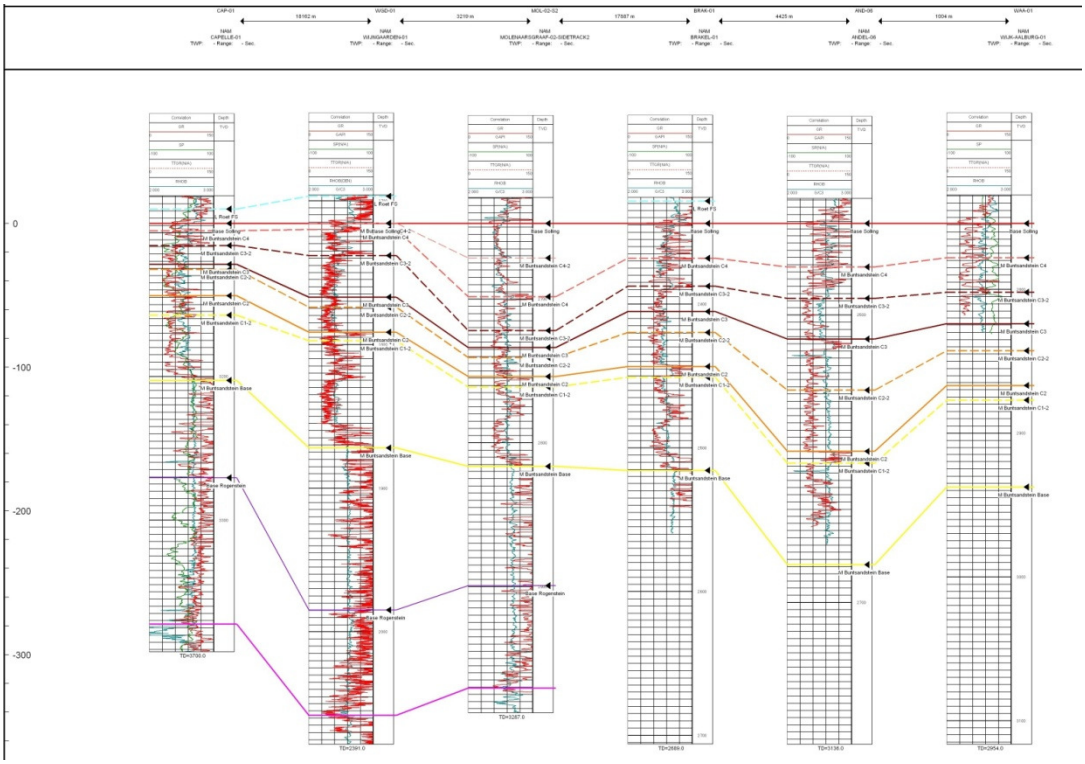

Figure 147: Strike section 6

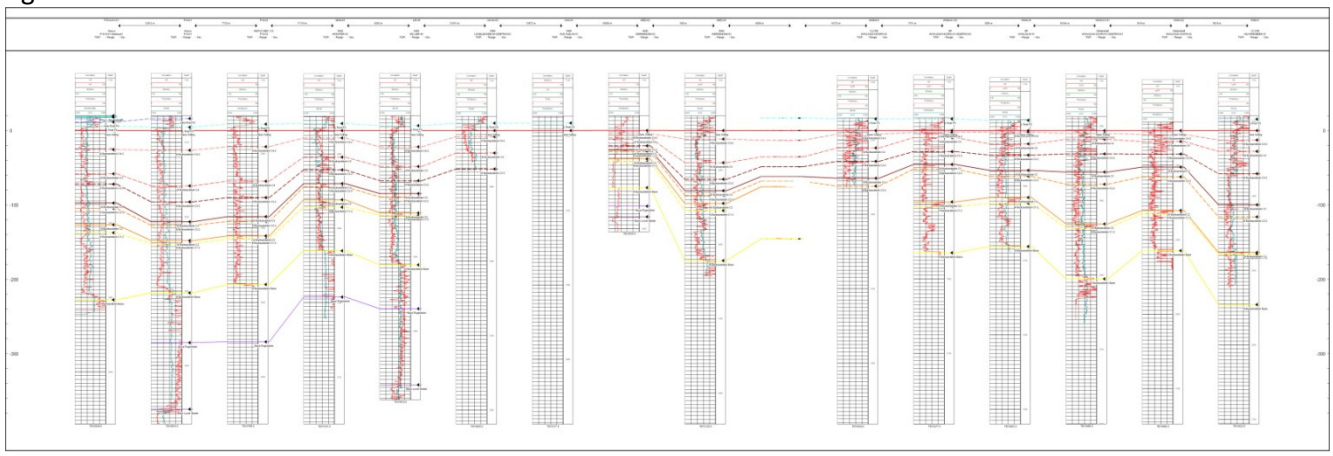

Figure 148: Strike section 7

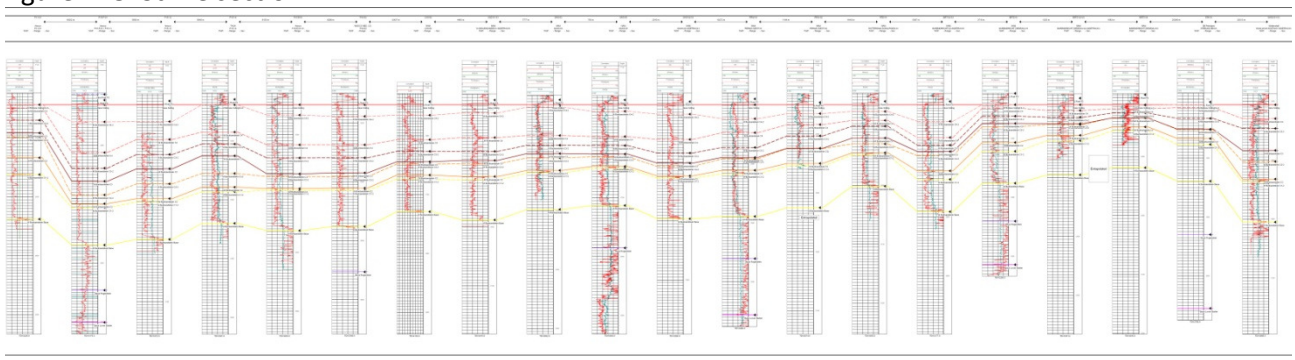

Figure 149: Strike section 8

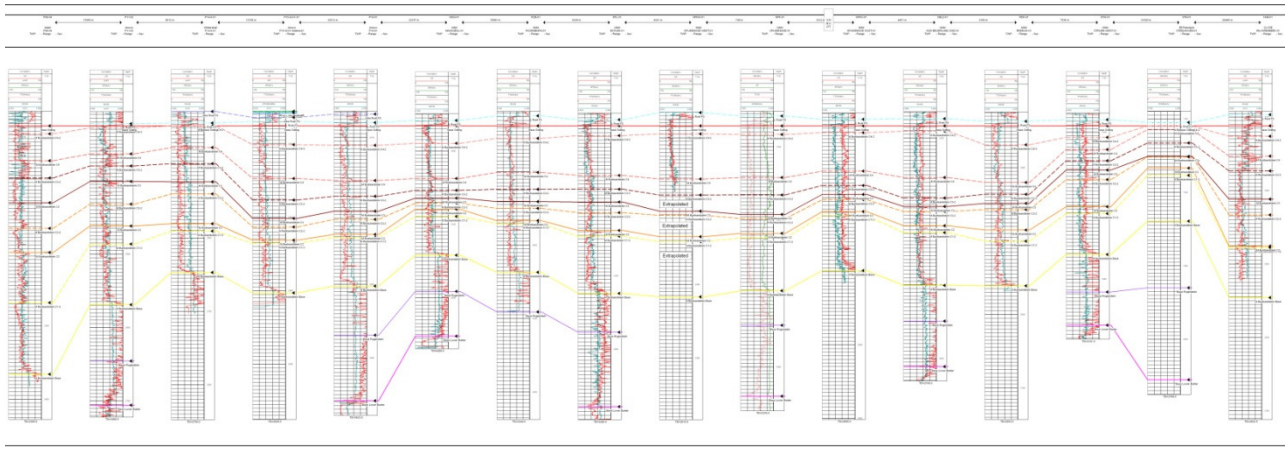

Figure 150: Dip section 17

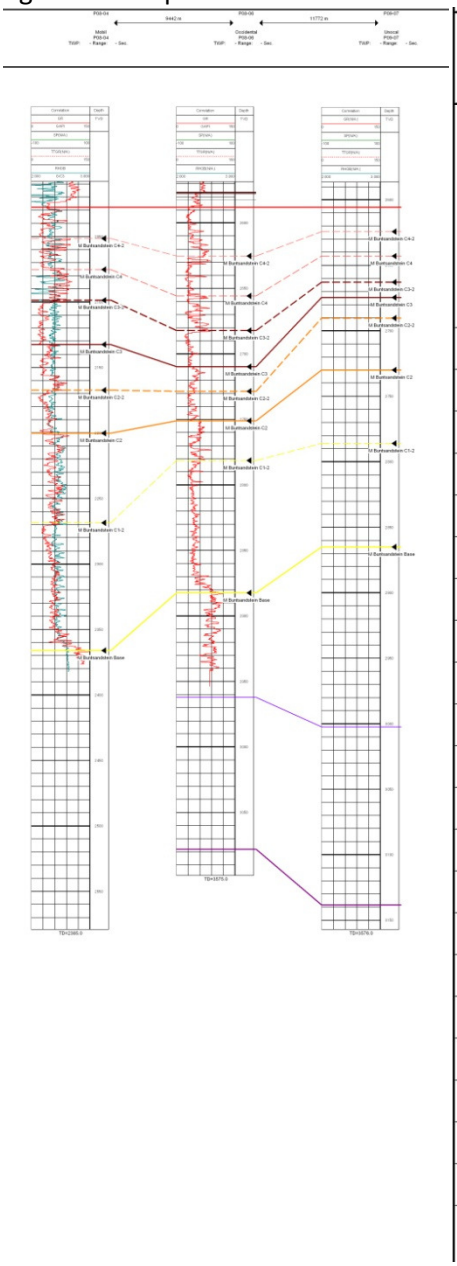

Figure 151: Dip section 16

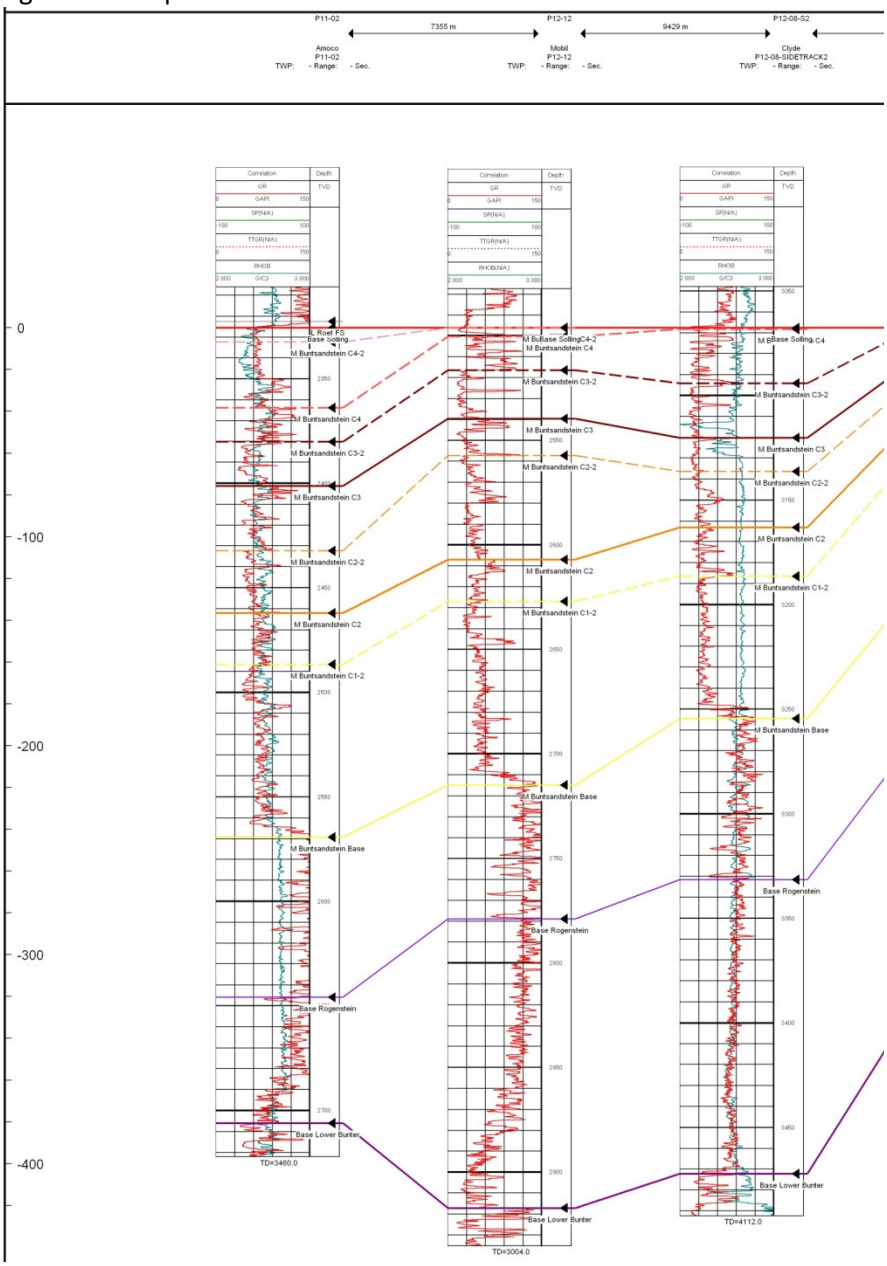

Figure 152: Dip section 15

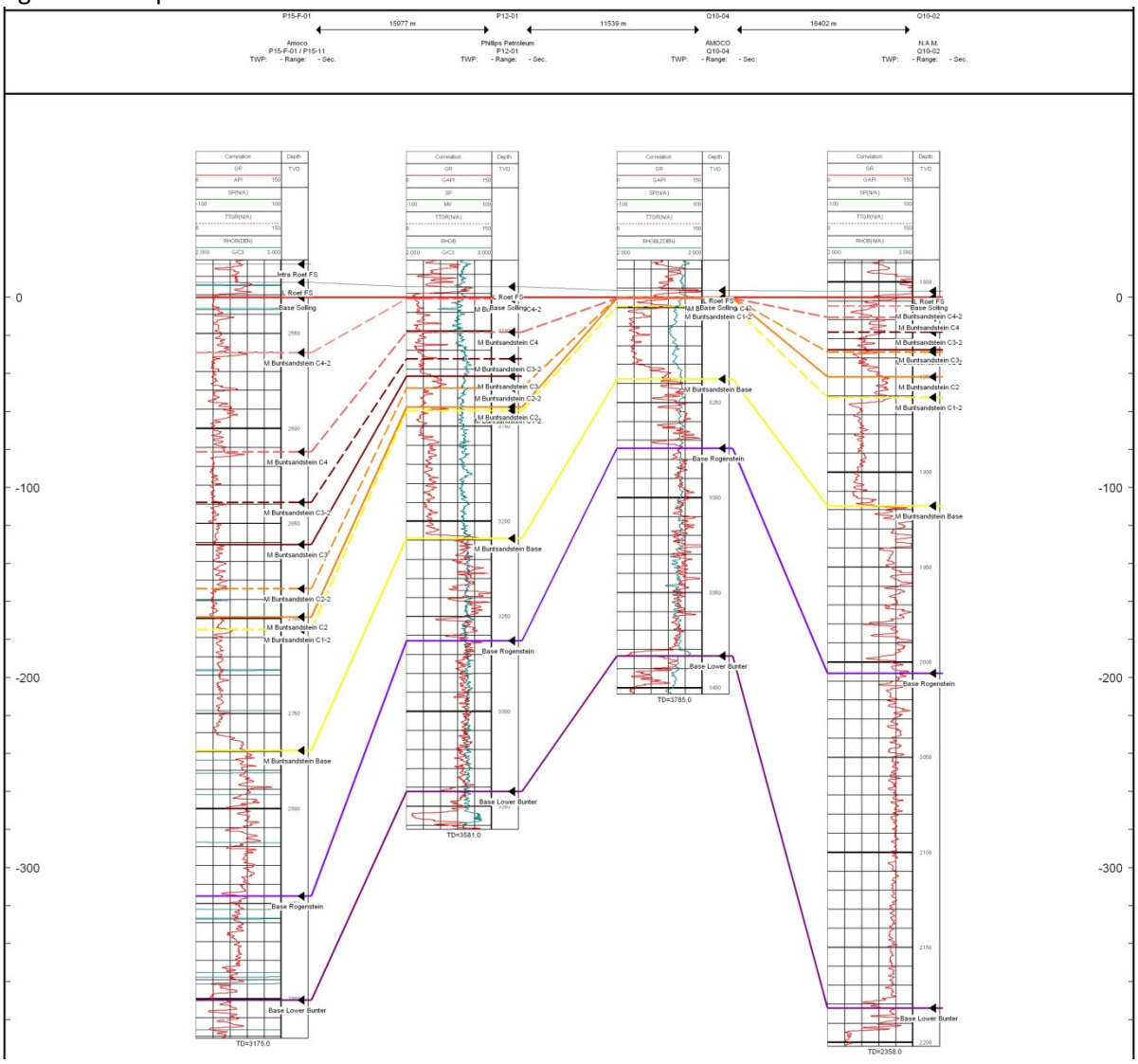

Figure 153: Dip section 14

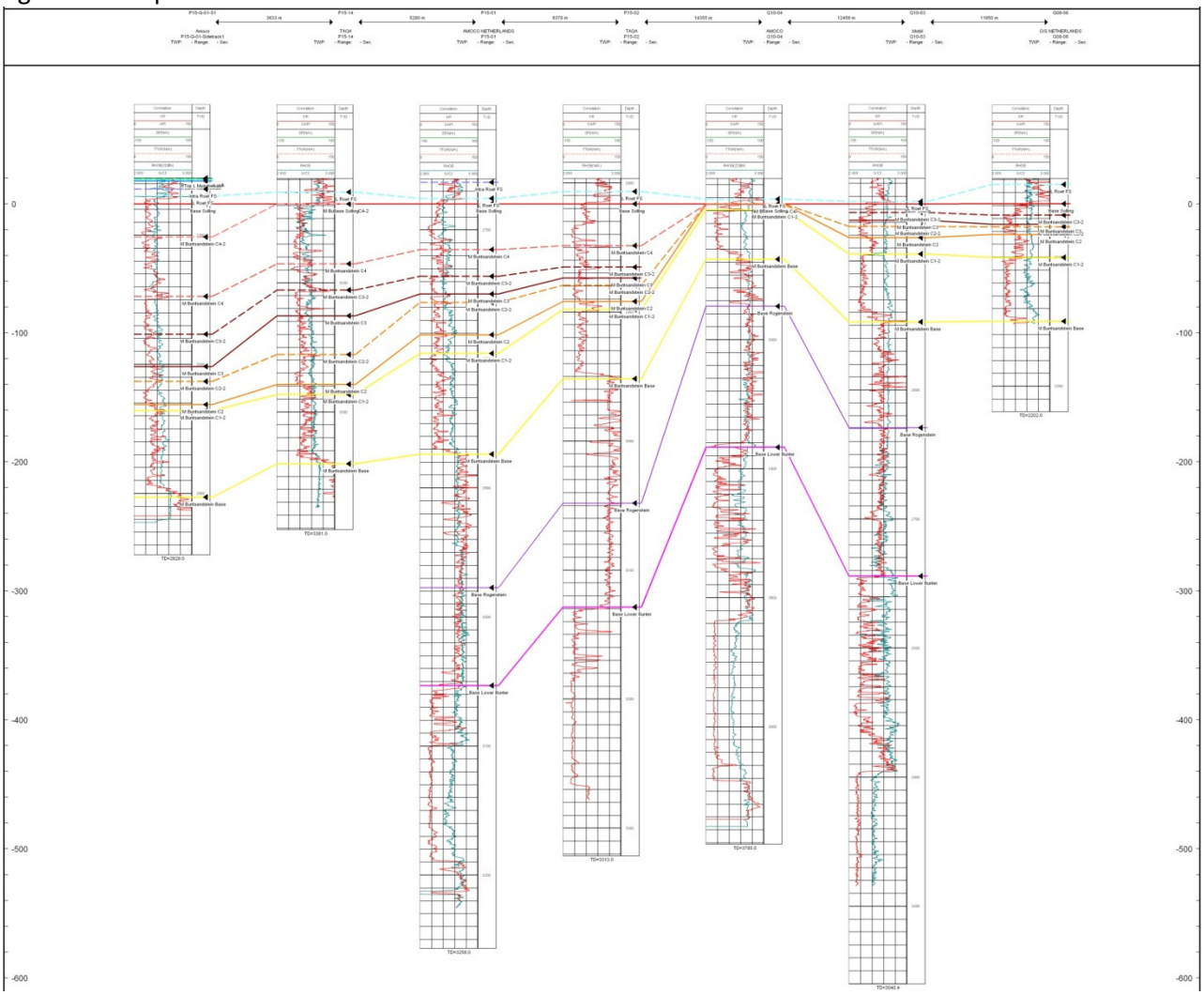

Figure 154: Dip section 13

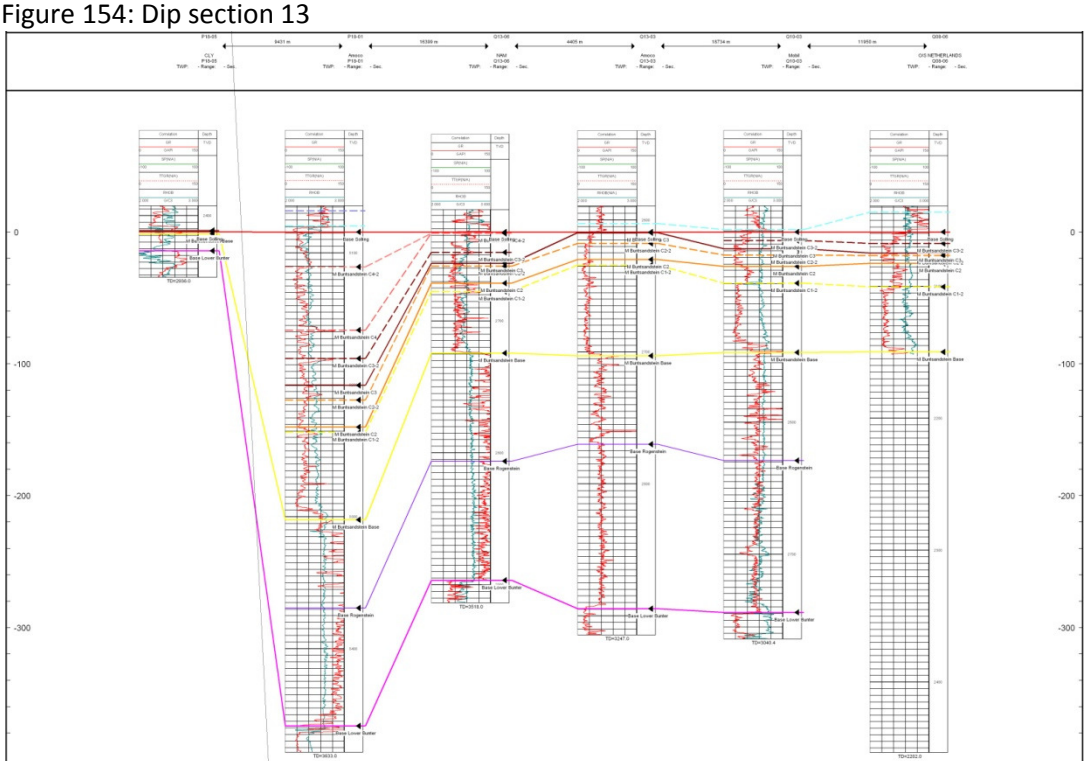

Figure 155: Dip section 12

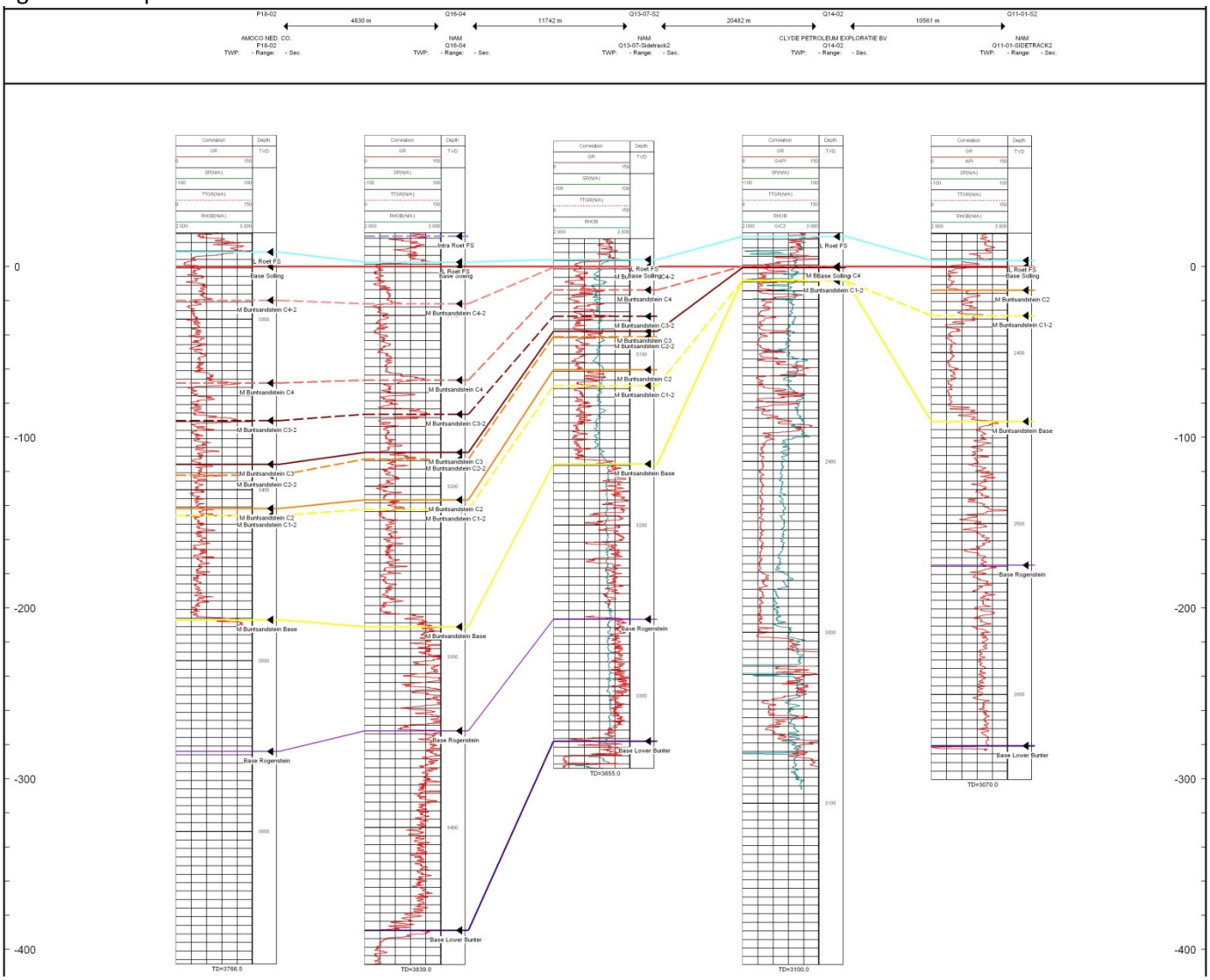

Figure 156: Dip section 11

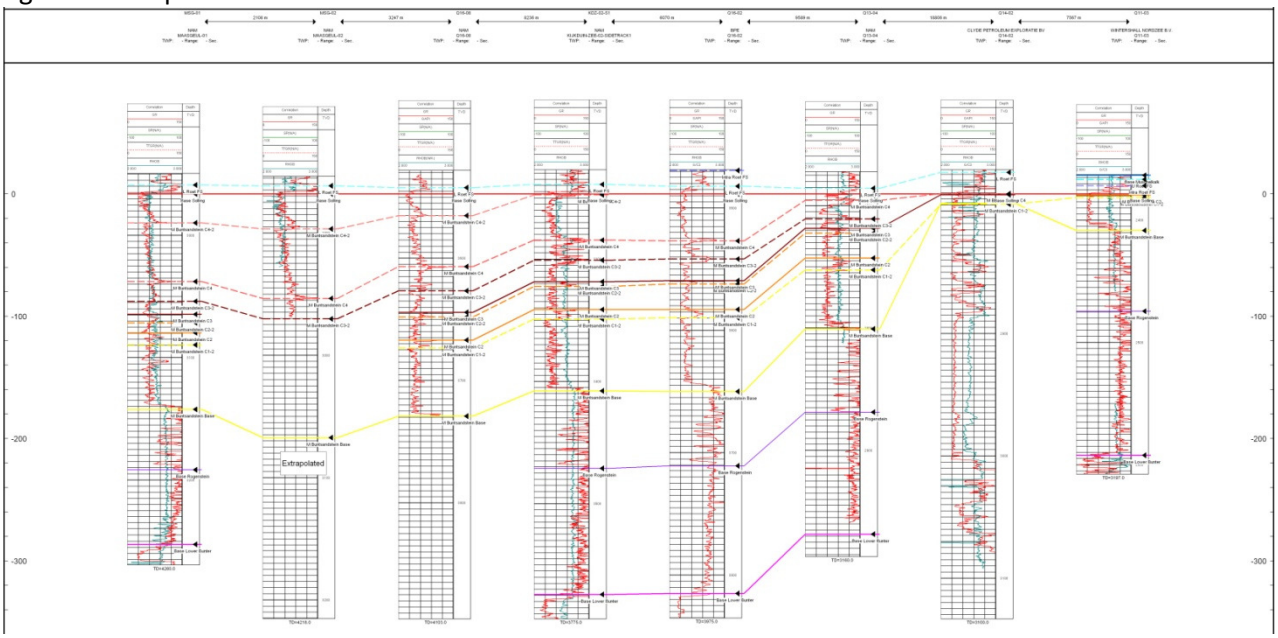

Figure 157: Dip section 10

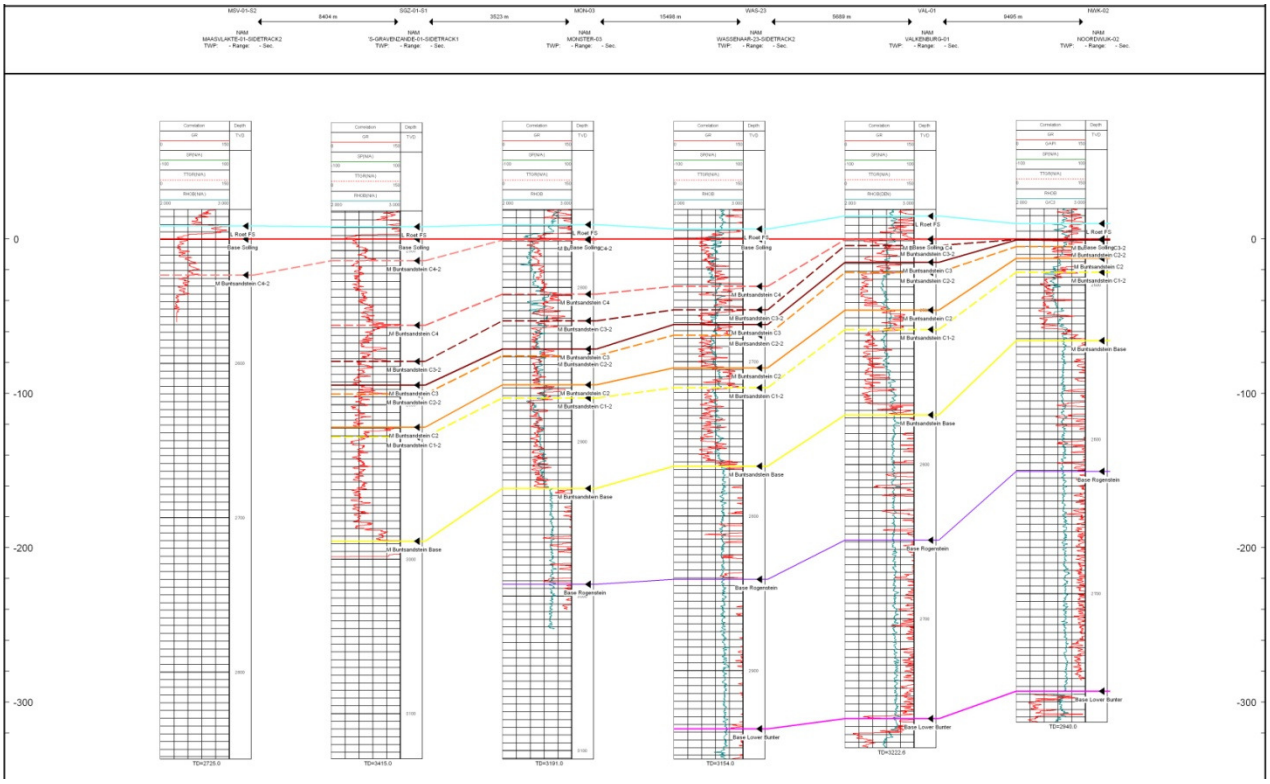

Figure 158: Dip section 2

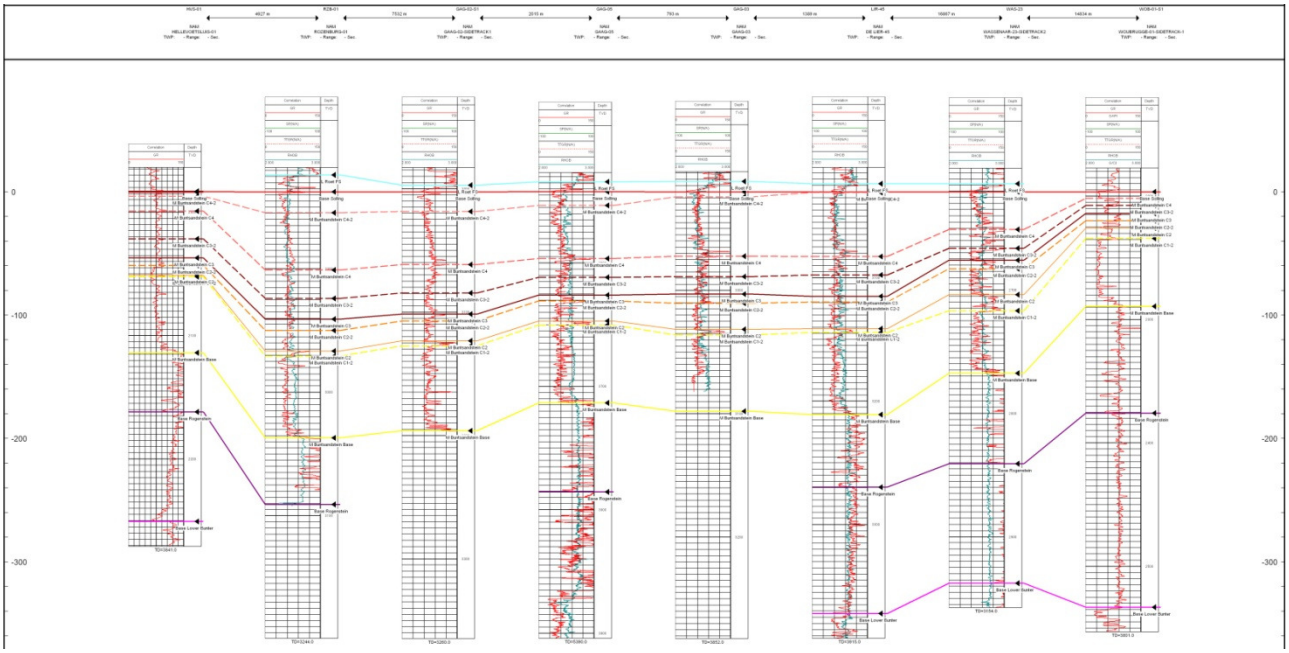

Figure 159: Dip section 3

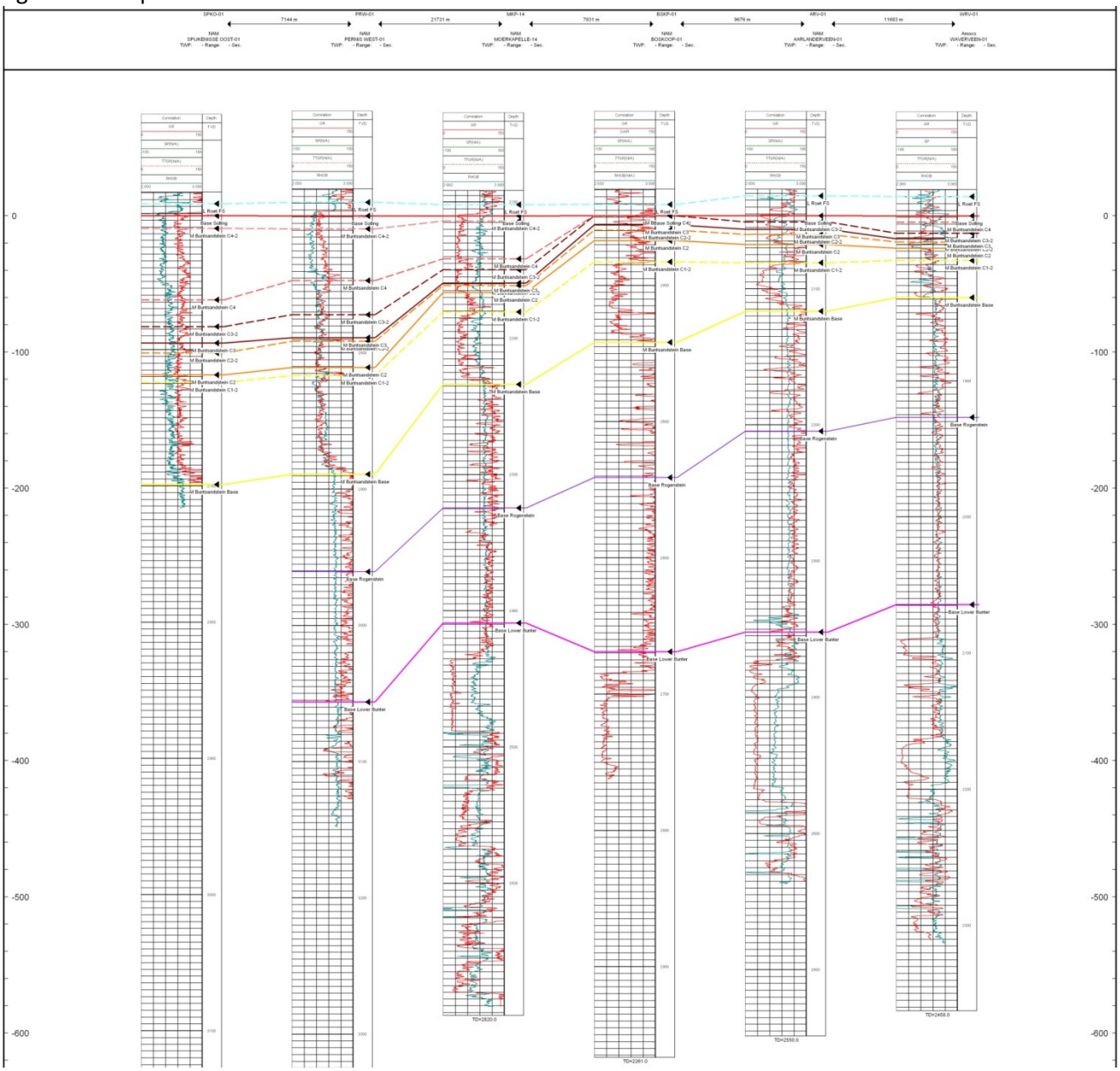

Figure 160: Dip section 4

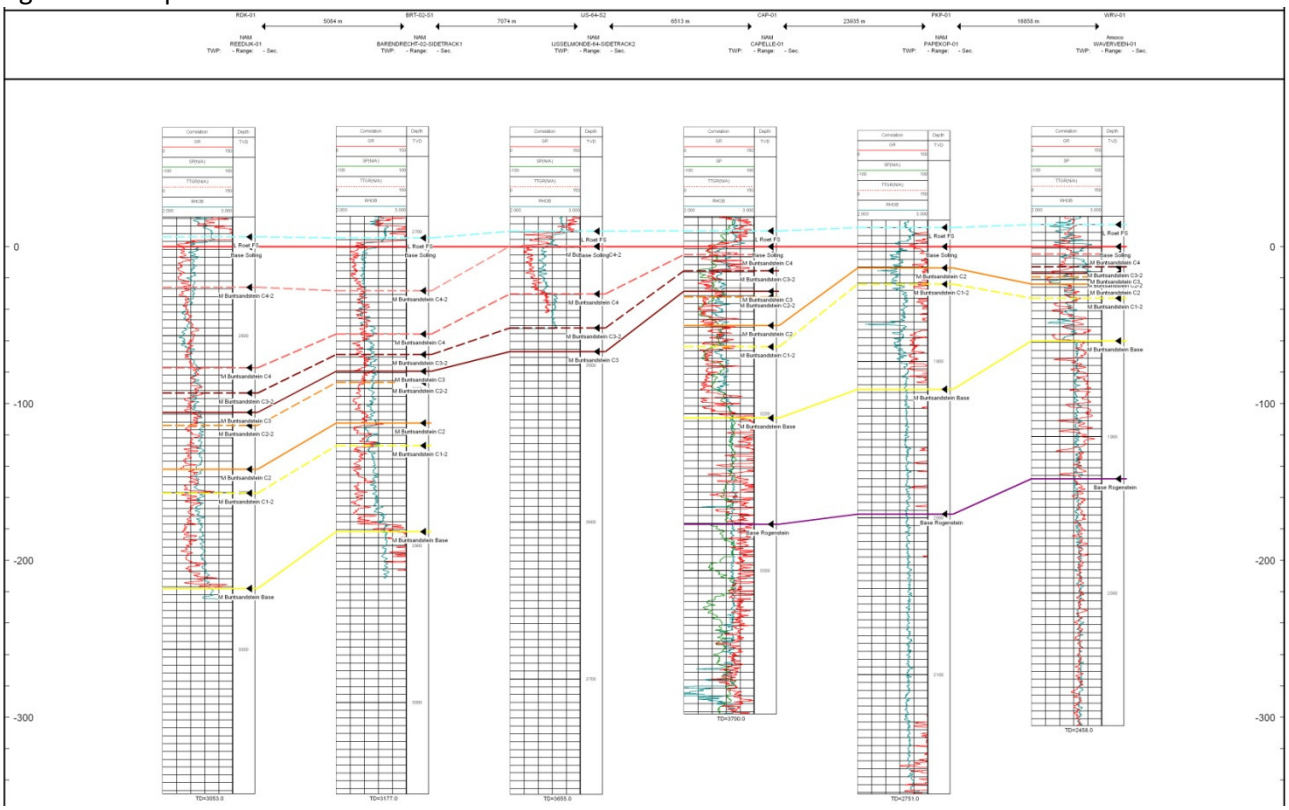

Figure 161: Dip section 5

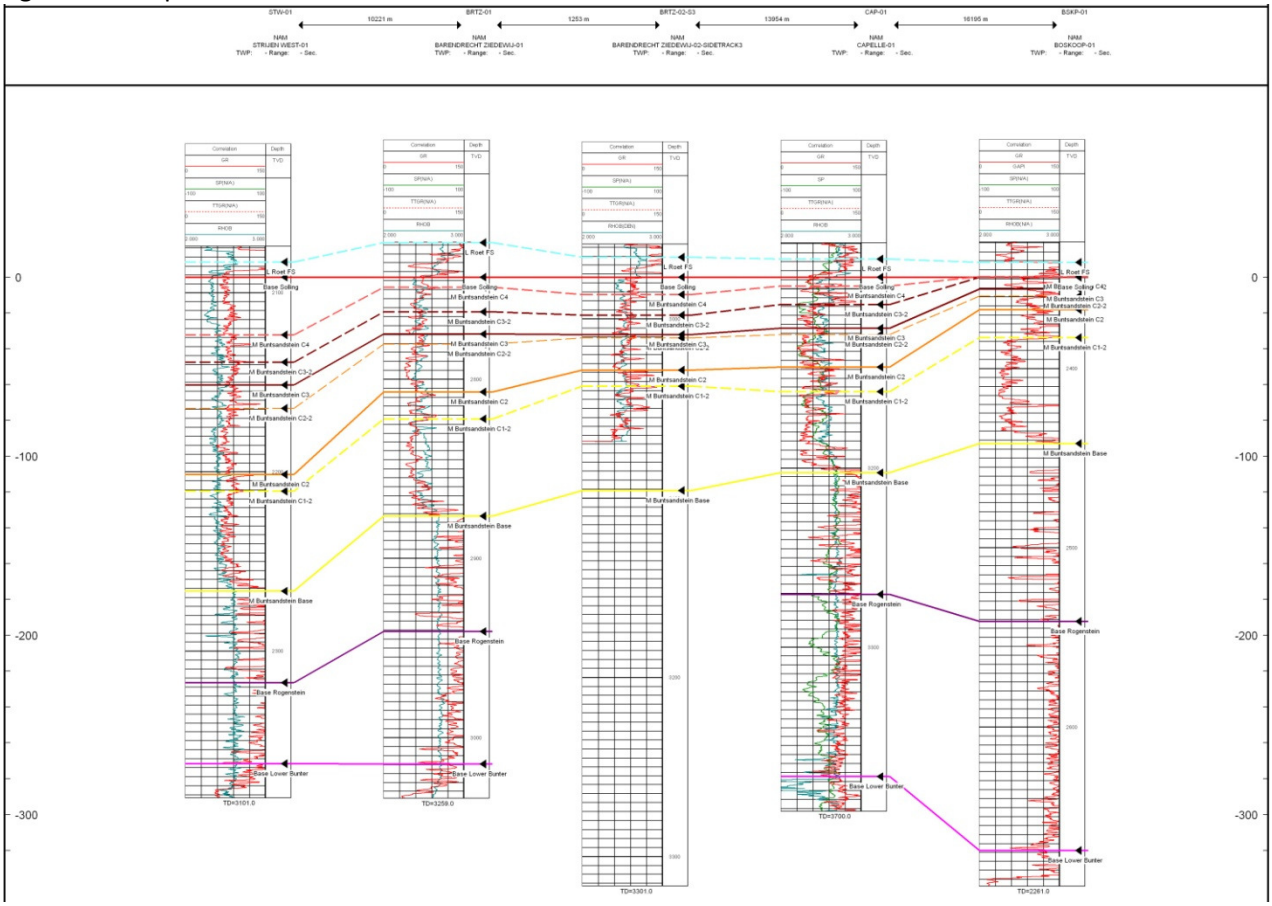

Figure 162: Dip section 6

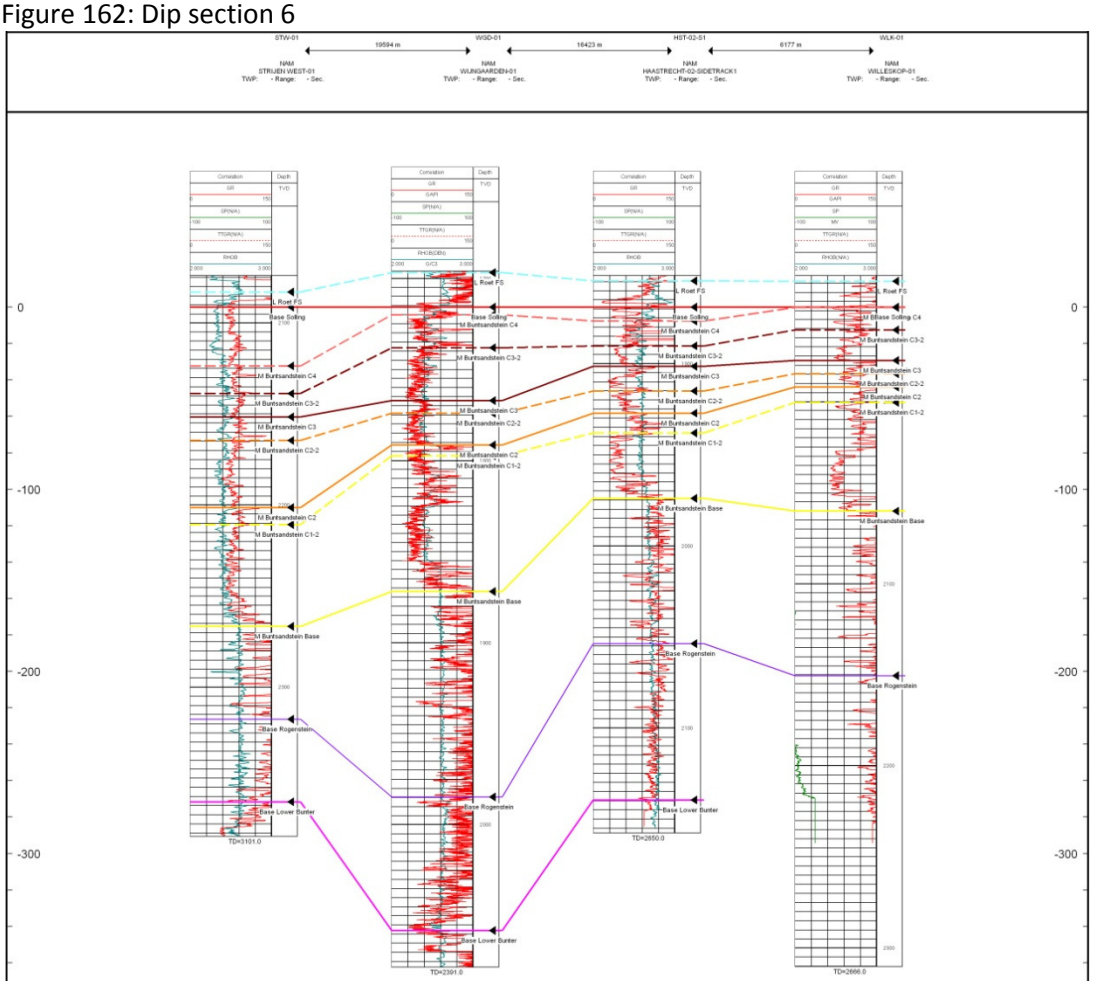

Figure 163: Dip section 7

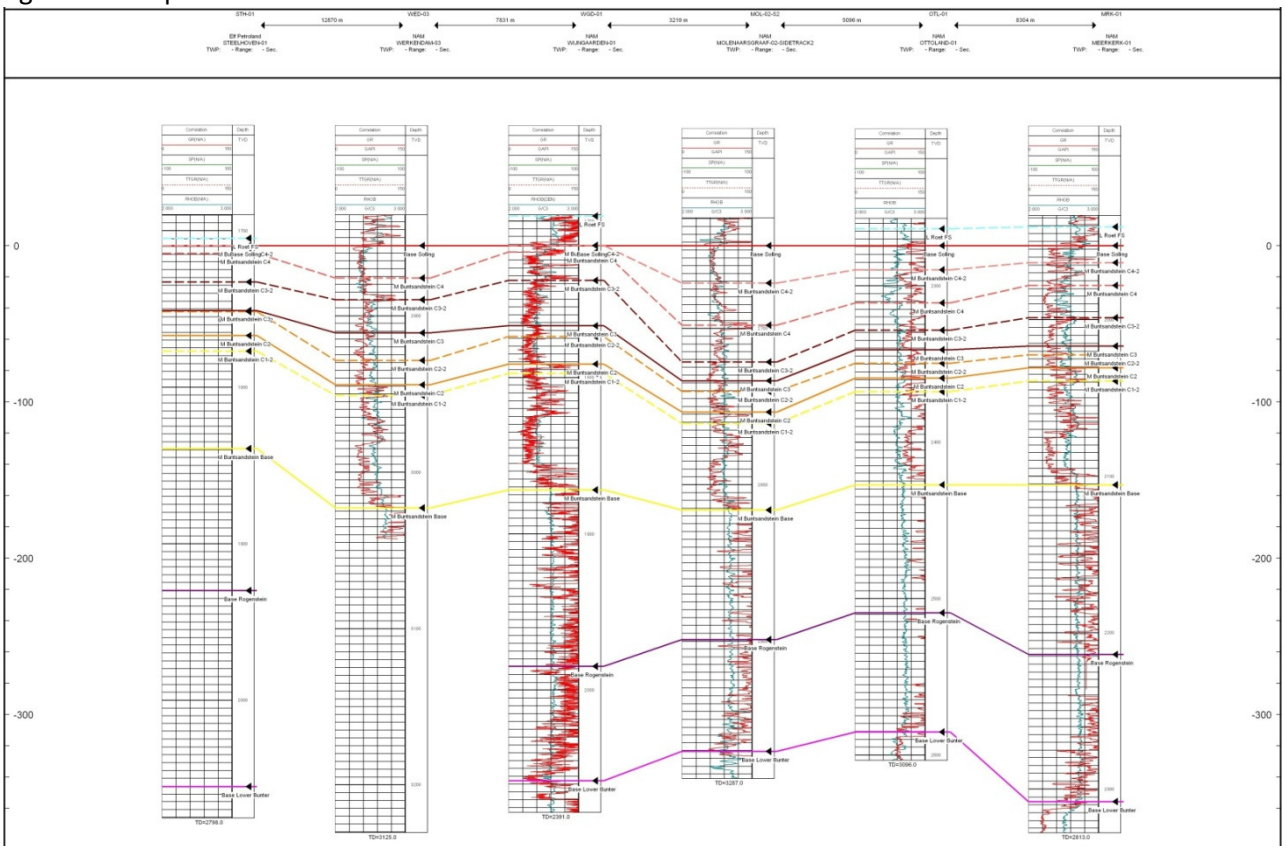

Figure 164: Dip section 9

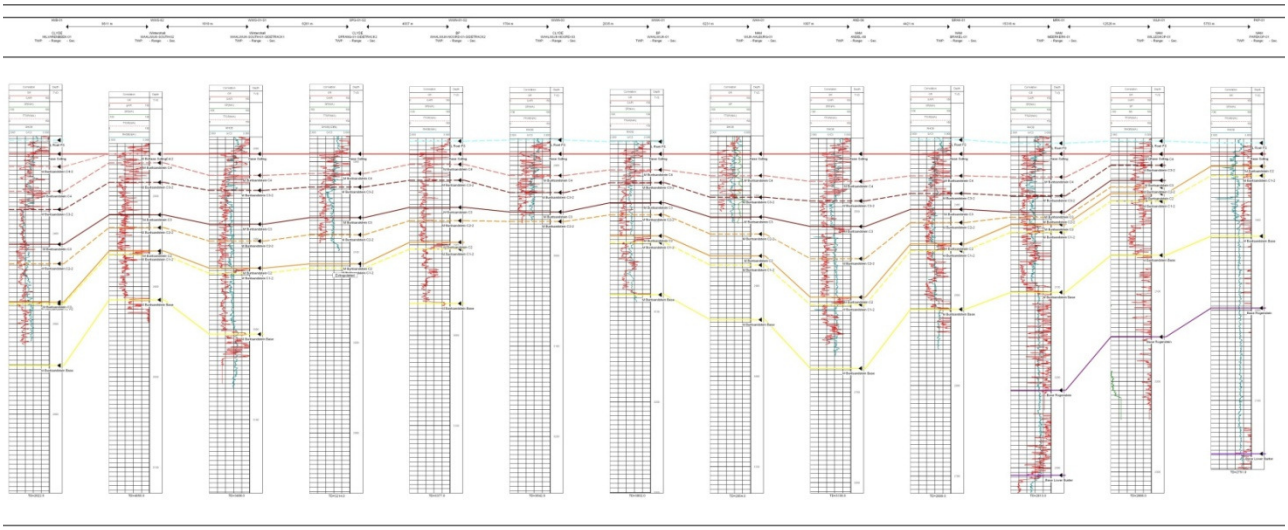

3. Dip Measurements

Table 19: Averaged Dip measurements in Main Buntsandstein separated by region and formation, sources are usually AST, MSD, SHDR, UBI or FMS/FMI tool measurements. Angles are in degrees.

Region	Well ID	Hardegsen				Detfurth				Volpriehausen			
		Dip Angle	Dip Orientation	Fractures Angle	Fractures Orientation	Dip Angle	Dip Orientation	Fractures Angle	Fractures Orientation	Dip Angle	Dip Orientation	Fractures Angle	Fractures Orientation
1	P11-02	25	240	35	270	15	235	32	180	15	260	50	270
	P12-12	30	230	X	X	22	230	X	X	23	245	X	X
2	P12-01	15	235	X	X	15	220	X	X	15	250	23	X
	Q10-04	X	X	X	X	X	X	X	X	18	200	X	X
3	P15-12	25	80	X	X	12	80	X	X	15	90	X	X
	P15-14	22	235	40	320	12	250	35	200	5	180	30	135
	P15-10	35	100	70	120	15	80	35	135	20	90	75	70
	P15-01	25	100	35	110	20	100	35	135	20	90	35	170
4	Q13-06	X	X	X	X	30	35	X	X	33	45	X	X
	Q13-04	X	X	X	X	10	235	55	80	12	220	45	330
	Q13-07	15	235	80	45	18	235	75	40	20	235	75	50
5	Q14-02	X	X	X	X	X	X	X	X	22	225	35	220
	NWK-02	X	X	X	X	X	X	X	X	8	55	15	90
	VAL-	X	X	X	X	12	255	75	125	12	265	85	35

*

	01												
6	Q16-04	6	235	X	X	8	235	X	X	6	240	X	X
	P18-02	12	50	X	X	15	50	X	X	18	60	X	X
	P18-A-06	10	90	75	120	12	120	75	95	10	110	75	95
7	Q16-02	12	340	22	45	12	345	70	265	5	350	45	235
	Q16-08	10	95	X	X	10	125	X	X	10	95	X	X
	KDZ-02	5	355	20	270	8	20	X	X	7	15	12	180
	MON-02	20	50	X	X	22	45	40	30	25	50	X	X
8	WAS-23	8	45	X	X	8	75	X	X	10	50	15	90
	MKP-14	15	225	30	180	11	220	X	X	12	215	22	180
	BSKP-01	X	X	X	X	27	225	X	X	23	225	X	X
9	ARV-01	X	X	X	X	0	100	X	X	0	100	X	X
	PKP-01	X	X	X	X	22	235	40	200	6	270	20	100
	WLK-01	X	X	X	X	X	X	X	X	25	35	45	55
	HST-02	10	190	18	80	8	200	X	X	8	195	30	75
10	MSG-01	15	235	X	X	12	235	X	X	12	235	X	X

!

	MSG-02	15	215	30	270	X	X	X	X	X	X	X	X
	SGZ-01	25	5	X	X	23	355	X	X	18	355	X	X
	RZB-01	4	20	20	0	6	25	X	X	6	15	18	20
	GAG-01	4	55	15	345	4	55	10	90	6	75	22	0
11	IJS-64	12	40	18	20	X	X	X	X	X	X	X	X
	PRW-01	8	345	X	X	10	340	X	X	10	350	X	X
	BTL-01	15	30	20	50	13	40	18	45	18	35	25	35
	SPKO-02	6	255	15	180	X	X	X	X	X	X	X	X
	BRTZ-01	22	350	X	X	18	345	X	X	15	315	X	X
12	OTL-01	28	40	45	355	30	40	80	355	25	40	X	X
	MOL-02	15	45	25	35	18	40	25	10	20	45	22	25
	WGD-01	10	235	X	X	8	210	X	X	8	210	X	X

Appendix III – Reservoir modelling, simulations, and evaluation data

1. Facie interpretations

Name of Well	Core top useful section (MD)	Core length (m)	Formation name	General thickness (m)	Photos available	Encountered facies in core	Formation Vshale	Formation Vsand
BRTZ-01	2755	35	Hardegsen	25	no	lacustrine silts and clays; sand flats; floodpain	145	50
CAP-01	3154	12	(lake, north) Hardegsen		yes	lacustrine silts and clays; sand flats; floodpain	120	40
GAG-02-S1	3080	15	Hardegsen	65	no	dry and damp sand flat	90	45
GAG-03	3655		Hardegsen	65	no	dry and damp sand flat	90	45
GAG-05	4095		Hardegsen	65	**yes**	dry and damp sand flat	90	45
IJS-64	3605	25	Hardegsen	35	no	dry and damp sand flat	75	30
KDZ-02-S1	3255	18	(both) Hardegsen	32	**yes**	sand dunes; dry and damp sand flat	72	28
MSG-01	3753	25	(both) Hardegsen	75	**yes**	sand dunes; dry and damp sand flat	75	30
MSG-02	4082	2	Hardegsen	75	no	dry and damp sand flat	75	30
MSV-01-S1	2684	15	Hardegsen	75	no	dry and damp sand flat	75	30
OTL-01	2578	17	Hardegsen	47	no (description)	lacustrine silts and clays; sand flats; floodpain	90	60
P11-02	2342	30	Hardegsen	30	no (tiff data)	dry and damp sand flat	105	60
P14-A-01	2485	27	(lower) Hardegsen	35	**no (description)**	lacustrine silts and clays; sand flats; floodpain	120	30
P15-01	2708	11	Hardegsen	47	no	sand flat	75	30
P15-02	2825	20	Hardegsen	29	no	dry and damp sand flat	80	25
P15-10	2656	153	Hardegsen	??	no	????????	??	??

P15-12	3147	17	Hardegsen (?)	44	no	????????	??	??
P15-14	3145	37	Hardegsen	38	no	sand flat	75	60
P15-F-01	2544	40	Hardegsen	30	no	dry and damp sand flat	75	30
P15-F-02	2545	22	Hardegsen	30	no	dry and damp sand flat	75	30
P18-02	3284	15	Hardegsen	69	no	dry and damp sand flat	73	20
P18-A-01	3626	26	(base of lower) Hardegsen	80	**no (description)**	dry and damp sand flat	75	30
PRW-01	2970	44	Hardegsen	44	**no (other info)**	dry and damp sand flat; floodplain	85	45
Q13-07-S2	3170	17	Hardegsen	45	**yes**	sand flat; lacustrine silts and clays; floodplain	90	30
RTD-01	3105	18	Hardegsen	40	**no (description)**	dry and damp sand flat	90	50
RZB-01	2947	57	Hardegsen	55	no	dry and damp sand flat	80	45
SGZ-01-S1	3206	10	Hardegsen	65	no **	dry and damp sand flat	90	45
SPKO-01-S1	2720	27	Hardegsen	80	no	sand dune, dry and damp sand flat		
SPKW-01	2817	18	Hardegsen	85	**no (description)**	sand dune, dry and damp sand flat	75	35
STW-01	2546	18	Hardegsen	28	no	dry and damp sand flat	75	60
WWN-01-S2		153	Hardegsen - RVG					
AND-06	2894	19	Upper Detfurth	30	**yes**	lacustrine silts and clays; sand flats; floodpain	150	60
CAP-01	3162	12		20	yes	lacustrine silts and clays; sand flats; floodpain		
P14-A-01	2510	27	Upper Detfurth	55	**no (description)**	lacustrine silts and clays; sand flats; floodpain		
P15-02	2877	12	Upper + Lower Detfurth	20	no	lacustrine silts and clays; sand flats; floodpain		

PRW-01	3066	20	Upper Detfurth	20	no	lacustrine silts and clays; sand flats; floodpain		
Q13-06	2752	30	Upper Detfurth	15	**yes**	lacustrine silts and clays; sand flats; floodpain		
Q16-08	3930	13	Upper Detfurth (Bs HRD)	20	**yes**	lacustrine silts and clays; sand flats; floodpain		
WWN-01-S2	3169	153	Upper Detfurth - RVG	30	**no (description)**	lacustrine silts and clays; sand flats; floodpain		
PRW-01	3085	255	Lower Detfurth	18	**yes**	fluvial bars		
Q13-04	2785	15	Upper + Lower Detfurth	16	**yes**	fluvial bars		
Q13-06	2763	10	Lower Detfurth	10	**yes**	fluvial bars		
Q16-02	3570	5	Base Lower Detfurth	16	**yes**	fluvial bars		
WWN-01-S2	3202	153	Lower Detfurth	18	**no (description)**	fluvial bars		
BTL-01	2818	18	Upper Volpriehausen	40	**no (description)**	fluvial bars; sand flats		
P14-A-01	2587	36	Upper Volpriehausen	45	**no (description)**	fluvial bars; sand flats		
PKP-01	2126	10	Upper Volpriehausen	40	**yes**	sand flats; lacustrine clays; floodplain		
PRW-01	3100	255	Upper Volpriehausen	25	no	fluvial bars; sand flats; floodplain		
Q13-06	2774	30	Upper Volpriehausen	15	**yes**	fluvial bars; sand flats; floodplain		
VAL-01	2821	60	Up Vol + Low Vol	40	**yes**	fluvial bars; sand flats; lacustrine clays; floodplain		
WWN-01-S2	3220	153	Upper Volpriehausen	50	**no (description)**	fluvial bars; sand flats; lacustrine clays; floodplain		
CAP-01	3205	25	L VLPR CLaySST and SST	50	yes	fluvial bars; sand flats; floodplain		
HST-02-S1	2127	25	Lower Volpriehausen	55	no	fluvial bars; sand flats; floodplain	75	30

			SST			
P18-02	3434	8	Lower Volpriehausen SST	60	no	fluvial bars; sand flats
PRW-01	3126	255	Lower Volpriehausen SST	70	no	fluvial bars; sand flats
Q16-02	3629	6	Lower Volpriehausen SST	55	**yes**	fluvial bars; sand flats
WWN-01-S2	3279	153	Lower Volpriehausen Clay -RVG	55	**no (description)**	fluvial bars; sand flats; lacustrine clays; floodplain

List of facies	
A	**desert sand dune**
B	**dry desert sand flat**
C	**fluvial braid bar**
D	**damp desert sand flat**
E	**fluvial fan/sand flat**
F	**floodplain/overbank**
G	**lacustrine clay/silt**

VISUAL INTERPRETATION OF CORE PHOTOGRAPHS

Well	Plug Num	Depth m MD	Porosity %	Kh mD	Kv mD	RHOB g/cm3	GR API	Formation	Facies
GAG-05	NM0001	4085.10	10.2	2.95		2.68	120	Solling	E
GAG-05	NM0002	4085.40	9.5	7.83		2.67	110	Solling	E
GAG-05	NM0003	4085.70	8.4	1.18		2.68	95	Solling	D
GAG-05	NM0004	4086.00	9.6	3.23		2.67	75	Hardegsen	D
GAG-05	NM0005	4086.30	10.6	6.25		2.67	60	Hardegsen	D
GAG-05	NM0006	4086.65	13.3	41.98		2.67	45	Hardegsen	D
GAG-05	NM0007	4086.90	11.4	13.78		2.67	30	Hardegsen	D
GAG-05	NM0008	4087.20	10.2	6.66		2.67	60	Hardegsen	D
GAG-05	NM0009	4087.50	13.8	51.32		2.67	65	Hardegsen	E
GAG-05	NM0010	4087.80	14.2	91.91		2.66	60	Hardegsen	D
GAG-05	NM0011	4088.10	12.1	14.92		2.67	75	Hardegsen	E
GAG-05	NM0012	4088.40	13.4	15.34		2.67	65	Hardegsen	E
GAG-05	NM0013	4088.75	10.9	5.25		2.68	60	Hardegsen	D
GAG-05	NM0014	4089.10	10.4	11.43		2.68	55	Hardegsen	D
GAG-05	NM0015	4089.40	17.0	62.22		2.66	45	Hardegsen	E
GAG-05	NM0016	4089.70	15.4	77.01		2.66	45	Hardegsen	E
GAG-05	NM0017	4089.95	13.5	13.83		2.67	35	Hardegsen	D
GAG-05	NM0018	4090.25	12.9	37.81		2.67	40	Hardegsen	D
GAG-05	NM0019	4090.55	10.0	13.97		2.67	40	Hardegsen	D
GAG-05	NM0020	4090.85	9.5	5.85		2.67	50	Hardegsen	D

GAG-05	NM0021	4091.15	12.9	30.75	2.67	45	Hardegsen	D
GAG-05	NM0022	4091.45	12.4	15.71	2.67	40	Hardegsen	E
GAG-05	NM0023	4091.75	9.7	5.73	2.67	35	Hardegsen	D
GAG-05	NM0024	4092.05	5.2	4.00	2.70	40	Hardegsen	E
GAG-05	NM0025	4092.35	10.6	14.06	2.67	40	Hardegsen	E
GAG-05	NM0026	4092.60	12.8	15.96	2.66	45	Hardegsen	D
GAG-05	NM0027	4092.90	8.4	0.20	2.68	75	Hardegsen	E
GAG-05	NM0028	4093.20	8.3	0.95	2.66	65	Hardegsen	D
GAG-05	NM0029	4093.50	6.3	0.13	2.66	60	Hardegsen	D
GAG-05	NM0030	4093.75	6.8	0.91	2.66	45	Hardegsen	D
GAG-05	NM0031	4094.05	9.6	9.90	2.67	45	Hardegsen	D
GAG-05	NM0032	4094.35	7.4	0.76	2.67	50	Hardegsen	E
GAG-05	NM0033	4094.85	7.9	1.01	2.66	50	Hardegsen	E
GAG-05	NM0034	4095.15	7.3	2.24	2.67	60	Hardegsen	D
GAG-05	NM0035	4095.40	9.3	4.67	2.66	75	Hardegsen	D
GAG-05	NM0036	4095.60	8.7	17.54	2.67	90	Hardegsen	D
GAG-05	NM0037	4095.90	11.7	39.30	2.67	90	Hardegsen	D
GAG-05	NM0038	4096.20	6.6	4.22	2.67	85	Hardegsen	E
GAG-05	NM0039	4096.60	5.1	0.17	2.67	80	Hardegsen	D
GAG-05	NM0040	4096.90	5.7	0.23	2.67	80	Hardegsen	D
GAG-05	NM0041	4097.30	5.6	0.73	2.67	80	Hardegsen	D
GAG-05	NM0042	4097.50	4.3	0.35	2.67	75	Hardegsen	D
GAG-05	NM0043	4097.85	8.5	2.35	2.68	75	Hardegsen	E
GAG-05	NM0044	4100.20	7.9	0.49	2.67	75	Hardegsen	D
GAG-05	NM0045	4100.55	5.3	0.11	2.67	75	Hardegsen	D
GAG-05	NM0046	4100.80	7.7	0.42	2.66	80	Hardegsen	D
GAG-05	NM0047	4101.15	6.6	0.26	2.67	70	Hardegsen	D
GAG-05	NM0048	4101.45	5.5	0.66	2.66	75	Hardegsen	E
GAG-05	NM0049	4101.80	3.2	0.39	2.69	75	Hardegsen	E
GAG-05	NM0050	4102.10	6.9	1.00	2.67	90	Hardegsen	F
GAG-05	NM0051	4102.57	5.0	0.42	2.70	90	Hardegsen	F
GAG-05	NM0052	4102.92	2.6	0.32	2.70	90	Hardegsen	F

GAG-05	NM0053	4103.32	11.6	15.96	2.67	90	Hardegsen	F
GAG-05	NM0054	4103.50	11.1	2.52	2.66	85	Hardegsen	E
GAG-05	NM0055	4103.80	9.1	32.34	2.67	80	Hardegsen	D
GAG-05	NM0056	4104.13	11.1	38.32	2.66	75	Hardegsen	D
KDZ-02-S1	NM0001	3255.10	13.8	28.10	2.65	45	Hardegsen	A
KDZ-02-S1	NM0004	3256.00	13.5	25.40	2.66	45	Hardegsen	A
KDZ-02-S1	NM0005	3256.30	12.0	25.00	2.67	40	Hardegsen	A
KDZ-02-S1	NM0007	3256.90	17.5	210.50	2.65	45	Hardegsen	B
KDZ-02-S1	NM0008	3257.20	7.3		2.75	45	Hardegsen	D
KDZ-02-S1	NM0009	3257.50	6.5	6.50	2.74	50	Hardegsen	D
KDZ-02-S1	NM0010	3257.80	14.0	43.60	2.66	45	Hardegsen	D
KDZ-02-S1	NM0011	3258.10	12.8	31.10	2.65	40	Hardegsen	B
KDZ-02-S1	NM0012	3258.40	11.2	22.00	2.65	45	Hardegsen	D
KDZ-02-S1	NM0013	3258.70	11.5	23.60	2.65	45	Hardegsen	D
KDZ-02-S1	NM0014	3259.00	7.1	1.50	2.67	45	Hardegsen	D
KDZ-02-S1	NM0015	3259.30	7.4	2.50	2.67	45	Hardegsen	D
KDZ-02-S1	NM0016	3259.60	10.8	9.20	2.67	45	Hardegsen	D
KDZ-02-S1	NM0017	3259.90	9.7	6.20	2.66	45	Hardegsen	D
KDZ-02-S1	NM0018	3260.20	11.2	43.60	2.67	45	Hardegsen	D
KDZ-02-S1	NM0019	3260.50	15.2	155.60	2.66	40	Hardegsen	B
KDZ-02-S1	NM0020	3260.80	13.5	367.10	2.67	40	Hardegsen	B
KDZ-02-S1	NM0021	3261.10	17.1	**637.60**	2.66	40	Hardegsen	B
KDZ-02-S1	NM0022	3261.40	14.6	93.60	2.66	45	Hardegsen	B
KDZ-02-S1	NM0023	3261.70	13.1	103.70	2.81	45	Hardegsen	D
KDZ-02-S1	NM0024	3262.00	9.9	81.40	2.68	45	Hardegsen	D
KDZ-02-S1	NM0025	3262.30	15.6	233.90	2.66	45	Hardegsen	B
KDZ-02-S1	NM0026	3262.60	13.3	69.90	2.67	45	Hardegsen	B
KDZ-02-S1	NM0027	3262.90	13.2	30.90	2.66	45	Hardegsen	D
KDZ-02-S1	NM0028	3263.20	13.3	91.80	2.66	45	Hardegsen	D
KDZ-02-S1	NM0029	3263.50	10.1	22.20	2.66	40	Hardegsen	D
KDZ-02-S1	NM0030	3263.80	14.4	60.10	2.67	40	Hardegsen	B
KDZ-02-S1	NM0031	3264.10	14.0	215.50	2.65	30	Hardegsen	D

KDZ-02-S1	NM0032	3264.40	12.8	47.10	2.68	30	Hardegsen	D
KDZ-02-S1	NM0033	3264.70	13.8	260.40	2.66	30	Hardegsen	B
KDZ-02-S1	NM0034	3265.00	11.2	41.90	2.66	40	Hardegsen	D
KDZ-02-S1	NM0035	3265.30	14.2	32.90	2.66	45	Hardegsen	B
KDZ-02-S1	NM0036	3265.60	14.8	183.50	2.66	45	Hardegsen	B
KDZ-02-S1	NM0037	3265.90	15.9	**598.20**	2.67	45	Hardegsen	B
KDZ-02-S1	NM0038	3266.20	9.4	2.50	2.67	45	Hardegsen	D
KDZ-02-S1	NM0039	3266.50	12.5	6.80	2.66	45	Hardegsen	D
KDZ-02-S1	NM0040	3266.80	12.2	35.10	2.66	45	Hardegsen	D
KDZ-02-S1	NM0041	3267.10	11.1	6.20	2.66	45	Hardegsen	D
KDZ-02-S1	NM0042	3267.40	9.0	4.10	2.66	45	Hardegsen	D
KDZ-02-S1	NM0043	3267.70	13.1	122.10	2.66	45	Hardegsen	B
KDZ-02-S1	NM0044	3268.00	9.3	22.20	2.67	45	Hardegsen	D
KDZ-02-S1	NM0045	3268.30	9.0	1.80	2.66	45	Hardegsen	B
KDZ-02-S1	NM0046	3268.60	17.8	123.10	2.65	45	Hardegsen	B
KDZ-02-S1	NM0047	3268.90	8.1	18.20	2.67	45	Hardegsen	B
KDZ-02-S1	NM0048	3269.20	10.6	30.60	2.68	50	Hardegsen	D
KDZ-02-S1	NM0049	3269.50	7.3	8.80	2.68	55	Hardegsen	D
KDZ-02-S1	NM0050	3269.80	16.8	**1027.90**	2.67	40	Hardegsen	A
KDZ-02-S1	NM0051	3270.10	11.6	108.20	2.66	45	Hardegsen	B
KDZ-02-S1	NM0052	3270.40	12.2	8.00	2.66	50	Hardegsen	D
KDZ-02-S1	NM0053	3270.70	13.4	30.70	2.68	45	Hardegsen	D
KDZ-02-S1	NM0054	3271.00	13.8	25.50	2.66	45	Hardegsen	D
KDZ-02-S1	NM0055	3271.30	14.6	9.80	2.65	45	Hardegsen	D
KDZ-02-S1	NM0056	3271.60	15.2	52.80	2.65	45	Hardegsen	D
KDZ-02-S1	NM0057	3271.90	14.4	105.40	2.65	45	Hardegsen	B
KDZ-02-S1	NM0058	3272.20	12.4	19.60	2.66	45	Hardegsen	D
KDZ-02-S1	NM0059	3272.50	12.1	10.30	2.66	45	Hardegsen	D
KDZ-02-S1	NM0060	3272.80	12.7	31.00	2.66	45	Hardegsen	D
KDZ-02-S1	NM0061	3273.10	15.8	9.40	2.66	45	Hardegsen	D
KDZ-02-S1	NM0062	3273.40	13.6	16.80	2.66	45	Hardegsen	D
MSG-01	NM0001	3753.10	9.5	25.55	2.68	45	Hardegsen	D

MSG-01	NM0002	3753.40	6.4	0.09	2.67	45	Hardegsen	D
MSG-01	NM0003	3753.70	25.4	**9524.41**	2.64	40	Hardegsen	B
MSG-01	NM0004	3754.00	21.8	**8451.03**	2.64	40	Hardegsen	B
MSG-01	NM0005	3754.30	10.9	80.59	2.65	50	Hardegsen	D
MSG-01	NM0006	3754.60	11.8	260.75	2.65	50	Hardegsen	D
MSG-01	NM0007	3754.95	11	96.23	2.65	55	Hardegsen	D
MSG-01	NM0008	3755.25	12.6	136.92	2.65	60	Hardegsen	D
MSG-01	NM0009	3755.60	22.5	**4616.90**	2.64	35	Hardegsen	B
MSG-01	NM0010	3755.90	11.6	524.22	2.69	30	Hardegsen	B
MSG-01	NM0011	3756.20	18.6	**4717.79**	2.66	30	Hardegsen	B
MSG-01	NM0012	3756.50	15	**1951.89**	2.66	35	Hardegsen	B
MSG-01	NM0013	3756.80	15.8	**1017.73**	2.65	35	Hardegsen	B
MSG-01	NM0014	3757.10	15.9	71.22	2.65	40	Hardegsen	D
MSG-01	NM0015	3757.40	13.5	61.76	2.65	40	Hardegsen	D
MSG-01	NM0016	3757.70	22.5	**1112.31**	2.64	40	Hardegsen	B
MSG-01	NM0017	3758.00	16.3	456.95	2.64	40	Hardegsen	D
MSG-01	NM0018	3758.30	24.3	**4446.89**	2.63	30	Hardegsen	B
MSG-01	NM0019	3758.60	25.8	**7210.83**	2.64	30	Hardegsen	B
MSG-01	NM0020	3758.95	25.1	**14561.66**	2.64	30	Hardegsen	B
MSG-01	NM0021	3759.20	25.6	**13182.79**	2.64	30	Hardegsen	B
MSG-01	NM0022	3759.50	14.6	**2249.04**	2.65	30	Hardegsen	B
MSG-01	NM0023	3759.80	14.7	360.77	2.65	50	Hardegsen	D
MSG-01	NM0024	3760.10	15.4	777.80	2.64	60	Hardegsen	D
MSG-01	NM0025	3760.40	17.3	**1165.91**	2.65	50	Hardegsen	B
MSG-01	NM0026	3760.70	17	**931.82**	2.64	40	Hardegsen	B
MSG-01	NM0027	3761.00	16.4	**803.98**	2.65	35	Hardegsen	B
MSG-01	NM0028	3761.30	12.9	46.09	2.66	50	Hardegsen	D
MSG-01	NM0029	3761.60	18.4	171.31	2.64	50	Hardegsen	D
MSG-01	NM0030	3761.90	20.1	**1297.74**	2.65	40	Hardegsen	B
MSG-01	NM0031	3762.20	12.8	562.17	2.66	45	Hardegsen	D
MSG-01	NM0032	3762.50	11.5	17.38	2.67	50	Hardegsen	D

MSG-01	NM0033	3762.80	15.9	135.03	2.65	50	Hardegsen	D
MSG-01	NM0034	3763.10	14.8	134.87	2.65	55	Hardegsen	D
MSG-01	NM0035	3763.40	21.8		2.65	50	Hardegsen	B
MSG-01	NM0036	3763.70	23.5	**6268.69**	2.65	45	Hardegsen	B
MSG-01	NM0037	3764.00	24	**18680.39**	2.64	40	Hardegsen	B
MSG-01	NM0038	3764.30	12.1	1.54	2.65	60	Hardegsen	D
MSG-01	NM0039	3764.60	15.5	171.69	2.65	55	Hardegsen	D
MSG-01	NM0040	3764.90	16.9	**932.73**	2.65	50	Hardegsen	B
MSG-01	NM0041	3765.20	16.9	**1372.34**	2.64	45	Hardegsen	B
MSG-01	NM0042	3765.50	18.4	**2882.22**	2.65	40	Hardegsen	B
MSG-01	NM0043	3765.80	16.3	49.20	2.65	45	Hardegsen	D
MSG-01	NM0044	3766.15	16.8	138.25	2.65	45	Hardegsen	D
MSG-01	NM0045	3766.55	19.6	**4128.80**	2.65	40	Hardegsen	B
MSG-01	NM0046	3766.85	13.4	56.26	2.66	45	Hardegsen	D
MSG-01	NM0047	3767.20	20.1	555.76	2.64	40	Hardegsen	B
MSG-01	NM0048	3767.50	17.1	368.43	2.64	40	Hardegsen	B
MSG-01	NM0049	3767.80	15.6	440.37	2.65	45	Hardegsen	B
MSG-01	NM0050	3768.15	16.6	472.94	2.65	45	Hardegsen	B
MSG-01	NM0051	3768.45	12.8	148.32	2.65	50	Hardegsen	D
MSG-01	NM0052	3768.75	14.8	20.00	2.65	55	Hardegsen	D
MSG-01	NM0053	3769.10	15.1	50.68	2.66	55	Hardegsen	D
MSG-01	NM0054	3769.40	17.5	519.93	2.65	45	Hardegsen	B
MSG-01	NM0055	3769.70	18.4	691.85	2.65	45	Hardegsen	B
MSG-01	NM0056	3770.00	15.7	128.45	2.66	50	Hardegsen	D
MSG-01	NM0057	3770.30	15.8	90.21	2.66	55	Hardegsen	D
MSG-01	NM0058	3770.60	17.1	122.04	2.65	55	Hardegsen	D
MSG-01	NM0059	3770.90	18.4	260.02	2.65	50	Hardegsen	D
MSG-01	NM0060	3771.05	18.4	670.51	2.65	45	Hardegsen	B
MSG-01	NM0061	3771.70	16.7	154.59	2.65	50	Hardegsen	D
MSG-01	NM0062	3772.00	18.7	240.73	2.65	55	Hardegsen	D
MSG-01	NM0063	3772.30	17	103.54	2.66	60	Hardegsen	D
MSG-01	NM0064	3772.60	16.6	92.35	2.65	60	Hardegsen	D

MSG-01	NM0065	3772.90	18.2	240.58	2.66	60	Hardegsen	D
MSG-01	NM0066	3773.20	15.5	52.05	2.67	65	Hardegsen	D
MSG-01	NM0067	3773.50	16.8	44.98	2.66	65	Hardegsen	D
MSG-01	NM0068	3773.80	18.2	221.38	2.65	60	Hardegsen	B
MSG-01	NM0069	3774.10	15.7	99.14	2.66	65	Hardegsen	D
MSG-01	NM0070	3774.40	15.3	17.71	2.66	70	Hardegsen	D
MSG-01	NM0071	3774.70	17.3	119.62	2.65	70	Hardegsen	D
MSG-01	NM0072	3775.00	16.4	113.79	2.65	70	Hardegsen	D
MSG-01	NM0073	3775.30	17.8	66.22	2.64	70	Hardegsen	D
MSG-01	NM0074	3775.65	15.7	51.07	2.66	75	Hardegsen	D
MSG-01	NM0075	3775.95	18.5	99.63	2.65	75	Hardegsen	D
MSG-01	NM0076	3776.20	17.2	208.42	2.65	80	Hardegsen	D
MSG-01	NM0077	3776.50	15.9	38.45	2.65	80	Hardegsen	D
MSG-01	NM0078	3776.80	15.6	30.87	2.66	85	Hardegsen	D
MSG-01	NM0079	3777.10	16	40.99	2.66	85	Hardegsen	D
MSG-01	NM0080	3777.40	10.5	17.23	2.68	90	Hardegsen	G
MSG-01	NM0081	3777.70	15.6	148.83	2.66	90	Hardegsen	D
MSG-01	NM0082	3778.00	19.3	236.78	2.65	90	Hardegsen	D
MSG-01	NM0083	3778.30	15.7	6.38	2.65	100	Hardegsen	G
MSG-01	NM0084	3778.60	19.5	137.44	2.64	90	Hardegsen	D
MSG-01	NM0085	3778.85	14.5	16.30	2.66	90	Hardegsen	D
MSG-01	NM0086	3779.15	17.5	49.19	2.65	75	Hardegsen	B
MSG-01	NM0087	3779.45	16.2	489.94	2.65	95	Hardegsen	D
MSG-01	NM0088	3779.75	18.1	153.36	2.65	115	Hardegsen	G
MSG-01	NM0089	3780.05	7.4	0.22	2.69	120	Hardegsen	G
MSG-01	NM0090	3780.35	10.5	1.43	2.66	50	Hardegsen	D
MSG-01	NM0091	3780.70	9.1	15.43	2.65	45	Hardegsen	D
MSG-01	NM0092	3780.95	13.4	121.91	2.65	50	Hardegsen	D
MSG-01	NM0093	3781.25	10.2	12.01	2.66	55	Hardegsen	D
MSG-01	NM0094	3781.55	12.7	82.68	2.65	50	Hardegsen	D
MSG-01	NM0095	3781.85	11	10.30	2.65	60	Hardegsen	D
MSG-01	NM0096	3782.15	14.1		2.65	55	Hardegsen	D

MSG-01	NM0097	3782.45	12.7	40.25		2.65	60	Hardegsen	D
MSG-01	NM0098	3782.80	14.8	112.83		2.64	55	Hardegsen	D
MSG-01	NM0099	3783.10	13.4	69.26		2.65	55	Hardegsen	D
MSG-01	NM0100	3783.40	11.7	9.22		2.65	55	Hardegsen	D
MSG-01	NM0101	3783.75	15.2	163.50		2.64	50	Hardegsen	D
MSG-01	NM0102	3784.05	9.4			2.65	40	Hardegsen	B
MSG-01	NM0103	3784.30	12.2	239.42		2.66	45	Hardegsen	B
MSG-01	NM0104	3784.60	11	27.38		2.65	55	Hardegsen	D
MSG-01	NM0105	3784.90	14.8	109.98		2.65	55	Hardegsen	D
MSG-01	NM0106	3785.20	18.7	177.00		2.65	45	Hardegsen	B
MSG-01	NM0107	3785.50	9.7	1.27		2.66	55	Hardegsen	D
MSG-01	NM0108	3785.75	12.5	74.26		2.65	50	Hardegsen	D
MSG-01	NM0109	3786.05	13.3	58.49		2.65	50	Hardegsen	D
MSG-01	NM0110	3786.35	12.4	102.82		2.65	50	Hardegsen	D
MSG-01	NM0111	3786.65	12.7	26.28		2.65	50	Hardegsen	D
MSG-01	NM0112	3786.95	12.3	197.37		2.66	45	Hardegsen	B
MSG-01	NM0113	3787.25	9.7	25.98		2.66	50	Hardegsen	D
MSG-01	NM0114	3787.55	10.9	4.08		2.65	50	Hardegsen	D
MSG-01	NM0115	3787.85	10.8	19.15		2.66	45	Hardegsen	D
MSG-01	NM0116	3788.15	14.5	167.93		2.65	45	Hardegsen	D
MSG-01	NM0117	3788.40	11.4	7.10		2.65	45	Hardegsen	D
MSG-01	NM0118	3788.70	16.2	202.05		2.65	45	Hardegsen	B
P14-A-01	1	2485.00	18.2	**860**	228	2.65		Hardegsen	B
P14-A-01	2	2485.25	18.9	**1092**	0	2.64		Hardegsen	B
P14-A-01	3	2485.50	18.2	397	31	2.64		Hardegsen	E
P14-A-01	4	2485.75	20	730	0	2.64		Hardegsen	B
P14-A-01	5	2486.00	15.8	188	30	2.64		Hardegsen	E
P14-A-01	6	2486.25	12.5	198	0	2.66		Hardegsen	E
P14-A-01	7	2486.50	15.3	90	3.9	2.64		Hardegsen	E
P14-A-01	8	2486.75	21.3	**1083**	0	2.64		Hardegsen	B
P14-A-01	9	2487.00	16.2	112	74	2.64		Hardegsen	E
P14-A-01	10	2487.25	14	53	0	2.65		Hardegsen	E

P14-A-01	11	2487.50	12.8	58	4.7	2.65	Hardegsen	E
P14-A-01	12	2487.75	13.1	79	0	2.64	Hardegsen	E
P14-A-01	13	2488.00	15.7	76	6.9	2.64	Hardegsen	E
P14-A-01	14	2488.25	17.2	697	0	2.65	Hardegsen	C
P14-A-01	15	2488.50	15.7	328	45	2.65	Hardegsen	C
P14-A-01	16	2488.75	15.5	337	0	2.65	Hardegsen	B
P14-A-01	17	2489.00	14.4	320	110	2.66	Hardegsen	B
P14-A-01	18	2489.25	17.6	**1333**	0	2.65	Hardegsen	B
P14-A-01	19	2489.50	15.2	405	148	2.65	Hardegsen	B
P14-A-01	20	2489.75	14.7	336	0	2.65	Hardegsen	D
P14-A-01	21	2490.00	16.5	638	348	2.66	Hardegsen	C
P14-A-01	22	2490.25	14	306	0	2.65	Hardegsen	C
P14-A-01	23	2490.50	14.6	387	113	2.65	Hardegsen	C
P14-A-01	24	2490.75	15.7	603	0	2.65	Hardegsen	C
P14-A-01	25	2491.00	13.7	512	260	2.67	Hardegsen	C
P14-A-01	26	2491.25	12.8	330	0	2.68	Hardegsen	C
P14-A-01	27	2491.50	15.4	608	424	2.65	Hardegsen	C
P14-A-01	28	2491.75	16.6	731	0	2.65	Hardegsen	C
P14-A-01	29	2492.00	16.6	680	419	2.65	Hardegsen	C
P14-A-01	30	2492.25	17.1	155	0	2.65	Hardegsen	E
P14-A-01	31	2492.50	16.2	124	26	2.65	Hardegsen	E
P14-A-01	32	2492.75	16.2	407	0	2.65	Hardegsen	D
P14-A-01	33	2493.00	16.9	582	228	2.65	Hardegsen	B
P14-A-01	34	2493.25	16.3	**852**	0	2.66	Hardegsen	B
P14-A-01	35	2493.50	12.9	62	2.8	2.64	Hardegsen	E
P14-A-01	36	2493.75	12.4	45	0	2.64	Hardegsen	E
P14-A-01	37	2494.00	14.9	261	1.8	2.64	Hardegsen	D
P14-A-01	38	2494.25	16.9	194	0	2.64	Hardegsen	D
P14-A-01	39	2494.50	11	31	0.6	2.66	Hardegsen	E
P14-A-01	40	2494.75	12.4	139	0	2.67	Hardegsen	E
P14-A-01	41	2495.00	16.8	152	10	2.64	Hardegsen	D
P14-A-01	42	2495.25	15.6	198	0	2.65	Hardegsen	D

P14-A-01	43	2495.50	15.7	135	2.1	2.64	Hardegsen	E
P14-A-01	44	2495.75	13.2	22	0	2.66	Hardegsen	E
P14-A-01	45	2496.00	14.1	82	1	2.65	Hardegsen	E
P14-A-01	46	2496.25	15.7	79	0	2.65	Hardegsen	E
P14-A-01	47	2496.50	15.6	93	4.4	2.65	Hardegsen	E
P14-A-01	48	2496.75	17.9	349	0	2.65	Hardegsen	D
P14-A-01	49	2497.00	17	148	8.8	2.65	Hardegsen	D
P14-A-01	50	2497.25	13.2	120	0	2.66	Hardegsen	E
P14-A-01	51	2497.50	14.5	25	7.3	2.65	Hardegsen	F
P14-A-01	52	2497.75	4.9	0.69	0	2.66	Hardegsen	F
P14-A-01	53	2498.00	5.4	0.15	0.02	2.69	Hardegsen	G
P14-A-01	54	2498.25	9.3	5.4	0	2.66	Hardegsen	G
P14-A-01	55	2498.50	7.5	0.18	0.22	2.69	Hardegsen	G
P14-A-01	56	2498.75	14.4	217	0	2.67	Hardegsen	G
P14-A-01	57	2499.00	14.9	237	98	2.66	Hardegsen	C
P14-A-01	58	2499.25	13	90	0	2.66	Hardegsen	F
P14-A-01	59	2499.50	13.2	134	38	2.66	Hardegsen	C
P14-A-01	60	2499.75	15.1	355	0	2.66	Hardegsen	C
P14-A-01	61	2500.00	13.4	210	33	2.66	Hardegsen	E
P14-A-01	62	2500.25	8.3	1.8	0	2.66	Hardegsen	F
P14-A-01	63	2500.50	16.2	331	236	2.65	Hardegsen	E
P14-A-01	64	2500.75	16.5	175	0	2.64	Hardegsen	E
P14-A-01	65	2501.00	13.6	26	16	2.65	Hardegsen	F
P14-A-01	66	2501.25	12.7	40	0	2.65	Hardegsen	F
P14-A-01	67	2501.50	15.5	244	85	2.65	Hardegsen	E
P14-A-01	68	2501.75	15	205	0	2.65	Hardegsen	E
P14-A-01	69	2502.00	15.1	295	118	2.66	Hardegsen	E
P14-A-01	70	2502.25	13.6	243	0	2.66	Hardegsen	E
P14-A-01	71	2502.50	13.7	367	114	2.66	Hardegsen	E
P14-A-01	72	2502.75	7.3	8.4	0	2.7	Hardegsen	F
P14-A-01	73	2503.00	3.5	0.25	0.26	2.65	Hardegsen	F
P14-A-01	74	2503.25	7	1	0	2.66	Hardegsen	F

P14-A-01	75	2503.50	15.5	728	185	2.68		Hardegsen	C
P14-A-01	76	2503.75	17.4	**839**	0	2.66		Hardegsen	C
P14-A-01	77	2504.00	16.3	614	358	2.66		Hardegsen	C
P14-A-01	78	2504.25	15.2	560	0	2.66		Hardegsen	C
P14-A-01	79	2504.50	15.5	673	200	2.65		Hardegsen	C
P14-A-01	80	2504.75	14.7	333	0	2.66		Hardegsen	E
P14-A-01	81	2505.00	14.3	356	86	2.66		Hardegsen	E
P14-A-01	82	2505.25	14.4	399	0	2.66		Hardegsen	E
P14-A-01	83	2505.50	13.7	325	116	2.66		Hardegsen	E
P14-A-01	84	2505.75	10.5	78	0	2.69		Hardegsen	F
P14-A-01	85	2506.00	13.1	329	33	2.66		Hardegsen	E
P14-A-01	86	2506.25	5.5	0.14	0	2.69		Hardegsen	F
P14-A-01	87	2506.50	12.4	199	47	2.66		Hardegsen	E
P14-A-01	88	2506.75	15.2	338	0	2.67		Hardegsen	E
P14-A-01	89	2507.00	15	191	15	2.67		Hardegsen	E
P14-A-01	90	2507.25	13.8	137	0	2.67		Hardegsen	E
P14-A-01	91	2507.50	12.2	161	25	2.67		Hardegsen	E
P14-A-01	92	2507.75	11.6	138	0	2.68		Hardegsen	E
P14-A-01	93	2508.00	12.5	84	26	2.67		Hardegsen	E
P14-A-01	94	2508.25	11.3	88	0	2.68		Hardegsen	E
P14-A-01	95	2508.50	11.5	61	5.8	2.68		Hardegsen	E
P14-A-01	96	2508.75	14.1	111	0	2.65		Hardegsen	E
P14-A-01	97	2509.00	12.3	133	44	2.67		Hardegsen	E
PRW-01	CL0173	3007.18	21.7	**1920.00**		2.74	45	Hardegsen	B
PRW-01	CL0174C	3007.46	16.7	191.00		2.79	45	Hardegsen	B
PRW-01	CL0072	3007.50	20.3	141.00		2.69	45	Hardegsen	D
PRW-01	CL0175C	3007.76	15.7	446.00		2.67	45	Hardegsen	B
PRW-01	CL0176	3008.08	14.3	27.00		2.69	50	Hardegsen	D
PRW-01	CL0177	3008.37	14.9	367.00		2.68	50	Hardegsen	D
PRW-01	CL0178C	3008.65	16.9	267.00		2.68	50	Hardegsen	B
PRW-01	CL0179	3008.97	16.1	238.00		2.67	55	Hardegsen	B
PRW-01	CL0180	3009.25	16.1	340.00		2.66	55	Hardegsen	B

PRW-01	CL0181	3009.55	10.2	37.00		2.68	60	Hardegsen	D
PRW-01	CL0181V	3009.56			1.30		60	Hardegsen	B
PRW-01	CL0182	3009.86	18.5	549.00		2.66	60	Hardegsen	B
PRW-01	CL0183V	3010.03			**915.00**		60	Hardegsen	B
PRW-01	CL0183	3010.16	21.8	**1680.00**		2.66	60	Hardegsen	B
PRW-01	CL0184V	3010.26			4.60		60	Hardegsen	B
PRW-01	CL0184	3010.45	18.8	322.00		2.67	65	Hardegsen	B
PRW-01	CL0185	3010.68	21.5	**1100.00**		2.65	55	Hardegsen	B
PRW-01	CL0186	3011.00	15.7	65.00		2.67	55	Hardegsen	D
PRW-01	CL0187	3011.30	19.8	308.00		2.68	55	Hardegsen	B
PRW-01	CL0188	3011.59	19.5	275.00		2.67	55	Hardegsen	D
PRW-01	CL0189	3011.86	17.6	110.00		2.67	55	Hardegsen	D
PRW-01	CL0190V	3012.01			4.00		55	Hardegsen	B
PRW-01	CL0190	3012.18	18.9	141.00		2.65	55	Hardegsen	B
PRW-01	CL0191	3012.47	15.7	124.00		2.68	55	Hardegsen	D
PRW-01	CL0192	3012.70	18.0	352.00		2.66	55	Hardegsen	B
PRW-01	CL0193	3013.04	16.2	158.00		2.66	55	Hardegsen	D
PRW-01	CL0194	3013.32	16.7	446.00		2.66	55	Hardegsen	B
PRW-01	CL0195V	3013.63	18.0		5.90	2.66	55	Hardegsen	B
PRW-01	CL0196B	3013.93	14.4	273.00		2.66	55	Hardegsen	D
PRW-01	CL0197V	3014.16			73.00		55	Hardegsen	B
PRW-01	CL0197	3014.21	20.4	851.00		2.66	50	Hardegsen	B
PRW-01	CL0198	3014.50	15.3	272.00		2.66	55	Hardegsen	D
PRW-01	CL0199	3014.78	17.2	**888.00**		2.67	55	Hardegsen	B
PRW-01	CL0200	3015.08	16.9	300.00		2.66	55	Hardegsen	B
PRW-01	CL0200V	3015.11			14.00		55	Hardegsen	B
PRW-01	CL0201	3015.40	21.8	**1300.00**		2.65	50	Hardegsen	B
PRW-01	CL0202	3015.72	11.9	100.00		2.68	55	Hardegsen	D
PRW-01	CL0074	3015.97	15.9	392.00		2.67	55	Hardegsen	D
PRW-01	CL0203	3016.00	13.2	37.00		2.68	55	Hardegsen	D
PRW-01	CL0204V	3016.26			3.00		55	Hardegsen	D
PRW-01	CL0204	3016.31	17.6	162.00		2.66	55	Hardegsen	B

PRW-01	CL0205	3016.62	17.0	477.00		2.66	55	Hardegsen	B
PRW-01	CL0206	3016.93	21.0	**1010.00**		2.67	50	Hardegsen	B
PRW-01	CL0207B	3017.25	17.9	119.00		2.66	55	Hardegsen	D
PRW-01	CL0208V	3017.51			21.00		55	Hardegsen	D
PRW-01	CL0208	3017.52	17.9	324.00		2.66	55	Hardegsen	B
PRW-01	CL0209B	3017.81	21.1	**796.00**		2.66	55	Hardegsen	B
PRW-01	CL0210C	3018.16	17.9	596.00		2.66	55	Hardegsen	B
PRW-01	CL0211	3018.43	19.3	401.00		2.65	55	Hardegsen	B
PRW-01	CL0212B	3018.72	19.2	236.00		2.65	55	Hardegsen	B
PRW-01	CL0213	3019.03	21.0	123.00		2.67	55	Hardegsen	D
PRW-01	CL0214	3019.32	22.9	602.00		2.67	50	Hardegsen	B
PRW-01	CL0214V	3019.36			6.60		55	Hardegsen	B
PRW-01	CL0215	3019.60	20.3	258.00		2.66	55	Hardegsen	B
PRW-01	CL0216	3019.89	17.5	416.00		2.66	55	Hardegsen	B
PRW-01	CL0075	3019.95	20.4	**1660.00**		2.68	55	Hardegsen	B
PRW-01	CL0217B	3020.11	18.4	**939.00**		2.65	55	Hardegsen	B
PRW-01	CL0218V	3020.26			20.00		55	Hardegsen	B
PRW-01	CL0218	3020.40	20.6	284.00		2.66	55	Hardegsen	B
PRW-01	CL0219	3020.70	20.6	581.00		2.66	55	Hardegsen	B
PRW-01	CL0220	3021.05	15.5	179.00		2.66	55	Hardegsen	D
PRW-01	CL0221	3021.37	16.9	43.00		2.65	55	Hardegsen	D
PRW-01	CL0222V	3021.46			7.60		55	Hardegsen	D
PRW-01	CL0222	3021.65	17.2	199.00		2.66	55	Hardegsen	B
PRW-01	CL0223	3021.93	16.9	56.00		2.66	55	Hardegsen	B
PRW-01	CL0224	3022.23	19.2	372.00		2.66	55	Hardegsen	B
PRW-01	CL0225	3022.53	16.0	62.00		2.66	55	Hardegsen	D
PRW-01	CL0226V	3022.80	22.6		201.00	2.66	55	Hardegsen	B
PRW-01	CL0227	3023.12	18.8	169.00		2.66	55	Hardegsen	D
PRW-01	CL0228	3023.43	15.1	18.00		2.66	55	Hardegsen	D
PRW-01	CL0229	3023.78	16.1	351.00		2.67	55	Hardegsen	B
PRW-01	CL0230	3024.08	14.7	551.00		2.67	55	Hardegsen	B
PRW-01	CL0231B	3024.39	16.8	413.00		2.66	55	Hardegsen	B

PRW-01	CL0232	3024.68	18.9	165.00		2.67	55	Hardegsen	B
PRW-01	CL0233	3024.99	17.9	235.00		2.66	55	Hardegsen	B
PRW-01	CL0234B	3025.28	19.7	344.00		2.66	55	Hardegsen	B
PRW-01	CL0235	3025.58	17.3	81.00		2.67	55	Hardegsen	D
PRW-01	CL0236V	3025.76			11.00		55	Hardegsen	D
PRW-01	CL0236	3025.86	18.7	280.00		2.65	55	Hardegsen	D
PRW-01	CL0237	3026.15	18.5	495.00		2.66	55	Hardegsen	B
PRW-01	CL0237V	3026.16			270.00		55	Hardegsen	B
PRW-01	CL0238	3026.49	18.1	549.00		2.66	55	Hardegsen	B
PRW-01	CL0239	3026.76	22.0	**830.00**		2.65	55	Hardegsen	B
PRW-01	CL0076	3027.05	19.8	408.00		2.68	55	Hardegsen	B
PRW-01	CL0240	3027.10	17.1	**750.00**		2.67	55	Hardegsen	B
PRW-01	CL0241	3027.35	18.9	271.00		2.66	55	Hardegsen	B
PRW-01	CL0242V	3027.64	20.0		375.00	2.65	55	Hardegsen	B
PRW-01	CL0243	3027.95	17.3	**879.00**		2.67	55	Hardegsen	B
PRW-01	CL0244	3028.23	18.8	193.00		2.66	55	Hardegsen	B
PRW-01	CL0245	3028.52	19.5	206.00		2.66	60	Hardegsen	B
PRW-01	CL0246	3028.81	17.7	102.00		2.65	60	Hardegsen	D
PRW-01	CL0247	3029.10	16.6	72.00		2.66	60	Hardegsen	D
PRW-01	CL0248V	3029.39	17.0		2.10	2.65	60	Hardegsen	D
PRW-01	CL0249	3029.69	16.9	28.00		2.66	60	Hardegsen	D
PRW-01	CL0250	3029.97	19.4	231.00		2.66	60	Hardegsen	B
PRW-01	CL0251	3030.33	18.0	108.00		2.67	60	Hardegsen	D
PRW-01	CL0252	3030.61	16.7	111.00		2.66	60	Hardegsen	D
PRW-01	CL0253V	3030.96			**895.00**		60	Hardegsen	B
PRW-01	CL0253B	3030.97	22.3	**4960.00**		2.66	60	Hardegsen	B
PRW-01	CL0254C	3031.28	16.2	163.00		2.65	60	Hardegsen	D
PRW-01	CL0255B	3031.54	16.4	28.00		2.66	60	Hardegsen	D
PRW-01	CL0078	3031.77	18.6	58.00		2.68	60	Hardegsen	D
PRW-01	CL0256	3031.85	20.9	**1990.00**		2.66	60	Hardegsen	B
PRW-01	CL0257	3032.07	19.2	412.00		2.66	60	Hardegsen	B

PRW-01	CL0258V	3032.38	19.3		57.00	2.65	60	Hardegsen	B
PRW-01	CL0259	3032.66	18.0	25.00		2.68	60	Hardegsen	D
PRW-01	CL0260	3032.92	21.5	685.00		2.65	60	Hardegsen	B
PRW-01	CL0261	3033.20	17.9	68.00		2.67	60	Hardegsen	D
PRW-01	CL0262	3033.52	17.6	155.00		2.66	60	Hardegsen	D
PRW-01	CL0263	3033.85	17.7	192.00		2.67	60	Hardegsen	D
PRW-01	CL0264	3034.14	16.9	23.00		2.67	60	Hardegsen	D
PRW-01	CL0265	3034.46	20.4	312.00		2.66	60	Hardegsen	B
PRW-01	CL0266	3034.71	18.6	216.00		2.66	60	Hardegsen	B
PRW-01	CL0267	3035.02	19.2	94.00		2.66	60	Hardegsen	D
PRW-01	CL0268V	3035.31			6.50		60	Hardegsen	D
PRW-01	CL0268	3035.33	20.6	724.00		2.66	60	Hardegsen	B
PRW-01	CL0269C	3035.62	19.2	**2408.00**		2.65	60	Hardegsen	B
PRW-01	CL0270V	3035.84			18.00		60	Hardegsen	B
PRW-01	CL0270	3035.93	19.2	402.00		2.66	60	Hardegsen	B
PRW-01	CL0271V	3036.01			82.00		60	Hardegsen	B
PRW-01	CL0271	3036.20	20.1	**939.00**		2.66	60	Hardegsen	B
PRW-01	CL0272	3036.52	18.2	402.00		2.67	60	Hardegsen	D
PRW-01	CL0273	3036.80	19.4	119.00		2.68	60	Hardegsen	D
PRW-01	CL0274	3037.11	16.9	20.00		2.67	60	Hardegsen	D
PRW-01	CL0275V	3037.26			1.00		60	Hardegsen	D
PRW-01	CL0275	3037.42	15.9	44.00		2.66	60	Hardegsen	D
PRW-01	CL0276	3037.69	17.3	46.00		2.66	60	Hardegsen	D
PRW-01	CL0277	3038.00	20.3	210.00		2.66	60	Hardegsen	B
PRW-01	CL0278	3038.36	17.4	9.10		2.66	60	Hardegsen	D
PRW-01	CL0279V	3038.61			10.00		60	Hardegsen	D
PRW-01	CL0279	3038.67	20.7	105.00		2.65	60	Hardegsen	B
PRW-01	CL0280	3038.94	19.1	711.00		2.68	60	Hardegsen	B
PRW-01	CL0281	3039.23	19.1	56.00		2.67	60	Hardegsen	D
PRW-01	CL0282	3039.53	20.9	243.00		2.65	60	Hardegsen	B
PRW-01	CL0283V	3039.81			3.90		60	Hardegsen	B
PRW-01	CL0283	3039.82	18.2	77.00		2.66	60	Hardegsen	D

PRW-01	CL0284	3040.14	21.8	204.00		2.66	60	Hardegsen	B
PRW-01	CL0285	3040.45	19.3	236.00		2.66	60	Hardegsen	B
PRW-01	CL0286	3040.79	21.2	**870.00**		2.66	60	Hardegsen	B
PRW-01	CL0287V	3040.96			12.00		60	Hardegsen	B
PRW-01	CL0287	3041.08	21.3	349.00		2.65	60	Hardegsen	B
PRW-01	CL0288	3041.40	19.9	313.00		2.66	60	Hardegsen	D
PRW-01	CL0289	3041.70	19.3	120.00		2.67	60	Hardegsen	D
PRW-01	CL0290	3042.04	19.7	209.00		2.66	60	Hardegsen	D
PRW-01	CL0291	3042.35	21.4	502.00		2.66	60	Hardegsen	B
PRW-01	CL0292V	3042.60	19.1		2.30	2.67	60	Hardegsen	B
PRW-01	CL0293	3042.91	20.7	593.00		2.66	60	Hardegsen	B
PRW-01	CL0294	3043.17	18.0	137.00		2.66	60	Hardegsen	D
PRW-01	CL0295	3043.46	21.0	**693.00**		2.66	60	Hardegsen	B
PRW-01	CL0296	3043.77	19.4	259.00		2.66	60	Hardegsen	B
PRW-01	CL0297V	3043.91			2.50		60	Hardegsen	B
PRW-01	CL0297	3044.06	21.0	**932.00**		2.67	60	Hardegsen	B
PRW-01	CL0298	3044.31	21.3	**823.00**		2.65	60	Hardegsen	B
PRW-01	CL0299	3044.62	20.1	547.00		2.67	60	Hardegsen	B
PRW-01	CL0300	3044.91	18.5	68.00		2.67	60	Hardegsen	D
PRW-01	CL0301V	3045.06			0.95		60	Hardegsen	D
PRW-01	CL0301C	3045.20	18.7	477.00		2.66	60	Hardegsen	B
PRW-01	CL0302	3045.51	18.8	77.00		2.66	60	Hardegsen	D
PRW-01	CL0303V	3045.82	18.8		1.80	2.65	60	Hardegsen	D
PRW-01	CL0304	3046.14	15.8	23.00		2.66	60	Hardegsen	D
PRW-01	CL0304V	3046.21			0.47		60	Hardegsen	D
PRW-01	CL0305	3046.47	20.4	146.00		2.67	60	Hardegsen	D
PRW-01	CL0306	3046.76	16.4	9.00		2.67	60	Hardegsen	D
PRW-01	CL0307	3047.09	23.1	453.00		2.66	60	Hardegsen	B
PRW-01	CL0308	3047.40	22.1	**771.00**		2.67	60	Hardegsen	B
PRW-01	CL0309	3047.73	19.6	282.00		2.67	60	Hardegsen	B
PRW-01	CL0310V	3047.89			33.00		60	Hardegsen	B
PRW-01	CL0310	3048.03	22.0	497.00		2.66	55	Hardegsen	B

PRW-01	CL0311	3048.35	21.2	572.00		2.67	55	Hardegsen	B
PRW-01	CL0312	3048.61	18.3	68.00		2.66	60	Hardegsen	D
PRW-01	CL0313	3048.92	23.7	671.00		2.66	55	Hardegsen	B
PRW-01	CL0314	3049.22	19.5	78.00		2.66	60	Hardegsen	D
PRW-01	CL0315	3049.50	18.5	98.00		2.67	60	Hardegsen	D
PRW-01	CL0316	3049.81	20.3	106.00		2.67	60	Hardegsen	D
PRW-01	CL0317	3050.13	8.7	0.14		2.67	60	Hardegsen	D
PRW-01	CL0318	3050.39	19.4	41.00		2.67	55	Hardegsen	D
PRW-01	CL0319	3050.70	9.8	1.10		2.71	60	Hardegsen	D
PRW-01	CL0320	3051.05	20.6	127.00		2.66	60	Hardegsen	D
PRW-01	CL0321	3051.33	25.5	623.00		2.65	55	Hardegsen	B
PRW-01	CL0322	3051.63	25.4	664.00		2.65	55	Hardegsen	B
PRW-01	CL0323	3051.91	18.7	17.00		2.66	60	Hardegsen	D
PRW-01	CL0324V	3052.19	11.5		0.21	2.68	60	Hardegsen	D
PRW-01	CL0325	3052.50	20.8	46.00		2.67	60	Hardegsen	B
PRW-01	CL0326	3052.80	15.6	1.00		2.68	60	Hardegsen	D
PRW-01	CL0327B	3053.06	15.0	10.00		2.70	60	Hardegsen	D
PRW-01	CL0328	3053.36	16.3	1.40		2.69	60	Hardegsen	D
PRW-01	CL0329	3053.67	11.9	0.34		2.74	60	Hardegsen	D
PRW-01	CL0330	3053.95	5.8	0.07		2.76	65	Hardegsen	D
PRW-01	CL0331	3054.29	13.3	12.00		2.70	65	Hardegsen	D
PRW-01	CL0332	3054.58	14.6	10.00		2.71	70	Hardegsen	D
PRW-01	CL0333B	3054.85	8.3	0.34		2.73	75	Hardegsen	D
PRW-01	CL0334	3055.17	11.1	3.10		2.72	70	Hardegsen	D
PRW-01	CL0335	3055.47	13.7	4.00		2.69	70	Hardegsen	D
PRW-01	CL0336	3055.78	13.4	1.10		2.68	75	Hardegsen	D
PRW-01	CL0337	3056.05	8.2	0.49		2.73	75	Hardegsen	D
PRW-01	CL0338	3056.37	10.3	1.20		2.69	70	Hardegsen	D
PRW-01	CL0339	3056.67	13.4	7.10		2.69	70	Hardegsen	D
PRW-01	CL0340	3056.95	14.0	17.00		2.69	70	Hardegsen	D
PRW-01	CL0341	3057.18	8.8	0.43		2.71	75	Hardegsen	D
PRW-01	CL0342	3057.50	16.7	10.00		2.68	65	Hardegsen	D

PRW-01	CL0343	3057.81	9.6	0.61	2.74	70	Hardegsen	D
PRW-01	CL0344	3058.07	8.6	0.52	2.79	70	Hardegsen	D
PRW-01	CL0345	3058.39	15.7	20.00	2.70	75	Hardegsen	D
PRW-01	CL0346	3058.63	18.6	25.00	2.71	70	Hardegsen	D
PRW-01	CL0347B	3058.94	15.6	6.00	2.68	70	Hardegsen	D
PRW-01	CL0349	3059.06	22.0	26.00	2.65	70	Hardegsen	D
PRW-01	CL0348	3059.24	18.4	8.10	2.67	75	Hardegsen	D
PRW-01	CL0350	3059.34	19.7	37.00	2.66	70	Hardegsen	D
PRW-01	CL0351	3059.67	11.2	0.74	2.68	75	Hardegsen	D
PRW-01	CL0352	3059.99	22.2	127.00	2.65	70	Hardegsen	B
PRW-01	CL0353	3060.32	18.4	52.00	2.67	75	Hardegsen	D
PRW-01	CL0354	3060.58	16.8	102.00	2.66	75	Hardegsen	B
PRW-01	CL0355	3060.85	18.3	105.00	2.68	75	Hardegsen	B
PRW-01	CL0356	3061.15	16.6	6.50	2.67	90	Hardegsen	G
PRW-01	CL0357	3061.44	20.1	129.00	2.65	75	Hardegsen	B
PRW-01	CL0358B	3061.73	17.0	71.00	2.67	75	Hardegsen	D
PRW-01	CL0359	3062.04	16.0	12.00	2.67	75	Hardegsen	D
PRW-01	CL0360	3062.32	14.8	8.80	2.66	80	Hardegsen	G
PRW-01	CL0361B	3062.64	16.5	50.00	2.66	80	Hardegsen	G
PRW-01	CL0362	3062.93	16.9	13.00	2.66	75	Hardegsen	D
PRW-01	CL0363	3063.22	16.3	5.30	2.66	75	Hardegsen	D
PRW-01	CL0364	3063.52	18.6	200.00	2.66	70	Hardegsen	B
PRW-01	CL0365	3063.80	16.6	23.00	2.66	70	Hardegsen	D
PRW-01	CL0366	3064.10	19.6	134.00	2.67	70	Hardegsen	B
PRW-01	CL0367	3064.41	14.2	20.00	2.68	70	Hardegsen	D
Q13-07-S2	NM0001A	3170.05	0.073	0.38	2.667		Hardegsen	F
Q13-07-S2	NM0002A	3170.35	0.079	0.34	2.671		Hardegsen	F
Q13-07-S2	NM0003A	3170.65	0.079	0.18	2.670		Hardegsen	F
Q13-07-S2	NM0004A	3170.95	0.074	0.05	2.663		Hardegsen	F
Q13-07-S2	NM0006	3171.65	0.059	2.95	2.704		Hardegsen	F

	A						
Q13-07-S2	NM0007 A	3171.95	0.065	0.47	2.664	Hardegsen	F
Q13-07-S2	NM0008 A	3172.25	0.059	0.24	2.696	Hardegsen	F
Q13-07-S2	NM0009 A	3172.55	0.047		2.710	Hardegsen	G
Q13-07-S2	NM0010 A	3172.90	0.028	0.05	2.644	Hardegsen	G
Q13-07-S2	NM0011 A	3173.20	0.047		2.719	Hardegsen	G
Q13-07-S2	NM0012 A	3173.50	0.035	0.03	2.696	Hardegsen	F
Q13-07-S2	NM0013 A	3173.80	0.05	0.15	2.674	Hardegsen	G
Q13-07-S2	NM0014 A	3174.10	0.082	3.47	2.669	Hardegsen	G
Q13-07-S2	NM0015 A	3174.40	0.094	1.66	2.653	Hardegsen	G
Q13-07-S2	NM0016 A	3174.75	0.051	0.24	2.661	Hardegsen	F
Q13-07-S2	NM0017 A	3175.05	0.087	2.46	2.653	Hardegsen	F
Q13-07-S2	NM0018 A	3175.35	0.062	0.18	2.661	Hardegsen	F
Q13-07-S2	NM0019 A	3175.65	0.063	0.28	2.661	Hardegsen	F
Q13-07-S2	NM0020 A	3175.95	0.048	0.44	2.683	Hardegsen	F
Q13-07-S2	NM0021 A	3176.25	0.074	1.37	2.662	Hardegsen	E
Q13-07-S2	NM0022 A	3176.50	0.019		2.732	Hardegsen	G
Q13-07-S2	NM0023 A	3176.80	0.043	0.02	2.649	Hardegsen	F
Q13-07-S2	NM0024 A	3177.10	0.114	20.16	2.646	Hardegsen	E
Q13-07-S2	NM0025 A	3177.40	0.047	0.22	2.686	Hardegsen	F
Q13-07-S2	NM0026 A	3177.70	0.022	0.05	2.706	Hardegsen	F

Q13-07-S2	NM0027A	3178.00	0.082	2.88	2.654	Hardegsen	E
Q13-07-S2	NM0028A	3178.30	0.023	0.07	2.712	Hardegsen	F
Q13-07-S2	NM0029A	3178.60	0.046	0.40	2.701	Hardegsen	F
Q13-07-S2	NM0030A	3178.90	0.072	6.42	2.662	Hardegsen	F
Q13-07-S2	NM0031A	3179.20	0.069	2.59	2.651	Hardegsen	G
Q13-07-S2	NM0032A	3179.50	0.052	0.11	2.649	Hardegsen	G
Q13-07-S2	NM0033A	3179.80	0.063	0.10	2.657	Hardegsen	E
Q13-07-S2	NM0034A	3180.10	0.049	0.02	2.664	Hardegsen	E
Q13-07-S2	NM0035A	3180.40	0.035	0.01	2.673	Hardegsen	E
Q13-07-S2	NM0036A	3180.65	0.047	0.04	2.665	Hardegsen	F
Q13-07-S2	NM0037A	3180.95	0.047	0.29	2.681	Hardegsen	F
Q13-07-S2	NM0038A	3181.25	0.06	0.65	2.665	Hardegsen	G
Q13-07-S2	NM0039A	3181.55	0.04		2.689	Hardegsen	G
Q13-07-S2	NM0040A	3181.85	0.025	0.01	2.657	Hardegsen	G
Q13-07-S2	NM0041A	3182.15	0.033		2.734	Hardegsen	G
Q13-07-S2	NM0042A	3182.45	0.032		2.705	Hardegsen	G
Q13-07-S2	NM0043A	3182.75	0.03		2.692	Hardegsen	G
Q13-07-S2	NM0044A	3183.05	0.04	0.01	2.667	Hardegsen	G
Q13-07-S2	NM0045A	3183.35	0.035	0.04	2.690	Hardegsen	F
Q13-07-S2	NM0046A	3183.65	0.066	0.73	2.668	Hardegsen	E
Q13-07-S2	NM0047A	3183.95	0.066	0.13	2.659	Hardegsen	F

Q13-07-S2	NM0048A	3184.25	0.035	0.39	2.689		Hardegsen	F
Q13-07-S2	NM0049A	3184.55	0.04	0.24	2.703		Hardegsen	G
Q13-07-S2	NM0050A	3184.85	0.038	0.08	2.696		Hardegsen	G
Q13-07-S2	NM0051A	3185.15	0.049	0.98	2.697		Hardegsen	F
Q13-07-S2	NM0052A	3185.45	0.073	2.53	2.680		Hardegsen	G
Q13-07-S2	NM0053A	3185.80	0.038		2.657		Hardegsen	E
Q13-07-S2	NM0054A	3186.05	0.035	0.01	2.669		Hardegsen	F
Q13-07-S2	NM0055A	3186.35	0.042		2.722		Hardegsen	F
Q13-07-S2	NM0056A	3186.65	0.027		2.671		Hardegsen	G
Q13-07-S2	NM0057A	3186.95	0.062		2.752		Hardegsen	G
Q13-07-S2	NM0058A	3187.25	0.043	0.03	2.674		Hardegsen	F
Q13-07-S2	NM0059A	3187.55	0.059	0.12	2.665		Hardegsen	F
Q13-07-S2	NM0060A	3187.80	0.083	8.96	2.660		Hardegsen	E
SPKW-01	NM0063	2815.10	16.8	50.12	2.66	60	Hardegsen	D
SPKW-01	NM0064	2815.40	11.9	86.41	2.67	60	Hardegsen	D
SPKW-01	NM0065	2815.71	17.2	65.24	2.68	55	Hardegsen	D
SPKW-01	NM0066	2816.00	18.2	565.93	2.65	50	Hardegsen	B
SPKW-01	NM0067	2816.30	17.5	**1454.48**	2.66	50	Hardegsen	B
SPKW-01	NM0068	2816.55	15.6	20.99	2.66	60	Hardegsen	D
SPKW-01	NM0069	2816.90	17.0	75.05	2.66	60	Hardegsen	D
SPKW-01	NM0070	2817.20	16.0	58.56	2.66	60	Hardegsen	D
SPKW-01	NM0071	2817.45	18.7	**1948.78**	2.65	50	Hardegsen	A
SPKW-01	NM0072	2817.80	16.3	418.71	2.66	50	Hardegsen	A
SPKW-01	NM0073	2818.10	17.7	104.72	2.65	50	Hardegsen	B
SPKW-01	NM0074	2818.45	18.7	548.88	2.65	50	Hardegsen	B

SPKW-01	NM0075	2818.75	16.8	119.04	2.65	55	Hardegsen	B
SPKW-01	NM0076	2819.00	17.1	110.45	2.66	55	Hardegsen	B
SPKW-01	NM0077	2819.35	19.8	**2053.71**	2.66	50	Hardegsen	A
SPKW-01	NM0078	2819.65	12.2	93.17	2.68	55	Hardegsen	B
SPKW-01	NM0079	2819.95	15.5	267.74	2.65	55	Hardegsen	B
SPKW-01	NM0080	2820.25	13.0	79.54	2.67	60	Hardegsen	B
SPKW-01	NM0081	2820.50	17.9	355.16	2.66	65	Hardegsen	B
SPKW-01	NM0082	2820.80	16.9	29.22	2.66	75	Hardegsen	D
SPKW-01	NM0083	2821.05	17.8	62.56	2.67	75	Hardegsen	D
SPKW-01	NM0084	2821.35	11.5	0.90	2.66	75	Hardegsen	D
SPKW-01	NM0085	2821.70	18.5	**613.02**	2.66	75	Hardegsen	B
SPKW-01	NM0086	2822.00	16.1	104.15	2.66	75	Hardegsen	D
SPKW-01	NM0087	2822.30	17.8	57.26	2.66	75	Hardegsen	D
SPKW-01	NM0088	2822.60	10.3	10.97	2.67	75	Hardegsen	D
SPKW-01	NM0089	2822.92	15.4	224.18	2.67	75	Hardegsen	D
SPKW-01	NM0090	2823.15	18.1	**1076.57**	2.67	60	Hardegsen	B
SPKW-01	NM0091	2823.45	18.5	266.51	2.65	60	Hardegsen	B
SPKW-01	NM0092	2823.75	13.0	1.85	2.66	75	Hardegsen	D
SPKW-01	NM0093	2824.05	16.9	68.03	2.64	75	Hardegsen	D
SPKW-01	NM0094	2824.35	15.4	26.87	2.65	75	Hardegsen	D
SPKW-01	NM0095	2824.65	16.7	230.90	2.65	60	Hardegsen	D
SPKW-01	NM0096	2825.10	15.0	68.02	2.65	50	Hardegsen	D
SPKW-01	NM0097	2825.35	21.2	281.92	2.64	45	Hardegsen	B
SPKW-01	NM0098	2825.65	21.5	379.11	2.64	45	Hardegsen	B
SPKW-01	NM0099	2826.00	17.9	344.57	2.64	50	Hardegsen	D
SPKW-01	NM0100	2826.30	17.0	209.89	2.65	55	Hardegsen	D
SPKW-01	NM0101	2826.65	19.6	**1945.30**	2.68	45	Hardegsen	B
SPKW-01	NM0102	2826.95	17.7	203.25	2.65	50	Hardegsen	B
SPKW-01	NM0103	2827.25	17.3	500.58	2.66	50	Hardegsen	B
SPKW-01	NM0104	2827.55	14.5	340.20	2.69	50	Hardegsen	D
SPKW-01	NM0105	2827.90	20.1	**1409.93**	2.67	45	Hardegsen	B
SPKW-01	NM0106	2828.20	20.2	2221.31	2.67	45	Hardegsen	B

SPKW-01	NM0107	2828.50	20.2	432.77		2.64	45	Hardegsen	B
SPKW-01	NM0108	2828.80	15.2	341.99		2.66	50	Hardegsen	B
SPKW-01	NM0109	2829.10	16.1	56.64		2.66	55	Hardegsen	D
SPKW-01	NM0110	2829.40	18.3	225.29		2.65	50	Hardegsen	B
SPKW-01	NM0111	2829.70	16.5	86.21		2.65	55	Hardegsen	D
SPKW-01	NM0112	2829.95	15.0	69.13		2.65	60	Hardegsen	D
SPKW-01	NM0113	2830.30	16.7	117.83		2.65	65	Hardegsen	D
SPKW-01	NM0114	2830.60	17.8	**601.35**		2.66	55	Hardegsen	B
SPKW-01	NM0115	2830.90	12.2	68.32		2.68	55	Hardegsen	B
SPKW-01	NM0116	2831.20	17.3	423.25		2.66	55	Hardegsen	B
SPKW-01	NM0117	2831.55	13.7	61.39		2.67	55	Hardegsen	B
SPKW-01	NM0118	2831.80	14.8	139.25		2.64	55	Hardegsen	B
SPKW-01	NM0119	2832.10	18.6	385.87		2.65	55	Hardegsen	B
SPKW-01	NM0120	2832.55	15.6	24.74		2.64	60	Hardegsen	D
SPKW-01	NM0121	2832.80	11.7	6.49		2.66	65	Hardegsen	D
SPKW-01	NM0122	2833.00	16.1	33.33		2.65	70	Hardegsen	D

P14-A-01	98	2509.25	6.5	1.3	0	2.67	Detfurth	F
P14-A-01	99	2509.5	5.5	0.08	0.02	2.72	Detfurth	F
P14-A-01	100	2509.75	6.7	0.31	0	2.68	Detfurth	F
P14-A-01	101	2510	4.8	0.07	0.08	2.72	Detfurth	F
P14-A-01	102	2510.25	5.5	0.15	0	2.68	Detfurth	F
P14-A-01	103	2510.5	3.8	0.27	0.09	2.63	Detfurth	F
P14-A-01	104	2510.75	8.8	15	0	2.75	Detfurth	E
P14-A-01	105	2511	10.3	6.2	3.8	2.69	Detfurth	F
P14-A-01	106	2511.25	12.6	35	0	2.68	Detfurth	E
P14-A-01	107	2511.5	11.6	16	6.8	2.68	Detfurth	E
P14-A-01	108	2511.75	9.2	14	0	2.68	Detfurth	E
P14-A-01	109	2512	9.3	4	0.7	2.66	Detfurth	F
P14-A-01	110	2512.25	11.3	89	0	2.67	Detfurth	E
P14-A-01	111	2512.5	10.1	15	6.8	2.68	Detfurth	E
P14-A-01	112	2512.75	5.2	0.75	0	2.7	Detfurth	F

P14-A-01	113	2513	7.1	0.79	7	2.7	Detfurth	F
P14-A-01	114	2513.25	4.7	0.28	0	2.77	Detfurth	F
P14-A-01	115	2513.5	4.3	0.08	0.1	2.71	Detfurth	F
P14-A-01	116	2513.75	4.2	0.08	0	2.74	Detfurth	F
P14-A-01	117	2514	6.5	5.2	9.7	2.68	Detfurth	E
P14-A-01	118	2514.25	7	0.42	0	2.68	Detfurth	F
P14-A-01	119	2514.5	12.4	94	6.2	2.69	Detfurth	C
P14-A-01	120	2514.75	13.4	199	0	2.67	Detfurth	C
P14-A-01	121	2515	13.5	307	0.24	2.67	Detfurth	C
P14-A-01	122	2515.25	16	336	0	2.66	Detfurth	C
P14-A-01	123	2515.5	14	145	20	2.68	Detfurth	C
P14-A-01	124	2515.75	12.3	65	0	2.69	Detfurth	C
P14-A-01	125	2516	8.1	17	4.4	2.66	Detfurth	E
P14-A-01	126	2516.25	11.7	57	0	2.67	Detfurth	C
P14-A-01	127	2516.5	14.1	38	0.26	2.65	Detfurth	C
P14-A-01	128	2516.75	10.6	0.59	0	2.65	Detfurth	F
P14-A-01	129	2517	9.4	57	16	2.67	Detfurth	E
P14-A-01	130	2517.25	13.5	170	0	2.66	Detfurth	C
P14-A-01	131	2517.5	9.4	3.5	0.86	2.67	Detfurth	C
P14-A-01	132	2517.75	12.3	195	0	2.66	Detfurth	C
P14-A-01	133	2518	9.4	25	5.2	2.67	Detfurth	C
P14-A-01	134	2518.25	13.8	380	0	2.67	Detfurth	C
P14-A-01	135	2518.5	12.4	140	42	2.67	Detfurth	C
P14-A-01	136	2518.75	13.3	187	0	2.67	Detfurth	C
P14-A-01	137	2519	13.8	113	30	2.66	Detfurth	C
P14-A-01	138	2519.5	11.8	133	40	2.67	Detfurth	E
P14-A-01	139	2519.75	12	221	0	2.67	Detfurth	E
P14-A-01	140	2520	11.1	221	67	2.69	Detfurth	E
P14-A-01	141	2520.25	12.4	172	0	2.67	Detfurth	E
P14-A-01	142	2520.5	13.6	290	125	2.67	Detfurth	E
P14-A-01	143	2520.75	15.5	460	0	2.67	Detfurth	E
P14-A-01	144	2521	15.3	413	204	2.67	Detfurth	C

P14-A-01	145	2521.25	15.2	408	0	2.67	Detfurth	E
P14-A-01	146	2521.5	14.4	368	197	2.67	Detfurth	E
P14-A-01	147	2521.75	13.4	318	0	2.67	Detfurth	E
P14-A-01	148	2522	13.7	293	58	2.67	Detfurth	C
P14-A-01	149	2522.25	10.8	75	0	2.67	Detfurth	E
P14-A-01	150	2522.5	13.6	221	6.6	2.66	Detfurth	C
P14-A-01	151	2522.75	14.4	283	0	2.67	Detfurth	C
P14-A-01	152	2523	10.1	22	2.7	2.69	Detfurth	C
P14-A-01	153	2523.25	5.9	0.66	0	2.69	Detfurth	F
P14-A-01	154	2523.5	7.2	7.3	0.87	2.69	Detfurth	F
P14-A-01	155	2523.75	12.4	150	0	2.67	Detfurth	C
P14-A-01	156	2524	9.8	8	5.7	2.67	Detfurth	C
P14-A-01	157	2524.25	14	383	0	2.65	Detfurth	C
P14-A-01	158	2524.5	15.1	468	139	2.66	Detfurth	E
P14-A-01	159	2524.75	16.1	626	0	2.66	Detfurth	E
P14-A-01	160	2525	14	350	184	2.65	Detfurth	E
P14-A-01	161	2525.25	6.7	0.41	0	2.64	Detfurth	F
P14-A-01	162	2525.5	14.8	393	29	2.65	Detfurth	E
P14-A-01	163	2525.75	15.1	549	0	2.65	Detfurth	E
P14-A-01	164	2526	14.7	552	118	2.65	Detfurth	C
P14-A-01	165	2526.25	16.4	502	0	2.66	Detfurth	C
P14-A-01	166	2526.5	14.1	116	29	2.65	Detfurth	C
P14-A-01	167	2526.75	15.7	471	0	2.65	Detfurth	C
P14-A-01	168	2527	15.2	318	139	2.65	Detfurth	C
P14-A-01	169	2527.25	15.3	189	0	2.65	Detfurth	C
P14-A-01	170	2527.5	9.7	0.41	0.16	2.64	Detfurth	F
P14-A-01	171	2527.75	9.9	1.3	0	2.64	Detfurth	E
P14-A-01	172	2528	16.3	72	18	2.65	Detfurth	C
P14-A-01	173	2528.25	13.8	23	0	2.65	Detfurth	E
P14-A-01	174	2528.5	13.9	149	19	2.66	Detfurth	E
P14-A-01	175	2528.75	13.2	2.5	0	2.65	Detfurth	E
P14-A-01	176	2529	16.1	115	67	2.66	Detfurth	C

P14-A-01	177	2529.25	12	3.1	0	2.65	Detfurth	C
P14-A-01	178	2529.5	11.5	9	0.41	2.65	Detfurth	E
P14-A-01	179	2529.75	9.7	3.6	0	2.65	Detfurth	F
P14-A-01	180	2530	13.9	16	0.53	2.65	Detfurth	E
P14-A-01	181	2530.25	13.6	88	0	2.66	Detfurth	E
P14-A-01	182	2530.5	12.7	29	0.31	2.66	Detfurth	E
P14-A-01	183	2530.75	13.1	7.4	0	2.66	Detfurth	F
P14-A-01	184	2531	14.2	3.2	26	2.65	Detfurth	F
P14-A-01	185	2531.25	15.6	247	0	2.65	Detfurth	E
P14-A-01	186	2531.5	9.8	33	23	2.66	Detfurth	E
P14-A-01	187	2531.75	17.2	86	0	2.64	Detfurth	E
P14-A-01	188	2532	14.3	1.9	1.1	2.65	Detfurth	E
P14-A-01	189	2532.25	12.3	3.3	0	2.67	Detfurth	F
P14-A-01	190	2532.5	11.8	3.5	0.92	2.66	Detfurth	F
P14-A-01	191	2532.75	10	7.1	0	2.66	Detfurth	E
P14-A-01	192	2533	14	11	4.1	2.66	Detfurth	C
P14-A-01	193	2533.25	8.9	0.53	0	2.66	Detfurth	F
P14-A-01	194	2533.5	9.7	3.1	2.9	2.67	Detfurth	F
P14-A-01	195	2533.75	13.6	16	0	2.68	Detfurth	F
P14-A-01	196	2534	10	2.3	1.6	2.69	Detfurth	F
P14-A-01	197	2534.25	2.7	0.01	0	2.64	Detfurth	F
P14-A-01	198	2534.5	5.2	0.27	0.01	2.69	Detfurth	F
P14-A-01	199	2534.75	4.9	0.01	0	2.71	Detfurth	F
P14-A-01	200	2535	6.4	0.11	0.03	2.72	Detfurth	F
P14-A-01	201	2535.25	7.4	1.1	0	2.69	Detfurth	F
P14-A-01	202	2535.5	7	0.05	0.06	2.74	Detfurth	F
P14-A-01	203	2535.75	7	0.18	0	2.68	Detfurth	F
P14-A-01	204	2536	18.6	245	227	2.66	Detfurth	C
P14-A-01	205	2536.25	18.6	583	0	2.65	Detfurth	C
P14-A-01	206	2536.5	17.9	198	21	2.65	Detfurth	C
P14-A-01	207	2536.75	19.9	525	0	2.65	Detfurth	C
P14-A-01	208	2537	17.5	84	69	2.66	Detfurth	C

P14-A-01	209	2537.25	18.7	494	0	2.65	Detfurth	C
P14-A-01	210	2537.5	18.9	759	646	2.65	Detfurth	C
PRW-01	CL0437	3085.07	13.9	1.6		2.69	Detfurth	E
PRW-01	CL0438	3085.36	13.6	15		2.69	Detfurth	E
PRW-01	CL0439	3085.66	17.4	95		2.69	Detfurth	E
PRW-01	CL0440	3085.95	14.9	20		2.71	Detfurth	E
PRW-01	CL0442B	3086.04	12.6	23		2.72	Detfurth	E
PRW-01	CL0441	3086.24	10.5	0.4		2.71	Detfurth	F
PRW-01	CL0443	3086.32	9	1.4		2.73	Detfurth	E
PRW-01	CL0444	3086.64	10.9	2.5		2.7	Detfurth	E
PRW-01	CL0445	3086.91	12.3	1.5		2.68	Detfurth	C
PRW-01	CL0446	3087.21	13.9	29		2.68	Detfurth	E
PRW-01	CL0447	3087.56	16	79		2.68	Detfurth	E
PRW-01	CL0448V	3087.82	14		0.49	2.7	Detfurth	E
PRW-01	CL0449	3088.1	15.1	27		2.65	Detfurth	C
PRW-01	CL0450	3088.39	15.3	82		2.67	Detfurth	E
PRW-01	CL0451	3088.69	13.6	27		2.7	Detfurth	E
PRW-01	CL0452	3089	16.4	98		2.66	Detfurth	C
PRW-01	CL0453	3089.29	17	136		2.67	Detfurth	E
PRW-01	CL0454	3089.58	11.8	2.4		2.67	Detfurth	E
PRW-01	CL0455	3089.89	16.3	103		2.67	Detfurth	E
PRW-01	CL0456	3090.16	17.8	171		2.67	Detfurth	E
PRW-01	CL0457	3090.45	17.6	294		2.67	Detfurth	E
PRW-01	CL0458	3090.76	17.3	391		2.66	Detfurth	C
PRW-01	CL0459	3091.05	13	36		2.69	Detfurth	C
PRW-01	CL0460	3091.35	17.1	289		2.69	Detfurth	C
PRW-01	CL0461	3091.65	13.6	48		2.69	Detfurth	C
PRW-01	CL0462	3091.94	16.2	152		2.68	Detfurth	C
PRW-01	CL0463	3092.25	18.4	288		2.67	Detfurth	C
PRW-01	CL0464	3092.51	18.9	336		2.65	Detfurth	C
PRW-01	CL0465	3092.86	8.4	0.24		2.74	Detfurth	F
PRW-01	CL0466	3093.1	8.6	0.23		2.71	Detfurth	F

PRW-01	CL0467	3093.37	6.3	0.03		2.71	Detfurth	F
PRW-01	CL0468	3093.71	18.8	200		2.65	Detfurth	E
PRW-01	CL0469	3094.03	11.5	0.54		2.75	Detfurth	F
PRW-01	CL0470	3094.3	12.6	4.5		2.75	Detfurth	E
PRW-01	CL0471	3094.6	14.1	6.5		2.7	Detfurth	E
PRW-01	CL0472	3094.9	13.6	4.3		2.71	Detfurth	C
PRW-01	CL0473	3095.22	13.6	4.1		2.65	Detfurth	C
PRW-01	CL0474	3095.5	13	2.5		2.71	Detfurth	E
PRW-01	CL0475	3095.79	13.5	4.5		2.7	Detfurth	E
PRW-01	CL0476	3096.1	14.3	8.2		2.7	Detfurth	E
PRW-01	CL0477	3096.38	14.7	7.3		2.71	Detfurth	E
PRW-01	CL0478	3096.69	14.5	4.5		2.71	Detfurth	E
PRW-01	CL0479	3096.99	15.1	8.8		2.71	Detfurth	E
PRW-01	CL0480	3097.28	8.9	0.07		2.74	Detfurth	F
PRW-01	CL0481	3097.59	17.2	29		2.71	Detfurth	E
PRW-01	CL0482	3097.88	17	32		2.7	Detfurth	E
PRW-01	CL0483	3098.18	16	22		2.75	Detfurth	E
PRW-01	CL0484	3098.46	15.6	19		2.71	Detfurth	E
PRW-01	CL0485	3098.76	17	40		2.79	Detfurth	E
PRW-01	CL0486V	3099.06	13.7		0.13	2.7	Detfurth	F
PRW-01	CL0487	3099.37	15	1		2.71	Detfurth	C
PRW-01	CL0488	3099.64	13.4	4.5		2.74	Detfurth	C
PRW-01	CL0489	3099.92	15.5	2.2		2.7	Detfurth	E
PRW-01	CL0490	3100.24	15.9	6.5		2.69	Detfurth	E
PRW-01	CL0491	3100.54	15.7	7.9		2.7	Detfurth	E
PRW-01	CL0492	3100.86	18.1	13		2.69	Detfurth	E
PRW-01	CL0493	3101.03	5.7			2.74	Detfurth	F
PRW-01	CL0494	3101.32	6.2	0.02		2.72	Detfurth	F
PRW-01	CL0495	3101.59	4.5			2.73	Detfurth	F
PRW-01	CL0496	3101.91	18.3	85		2.69	Detfurth	C
PRW-01	CL0497	3102.2	21.3	208		2.67	Detfurth	E
PRW-01	CL0498	3102.51	16	15		2.67	Detfurth	E

PRW-01	CL0499	3102.8	11.6	1.4	2.73	Detfurth	F
Q13-04	NM0005	2785.2	1.4		2.704	Detfurth	E
Q13-04	NM0006	2785.5	5.3		2.657	Detfurth	E
Q13-04	NM0007	2785.8	4		2.702	Detfurth	E
Q13-04	NM0008	2786.1	4.4		2.694	Detfurth	E
Q13-04	NM0009	2786.4	3.7		2.689	Detfurth	E
Q13-04	NM0010	2786.7	2.3		2.683	Detfurth	E
Q13-04	NM0011	2787	7.2		2.659	Detfurth	E
Q13-04	NM0012	2787.3	4.3		2.678	Detfurth	E
Q13-04	NM0013	2787.6	3.4		2.687	Detfurth	E
Q13-04	NM0014	2787.9	1.6		2.726	Detfurth	C
Q13-04	NM0015	2788.2	1.6		2.709	Detfurth	E
Q13-04	NM0016	2788.5	2.6		2.691	Detfurth	C
Q13-04	NM0017	2788.8	1.2		2.723	Detfurth	E
Q13-04	NM0018	2789.1	1.2		2.734	Detfurth	E
Q13-04	NM0019	2789.4	1.4		2.725	Detfurth	E
Q13-04	NM0020	2789.7	1.7		2.708	Detfurth	E
Q13-04	NM0021	2790	2.2		2.697	Detfurth	E
Q13-04	NM0022	2790.3	2.4		2.8	Detfurth	E
Q13-04	NM0023	2790.6	1.3		2.697	Detfurth	E
Q13-04	NM0024	2790.9	1.2		2.686	Detfurth	C
Q13-04	NM0025	2791.2	1.4		2.694	Detfurth	C
Q13-04	NM0026	2791.5	1.2		2.725	Detfurth	
Q13-04	NM0027	2791.8	1.4		2.712	Detfurth	C
Q13-04	NM0028	2792.1	2.6		2.686	Detfurth	E
Q13-04	NM0029	2792.4	2.7		2.686	Detfurth	E
Q13-04	NM0030	2792.7	5.1		2.691	Detfurth	E
Q13-04	NM0031	2793	4.1		2.733	Detfurth	F
Q13-04	NM0032	2793.3	2.4		2.701	Detfurth	F
Q13-04	NM0033	2793.6	1.1		2.712	Detfurth	F
Q13-04	NM0034	2793.9	2.5		2.713	Detfurth	F
Q13-04	NM0035	2794.2	3.8		2.687	Detfurth	F

Q13-04	NM0036	2794.5	3.5	2.713	Detfurth	F
Q13-04	NM0038	2795.1	3.5	2.689	Detfurth	F
Q13-04	NM0039	2795.4	3.8	2.695	Detfurth	F
Q13-04	NM0040	2795.7	2.8	2.717	Detfurth	F
Q13-04	NM0041	2796	3.2	2.7	Detfurth	F
Q13-04	NM0042	2796.3	3.5	2.719	Detfurth	F
Q13-04	NM0043	2796.6	2.7	2.718	Detfurth	F
Q13-04	NM0044	2796.9	2.3	2.734	Detfurth	F
Q13-04	NM0045	2797.2	2.7	2.698	Detfurth	F
Q13-04	NM0046	2797.5	2.2	2.713	Detfurth	F
Q13-04	NM0047	2797.8	2	2.719	Detfurth	F
Q13-04	NM0048	2798.1	3.1	2.687	Detfurth	F
Q13-04	NM0049	2798.4	2.2	2.708	Detfurth	F
Q13-04	NM0050	2798.7	2.2	2.703	Detfurth	F
Q13-04	NM0051	2799	1.6	2.706	Detfurth	F
Q13-04	NM0052	2799.3	1.7	2.715	Detfurth	F
Q13-04	NM0053	2799.6	2.6	2.683	Detfurth	F
Q13-04	NM0054	2799.9	1.4	2.71	Detfurth	F
Q13-06	NM0027	2752	3.5	2.72	Detfurth	F
Q13-06	NM0028	2752.3	4.6	2.704	Detfurth	F
Q13-06	NM0029	2752.6	3.7	2.732	Detfurth	F
Q13-06	NM0030	2752.9	4.4	2.716	Detfurth	F
Q13-06	NM0031	2753.2	5.7	2.687	Detfurth	E
Q13-06	NM0032	2753.5	5	2.689	Detfurth	E
Q13-06	NM0033	2753.8	4.5	2.718	Detfurth	E
Q13-06	NM0034	2754.1	5.1	2.697	Detfurth	E
Q13-06	NM0035	2754.4	4.6	2.707	Detfurth	E
Q13-06	NM0036	2754.7	4.1	2.72	Detfurth	E
Q13-06	NM0037	2755	5	2.701	Detfurth	E
Q13-06	NM0038	2755.3	4.6	2.701	Detfurth	E
Q13-06	NM0039	2755.6	5.7	2.681	Detfurth	E
Q13-06	NM0040	2755.8	5.8	2.687	Detfurth	E

Q13-06	NM0041	2756.1	5.7	2.806	Detfurth	G
Q13-06	NM0042	2756.4	4.1	2.708	Detfurth	G
Q13-06	NM0043	2756.7	5.1	2.665	Detfurth	G
Q13-06	NM0044	2757	6.4	2.673	Detfurth	G
Q13-06	NM0045	2757.3	7.5	2.672	Detfurth	G
Q13-06	NM0046	2757.6	4.7	2.708	Detfurth	G
Q13-06	NM0047	2757.9	3.6	2.719	Detfurth	G
Q13-06	NM0048	2758.2	4.6	2.787	Detfurth	F
Q13-06	NM0049	2758.5	6.3	2.685	Detfurth	G
Q13-06	NM0050	2758.8	4.2	2.74	Detfurth	F
Q13-06	NM0051	2759.1	5.5	2.684	Detfurth	F
Q13-06	NM0052	2759.4	4.9	2.703	Detfurth	G
Q13-06	NM0053	2759.7	5.5	2.691	Detfurth	G
Q13-06	NM0054	2760	4.8	2.704	Detfurth	F
Q13-06	NM0055	2760.3	4.8	2.734	Detfurth	G
Q13-06	NM0056	2760.7	5.7	2.694	Detfurth	G
Q13-06	NM0057	2761	7	2.706	Detfurth	E
Q13-06	NM0058	2761.3	4.7	2.715	Detfurth	E
Q13-06	NM0059	2761.5	4.9	2.701	Detfurth	E
Q13-06	NM0060	2761.8	4.6	2.686	Detfurth	E
Q13-06	NM0061	2762.1	4.7	2.814	Detfurth	E
Q13-06	NM0062	2762.4	5.3	2.73	Detfurth	E
Q13-06	NM0063	2762.7	7.1	2.707	Detfurth	E
Q13-06	NM0064	2763	7.5	2.696	Detfurth	E
Q13-06	NM0065	2763.3	4.3	2.668	Detfurth	E
Q13-06	NM0066	2763.6	8.4	2.722	Detfurth	E
Q13-06	NM0067	2763.9	8.8	2.701	Detfurth	E
Q13-06	NM0068	2764.2	6.2	2.7	Detfurth	E
Q13-06	NM0069	2764.5	6.8	2.714	Detfurth	E
Q13-06	NM0070	2764.8	8.3	2.72	Detfurth	E
Q13-06	NM0071	2765.1	9	2.709	Detfurth	E
Q13-06	NM0072	2765.4	7.5	2.697	Detfurth	E

Q13-06	NM0002A	2765.7	11.2	1.22	2.688	Detfurth	E
Q13-06	NM0073	2765.8	10.1		2.692	Detfurth	E
Q13-06	NM0074	2766.1	8.1		2.692	Detfurth	E
Q13-06	NM0075	2766.4	8		2.699	Detfurth	E
Q13-06	NM0076	2766.7	4.2		2.668	Detfurth	C
Q13-06	NM0077	2767	4.2		2.666	Detfurth	E
Q13-06	NM0078	2767.3	6.8		2.694	Detfurth	E
Q13-06	NM0079	2767.6	9.1		2.691	Detfurth	E
Q13-06	NM0080	2767.9	10.1	0.91	2.675	Detfurth	E
Q13-06	NM0081	2768.2	9.1		2.688	Detfurth	E
Q13-06	NM0082	2768.4	9.8		2.678	Detfurth	E
Q13-06	NM0083	2768.7	8.5		2.691	Detfurth	E
Q13-06	NM0003A	2768.8	9.9		2.693	Detfurth	E
Q13-06	NM0084	2769	2.8		2.649	Detfurth	E
Q13-06	NM0085	2769.3	10.7		2.675	Detfurth	E
Q13-06	NM0086	2769.7	11.8	1.22	2.669	Detfurth	E
Q13-06	NM0004A	2769.8	11.1	1.01	2.685	Detfurth	E
Q13-06	NM0087	2770	10.4		2.691	Detfurth	E
Q13-06	NM0088	2770.3	9.5		2.684	Detfurth	E
Q13-06	NM0089	2770.6	3.5		2.672	Detfurth	F
Q13-06	NM0090	2770.9	8.6		2.724	Detfurth	E
Q13-06	NM0091	2771.2	8.3		2.701	Detfurth	E
Q13-06	NM0092	2771.5	8.3		2.724	Detfurth	E
Q13-06	NM0093	2771.8	8.6		2.703	Detfurth	E
Q13-06	NM0094	2772.1	5.9		2.676	Detfurth	E
Q13-06	NM0095	2772.4	9.2		2.675	Detfurth	E
Q13-06	NM0096	2772.9	9.8		2.675	Detfurth	E
Q13-06	NM0097	2773	9.3		2.67	Detfurth	E
Q13-06	NM0098	2773.3	10.2		2.68	Detfurth	E
Q13-06	NM0099	2773.6	9.4		2.678	Detfurth	E
Q13-06	NM0100	2773.9	9.5		2.661	Detfurth	E

Q13-06	NM0101	2774.2	9.9			2.699	Detfurth	E
Q13-06	NM0102	2774.5	11.1	0.91		2.67	Detfurth	E
Q16-02	1	3570.1	3.9	0.02	0.02	2.67	Detfurth	E
Q16-02	2	3570.7	4	0.03	0.02	2.66	Detfurth	E
Q16-02	3	3571	3.9	0.02	0.02	2.67	Detfurth	E
Q16-02	4	3571.3	3	0.01	0.01	2.7	Detfurth	E
Q16-02	5	3571.9	4.2	0.03	0.03	2.69	Detfurth	E
Q16-02	6	3572.5	5.6	0.02	0	2.66	Detfurth	E
Q16-02	7	3572.76	6.5	0.03	0.01	2.67	Detfurth	C
Q16-02	8	3573.1	6.3	0.08	0.01	2.67	Detfurth	F
Q16-02	9	3573.3	6.6	0.03	0.02	2.68	Detfurth	C
Q16-02	10	3574	2.9	0.01	0.01	2.69	Detfurth	F
Q16-02	11	3574.15	3	0.01	0.01	2.69	Detfurth	F
Q16-02	12	3574.8	6.4	0.05	0.03	2.67	Detfurth	C
Q16-02	13	3574.85	4.5	0.03	0.03	2.68	Detfurth	E
Q16-02	14	3575.1	5.5	0.04	0.04	2.68	Detfurth	E
Q16-02	15	3575.7	6.2	0.05	0.04	2.67	Detfurth	C
Q16-08	NM0023	3939.5	3.2			2.670	Detfurth	E
Q16-08	NM0024	3939.8	2.7			2.676	Detfurth	E
Q16-08	NM0025	3940.1	2.1			2.674	Detfurth	E
Q16-08	NM0026	3940.45	2.1			2.709	Detfurth	F
Q16-08	NM0027	3940.75	2.6			2.694	Detfurth	F
Q16-08	NM0028	3941.15	2.6			2.669	Detfurth	E
Q16-08	NM0029	3941.45	2.9			2.669	Detfurth	E
Q16-08	NM0030	3941.8	2.5	0.04		2.675	Detfurth	B
Q16-08	NM0031	3942.15	2			2.675	Detfurth	E
Q16-08	NM0032	3942.45	2.5			2.669	Detfurth	E
Q16-08	NM0033	3942.75	2.2			2.685	Detfurth	G
Q16-08	NM0034	3943.05	2.2	0.04		2.674	Detfurth	E
Q16-08	NM0035	3943.45	4			2.673	Detfurth	E
Q16-08	NM0036	3943.75	5.7	0.05		2.668	Detfurth	E
Q16-08	NM0037	3943.95	6	0.08		2.658	Detfurth	E

Q16-08	NM0038	3944.35	4.9	0.1		2.668	Detfurth	E
Q16-08	NM0039	3944.85	2.9	0.02		2.675	Detfurth	E
Q16-08	NM0040	3944.93	3.5	0.03		2.670	Detfurth	E
Q16-08	NM0041	3945.23	3.5	0.02		2.668	Detfurth	E
Q16-08	NM0042	3945.53	2.2	0.03		2.663	Detfurth	E
Q16-08	NM0043	3945.82	3.1			2.676	Detfurth	G
Q16-08	NM0044	3946.17	8.3	0.55		2.682	Detfurth	E
Q16-08	NM0045	3946.42	8.5	0.41		2.670	Detfurth	E
Q16-08	NM0046	3946.73	6.9	0.52		2.692	Detfurth	E
Q16-08	NM0047	3946.93	6.5	0.35		2.693	Detfurth	E
Q16-08	NM0048	3947.13	5.5	0.17		2.700	Detfurth	E
WWN-01-S2	327	3201.00	8.4	0.11	0.07	2.660	Detfurth	E
WWN-01-S2	328	3201.25	8.4	0.15		2.650	Detfurth	E
WWN-01-S2	329	3201.50	5.0	0.04		2.690	Detfurth	E
WWN-01-S2	330	3201.75	15.3	6.80		2.640	Detfurth	C
WWN-01-S2	331	3202.00	14.7	32.00	28.00	2.700	Detfurth	C
WWN-01-S2	332	3202.25	15.1	46.00		2.690	Detfurth	C
WWN-01-S2	333	3202.50	15.0	37.00		2.720	Detfurth	C
WWN-01-S2	334	3202.75	16.2	82.00		2.710	Detfurth	C
WWN-01-S2	335	3203.00	13.4	34.00	2.00	2.750	Detfurth	C
WWN-01-S2	336	3203.25	17.1	52.00		2.680	Detfurth	C
WWN-01-S2	337	3203.50	16.9	60.00		2.680	Detfurth	C
WWN-01-S2	338	3203.75	12.6	4.10		2.660	Detfurth	E
WWN-01-S2	339	3204.00	14.9	11.00	1.90	2.670	Detfurth	E
WWN-01-S2	340	3204.50	14.5	8.20		2.660	Detfurth	E

WWN-01-S2	341	3204.75	15.4	13.00		2.660	Detfurth	E
WWN-01-S2	342	3205.00	12.3	3.80	0.41	2.680	Detfurth	E
WWN-01-S2	343	3205.25	10.1	0.97		2.680	Detfurth	E
WWN-01-S2	344	3205.50	13.6	9.20		2.710	Detfurth	E
WWN-01-S2	345	3205.75	14.4	16.00		2.710	Detfurth	C
WWN-01-S2	346	3206.00	16.6	22.00	16.00	2.680	Detfurth	C
WWN-01-S2	347	3206.25	16.0	16.00		2.690	Detfurth	E
WWN-01-S2	348	3206.50	10.8	2.30		2.710	Detfurth	E
WWN-01-S2	349	3206.75	6.1	0.07		2.690	Detfurth	E
WWN-01-S2	350	3207.00	12.0	1.40	8.60	2.670	Detfurth	E
WWN-01-S2	351	3207.25	11.5	1.10		2.670	Detfurth	E
WWN-01-S2	352	3207.50	12.1	3.40		2.710	Detfurth	E
WWN-01-S2	353	3207.75	15.1	51.00		2.700	Detfurth	C
WWN-01-S2	354	3208.00	15.3	15.00	1.90	2.730	Detfurth	C
WWN-01-S2	355	3208.25	15.0	14.00		2.710	Detfurth	E
WWN-01-S2	356	3208.50	9.4	0.43		2.760	Detfurth	E
WWN-01-S2	357	3208.75	8.9	0.47		2.700	Detfurth	E
WWN-01-S2	358	3209.00	14.0	13.00	3.90	2.700	Detfurth	E
WWN-01-S2	359	3209.25	11.5	2.30		2.730	Detfurth	E
WWN-01-S2	360	3209.50	12.3	2.30		2.710	Detfurth	E
WWN-01-S2	361	3209.75	12.3	2.10		2.720	Detfurth	E

WWN-01-S2	362	3210.00	12.4	2.10	1.40	2.710	Detfurth	E
WWN-01-S2	363	3210.25	12.1	2.20		2.690	Detfurth	E
WWN-01-S2	364	3210.50	12.7	2.80		2.690	Detfurth	E
WWN-01-S2	365	3210.75	15.4	12.00		2.690	Detfurth	E
WWN-01-S2	366	3211.00	16.0	13.00	5.00	2.680	Detfurth	E
WWN-01-S2	367	3211.25	12.2	2.20		2.710	Detfurth	E
WWN-01-S2	368	3211.50	13.8	4.80		2.690	Detfurth	E
WWN-01-S2	369	3211.75	11.0	0.70		2.680	Detfurth	E
WWN-01-S2	370	3212.00	12.8	1.80	1.50	2.670	Detfurth	E
WWN-01-S2	371	3212.25	13.5	2.30		2.670	Detfurth	E
WWN-01-S2	372	3212.50	13.5	2.00		2.690	Detfurth	E
WWN-01-S2	373	3212.75	15.9	15.00		2.670	Detfurth	E
WWN-01-S2	374	3213.00	14.0	4.40	1.90	2.670	Detfurth	E
WWN-01-S2	375	3213.25	15.6	9.40		2.660	Detfurth	E
WWN-01-S2	376	3213.50	11.8	21.00		2.670	Detfurth	E
WWN-01-S2	377	3213.75	13.5	14.00		2.670	Detfurth	E
WWN-01-S2	378	3214.00	6.0	0.10	0.06	2.680	Detfurth	E
WWN-01-S2	379	3214.25	8.3	0.51		2.680	Detfurth	E
WWN-01-S2	380	3214.50	8.5	0.81		2.690	Detfurth	E
WWN-01-S2	381	3214.75	16.3	50.00		2.670	Detfurth	C
WWN-01-S2	382	3215.00	19.5	107.00	62.00	2.660	Detfurth	C

WWN-01-S2	383	3215.25	19.5	88.00		2.670	Detfurth	C
WWN-01-S2	384	3215.50	19.6	162.00		2.660	Detfurth	C
WWN-01-S2	385	3215.75	10.7	1.30		2.690	Detfurth	E
WWN-01-S2	386	3216.00	16.4	64.00	36.00	2.670	Detfurth	C
WWN-01-S2	387	3216.25	10.1	10.00		2.720	Detfurth	E
WWN-01-S2	388	3216.50	21.1	365.00		2.660	Detfurth	C
WWN-01-S2	389	3216.75	19.1	85.00		2.660	Detfurth	C
WWN-01-S2	390	3217.00	15.7	29.00	0.68	2.690	Detfurth	C
WWN-01-S2	391	3217.25	7.8	0.02		2.720	Detfurth	E
WWN-01-S2	392	3217.50	6.8	0.04		2.770	Detfurth	E
WWN-01-S2	393	3217.75	9.1	0.10		2.660	Detfurth	E
WWN-01-S2	394	3218.00	11.6	0.31	0.31	2.660	Detfurth	E
WWN-01-S2	395	3218.25	7.9	0.03		2.670	Detfurth	E
WWN-01-S2	396	3218.50	9.8	0.10		2.670	Detfurth	E
WWN-01-S2	397	3218.75	11.5	0.41		2.660	Detfurth	C
WWN-01-S2	398	3219.00	8.9	0.07	0.04	2.670	Detfurth	E
WWN-01-S2	399	3219.25	7.3	0.07		2.710	Detfurth	E
WWN-01-S2	400	3219.50	8.8	0.06		2.660	Detfurth	E
WWN-01-S2	401	3219.75	9.7	0.06		2.650	Detfurth	E
WWN-01-S2	402	3220.00	8.3	0.07	0.05	2.690	Detfurth	E
WWN-01-S2	403	3220.25	10.3	0.24		2.670	Detfurth	E

WWN-01-S2	404	3220.50	9.4	0.06		2.650	Detfurth	E
WWN-01-S2	405	3220.75	11.8	0.46		2.680	Detfurth	E
WWN-01-S2	406	3221.00	11.1	0.26	0.13	2.680	Detfurth	E
WWN-01-S2	407	3221.25	10.7	0.29		2.690	Detfurth	E
WWN-01-S2	408	3221.50	10.2	0.16		2.710	Detfurth	E
WWN-01-S2	409	3221.75	8.4	0.08		2.720	Detfurth	C
WWN-01-S2	410	3222.00	10.1	0.34	0.07	2.700	Detfurth	C
WWN-01-S2	411	3222.25	10.4	0.24		2.690	Detfurth	C
WWN-01-S2	412	3222.50	7.9	0.17		2.750	Detfurth	F
WWN-01-S2	413	3222.75	11.4	0.89		2.700	Detfurth	F
BTL-01	K-0157A	2819.6	13.6	22		2.71	U Volpriehausen	E
BTL-01	K-0157C	2819.7	13.2	9.3			U Volpriehausen	E
BTL-01	K-0158A	2819.9	15.7	88		2.7	U Volpriehausen	E
BTL-01	K-0160A	2820.5	18.6	230		2.68	U Volpriehausen	E
BTL-01	K-0163A	2821.4	15.9	47		2.69	U Volpriehausen	E
BTL-01	K-0166A	2822.3	19.02	**300**		2.69	U Volpriehausen	E
BTL-01	K-0169A	2823.2	17.9	180		2.7	U Volpriehausen	C
BTL-01	K-0169C	2823.3	17.8	120			U Volpriehausen	C
BTL-01	K-0173A	2824.4	12.62	2.7		2.69	U Volpriehausen	E
BTL-01	K-0175A	2825	21.8	**640**		2.67	U Volpriehausen	C
BTL-01	K-0180A	2826.5	19.41	160		2.68	U Volpriehausen	C
BTL-01	K-0184A	2827.7	18.8	190		2.69	U Volpriehausen	C
BTL-01	K-0184C	2827.8	18.6	94			U Volpriehausen	E
BTL-01	K-0185A	2828	16.02	94		2.69	U Volpriehausen	E
BTL-01	K-0190A	2829.5	20.7	**490**		2.68	U Volpriehausen	C
BTL-01	K-0192A	2830.1	16.63	100		2.69	U Volpriehausen	C

BTL-01	K-0196A	2831.3	22.6	**700**		2.69	U Volpriehausen	C
BTL-01	K-0196C	2831.4	22.5	**470**			U Volpriehausen	C
BTL-01	K-0197A	2831.6	11.82	4		2.74	U Volpriehausen	E
BTL-01	K-0202A	2833.1	20.6	**350**		2.68	U Volpriehausen	C
BTL-01	K-0202C	2833.2	20.6	170			U Volpriehausen	C
BTL-01	K-0204A	2833.7	7.5	0.08		2.72	U Volpriehausen	E
BTL-01	K-0205A	2834	14.75	48		2.69	U Volpriehausen	E
BTL-01	K-0206A	2834.3	8.6	0.06		2.71	U Volpriehausen	E
BTL-01	K-0206C	2834.4	8.5				U Volpriehausen	E
P14-A-01	211	2587	8.4	0.19	0.18	2.69	U Volpriehausen	E
P14-A-01	212	2587.25	6	0.07	0	2.69	U Volpriehausen	E
P14-A-01	213	2587.5	6	0.11	0.05	2.7	U Volpriehausen	E
P14-A-01	214	2587.75	4.8	0.06	0	2.72	U Volpriehausen	E
P14-A-01	215	2588	5.7	0.05	0.04	2.68	U Volpriehausen	E
P14-A-01	216	2588.25	5.2	0.03	0	2.7	U Volpriehausen	E
P14-A-01	217	2588.5	8	0.03	0.05	2.66	U Volpriehausen	E
P14-A-01	218	2588.75	4.8	0.11	0	2.69	U Volpriehausen	E
P14-A-01	219	2589	6.1	0.23	0.14	2.71	U Volpriehausen	E
P14-A-01	220	2589.25	4.2	0.12	0	2.71	U Volpriehausen	E
P14-A-01	221	2589.5	4.3	0.07	0.07	2.71	U Volpriehausen	E
P14-A-01	222	2589.75	6.4	0.12	0	2.71	U Volpriehausen	E
P14-A-01	223	2590	5.3	0.08	0.06	2.71	U Volpriehausen	E
P14-A-01	224	2590.25	5.1	0.08	0	2.71	U Volpriehausen	E
P14-A-01	225	2590.5	5.7	0.05	0.03	2.71	U Volpriehausen	E
P14-A-01	226	2590.75	6.1	0.09	0	2.7	U Volpriehausen	E
P14-A-01	227	2591	5.6	0.03	0.02	2.67	U Volpriehausen	E
P14-A-01	228	2591.25	7.3	0.01	0	2.65	U Volpriehausen	E
P14-A-01	229	2591.5	6.7	0.03	0	2.66	U Volpriehausen	E
P14-A-01	230	2591.75	8.4	0.07	0	2.66	U Volpriehausen	E
P14-A-01	231	2592	6.3	0.03	0	2.7	U Volpriehausen	E
P14-A-01	232	2592.25	8.7	0.16	0	2.69	U Volpriehausen	E
P14-A-01	233	2592.5	8.3	0.14	0.09	2.68	U Volpriehausen	E

P14-A-01	234	2592.75	6.2	0.1	0	2.7	U Volpriehausen	E
P14-A-01	235	2593	5.6	0.03	0.04	2.72	U Volpriehausen	E
P14-A-01	236	2593.25	6.6	0.26	0	2.7	U Volpriehausen	E
P14-A-01	237	2593.5	3.7	0.06	0	2.71	U Volpriehausen	E
P14-A-01	238	2593.75	4.6	0.15	0	2.72	U Volpriehausen	E
P14-A-01	239	2594	12.7	1.5	0.96	2.67	U Volpriehausen	C
P14-A-01	240	2594.25	12.4	2.4	0	2.67	U Volpriehausen	C
P14-A-01	241	2594.5	10.3	0.7	0.49	2.68	U Volpriehausen	C
P14-A-01	242	2594.75	8.8	0.34	0	2.69	U Volpriehausen	C
P14-A-01	243	2595	7.3	0.12	0.07	2.7	U Volpriehausen	E
P14-A-01	244	2595.25	7.7	0.13	0	2.69	U Volpriehausen	E
P14-A-01	245	2595.5	7	0.09	0.06	2.69	U Volpriehausen	E
P14-A-01	246	2595.75	5.6	0.03	0	2.68	U Volpriehausen	E
P14-A-01	247	2596	3.1	0.04	0.03	2.66	U Volpriehausen	E
P14-A-01	248	2596.25	3.6	0	0	2.68	U Volpriehausen	E
P14-A-01	249	2596.5	3.7	0.04	0	2.7	U Volpriehausen	E
P14-A-01	250	2596.75	6.7	0.13	0	2.69	U Volpriehausen	E
P14-A-01	251	2597	8.9	0.48	0.31	2.68	U Volpriehausen	E
P14-A-01	252	2597.25	6.6	0.09	0	2.68	U Volpriehausen	E
P14-A-01	253	2597.5	9	0.45	0.25	2.68	U Volpriehausen	E
P14-A-01	254	2597.75	7.7	0.2	0	2.69	U Volpriehausen	E
P14-A-01	255	2598	10.2	0.37	0.31	2.68	U Volpriehausen	E
P14-A-01	256	2598.25	9.5	0.52	0	2.69	U Volpriehausen	E
P14-A-01	257	2598.5	8.5	0.61	0.5	2.67	U Volpriehausen	E
P14-A-01	258	2598.75	8.5	0.19	0	2.68	U Volpriehausen	E
P14-A-01	259	2599	8	0.17	0.14	2.69	U Volpriehausen	E
P14-A-01	260	2599.25	7.1	0.21	0	2.69	U Volpriehausen	E
P14-A-01	261	2599.5	5.7	0.08	0.08	2.73	U Volpriehausen	E
P14-A-01	262	2599.75	5.4	0.01	0	2.68	U Volpriehausen	E
P14-A-01	263	2600	6	0.02	0	2.66	U Volpriehausen	E
P14-A-01	264	2600.25	8.1	0.07	0	2.69	U Volpriehausen	E
P14-A-01	265	2600.5	10.3	0.18	0.18	2.68	U Volpriehausen	E

P14-A-01	266	2600.75	9.7	0.09	0	2.66	U Volpriehausen	E
P14-A-01	267	2601	10.7	0.4	0.32	2.68	U Volpriehausen	E
P14-A-01	268	2601.25	10	0.26	0	2.7	U Volpriehausen	E
P14-A-01	269	2601.5	8.5	0.06	0.03	2.65	U Volpriehausen	E
P14-A-01	270	2601.75	9.4	0.14	0	2.67	U Volpriehausen	E
P14-A-01	271	2602	6.1	0.01	0	2.68	U Volpriehausen	E
P14-A-01	272	2602.25	8	0.44	0	2.7	U Volpriehausen	C
P14-A-01	273	2602.5	6.8	0.24	0.22	2.71	U Volpriehausen	C
P14-A-01	274	2602.75	8.8	0.29	0	2.68	U Volpriehausen	C
P14-A-01	275	2603	8	0.47	0.33	2.69	U Volpriehausen	C
P14-A-01	276	2603.25	7.5	0.31	0	2.7	U Volpriehausen	C
P14-A-01	277	2603.5	9.9	0.63	0.37	2.68	U Volpriehausen	E
P14-A-01	278	2603.75	9.2	0.38	0	2.7	U Volpriehausen	E
P14-A-01	279	2604	8.1	0.34	0.27	2.69	U Volpriehausen	E
P14-A-01	280	2604.25	10.1	0.49	0	2.68	U Volpriehausen	E
P14-A-01	281	2604.5	4.8	0.04	0.02	2.65	U Volpriehausen	E
P14-A-01	282	2604.75	8	0.1	0	2.67	U Volpriehausen	E
P14-A-01	283	2605	7.4	0.07	0	2.68	U Volpriehausen	E
P14-A-01	284	2605.25	10.5	3	0	2.69	L Volpriehausen SST	E
P14-A-01	285	2605.5	13.5	18	15	2.68	L Volpriehausen SST	E
P14-A-01	286	2605.75	11.3	6.4	0	2.67	L Volpriehausen SST	E
P14-A-01	287	2606	14.4	64	44	2.67	L Volpriehausen SST	E
P14-A-01	288	2606.25	9.8	4.1	0	2.69	L Volpriehausen SST	E
P14-A-01	289	2606.5	10.9	21	11	2.69	L Volpriehausen SST	E
P14-A-01	290	2606.75	15.5	126	0	2.66	L Volpriehausen SST	C
P14-A-01	291	2607	18.1	**394**	315	2.66	L Volpriehausen SST	C
P14-A-01	292	2607.25	14.6	128	0	2.67	L Volpriehausen SST	C

P14-A-01	293	2607.5	14.7	135	81	2.67	L Volpriehausen SST	E
P14-A-01	294	2607.75	13.5	49	0	2.67	L Volpriehausen SST	E
P14-A-01	295	2608	13.6	44	15	2.67	L Volpriehausen SST	C
P14-A-01	296	2608.25	11.7	41	0	2.68	L Volpriehausen SST	C
P14-A-01	297	2608.5	9.5	5.9	1.7	2.67	L Volpriehausen SST	C
P14-A-01	298	2608.75	14.6	88	0	2.67	L Volpriehausen SST	C
P14-A-01	299	2609	13	29	29	2.68	L Volpriehausen SST	C
P14-A-01	300	2609.25	9.7	5.5	0	2.69	L Volpriehausen SST	C
P14-A-01	301	2609.5	3.4	0.03	0.02	2.66	L Volpriehausen SST	E
P14-A-01	302	2609.75	5.1	0.11	0	2.68	L Volpriehausen SST	E
P14-A-01	303	2610	9.4	6.7	1.5	2.68	L Volpriehausen SST	E
P14-A-01	304	2610.25	10.6	15	0	2.68	L Volpriehausen SST	E
P14-A-01	305	2610.5	12	23	15	2.68	L Volpriehausen SST	E
P14-A-01	306	2610.75	10.5	7.2	0	2.68	L Volpriehausen SST	E
P14-A-01	307	2611	7.4	0.41	0.14	2.67	L Volpriehausen SST	E
P14-A-01	308	2611.25	9.5	3.9	0	2.69	L Volpriehausen SST	E
P14-A-01	309	2611.5	8.2	0.51	0.21	2.69	L Volpriehausen SST	E
P14-A-01	310	2611.75	6.6	0.46	0	2.71	L Volpriehausen SST	E
P14-A-01	311	2612	7.3	0.29	0.45	2.69	L Volpriehausen SST	E
P14-A-01	312	2612.25	9.7	4.7	0	2.69	L Volpriehausen SST	E
P14-A-01	313	2612.5	7.1	0.41	0.35	2.7	L Volpriehausen SST	E

P14-A-01	314	2612.75	8.4	0.64	0	2.69	L Volpriehausen SST	E
P14-A-01	315	2613	6.8	0.15	0.07	2.69	L Volpriehausen SST	E
P14-A-01	316	2613.25	5.6	0.09	0	2.71	L Volpriehausen SST	E
P14-A-01	317	2613.5	8.8	0.85	0.16	2.68	L Volpriehausen SST	E
P14-A-01	318	2613.75	9.7	5	0	2.69	L Volpriehausen SST	E
P14-A-01	319	2614	8.2	0.92	0	2.7	L Volpriehausen SST	E
P14-A-01	320	2614.25	8.8	9.3	0	2.69	L Volpriehausen SST	E
P14-A-01	321	2614.5	8.6	5	0	2.7	L Volpriehausen SST	E
P14-A-01	322	2614.75	9.2	10	0	2.68	L Volpriehausen SST	E
P14-A-01	323	2615	7.7	0	0	2.68	L Volpriehausen SST	E
P14-A-01	324	2615.25	10.8	19	0	2.69	L Volpriehausen SST	C
P14-A-01	325	2615.5	9.5	18	0	2.7	L Volpriehausen SST	C
P14-A-01	326	2615.75	11.1	32	0	2.69	L Volpriehausen SST	C
P14-A-01	327	2616	10.1	2	0	2.68	L Volpriehausen SST	C
P14-A-01	328	2616.25	6.4	0.09	0	2.69	L Volpriehausen SST	C
P14-A-01	329	2616.5	5.9	0.11	0.04	2.7	L Volpriehausen SST	C
P14-A-01	330	2616.75	7.4	1	0	2.69	L Volpriehausen SST	C
P14-A-01	331	2617	8.3	0.86	0.57	2.7	L Volpriehausen SST	C
P14-A-01	332	2617.25	9.3	0.88	0	2.69	L Volpriehausen SST	C
P14-A-01	333	2617.5	10	1.9	0.91	2.68	L Volpriehausen SST	C
P14-A-01	334	2617.75	9.8	1.6	0	2.68	L Volpriehausen SST	C

P14-A-01	335	2618	8.7	0.94	0.79	2.7	L Volpriehausen SST	C
P14-A-01	336	2618.25	8.3	0.54	0	2.67	L Volpriehausen SST	C
P14-A-01	337	2618.5	8.1	1.4	0.51	2.69	L Volpriehausen SST	C
P14-A-01	338	2618.75	9.1	1.8	0	2.69	L Volpriehausen SST	E
P14-A-01	339	2619	9	3.6	0.86	2.69	L Volpriehausen SST	C
P14-A-01	340	2619.25	11.4	18	0	2.68	L Volpriehausen SST	C
P14-A-01	341	2619.5	10.5	1.8	2.3	2.68	L Volpriehausen SST	C
P14-A-01	342	2619.75	5.4	0.04	0	2.66	L Volpriehausen SST	C
P14-A-01	343	2620	11.3	7.2	4.9	2.68	L Volpriehausen SST	C
P14-A-01	344	2620.25	11.1	2.9	0	2.69	L Volpriehausen SST	C
P14-A-01	345	2620.5	10.8	1.4	0.19	2.68	L Volpriehausen SST	C
P14-A-01	346	2620.75	3.3	0.01	0	2.67	L Volpriehausen SST	C
P14-A-01	347	2621	4.7	0	0.02	2.65	L Volpriehausen SST	C
P14-A-01	348	2621.25	7.6	0.16	0	2.7	L Volpriehausen SST	E
P14-A-01	349	2621.5	10.1	1	0.72	2.68	L Volpriehausen SST	E
P14-A-01	350	2621.75	9.7	0.62	0	2.69	L Volpriehausen SST	C
P14-A-01	351	2622	8.9	0.36	0.29	2.69	L Volpriehausen SST	C
P14-A-01	352	2622.25	13.5	4.5	0	2.67	L Volpriehausen SST	C
P14-A-01	353	2622.5	12.1	3.5	3.4	2.67	L Volpriehausen SST	C
P14-A-01	354	2622.75	10.4	2.2	0	2.68	L Volpriehausen SST	E
P14-A-01	355	2623	11	4.3	1.3	2.68	L Volpriehausen SST	E

PKP-01	61	2126.1	2.6	2.728	U Volpriehausen	F
PKP-01	62	2126.4	1.9	2.736	U Volpriehausen	F
PKP-01	63	2126.7	1.7	2.716	U Volpriehausen	F
PKP-01	64	2127	1.1	2.717	U Volpriehausen	G
PKP-01	65	2127.3	1.5	2.688	U Volpriehausen	G
PKP-01	66	2127.6	3.2	2.69	U Volpriehausen	G
PKP-01	67	2127.9	2.5	2.721	U Volpriehausen	G
PKP-01	70	2128.8	2.1	2.712	U Volpriehausen	G
PKP-01	71	2129.1	1.8	2.759	U Volpriehausen	G
PKP-01	72	2129.4	2.7	2.677	U Volpriehausen	G
PKP-01	73	2129.7	2.6	2.693	U Volpriehausen	E
PKP-01	74	2130	4.1	2.683	U Volpriehausen	G
PKP-01	75	2130.3	2	2.649	U Volpriehausen	G
PKP-01	77	2130.9	4.4	2.686	U Volpriehausen	G
PKP-01	78	2131.2	1.6	2.7	U Volpriehausen	G
PKP-01	79	2131.5	2.9	2.672	U Volpriehausen	G
PKP-01	80	2131.8	1.8	2.723	U Volpriehausen	G
PKP-01	81	2132.1	2.5	2.707	U Volpriehausen	G
PKP-01	82	2132.4	2.7	2.713	U Volpriehausen	E
PKP-01	83	2132.7	1.6	2.708	U Volpriehausen	G
PKP-01	84	2133	3.6	2.716	U Volpriehausen	G
PKP-01	85	2133.3	3.9	2.731	U Volpriehausen	G
PKP-01	86	2133.6	2.2	2.7	U Volpriehausen	G
PKP-01	87	2133.9	4	2.683	U Volpriehausen	G
PKP-01	88	2134.2	2.4	2.707	U Volpriehausen	G
PKP-01	89	2134.5	3.4	2.702	U Volpriehausen	G
PKP-01	90	2134.8	2.5	2.667	U Volpriehausen	G
PKP-01	91	2135.1	3.9	2.673	U Volpriehausen	G
PKP-01	92	2135.4	4.4	2.722	U Volpriehausen	G
Q13-06	NM0103	2774.8	8.9	2.667	U Volpriehausen	C
Q13-06	NM0104	2775.1	6.9	2.664	U Volpriehausen	E
Q13-06	NM0105	2775.4	9.7	2.672	U Volpriehausen	E

Q13-06	NM0106	2775.7	11.2	1.11	2.664	U Volpriehausen	E
Q13-06	NM0107	2776	11.5	1.01	2.676	U Volpriehausen	E
Q13-06	NM0108	2776.3	9.8		2.674	U Volpriehausen	E
Q13-06	NM0109	2776.6	10.4	2.43	2.674	U Volpriehausen	E
Q13-06	NM0110	2776.9	10		2.667	U Volpriehausen	C
Q13-06	NM0111	2777.2	11.1	1.52	2.676	U Volpriehausen	C
Q13-06	NM0112	2777.5	11.5	2.23	2.67	U Volpriehausen	E
Q13-06	NM0113	2777.8	10.5	1.01	2.67	U Volpriehausen	E
Q13-06	NM0114	2778.1	11.8	4.56	2.665	U Volpriehausen	E
Q13-06	NM0115	2778.4	9.3		2.669	U Volpriehausen	E
Q13-06	NM0116	2778.7	9.9		2.669	U Volpriehausen	E
Q13-06	NM0117	2779	9.3		2.667	U Volpriehausen	E
Q13-06	NM0118	2779.3	9.9		25.675	U Volpriehausen	E
Q13-06	NM0119	2779.6	9.1		2.681	U Volpriehausen	E
Q13-06	NM0120	2779.9	9.7		2.674	U Volpriehausen	E
VAL-01	NM0001	2821.5	2.4	0.01	2.724	U + L Volpriehausen	E
VAL-01	NM0002	2821.8	4.9	0.02	2.729	U + L Volpriehausen	E
VAL-01	NM0003	2822.1	3.8	0.03	2.721	U + L Volpriehausen	E
VAL-01	NM0004	2822.4	5.3	0.03	2.714	U + L Volpriehausen	E
VAL-01	NM0005	2822.7	6.2	0.04	2.704	U + L Volpriehausen	E
VAL-01	NM0006	2823	7.7	0.09	2.671	U + L Volpriehausen	E
VAL-01	NM0007	2823.3	5.6	0.14	2.687	U + L Volpriehausen	C
VAL-01	NM0008	2823.6	7.3	0.09	2.693	U + L Volpriehausen	E
VAL-01	NM0009	2823.9	6.6	0.05	2.718	U + L Volpriehausen	F
VAL-01	NM0010	2824.25	9.8	0.14	2.68	U + L Volpriehausen	E
VAL-01	NM0011	2824.55	6.1	0.04	2.755	U + L Volpriehausen	F

VAL-01	NM0012	2824.8	6.4	0.03	2.73	U + L Volpriehausen	E
VAL-01	NM0013	2825.1	4.4	0.01	2.744	U + L Volpriehausen	F
VAL-01	NM0014	2825.4	6.7	0.03	2.701	U + L Volpriehausen	E
VAL-01	NM0015	2825.65	7	0.02	2.707	U + L Volpriehausen	F
VAL-01	NM0016	2826.05	8.2	0.17	2.699	U + L Volpriehausen	E
VAL-01	NM0017	2826.35	5.5	0.02	2.716	U + L Volpriehausen	F
VAL-01	NM0018	2826.65	5.3	0.02	2.721	U + L Volpriehausen	F
VAL-01	NM0019	2826.95	5.6	0.03	2.719	U + L Volpriehausen	E
VAL-01	NM0020	2827.25	5.9	0.03	2.718	U + L Volpriehausen	E
VAL-01	NM0021	2827.5	4.9	0.02	2.724	U + L Volpriehausen	F
VAL-01	NM0022	2827.75	6.6	0.03	2.699	U + L Volpriehausen	E
VAL-01	NM0023	2828.1	6.1	0.04	2.725	U + L Volpriehausen	F
VAL-01	NM0024	2828.4	6.2	0.12	2.744	U + L Volpriehausen	F
VAL-01	NM0025	2828.75	5.3	0.57	2.741	U + L Volpriehausen	F
VAL-01	NM0026	2829.15	7.5	0.02	2.702	U + L Volpriehausen	E
VAL-01	NM0027	2829.45	7.6	0.03	2.689	U + L Volpriehausen	E
VAL-01	NM0028	2829.8	7.4	0.02	2.691	U + L Volpriehausen	E
VAL-01	NM0029	2830.1	5.3	0.03	2.733	U + L Volpriehausen	E
VAL-01	NM0030	2830.45	5.6	0.07	2.71	U + L Volpriehausen	E
VAL-01	NM0031	2830.75	5.6	0.03	2.746	U + L Volpriehausen	F
VAL-01	NM0032	2831.1	7.1	0.03	2.69	U + L Volpriehausen	E

VAL-01	NM0033	2831.4	5.4		2.702	U + L Volpriehausen	E
VAL-01	NM0034	2831.65	6.7	0.03	2.682	U + L Volpriehausen	E
VAL-01	NM0035	2831.95	7.3	0.25	2.667	U + L Volpriehausen	E
VAL-01	NM0036	2832.25	3.1	0.02	2.71	U + L Volpriehausen	E
VAL-01	NM0037	2832.55	3.4	0.03	2.72	U + L Volpriehausen	E
VAL-01	NM0038	2832.85	4.6	0.03	2.709	U + L Volpriehausen	E
VAL-01	NM0039	2833.15	8.1	0.46	2.711	U + L Volpriehausen	E
VAL-01	NM0040	2833.45	9.8	2.02	2.694	U + L Volpriehausen	E
VAL-01	NM0041	2833.75	7.9	0.21	2.679	U + L Volpriehausen	E
VAL-01	NM0042	2834.05	5.4	0.09	2.703	U + L Volpriehausen	E
VAL-01	NM0043	2834.35	8	0.48	2.68	U + L Volpriehausen	E
VAL-01	NM0044	2834.65	8.2	0.86	2.688	U + L Volpriehausen	C
VAL-01	NM0045	2834.95	8.2	0.15	2.696	U + L Volpriehausen	C
VAL-01	NM0046	2835.25	7.1	0.08	2.682	U + L Volpriehausen	E
VAL-01	NM0047	2835.55	6.7	0.06	2.683	U + L Volpriehausen	E
VAL-01	NM0048	2835.85	6	0.04	2.685	U + L Volpriehausen	E
VAL-01	NM0049	2836.3	7.9	0.19	2.681	U + L Volpriehausen	E
VAL-01	NM0050	2836.6	6.6	0.07	2.686	U + L Volpriehausen	E
VAL-01	NM0051	2836.9	8.2	0.28	2.691	U + L Volpriehausen	E
VAL-01	NM0052	2837.2	9	1.07	2.68	U + L Volpriehausen	E
VAL-01	NM0053	2837.5	7.2	0.1	2.69	U + L Volpriehausen	E

VAL-01	NM0054	2837.8	9.5	2.55	2.681	U + L Volpriehausen	E
VAL-01	NM0055	2838.05	8.7	0.52	2.698	U + L Volpriehausen	E
VAL-01	NM0056	2838.4	6.8	0.09	2.692	U + L Volpriehausen	E
VAL-01	NM0057	2839.1	9.8	3.34	2.689	U + L Volpriehausen	E
VAL-01	NM0058	2839.4	4.9	0.07	2.717	U + L Volpriehausen	E
VAL-01	NM0059	2839.7	5.8	0.03	2.676	U + L Volpriehausen	E
VAL-01	NM0060	2840	9.2	0.95	2.681	U + L Volpriehausen	E
VAL-01	NM0061	2840.3	9.3	1.31	2.675	U + L Volpriehausen	E
VAL-01	NM0062	2840.6	7.3	0.19	2.678	U + L Volpriehausen	E
VAL-01	NM0063	2840.9	9.1	1.23	2.68	U + L Volpriehausen	E
VAL-01	NM0064	2841.2	9.4	2.64	2.692	U + L Volpriehausen	C
VAL-01	NM0065	2841.5	8.6	2.58	2.699	U + L Volpriehausen	E
VAL-01	NM0066	2841.8	7.7	0.85	2.71	U + L Volpriehausen	E
VAL-01	NM0067	2842.1	8.5	0.41	2.679	U + L Volpriehausen	C
VAL-01	NM0068	2842.4	8.5	0.66	2.678	U + L Volpriehausen	C
VAL-01	NM0069	2842.7	8	0.3	2.691	U + L Volpriehausen	C
VAL-01	NM0070	2843	6.6	0.06	2.686	U + L Volpriehausen	E
VAL-01	NM0071	2843.3	4.7	0.02	2.69	U + L Volpriehausen	E
VAL-01	NM0072	2843.6	6.8	0.33	2.713	U + L Volpriehausen	E
VAL-01	NM0073	2843.9	8.4	0.81	2.694	U + L Volpriehausen	C
VAL-01	NM0074	2844.2	8.3	0.56	2.697	U + L Volpriehausen	C

VAL-01	NM0075	2844.5	7.7	0.39	2.695	U + L Volpriehausen	E
VAL-01	NM0076	2844.8	8	0.41	2.713	U + L Volpriehausen	E
VAL-01	NM0077	2845.1	7.6	0.26	2.714	U + L Volpriehausen	E
VAL-01	NM0078	2845.4	6.2	0.05	2.732	U + L Volpriehausen	E
VAL-01	NM0079	2845.7	7.3	0.14	2.708	U + L Volpriehausen	E
VAL-01	NM0080	2846.05	7.7	0.13	2.715	U + L Volpriehausen	E
VAL-01	NM0081	2846.35	7	0.07	2.705	U + L Volpriehausen	E
VAL-01	NM0082	2846.65	7.3	0.11	2.711	U + L Volpriehausen	E
VAL-01	NM0083	2846.95	6.8	0.04	2.698	U + L Volpriehausen	E
VAL-01	NM0084	2847.25	6.5	0.04	2.7	U + L Volpriehausen	E
VAL-01	NM0085	2847.55	4.5	0.01	2.685	U + L Volpriehausen	E
VAL-01	NM0086	2847.85	5.9	0.04	2.692	U + L Volpriehausen	E
VAL-01	NM0087	2848.15	4.9	0.02	2.717	U + L Volpriehausen	E
VAL-01	NM0088	2848.45	4.7	0.02	2.722	U + L Volpriehausen	E
VAL-01	NM0089	2848.83	6.4	0.03	2.682	U + L Volpriehausen	E
VAL-01	NM0090	2849.1	7.1	0.04	2.708	U + L Volpriehausen	E
VAL-01	NM0091	2849.4	7.4	0.13	2.706	U + L Volpriehausen	E
VAL-01	NM0092	2849.7	6.7	0.07	2.711	U + L Volpriehausen	E
VAL-01	NM0093	2850	6.3	0.04	2.684	U + L Volpriehausen	E
VAL-01	NM0094	2850.3	8.7	0.34	2.69	U + L Volpriehausen	E
VAL-01	NM0095	2850.6	8.6	0.37	2.697	U + L Volpriehausen	E

VAL-01	NM0096	2850.9	9.2	0.28	2.692	U + L Volpriehausen	E
VAL-01	NM0097	2851.2	9.1	0.27	2.683	U + L Volpriehausen	E
VAL-01	NM0098	2851.5	3.3		2.718	U + L Volpriehausen	G
VAL-01	NM0099	2851.8	7.6	0.06	2.694	U + L Volpriehausen	E
VAL-01	NM0100	2852.1	7.6	0.06	2.692	U + L Volpriehausen	E
VAL-01	NM0101	2852.4	7.7	0.09	2.683	U + L Volpriehausen	E
VAL-01	NM0102	2852.7	7.8	0.06	2.693	U + L Volpriehausen	E
VAL-01	NM0103	2853	5.6	0.02	2.687	U + L Volpriehausen	E
VAL-01	NM0104	2853.4	4.4		2.716	U + L Volpriehausen	F
VAL-01	NM0105	2853.75	3.3	0.02	2.742	U + L Volpriehausen	F
VAL-01	NM0106	2854.1	5.7	0.06	2.753	U + L Volpriehausen	F
VAL-01	NM0107	2854.45	6.5		2.746	U + L Volpriehausen	F
VAL-01	NM0108	2854.75	4.6	0.02	2.757	U + L Volpriehausen	F
VAL-01	NM0109	2855.05	5.3	0.03	2.709	U + L Volpriehausen	E
VAL-01	NM0110	2855.35	5.2	0.02	2.711	U + L Volpriehausen	E
VAL-01	NM0111	2855.65	4.7		2.738	U + L Volpriehausen	F
VAL-01	NM0112	2855.95	5.6		2.767	U + L Volpriehausen	F
VAL-01	NM0113	2856.25	5.7	0.01	2.717	U + L Volpriehausen	F
VAL-01	NM0114	2856.6	5.3		2.774	U + L Volpriehausen	F
VAL-01	NM0115	2856.9	5.7		2.758	U + L Volpriehausen	F
VAL-01	NM0116	2857.3	4	0.02	2.746	U + L Volpriehausen	F

VAL-01	NM0117	2857.85	5.3		2.73	U + L Volpriehausen	F
VAL-01	NM0118	2858.4	4.2	0.02	2.74	U + L Volpriehausen	F
VAL-01	NM0119	2858.75	5.4		2.746	U + L Volpriehausen	F
VAL-01	NM0120	2859.2	4.8		2.783	U + L Volpriehausen	F
VAL-01	NM0121	2859.5	5.4		2.749	U + L Volpriehausen	F
VAL-01	NM0122	2859.8	4		2.749	U + L Volpriehausen	F
VAL-01	NM0123	2860.1	4.4		2.721	U + L Volpriehausen	F
VAL-01	NM0124	2860.4	3.5		2.753	U + L Volpriehausen	F
VAL-01	NM0125	2860.7	4.9		2.772	U + L Volpriehausen	F
VAL-01	NM0126	2861.35	4.4		2.741	U + L Volpriehausen	G
VAL-01	NM0127	2861.9	4.2		2.747	U + L Volpriehausen	F
VAL-01	NM0128	2862.5	4.3	0.02	2.705	U + L Volpriehausen	F
VAL-01	NM0129	2863.3	4.1		2.752	U + L Volpriehausen	G
VAL-01	NM0130	2863.65	7.3	0.05	2.709	U + L Volpriehausen	E
VAL-01	NM0131	2863.95	4.6	0.13	2.725	U + L Volpriehausen	F
VAL-01	NM0132	2864.35	2.8	0.01	2.745	U + L Volpriehausen	F
VAL-01	NM0133	2864.55	5.6	0.01	2.694	U + L Volpriehausen	F
VAL-01	NM0134	2864.9	5.2		2.744	U + L Volpriehausen	F
VAL-01	NM0135	2865.15	4.4		2.716	U + L Volpriehausen	F
VAL-01	NM0136	2865.55	4.3	0.03	2.725	U + L Volpriehausen	F
VAL-01	NM0137	2865.95	4.7	0.09	2.725	U + L Volpriehausen	F

VAL-01	NM0138	2866.25	5.1		2.744	U + L Volpriehausen	G
VAL-01	NM0139	2866.75	4.4		2.728	U + L Volpriehausen	F
VAL-01	NM0140	2867.05	5.4		2.77	U + L Volpriehausen	F
VAL-01	NM0141	2867.45	5.3		2.734	U + L Volpriehausen	F
VAL-01	NM0142	2867.75	4.4		2.732	U + L Volpriehausen	F
VAL-01	NM0143	2868.25	7	0.13	2.691	U + L Volpriehausen	F
VAL-01	NM0144	2868.55	4.3		2.775	U + L Volpriehausen	F
VAL-01	NM0145	2868.9	5.1		2.775	U + L Volpriehausen	F
VAL-01	NM0146	2869.1	4.6		2.729	U + L Volpriehausen	F
VAL-01	NM0147	2869.45	7.7	0.05	2.681	U + L Volpriehausen	E
VAL-01	NM0148	2869.75	3.9	0.03	2.723	U + L Volpriehausen	E
VAL-01	NM0149	2870.15	7.1	0.6	2.704	U + L Volpriehausen	E
VAL-01	NM0150	2870.45	7.7	0.21	2.701	U + L Volpriehausen	E
VAL-01	NM0151	2870.8	9.7	0.22	2.7	U + L Volpriehausen	C
VAL-01	NM0152	2871.25	6.1	0.11	2.722	U + L Volpriehausen	E
VAL-01	NM0153	2871.55	7.1	0.07	2.716	U + L Volpriehausen	E
VAL-01	NM0154	2871.85	7.1	0.11	2.726	U + L Volpriehausen	E
VAL-01	NM0155	2872.15	7.1	0.14	2.728	U + L Volpriehausen	E
VAL-01	NM0156	2872.45	6.6	0.03	2.703	U + L Volpriehausen	E
VAL-01	NM0157	2872.75	6.7	0.02	2.705	U + L Volpriehausen	E
VAL-01	NM0158	2873.1	8.9	0.09	2.692	U + L Volpriehausen	C

VAL-01	NM0159	2873.4	9.1	0.08	2.697	U + L Volpriehausen	C
VAL-01	NM0160	2873.6	7.3	0.03	2.719	U + L Volpriehausen	E
VAL-01	NM0161	2873.9	7.4	0.04	2.708	U + L Volpriehausen	E
VAL-01	NM0162	2874.2	7.6	0.08	2.705	U + L Volpriehausen	E
VAL-01	NM0163	2874.5	4.5		2.702	U + L Volpriehausen	E
VAL-01	NM0164	2874.8	6.8	0.02	2.694	U + L Volpriehausen	E
VAL-01	NM0165	2875.1	9.1	0.11	2.695	U + L Volpriehausen	E
VAL-01	NM0166	2875.4	9.2	0.12	2.695	U + L Volpriehausen	E
VAL-01	NM0167	2875.7	9.4	0.24	2.695	U + L Volpriehausen	E
VAL-01	NM0168	2876	7.2	0.07	2.724	U + L Volpriehausen	E
VAL-01	NM0169	2876.3	6.6	0.03	2.7	U + L Volpriehausen	C
VAL-01	NM0170	2876.6	7.4	0.09	2.715	U + L Volpriehausen	E
VAL-01	NM0171	2876.9	8.2	0.1	2.702	U + L Volpriehausen	C
VAL-01	NM0172	2877.2	7.7	0.12	2.71	U + L Volpriehausen	E
VAL-01	NM0173	2877.5	7.5	0.06	2.706	U + L Volpriehausen	E
VAL-01	NM0174	2877.8	4.4		2.697	U + L Volpriehausen	E
VAL-01	NM0175	2878.1	7.1	0.07	2.722	U + L Volpriehausen	E
VAL-01	NM0176	2878.4	7.7	0.13	2.713	U + L Volpriehausen	E
VAL-01	NM0177	2878.7	8.2	0.12	2.7	U + L Volpriehausen	E
VAL-01	NM0178	2879	4.4		2.714	U + L Volpriehausen	E
VAL-01	NM0179	2879.3	8.6	0.11	2.706	U + L Volpriehausen	C

VAL-01	NM0180	2879.6	8.3	0.17		2.708	U + L Volpriehausen	C
VAL-01	NM0181	2879.9	6.9	0.11		2.727	U + L Volpriehausen	E
VAL-01	NM0182	2880.2	6.8	0.08		2.731	U + L Volpriehausen	E
VAL-01	NM0183	2880.55	8.6	0.11		2.693	U + L Volpriehausen	E
WWN-01-S2	414	3223.00	9.3	0.19	0.22	2.720	U Volpriehausen	E
WWN-01-S2	415	3223.25	7.1	0.03		2.690	U Volpriehausen	E
WWN-01-S2	416	3223.50	0.8	0.12		2.660	U Volpriehausen	F
WWN-01-S2	417	3223.75	2.5	0.01		2.670	U Volpriehausen	E
WWN-01-S2	418	3224.00	8.8	0.14	0.02	2.670	U Volpriehausen	E
WWN-01-S2	419	3224.25	10.3	0.20		2.690	U Volpriehausen	E
WWN-01-S2	420	3224.50	6.8	0.12		2.720	U Volpriehausen	E
WWN-01-S2	421	3224.75	9.6	0.53		2.710	U Volpriehausen	E
WWN-01-S2	422	3225.00	8.3	0.22	0.45	2.700	U Volpriehausen	E
WWN-01-S2	423	3225.25	9.0	0.28		2.710	U Volpriehausen	E
WWN-01-S2	424	3225.50	10.4	1.20		2.710	U Volpriehausen	C
WWN-01-S2	425	3225.75	14.7	37.00		2.690	U Volpriehausen	C
WWN-01-S2	426	3226.00	10.0	0.14	0.08	2.670	U Volpriehausen	C
WWN-01-S2	427	3226.25	12.2	0.68		2.680	U Volpriehausen	C
WWN-01-S2	428	3226.50	7.6	0.12		2.690	U Volpriehausen	E
WWN-01-S2	429	3226.75	5.8	0.01		2.660	U Volpriehausen	E
WWN-01-S2	430	3227.00	11.7	0.81	0.68	2.670	U Volpriehausen	E

WWN-01-S2	431	3227.50	9.8	0.22		2.670	U Volpriehausen	E
WWN-01-S2	432	3227.75	13.7	4.20		2.670	U Volpriehausen	E
WWN-01-S2	433	3228.00	9.1	0.15	0.06	2.660	U Volpriehausen	E
WWN-01-S2	434	3228.25	11.1	0.41		2.670	U Volpriehausen	E
WWN-01-S2	435	3228.50	8.5	0.07		2.670	U Volpriehausen	E
WWN-01-S2	436	3228.75	9.7	0.16		2.660	U Volpriehausen	E
WWN-01-S2	437	3229.00	10.8	0.37	0.17	2.670	U Volpriehausen	C
WWN-01-S2	438	3229.25	12.0	0.82		2.660	U Volpriehausen	C
WWN-01-S2	439	3229.50	12.1	0.83		2.670	U Volpriehausen	C
WWN-01-S2	440	3229.75	11.0	0.67		2.690	U Volpriehausen	C
WWN-01-S2	441	3230.00	12.3	1.50	0.49	2.700	U Volpriehausen	C
WWN-01-S2	442	3230.25	10.2	0.68		2.710	U Volpriehausen	C
WWN-01-S2	443	3230.50	9.6	0.20		2.680	U Volpriehausen	C
WWN-01-S2	444	3230.75	9.2	0.14		2.660	U Volpriehausen	C
WWN-01-S2	445	3231.00	5.3	0.02	0.02	2.660	U Volpriehausen	F
WWN-01-S2	446	3231.25	13.2	9.50		2.690	U Volpriehausen	C
WWN-01-S2	447	3231.50	10.6	9.76		2.710	U Volpriehausen	C
WWN-01-S2	448	3231.75	6.3	0.01		2.670	U Volpriehausen	C
WWN-01-S2	449	3232.00	6.0	0.03	0.02	2.660	U Volpriehausen	C
WWN-01-S2	450	3232.25	12.1	1.40		2.690	U Volpriehausen	C
WWN-01-S2	451	3232.50	13.1	3.00		2.680	U Volpriehausen	C

WWN-01-S2	452	3232.75	10.3	0.40		2.660	U Volpriehausen	C
WWN-01-S2	453	3233.00	9.1	0.36	0.04	2.660	U Volpriehausen	C
WWN-01-S2	454	3233.25	10.7	1.30		2.710	U Volpriehausen	C
WWN-01-S2	455	3233.50	12.2	2.60		2.690	U Volpriehausen	C
WWN-01-S2	456	3233.75	10.8	0.81		2.690	U Volpriehausen	C
WWN-01-S2	457	3234.00	10.0	0.85	0.39	2.700	U Volpriehausen	C
WWN-01-S2	458	3234.25	8.1	0.46		2.700	U Volpriehausen	C
WWN-01-S2	459	3234.50	9.2	0.43		2.700	U Volpriehausen	C
WWN-01-S2	460	3234.75	11.5	0.70		2.660	U Volpriehausen	C
WWN-01-S2	461	3235.00	7.7	0.03	0.01	2.660	U Volpriehausen	C
WWN-01-S2	462	3235.25	9.0	0.05		2.660	U Volpriehausen	C
WWN-01-S2	463	3235.50	11.2	0.40		2.680	U Volpriehausen	C
WWN-01-S2	464	3235.75	10.2	0.23		2.690	U Volpriehausen	C
WWN-01-S2	465	3236.00	10.3	0.25	0.13	2.680	U Volpriehausen	C
WWN-01-S2	466	3236.25	7.7	0.03		2.680	U Volpriehausen	E
WWN-01-S2	467	3236.50	10.5	0.22		2.690	U Volpriehausen	E
WWN-01-S2	468	3236.75	8.8	0.11		2.680	U Volpriehausen	E
WWN-01-S2	469	3237.00	7.1	0.02	0.01	2.670	U Volpriehausen	E
WWN-01-S2	470	3237.25	7.8	0.04		2.660	U Volpriehausen	E
WWN-01-S2	471	3237.50	5.0	0.01		2.680	U Volpriehausen	E
WWN-01-S2	472	3237.75	8.6	0.15		2.710	U Volpriehausen	E

WWN-01-S2	473	3238.00	10.5	0.15	0.18	2.690	U Volpriehausen	E
WWN-01-S2	474	3238.25	9.0	0.11		2.690	U Volpriehausen	E
WWN-01-S2	475	3238.50	9.7	0.16		2.700	U Volpriehausen	E
WWN-01-S2	476	3238.75	7.9	0.04		2.670	U Volpriehausen	E
WWN-01-S2	477	3239.00	9.7	0.11	0.05	2.680	U Volpriehausen	E
WWN-01-S2	478	3239.25	8.9	0.06		2.690	U Volpriehausen	C
WWN-01-S2	479	3239.50	6.7	0.05		2.690	U Volpriehausen	C
WWN-01-S2	480	3239.75	10.9	0.46		2.680	U Volpriehausen	C
WWN-01-S2	481	3240.00	10.5	0.27	0.24	2.680	U Volpriehausen	C
WWN-01-S2	482	3240.25	3.2	0.01		2.690	U Volpriehausen	F
WWN-01-S2	483	3240.50	8.8	0.61		2.710	U Volpriehausen	E
WWN-01-S2	484	3240.75	8.0	0.06		2.680	U Volpriehausen	E
WWN-01-S2	485	3241.00	9.9	0.12	0.08	2.700	U Volpriehausen	E
WWN-01-S2	486	3241.25	8.1	0.10		2.720	U Volpriehausen	E
WWN-01-S2	487	3241.50	10.4	0.30		2.680	U Volpriehausen	E
WWN-01-S2	488	3241.75	9.1	0.18		2.710	U Volpriehausen	E
WWN-01-S2	489	3242.00	8.9	0.13	0.15	2.680	U Volpriehausen	E
WWN-01-S2	490	3242.25	10.5	0.26		2.680	U Volpriehausen	E
WWN-01-S2	491	3242.50	6.1	0.02		2.680	U Volpriehausen	E
WWN-01-S2	492	3242.75	9.8	0.23		2.680	U Volpriehausen	E
WWN-01-S2	493	3243.00	7.8	0.19	0.11	2.720	U Volpriehausen	E

WWN-01-S2	494	3243.25	9.3	0.34		2.690	U Volpriehausen	E
WWN-01-S2	495	3243.50	9.0	0.21		2.700	U Volpriehausen	C
WWN-01-S2	496	3243.75	6.8	0.01		2.660	U Volpriehausen	C
WWN-01-S2	497	3244.00	5.6	0.02	0.01	2.650	U Volpriehausen	C
WWN-01-S2	498	3244.25	0.8	0.01		2.640	U Volpriehausen	F
WWN-01-S2	499	3244.50	4.0	0.01		2.650	U Volpriehausen	F
WWN-01-S2	500	3244.75	8.1	0.04		2.670	U Volpriehausen	C
WWN-01-S2	501	3245.00	8.0	0.03	0.03	2.690	U Volpriehausen	C
WWN-01-S2	502	3245.25	8.1	0.07		2.710	U Volpriehausen	C
WWN-01-S2	503	3245.50	8.6	0.24		2.730	U Volpriehausen	C
WWN-01-S2	504	3245.75	6.6	0.12		2.770	U Volpriehausen	C
WWN-01-S2	505	3246.00	7.1	0.02	0.01	2.660	U Volpriehausen	C
WWN-01-S2	506	3246.25	10.3	0.17		2.680	U Volpriehausen	C
WWN-01-S2	507	3246.50	8.6	0.16		2.690	U Volpriehausen	C
WWN-01-S2	508	3246.75	5.5	0.01		2.660	U Volpriehausen	C
WWN-01-S2	509	3247.00	10.3	0.14	0.10	2.670	U Volpriehausen	C
WWN-01-S2	510	3247.25	8.1	0.05		2.660	U Volpriehausen	C
WWN-01-S2	511	3247.50	9.4	0.15		2.680	U Volpriehausen	C
WWN-01-S2	512	3247.75	7.1	0.01		2.660	U Volpriehausen	C
WWN-01-S2	513	3248.00	5.5	0.02	0.01	2.680	U Volpriehausen	C
WWN-01-S2	514	3248.25	7.8	0.14		2.680	U Volpriehausen	C

WWN-01-S2	515	3248.50	6.4	10.00		2.730	U Volpriehausen	E
WWN-01-S2	516	3248.75	6.0	0.24		2.690	U Volpriehausen	E
WWN-01-S2	517	3249.00	4.9	0.01	0.01	2.690	U Volpriehausen	E
WWN-01-S2	518	3249.25	10.1	0.19		2.700	U Volpriehausen	E
WWN-01-S2	519	3249.50	8.9	0.10		2.700	U Volpriehausen	E
WWN-01-S2	520	3249.75	8.6	0.07		2.690	U Volpriehausen	E
WWN-01-S2	521	3250.00	10.6	0.26	0.14	2.690	U Volpriehausen	F
WWN-01-S2	522	3250.25	5.7	0.01		2.680	U Volpriehausen	C
WWN-01-S2	523	3250.50	9.4	0.07		2.690	U Volpriehausen	C
WWN-01-S2	524	3250.75	9.4	0.08		2.680	U Volpriehausen	C
WWN-01-S2	525	3251.00	8.1	0.04	0.02	2.670	U Volpriehausen	C
WWN-01-S2	526	3251.25	8.0	0.02		2.680	U Volpriehausen	C
WWN-01-S2	527	3251.50	8.3	0.03		2.690	U Volpriehausen	C
WWN-01-S2	528	3252.00	2.8	0.01	0.01	2.690	U Volpriehausen	F
WWN-01-S2	529	3252.25	3.8	0.01		2.670	U Volpriehausen	F
WWN-01-S2	530	3252.50	8.4	0.04		2.670	U Volpriehausen	C
WWN-01-S2	531	3252.75	6.1	0.01		2.670	U Volpriehausen	C
WWN-01-S2	532	3253.00	9.9	0.12	0.07	2.690	U Volpriehausen	C
WWN-01-S2	533	3253.25	8.4	0.08		2.710	U Volpriehausen	C
WWN-01-S2	534	3253.50	1.1	0.01		2.660	U Volpriehausen	F
WWN-01-S2	535	3253.75	7.3	0.02		2.700	U Volpriehausen	C

WWN-01-S2	536	3254.00	8.6	0.04	0.05	2.680	U Volpriehausen	C
WWN-01-S2	537	3254.25	9.0	0.08		2.660	U Volpriehausen	C
WWN-01-S2	538	3254.50	1.1	0.02		2.680	U Volpriehausen	F
WWN-01-S2	539	3254.75	7.6	0.10		2.700	U Volpriehausen	C
WWN-01-S2	540	3255.00	8.8	0.12	0.06	2.670	U Volpriehausen	C
WWN-01-S2	541	3255.25	9.7	0.46		2.690	U Volpriehausen	C
WWN-01-S2	542	3255.50	7.9	0.12		2.670	U Volpriehausen	C
WWN-01-S2	543	3255.75	6.9	0.02		2.680	U Volpriehausen	C
WWN-01-S2	544	3256.00	8.9	0.65	0.57	2.690	U Volpriehausen	C
WWN-01-S2	545	3256.25	8.0	0.14		2.700	U Volpriehausen	C
WWN-01-S2	546	3256.50	9.5	0.17		2.670	U Volpriehausen	C
WWN-01-S2	547	3256.75	7.5	0.09		2.710	U Volpriehausen	C
WWN-01-S2	548	3257.00	5.8	0.17	0.07	2.730	U Volpriehausen	C
WWN-01-S2	549	3257.25	7.9	0.16		2.690	U Volpriehausen	C
WWN-01-S2	550	3257.50	8.1	0.17		2.700	U Volpriehausen	C
WWN-01-S2	551	3257.75	2.4	0.04		2.670	U Volpriehausen	F
WWN-01-S2	552	3258.00	6.7	0.04	0.01	2.760	U Volpriehausen	C
WWN-01-S2	553	3258.25	0.6	0.01		2.660	U Volpriehausen	C
WWN-01-S2	554	3258.50	9.9	3.50		2.680	U Volpriehausen	C
WWN-01-S2	555	3259.00	6.7	0.21	0.08	2.690	U Volpriehausen	C
WWN-01-S2	556	3259.25	5.3	0.02		2.670	U Volpriehausen	C

WWN-01-S2	557	3259.50	7.9	0.04		2.700	U Volpriehausen	C
WWN-01-S2	558	3260.00	8.1	0.42	0.22	2.690	U Volpriehausen	C
WWN-01-S2	559	3260.25	7.3	0.03		2.700	U Volpriehausen	C
WWN-01-S2	560	3260.50	7.8	0.04		2.710	U Volpriehausen	C
WWN-01-S2	561	3260.75	4.0	0.01		2.660	U Volpriehausen	F
WWN-01-S2	562	3261.00	3.7	0.01	0.01	2.680	U Volpriehausen	F
WWN-01-S2	563	3261.25	8.1	0.05		2.660	U Volpriehausen	C
WWN-01-S2	564	3261.50	8.5	0.06		2.690	U Volpriehausen	C
WWN-01-S2	565	3261.75	7.1	0.02		2.710	U Volpriehausen	C
WWN-01-S2	566	3262.00	5.4	0.01	0.04	2.670	U Volpriehausen	C
WWN-01-S2	567	3262.25	7.9	0.07		2.700	U Volpriehausen	C
WWN-01-S2	568	3262.50	5.4	0.01		2.690	U Volpriehausen	C
WWN-01-S2	569	3262.75	6.2	0.01		2.670	U Volpriehausen	C
WWN-01-S2	570	3263.00	7.4	0.01	0.01	2.680	U Volpriehausen	C
WWN-01-S2	571	3263.25	8.0	0.02		2.700	U Volpriehausen	C
WWN-01-S2	572	3263.50	7.7	0.03		2.690	U Volpriehausen	C
WWN-01-S2	573	3263.75	5.8	0.01		2.680	U Volpriehausen	C
WWN-01-S2	574	3264.00	5.6	0.01	0.01	2.680	U Volpriehausen	C
WWN-01-S2	575	3264.25	8.3	0.01		2.690	U Volpriehausen	C
WWN-01-S2	576	3264.50	7.6	0.07		2.720	U Volpriehausen	C
WWN-01-S2	577	3264.75	7.9	0.01		2.700	U Volpriehausen	C

WWN-01-S2	578	3265.00	7.8	0.06	0.05	2.700	U Volpriehausen	C
WWN-01-S2	579	3265.25	1.9	0.01		2.670	U Volpriehausen	F
WWN-01-S2	580	3265.50	3.3	0.01		2.680	U Volpriehausen	F
WWN-01-S2	581	3265.75	5.8	0.01		2.670	U Volpriehausen	C
WWN-01-S2	582	3266.00	7.9	0.05	0.03	2.700	U Volpriehausen	C
WWN-01-S2	583	3266.25	8.1	0.08		2.670	U Volpriehausen	C
WWN-01-S2	584	3266.50	8.6	0.13		2.690	U Volpriehausen	C
WWN-01-S2	585	3266.75	9.4	0.16		2.690	U Volpriehausen	C
WWN-01-S2	586	3267.00	8.9	0.15	0.12	2.680	U Volpriehausen	C
WWN-01-S2	587	3267.25	9.7	0.38		2.660	U Volpriehausen	C
WWN-01-S2	588	3267.50	9.7	0.27		2.680	U Volpriehausen	C
WWN-01-S2	589	3267.75	8.6	0.26		2.750	U Volpriehausen	C
WWN-01-S2	590	3268.00	7.2	0.02	0.01	2.660	U Volpriehausen	C
WWN-01-S2	591	3268.25	8.0	0.03		2.650	U Volpriehausen	C
WWN-01-S2	592	3268.75	11.0	0.98		2.670	U Volpriehausen	C
WWN-01-S2	593	3269.00	10.7	0.97	0.61	2.690	U Volpriehausen	C
WWN-01-S2	594	3269.25	3.9	0.01		2.660	U Volpriehausen	F
WWN-01-S2	595	3269.50	7.2	0.03		2.660	U Volpriehausen	C
WWN-01-S2	596	3269.75	8.0	0.07		2.680	U Volpriehausen	C
WWN-01-S2	597	3270.00	8.8	0.33	0.24	2.760	U Volpriehausen	C
WWN-01-S2	598	3270.25	9.1	1.80		2.740	U Volpriehausen	C

WWN-01-S2	599	3270.50	10.1	0.91		2.700	U Volpriehausen	C
WWN-01-S2	600	3270.75	10.5	0.77		2.740	U Volpriehausen	C
WWN-01-S2	601	3271.00	8.7	0.11	0.09	2.690	U Volpriehausen	C
WWN-01-S2	602	3271.25	7.8	0.08		2.680	U Volpriehausen	E
WWN-01-S2	603	3271.50	8.3	0.11		2.700	U Volpriehausen	E
WWN-01-S2	604	3271.75	9.5	0.22		2.670	U Volpriehausen	E
WWN-01-S2	605	3272.00	7.3	0.07	0.11	2.680	U Volpriehausen	E
WWN-01-S2	606	3272.25	8.8	0.10		2.680	U Volpriehausen	E
WWN-01-S2	607	3272.50	3.3	0.01		2.670	U Volpriehausen	F
WWN-01-S2	608	3272.75	7.1	0.03		2.670	U Volpriehausen	E
WWN-01-S2	609	3273.25	9.9	0.55	0.22	2.670	U Volpriehausen	E
WWN-01-S2	610	3273.50	5.7	0.01		2.660	U Volpriehausen	E
WWN-01-S2	611	3273.75	3.0	0.01		2.670	U Volpriehausen	F
WWN-01-S2	612	3274.25	10.1	0.32		2.690	U Volpriehausen	C
WWN-01-S2	613	3274.50	10.2	0.32	0.18	2.680	U Volpriehausen	C
WWN-01-S2	614	3274.75	9.5	0.17		2.680	U Volpriehausen	E
WWN-01-S2	615	3275.25	9.8	0.18	0.14	2.660	U Volpriehausen	E
WWN-01-S2	616	3275.50	9.7	0.16		2.690	U Volpriehausen	E
WWN-01-S2	617	3275.75	10.3	0.28		2.690	U Volpriehausen	C
WWN-01-S2	618	3276.00	9.8	0.16	0.14	2.680	U Volpriehausen	C
WWN-01-S2	619	3276.25	9.8	0.10		2.680	U Volpriehausen	C

WWN-01-S2	620	3276.50	7.5	0.01		2.690	U Volpriehausen	E
WWN-01-S2	621	3276.75	9.9	0.22		2.680	U Volpriehausen	E
WWN-01-S2	622	3277.00	8.8	0.60	0.10	2.690	U Volpriehausen	E
WWN-01-S2	623	3277.25	2.8	0.01		2.680	U Volpriehausen	E
WWN-01-S2	624	3277.50	9.4	0.13		2.700	U Volpriehausen	E
WWN-01-S2	625	3277.75	4.5	0.01		2.680	U Volpriehausen	F
WWN-01-S2	626	3278.00	9.0	0.13	0.09	2.700	U Volpriehausen	E
WWN-01-S2	627	3278.25	7.8	0.04		2.720	U Volpriehausen	E
WWN-01-S2	628	3278.50	0.8	0.01		2.670	U Volpriehausen	E
WWN-01-S2	629	3278.75	7.4	0.01		2.710	U Volpriehausen	E
WWN-01-S2	630	3279.00	4.1	0.05	0.01	2.740	U Volpriehausen	F
WWN-01-S2	631	3279.25	0.7	0.27		2.680	U Volpriehausen	F
WWN-01-S2	632	3279.50	0.6	0.40		2.660	U Volpriehausen	F
WWN-01-S2	633	3279.75	0.6			2.670	U Volpriehausen	F
WWN-01-S2	634	3280.00	1.4		0.01	2.660	U Volpriehausen	F
WWN-01-S2	635	3280.25	2.2	0.01		2.690	U Volpriehausen	F
WWN-01-S2	636	3280.50	1.9			2.680	U Volpriehausen	F
Q16-02	16	3629.4	4.3	0.02	0.02	2.69	L Volpriehausen SST	C
Q16-02	17	3630	3.6	0.02	0.02	2.69	L Volpriehausen SST	C
Q16-02	18	3630.6	4	0.03	0.02	2.69	L Volpriehausen SST	C
Q16-02	19	3631.2	4.2	0.03	0.02	2.68	L Volpriehausen SST	C

Q16-02	20	3631.8	3.3	0.02	0.02	2.69	L Volpriehausen SST	C
Q16-02	21	3632.4	3.8	0.04	0.02	2.7	L Volpriehausen SST	C
Q16-02	22	3633	4	0.03	0.02	2.68	L Volpriehausen SST	C
Q16-02	23	3633.6	3.7	0.02	0.02	2.71	L Volpriehausen SST	C
Q16-02	24	3634.2	3.3	0.03	0.02	2.7	L Volpriehausen SST	C
Q16-02	25	3634.75	3.4	0.02	0.02	2.69	L Volpriehausen SST	C

2. Property graphs and trends

Hardegsen

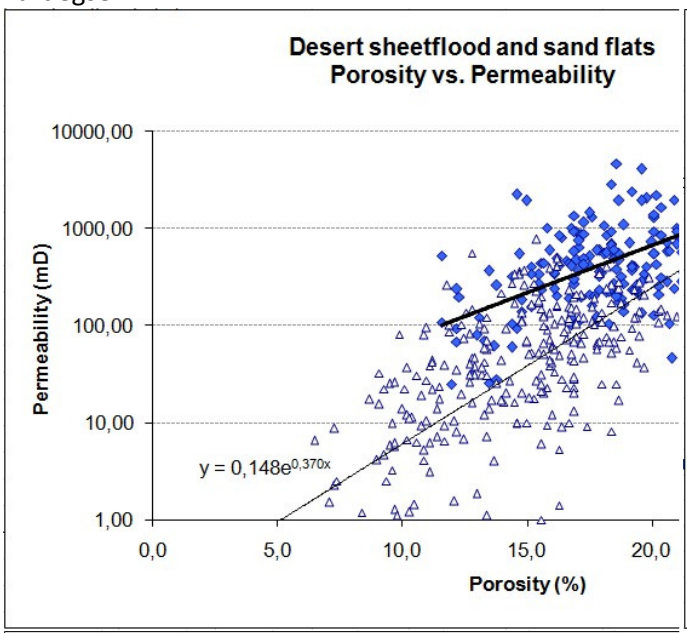

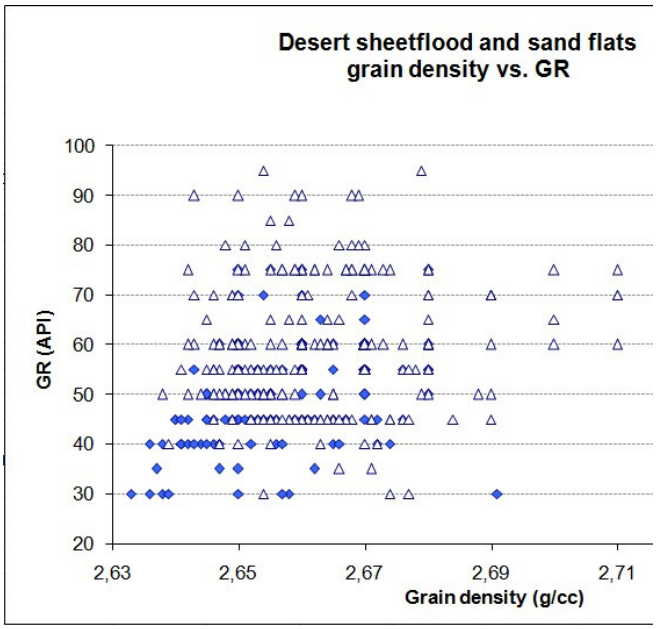

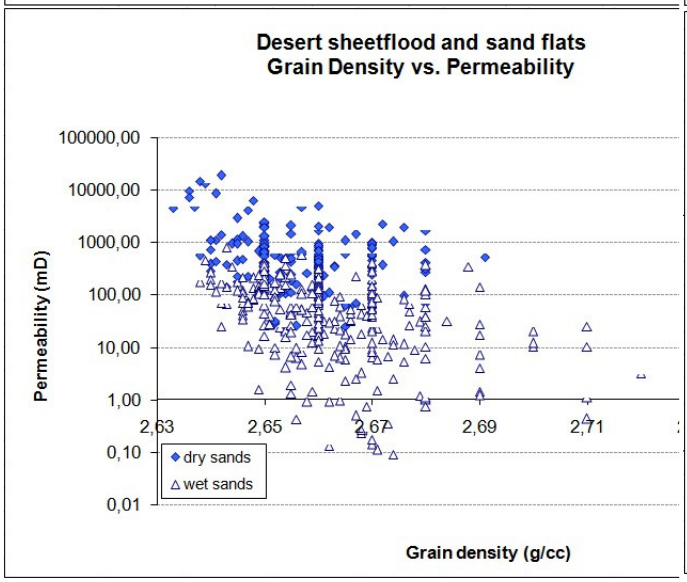

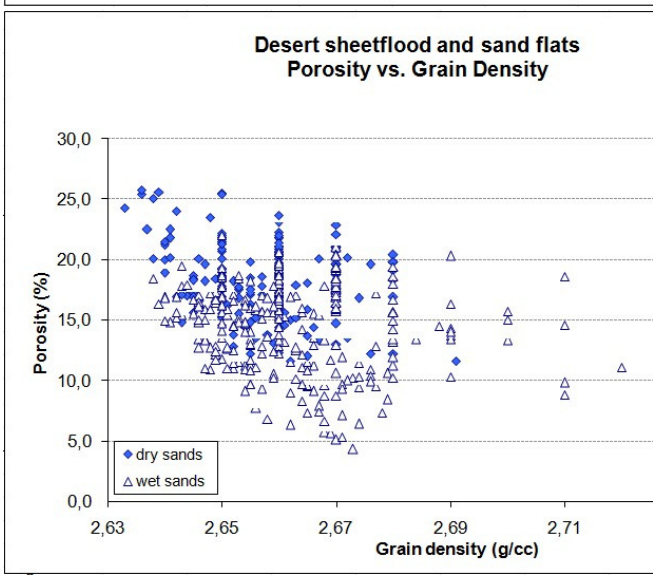

Detfurth

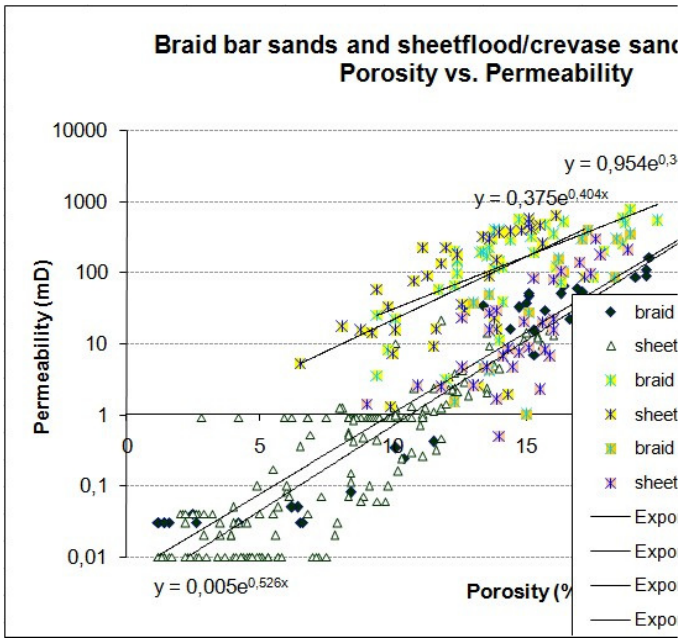

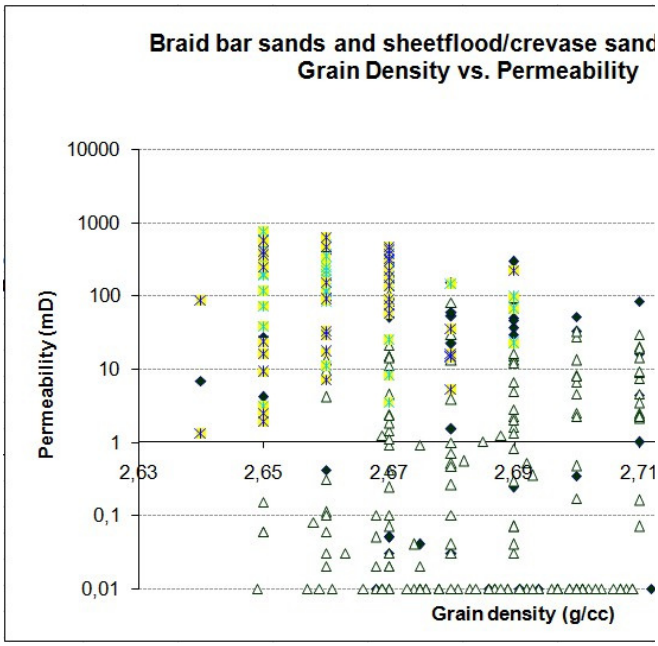

Volpriehausen

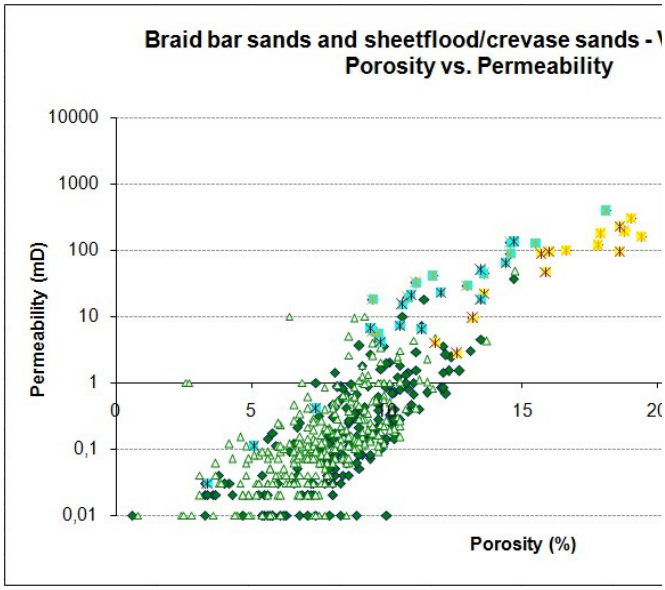

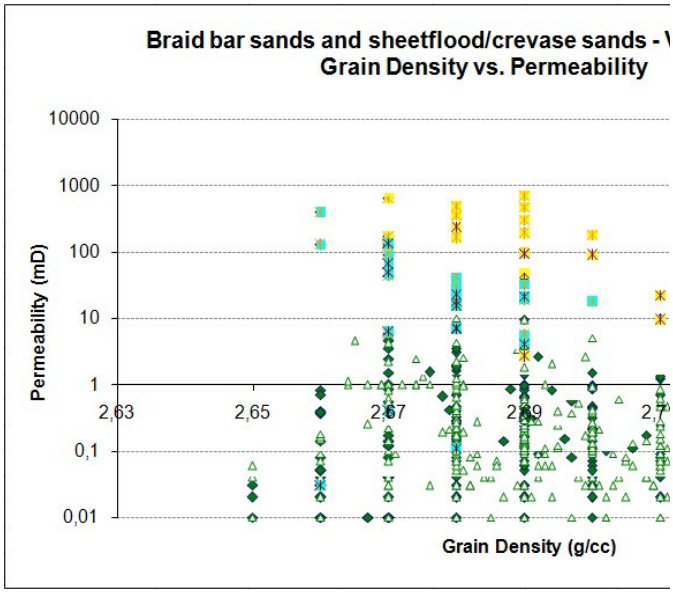

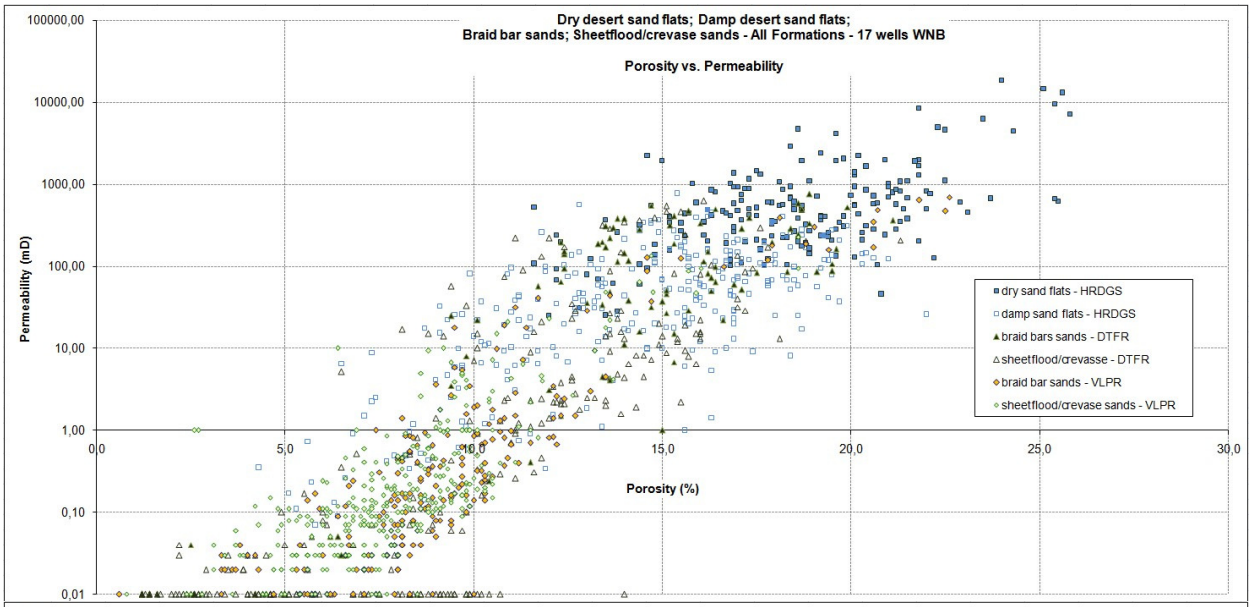
Dry desert sand flats; Damp desert sand flats;
Braid bar sands; Sheetflood/crevase sands - All Formations - 17 wells WNB
Porosity vs. Permeability
Permeability (mD)
100000,00
10000,00
1000,00
100,00
10,00
1,00
0,10
0,01
0,0
5,0
10,0
15,0
20,0
25,0
30,0
Porosity (%)
dry sand flats - HRDGS
damp sand flats - HRDGS
braid bars sands - DTFR
sheetflood/crevasse - DTFR
braid bar sands - VLPR
sheetflood/crevase sands - VLPR

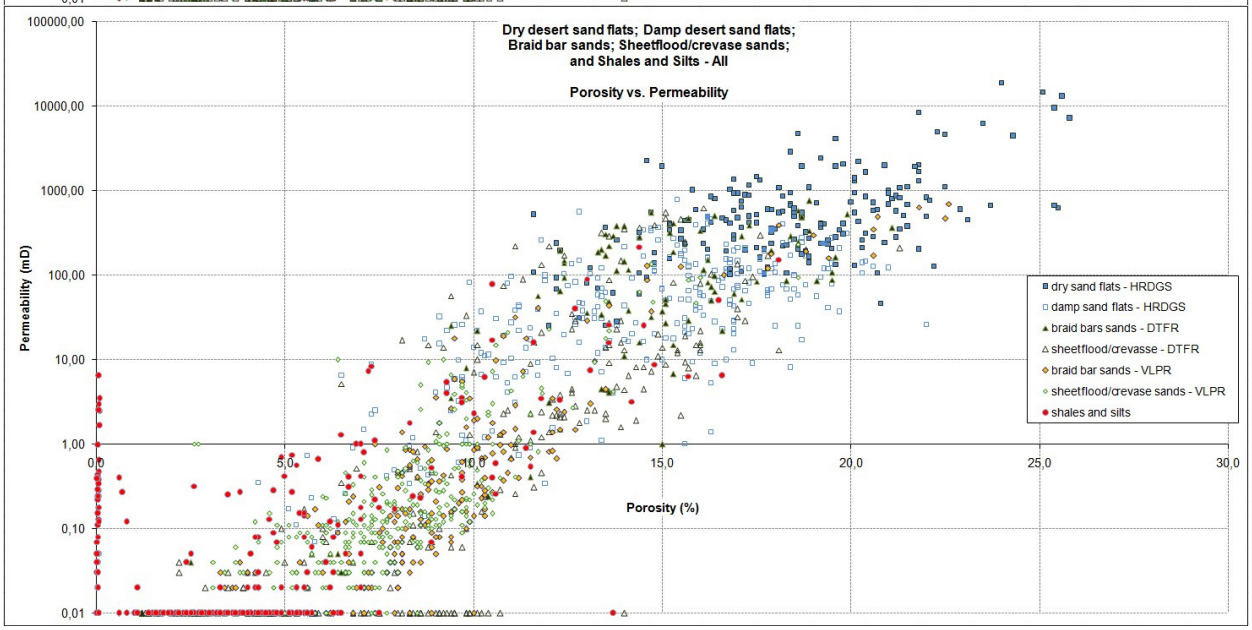
Dry desert sand flats; Damp desert sand flats;
Braid bar sands; Sheetflood/crevase sands;
and Shales and Silts - All
Porosity vs. Permeability
Permeability (mD)
100000,00
10000,00
1000,00
100,00
10,00
1,00
0,10
0,01
0,0
5,0
10,0
15,0
20,0
25,0
30,0
Porosity (%)
dry sand flats - HRDGS
damp sand flats - HRDGS
braid bars sands - DTFR
sheetflood/crevasse - DTFR
braid bar sands - VLPR
sheetflood/crevase sands - VLPR
shales and silts

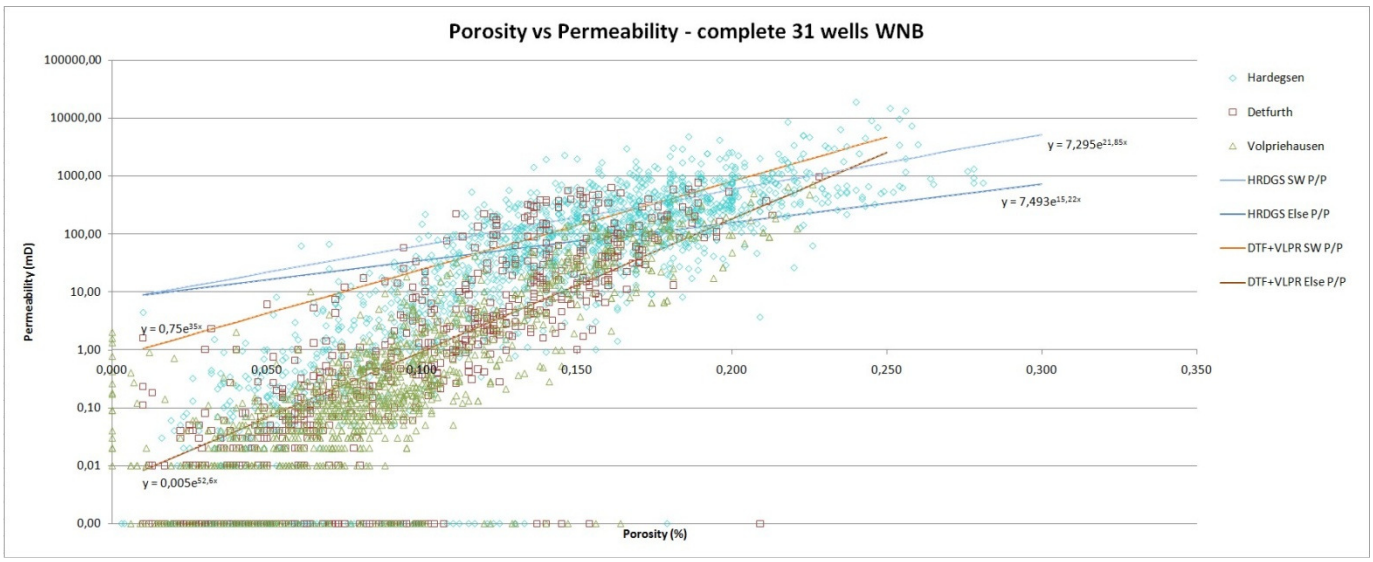
Porosity vs Permeability - complete 31 wells WNB
Permeability (mD)
Porosity (%)
y = 7,295e21,85x
y = 7,493e15,22x
y = 0,75e35x
y = 0,005e52,6x
Hardegsen
Detfurth
Volpriehausen
HRDGS SW P/P
HRDGS Else P/P
DTF+VLPR SW P/P
DTF+VLPR Else P/P

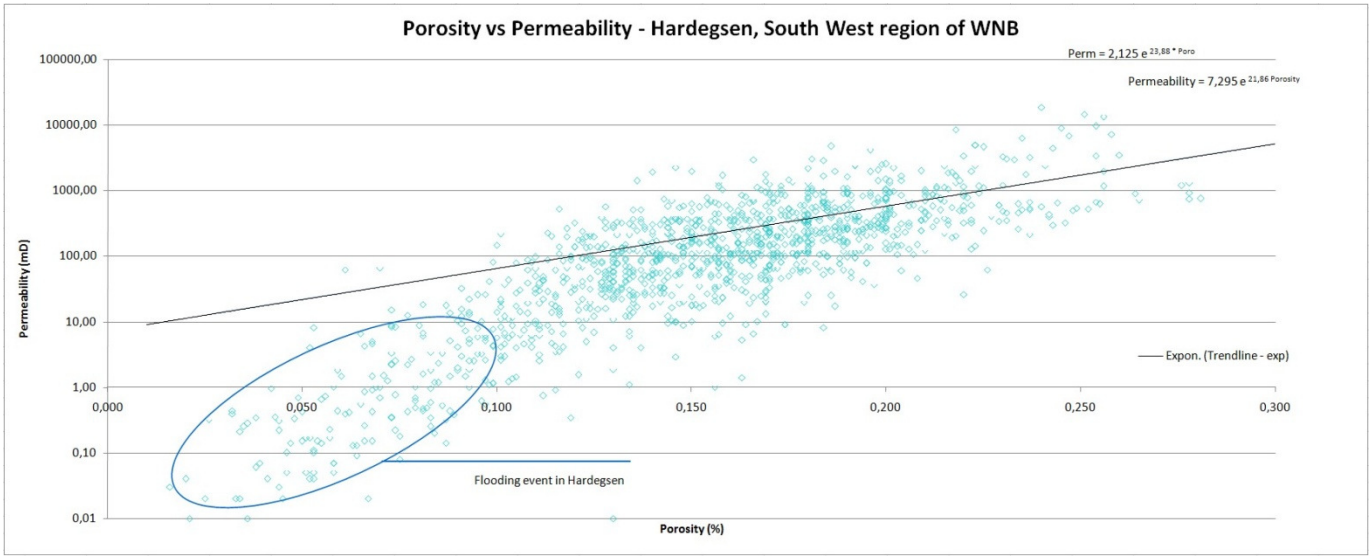
Porosity vs Permeability - Hardegsen, South West region of WNB
Perm = 2,125 e 23,88 * Poro
Permeability = 7,295 e 21,86 Porosity
Permeability (mD)
Porosity (%)
Expon. (Trendline - exp)
Flooding event in Hardegsen